

The University of Greenwich



the
UNIVERSITY
of
GREENWICH



Self-incompatibility in *Cosmos atrosanguineus*:
a rare Mexican endemic species
of Asteraceae

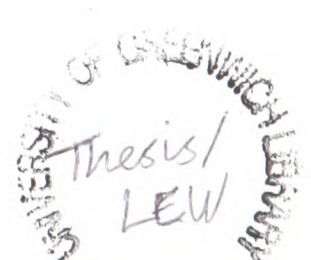
A thesis submitted by

Sarah LEWENDON

for the degree of
Doctor of Philosophy

Biological, Chemical and Life Sciences
The University of Greenwich
&
Jodrell Laboratory
Royal Botanic Gardens, Kew

July 2005



ABSTRACT

This work centres on *Cosmos atrosanguineus*, a rare Mexican endemic self-incompatible species of Asteraceae that is now believed to be extinct in the wild. The two known wild *C. atrosanguineus* collections, made in the 19th century, localise the species to the pine-oak mountain forest ecological region in two areas of central Mexico. Its disappearance from the natural environment is attributed to habitat destruction by the copper mining industry and subsequent urbanisation, so that *C. atrosanguineus* is now known only as a cultivated species. European and American *C. atrosanguineus* populations are probably the progeny of seed collected in the 1860s by Benedict Roezl and brought to Europe for plant verification. Sir William Jackson Hooker (1785-1865), Director of the Royal Botanic Gardens, Kew initially identified the Roezl specimen as *Cosmos diversifolius* var. *atrosanguineus*, but it was classified as the distinct species, *Cosmos atrosanguineus* by Andreas Voss in 1894. *Cosmos atrosanguineus* is much prized in horticulture for its deep-red “atrosanguinate” blooms, which are deliciously chocolate scented, giving rise to its common name, “the Hot Chocolate Plant”. From 1885 to 1942, *C. atrosanguineus* was sold as seed in England by Thompson and Morgan Seed Merchants, under the name of *C. diversifolius atrosanguineus*, but disappeared from the Thompson and Morgan seed catalogue thereafter. *Cosmos atrosanguineus* exhibits strong sporophytic self-incompatibility (SSI), does not set seed, and must be propagated vegetatively, a factor that has contributed to the proliferation of closely related or identical genotypes. Microsporogenesis within the species appears normal, with no discernible differences between microsporogenesis in *C. atrosanguineus* and two seed-producing *Cosmos* species. The *C. atrosanguineus* karyotype and chromosome associations at meiosis identify the species as an allotetraploid that produces viable gametes with ~30% pollen viability. Self- and cross-pollinations of *C. atrosanguineus* are strongly incompatible with an average of zero pollen grains germinating per stigma. In contrast, cross and self-pollinations in *C. bipinnatus* and *C. sulphureus* produced three compatibility groups; incompatible (-), compatible (+) and semi-compatible (\pm), and four categories of pollen-stigma interaction that putatively identify a gametophytic-sporophytic (G-S) incompatibility system in *Cosmos*. Dominance interactions of S-alleles are prevalent in the genus and pseudo-self-compatibility was observed in *C. bipinnatus* but not *C. atrosanguineus*. The *Cosmos* stigma is dry, papillate and becomes receptive only after stigmas become reflexed. Prior to this period, the stigmas do not respond to pollination and selfed bud pollinations and crossed bud pollinations are incompatible. Degenerate S-specific primers identified 41 S-domain-encoding sequences from *Cosmos* and four other genera of Asteraceae. These 41 Asteraceae sequences encoded S-domains related to *Brassica* S-domain proteins, but none identified as a putative self-incompatible molecule, indicating the control of SI in *Cosmos* is probably different to that in *Brassica*. Genetic fingerprinting studies (AFLP) of various European sources of *C. atrosanguineus* showed no genetic variation. In conclusion, *Cosmos atrosanguineus* is a strongly self-incompatible species with a reduced genome. It does not set seed because the gene pool of cultivated individuals has narrowed to a level where S-allele numbers are too few to produce cross compatible genotypes. For this to have occurred, the genetic diversity of plants at the Royal Botanic Gardens Kew and in commercial cultivation must have been reduced to genets that share one, but more probably both S-alleles, thus preventing germination of pollen and formation of seed.

ACKNOWLEDGMENTS

The ten years that have passed since I embarked on this part-time route to a PhD have led me down many paths, none of which I could have completed without the support, advice and kindness of the many individuals. First and foremost I would like to thank my two supervisors, Prof. Simon Owens, at the Royal Botanic Gardens Kew, for his unstinting support and guidance throughout this work, and for setting me such a captivating project, and Dr Ivor Evans, at the University of Greenwich, for his enthusiasm, encouragement and awesome editing skills.

I would also like to thank my colleagues at the Jodrell Laboratory and the Herbarium of the Royal Botanic Gardens Kew for their help and hospitality while pursuing the various components of this work. In particular Dr Paula Rudall, Dr Hazel Wilkinson, Dr Carol Furness, Dr Mary Clare Sheahan, Chrissie Prychid, and Tim Lawrence for their skills and wisdom in plant anatomy; Dr Peter Brandham, Dr Ilia Leitch, Lynda Hanson and Margaret Johnson for opening my eyes to the value of plant cytology, with a special debt of gratitude to Dr Peter Brandham, who took me from apprentice to journeyman in the fields of plant cytology and botanical photography; Prof Mark Chase, and Dr Vincent Savolainen for allowing me to develop the molecular component of the thesis, and to the indefatigable team of the Molecular Systematics section, Dr Dolores Lledó (Lola), Dr Tim Fulcher, Robyn Cowan, Jeffrey Joseph, Edith Kapinos, Laszlo Csiba, Martyn Powell, Jim Clarkson, Dion Devey and Olivier Maurin. I am grateful to Dr Alison Scott-Brown, Dr Paul Green and Dr Elaine Porter for their help and encouragement throughout the PhD, as fellow part-time PhDs, I truly appreciated your advice and support, and to Dr Tetsuo Kokubun, Dr Melanie Howes and Dr Stephen Graham who were always at hand for advice. I am grateful to Dr Nicholas Hind for providing herbarium material for DNA extraction and for archiving my research material at the Herbarium, Royal Botanic Gardens Kew, Dr Dick Brummitt for his advice on matters of taxonomy, and to Linda Jenkins and John Sitch of Jodrell Glass for growing and attending to my research plants. Special thanks to Dr Lourdes Rico-Arce (Lulu) who was a fountain of knowledge regarding the flora of Mexico, and a conduit for the many productive research collaborations in Mexico. Many thanks also to Prof. Rzedowski and Maestra Rzedowski for their warmth and hospitality during our plant collecting trip in Mexico 2001.

I am indebted to all those visitors who passed through the Jodrell Laboratory and dropped their pearls of wisdom. In particular the members of the 'Weekend Crew', also known as "*the Usual Suspects*" who made working in the lab at the weekends so much fun; Dr Gerardo Salazar, Lidia Salazar, Dr Félix Forest, Dr Adrian Loo, Dr Caroline Van

den Heede, Dr Ng Yan Peng, Dr Philippe Cuenoud, Dr Helga Ochoterena, Dr Hilda Flores Olvera, Dr Cassio van den Berg, Dr Chris Pires, Dr Doug Goldman and Esther Francis. Your company was inspiring.

Many thanks also to Rosemary McClenaghan at HRI (Horticulture Research International) Wellesbourne for providing *Brassica* and *Arabidopsis* material for DNA extraction and Clare Horne, Horticultural Quality Control Manager of Thompson and Morgan (UK) Ltd, for providing copies of archived Thompson and Morgan seed catalogues.

I would also like to acknowledge the financial support provided by the Wingate Foundation, who partly funded one year of my PhD studies through a Wingate Scholarship.

I owe a tremendous debt of gratitude to my work colleagues in the Science Department of City and Islington College, who supported me in deed and spirit; Sue Addinell, Jill White, June Moseley, Christoforo Pambou, Dr Pedro Montiel, Roger Green, Avi Puri, Ian Taylor, Jane Hartley, Vanessa Nottage and Tom McGoldrick, your encouragement and kindness contributed significantly to my ability to complete this project. I remain eternally grateful to my Head of Department, Dave Swinscoe, my former Head of Department, Jon Duveen, and my confidant and Head of Biology, Dr Barry Brinklow for organising my teaching timetable so as to maximise both my teaching and research aspirations.

To my family, some of whom were children when I started the PhD, but were driving themselves to vote by its completion, thanks for your constant and unconditional support, and for making sure I had nourishing food more than once in a while.

London, July 2005

to *Vanessa* and *Gwen* for all their love and support

In memory of my Father
Carlton Herbert Bayley Harris

and my Grandparents
Edward and Violet Lewendon

TABLE OF CONTENTS

Declaration	1
Abstract.....	2
Acknowledgements.....	3
Dedications.....	5
Table of Contents.....	6
List of Tables.....	12
List of Figures.....	14
List of Plates.....	16
Chapter 1 – Introduction and review of literature	
1.1 – The study.....	18
1.1.1 – Rationale for the study.....	19
1.1.2 – Research methodology.....	20
1.1.3 – Description of <i>Cosmos bipinnatus</i> , <i>C. carvifolius</i> and <i>C. sulphureus</i>	21
(i) <i>Cosmos bipinnatus</i>	21
(ii) <i>Cosmos carvifolius</i>	24
(iii) <i>Cosmos sulphureus</i>	25
1.2 – Origins and Classification of Asteraceae.....	28
1.2.1 – Introduction.....	28
1.2.2 – Tribal relationships in Asteraceae: a review of recent phylogenies.....	32
1.3 – Polyploidy: genome duplication and evolution	41
1.3.1 – Introduction.....	41
1.3.2 – Hybridization, polyploidization and genome change.....	42
1.3.3 – Autopolyploidy and allopolyploidy: extremes of a polyploid continuum....	45
1.4 – Asteraceae cytology.....	48
1.4.1 – Chromosome numbers in Asteraceae.....	48
1.4.2 – Chromosome numbers in Heliantheae.....	48
1.4.3 – Previous cytological investigations in <i>Cosmos</i>	50
1.5 – Self-incompatibility in plants.....	54
1.5.1 – Introduction.....	54
1.5.2 – Homomorphic self-incompatibility: an intraspecific rejection system.....	60
1.5.3 – Molecular genetics of gametophytic self-incompatibility model.....	64
1.5.4 – Sporophytic self-incompatibility: the <i>Brassica</i> model.....	69
1.5.5 – Identifying sporophytic self-incompatibility (SSI) in plants.....	73
1.5.6 – SSI molecules in <i>Brassica</i> : structure and function.....	74
1.5.7 – <i>Brassica</i> S-receptor kinase (SRK) and the SRK S-domain.....	77
1.5.8 – Plant receptor-like kinases (RLKs).....	81
1.5.9 – Molecular mechanisms of SI in <i>Brassica</i>	93

1.5.10 – SI signal transduction and SRK substrate molecules.....	95
1.6 – Ecology of Mexico: a general overview.....	103
1.6.1 – Physical geography of Mexico.....	103
1.6.2 – Floristic richness and megadiversity of Mexico.....	111
1.6.3 – Loss of biodiversity in Mexico	115
1.6.4 – Summary.....	117

Chapter 2 – The story of *Cosmos atrosanguineus*

2.1 – <i>Cosmos atrosanguineus</i> in the natural environment.....	118
2.2 – Horticultural importance of <i>Cosmos atrosanguineus</i>	120
2.3 – Emergence of <i>Cosmos atrosanguineus</i> as a cultivated species.....	121
2.4 – <i>Cosmos atrosanguineus</i> : a possible self-incompatible clone.....	122
2.5 – Summary.....	124

Chapter 3 – *Cosmos* floral biology

3.1 – Introduction.....	125
3.2 – Materials and Methods.....	125
3.2.1 – Light microscopy.....	125
3.2.2 – CryoSEM and Ambient SEM.....	126
3.2.3 – Semi-thin resin sections (smRS).....	126
3.2.4 – Light macroscopy.....	126
3.3 – Results and Discussion.....	127
3.3.1 – <i>Cosmos</i> floral morphology.....	127
3.3.2 – Comparison of disk-floret development in <i>Cosmos atrosanguineus</i> and <i>C. bipinnatus</i>	129
(i) Stage-1 florets.....	129
(ii) Stage-2 florets.....	130
(iii) Stage-3 florets.....	131
3.3.2 – Microsporogenesis and disk floret development in <i>Cosmos</i>	135
(i) Early stage-1 – Pre-meiosis.....	135
(ii) Mid stage-1 – From meiosis to free microspores	138
(iii) Late stage-1 – From invasive tapetum to binucleate pollen.....	142
(iv) Early stage-2 – from engorging pollen grains to second mitosis.....	158
(v) Mid to Late stage-2 – Anther dehiscence.....	161
(vi) Early to Mid stage-3 – Emergence of anther tube from corolla and separation of stigma lobes.....	164
(vii) Late stage-3 – From arched to fully reflexed stigmas.....	169
3.3.3 – Conclusion.....	171

Chapter 4 – Cytological investigations in *Cosmos*

4.1 – Introduction.....	172
4.1.1 – Pollen viability: a discussion of methods.....	173
4.2 – Materials and Methods.....	176
4.2.1 – Chromosome counts: mitosis in root tip cells.....	176
4.2.2 – Chromosome counts: meiosis in pollen mother cells (PMCs).....	176
4.2.3 – Meiotic index.....	176
4.2.4 – Permanizing slides	177
4.2.5 – Preparation of karyotypes.....	177
4.2.6 – Idiograms of chromosomes at diakinesis-metaphase 1.....	178
4.2.7 – Fluorescein diacetate (FDA) determination of pollen viability	178
4.2.8 – Estimating pollen-grain number per disk floret	179
4.2.9 – Calculating pollen-grain size	180
4.2.10 – Statistical methods.....	180
4.3 – Results and Discussion.....	180
4.3.1 – Introduction.....	180
4.3.2 – Karyotypes of <i>Cosmos</i> mitosis (root-tip) chromosomes.....	182
(i) <i>Cosmos atrosanguineus</i>	182
(ii) <i>Cosmos bipinnatus</i>	183
(iii) <i>Cosmos carvifolius</i>	184
(iv) <i>Cosmos sulphureus</i>	185
4.3.3 – Idiograms of chromosomes at diakinesis-metaphase I.....	188
(i) <i>Cosmos atrosanguineus</i>	189
(ii) <i>Cosmos bipinnatus</i>	189
(iii) <i>Cosmos sulphureus</i>	189
4.3.4 – Pollen viability in three <i>Cosmos</i> species.....	192
4.3.5 – Pollen-grain number in three <i>Cosmos</i> species.....	196
4.3.6 – Analysis of pollen viability and pollen-grain number.....	199
4.3.7 – Pollen-grain size in three <i>Cosmos</i> species.....	200
4.3.8 – Summary.....	201
4.3.9 – Conclusion.....	204
4.3.10 – Possible progenitor species of <i>Cosmos atrosanguineus</i>	204
4.3.11 – Possible centre of origin of atrosanguinate <i>Cosmos</i> species.....	215
Chapter 5 – Pollen-stigma interactions in <i>Cosmos</i>	
5.1 – Introduction.....	217
5.1.1 – Pollen-stigma Interactions in SSI species: the <i>Brassica</i> model	217
5.1.2 – Pollen-stigma Interactions in SSI species: the Asteraceae model.....	218
5.2 – Materials and Methods.....	221
5.2.1 – <i>Cosmos</i> reproductive Biology: cross- and self-pollinations	221

5.2.2 – Forced self-pollinations	
(i) Saline treatment.....	222
(ii) Bud pollinations.....	222
5.2.3 – Pollen-stigma Interactions in <i>Cosmos</i>	223
5.2.4 – Interspecific pollinations: <i>C. atrosanguineus</i> and <i>C. bipinnatus</i>	223
5.3 – Results.....	223
5.3.1 – Forced self-pollinations	223
(i) Saline treatment.....	223
(ii) Bud pollinations.....	224
5.3.2 – Stigma receptivity in <i>Cosmos</i>	225
5.3.3 – The <i>Cosmos</i> pollen-stigma interaction	227
5.3.4 – Interspecific pollinations: <i>C. atrosanguineus</i> x <i>C. bipinnatus</i>	236
5.3.5 – Pollination experiments in populations of <i>C. atrosanguineus</i> , <i>C. bipinnatus</i> and <i>C. sulphureus</i>	237
5.3.6 – Analysis of pollination experiments in <i>Cosmos</i>	247
(i) Introduction.....	247
(ii) Pollination in five <i>Cosmos bipinnatus</i> individuals.....	247
(iii) Estimating possible S-allele specificities in five <i>Cosmos bipinnatus</i> (1996 582) individuals Bip 1 to Bip 5.....	252
5.4 – Discussion.....	256
5.4.1 – Introduction.....	256
5.4.2 – Interspecific pollinations between <i>C. atrosanguineus</i> x <i>C. bipinnatus</i>	258
5.4.3 – Pollen-stigma interactions in <i>Cosmos</i>	259
5.4.4 – Conclusion.....	259
Chapter 6 – In search of the <i>Cosmos</i> self-incompatibility gene	
6.1 – Introduction.....	260
6.1.1 – The S-domain multigene family.....	260
6.1.2 – S-gene and S-domain morphology	262
6.1.3 – Diagnostic features of the S-domain	263
6.1.4 – Using sequence conservation to isolate S-genes.....	265
6.2 – Materials and Methods.....	266
6.2.1 – Plant material	266
6.2.2 – Primers	268
6.2.3 – DNA extraction.....	269
6.2.4 – PCR amplification.....	270
6.2.5 – Cycle sequencing	270
6.2.6 – Sequence editing and analysis.....	271
6.2.7 – Tree-building methods.....	272

6.3 – Results.....	273
6.3.1 – Introduction	273
(i) Assessment of DNA quality.....	273
(ii) Assessment of amplification and cycle-sequencing reactions.....	273
(iii) Sequence quality	273
(iv) Open Reading Frames (ORFs) and longest length ORFS.....	273
6.3.2 – Analysis of Results	275
(i) PCR amplification and cycle-sequencing reactions	275
(ii) Control species	275
(iii) Analysis of taxa-specific nucleotide sequences and encoded protein sequences	276
6.3.3 – Analysis of encoded <i>Arabidopsis thaliana</i> and <i>Brassica oleracea</i> CosPS protein sequences.....	286
6.3.4 – Analysis of encoded Asteraceae CosPS protein sequences.....	287
6.3.5 – Criteria for identifying S-domain CosPS sequences.....	288
6.4 – Discussion.....	294
6.4.1 – Trends and Patterns in CosPS sequences.....	294
6.4.2 – Homology of CosPS Sequences	
(i) <i>Brassica oleracea</i> CosPS sequences 5+6 (band 2), and 9 (band 2) are SLR3-1 homologues.....	295
(ii) Primer Pair 2 generates <i>BcRL3</i> homologues in <i>B. oleracea</i> , <i>Cosmos</i> <i>bipinnatus</i> and two species of <i>Senecio</i> . Primer Pair 13 generates <i>BcRL3</i> homologues in <i>Brassica oleracea</i>	296
(iii) Primer Pair 12 generates <i>BcRK1</i> homologues in <i>B. oleracea</i>	298
6.4.3 – Pairwise percentage identities of encoded CosPS protein sequences generated by primer pairs 1-15 in species of Asteraceae and <i>Diplotaxis</i> <i>tenuifolia</i>	299
6.5 – Analysis of encoded CosPS S-domain sequences.....	303
6.5.1 – Introduction.....	303
6.5.2 – Distance relationships of 41 encoded CosPS S-domains of Asteraceae and <i>Diplotaxis tenuifolia</i>	306
6.5.3 – Distance relationships of 88 encoded CosPS S-domains with Brassicaceae, Convolvulaceae and Fabaceae S-domains	310
6.4.6 – Summary.....	331

Chapter 7 – Concluding comments and future prospects

7.1 - Discussion.....	333
-----------------------	-----

Bibliography	340
---------------------------	-----

Appendices

Appendix 1 - Names, descriptions and abbreviations of RLKs, RTKs and associated molecules.....	i
Appendix 2 - The story of <i>Cosmos atrosanguineus</i>	vii
2.1 - Life and times of Benedict Roezl.....	vii
(a) Reproduction of an article on the life of Benedict Roezl printed in <i>The Gardeners Chronicle</i> , July 18, 1874. (p.73).....	vii

(b) Enlarged extract of columns 1 and 2 from the Article on the Life of Benedict Roezl printed in <i>The Gardeners Chronicle</i> , July 18, 1874. (p.73).....	viii
(c) Enlarged extract of columns 2 and 3 from the Article on the Life of Benedict Roezl printed in <i>The Gardeners Chronicle</i> , July 18, 1874. (p.73).....	ix
2.2 - Front cover of the fax that accompanied copies of the 1885, 1902 Thompson's seed catalogues and the 1942 Thompson and Morgan seed catalogue.....	x
2.3 - Thompson's 1885 Seed Catalogue.....	xi
(a) Front Cover.....	xi
(b) Pages 12-13.....	xii
2.4 - Thompson's 1902 Seed Catalogue (pages 24-25).....	xiii
2.5 - Thompson and Morgan's 1942 Seed Catalogue.....	xiv
(a) Front and back pages.	xiv
(b) Pages 12-13.....	xv
2.6 - Correspondence between Sarah Lewendon and Brian Halliwell.....	xvi
(a) - Letter from Sarah Lewendon (28-3-99) to Brian Halliwell requesting information on the <i>Cosmos atrosanguineus</i> ' accessions at the Royal Botanic Gardens, Kew.	xvi
(b) - Reply from Brian Halliwell (5-4-99) to Sarah Lewendon's letter dated (28-3-99).....	xvii
Appendix 3 - Anatomy protocols	
3.1 - Protocol 1: Wax embedding.....	xviii
3.2 - Protocol 2: Staining schedule (safranin and alcian blue).....	xviii
3.3 - Protocol 3: Alcohol series for CPD.....	xix
3.4 - Protocol 4: Resin embedding.....	xix
Appendix 4 - Statistical analyses for Chapter 4	
4.1 - Descriptive statistics for pollen viability, pollen number and pollen size.....	xx
4.2 - Statistical analysis of pollen viability, pollen number and pollen size in <i>Cosmos</i>	xxii
Appendix 5 - Statistical analyses and plant data for Chapter 5	
5.1 - Descriptive Statistics for compatible pollen tubes and incompatible pollen tubes produced in all <i>Cosmos bipinnatus</i> compatibility groups.....	xxix
5.2 - Statistical analysis of compatible pollen tubes and incompatible pollen tubes produced in all <i>Cosmos bipinnatus</i> compatibility groups.....	xxxii
5.3 - Statistical analysis of <i>Cosmos bipinnatus</i> pollination groups.....	xxxii
5.4 - Royal Botanic Gardens, Kew (RBG, Kew) Plant Data for <i>Cosmos</i> accessions used in POLL-01 pollinations (Chapter 5)	xlii
(a) <i>Cosmos atrosanguineus</i>	xlii
(b) <i>Cosmos bipinnatus</i>	xliv
(a) <i>Cosmos sulphureus</i>	xlvi
(a) <i>Cosmos carvifolius</i>	xlvii
Appendix 6 - Review of <i>Brassica</i> S-primers.....	xlix
6.1 - Published <i>Brassica</i> S-primers used in PCR-amplification and cycle sequencing of S-genes in <i>Brassica</i> and <i>Arabidopsis</i> species.....	xl
6.2 - Analysis of priming characteristics of published <i>Brassica</i> S-primer pairs	xli

LIST OF TABLES

CHAPTER 1

TABLE 1.1 – Flowering times in Mexico and England of four <i>Cosmos</i> species.....	27
TABLE 1.2 – Reported chromosome numbers for <i>Cosmos</i> species.....	52
TABLE 1.3 – Homomorphic self-incompatibility in angiosperms	55
TABLE 1.4 – Comparison of the genotype and phenotype of gametophytic-sporophytic (G-S) incompatibility in Brassicaceae and Asteraceae	74
TABLE 1.5 – Classification, expression and specificity of plant receptor-like kinases (RLKs).....	86
TABLE 1.6 – Best-represented plant families in Mexico	112
TABLE 1.7 – Plant diversity and endemism versus ecological zones of Mexico.....	113
TABLE 1.8 – Approximate percentage of Mexican endemism in some families of flowering plants	114
TABLE 1.9 – Deforestation rate by forest type in Mexico.....	116
TABLE 1.10 – Types of forest and causes of deforestation in Mexico.....	116

CHAPTER 4

TABLE 4.1 - <i>Cosmos</i> plant material and photomicrographs used in cytology investigation.....	178
TABLE 4.2 - Summary of cytological investigations of four <i>Cosmos</i> species	187
TABLE 4.3 – C-DNA values of four <i>Cosmos</i> species	187
TABLE 4.4 – Numbers of normal tetrads, anaphase-I laggards and bridges observed in accessions of <i>C. atrosanguineus</i> and <i>C. bipinnatus</i>	190
TABLE 4.5 – Chromosome associations at diakinesis in three <i>Cosmos</i> species	190
TABLE 4.6 – Pollen-viability: <i>Cosmos atrosanguineus</i>	192
TABLE 4.7 – Pollen-viability: <i>Cosmos bipinnatus</i> 1996 582.....	193
TABLE 4.8 – Pollen-viability: <i>Cosmos sulphureus</i> 1996 980 (Autumn).....	194
TABLE 4.9 – Pollen-viability: <i>Cosmos sulphureus</i> 1996 980 (Spring).....	194
TABLE 4.10 – <i>Cosmos</i> pollen-grain numbers per 4- μ l sample of vortexed anther solution	196
TABLE 4.11 – Size of mature pollen grains in three <i>Cosmos</i> species	200
TABLE 4.12 – Flowering times in Mexico of thirteen <i>Cosmos</i> species	212

CHAPTER 5

TABLES 5.1a-e – Pollination results: POLL-01 <i>Cosmos bipinnatus</i> (1995 582) Bip 1 to Bip 5... 238	238
TABLE 5.2 – Compatibility relationships: POLL-01 <i>Cosmos bipinnatus</i> (1995 582) Bip 1 to Bip.. 241	241
TABLES 5.3a-e – Pollination results of POLL-01 <i>Cosmos atrosanguineus</i> (1999 3819) Atro 1 to Atro 5..... 242	242
TABLE 5.4 – Compatibility relationships of POLL-01 <i>Cosmos atrosanguineus</i> Atro 1 to Atro 5... 244	244
TABLES 5.5a-d – Pollination results of POLL-01 <i>Cosmos sulphureus</i> (1996 980) Sul 1 to Sul 4..... 245	245
TABLE 5.4 – Compatibility relationships of POLL-01 <i>Cosmos sulphureus</i> (1996 980) Sul 1 to Sul 4..... 246	246
TABLE 5.7 – Possible S and G alleles in <i>C. bipinnatus</i> (1995 582) individuals Bip 1 to Bip 5..... 253	253
TABLE 5.8 – Compatibility relationships in POLL-01 <i>Cosmos bipinnatus</i> (1995 582) Bip 1 to Bip 5 with possible dominance interactions of S alleles in stigma and pollen..... 253	253

CHAPTER 6

TABLE 6.1 – S- genes: abbreviations, names and plant origin.....	260
TABLE 6.2 – Plant material	267
TABLE 6.3 – Primer pairs	269
TABLE 6.4 – Results of amplification and cycle-sequencing reactions in species of Asteraceae and Brassicaceae	274
TABLE 6.5 – Longest ORFs of nucleotide sequences generated by primer pairs 1-15 in species of Asteraceae and Brassicaceae.....	276
TABLE 6.6 – List of the 88 distinct CosPS nucleotide sequences generated by primer pairs 1-15 in species of Asteraceae and Brassicaceae.....	284
TABLE 6.7 – Location of S-associated conserved domains in fifty full-length S-protein and S-like protein sequences	289
TABLE 6.8 – Positions of S-associated conserved domains in predicted CosPS protein sequences of Asteraceae species and <i>Diplotaxis tenuifolia</i>	291
TABLE 6.9a – Percentage pairwise identities of <i>SLR3-1</i> homologues generated by primer pairs 5+6 and 9 in <i>Brassica oleracea</i> haplotypes S3, S5, S6, S13, S15 compared with <i>Brassica oleracea SLR3-1</i> (X81833).....	296
TABLE 6.9b – Percentage pairwise identities of <i>SLR3-1</i> homologues of <i>Brassica oleracea</i> haplotypes S3, S5, S6, S13, S15 and <i>Brassica oleracea SLR3-1</i> (CAA57427).....	296
TABLE 6.10a – Percentage pairwise identities of <i>BcRL3</i> homologues generated by primer pairs 2 and 13 in <i>Brassica oleracea</i> haplotypes S2, S3, S6, S9, S13, <i>Cosmos bipinnatus</i> , <i>Senecio squalidus</i> , <i>S. vulgaris</i> compared with <i>Brassica rapa BcRL3</i> (AB041620)	298
TABLE 6.10b – Percentage pairwise identities of <i>BcRK3</i> homologues of <i>Brassica oleracea</i> haplotypes S2, S3, S6, S9, S13, <i>Cosmos bipinnatus</i> , <i>Senecio squalidus</i> , <i>S. vulgaris</i> and <i>Brassica rapa BcRk3</i> (BAB69682)	298
TABLE 6.11a – Percentage pairwise identities of <i>BcRK1</i> homologues of <i>Brassica oleracea</i> haplotypes S2, S3, S6, S9, S13, S15, S29, and <i>Brassica rapa BcRK1</i> (AB000970)	299
TABLE 6.11b – Percentage pairwise identities of <i>SRK1</i> homologues of <i>Brassica oleracea</i> haplotypes S2, S3, S6, S9, S13, S15, S29, and <i>Brassica rapa SRK1</i> (BAB69682)	299
TABLE 6.12 – Percentage pairwise identities of predicted CosPS protein sequences generated by primer pairs 1-15 in Asteraceae species and <i>Diplotaxis tenuifolia</i>	301
TABLE 6.13a –List of NCBI S-domain protein sequences form Asteraceae, Brassicaceae, Convolvulaceae and Fabaceae used to construct Neighbour-Joining (NJ) trees of plant S-domains.....	310
TABLE 6.13b – List of encoded CosPS sequences, generated by Primer Pairs 1-15, and used to construct Neighbour-Joining (NJ) trees of plant S-domains.....	317
TABLE 6.13c – List of NCBI S-domain protein sequences used as outgroup sequences in the construction the Neighbour-Joining (NJ) trees of plant S-domains.....	319
TABLE 6.14 – Four Brassicaceae tribes and some respective genera.....	327

LIST OF FIGURES

CHAPTER 1

FIGURE 1.1 – Distribution map of <i>Cosmos bipinnatus</i> in Mexico.....	21
FIGURE 1.2 – Distribution map of <i>Cosmos carvifolius</i> in Mexico.....	24
FIGURE 1.3 – Distribution map of <i>Cosmos sulphureus</i> in Mexico.....	26
FIGURE 1.4 – Comparison of five suprageneric classifications of Asteraceae.....	31
FIGURE 1.5 – (Kim and Jansen, 1995). Phylogeny of Asteraceae tribes resolved using the chloroplast <i>ndhF</i> gene	37
FIGURE 1.6 – (Bremer 1996). Phylogeny of Asteraceae tribes resolved using morphological and molecular data	37
FIGURE 1.7 – (Bayer and Starr, 1998). Phylogeny of Asteraceae tribes resolved using <i>trnL</i> intron and <i>trnL/trnF</i> intergenic spacer	38
FIGURE 1.8 – (Wagstaff and Breitwieser 2002). Phylogeny of Asteraceae tribes resolved using ITS	39
FIGURE 1.9 – (Goertzen <i>et al.</i> , 2003). Phylogeny of Asteraceae tribes resolved using <i>ndrF</i> and ITS.....	39
FIGURE 1.10 – (Panero and Funk, 2002). Phylogeny of Asteraceae tribes resolved using <i>ndhF</i> , <i>trnL-trnF</i> , <i>matK</i> , <i>ndhD</i> , <i>rbcl</i> , <i>rpoB</i> , <i>rpoC1</i> exon 1, 23S- <i>trnL</i> and <i>ndhI</i>	40
FIGURE 1.11 – Sub-tribal relationships in the Heliantheae.....	51
FIGURE 1.12a – GSI with independent interaction of S-alleles.....	61
FIGURE 1.12b – GSI with dominance interaction of S-alleles in the pistil and independent action of S-alleles in the pollen S-alleles.....	61
FIGURE 1.12c – SSI with independent interaction of S-alleles	62
FIGURE 1.12d – SSI with dominance interaction of S-alleles in the pollen and Independent action in the pistil S-alleles.....	62
FIGURE 1.13 – Dominance interactions of some S alleles in the pollen and stigma of <i>Iberis amara</i> , <i>Cosmos bipinnatus</i> , <i>Ipomoea trifida</i> , <i>Arabidopsis lyrata</i> and <i>Senecio squalidus</i>	72
FIGURE 1.14 – Schematic representation of the S locus with emphasis on the locations of <i>SRK</i> , <i>SCR</i> and <i>SLG</i>	77
FIGURE 1.15 – Generalised structure of <i>Brassica oleracea</i> SRK6	79
FIGURE 1.16 – Generalised plan of Mexico	105
FIGURE 1.17 – Physical maps of Mexico.....	107
FIGURE 1.18 – Climate maps of Mexico	110
FIGURE 1.19 – Map of the principal types of vegetation in Mexico	111
FIGURE 1.20 – Map showing floristic diversity in the 20 main floristic treatments of Mexico.....	112

CHAPTER 2

FIGURE 2.1 – <i>Cosmos atrosanguineus</i> plate 5227 from <i>Curtis's Botanical Magazine</i>	119
FIGURE 2.2 – Distribution map of <i>Cosmos atrosanguineus</i> in Mexico	120

CHAPTER 4

FIGURE 4.1 – Somatic (root) cell showing chromosomes of <i>Cosmos atrosanguineus</i> (98-69)	182
FIGURE 4.2 – Somatic (root) cell showing chromosomes of <i>Cosmos atrosanguineus</i> (98-82).....	182
FIGURE 4.3 – Karyotype drawing of <i>Cosmos atrosanguineus</i> (98-82).....	182
FIGURE 4.4 – Somatic (root) cell showing chromosomes of <i>Cosmos bipinnatus</i> (98-86).....	183

FIGURE 4.5 – Karyotype drawing of <i>Cosmos bipinnatus</i> (98-86)	183
FIGURE 4.6 – Somatic (root) cell showing chromosomes of <i>Cosmos carvifolius</i> (98-136)	184
FIGURE 4.7 – Karyotype drawing of <i>Cosmos carvifolius</i> (98-136).....	184
FIGURE 4.8 – Somatic (root) cell showing chromosomes of <i>Cosmos sulphureus</i> (98-49).....	185
FIGURE 4.9 – Karyotype drawing of <i>Cosmos sulphureus</i> (98-49).....	185
FIGURE 4.10 – <i>Cosmos</i> chromosomes at diakinesis-metaphase-I with associated drawing.....	188
FIGURE 4.11 – Idiogram of <i>Cosmos atrosanguineus</i> chromosomes at diakinesis-metaphase.....	189
FIGURE 4.12 – Idiogram of <i>Cosmos bipinnatus</i> chromosomes at diakinesis-metaphase I	189
FIGURE 4.13 – Idiogram of <i>Cosmos sulphureus</i> chromosomes at diakinesis-metaphase I	189
FIGURE 4.14 – Bar chart showing pollen viability of three <i>Cosmos</i> species.....	195
FIGURE 4.15 – Boxplot comparing number of pollen grains produced in three <i>Cosmos</i> species...	198
FIGURE 4.16 – Barchart of pollen volume in <i>Cosmos atrosanguineus</i> , <i>C. bipinnatus</i> and <i>C. sulphureus</i>	201
FIGURE 4.17 – Map showing distribution of <i>Cosmos scabiosoides</i> in Mexico.....	206
FIGURE 4.18 – Map show distribution of <i>Cosmos jaliscensis</i> in Mexico	207
FIGURE 4.19 – Map show distribution of <i>Cosmos concolor</i> in Mexico	208
FIGURE 4.20 – Map show distribution of <i>Cosmos montanus</i> in Mexico	208
FIGURE 4.21 – Map show distribution of <i>Cosmos purpureus</i> var. <i>purpureus</i> in Mexico.....	209
FIGURE 4.22 – Map show distribution of <i>Cosmos palmerii</i> var. <i>odontophyllus</i> in Mexico	210
FIGURE 4.23 – Map show distribution of <i>Cosmos diversifolius</i> in Mexico	211
FIGURE 4.24 – Map showing the known distribution of atrosanguinate <i>Cosmos</i> species in Mexico.....	215

CHAPTER 5

FIGURE 5.1 – Bar chart of compatible pollen tubes produced in all <i>Cosmos bipinnatus</i> crosses in pollination experiment POLL-01.....	241
FIGURE 5.2 – Scatter plot of compatible pollen tubes versus incompatible pollen tubes in all compatibility groups of the <i>Cosmos-bipinnatus</i> pollination experiment POLL-01....	250

CHAPTER 6

FIGURE 6.1. – Generalised structure of <i>Brassica oleracea</i> SLG6.....	264
FIGURE 6.2 – Schematic structure comparing S-domains of <i>Brassica oleracea</i> SLG6 and SLR1-22	264
FIGURE 6.3 – A phylogeny of core Eudicots emphasising the relationship of Brassicaceae, Fabaceae Convolvulaceae and Asteraceae.....	302
FIGURE 6.4a – A majority-rule neighbour-joining (NJ) Tree comparing distance relationships of deduced CosPS protein sequences generated by primer pairs 1-10, 12-13 and 15 in species of Asteraceae and <i>Diplotaxis tenuifolia</i>	304
FIGURE 6.4b – A phylogram of NJ Tree comparing distance relationships of deduced CosPSprotein sequences generated by primer pairs 1-10, 12-13 and 15 in species of Asteraceae and <i>Diplotaxis tenuifolia</i>	305
FIGURE 6.5a – NJ Tree of deduced CosPS S-domain sequences and S-domains from Brassicaceae, Convolvulaceae and Fabaceae.....	320
FIGURE 6.5b – A phylogram of NJ Tree of deduced CosPS S-domain sequences and S-domains from Brassicaceae, Convolvulaceae and Fabaceae.....	322

LIST OF PLATES

CHAPTER 1

- PLATE 1.1 – *Cosmos bipinnatus*: single weedy individual growing on fallow arable land in the state of Queretaro, Mexico 22
- PLATE 1.2 – *Cosmos bipinnatus*. Population of weedy plants growing in a grassy meadow in the state of Queretaro, Mexico 22
- PLATE 1.3 – A single capitulum of *Cosmos bipinnatus* 23
- PLATE 1.4 – A single capitulum of *Cosmos carvifolius* 25
- PLATE 1.5 – A single capitulum of *Cosmos sulphureus* 27

CHAPTER 2

- PLATE 2.1 – *Cosmos atrosanguineus* single capitulum 121

CHAPTER 3

- PLATE 3.1 – *Cosmos atrosanguineus* stage-1 capitulum 127
- PLATE 3.2 – *Cosmos atrosanguineus* disk florets 128
- PLATE 3.3 – *Cosmos atrosanguineus* fully reflexed stigma lobe 129
- PLATE 3.4 – Morphological stages in the development of *Cosmos* disk florets..... 132
- PLATE 3.5 – TS stage-1, -2 and -3 disk florets of *Cosmos atrosanguineus* and *C. bipinnatus*..... 133
- PLATE 3.6 – Stage-3 disk florets of *Cosmos atrosanguineus*, showing the distinction between early, mid and late stage-3 disk florets 134
- PLATE 3.7 – *Cosmos atrosanguineus* stage-3 disk floret displayed..... 134
- PLATE 3.8 – *Cosmos atrosanguineus* early stage-1 disk florets..... 136
- PLATE 3.9 – *Cosmos atrosanguineus* LS early stage-1 disk florets..... 137
- PLATE 3.10 – *Cosmos* early to mid stage-1 disk florets..... 139
- PLATE 3.11 – *Cosmos atrosanguineus* LS mid stage-1 anthers..... 141
- PLATE 3.12 – Late stage-1 *Cosmos* disk florets..... 146
- PLATE 3.13a – Late stage-1 *Cosmos atrosanguineus* disk florets..... 147
- PLATE 3.13b – Enlarged Images of C and D from 3.13a showing detail of pollen wall layers in late stage-1 *Cosmos atrosanguineus* disk florets 148
- PLATE 3.14 – Late stage-1 *Cosmos* anthers..... 149
- PLATE 3.15 – Late stage-1 *Cosmos sulphureus* anthers..... 154
- PLATE 3.16 – LS Late stage-1 *Cosmos atrosanguineus* anthers..... 155
- PLATE 3.17 – Early stage-2 *Cosmos* pollen grains showing deposition of pollen coat..... 156
- PLATE 3.18 – Stage-1 and stage-2 *Cosmos* anthers..... 157
- PLATE 3.19 – TS *Cosmos atrosanguineus* disk florets, showing the transition from tetrasporangiate stage-1 to bisporangiate stage-2 anthers. 159
- PLATE 3.20 – Early and mid-stage-2 *Cosmos* anthers..... 160
- PLATE 3.21 – Late stage-2 *Cosmos* anthers..... 162
- PLATE 3.22 – *Cosmos* early to mid stage-3 stigmas..... 165
- PLATE 3.23 – Morphology of stage-3 *Cosmos* stigma..... 167
- PLATE 3.24 – Morphology of stage-3 *Cosmos* stigma 168
- PLATE 3.25 – Stage-3 *Cosmos* stigma papillae showing pellicle-cuticle layer 170

CHAPTER 5

PLATE 5.1 – <i>Cosmos bipinnatus</i> stage-2 disk florets with corolla and anther tube dissected open to show stage-2 stigma.....	223
PLATE 5.2 – <i>Cosmos</i> selfed bud pollinations	224
PLATE 5.3 – <i>Cosmos sulphureus</i> stage-3 disk florets showing stages in the development of the receptive stigma.....	225
PLATE 5.4 – <i>Cosmos bipinnatus</i> mid to late stage-3 stigmas revealing the onset of stigma receptivity.....	226
PLATE 5.5 – <i>Cosmos</i> pollen-stigma interaction, observed on short stigma papillae 15 to 45 minutes after cross pollination stage-1 inflorescence.....	227
PLATE 5.6 – Self-pollinated <i>Cosmos</i> stigmas showing category-1 type incompatibility 4 hours after pollination.....	228
PLATE 5.7 – Self-pollinated <i>Cosmos</i> stigmas, exhibiting a category-1 type incompatibility reactions observed 4 hours after pollination.....	229
PLATE 5.8 – <i>Cosmos atrosanguineus</i> cross-pollinated stigmas showing category-2 and category-3 type incompatibility reactions 8 hours after pollination.....	231
PLATE 5.9 – Cross-pollinated <i>Cosmos</i> stigmas.....	232
PLATE 5.10 – <i>Cosmos</i> cross-pollinated stigmas showing category-1 and category-2 type incompatibility reactions 8 hours after pollination.....	233
PLATE 5.11 – <i>Cosmos bipinnatus</i> cross-pollinated stigmas 8 hours after pollination, comparing category-2 and category-3 type incompatibility reactions in <i>Cosmos</i>	234
PLATE 5.12 – <i>Cosmos bipinnatus</i> stage-3 cross-pollinated stigmas 8 hours after pollination showing the segregation of incompatible and compatible pollen tubes.....	235
PLATE 5.13 – Interspecific pollinations between <i>Cosmos atrosanguineus</i> and <i>C. bipinnatus</i>	237

CHAPTER 1 – Introduction and review of literature

1.1 - The Study

The research reported here concerns self-incompatibility (SI) in a rare Mexican species of Compositae, *Cosmos atrosanguineus* (Asteraceae, Heliantheae), a species now apparently extinct in the wild (Ortega-Larrocea *et al.*, 1997; Wilkinson *et al.*, 1998, 2003). The circumstances for its disappearance from the natural environment are not known. Evidence from herbaria is consistent with a very narrow geographical and temporal distribution for the species, with wild collections limited to two localities; an 1878 collection from the state of San Luis Potosí and the original 1861 collection from Zimapán, a town in the state of Hidalgo, 200 kilometres south-east of San Luis Potosí, (Sherff, 1932; Sherff and Alexander, 1955). The loss of *C. atrosanguineus* from its wild habitat, whether through habitat destruction, over-zealous plant collecting or a deleterious natural bottleneck, has led to a predominance of cultivated specimens in the herbarium record (Roezl, 1874; Sherff, 1932; McVaugh, 1984; Ortega-Larrocea *et al.*, 1997; Wilkinson *et al.*, 1998).

Cosmos atrosanguineus is a self-incompatible (SI) perennial much prized in horticulture for its deep blood-red blooms, subtended singularly on long peduncles emerging from broad simply pinnate foliage (Brickell and Sharman, 1986; Wilkinson *et al.*, 1998). The daisy-like blooms range from 4-6 cm in diameter and are “deliciously chocolate scented” (Brickell and Sharman, 1986), giving rise to its common name, “The Hot Chocolate Plant”. *Cosmos atrosanguineus* does not set seed, and must be propagated vegetatively, a factor that has contributed to the proliferation of closely related and/or identical horticultural genotypes (Wilkinson *et al.*, 1998). Pollination experiments confirm a strong sporophytic self-incompatibility system in *Cosmos* (Little *et al.* 1940; Crowe, 1954). Strong self-incompatibility, combined with a reduced S-allele numbers may account for the inability of *C. atrosanguineus* to produce seed (Ortega-Larrocea *et al.*, 1997; Wilkinson, *et al.* 1998). This supposition requires investigation, as the putative *Cosmos* SI gene has not been identified, and the production of viable seed includes many components independent of SI. An outward appearance of self-incompatibility may actually be a consequence of failure in one or more of the many non-SI processes required for successful pollination. Aberrant chromosome pairing at meiosis can lead to problems in the production of viable gametes, and is a cause of sterility often encountered in polyploids (Stebbins, 1950, 1971). The pollen viability, reproductive biology and chromosomal behaviour at

meiosis need to be assessed in order to ascertain the reasons for the loss of fertility in *C. atrosanguineus*. This study set out to answer the questions, why *Cosmos atrosanguineus* does not set seed, and whether the molecular mechanism of SI in *Cosmos* and *Brassica* are the same. The two aims of the thesis were: to identify factors responsible for loss of seed production in *C. atrosanguineus*, through an examination of *Cosmos* floral biology (Chapter 3), cytology, (Chapter 4) and reproductive biology (Chapter 5), and the isolation, using degenerate primers, of the putative *Cosmos* SI gene (Chapter 6). In addition, the origins, history and geographical distribution of *Cosmos atrosanguineus* have been reviewed (Chapter 2), and the processes pertinent to the transition of *C. atrosanguineus* from a wild viable species to a cultivated non-viable putative clone have been discussed.

1.1.1 - Rationale for the Study

Studies of SI arose principally from the interests of plant breeders to manipulate self-incompatible plants (East and Mangelsdorf, 1925). It became apparent to early plant breeders that high proportions of plant species were self-incompatible and that an understanding of the causes SI could reap commercial rewards. The search for improved breeding techniques and new commercial varieties has driven and funded much of the research into self-incompatibility and consequently the majority of this research has focused on commercially important species in plant families such as the Brassicaceae, Solanaceae, Rosaceae and Poaceae.

For the academic community, studies of SI have provided a vehicle for broadening the foundations of plant biology, and the understanding the complexity and inter-relatedness of plant genomes, and is a paradigm for cell signalling in plants (Lewis, 1954; Ride, 1992; Kahmann and Bölker, 1996; Hiscock *et al.*, 1996; Hiscock and Kües, 1999). The emergence of the S-multigene family and the elucidation of the complex structure of the *Brassica* and *Arabidopsis* S loci exemplify this latter point (Dwyer *et al.*, 1989; Kianian and Quiros, 1992; Kumar and Trick, 1994; Bell, 1995; Boyes *et al.*, 1997; Pastuglia *et al.*, 1997, 2002). The S-multigene family comprises one of the most interesting plant-gene families, with S genes being associated with cell-cell recognition in compatibility relationships, plant defence mechanisms, plant development, and symbiosis (Harris *et al.*, 1984; Dangl 1995; Franklin *et al.* 1995, Schierup *et al.* 2001). Elucidating the nature, function and evolution of S-genes involved in these cell-cell recognition processes is aided through the identification of S-genes from a wide range of angiosperms. Consequently, hunting for S-genes is a

growing area of research and their isolation, identification and expression has become a prerequisite to studies in S-gene phylogeny and function (Pastuglia *et al.*, 1997, 2002; Bouchez and Höfte, 1998; Schierup *et al.* 2001). In addition, the dual role of certain S genes in plant signalling and plant development has analogies with the functional duality demonstrated by the Toll signalling pathway in *Drosophila* and the interleukin-1 (IL-1) response pathway in mammals (Pastuglia *et al.* 1997; see Section 1.5.7 below). Thus, in a broader scientific context, SI studies contribute to an understanding of self and non-self-recognition encompassing plant and animal research, in areas as diverse and important as sexual recognition, disease-resistance, plant development, and immune systems (Dzelzkalns, *et al.* 1992; Ellard-Ivey *et al.*, 1997). The study of self-incompatibility in *C. atrosanguineus* has offered a versatile and manageable PhD project that relates to pure and applied elements of research.

Cosmos atrosanguineus has high horticultural value as a garden species and cut flowers (Brickell and Sharman, 1986) and is the focus of a conservation and reintroduction programme under the direction of the Autonomous University of Mexico (UNAM) (Ortega-Larrocea *et al.*, 1997). However, before successful reintroduction to the natural environment can be achieved, the problems of self-incompatibility will need to be addressed, and thus identification of the molecules responsible for *Cosmos* SI would facilitate such studies.

1.1.2 - Research Methodology

A comparative research methodology was adopted in this study, by including additional Asteraceae taxa from *Centaurea*, *Conyza*, *Cosmos*, *Picris* and *Senecio*. The inclusion of additional species increased the workload, but offered flexibility to the research. These Asteraceae taxa were: *Centaurea cyanus* (subfamily either Cichorioideae or Carduoideae), *Conyza canadensis*, *C. sumatrensis* (Asteroideae) *Picris echioides* (Cichorioideae), *Senecio squalidus* and *S. vulgaris* (Asteroideae) and permitted comparison of putative S/SI-gene sequences from representative taxa of Asteraceae subfamilies. The main consideration in selecting these taxa was their availability, whereas the selection criteria for *Cosmos* species included availability, Mexican origin and flowering-time. The three *Cosmos* species used for comparison are described below.

1.1.3 – Descriptions of *Cosmos bipinnatus*, *C. carvifolius* and *C. sulphureus*

(i) *Cosmos bipinnatus*

Cosmos bipinnatus Cav. Ic. 1:10 pl. 14. 1791.

Coreopsis formosa Bonato, Pis. Autom 22. 1793.

Cosmea bipinnata Willd. Sp. Pl. 3 : 2250. 1840.

Georgia bipinnata Spreng. Syst. 3 : 611. 1826.

Cosmos tenuifolius Lindl. Bot. Reg. 23 : pl. 2007. 1837.

Cosmea tenuifolia Lindl. in Heynh. Nom. 1 : 223. 1840.

Bidens formosa Schultz-Bip. in Seem. Bot. Voy. Herald 307. 1856

Bidens lindleyi Schultz-Bip. in Seem. Bot. Voy. Herald 307. 1856

Cosmos bipinnatus is a self-incompatible herbaceous annual available as living and herbarium material at the Royal Botanic Gardens, Kew. It is native to Mexico (McVaugh, 1984; Sherff, 1932) where it is known as the Mexican Aster (Garg and Sastry, 1996). It has a distribution from Arizona in the USA, south-eastward into the Mexican states of Sinaloa (8), Durango (9), Zacatecas (10), Jalisco (13), Aguascalientes (14), Nayarit (12), Guanajuato (15), Hidalgo (17), Michoacán (20), Mexico state (21) Distrito Federal D.F (24), Puebla (25), Oaxaca (27) and Chiapas (28) (Sherff 1932; Sherff and Alexander, 1955; McVaugh, 1984; Figure 1.1).



Figure 1.1 - Distribution map of *Cosmos bipinnatus* in Mexico

Cosmos bipinnatus has a distribution from Arizona in the USA south-eastwards through Mexico to Guatemala (green shading). (Map of Mexico amended from © pickatrail.com).

Key to names of states: 1 – Baja California, 2 – Baja California Sur, 3 – Sonora, 4 – Chihuahua, 5 – Coahuila, 6 – Nuevo Leon, 7 – Tamaulipas, 8 – Sinaloa, 9 – Durango, 10 – Zacatecas, 11 – San Luis Potosí, 12 – Nayarit, 13 – Jalisco, 14 – Aguascalientes, 15 – Guanajuato, 16 – Queretaro, 17 – Hidalgo, 18 – Veracruz, 19 – Colima, 20 – Michoacán, 21 – Estado de México, 22 – Morelos, 23 – Tlaxcala, 24 – Distrito Federal (D.F.), 25 – Puebla, 26 – Guerrero, 27 – Oaxaca, 28 – Chiapas, 29 – Tabasco, 30 – Campeche, 31 – Yucatán, 32 – Quintana Roo.

Cosmos bipinnatus thrives as vast natural populations on disturbed open land and roadside embankments at altitudes between 2000–2500 metres, and is often intermingled with other Asteraceae taxa, particularly species of *Tagetes* and *Bidens*. It is a persistent weed of arable land, where it is the Mexican equivalent of the European poppy (Plate 1.2).



Photos: Sarah Lewendon



Cosmos bipinnatus

Plate 1.1. (above) A single weedy *C. bipinnatus* plant, (height 25 cm) on fallow arable land 25 km north of Villa del Pueblito on the road to Huimilpan, in the state of Queretaro, Mexico. Mexico Scale bar = 5 cm

Plate 1.2 (left)

Population of weedy *Cosmos bipinnatus* plants (average height 35 cm) growing on a roadside embankment at ~2300 metres, 20 km north of Villa del Pueblito, Queretaro, Mexico. Scale bar = 5 cm

In Mexico, *C. bipinnatus* flowers from September to November (McVaugh, 1984). Its flowering period in England, May to September, corresponds to that of *C. atrosanguineus* and allows concurrency in pollination experiments (Table 1.1). *C. bipinnatus* has been studied extensively in terms of its pollen chemistry (Knox and Heslop-Harrison 1970; Howlett *et al.*, 1973; Knox 1973; Howlett *et al.*, 1975), stigma, anther and pollen morphology (Heslop-Harrison, 1969; Dickinson and Potter, 1976; Dickinson and Potter, 1979; Blackmore and Barnes, 1985), and self-incompatibility (Little *et al.*, 1940; Crowe, 1954; Howlett *et al.*, 1975). It exhibits sporophytic self-incompatibility, with an estimated 8 S-alleles in a sample population of 12 individuals (Crowe, 1954; see Section 1.5.4 below). Cytological data on the species include chromosome counts, karyotypes and idiograms, and reveal *C. bipinnatus* to be a diploid species where $2n = 2x = 24$ (Sugiura, 1936; Sharma, 1947; Powell and Turner, 1963; Melchert, 1968; Banerjee, 1971; Gupta *et al.*, 1972; Solbrig *et al.*, 1972; Koul and Gohil, 1973; Mehra and Remanandan, 1974; Keil and Stuessy, 1977; Srivastava,

1983; Mathew and Mathew, 1988; Ohri *et al.*, 1988; Murín, 1993; Bennett and Leach, 1995). It is the type species for the genus (Sherff and Alexander, 1955) and the most comprehensively studied species within *Cosmos*. It has served as the principal species for comparison in this study.



Plate 1.3. A single inflorescence (capitulum) of *Cosmos bipinnatus*. The inflorescence measures 65 mm across extended rays. Note the copious amounts of pollen on the tips of newly emerged anthers, with a few pollen grains scattered on the sterile ray florets. Scale bar = 2 cm. (Photo: Sarah Lewendon)

Cosmos bipinnatus is a popular garden annual cultivated for its attractive bipinnate foliage and its showy composite flower heads - generally referred to as capitula or inflorescences - composed of an outer whorl of sterile (neutral) ray florets, which fan out from a central circle of yellow densely packed fertile hermaphrodite disk florets (see Chapter 3 for details on *Cosmos* floral structure). Horticultural specimens range in height from 0.6-2.0 metres. Natural populations may become weedy (Plates 1.1 and 1.2), ranging from 20-40 cm in height with correspondingly smaller capitula. In non-weedy cultivated types the capitula measure 4-8 cm across extended rays (Plate 1.3). The 8 neutral ray florets range in colour from crimson through pink to pure white and contrast sharply with the 50-80 yellow hermaphrodite central disk florets. The pollen is conspicuously bright yellow at anthesis and it collects on the top of the protruding yellow bi-lobed stigma. There are two varieties of *C. bipinnatus*: *C. bipinnatus* var. *bipinnatus*, with awned achenes, and *C. bipinnatus* var. *exaristatus* in which the achenes are awnless. Most cultivars are of the latter type, with both types being found in the wild (Sherff 1932; Sherff and Alexander, 1955; McVaugh, 1984).

(ii) *Cosmos carvifolius*

Cosmos carvifolius Benth. Bot.Voy. Sulph. 117. 1844.

Bidens seemannii Schultz-Bip. in Seem. Bot. Voy. Herald 307. 1856

Bidens carvifolia Schultz-Bip. in Seem. Bot. Voy. Herald 308. 1856

Cosmos seemannii A.gray, Proc. Am. Acad. **19**: 16. 1883.

Cosmos carvifolius is a self-incompatible perennial herb available as fresh and herbarium material at RBG, Kew. It is a many-stemmed shrub or half-shrub. It is native to Mexico with a distribution from the Sierra Madre in north-western Mexico, south-eastwards through the states of Sinaloa (8), Durango (9), Nayarit (12), Jalisco (13), Michoacán (20), to Mexico State (21) (Figure 1.2). It is characteristic of open oak and pine forests, on hillsides and steep slopes at altitudes of 1000-2000 metres (McVaugh, 1984; Sherff 1932). Its flowering time in Mexico is August to December as it is able to tolerate quite cold ground conditions from 10-12°C (Sherff, 1932). In England it flowers from June to September but will continue to flower under glass until December, by which time the stems become woody and brittle (Table 1.1).



Figure 1.2. Distribution map of *Cosmos carvifolius* in Mexico

Distribution of *Cosmos carvifolius* is restricted to the southwestern states of Mexico on the Pacific slopes of the Sierra Madre (green shading). (See Figure 1.1 for key to the names of Mexican states). (Map of Mexico amended from © pickatrail.com).

Cosmos carvifolius has little horticultural importance due to its shrubby, weedy habit. Its slender erect simple stems ascend from a woody rootstock to 1.5 m, but tend to fall to the ground, resulting in damage to capitula and to the finely pinnate foliage.

Capitula are few in number, with an average of 4-5 capitula per plant. The capitulum consists of 8 outer sterile (neutral) ray florets that surround 20-25 central fertile hermaphrodite disk florets. Flower colour ranges from dark purple through lavender to rose purple, with central disk florets being slightly darker in hue than the outer rays. The capitulum is small to medium, measuring 2.5-5.5 cm across extended rays (Sherff 1932; Sherff and Alexander, 1955; McVauch, 1984). An attractive feature of this species is the abundant production of snow-like pollen. The pollen is deposited heavily on the top of the dark purple stigmas giving the disk florets a beautifully frosted appearance at anthesis (Plate 1.4). Due to the relative smallness of the flower this attractive feature is best observed with the aid of a magnifying glass. Aside from its inclusion in floras of Mexico (Sherff 1932; Sherff and Alexander, 1955; McVauch, 1984), there is no other published material on this species.



Plate 1.4 A single capitulum of *Cosmos carvifolius*
The inflorescence measures 35 mm across extended rays. Six disk florets at the centre of the inflorescence are closed, while those on the periphery have opened and present copious amounts of white pollen on the tips of emerged anthers and stigmas. Scale bar = 1 cm. (Photo: Sarah Lewendon).

(iii) *Cosmos sulphureus*

Cosmos sulphureus Cav. Ic. 1 : 56. 1791.

Coreopsis artemisiaefolia Jacq. Ic. Pl. Rar. 3 : 16. 1793.

Cosmea sulphura Willd. Sp. Pl. 3 : 2250. 1804.

Bidens sulphurea Schultz-Bip. in Seem. Bot. Voy. Herald 308. 1856.

Cosmos aurantacus Klatt, Leopoldina 25 : 105. 1889.

Coreopsis artemisifolia Sessé & Moc. Pl. Nov. Hisp. 148. 1890.

Cosmos sulphureus is a self-incompatible herbaceous annual that is available as fresh and herbarium material at RGB, Kew. It is native to Mexico where it is known by its Aztec name, *xochipali* (flower paint), and is used as a dye (Sherff, 1932; McVaugh, 1984; Heinrich, 1996). Its distribution is extensive and it is found throughout Mexico, particularly the states of Sonora (3), Sinaloa (8), Durango (9), Zacatecas (10), Jalisco (13), Aguascalientes (14), Nayarit (12), Colima (19), Michoacán (20), Mexico state (21), Guerrero (26), Morelos (22), Oaxaca (27) and Chiapas (28) (Figure 1.3), and southwards into Guatemala, El Salvador, Panama, Colombia, Guyana and the State of Minas Geraes in northern Brazil. It is found on ridges, hillsides, and open spaces, and also along roadsides and streams at altitudes of 450-1000 metres, but is occasionally associated with oak or pine-oak forests at altitudes of 1200-1500 metres (Sherff 1932; Sherff and Alexander, 1955; McVaugh, 1984).



Figure 1.3. Distribution map of *Cosmos sulphureus* in Mexico
Cosmos sulphureus is distributed almost throughout Mexico and in Guatemala, Panama, Salvador, Guayana and Brazil (Minas Geraes). (See Figure 1.1 for key to the names of Mexican states). (Map of Mexico amended from © pickatrail.com).

Cosmos sulphureus has a shrubby weedy habit and little horticultural importance. It is an annual with a much-branched bushy habit ranging from 0.5-2.0 m high. Leaves are petiolate, ovate and 2-3 times pinnatisect, with blades 2-15 cm long. Capitula are scattered profusely throughout the foliage, and range from 2.5-6.5 cm wide across extended rays. Each capitulum consists of 8 orange or orange-yellow sterile (neutral) ray florets with 20-40 central orange-yellow fertile hermaphrodite disk florets (Sherff 1932; Sherff and Alexander, 1955; McVaugh, 1984; Plate 1.5).



Plate 1.5 A single capitulum of *Cosmos sulphureus*

The inflorescence measures 40 mm across extended rays. This inflorescence is exceptional in having nine sterile ray flowers while others from the same plant possessed the common complement of eight rays. Scale bar = 1 cm.

(Photo: Sarah Lewendon).

The flowering time of the *C. sulphureus* accession used in this study does not correspond with *C. atrosanguineus*: it appears to be a short-day plant, flowering in England from October to December, and March to May, and in Mexico from August to November (McVaugh, 1984; Table 1.1). This late flowering time added an advantage to the research as it allowed work to be carried out on this species throughout the winter months, when other *Cosmos* floral material was not available. Literature on *C. sulphureus* focuses predominantly on its ethno-botanical uses (Heinrich, 1996) and cytology, and has been shown to be a diploid species, $2n = 2x = 24$ (Sharma, 1947; Turner and Flyr, 1966; Melchert, 1968; Koul and Gohil, 1973; Mehra and Remanandan 1974; Pinkava and Keil, 1977; Olsen, 1980; Srivastava, 1983; Mathew and Thompson, 1984; Mathew and Mathew, 1988; Husani and Iwo, 1990; Bennett and Leach 1995).

Table 1.1 - Flowering times in Mexico and England of four *Cosmos* species

<i>Cosmos</i> species	Jan	Feb	Mar	Apr	May	Jun	Jul	Aug	Sept	Oct	Nov	Dec
<i>C. atrosanguineus</i>					Blue	Blue	Blue	Blue	Blue			
<i>C. bipinnatus</i>					Blue	Blue	Blue	Blue	Blue			
<i>C. carvifolius</i>								Blue	Blue	Blue	Blue	Blue
<i>C. sulphureus</i>			Blue	Blue	Blue					Blue	Blue	Blue

Key: blue bars, flowering time in England; orange bars, flowering time in Mexico. The wet season in Mexico runs from June to September, and the dry season from October to May.

1.2 - Origins and Classification of Asteraceae

1.2.2 - Introduction

The Asteraceae or daisy family contains approximately 1400 genera and 23 000 species that occur in all continents apart from Antarctica (Bremer, 1996; Bayer and Starr, 1998). They are found in arid and temperate regions, and mountainous areas of the tropics and subtropics (Heywood *et al.*, 1977; Bremer, 1994; Wagstaff and Breitwieser, 2002). The fossil record, morphological characteristics and paleoclimatic data place the origins of the Asteraceae at 43 million years ago (late Eocene) on the continental plate of South America (Raven and Axelrod, 1974; Bremer, 1994), while in Eurasia and the USA, fossil pollen attributed to Asteraceae first appears in Oligocene deposits approximately 39 million years ago. The Asteraceae underwent rapid diversification throughout the lower Miocene, 16-25 million years ago, a period associated with the radiation of Asteraceae tribes (Muller, 1981; Goertzen *et al.*, 2003). The numerous and widely-separated fossil records existing from this relatively short time period are attributed to many disparate dispersal events (Muller, 1981; Wagstaff and Breitwieser, 2002). The entire diversification of the Asteraceae has taken place within the last 50 million years, and as a consequence its evolutionary history is difficult to discern (Goertzen, *et al.*, 2003). Various molecular and cladistical methods have elucidated the origins of the Asteraceae and the relationships among tribes, but have not been able to clarify the evolutionary order in which the tribes emerged (Jansen *et al.*, 1991; Kim *et al.*, 1992; Bremer, 1994, 1996; Kim and Jansen, 1995; Bayer and Starr, 1998). Although, the recent work of Panero and Funk (2002), using a combination of nine genes, has produced a monophyletic phylogeny for the family composed of 36 tribes and 11 subfamilies, controversy remains as to the robustness of this phylogeny, particularly regarding its basal nodes (Panero and Funk, 2002).

Cassini is credited with the first systematic classification of the Asteraceae in 1816, organising the family into 19 tribes (Bremer, 1994). In 1821 Cassini revised his earlier classification to include 20 tribes by subsuming his 16th tribe Xeranthemeae into the tribe Carlineae, and adding the two new tribes Tageteae and Nassauvieae (Bremer, 1994). Lessing in 1832 and De Candolle in 1836 developed alternative classifications for the Asteraceae which recognised many of Cassini's subtribes, but segregated the family into eight and seven tribes respectively by using widely different tribal circumscriptions to Cassini (Stuessy, 1977; Bremer, 1994). In 1873, Bentham revised the tribal classification, delimiting the family to 13 tribes that affirmed much of Cassini's earlier work. Hoffman (1890) made some minor alterations to subtribes, but maintained and repeated Bentham's 13 tribal classifications (Heywood *et al.*, 1977; Turner, 1977a;

Stuessy, 1977; Bremer, 1994). Della Torre and Harms (1907) catalogued Hoffman's classification, amending it to 14 tribes by elevating the subtribe Tagetinae to the tribe Tageteae (Turner, 1977a). The 1907 classification of Della Torre and Harms comprised some 887 genera and 10, 000 species and is essentially that of Bentham (Heywood *et al.*, 1977; Turner, 1977a; Bremer, 1994). It persisted for 70 years, being expanded, but fundamentally unchanged, by piecemeal additions from many disparate contributors, inflating the number of genera and species within the family to approximately 1400 and 23 000 respectively (Turner, 1977a; Bremer, 1996).

The 1975 Reading Symposium, *The Biology and Chemistry of the Compositae* (Heywood *et al.*, 1977), was the first major review undertaken of the family in the twentieth century. Although the Symposium did not have the benefit of molecular methods available to today's taxonomists, it did seek to broaden the systematic analysis of the family by augmenting the traditional morphological/anatomical parameters with chemical characteristics specific to the Asteraceae. Sesquiterpene lactones and flavenols in particular were utilised in the phylogenetic analysis of the family (Heywood *et al.*, 1977; Bremer 1994). The Reading Symposium recognised the 14 tribes from the 1907 classification of Della Torre and Harms, and considered proposals to divide the family alternatively into 2 subfamilies; Cichorioideae and Asteroideae, or three subfamilies; Cichorioideae, Vernonioideae and Asteroideae (Turner 1977a). At the conclusion of the Reading Symposium the 14 tribes were maintained, but the delimitation of subfamilies remained unresolved (Heywood *et al.*, 1977; Turner, 1977a). Bremer (1994), using morphological and anatomical characters, produced a classification that divided the Asteraceae into 3 subfamilies and 17 tribes. After the *International Compositae Conference* at RBG Kew in 1994, Bremer, incorporating data from molecular systematics, revised his earlier classification, dividing it into 4 subfamilies wherein the 17 tribes are maintained, but rearranged (Bremer, 1996; Figure 1.4). Bremer (1996) distinguishes four subfamilies in Asteraceae: Asteroideae, Cichorioideae, Carduoideae and Barnadesioideae (Figures 1.4 and 1.6) of which the Asteroideae constitutes the largest subfamily of 1135 genera and 16, 200 species, the Cichorioideae 232 genera and 3, 230 species, and the Carduoideae 83 genera and 2, 500 species. These three higher Asteraceae subfamilies in the Bremer classification are fairly well resolved, in contrast to the basal phylogeny of Asteraceae that lacks clarity due predominantly to the poorly resolved Mutisieae group. The Mutisieae is a cosmopolitan paraphyletic group of 76 genera and 970 species not assigned by Bremer to a subfamily due to its unresolved phylogeny (Figure 1.4). The South American subfamily Barnadesioideae, consisting of 9 genera

and 92 species, is a well-resolved monophyletic group of morphologically diverse forms ranging from annuals to large trees.

Cosmos Cav. 1791 is a member of the tribe Heliantheae, one of the largest and morphologically diverse tribes of the Asteraceae comprising 2,500 species and 189 genera (Bremer, 1996; Karis and Ryding, 1994; Stuessy, 1977; Wagstaff and Breitwieser, 2002). Like all members of the Heliantheae, *Cosmos* is predominantly neotropical, distributed principally in South America, and those parts of North and Central America that lie south of the tropic of Cancer (Bremer, 1994; Karis and Ryding, 1994). Mexico is the centre of diversification of the Heliantheae, having 165 genera and 1150 species of which 740 are endemics (Villaseñor, 1991). Helenieae and Eupatorieae are the closest sister tribes to the Heliantheae, and these three tribes, with their characteristic carbonised fruits and trinerved leaves, constitute the Helianthoid group (Heliantheae *sensu lato*) of Asteraceae (Bremer, 1996; Wagstaff and Breitwieser, 2002; Figure 1.6 and 1.7). The main feature distinguishing the Heliantheae from all species of Helenieae and Eupatorieae is the presence in the capitulum of receptacle paleae (Karis and Ryding, 1994; Plate 3.3). *Cosmos*, comprising 26-36¹ species, is one of the smallest genera of the Heliantheae (Karis and Ryding, 1994). It is located in the subtribe Coreopsidinae Less. with *Heterosperma* and *Henricksonia* recognised as the most closely related genera (Ryding and Karis, 1992; Bremer 1994; Karis and Ryding, 1994). Of the 34 *Cosmos* species identified by Villaseñor (1991), 28 are endemic to Mexico, with *C. atrosanguineus* belonging to section 4 – Discopoda of the subtribe Coreopsidinae. This section contains six other dark-sanguineous ligulate *Cosmos* species *C. concolor*, *C. jaliscensis*, *C. montanus*, *C. modestus*, *C. purpuerus*, and *C. scabiosoides* that like *C. atrosanguineus* are endemic to pine-oak forest ecoregions of Mexico (Sherff and Alexander, 1955).

¹ Melchert (1968) identifies 36 species for the genus *Cosmos*; Villasenor (1991) describes 34 taxa; Bremer (1994) records 26 species, and the Index Kewensis (Royal Botanic Gardens, Kew Database 2003) lists 59 *Cosmos* species.

Cassini 1821	Bentham 1873	Della Torre & Harms 1907/ Reading 1977	Bremer 1994	Bremer 1996
Adenostyleae ⁽³⁾ Tussilagineae ⁽⁴⁾ Ambrosiaceae ⁽⁹⁾ Echinopseae ⁽¹³⁾ Centaureae ⁽¹⁵⁾ Carlineae ⁽¹⁶⁾ Nassauvieae ⁽²⁰⁾				
			Asteroideae	Asteroideae
Inuleae ⁽⁷⁾	Inuleae ⁽⁴⁾	Inuleae ⁽⁴⁾	Inuleae	Inuleae
			Pulcheae	Pulcheae
			Gnaphalieae	Gnaphalieae
Calenduleae ⁽¹¹⁾	Calenduleae ⁽¹⁹⁾	Calenduleae ⁽¹¹⁾	Calenduleae	Calenduleae
Astereae ⁽⁶⁾	Astereae ⁽³⁾	Astereae ⁽³⁾	Astereae	Astereae
Anthemideae ⁽⁸⁾	Anthemideae ⁽⁷⁾	Anthemideae ⁽⁷⁾	Anthemideae	Anthemideae
Senecioneae ⁽⁵⁾	Senecioneae ⁽⁸⁾	Senecioneae ⁽⁸⁾	Senecioneae	Senecioneae
	Helenieae ⁽⁶⁾	Helenieae ⁽⁶⁾	Helenieae	Helenieae
Heliantheae ⁽¹⁰⁾	Heliantheae ⁽⁵⁾	Heliantheae ⁽⁵⁾	Heliantheae	Heliantheae
Eupatorieae ⁽²⁾	Eupatorieae ⁽²⁾	Eupatorieae ⁽²⁾	Eupatorieae	Eupatorieae
Tageteae ⁽¹⁹⁾		Tageteae ⁽⁹⁾		
			Cichorioideae	Cichorioideae
Mutisieae ⁽¹⁷⁾	Mutisieae ⁽¹²⁾	Mutisieae ⁽¹³⁾	Mutisieae	
Cardueae ⁽¹⁴⁾	Cynareae ⁽¹¹⁾ (Cardueae)	Cynareae ⁽¹²⁾ (Cardueae)	Cardueae	
Lactuceae ⁽¹⁸⁾	Cichorieae ⁽¹³⁾ (Lactuceae)	Lactuceae ⁽¹⁴⁾	Lactuceae	Lactuceae
Vernonieae ⁽¹⁾	Vernonieae ⁽¹⁾	Vernonieae ⁽¹⁾	Vernonieae	Vernonieae
		Liabeae	Liabeae	Liabeae
Arctotideae ⁽¹²⁾	Arctotideae ⁽¹⁰⁾	Arctoteae ⁽¹⁰⁾	Arctoteae	Arctoteae
				Carduoideae
				Cardueae
				Mutisieae
			Barnadesioideae	Barnadesioideae
			Barnadesieae	Barnadesieae

Figure 1.4- Comparison of five suprageneric classifications of Asteraceae

Numbers in brackets refer to the numbering of tribes by Cassini; Bentham; Della Torre & Harms. Tribes have been arranged to align with the classification systems of Bremer 1994, 1996. Original tribal spellings have been updated, e.g. Cassini's Asterees to Astereae, and Bentham's Helianthoideae to Heliantheae. Bracketed tribe names denote the present delimitation of the tribe e.g. Cassini's Adenostyleae⁽³⁾ and Tussilagineae⁽⁴⁾ have since been assigned to the Senecioneae; his Ambrosiaceae⁽⁹⁾ to the Heliantheae; the three tribes Echinopseae⁽¹³⁾, Centaureae⁽¹⁵⁾, Carlineae⁽¹⁶⁾ to Cardueae, and Nassavieae⁽²⁰⁾ to Mutisieae. The tribe Mutisieae (Bremer, 1996) is shaded as it remains unclassified with respect to subfamily pending resolution of its phylogeny. Figure 1.4 compiled using data from: Bremer, 1994, 1996; Heywood *et al.*, 1977; Turner, 1977a)

1.2.2 - Tribal relationships in Asteraceae: a review of recent phylogenies

Asteraceae is a taxonomically complex family. The parallel morphology that occurs throughout the family has proved an obstacle to finding conservative, non-homoplasious - i.e. non-analogous - characters with which to produce a reliable phylogeny for the family. Prior to the recent phylogeny of Panero and Funk (2002) (Figure 1.10), the tribal phylogeny of Asteraceae was unresolved. The main areas of debate concerned the phylogenetic relationships of members within the paraphyletic tribe Mutisieae, the tribal relationships within the paraphyletic Cichorioideae subfamily, and the tribal circumscription of the tribes Helenieae and Eupatorieae.

Molecular phylogenetic studies in the Asteraceae have sought to overcome the morphological limitations that exist within the family, and have concerned themselves with the appropriateness of respective genes in constructing a reliable phylogeny for this rapidly-radiated plant family (Kim and Jansen, 1995). The plastid gene coding for the large subunit of the Rubisco enzyme (*rbcL*) has been the most widely sequenced gene in phylogenetic reconstruction. However, due to its slow evolutionary rate, *rbcL* has a limited use in Asteraceae phylogeny, restricted in the main to studies above the family level (Kim and Jansen, 1995; APG 1998, 2003). On the strength of *rbcL*, the closest relatives of the Asteraceae were found to lie within the order Asterales, with sister families being Calyceraceae and Goodeniaceae (Chase *et al.*, 1993; Kim and Jansen, 1995; Bremer, 1996; Panero and Funk, 2002; and Figure 6.3). Some researchers have used more rapidly evolving gene sequences, such as the internal transcribed regions of nuclear ribosomal RNA, ITS-1 and ITS-2, to reconstruct an Asteraceae phylogeny (Wagstaff and Breitwieser, 2002; Goertzen *et al.* 2003). Although ITS sequences have been used successfully at infrageneric levels in the Asteraceae, and to a lesser degree at the tribal level, their high divergence and length variation means they are not often useful at higher taxonomic levels (Kim and Jansen, 1995; Wagstaff and Breitwieser, 2002; Goertzen *et al.* 2003). The plastid *ndhF* gene, coding for a subunit of the plastid NDH (NAD(P)H dehydrogenase) complex is longer (2133 kb) than ITS, and shows higher sequence divergence than other phylogenetically informative plastid genes. It is particularly useful in that its 5' region is relatively conserved, and shows similar evolutionary patterns to *rbcL*, while its 3' region shows a much more rapid rate of sequence evolution (Kim and Jansen, 1995). As a consequence *ndhF* provides more phylogenetic information than *rbcL*, and is less capricious than ITS.

The first use of a molecular marker to reconstruct an Asteraceae phylogeny was by Jansen and Palmer (1987), and involved restriction fragment length polymorphisms (RFLP) of the Asteraceae chloroplast genome that identified a 22-kb inversion present in all Asteraceae aside from the members of Mutisieae subtribe Barnadesiinae. On the strength of this omission, the Barnadesiinae was raised to the subfamily Barnadesioideae and identified as ancestral and sister to the rest of the Asteraceae (Jansen and Palmer, 1987).

In 1995, Kim and Jansen, using the chloroplast *ndhF* sequences of 94 taxa, produced a phylogeny that recognised 15 tribes and three subfamilies: Asteroideae, Cichorioideae and Barnadesioideae, with the Asteroideae dividing into 2 main clades (Figure 1.5). In the first clade, the Athroisma group is sister to the Heliantheae, and together with the Inuleae, into which the Pulcheae is collapsed, forms a monophyletic group that is sister to remaining tribes of the Asteroideae. The paraphyletic Cichorioideae subfamily is divided into three main clades. The first clade encompasses the tribes Vernonieae, Liabeae, Arctoteae and Lactuceae that form a monophyletic group sister to the Asteroideae. The second and third clades are composed respectively of the tribes Cardueae and Mutisieae, with Barnadesioideae forming the basal clade.

Bremer (1996), used predominantly morphological characters supplemented with molecular data from chloroplast DNA inversions, *ndhF* and *rbcL*, to produce a phylogeny composed of four subfamilies; Asteroideae, Cichorioideae, Carduoideae and Barnadesioideae. The subfamily Asteroideae contains the Helianthoid group, which is sister to the remaining tribes of the Asteroideae subfamily (Figure 1.6). The subfamily Cichorioideae is restricted to the four tribes, Vernonieae, Liabeae, Lactuceae and Arctoteae, and is sister to the subfamily Asteroideae. In Bremer's phylogeny a new subfamily Carduoideae, consisting of the single tribe Cardueae, is created that is equally sister to the subfamilies Asteroideae and Cichorioideae *sensu stricto*. A basal dichotomy exists between the Barnadesioideae and the other three Asteraceae subfamilies. Although Barnadesioideae lies close to the root of the tree, it was not considered by Bremer to be primitive or ancestral to the other Asteraceae. Its basal position is a consequence of the lack of resolution in the Mutiseae, within which the basal phylogeny of the Asteraceae is believed to reside.

Bayer and Starr (1998), opted to use two non-coding, relatively short chloroplast tRNA DNA sequences, the *trnL* intron (~424-453 bp) and *trnL/trnF* intergenic spacer (~255-

345 bp) to resolve tribal relationships of Asteraceae. By choosing non-coding DNA sequences that are under less evolutionary constraint, they sought to overcome the deficiencies in information encountered by using protein-coding regions. Bayer and Starr's (1998) phylogeny (Figure 1.7) agrees principally with the phylogenies of Bremer (1996) and Kim and Jansen (1995). The Asteroideae represent a monophyletic group that contain the same tribes as Bremer (1996) and Kim and Jansen (1995), but with the Inuleae *sensu stricto* (*s. str.*) and Pulcheae separated as sister tribes that are sister to the remainder of the Asteroideae. Within the Asteroideae, the helianthoid clade forms a fairly well-supported monophyletic group consisting of Heliantheae, Eupatorieae and the Helenieae, but also contains some problem taxa in its basal branches that suggest some of the tribes in the helianthoid clade are paraphyletic. In keeping with other phylogenies, the Mutisieae and Cardueae form a very well supported (100% bootstrap value) monophyletic basal group that is sister to a clade that contains the remaining members of the Cichorioideae. However, the resolution of the Lactuaceae (L), Arctoceae (A), Liabeae (L), and Vernonieae (V) clades is low, with bootstrap values of 50% or less, and hence the LALV monophyletic group identified by Kim and Jansen (1995) is not resolved in this tree. In addition, the paraphyletic Cichorioideae shows slightly different tribal relationships than Kim and Jansen (1995).

The phylogeny of Wagstaff and Breitwieser (2002) focussed on the ITS region² of 92 New Zealand species of Asteraceae and as a consequence species sampling was limited. The main problem with the Wagstaff and Breitwieser tree is that representative species from the tribes Pulcheae Vernonieae and Liabeae were not included, and informative characters were reduced to a single relatively short nuclear region (Figure 1.8). Omissions of the Pulcheae Vernonieae and Liabeae are known to cause topological differences within the Asteroideae and Cichorioideae subfamilies (Bayer and Starr, 1998). Despite these limitations, the phylogeny of Wagstaff and Breitwieser (2002) is not vastly different to that of Bremer (1996) or Kim and Jansen (1995), with an Asteroideae subfamily consisting of ten fully resolved tribes. In keeping with the majority of phylogenies, Cardueae is subsumed into the Cichorioideae and the three Asteraceae subfamilies are retained (Figure 1.8).

Using ITS and *ndhF* sequences from 82 taxa, Goertzen *et al.* (2003), produced a fairly well resolved, more inclusive tribal phylogeny in which all Asteraceae tribes were

² The ITS region used by Wagstaff and Breitwieser (2002), included the conservative regions at the 3' end of the 18S gene, the entire 5.8S gene and the 5' end of the 26S gene in conjunction with the intervening internal transcribed spacers ITS-1 and ITS-2.

represented (Figure 1.9): though the ITS data produced a much less resolved tree than that of Wagstaff and Breitwieser (2002), the ITS and *ndhF* trees showed some general consistencies in terms of tribal relationships. In both the ITS and *ndhF* trees the Barnadesioideae is the basal group, the Mutisieae forms the earliest branching lineage within the Cichorioideae, and the tribes Arctoteae, Lactuceae, Liabeae and Vernonieae within the paraphyletic Cichorioideae are retained.

The phylogeny of Panero and Funk (2002) takes a more radical approach in both method and interpretation. These researchers used the nine chloroplast gene/markers *ndhF*, *trnL-trnF*, *matK*, *ndhD*, *rbcL*, *rpoB*, *rpoC1* exon 1, 23S-*trnL* and *ndhI*, to create a total data matrix of 13,380 base pairs (bp) composed of 122 genera representing most Asteraceae tribes. The phylogeny proposed contains 11 subfamilies and 36 tribes (Figure 1.10) and “represents the largest overhaul to the classification of the *Compositae* since *Bentham (1873)*” (Panero and Funk, 2002). Apart from the paraphyletic Mutisioideae, represented by two branches near the base of the tree, all groups are monophyletic, with high bootstrap support (>85%), and reflect the evolutionary history of the family. However, the tree represented in Panero and Funk (2002) is a reduced version of a much larger phylogeny that contained a greater number of sequences at the basal clades. Addition or removal of these sequences altered considerably the basal topology of the tree, so causing controversy and contradicting the robustness claimed by Panero and Funk (2002) for this phylogeny (Nicholas Hind, pers.comm.).

Of the six Asteraceae phylogenies presented in this chapter, only Bremer (1996) combines morphological and molecular characters. The other five phylogenies are based solely on molecular data. Molecular methods have enhanced analysis of evolutionary relationships, particularly when these methods are used in an eclectic process that includes chemotaxonomic markers, biogeography, comparative genomics (gene order, gene clusters, ploidy level), protein domain architectures and morphology. A phylogeny supported by an array of appropriate phylogenetic markers may be expected to reflect a more realistic model. Over reliance on one methodology, no matter how logistically appealing, may undermine the full potential of the methodology and lead to a narrowing of data and the production of incongruent results. There is a suggestion from some quarters of cladistics that the latter may be occurring in some Asteraceae phylogenies. Support for these concerns may be found in recent discussion papers on comparative genomics and its implications for the tree of life (Tatusov *et al.*, 2001; Koonin, 2003; Koonin *et al.*, 2000; Kurland *et al.*, 2003;

Lawrence and Hendrickson, 2003). Comparative genomics has revealed the fundamental plasticity of genomes, whereby only 80 (<5%) of the 2100 ancient orthologous gene families (predominantly associated with core components of the translation-transcription machinery) are ubiquitous in bacterial, archaeal, and eukaryote genomes (Koonin, *et al.*, 2000). The proposition that horizontal dissemination of genes - horizontal gene transfer (HGT) - and lineage-specific gene loss have played a major role in evolution, has dramatic consequences on our present understanding of the tree of life (Lawrence and Hendrickson 2003). Particularly so for those plant phylogenies constructed from mitochondrial (mt) genomes, as recent studies indicate that plant mtDNAs are conspicuously active in HGT compared with other organellar genomes and nuclear genomes of multicellular eukaryotes (Bergthorsson *et al.*, 2004). The evidence to date suggests that the main portion of extant chloroplast and nuclear genomes contain genes that have been vertically inherited from a universal common ancestor throughout their entire evolutionary history, as exemplified by the ribosomal proteins (Koonin, *et al.*, 2000; Bergthorsson *et al.*, 2004). However, if horizontal (lateral) gene transfer (HGT) does prove to have been prevalent in the evolutionary history of specific genes, then a phylogeny created using such genes would be misleading or meaningless (Kurland *et al.*, 2003). Furthermore, for those genes that code complex multidomain proteins, the evolutionary process might be better analysed in terms of protein domains rather than entire protein genes, as it is clear that portions of such proteins are related by vertical descent whereas other regions have accrued new domains and functions in different lineages. In such cases, "domain architectures" may serve as unique evolutionary markers, i.e. shared derived characters that may aid cladistics (Koonen *et al.*, 2000).

It is clear from the six phylogenies that the protracted problems of the family, particularly those regarding the Mutisieae and the basal nodes of the family have still to be resolved. The task of producing a fully resolved phylogeny may require a more extended range of markers and the development of integrated, sophisticated and robust analytical tools

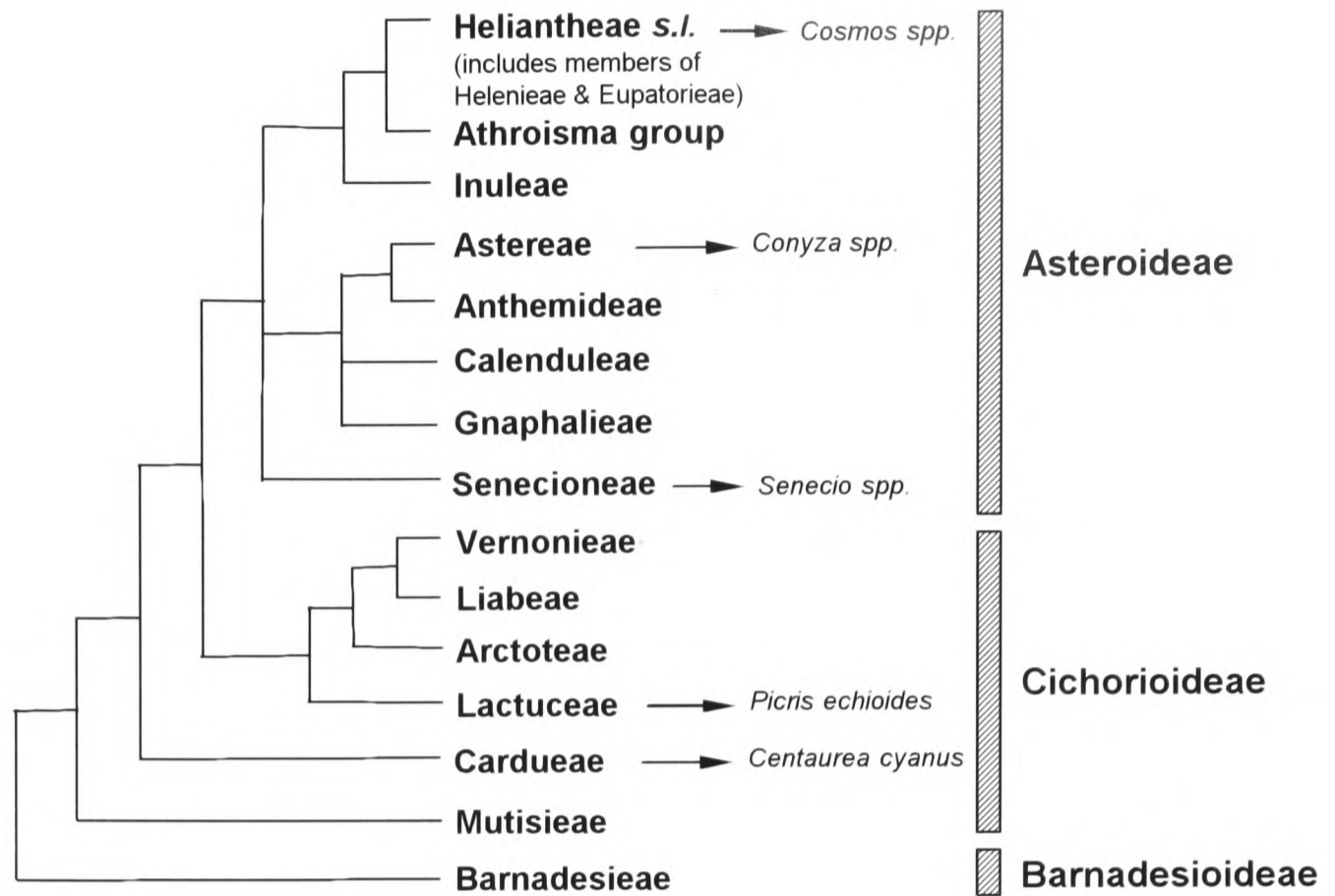


Figure 1.5 - (Kim and Jansen, 1995)
Phylogeny of Asteraceae tribes resolved using the chloroplast *ndhF* gene.

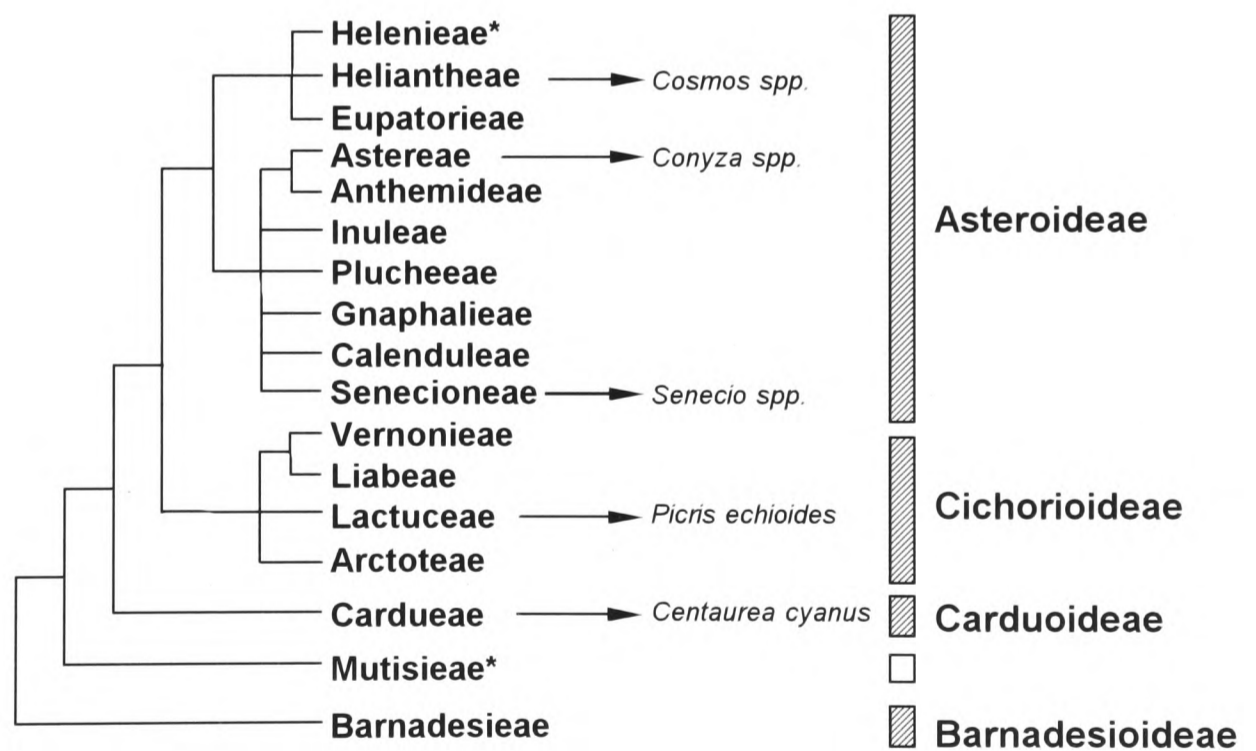


Figure 1.6 - (Bremer 1996)
Phylogeny of Asteraceae tribes resolved using using morphological and molecular data. Mutisieae forms a poorly understood grade at the base of the family tree and was not assigned to a subfamily by Bremer. The tribes containing Asteraceae genera used in this thesis i.e. *Centaurea*, *Conyza*, *Cosmos*, *Picris* and *Senecio*, are identified by arrows. (*indicates paraphyletic tribes). The number of taxa used in Bremer's 1996 phylogeny was not given.

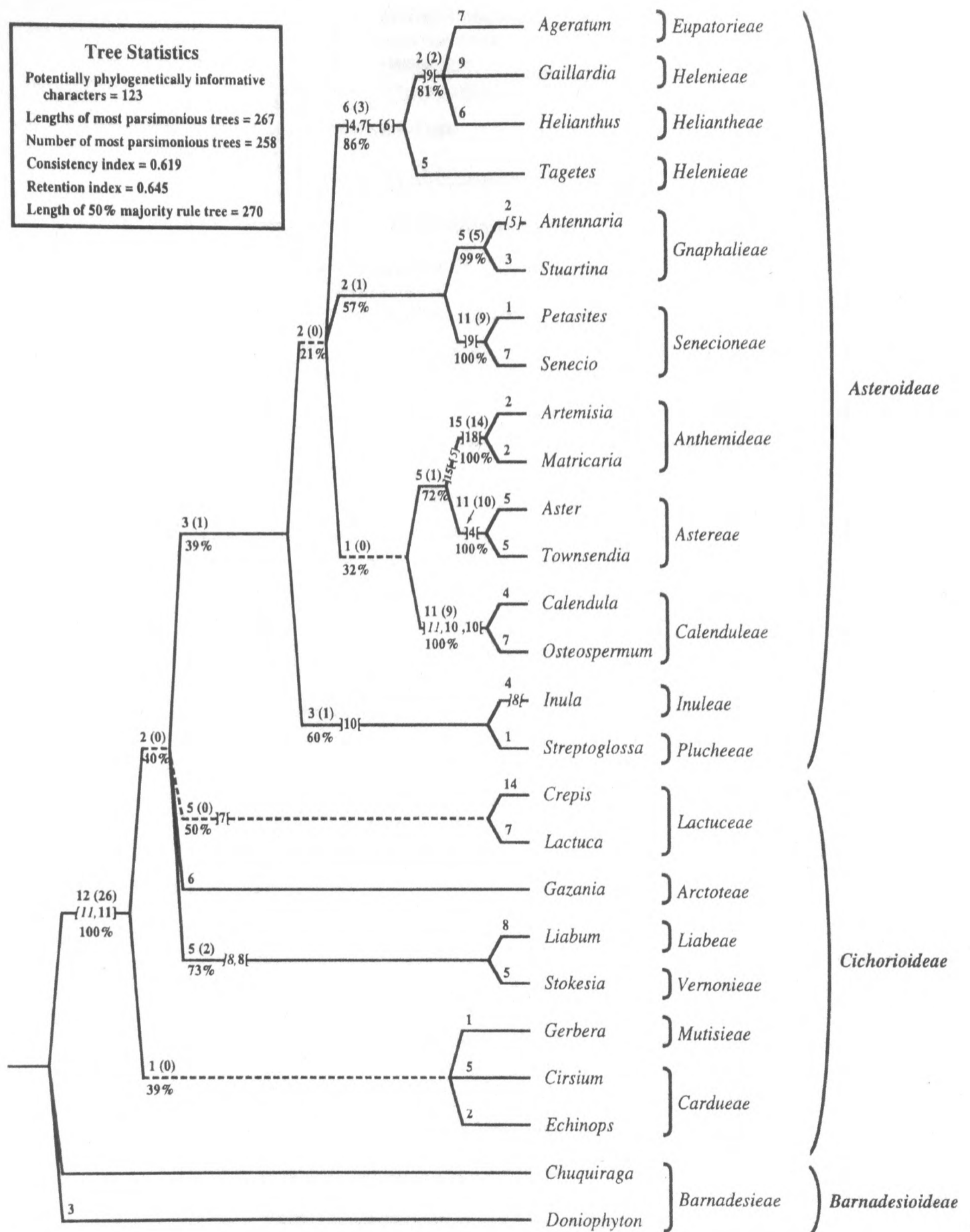


Figure 1.7 - (Bayer and Starr, 1998)

Phylogeny of Asteraceae tribes resolved using *trnL* intron and *trnL/trnF* intergenic spacer (after Bayer and Starr, 1998, Figure 2).

The tree represents the 50% majority rule consensus tree of 180 equally parsimonious trees. Dashed lines indicate branches that did not appear in the strict consensus. Numbers above the branches identify the number of apomorphies, and decay index values are in parentheses, also above branch lines. Bootstrap values are below branches. All indels were excluded from analysis.

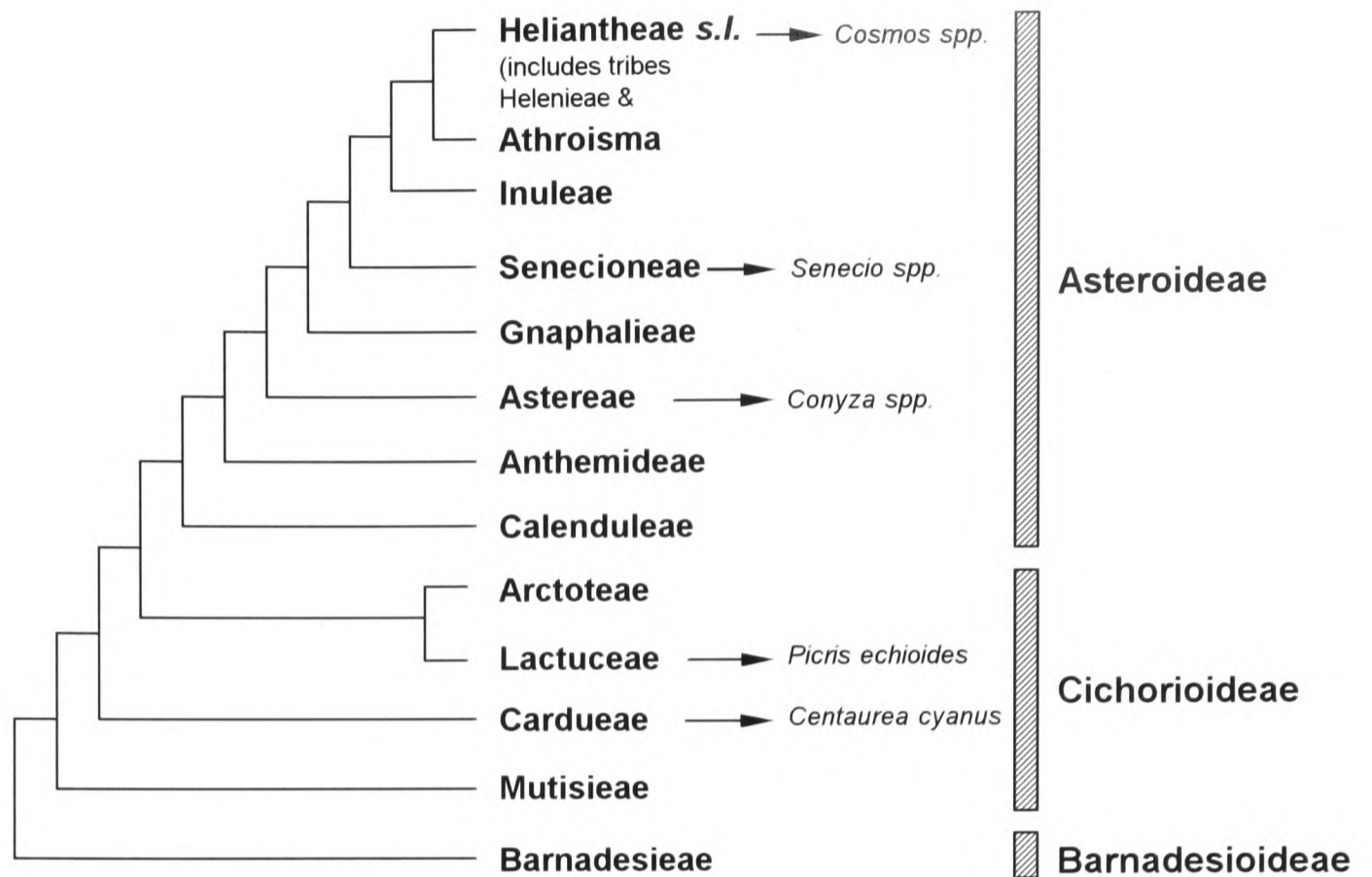


Figure 1.8 - (Wagstaff and Breitwieser 2002)
Phylogeny of Asteraceae tribes resolved using the ITS region.
 Representatives of Plucheeae, Vernonieae and Liabeae were not included in this ITS survey.

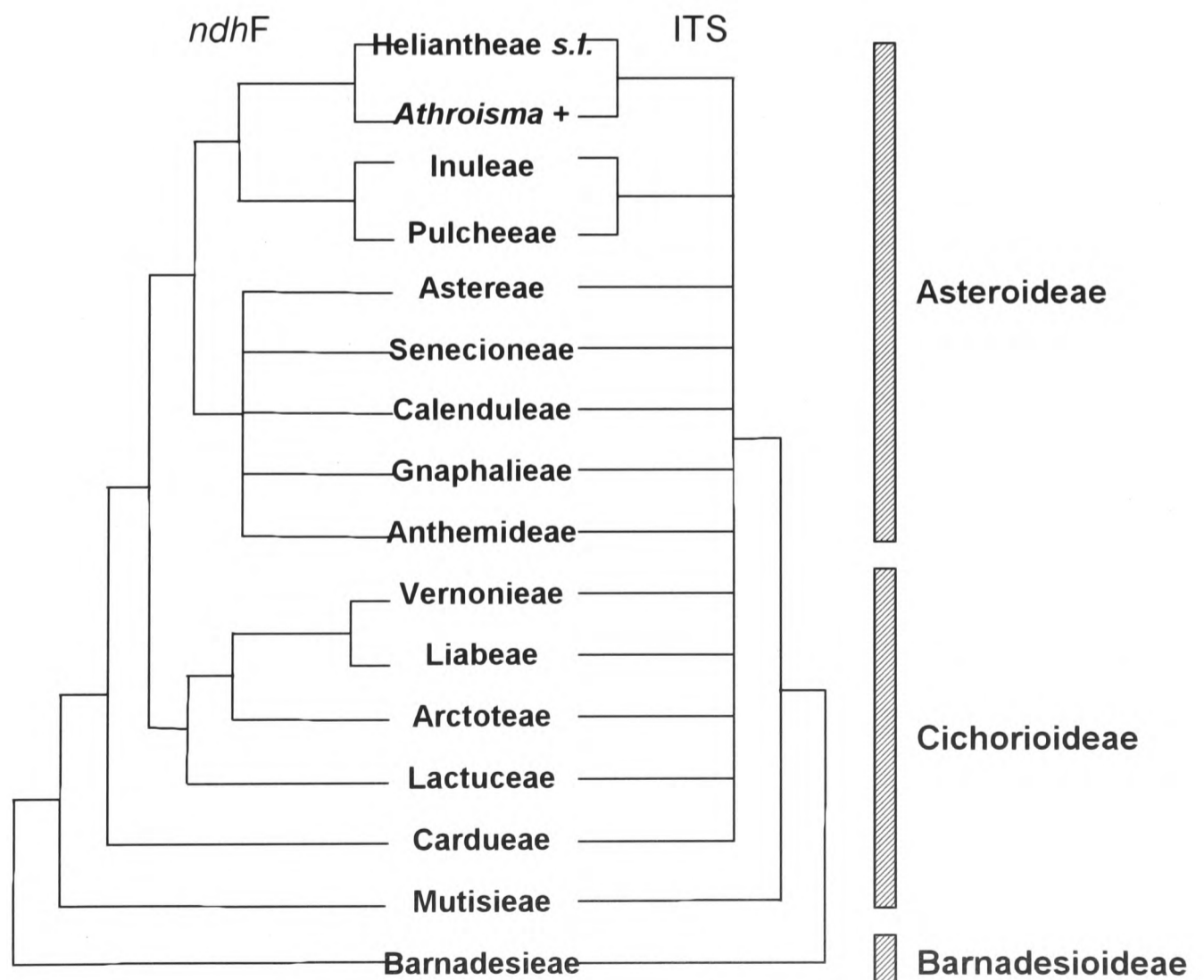


Figure 1.9 - (Goertzen et al., 2003)
Phylogeny of Asteraceae tribes resolved using *ndrF* and ITS regions.

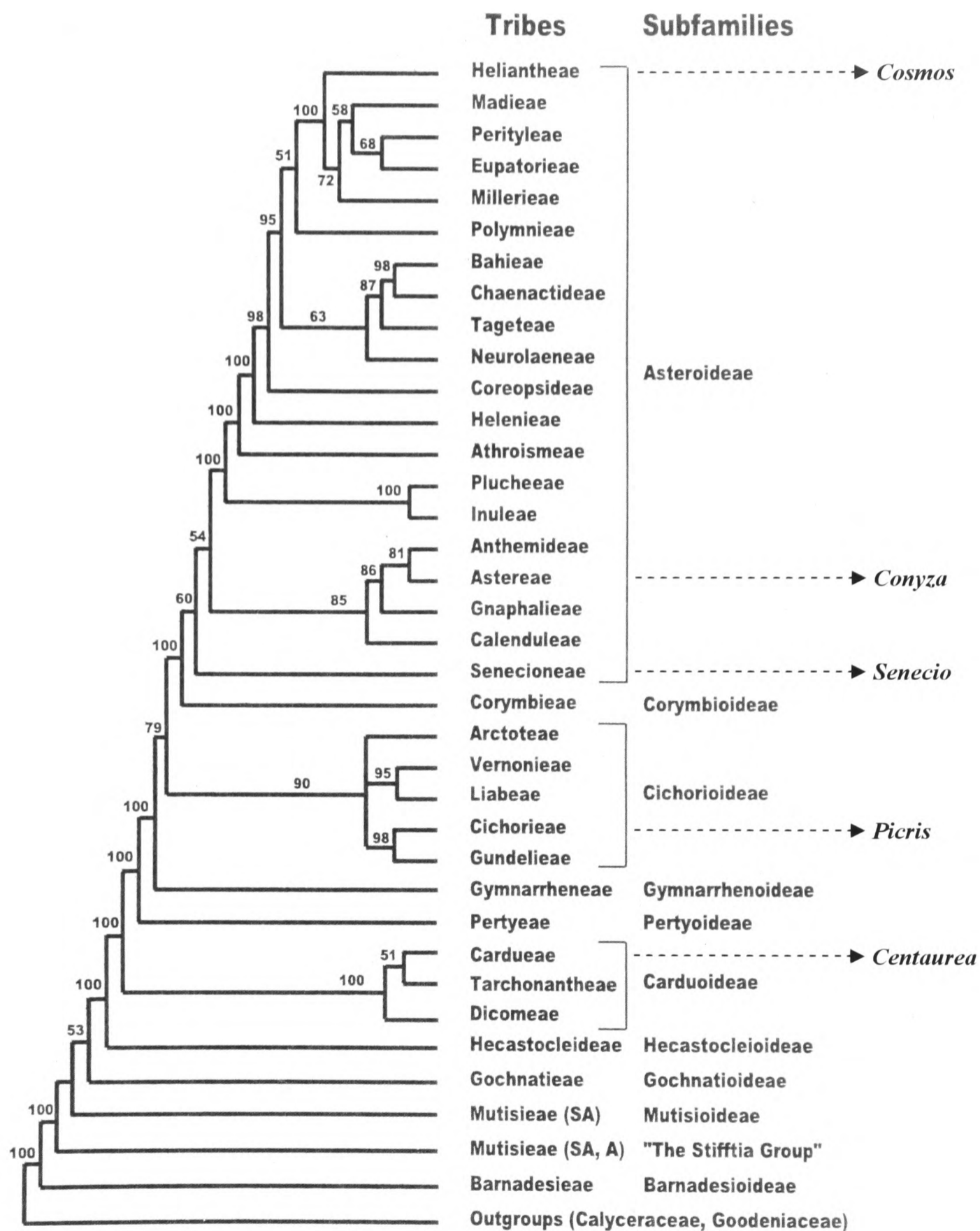


Figure 1.10 - (Panero and Funk 2002)

Phylogeny of Asteraceae tribes resolved using *ndhF*, *trnL-trnF*, *matK*, *ndhD*, *rbcl*, *rpoB*, *rpoC1* exon 1, 23S-*trnL* and *ndhI*.

The phylogeny tree is reproduced from Panero and Funk, 2002, and represents a strict consensus tree of 12 most parsimonious trees for 122 representative Compositae taxa based on sequence data from nine chloroplast DNA genes. The numbers above nodes represent bootstrap values. SA = South America, A = Asia. The tree is simplified to show only tribe and subfamily placement and arrangement. The positions on the tree of Asteraceae genera used in chapter 6 of this thesis are identified by broken-line arrows. Maximum parsimony without the coding of indels or character weighting was used to analyse the matrix.

1.3 – Polyploidy: genome duplication and evolution

1.3.1 Introduction

It is now accepted that polyploidy is a fundamental process in plant evolution, creating, within one generation, new plant races or species capable of existing and competing in the same spatial and temporal location as progenitor diploid species (Soltis and Soltis 1995, 1999, 2000; Song *et al.*, 1995a; Sybenga, 1996; Gaut and Doebley 1997; Ramsey and Schemske, 1998, 2002; Wendel, 2000; Boff and Schifino-Wittmann, 2003; Otto, 2003). The success of polyploid species is attributed to their increased level of heterozygosity and the presence of additional alleles, attributes that bestow vigour and durability that enable polyploids to colonize a wider range of habitats and extremes of climate than their diploid progenitors (Song *et al.*, 1995a; Osborn *et al.*, 2003). It is estimated that probably 50% and possibly 70% of angiosperms, and 95% of pteridophytes have undergone one or more episodes of chromosome doubling during the course of their evolution (Stebbins, 1950; Grant, 1963; Goldblatt, 1980; Masterson, 1994; Soltis and Soltis, 1999, 2000; Otto and Whitton 2000; Mavrodiev and Soltis 2001; Pikaard, 2001). Otto and Whitton, (2000), developed a formula to calculate the polyploid index (*PI*), a measure of the incidence of polyploidy in plants, and used it to estimate speciation events attributed to polyploidization in ferns and flowering plants. The *PI* for ferns (~42%) indicates that almost half the recent changes in the haploid chromosome number of ferns have been due to polyploidization and an estimated ~7% of fern speciation events involve polyploidization. For angiosperms, a *PI* of ~18-35% was calculated, and ~2-4% of speciation was attributed to polyploidization, implying that polyploidy is an important process in ferns and angiosperms, and is responsible for a substantial fraction of speciation events in both groups (Otto and Whitton, 2000).

Recent evidence indicates that the majority of polyploid species are formed by repeated polyploidization events from different parental genotypes of the same diploid species (Cook, *et al.* 1998; Mavrodiev and Soltis, 2001; Seagraves *et al.*, 1999; Soltis and Soltis, 1995; 1999, 2000). The seminal works on recurrent polyploid formation were undertaken in *Tragopogon mirus* and *T. miscellus* (Asteraceae) (Soltis *et al.* 1995; Cook *et al.* 1998), *Heuchera grossulariifolia* (Saxifragaceae) (Seagraves *et al.* 1999), *Draba norvegica* (Brassicaceae), (Brochmann and Elven, 1992; Brochmann *et al.*, 1992a; 1992b), *Senecio* (Asteraceae) (Lowe and Abbot, 1996; Abbot and Lowe, 2004; Abbot and Forbes 2002) and *Rubus* (Rosaceae) carried out by Maria Rozanova in the Soviet Union between 1934-1946 (Mavrodiev and Soltis 2001). The multiple origins of polyploid species generate a diverse array of polyploid genotypes that may

experience, in a relatively short time (e.g. 60 years), as many as 20 episodes of recurrent formation from different parental genets (Seagraves *et al.*, 1999; Soltis and Soltis, 1999). Genetic variability of polyploids may be enhanced further by subsequent hybridization of polyploid genotypes. Contrary to the classical view of polyploids as rare genetically uniform species of single origin, polyploidization has been demonstrated to be a dynamic force driving plant evolution, through its superhybridity and genomic malleability. The mechanisms responsible for polyploid evolution are not yet fully understood, but can result in loss, inactivation or divergence of redundant genes (Wendel, 2000).

1.3.2 – Hybridization, polyploidization and genome change

Classical theory assumed polyploids to be evolutionarily inert species, having fixed genomes with expression levels controlled equally by each gene member of duplicated genomes (Soltis and Soltis 1995; 2000; Wendel, 2000; Otto, 2003). Recent research refutes these notions, with evidence showing an essential feature of polyploidization to be immediate and rapid change in the polyploid genome (Song *et al.*, 1995a; Cronn *et al.*, 1999; Comai *et al.*, 2000; Weiss and Maluszynska, 2000; Ramsey and Schemske, 2002; Adams *et al.*, 2003; Osborn *et al.*, 2003; Otto, 2003). For example, four synthetic reciprocal homozygous *Brassica* polyploids analogous to the natural allopolyploids *Brassica juncea* (AB genomes) and *B. napus* (AC genomes), derived from *B. rapa* (A genome), *B. nigra* (B genome), and *B. oleracea* (C genome) were selfed for five generations (Song *et al.*, 1995a). The nuclear genome of F₅ selfed progeny diverged rapidly, showing approximately 6% pairwise genetic distance from their polyploid parents. Interestingly, the genetic distance between F₅ plants and their polyploid F₂ parents was significantly lower in the more closely related AC genomes (~4%) than in the more distantly related AB genomes (~8-9%), supporting the thesis that genetic change occurs more rapidly in more highly diverged polyploid genomes (Wendel, 2000). This trend was mirrored in the nuclear genomic variability within F₅ plants, with AC individuals exhibiting an average of 2.5% pairwise genetic difference whereas the more distantly related AB F₅-generation averaged 9% pairwise difference. The genomic variety was accompanied by morphological variation and differences in fertility. In contrast, chloroplast (*cp*) and mitochondrial (*mt*) genomes showed no differences between F₂ and F₅ generations, with both generations inheriting the maternal *cp* and *mt* genome without alteration. However, cytoplasmic-nuclear interactions were apparent in the more distantly related AB genomes, with the maternally-inherited genome causing directional changes away from the paternal genome. Hybridization and polyploidization in allotetraploid wheat showed similar

results, with ~14% of low-copy number DNA sequences being eliminated in the first generation through intra-chromosomal deletions (Ozkan *et al.*, 2001; Shaked *et al.*, 2001). In another example, newly-formed synthetic allotetraploids of *Arabidopsis suecica* produced from interspecific reciprocal crosses between the natural tetraploids *A. thaliana* and *A. arenosa* (also known as *Cardaminopsis arenosa*) displayed phenotypes and gene expression not apparent in natural allotetraploid populations (Comai *et al.*, 2000). These novel phenotypes and gene expressions were eliminated in F₂ polyploid plants through the apparent silencing or re-activation of genes in one or other of the constituent genomes (Comai *et al.*, 2000). Genomic changes, whether through silencing or re-activation of genes, appear to function by nullifying the destabilizations incurred by uniting distantly-related genomes in new allopolyploids. This stabilizing influence is observed not only in the F₂ polyploid generations, but proceeds through subsequent polyploid generations until balanced genomic interactions are achieved (Song *et al.*, 1995a; Comai *et al.*, 2000). Genomic stabilization may be brought about by reversible DNA modifications such as heterochromatinization, euchromatinization and methylation, or by permanent chromosomal changes such as duplication, deletion, insertion, inversion, and intergenomic translocations, but most probably involves a combination of reversible and permanent processes (White *et al.*, 1994; Britten, 1996; Kidwell and Lisch, 1997; Soltis and Soltis, 1999; Comai *et al.*, 2000; Pikaard, 2001). Transposable elements (TEs) also play a role in polyploid genomes, as they appear to increase in copy number after hybridization and/or polyploidization (McDonald, 1993, 1998; White *et al.*, 1994). TEs are implicated in gene silencing and also provide a source of genetic variation in genomes, initiating change through a sophisticated array of mechanisms that may result in subtle alterations in tissue-specific regulation of genes, or dramatic alterations in the development and phenotype of organs (White *et al.*, 1994; Kidwell and Lisch, 1997). Whatever the mechanisms responsible, rapid genomic change in newly-formed polyploids appears to be the norm and occurs as a response to instability between genomes. Hence, genomic change is more diverse and rapid in polyploids produced from distantly-related genomes than those from more closely-related ones. In many polyploids, the degree of gene silencing and chromosomal reorganisation proceeds to such a level that the polyploid genome becomes structurally and functionally indistinguishable from that of a diploid (Soltis and Soltis, 1999). These 'chromosomally diploidized' polyploids invoke a range of rapid and long-term mechanisms leading towards diploidization (Wendel, 2000). It is now understood that the majority of plant and animal species are the result of one or more cycles of polyploidization succeeded by diploidization, with ancient polyploidizations obscured

by subsequent diploidizations (Lagercrantz and Lydiate, 1996; Shoemaker, *et al.*, 1996; Cheun, *et al.*, 1997; Lagercrantz, 1998; Brubaker, *et al.*, 1999).

Classical assumptions of polyploidization supposed that duplicated gene copies freed from the restraints of selection rapidly degenerate (pseudogenization) or diverge (functional divergence) (Stebbins, 1950; Ohno, 1973; Ohta, 1991; Pickett and Meeks-Wagner, 1995; Cronn *et al.*, 1999; Force *et al.*, 1999; Otto and Whitton, 2000;). For many genes this is the case, with genome duplication leading either to degenerate nonsense-DNA base sequences or to functional diversity and the evolution of gene families (Ohno, 1973; Ferris and Whitt, 1977, 1979; Hughes, 1994; Ohta, 1994; Wendel, 2000). However, in naturally-occurring newly synthesized allotetraploids of cotton (*Gossypium*), homoeologues of A and D genomes were expressed at different levels in different tissues (Cronn *et al.*, 1999; Adams, *et al.*, 2003³). Moreover, differentiation in expression patterns among some duplicated genes occurred immediately, between 2 and 5 generations, as a result of hybridisation and/or tetraploidization, and was developmentally related such that one gene copy dominates expression at one time and the second copy dominates at another (Adams *et al.*, 2003). Since expression/silencing of homoeologous gene pairs was reciprocal in different organs, this cannot be due to sub-functionalization of gene copies. These observations of Adams *et al.* (2003) contradict the classical view regarding pseudogenization and functional divergence of redundant genes, and may explain the many accounts in which duplicated gene pairs are retained for millions of years following genome doubling (Ferris and Whitt, 1977; Pickett and Meeks-Wagner, 1995; Gibson and Spring, 1998; Force *et al.*, 1999; Otto and Whitton, 2000; Wendel, 2000). If, as in the case of cotton, duplicated gene copies do not cover fully for one another, then both copies will be retained by selection and a duplicate genic stasis may predominate at these loci after polyploidization (Song *et al.*, 1995a; Cronn *et al.*, 1999; Force *et al.*, 1999; Wendel, 2000; Adams *et al.*, 2003; Otto, 2003). The duplication-degeneration-complementation (DDC) model elaborates further by proposing that degenerate mutations in regulatory elements cause an *increase*, not a decrease, in the probability of duplicate gene preservation (Force *et al.* 1999). To summarise, the DDC process is a reminder that the polyploidization event duplicates not only chromosomes and genes but also the upstream regulatory regions that control the expression of

³Adams *et al.*, (2003) used natural allotetraploid cottons *Gossypium hirsutum*, *G. mustelinum* and *G. darwinii*. Model progenitor diploids used for the cotton A and D genomes were respectively *G. herbaceum* and *G. raimondii*. Synthetic allotetraploids were formed from *Gossypium arboreum* (A genome) and *G. thurberi* (D genome).

genes. Loss of function may occur at the level of the chromosome, the gene or individual regulatory elements. If duplicated genes lose different regulatory sub-functions, they may be able to complement this loss by retaining jointly the full set of regulatory sub-functions that were present in the ancestral gene (Force *et al.* 1999). Thus in the DDC model, the partitioning of ancestral-gene functions caused by the complementary loss of regulatory elements in duplicated genes, is the mechanism by which duplicate genes are preserved (Force *et al.* 1999).

The DDC model concerns itself with degeneration and loss of regulatory elements. However, it is also conceivable that redundant regulatory elements accumulate random mutations that bestow new elements in the transcription or expression of a gene. In such a situation, persistence of duplicate genes may not imply the retention of identical protein expression (Hughes, 1994; Cooke *et al.*, 1997). In baker's yeast *Saccharomyces cerevisiae*, the upstream regulation of duplicated genes evolves more rapidly than the downstream functions of their proteins, with an average 3% loss of common transcription factors for every 1% divergence of amino acid (protein) sequence (Maslov, *et al.*, 2004) This upstream plasticity and downstream robustness has also been demonstrated in *Helicobacter pylori* (Rain *et al.* 2001), *Drosophila melanogaster* (Giot *et al.*, 2003) and *Caenorhabditis elegans* (Kamath *et al.*, 2003). Even without the safety-net of redundancy, the same gene may code for an enzyme or a structural protein by acquiring new gene regulatory elements (Ohta, 1991). For example in birds, diversification of gene expression and post-translational modification allow the same gene to code the eye lens ϵ -crystallin and the enzyme lactate dehydrogenase, while the r -crystallin of fish and birds appears to be the same gene that encodes α -enolase (Wistow *et al.*, 1987). However, it is more common for multiple functions of a gene to evolve in tandem with gene duplication, principally via differential control of two mechanisms: transcript splicing, and post-translational modifications such as proteolytic cleavage of nascent proteins, and/or phosphorylation (Ohta, 1991). The retention of duplicated genes probably has many causes, but essentially redundancy enhances an individual's fitness in ways that may become apparent only at specific stages of the life cycle, or in particular environmental conditions, or at different hierarchical levels of biochemical pathways (Ohta, 1991; Doebley, 1993).

1.3.3 – Autopolyploidy and allopolyploidy: extremes of a polyploid continuum

Classically, polyploids were identified as autopolyploids or allopolyploids (Kihara and Ono, 1926 in Ramsey and Schemske, 1998). Autopolyploids were characterised as

having identical duplicated genomes, multivalents at meiosis, and polysomic inheritance at each locus, whereas allopolyploids have distinct (non-identical) duplicated genomes, fixed heterozygosity, bivalents at meiosis, and disomic inheritance (Ramsey and Schemske, 1998; Soltis and Soltis 2000). Autopolyploids were thought to occur rarely in the wild as their tendency to form multivalents at meiosis was deemed to reduce their reproductive success as a result of the formation of unbalanced non-viable gametes and infertile aneuploid offspring (Ramsey and Schemske, 2000; Soltis and Soltis 2000). However, empirical investigations show a higher than expected prevalence of autopolyploids in natural populations (Soltis and Soltis, 1993) and a lower than expected frequency of multivalents in natural and synthetic autopolyploids (Soltis and Soltis, 1993; 2000; Sybenga, 1992; 1996). In newly synthetic autotetraploids of *Arabidopsis thaliana* and *Crepis capillaris*, multivalent formation was suppressed within the first few generations of polyploidy (Jones and Vincent, 1994; Weiss and Maluzynska, 2000). Together with a combination of genomic and chromosomal changes discussed previously, it appears that autopolyploid genomes can be diploidized within as few as 20 to 30 generations after which preferential bivalent formation is observed at meiosis and disomic inheritance prevails (Weiss and Maluzynska, 2000).

Present theories view polyploidy more as a continuum from auto- to allopolyploidy, i.e. from identical to fully distinct genomes (Stebbins, 1950, 1971; Sybenga, 1996). In this continuum, autopolyploids have genomes arising from the same species that are all identical or very closely related, with homologues having equal opportunities of pairing at meiosis and a binomial distribution of multivalents observed in meiocytes. Allopolyploids may originate either from well-differentiated genomes, often termed as genomic allopolyploids, or from less well-differentiated genomes of closely-related species, known as segmental allopolyploids (Stebbins, 1950). Segmental allopolyploids are closer to autopolyploids than genomic allopolyploids in the polyploid continuum. In genomic allopolyploids, fully homologous chromosomes appear in pairs, there is a strong barrier to pairing between homoeologous chromosomes, and bivalents only are observed at meiosis. In segmental allopolyploids, the closeness of the interspecific genomes means that the pairing barrier between entirely homologous chromosomes and less fully homologous chromosomes occasionally breaks down, allowing a degree of pairing and partner switching to occur between homoeologous chromosomes of the parents (Sybenga, 1996). In such cases, homoeologous pairing over the entire chromosome length leads to homoeologous bivalents being formed, while recombined chromosomes consisting of segments derived from both parental

genomes occur when only parts of homoeologous chromosomes are paired and switched (Sybenga, 1994). These recombined chromosomes may form multivalents at diakinesis-metaphase-I (Sybenga, 1996). Recombination between homoeologous chromosomes has been observed often and appears to be a common occurrence in the stabilization of new polyploids (Brubaker *et al.*, 1979; Whitkus, *et al.*, 1992; Kenton, *et al.*, 1993; Chen and Armstrong, 1994; Reinisch *et al.*, 1994). For example, Zwierzykowski *et al.* (1998) observed between 0 to 7 inter-genomic translocations per chromosome in 20 out of the 28 chromosomes in a synthetic allotetraploid of *Festuca pratensis* and *Lolium multiflorum*. Segmental allopolyploids may take one of two routes to stabilization. One route envisages continued recombination through successive generations, resulting in a segmental allopolyploid becoming stabilized as a functional autopolyploid consisting of recombined chromosomes (Stebbins, 1950). By the end of this route of allopolyploid stabilization the original allopolyploid origins become completely obscured in the genome and may only be gleaned through aberrant chromosome numbers and karyotypes (Sybenga, 1996). Even though difficult to discern, many natural apparent autopolyploid species are believed to have originated from this type of allopolyploid (Stebbins, 1950; Sybenga, 1996). Alternatively, some sets of chromosomes in a segmental allopolyploid may become stabilized by evolving into fully homologous recombined chromosomes capable of forming multivalents, while other sets of more differentiated chromosomes develop into fully differentiated chromosomes forming bivalents at meiosis. This form of auto-allopolyploidy, termed stable secondary segmental allopolyploidy, is predicted to produce a combination of bivalent and multivalent associations at meiosis and to exhibit tetrasomic inheritance for some genes and disomic inheritance for others (Sybenga, 1996).

There is some doubt as to whether stable secondary segmental allopolyploids occur naturally (Sybenga, 1996). A low frequency of multivalents at meiosis is often used to identify segmental allopolyploids. However, caution is required with this observation since many true autopolyploids rarely form quadrivalents (Sybenga, 1996, Weiss and Maluszynska, 2000), and heterozygous chromosome translocations also have a tendency to form ring, chain and figure-of-eight quadrivalents at meiosis (Sybenga, 1992; 1994). Recent research compared patterns of sequence divergence of duplicated genes to identify segmental allopolyploids (Gaut and Doebley, 1997). These researchers calculated the coalescent times for 14 pairs of duplicated sequences in maize. The coalescent times for these duplicated genes fell into two distinct groups corresponding to 20.5 and 11.4 million years ago, suggesting that the maize genome is the product of a segmental allotetraploid event. The coalescent time

of 20.5 million years represents the time of divergence of the two diploid progenitors, while the allotetraploid event is deemed to have occurred 11.4 million years ago (Gaut and Doebley, 1997). The use of molecular-sequencing methods may offer a new approach in determining segmental allopolyploidy in plants. Non-molecular methods for identifying segmental allopolyploids rely on an assessment of the distribution of multivalents in cells. If all sets of homologous chromosomes have equal probabilities of forming multivalents, as in a true autopolyploid, then there should be normal distribution of multivalents in cells. If some sets of chromosomes consistently form multivalents while other sets never do, as occurs in a secondary segmental allopolyploid, then the distribution is skewed (Sybenga, 1996). A skewed distribution of multivalents across a statistically relevant number of cells suggests a stabilized segmental allopolyploid. However, this test is sensitive only when there are small numbers of consistently-formed multivalents at meiosis

1.4 – Asteraceae cytology

1.4.1- Chromosome numbers in Asteraceae

The chromosome numbers in the Asteraceae vary from $n = 2$ to 120 (Solbrig, 1977). The vast majority (~80%) of known chromosome counts for the family fall between $n = 4$ and $n = 18$, with high polyploid numbers and very low chromosome numbers occurring infrequently (Keil and Stuessy, 1977; Solbrig, 1977; Stuessy, 1977; Robinson *et al.*, 1981). Chromosome numbers above $n = 20$ are held to be the result of polyploidization and those below $n = 9$ the result of dysploid decrease (Solbrig, 1977).

1.4.2- Chromosome numbers in Heliantheae

Heliantheae, the tribe to which *Cosmos* belongs, reflects the distribution pattern of the family, having a modal chromosome number of $n = 18$, but a range from, $n = 4$ in *Calycadenia*, *Hemizonia* and *Holocarpha*, to $n = 120$ in *Melanthera* (Stuessy, 1977; Robinson, *et al.*, 1981). The Heliantheae show no correlation between chromosome number and phylogeny with closely-related taxa showing a wide diversity in chromosome number and vice versa. However, there appears to be a relationship between chromosome number and plant habit, with weedy short-lived herbaceous species having reduced DNA content and fewer chromosomes than woody perennial types (Stebbins, 1950; Keil and Stuessy, 1977; Solbrig, 1977; Robinson *et al.*, 1981). Polyploidy occurs commonly in the tribe and is the most prevalent evolutionary process affecting chromosome number, with the original base number being obscured by

repeated polyploidizations (Solbrig, 1977; Robinson *et al.*, 1981). Polyploidization in the tribe is associated predominantly with perennial herbs, supporting the thesis put forward by Stebbins (1950): “*that perennial herbs with alternative means of vegetative production have a greater probability of surviving when polyploidized (particularly in the case of segmental allopolyploids) than ephemeral annuals, or trees and shrubs that rely exclusively on sexual reproduction*”. Dysploidy – a situation where species in a genus have different diploid chromosome numbers, but do not represent a polyploid series occurs often in the Asteraceae. Dysploid increase occurs rarely in the tribe, but decrease is common, with long series being evident in many groups (Solbrig, 1977; Stuessy, 1977; Robinson *et al.*, 1981). Reduction in chromosome number appears to be associated with chromosomal rearrangement around fewer centromeres rather than with chromosomal loss (Solbrig, 1977; Robinson *et al.*, 1981). Although rare, polyhaploidy and dysploid increase may account for some of the chromosome numbers in subtribes such as Galinsoginae that show little evidence of ancient or recent polyploidy (Robinson *et al.*, 1981). Members of the Heliantheae are rarely apomictic, but allopolyploidy has contributed to chromosome variability in many groups (Robinson *et al.*, 1981). Infrageneric hybridization occurs naturally in the tribe but leads commonly to the production of sterile hybrids (Robinson *et al.*, 1981). Robinson *et al.* (1981) proposed Heliantheae *sensu lato* to be a group of ancient polyploid origin wherein lower chromosome numbers are associated with annuals and/or short-lived perennials. The chromosome number in Heliantheae is extremely varied, with chromosomal base numbers⁴, $x = 8, 9, 11, 12, 17, 18$ or 19 being present in all major genera of the tribe (Figure 1.11). The lowest commonly-observed chromosome numbers in the tribe are $n = 8$ and 9 , and thus an ancestral base number $x = 8$ was suggested for the tribe, from which the higher base numbers of $x = 17-19$ have been derived (Stuessy, 1977). However, Robinson *et al.* (1981) suggested that the base number for the tribe is more likely to be $x = 10$. They offer as evidence the observed base number of $x = 9$ and $x = 10$ for the entire Asteraceae family, with $x = 9$ being the most common chromosome number (Solbrig *et al.*, 1972, 1977). In addition, within the Asteraceae and Heliantheae there is extensive evidence of dysploid decrease and a tendency for higher chromosome numbers to stabilise at levels below the original base number, and for this reason the base number for Asteraceae and Heliantheae is $x =$

⁴ The terminology adopted follows the conventions used by Ramsey and Schemske 1998. and Otto and Whitton 2000. Throughout the thesis. x denotes the base number of a lineage. $2n$ represents the chromosome number in somatic tissue regardless of whether an individual is diploid, triploid or tetraploid. i.e. $2n = 2x$, $2n = 3x$ or $2n = 4x$. The gametic or haploid chromosome number is represented by n , and is the number of chromosomes expected after meiosis in a sexually reproducing organism.

10, from which $x = 9$ and 8 are derived by dysploid decrease, and the higher numbers of $x = 20, 22, 26, 24, 28, 32, 36$ that occur frequently in the tribe are the result of eupolyploidization or aneupolyploidization (Solbrig, 1977; Turner *et al.*, 1979; Robinson *et al.*, 1981).

The subtribe Coreopsidinae, to which *Cosmos* belongs, is assigned the base number $x = 12$. The lower chromosome numbers of $n = 8, 9, 10$ and 11 prevalent within the subtribe are viewed as the result of dysploid decrease, with polyploidy giving rise to the higher commonly-occurring chromosome numbers of $n = 24, 36, 48, 60$. Chromosome numbers of $n = 22, 23, 32, 30, 34, 56$, also common in the group, can be explained as being the result of polyploidy followed by dysploid decrease or vice versa. The prevalence of $n = 15$, and 16, that occur regularly in *Hidalgoa* and *Dahlia* is difficult to explain as a consequence of polyploidy and dysploid decrease from a base number of $x = 12$, since the lowest chromosome numbers identified so far for these two genera are $n = 15$ and 16 respectively. Likewise, chromosome numbers of $n = 13$ and 14, that occur in *Cosmos*, *Coreopsis* and *Heterosperma* suggest either an increase from $x = 12$, or an alternative base number for these genera. In response to these observations, a base number of $x = 14$ was suggested for *Coreopsis* with a high base number of $x = 17-19$ for the whole tribe (Smith, 1975). General opinion however, identifies a base chromosome number of $x = 12$ for Coreopsidinae, with higher numbers being characteristic of specific genera that encompass some of the most divergent members of the subtribe. Included in this group of divergent genera are *Hidalgoa* ($x = 15, 16$), *Dahlia* ($x = 16, 17, 18$) and *Henricksonia* ($x = 18$) (Turner and Flyr, 1966; Turner, *et al.*, 1973, 1979; Turner, 1977b; Stuessy, 1977; Robinson *et al.*, 1981; Karis and Ryding, 1994). Aside from these anomalies, it must be acknowledged that for many members of the Heliantheae and Coreopsidinae there are no chromosome counts, so the full range of chromosome numbers within Asteraceae tribes and subtribes has yet to be determined. When chromosome counts for the majority of Heliantheae are known, then more authoritative conclusions regarding anomalous genera and base numbers may be drawn.

1.4.3 - Previous cytological investigations in *Cosmos*

Cosmos bipinnatus and *C. sulphureus* have been the subjects of numerous cytological investigations (Table 1.2). Chromosome counts and karyotypes for these taxa identify them as diploid $2n = 2x = 24$. The karyotype of *C. bipinnatus* is characterised as having eight homologues with median centromeres (8 *m*) and four with submedian

centromeres (4 *sm*), with that of *C. sulphureus* having 6 *sm* homologues and 6 homologues with subterminal centromeres (6 *st*) (Ohri *et al.*, 1988), with both species having 12 bivalents at meiosis (Turner and Flyr, 1966; Banerjee 1971; Mathew and Mathew 1988; Ohri *et al.*, 1988). Base numbers of $x = 11$ and 12 have been proposed for the genus (Powell and Turner, 1963; Turner and Flyr, 1966; Gupta *et al.*, 1972; Solbrig *et al.*, 1972). In contrast, the cytology of *C. atrosanguineus* (Lawrence, 1930) and *C. carvifolius* (Melchert, 1968) have been investigated only once. *Cosmos carvifolius* is reported to be a diploid species $2n = 2x = 22$, with 11 bivalents present at meiosis (Melchert, 1968). Meiotic cells only of *C. carvifolius* were investigated and hence its karyotype was not described (Melchert, 1968). Lawrence (1930) made counts from mitotic and meiotic cells of *C. atrosanguineus*, identifying it as a tetraploid with $2n = 4x = 48$ chromosomes, but produced no drawings or karyotype for the species and made no comments about chromosome associations during meiosis. It seemed prudent therefore to investigate the cytology of *C. atrosanguineus* accessions used in this research as a means of eliminating, or establishing the chromosomes as the source of sterility in this species.

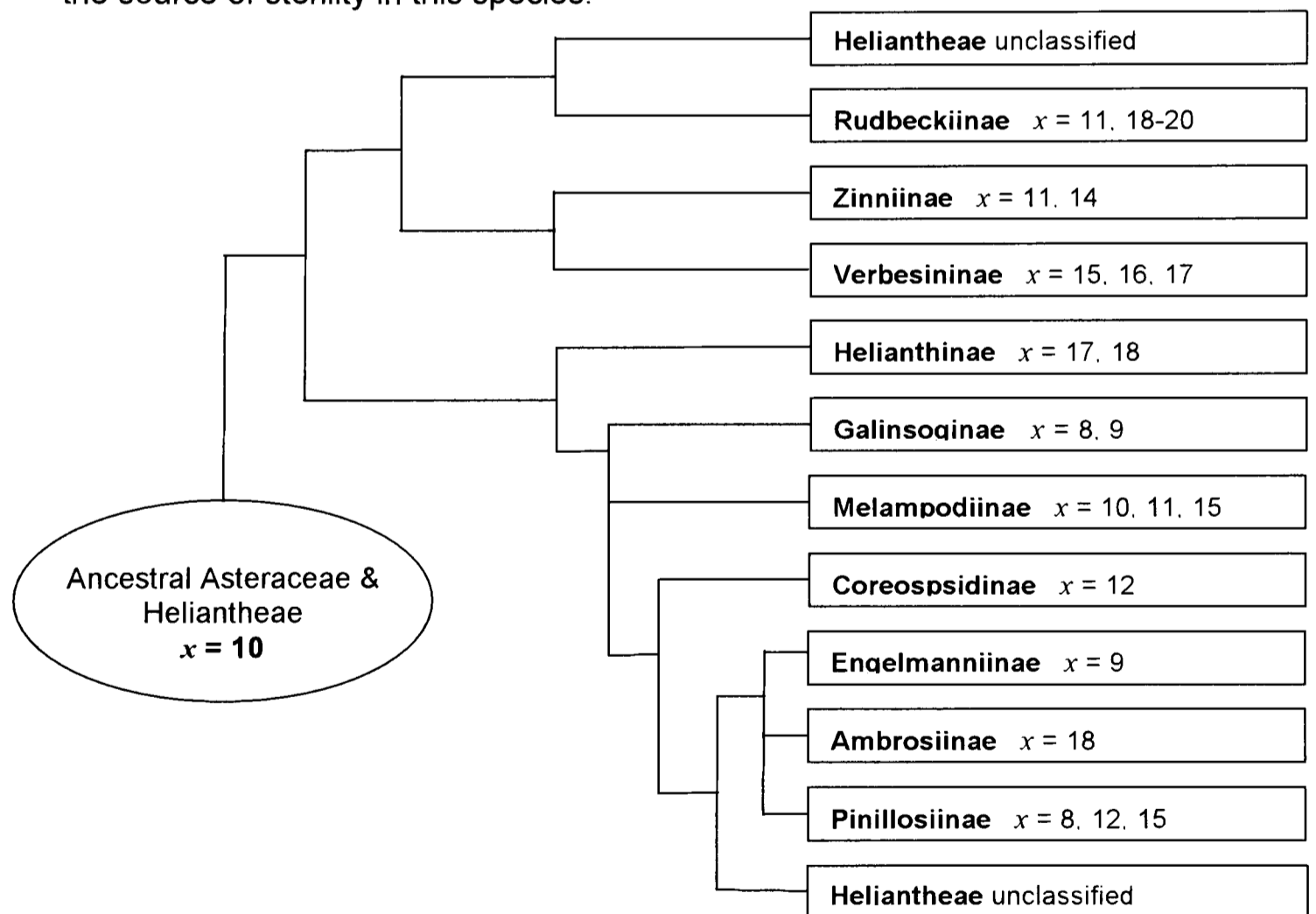


Figure 1.11. Sub-tribal relationships in the Heliantheae

Evolutionary relationships of the subtribes of Heliantheae, after Karis and Ryding 1994. Sixty-four genera of the Heliantheae were sampled using morphological cladistic analysis. In this analysis, Heliantheae is divided into 10 putatively monophyletic subtribes that form two main branches representing sister groups. One group contains the subtribe Verbessininae, its sister subtribe Zinniinae, and Rudbeckiinae. The other group contains the majority of the Heliantheae subtribes. The base numbers 'x' for each subtribe are included in accordance with Solbrig *et al.*, 1972; Stuessy, 1977; Keil and Stuessy, 1977; Solbrig, 1977; Robinson *et al.*, 1981.

Table 1.2 Reported chromosome numbers for *Cosmos species*

<i>Cosmos species</i>	Chromosome number		Ploidy	Reference
	<i>n.</i>	<i>2n</i>		
<i>C. atrosanguineus</i> (Hook.) Voss	24	48	4x	Lawrence, 1930
<i>C. bipinnatus</i> Cav.	---	24	2x	Sugiura, 1936
	12	---		Melchert, 1968
	12	24		Banerjee, 1971
	12, 12+	---		Gupta, <i>et al.</i> 1972
	---	24		Koul and Gohil, 1973
	12	---		Mehra and Remanandan, 1974
	12	---		Keil and Stuessy, 1977
	12 II	---		Lakshami <i>et al.</i> 1982
	12	---		Gupta and Gill, 1983
	---	24		Srivastava, 1983
	---	24		Nirmala and Rao, 1984, 1985
	12	---		Srivastava, 1986
	12	---		Mathew and Mathew, 1988
	---	24		Ohri, <i>et al.</i> 1988
	12	---		Gupta, and Gill, 1989
	---	24		Probatova, <i>et al.</i> 1991
	---	24		Razaq <i>et al.</i> 1994
		Zhang Y-x, 1994		
	12	24	Jose and Mathew, 1995	
<i>C. caudatus</i> Kunth	24 II	---	4x	Robinson <i>et al.</i> , 1981
	24 II	---		Keil <i>et al.</i> , 1988
	24 II	---		Melchert, 1990
	24 II	48		Jose and Mathew, 1995
<i>C. carvifolius</i> Benth.	11 II	---	2x	Melchert, 1968
<i>C. concolor</i> Sherff	36	---	6x	Melchert, 1968
<i>C. crithmifolius</i> H.B.K.	33	---	6x	Melchert, 1968
<i>C. diversifolius</i> Otto	12 II	---	2x	Melchert, 1968
<i>C. intercedens</i> Sherff	11 II	---	2x	Melchert, 1968
<i>C. jaliscensis</i> Sherff	36	---	6x	Melchert, 1968
<i>C. juxtlahuacensis</i> Panero & Villaseñor	13 II	26	2x	Strother and Panero, 2001
<i>C. landii</i> Sherff	22 II	---	4x	Melchert, 1968
<i>C. linearifolius</i> (Schultz-Bip)	22 II	---	2x	Melchert, 1968
<i>C. linearifolius</i> var. <i>magnifolius</i>	11 II	---	2x	Melchert, 1968
<i>C. marginatus</i> Klatt.	24 II	---	2x	Wulff <i>et al.</i> 1996
<i>C. mcvaughii</i> Sherff	12 II	---	2x	Melchert, 1968
<i>C. montanus</i> Sherff	12 II	---	2x	Melchert, 1968

Table 1.2 continued

<i>Cosmos</i> species	Chromosome Number		Ploidy	Reference
	<i>n.</i>	<i>2n</i>		
<i>C. pacificus</i> var. <i>chiapensis</i> Melchart	12 II	---	2x	Melchert, 1990
<i>C. pacificus</i> var. <i>pacificus</i>	12 II	---	2x	Melchert, 1990
<i>C. palmerii</i> B.L. Robinson	24	---	4x	Melchert, 1968
<i>C. parviflorus</i> (Jacq.) Kunth	12	---	2x	Ward and Spellenberg, 1988
	12 II	---	2x	Melchert, 1968
<i>C. peucedanifolius</i> Wedd.	12-14		2x	Robinson <i>et al.</i> , 1981
<i>C. peucedanifolius</i> var. <i>peucedanifolius</i>	18	36	2x	Kuzmanov <i>et al.</i> , 1989
	18	36	2x	Dabrowska, 1989
	12	---	2x	Hunziker <i>et al.</i> , 1990
<i>C. purpureus</i> (DC.) Hemsl. var. <i>purpureus</i>	12	---	2x	Melchert, 1968
<i>C. purpureus</i> var. <i>flavidiscus</i> Sherff	12	---	2x	Melchert, 1968
<i>C. ocellatus</i> Greenman	12 II	---	2x	Melchert, 1968
<i>C. ochroleucoflorus</i> Melchert	22	---	4x	Melchert, 1968
<i>C. scabiosoides</i> H.B.K.	12 II	---	2x	Melchert, 1968
	24 II	---	4x	Melchert, 1968
<i>C. schaffneri</i> Sherff	12	---	2x	Melchert, 1968
<i>C. sherffi</i> Melchert	12	---	2x	Melchert, 1968
<i>C. sulphureus</i> Cav.	12	---	2x	Turner and Flyr, 1966
	12	---		Melchert, 1968
	12	---		Solbrig <i>et al.</i> , 1972
	---	24		Koul and Gohil, 1973
	12	---		Turner <i>et al.</i> , 1973
	13	---		Mehra and Remanandan, 1974
	12	---		Pinkava and Keil, 1977
	12	---		Olsen, 1980
	12	24		Gupta. and Gill, 1983
	---	24		Srivastava, 1983
	12	---		Gupta. and Gill, 1984
	12, 24	24.		Mathew and Thomspn, 1984
	---	24		Nirmala and Rao, 1985
	---	24		Wang and Li, 1987
	---	24		Ohri, <i>et al.</i> 1988
	12	---		Mathew and Mathew, 1988
	12	---		Gupta and Gill, 1989
	12	---		Husaini and Iwo, 1990
---	24	Nirmala. and Rao, 1990		
12	24	Jose and Mathew, 1995		

1.5 - Self-incompatibility in Plants

1.5.1 - Introduction

Self-incompatibility (SI) is a mechanism employed by hermaphrodite plant species to promote outbreeding (Crowe, 1964; Mau *et al.*, 1991; Richards, 1997), and is defined as “the inability of a fertile hermaphrodite seed plant to produce zygotes after self-pollination” (De Nettancourt, 1977, 2001).

Diversity in organisms is generated through gamete formation and mutations (Lewis, 1979; Jones, 1999). The production of fertile genetically varied offspring is enhanced by ensuring the fusion of gametes from genetically diverse but related individuals. In higher animals, lower plants and approximately five percent of angiosperms this is achieved by segregating male and female reproductive structures into separate, often morphologically distinct, individuals (Mather, 1944; Crowe, 1964; Richards, 1997). The majority of angiosperms are hermaphrodite, with male and female sexual organs in close proximity within the same flower. Without a preventative mechanism to self-fertilization, levels of homozygosity would increase and lead to the deleterious effects of inbreeding depression (de Nettancourt, 1977; Dickinson, 1990; Mau *et al.*, 1991; Richards, 1997). In some plants, separation in time and space of mature reproductive structures is used to avoid self-fertilization (Charlesworth, 1985; Richards, 1997), however, for the vast majority of hermaphrodite plants; self-incompatibility is used alone or in combination with temporal or spatial mechanisms to ensure outbreeding (Crowe, 1964; de Nettancourt, 1977; Hinata *et al.*, 1993; Franklin *et al.*, 1995).

Two types of self-incompatibility are distinguished by flower morphology. Plants with heteromorphic self-incompatibility have a one or two S-locus gene system producing flowers with different morphologies (Charlesworth 1995). The heteromorphology commonly involves differences in the style length and anther height (Lewis, 1979; Mau *et al.*, 1991; Franklin *et al.*, 1995). Heteromorphic self-incompatibility predominates in the Primulaceae, Rubiaceae and Plumbaginaceae but is found to lesser degrees in a further twenty-one plant families (Crowe, 1964; Lewis, 1979; Mau *et al.*, 1991).

Homomorphic self-incompatibility is the more widespread form of self-incompatibility and refers to interbreeding self-incompatible species with flowers that are morphologically indistinguishable (de Nettancourt, 1977; Mau *et al.*, 1991; Newbigin, *et al.*, 1993; Franklin-Tong and Franklin, 2003). Homomorphic self-incompatibility is a genetically controlled phenomenon, estimated to occur in 90 plant families and more than 250 genera (Charlesworth, 1995; Franklin *et al.*, 1995; Table 1.3). Homomorphic

SI systems become effective after pollination takes place, but before zygote formation, and rely on a complex molecular interaction between pollen and pistil to produce a physiological barrier to self-fertilization (Bateman, 1952; Haring *et al.*, 1990; Kao and McCubbin 1997).

Table 1.3 Homomorphic self-incompatibility in angiosperms

Family	Genetic Control of SI	Species	Site of SI	S-locus component cloned	Catalytic activity implicated	Ploidy	No. S-alleles	Ref.
Asteraceae	SSI one locus	<i>Arnica montana</i>	Stigma	None	---	---	---	83
		<i>Aster furcatus</i>	Stigma	None	---	---	---	110
		<i>Carthamus flavescens</i>	Stigma	None	---	---	---	126
	Partial SSI	<i>Centaurea nigra</i>	Stigma	None	---	---	---	131-133
		<i>Centaurea scabiosa</i>	Stigma	None	---	---	---	131-133
		<i>Centaurea solstitialis</i>	Stigma	None	---	---	---	130
	SSI one locus	<i>Cichorium intybus</i>	Stigma	None	---	2x	---	1
		<i>Cosmos bipinnatus</i>	Stigma	None	---	2x	---	2
		<i>Crepis foetida ssp. Rhoeadifolia</i>	Stigma	None	---	2x	---	3
	Pseudo SSI	<i>Crepis sancta</i>	Stigma	None	---	---	---	87
	SSI one locus	<i>Erigeron kachinensis</i>	Stigma	None	---	---	---	80
		<i>Espeletia angustifolia</i>	Stigma	None	---	---	---	113
		<i>Espeletia atropurpurea</i>	Stigma	None	---	---	---	113
		<i>Espeletia badilloi</i>	Stigma	None	---	---	---	113
		<i>Espeletia batata</i>	Stigma	None	---	---	---	113
		<i>Espeletia lindenbergii</i>	Stigma	None	---	---	---	113
		<i>Espeletia marcescens</i>	Stigma	None	---	---	---	113
		<i>Espeletia neriifolia</i>	Stigma	None	---	---	---	113
		<i>Espeletia schultzii</i>	Stigma	None	---	---	---	113
		<i>Helenium virginicum</i>	Stigma	None	---	---	---	82
		<i>Helianthus annuus</i>	Stigma	None	---	---	---	107
		<i>Hymenoxys acaulis ver. glabra</i>	Stigma	None	---	---	---	128
		<i>Hypochoeris radicata</i>	Stigma	None	---	---	---	109
		<i>Liatris-helleri</i>	---	None	---	---	---	88
		<i>Parthenium argentatum</i>	Stigma	None	---	2x	---	4, 5, 109
		<i>Parthenium hysterophorus</i>	Stigma	None	---	---	---	109
	Partial SSI	<i>Pyrrhopappus carolinianus</i>	---	---	---	---	---	133
	SSI one locus	<i>Rutidosia leiolepis</i>	Stigma	None	---	2x	---	79
		<i>Rutidosia leptorrhynchoides</i>	Stigma/Style	None	---	2x & 4x	---	81
	Partial SSI	<i>Scalesia affinis</i>	Stigma	None	---	4x	---	86
SSI one locus	<i>Scalesia divisa</i>	Stigma	None	---	---	---	86, 129	
	<i>Senecio squalidus</i>	Stigma	None	---	2x	20	6, 108	

Key to abbreviations and symbols: ---, no data available; numbers in brackets indicates the size of the population from which S-allele numbers were estimated; GSI, gametophytic self-incompatibility; LSI late-acting self-incompatibility; OS ovarian sterility; SSI, sporophytic self-incompatibility. S receptor kinase is the female determinant of the sporophytic self-incompatibility in *Brassica*; RNase is the female determinant of the gametophytic self-incompatibility system identified in Solanaceae and Rosaceae.

Table 1.3 continued

Family	Genetic Control of SI	Species	Site of SI	S-locus component cloned	Catalytic activity implicated	Ploidy	No. S-alleles	Ref.
Bignoniaceae	LSI-OS GSI	<i>Dolichandra cynanchoides</i>	Style/ Ovary	None	---	---	---	92-93
		<i>Tabebuia nodosa</i>	Style/ Ovary	None	---	---	---	92-93
		<i>Pandorea baileyana</i>	Ovary	None	---	---	---	91-92
		<i>Pandorea jasminoides</i>	Ovary	None	---	---	---	91-92
		<i>Pandorea pandorana</i>	Ovary	None	---	---	---	91-92
Brassicaceae	SSI one locus	<i>Arabidopsis lyrata</i>	Stigma	Female	S- receptor	2x	26	57
		<i>Brassica oleracea</i>	Stigma	Male & Female	S- receptor kinase	2x	50	9-10
		<i>Brassica rapa</i>	Stigma	Male & Female	S- receptor kinase	2x	30	11
		<i>Brassica napus</i>	Stigma	Female	S- receptor	2x	---	12-13
		<i>Iberis amara</i>	Stigma	None	---	2x	22	14
		<i>Raphanus raphanistrum</i>	Stigma	None	---	2x	25-34	15
		<i>Raphanus sativus</i>	Stigma	Female	---	2x	20	16
		<i>Sinapsis arvensis</i>	Stigma	Female	---	2x	35 (52)	17-18
Campanulaceae	GSI one locus	<i>Campanula rapunculoides</i>	Style	Female	RNase	---	---	77, 92
Caryophyllaceae	SSI one locus	<i>Cerastium arvense</i> ssp. <i>Stictum</i>	Stigma	None	---	4x	---	19-20
		<i>Stellaria holostea</i>	Stigma	None	---	---	---	85
Chenopodiaceae	GSI four loci	<i>Beta vulgaris</i>	Stigma	None	---	2x	---	21, 118
Cistaceae	GSI	<i>Cistus carthagenensis</i>	Style	None	---	2x	---	76
Convolvulaceae	SSI one locus	<i>Ipomoea cairica</i>	---	None	---	---	---	123
		<i>Ipomoea-fistulosa</i>	---	None	---	---	---	84
		<i>Ipomea leucantha</i>	Stigma	None	---	2x	---	22
		<i>Ipomea setifera</i>	Stigma	None	---	2x	---	23
		<i>Ipomea trifida</i>	Stigma	None	---	2x	49	24
Corylaceae (Betulaceae)	SSI one locus	<i>Corylus avellana</i>	Stigma	None	---	2x	25	7, 66, 115
Ericaceae	GSI	<i>Vaccinium angustifolium</i>	Style	None	---	---	---	92, 95
		<i>Vaccinium corymbosum</i>	Style	None	---	---	---	92, 95
		<i>Vaccinium myrtilloides</i>	Style	None	---	---	---	92, 95

Table 1.3 continued

Family	Genetic Control of SI	Species	Site of SI	S-locus component cloned	Catalytic activity implicated	Ploidy	No. S-alleles	Ref.
Fagaceae	GSI	<i>Quercus ilex</i>	Style/Ovary	None	---	---	---	92, 100
Gesneriaceae	SSI	<i>Titanotrichum oldhamii</i>	Stigma	None	---	---	---	135
Leguminosae	GSI one locus	<i>Trifolium pratense</i>	Style	None	---	2x	129-215	25-26
		<i>Trifolium repens</i>	Style	None	---	2x	39 (101)	64
Liliaceae	GSI one locus	<i>Lilium longiflorum</i>	Style	None	---	---	---	27
	GSI four loci	<i>Lilium martagon</i>	Style	None	---	---	---	104
Malvaceae	GSI & (SSI)	<i>Luehea grandiflora</i>	Style	None	---	---	---	125
Melantheaceae	SSI	<i>Trillium grandiflorum</i>	Stigma	None	---	---	---	102-103, 122
		<i>Trillium erectum</i>	Stigma	None	---	---	---	
Oenotheraceae	GSI one locus	<i>Oenothera organensis</i>	Stigma	None	---	---	45	28
Oleaceae	GSI one locus	<i>Phillyrea angustifolia</i>	Style	None	---	---	---	94
Paeoniaceae	GSI Possibly	<i>Paeonia jishanensis</i>	Style	None	---	---	---	114
Papaveraceae	GSI one locus	<i>Papaver rhoeas</i>	Stigma	None	---	---	45 (66)	25, 29-33
Passifloraceae	SSI one locus	<i>Passiflora edulis</i>	Stigma	None	---	---	---	58
Poaceae	GSI	<i>Andropogon gerardii</i>	---	None	---	---	---	92, 101
	GSI two loci	<i>Lolium perenne</i>	Stigma	None	---	---	31S & 31Z (38-39)	34, 35, 124
		<i>Phalaris coerulea</i>	Stigma	Male	---	---	---	111
	GSI	<i>Sorghastrum nutans</i>	---	None	---	---	---	92, 101
Polemoniaceae	GSI one locus	<i>Phlox drummondii</i>	---	None	---	2x	30 (34)	73, 92
	SSI one locus	<i>Linanthus androsaccous</i>	---	None	---	---	---	112
		<i>Linanthus latisectus</i>	---	None	---	---	---	112
		<i>Linanthus montanum</i>	---	None	---	---	---	112
		<i>Linanthus nudotus</i>	---	None	---	---	---	112
		<i>Linanthus parviflorus</i>	---	None	---	---	---	92, 96
Primulaceae	GSI one locus	<i>Anagallis monellii</i>	---	None	---	---	134	

Table 1.3 continued

Family	Genetic Control of SI	Species	Site of SI	S-locus component cloned	Catalytic activity Implicated	Ploidy	No. S-alleles	Ref.
Ranunculaceae	GSI three loci	<i>Ranunculus acris</i>	---	None	---	2x	---	21
Rosaceae	GSI one locus	<i>Crataegus monogyna</i>	Style	Female	RNase	---	17 (13)	72
		<i>Malus domestica</i>	Style	Female	RNase	---	---	48-50
		<i>Prunus avium</i>	Style	Female	RNase	2x	8	59, 62, 71, 137
		<i>Prunus cerasus</i>	Style	Female	RNase	---	---	137
		<i>Prunus dulcis</i>	Style	Female	RNase	---	---	60-61
		<i>Prunus mume</i>	Style	Female	RNase	---	---	136
		<i>Pyrus pyrifolia</i>	Style	Female	RNase	---	---	49, 51-52
		<i>Pyrus serotina</i>	Style	Female	RNase	---	---	53, 63
		<i>Sorbus aucuparia</i>	Style	Female	RNase	---	20 (20)	72
Rubiaceae	GSI	<i>Coffea canephora</i>	Style	None	---	---	---	119
Saxifragaceae	LSI-OS GSI	<i>Heuchera micrantha</i> var. <i>diversifolia</i>	Style/Ovary	None	---	---	---	92, 97
		<i>Tolmeia menziesii</i>	Ovary	None	---	---	---	92, 98
Scrophulariaceae	GSI one locus	<i>Antirrhinum glutinosum</i>	---	None	---	---	8	69, 89
		<i>Antirrhinum hispanicum</i>	Style	Female	RNase	---	---	70, 89, 138
		<i>Nemesia strumosa</i>	---	None	---	---	6-7	92, 99, 121
		<i>Scrophularia fontqueri</i>	Style	None	---	---	---	90
Solanaceae	GSI one locus	<i>Lycopersicon peruvianum</i>	Style	Female	RNase	---	---	36, 127
		<i>Nicotiana alata</i>	Style	Female	RNase	2x	---	37-38, 120
		<i>Nicotiana tabacum</i>	style	Female	RNase	---	---	117
		<i>Petunia axillaris</i>	Style	Female	RNase	---	18 (30)	74-75
		<i>Petunia hybrida</i>	Style	Female	RNase	---	---	39
		<i>Petunia inflata</i>	Style	Female	RNase	---	---	40-43, 116
		<i>Physalis crassifolia</i>	Style	Female	RNase	2x	28 (45)	67, 68
		<i>Solanum carolinense</i>	Style	Female	RNase	2x	13 (14)	65
		<i>Solanum chacoense</i>	Style	Female	RNase	---	---	44-45
		<i>Solanum tuberosum</i>	Style	Female	RNase	---	---	46-47

Table 1.3 continued

Family	Genetic Control of SI	Species	Site of SI	S-locus component cloned	Catalytic activity Implicated	Ploidy	No. S-alleles	Ref.
Sterculiaceae	LSI-OS SSI one locus	<i>Dombeya species</i>	Ovule	None	---	---	---	105
	LSI-OS SSI one locus	<i>Dombeya acutangula ssp. Acutangula</i>	Ovule	None	---	---	---	106
	LSI-OS SSI one locus	<i>Theobroma cacao</i>	Ovule	None	---	---	---	54-55
	SSI one locus	<i>Cola nitida</i>	Stigma	None	---	---	---	56
Verbenaceae	GSI	<i>Tectona grandis</i>	Style	None	---	---	---	78

¹Varotto *et al.*, 1995; ²Crowe, 1954; Little, 1940; ³Hughes & Babcock, 1950; ⁴Gerstel, 1950; ⁵Gerstel & Riner, 1950; ⁶Hiscock *et al.* 2003 ⁷Thompson, 1979; ⁸Schierup *et al.*, 1979, 2001; ⁹Brace *et al.*, 1994; ¹⁰Stephenson, 1997; ¹¹Nou *et al.*, 1993; ¹²Goring *et al.*, 1992a; ¹³Goring & Rothstein 1992; ¹⁴Bateman, 1955; ¹⁵Sampson, 1967; ¹⁶Karron *et al.* 1990; ¹⁷Ford & Kay, 1985; ¹⁸Stevens & Kay 1988; ¹⁹Lundqvist, 1979, ²⁰Lundqvist 1990; ²¹Lundqvist *et al.*, 1973; ²²Kowyama, 1980; ²³Martin, 1968; ²⁴Kowyama, 1994; ²⁵O'Donnell & Lawrence 1984; ²⁶Paxman, 1963; ²⁷Tsuruhara and Tezuka, 2001; ²⁸Emerson, 1940; ²⁹Campbell & Lawrence, 1981; ³⁰Franklin-Tong *et al.*, 1989; ³¹Lawrence *et al.*, 1978, ³²Lawrence *et al.*, 1993; ³³Franklin-Tong *et al.* 1991; ³⁴Fearon *et al.*, 1994; ³⁵Lundqvist, 1962; ³⁵Mau *et al.*, 1986; ³⁷Anderson *et al.*, 1986; 1989; ³⁸Murfett *et al.*, 1996; ³⁹Broothaerts *et al.*, 1990; ⁴⁰Ai *et al.*, 1990; ⁴¹Clarke *et al.*, 1989; ⁴²Huang *et al.*, 1994; ⁴³Lee *et al.*, 1994; ⁴⁴Xu *et al.*, 1990; ⁴⁵Matton *et al.*, 1997; ⁴⁶Kirch *et al.*, 1989; ⁴⁷Kaufmann *et al.*, 1992; ⁴⁸Sassa *et al.*, 1994, ⁴⁹Sassa *et al.*, 1996; ⁵⁰Katoh *et al.*, 2002; ⁵¹Ishimizu *et al.*, 1995, 1996a & 1996b; ⁵²Norioka *et al.*, 1996; ⁵³Sassa *et al.*, 1993; ⁵⁴Cope, 1962a and 1962b; ⁵⁵Knight & Rogers, 1955; ⁵⁶Jacob, 1973; ⁵⁷Mable, *et al.*, 2003; ⁵⁸Bruckner, *et al.*, 1995; ⁵⁹Richman *et al.*, 1997; ⁶⁰Tao *et al.*, 1997; ⁶¹Ushijima *et al.*, 1998; ⁶²Tao *et al.*, 1999; ⁶³Sassa *et al.*, 1992; ⁶⁴Atwood, 1944; ⁶⁵Richman *et al.*, 1995; ⁶⁶Mehlenbacher, 1997; ⁶⁷Richman *et al.*, 1996a; ⁶⁸Richman *et al.*, 1996b; ⁶⁹Gruber, 1932; ⁷⁰Xue *et al.*, 1996; ⁷¹Crane and Brown, 1937; ⁷²Raspé and Kohn, 2002; ⁷³Levin, 1993; ⁷⁴Tsukamoto *et al.*, 1999; ⁷⁵Tsukamoto *et al.*, 2003; ⁷⁶Boscaiu and Guemes, 2001; ⁷⁷Stephenson *et al.*, 2000; ⁷⁸Tangmitcharoen and Owens, 1997; ⁷⁹Young *et al.*, 2002; ⁸⁰Allphin *et al.*, 2002; ⁸¹Young *et al.*, 2000; ⁸²Messmore and Knox, 1997; ⁸³Luijten *et al.*, 1996; ⁸⁴Prabha *et al.*, 1982; ⁸⁵Lundqvist, 1994; ⁸⁶Nielsen *et al.*, 2003; ⁸⁷Cheptou *et al.*, 2002; ⁸⁸Godt and Hamrick, 1995; ⁸⁹Ma *et al.*, 2003; ⁹⁰Ortega-Olivencia and Devesa, 1998; ⁹¹James and Knox, 1993; ⁹²Igic, and Kohn, 2001; ⁹³Gibbs and Bianchi, 1999; ⁹⁴Vassiliadis *et al.*, 2000; ⁹⁵Hokanson and Hancock, 2000; ⁹⁶Goodwillie, 1997; ⁹⁷Rabe and Soltis, 1999; ⁹⁸Weiblen and Brehm, 1996; ⁹⁹Henny and Ascher, 1977; ¹⁰⁰Yacine and Bouras, 1997; ¹⁰¹McKone *et al.*, 1998; ¹⁰²Steven *et al.*, 2003; ¹⁰³Sage *et al.*, 2001; ¹⁰⁴Lundqvist 1991; ¹⁰⁵Humeau *et al.*, 1999; ¹⁰⁶Gigord *et al.*, 1998; ¹⁰⁷Elleman, *et al.*, 1992; ¹⁰⁸Hiscock, 2000a; ¹⁰⁹Lewis, 1994; ¹¹⁰Reinartz and Les, 1994; ¹¹¹Li *et al.*, 1994; ¹¹²Goodwillie, 1999; ¹¹³Berry and Calvo, 1989; ¹¹⁴Zhou *et al.*, 1999; ¹¹⁵Ciampolini and Cresti, 1998; ¹¹⁶Karunanandaa *et al.*, 1994; ¹¹⁷Kirch *et al.*, 1995; ¹¹⁸Larsen, 1977; 1978 & 1983; ¹¹⁹Lashermes *et al.*, 1996; ¹²⁰Lantin *et al.*, 1997; ¹²¹Riley 1934; ¹²²Sage *et al.*, 1994; ¹²³Sood *et al.*, 1982; ¹²⁴Devey *et al.*, 1994; ¹²⁵Gibbs *et al.*, 2003; ¹²⁶Imrie and Knowles, 1971; ¹²⁷Chawla, *et al.*, 1997; ¹²⁸DeMauro, 1993; ¹²⁹Nielsen *et al.*, 2000; ¹³⁰Maddox *et al.*, 1996; ¹³¹Marsden-Jones and Turrill, 1954; ¹³²Lack, 1982; ¹³³Estes and Thorp, 1975; ¹³⁴Talavera *et al.*, 2001, ¹³⁵Wang *et al.*, 2004; ¹³⁶Entani *et al.*, 2003; ¹³⁷Yamane *et al.*, 2003; ¹³⁸Lai *et al.*, 2002.

1.5.2 - Homomorphic self-incompatibility: an intraspecific rejection system

Homomorphic self-incompatibility in higher plants is an intraspecific rejection system involving the recognition of self from non-self pollen (de Nettancourt, 1977 & 1997; Hinata *et al.*, 1993; Franklin *et al.*, 1995). The recognition event takes place at the pollen-pistil interface and involves specific molecules under the control of multiple S-alleles (for sterility alleles) at one, two or a few sterility loci (S-loci) (Hinata *et al.*, 1993; Table 1.3). A rejection event occurs when pistil and pollen phenotypes have been determined by identical S-alleles, and results in the arrest of normal pollen development (de Nettancourt, 1977; Hinata *et al.*, 1993). The pistil can be viewed as a genetic filter, inhibiting the development of certain pollen genotypes, while permitting others to grow and achieve fertilization (Mather, 1944).

Two systems of homomorphic self-incompatibility are distinguished by the genetic control operating in the pollen. In gametophytic self-incompatibility (GSI) the pollen grain expresses only the S-allele encoded by its own haploid genome, with transcription and translation of the S-allele occurring in the pollen grain after meiosis (Dodds *et al.*, 1996). The genetics of sporophytic self-incompatibility (SSI) is more complicated as the pollen grain is under maternal control, and therefore expresses both S-alleles of the diploid pollen donor, and may also express the single S-allele encoded by its own haploid genome (Kusaba *et al.*, 2002). Transcription and translation of the sporophytic S-gene occurs in the diploid sporophytic tissue of the tapetum and is transferred to the pollen coat (Heslop-Harrison, 1968; Lewis, 1994; Dodds *et al.*, 1996; Schopfer *et al.*, 1999). The difference in pollen behaviour between the two self-incompatibility systems can be interpreted as a shift in the timing of S-gene action (Pandey, 1958). Pollen under sporophytic control is imprinted with a higher number of S-allele specificities than pollen under gametophytic control and consequently is more likely to experience cross-incompatibility (Nasrallah and Nasrallah, 1989). However, dominance interactions of S-alleles, which commonly occur in the pollen grains and to a lesser degree in pistils of sporophytic SI systems, reduces the number of S-allele specificities expressed in the sporophytic phenotype, and reduces the incidence of cross-incompatibility (Franklin *et al.*, 1995; Figure 1.12c-d). In the gametophytic system, dominance in the diploid pistil would result in self-compatibility and so co-dominance of S-alleles in both pollen and pistil is the norm and the S-locus of GSI species is always heterozygous (Heslop-Harrison, 1975; Mau *et al.*, 1991; Figure 1.12a-b).

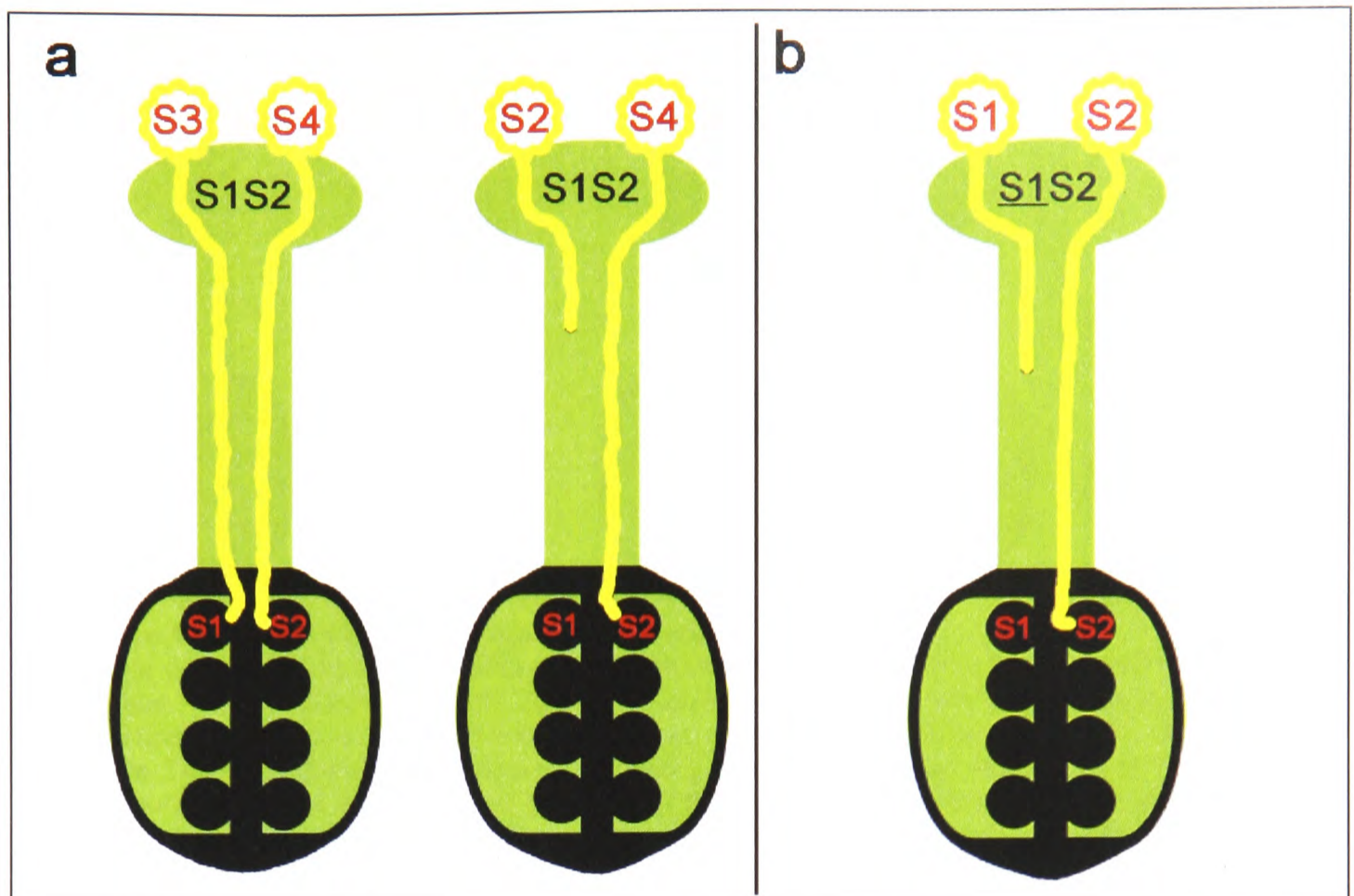


Figure 1.12a - GSI with independent interaction of S-alleles

Pollen from the S_3S_4 plant is fully compatible with the S_1S_2 pistil on the left. Pollen from S_2S_4 plants is semi-compatible with S_1S_2 pistil on the right, as only half the pollen is compatible i.e. S_4 pollen, which grows down the pistil and enters the ovary, while S_2 pollen is rejected halfway down the pistil. In GSI species, a fully compatible cross, where 100% of the viable pollen germinates pollen tubes, indicates the participants in the cross have completely different genotypes e.g. ($S_1S_2 \times S_3S_4$). Semi-compatibility, where a 1:1 segregation of compatible and incompatible pollen tubes is observed in the pistil, confirms the presence of a shared allele within the participants of a cross ($S_1S_2 \times S_2S_4$). Full incompatibility, when no compatible pollen tubes are observed, means the plants being crossed have identical genotypes ($S_1S_2 \times S_1S_2$).

Figure 1.12b - GSI with dominance interaction of S-alleles in the pistil and independent action of S-alleles in the pollen

If S_1 is dominant to S_2 ($S_1 > S_2$) in the pistil, but is codominant with S_2 ($S_1 = S_2$) in the pollen, then S_1S_2 pistils would accept S_2 pollen and SI would break down. In the scenario illustrated in Figure 1.12b, the S_1S_2 plants are semi self-compatible, i.e. compatible with S_2 pollen but incompatible with S_1 pollen. In such a selfed individual, a 1:1 segregation of compatible and incompatible pollen tubes would be observed in the pistil. In GSI, dominance interaction of S-alleles results in self-compatibility and consequently GSI species always exhibit independent action of S alleles and have a heterozygous S-locus.

(Key to figure: S-alleles printed in black represent the S-alleles of the diploid pollen donor i.e. the sporophytic generation; S-alleles printed in red represent those of the haploid gametophytic generation of the pollen and ovule; pollen grains are represented as yellow circles; the pistil is coloured green; ovules are represented as black circles within the ovary. Dominant S-alleles are underlined, e.g. S_1)

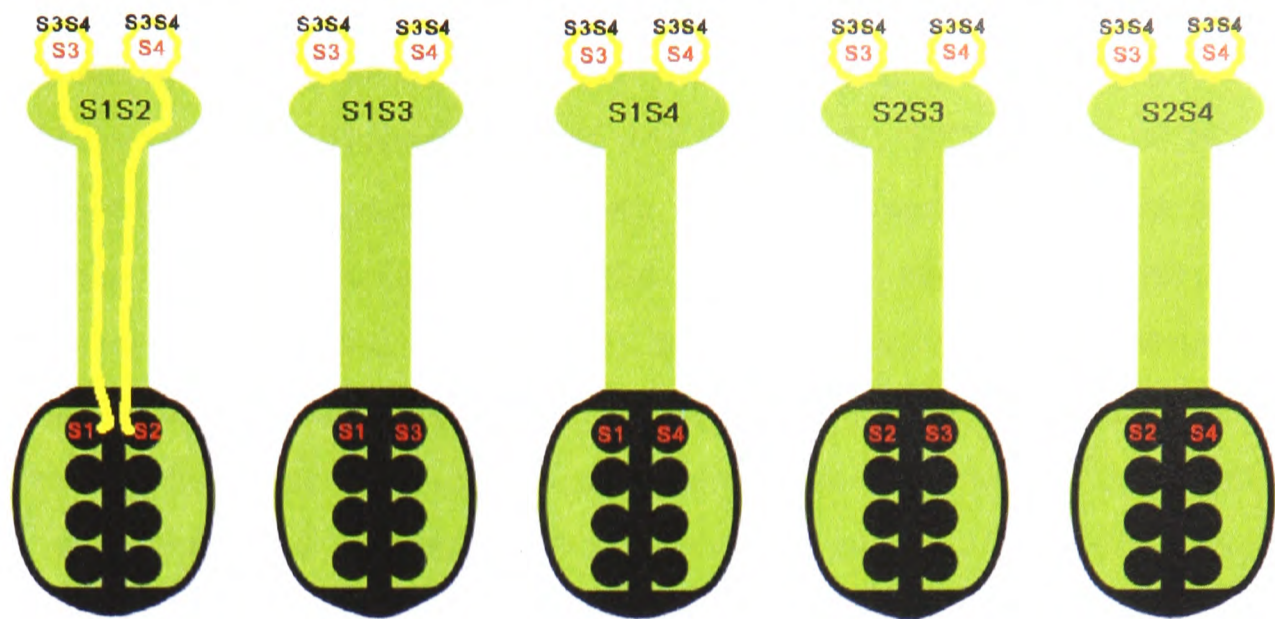


Figure 1.12c - SSI with independent interaction of S-alleles

SSI is determined by the expression of both S-alleles of the diploid pollen donor on the pollen surface. In SSI, pollen from an S_3S_4 plant is fully compatible with an S_1S_2 pistil, but is fully incompatible with any plant with which it shares an S-allele, e.g. S_1S_3 , S_1S_4 , S_2S_3 , S_2S_4 , etc. The single S-allele encoded by the pollen's haploid genome is either not expressed, or is masked by, or incorporated into the expressed genotype of the diploid (sporophytic) pollen donor at the pollen grain surface. SSI individuals having non-matching S-alleles are fully compatible, whereas those that share one S-allele, i.e. $S_1S_2 \times S_1S_3$ or $S_1S_2 \times S_2S_3$ or both S-alleles, i.e. $S_1S_2 \times S_1S_2$ or $S_2S_3 \times S_2S_3$ are fully incompatible, and pollen development in these crosses is arrested on the stigma surface. SSI with independent interaction of S-alleles achieves self-incompatibility, but also promotes cross-incompatibility between individuals that share one S-allele.

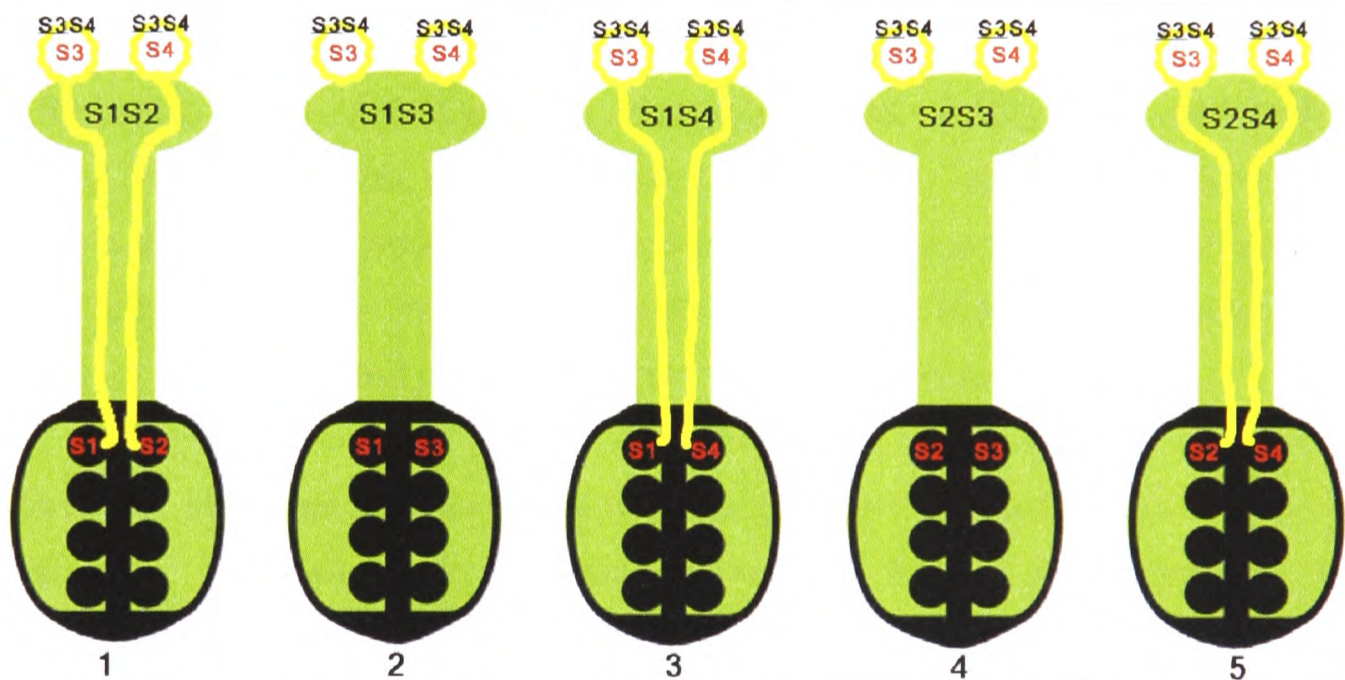


Figure 1.12d - SSI with dominance interaction of S-alleles in the pollen, and independent action in the pistil.

In SSI, if independent interaction of S-alleles occurs in the pistil e.g. $S_x = S_x$, but dominance occurs between S-alleles in the pollen e.g. $\underline{S}_3 > S_4$, then S_3S_4 pollen would be accepted not only by the S_1S_2 pistil, but also by the S_1S_4 pistil and the S_2S_4 pistil, reducing cross-incompatibility by 50%. Also, the presence of dominant S-alleles in either stigma or pollen permits the generation of homozygous S-loci. In Figure 1.12d, \underline{S}_3 is dominant to \underline{S}_4 on the pollen surface and so S_4S_4 genotypes will appear in the progeny of pistil 3 and pistil 5, as S_4 pollen is not rejected at the stigma surface and is able to fertilize S_4 ovules. In SSI, dominance interaction of S-alleles increases cross-compatibility, but also allows the generation of homozygous and heterozygous S-loci.

(Key to Figures 1.12c-d: S-alleles printed in black represent the S-alleles of the sporophytic generation; S-alleles printed in red represent those of the haploid gametophytic generation; pollen grains are represented as yellow circles; the pistil is coloured green; ovules are represented as black circles. Dominant S-alleles are underlined, e.g. \underline{S}_3 on the pollen surface of Fig. 1.12d).

The distinction in the genetic control of the two self-incompatibility systems is accompanied by differences in reproductive morphology and the site and type of the incompatibility reaction (Heslop-Harrison and Shivanna, 1977; Hinata *et al.*, 1993). Mature pollen of GSI species is usually binucleate and the stigma is wet, a consequence of stilar exudates from the transmitting tract (Clarke *et al.*, 1980; Franklin *et al.*, 1995; Mau *et al.*, 1986). In the majority of plants exhibiting GSI, compatible pollination leads to hydration, germination, and penetration of stigma papilla cells with subsequent growth of pollen tubes occurring in the intercellular spaces along the stilar transmitting tract (Newbigin *et al.*, 1993; Richards, 1997). During the growth of compatible pollen tubes, callose cross walls are laid down at regular intervals along the lengths of tubes creating a characteristic ladder-like pattern (Mau *et al.*, 1991; Newbigin *et al.*, 1993; Cheung, 1996). Hydration, germination and the initial growth of incompatible pollen tubes follows the same course as compatible pollinations, until the second pollen mitosis. Thereafter, callose deposition is disrupted, resulting in a disordered pattern of callose (Mau *et al.*, 1991; Newbigin *et al.*, 1993). Eventually, after 7-8 hours of growth, when pollen tubes have reached a third to half way along the style, the tips of pollen tubes swell, thicken with callose, and may burst, and subsequent growth is arrested (Anderson *et al.*, 1986, Mau *et al.*, 1991; Bell, 1995; Richards, 1997). In SSI species, mature pollen is usually trinucleate and the stigma dry (Heslop-Harrison, 1987). Compatible pollination leads to adhesion of the pollen grain to the stigma, followed by hydration and rapid germination of pollen tubes (Heslop-Harrison, 1992b). Incompatible pollen fails to adhere to the stigma and germinate, or germinates but produces a short stunted pollen tube.

Variations in the gametophytic self-incompatibility model are apparent in the Papaveraceae, Poaceae and Oenotheraceae. In these plant families self-incompatibility is gametophytic, but the incompatibility reaction occurs just beneath the stigma (Franklin *et al.* 1995). In Papaveraceae, GSI is under the control of a single S-locus, but the stigma surface is dry and the self-incompatibility response accords more closely with that of sporophytic systems, as it is rapid, occurring before or shortly after germination at the stigma surface. In addition, callose deposition is located in the colpal apertures of pollen grains or the tips of the short, distorted self-pollen tubes within 15-20 minutes of pollen germination (Newbigin *et al.*, 1993). Further variations exist in the GSI model of Poaceae, in that it is under the control of two unlinked S and Z self-incompatibility loci, has a dry stigma surface and pollen that is trinucleate at the time of anther dehiscence (Lundqvist, 1962; Newbigin *et al.*, 1993; Richards, 1997; Franklin-Tong and Franklin, 2003).

The molecular basis of GSI and SSI is also different. Self-rejection in the GSI system exhibited by species of Solanaceae Rosaceae and Scrophulariaceae is brought about by the cytotoxic action of S-RNases degrading ribosomal RNA (rRNA) in the pistil (McClure *et al.*, 1989; Foote *et al.*, 1994; Huang *et al.*, 1994; Murfett, 1996; Xue *et al.*, 1996;), whereas the GSI system of *Papaver rhoeas* of Papaveraceae is dependent on a calcium ion (Ca^{2+}) signalling network (Franklin-Tong *et al.*, 1993; Franklin-Tong and Franklin, 2003). In comparison, the sporophytic SI response is regulated by a cascade of biochemical pathways initiated by autophosphorylation of a serine/threonine S-receptor kinase (SRK) (de Nettancourt, 1977, 1997)

In many angiosperm species, genetic control of homomorphic SI is by a single multiallelic, polymorphic S locus (de Nettancourt, 1977 & 1997; Dickinson, 1990; Hinata *et al.*, 1993; Newbigin *et al.*, 1993; Nasrallah and Nasrallah, 1993; Franklin *et al.*, 1995; Kao and McCubbin, 1996a; 1996b). It is important to recognise however, that these investigations have concentrated on a few, predominantly cultivated species within the Brassicaceae, Solanaceae, Rosaceae, Scrophulariaceae and Papaveraceae (Franklin *et al.*, 1995; Franklin-Tong and Franklin, 2003)). Evidence from the grasses (Poaceae) where self-incompatibility is controlled by the two unlinked multiallelic S and Z loci, with allelic reactions at both S and Z loci being required for incompatibility to take place (Lundqvist, 1962; Østerbye, 1980 *et al.*; Li *et al.*, 1994; Wehling *et al.*, 1995), reports of three or four linked multiple SI-genes in species of Ranunculaceae (Østerbye, 1975; 1977; 1978; 1986; Lundqvist, 1973), *Lilium martagon* (Lundqvist, 1990) and Chenopodiaceae (Murray, 1974, 1979; Larsen, 1977, 1978, 1983; Lewis, 1977), and the S-gene behaviour observed in some Caryophyllaceae and Papaveraceae (Lundqvist, 1994, 1995; Hearn *et al.*, 1996) hint at a variety and sophistication in the genetic control of self-incompatibility that suggests multiple origins of self-incompatibility in plants (Hiscock *et al.*, 2003).

1.5.3- Molecular genetics of gametophytic self-incompatibility

The first S-locus products to be identified in GSI species were the *Nicotiana glauca* S-glycoproteins isolated from stylar extracts of *Nicotiana glauca* (Ornamental tobacco) (Anderson *et al.*, 1986). Pistil specific S-glycoproteins have since been identified in other members of the Solanaceae; *Solanum chacoense* (Xu *et al.*, 1990); *Solanum tuberosum* (Kirch *et al.*, 1989); *Petunia hybrida* (Broothaerts, *et al.*, 1990); *Lycopersicon peruvianum* (Mau *et al.*, 1986) and *Petunia inflata* (Anderson *et al.*, 1986; 1989) as well as in the Rosaceae; *Malus domestica* (Sassa *et al.*, 1994; 1996), *Pyrus pyrifolia* (Ishimizu *et al.*, 1996b; Norioka *et al.*, 1996; Sassa); *Pyrus serotina*

(Sassa *et al.*, 1992; 1993), the Scrophulariaceae; *antirrhinum hispanicum* (Xue *et al.*, 1996; Lai *et al.*, 2002; Zhou *et al.*, 2003; Qiao *et al.*, 2004a) and the Campanulaceae; *Campanula rapunculoides* (Stephenson *et al.*, 2000; Good-Avila *et al.*, 2001). Spatial and temporal localization of S-glycoproteins corresponds with the expression of self-incompatibility in styles (Kao and McCubbin, 1996a; 1996b). In addition, stelar extracts from immature self-compatible stigmas do not possess S-glycoproteins (Anderson *et al.*, 1986). Conclusive evidence that S-glycoproteins are the products of S-alleles was provided by loss of function and gain of function experiments in transgenic *Petunia inflata*, (Lee *et al.*, 1994) and transgenic *Nicotiana glauca* (Murfett *et al.*, 1994). The loss of function experiments created transgenic plants of the *Petunia inflata* S₂S₃ genotype, in which the normal S₃ allele was replaced by an antisense S₃-gene construct (Lee *et al.*, 1994). These S₂S_{3-antisense} transgenic plants produced normal levels of S₂ protein but undetectable amounts of S₃ protein and also rejected S₂ pollen but not S₃. In the gain of function experiment a genomic clone containing the normal S₃-gene of *Petunia inflata* was introduced into S₁S₂ genotypes of *P. inflata*. The S₁S₂ transgenic plants produced S₃ proteins in addition to S₁ and S₂ proteins, and completely rejected S₃ pollen (Lee *et al.*, 1994). Similar results were produced in loss of function experiments with transgenic *Nicotiana glauca* plants (Murfett *et al.*, 1994).

Complementary DNAs (cDNAs) of S-proteins from many solanaceous species have been reported (Ioerger *et al.* 1991; Green, 1994). All S-glycoproteins of solanaceous species so far studied are RNA-degrading enzymes, referred to as S-ribonucleases (S-RNases) (Kao and McCubbin, 1996). S-RNases have 1 to 5 N-linked glycans with characteristic conserved and variable regions in their amino acid sequence, and exhibit between ~18 to ~26% sequence diversity (Anderson *et al.*, 1989; Ai *et al.*, 1990). Five highly conserved regions, termed C-regions, exhibit more than 50% sequence identity and are concerned with the catalytic function of the S-glycoprotein, whereas the two non-conserved regions, termed hypervariable region-a (HVa) and hypervariable region-b (HVb) are thought to control allelic specificity (Anderson *et al.*, 1989; Ioerger *et al.*, 1991; Green, 1994; Kao and McCubbin, 1996; Matton *et al.*, 1997). Although the protein backbone has been identified as the site of S-RNase specificity, the precise location within the amino acid sequence has yet to be determined (Franklin-Tong and Franklin, 2003). Two conserved histidines, one in the C2 region and the other in the C3 region, are required for RNase activity and identify S-RNases as belonging to the T2-RNase family of genes, identified first in *Aspergillus oryzae*; (Kawata *et al.*, 1990; Green, 1994; Huang *et al.*, 1994; Golz *et al.*, 1995; Newbigin, 1996; Sassa *et al.*, 1996; Sato Matton *et al.*, 1997).

In S-RNase-mediated GSI, S-RNases are secreted by the stylar tissue and enter the pollen in a S-haplotype-independent manner, such that both S_1 and S_2 RNases of an S_1S_2 pistil will appear in S_1 pollen tubes and S_2 pollen tubes (Luu, *et al.*, 2000). S-RNase uptake appears to be mediated by stylar proteins, which may form molecular complexes that facilitate the movement of S-RNases into the pollen tube (Luu, *et al.*, 2000; Cruz-Garcia *et al.*, 2003). Inhibition in the growth of pollen tubes is brought about by the cytotoxic action of self-S-RNase, which degrades the RNA of incompatible self-pollen tubes. How non-self S-RNase is prevented from degrading pollen tube RNA is not known precisely, but hypotheses on the specificity of S-RNases activity have been refined since identification of the pollen S-determinant.

Pollen-expressed F-box genes (*SLFs*) were first suspected of being the male determinants of RNase-mediated GSI in Scrophulariaceae (Lai *et al.*, 2002; Zhou *et al.*, 2003) and Rosaceae (Entani *et al.*, 2003; Ushijima, *et al.*, 2003; Qiao *et al.*, 2004a), as they exhibit S-haplotype-specific sequence polymorphism, are linked to the S-locus, and their products, SLFs (for S-locus F-box proteins) interact with S-RNases and are expressed specifically in the pollen (Entani *et al.*, 2003; Ushijima, *et al.*, 2003. Qiao *et al.*, 2004a). *SLF* was conclusively identified as the male determinant of RNase-mediated GSI in the *Petunia inflata* S_2 haplotype (*PiSLF₂*) of Solanaceae (Sijacic *et al.*, 2004), and the *Antirrhinum hispanicum* S_2 haplotype (*AhSLF-S₂*) of Scrophulariaceae (Qiao *et al.*, 2004b). Also *AhSLF-S₂* (*Antirrhinum hispanicum* F-box S_2 protein) has been shown to interact directly with S-RNases (Qiao *et al.*, 2004a). Strong evidence indicates *SLF* to be the pollen S-determinant in *Prunus mume* and *P. avium* of Rosaceae (Entani, *et al.*, 2003; Yamane *et al.*, 2003), and thus *SLF* genes appear to control pollen function in three out of the four plant families known to exhibit RNase-mediated GSI (Entani, *et al.*, 2003; Franklin-Tong and Franklin, 2003; Qiao *et al.*, 2004a; 2004b; Sijacic *et al.*, 2004).

F-box proteins were first identified in yeast and human cells where they were shown to be components of a specific E3 ubiquitin ligase complex known as the Skp1p-Cdc53p-F-box protein complex (SCF complex) (Bai *et al.*, 1996; Skowyra *et al.*, 1997). The E3 ligase complex conjugates with E2 enzymes to bring about the ubiquitination of target proteins via the 26S proteasome (Hershkko and Ciechanover, 1998). The highly conserved F-box motif, located at the N terminus of SLFs, interacts with Skp1 (Gange *et al.*, 2002) and a variable region in the C terminal is expected to bind the target S-RNase protein. One hypothesis suggests that SLFs act as pollen S-determinant of S-

RNAse-mediated GSI by forming an SCF-type complex that targets non-self S-RNases for 26S-proteasome degradation, but leaves self S-RNase intact. The intact self S-RNase then brings about the inhibition of further pollen tube growth by functioning as a cytotoxin that degrades the RNA of self-pollen tubes (Entani *et al.*, 2003; Ushijima *et al.*, 2004). Evidence from fungi proffers a possible mechanism for the selective lack of interaction between SLF and S-RNase proteins of the same S-haplotype. In this hypothesis, non-self SLFs and S-RNases are able to form active heterodimers that trigger ubiquitin-mediated S-RNase protein degradation, whereas self SLFs and S-RNases are in some way inhibited from forming active heterodimers (Entani *et al.*, 2003; Ushijima *et al.*, 2004).

In the simple inhibitor model of S-RNase activity, SLF and S-RNase each contain two functional domains, an S-allele-specific domain that is unique to each S-RNase and SLF haplotype, and a second domain that is a common catalytic domain in S-RNases, but a common S-RNase inhibitor domain in SLFs (Kao and Tsukamoto, 2004). According to this model, the S-allele-specific domain of cognate SLF and S-RNase interact. This S-haplotype-specific binding prevents the interaction of the RNase inhibitor domain and the catalytic domain of the cognate SLF and S-RNase, and locks the S-RNase in an inactive form. In the reaction between non-cognate S-haplotypes, the S-RNase inhibitor domain of SLF and the catalytic domain of S-RNase are able to interact, because their S-allele-specific domains do not match, and S-RNase activity is inhibited, presumably via 26S-proteasome degradation (Gange *et al.*, 2002; Kao and Tsukamoto, 2004). The assumption in the simple inhibitor model is that the interaction between the S-allele-specific domains of SLF and its cognate S-RNase is stronger than the interaction between the S-RNase inhibitor domain of SLF and the catalytic domain of its cognate S-RNase. The modified inhibitor model proposes that SLFs contain only one domain; the S-allele-specific domain and that a general RNase inhibitor is responsible for the inhibition of S-RNases. It also predicts that the active form of SLF is a homotetramer. According to the modified inhibitor model, a general inhibitor binds and inactivates all S-RNases that are not bound to a cognate SLF via their matching S-allele-specific domain (Luu *et al.*, 2001a).

The attraction of modified inhibitor model is that it accommodates the observations of dual-specificity S-RNases, such as the *Solanum chacoense* S_{11/13}-RNase which is a chimer of S₁₁- S₁₃-RNases that rejects both S₁₁ and S₁₃ pollen as well as diploid S₁₁S₁₃ pollen (Luu *et al.*, 2001a). It also accomodates the phenomenum of competative interaction, in which the functioning of pollen SI breaks down when two S-loci of different haplotypes are expressed in the pollen (Kao and Tsukamoto, 2004). For

example, when a pollen grain expresses two different *SLF* genes, as occurs in competitive interaction, their products would form heterotetramers. These heterodtetrameric *SLF* molecules would not bind efficiently with either cognate *S*-RNase, and so the general RNase inhibitor would be free to bind both *S*-RNases resulting in the inhibition of RNase activity of both *S*-RNases in the pollen tube. Pollen tubes expressing two different *S*-alleles are therefore compatible with pistils expressing any *S*-genotype, as they cannot form homotetramers. On the other hand, dual-specificity *S*-RNases such as the *S*_{11/13}-RNase of *Solanum chacoense* would be able to bind the *SLF* homotetramers expressed by *S*₁₁ or *S*₁₂ pollen genotypes and the *SLF* heterotetramers expressed by *S*₁₁*S*₁₃ diploid pollen. Binding of *SLF* and *S*-RNase prohibits the binding of the general RNase inhibitor with the dual-specificity *S*-RNase, and so degradation of pollen tube RNA occurs and pollen tube growth stops (Kao and Tsukamoto, 2004).

The GSI of *Papaver rhoeas* (Papaveraceae) has little in common with *S*-RNase-mediated GSI. In *Papaver* GSI, small (~15kDa) secreted stigmatic *S*-proteins are believed to act as signalling ligands that interact with the allelic product of the pollen *S*-gene assumed to be a receptor located at the pollen plasma membrane (Franklin-Tong *et al.*, 1989; Franklin-Tong and Franklin, 2003). Although several *Papaver* stigmatic *S* proteins have been cloned, the male determinant of *Papaver* SI has yet to be identified (Franklin-Tong and Franklin, 2003) In *Papaver rhoeas* self-incompatibility brings about rapid increases in cytosolic free Ca^{2+} in the shank region of self-incompatible pollen tubes (Franklin-Tong and Franklin, 2003). The increases in cytosolic free Ca^{2+} initiates an intracellular signalling network with several targets, resulting in the rapid inhibition of pollen tube growth (Franklin-Tong and Franklin, 2003). One of these targets is believed to be the pollen actin cytoskeleton, specifically the F-actin bundles, which are crucial for the delivery of secretory vesicles to the growing apex of the pollen tube. SI in *Papaver rhoeas* has been shown to trigger rapid and large-scale depolymerisation of actin bundles possibly via SI-stimulated increases in cytosolic free Ca^{2+} , with F-actin depolymerisation possibly also stimulating cell apoptosis and programmed cell death (PCD) (Thomas and Franklin-Tong 2004). Another target of *Papaver* SI is a phosphorylated inorganic pyrophosphatase, p26, whose pyrophosphatase activity is reduced in conditions of high cytosolic free Ca^{2+} . Pyrophosphatase are important for the generation of ATP and polymers required in the making of new membranes and cell walls. The down regulation of p26 by SI-induced increases in high cytosolic free Ca^{2+} , could result in a depletion of long-chain carbohydrates and proteins needed to sustain pollen tube growth (Franklin-Tong and Franklin, 2003). Further work in other species of Papaveraceae and other GSI species will broaden understanding of mechanisms for

achieving self-incompatibility in plants. However S-RNase-mediated GSI, Papaver GSI, and the different forms of SSI that are becoming apparent in Brassicaceae, Asteraceae and Caryophyllaceae indicate multiple origins of self-incompatibility in plants

1.5.4- Sporophytic self-incompatibility: the *Brassica* model

Sporophytic self-incompatibility (SSI) is known to occur in 6 plant families: Asteraceae, Betulaceae (Corylaceae), Brassicaceae, Caryophyllaceae, Convolvulaceae, and Polemoniaceae, and has been reported also in Passifloraceae, Malvaceae and Sterculiaceae (Hiscock and McInnis, 2003; Hiscock and Tabah, 2003; Table 1.3). It was first observed in *Raphanus sativus* (Stout 1920) but has been studied extensively in *Brassica oleracea* (Roberts and Dickinson 1981; Nasrallah *et al.*, 1985a, 1985b, 1987, 1988; Chen and Nasrallah 1990; Stein *et al.*, 1991; Boyes *et al.*, 1991; Boyes and Nasrallah 1993, 1995; Delorme *et al.* 1995; Stephenson *et al.*, 1997; Kusaba and Nishio 1999; Kusaba *et al.*, 1997), *Brassica rapa* (syn. *campestris*) (Hinata and Nishio 1978; Isogai *et al.*, 1987; 1988; Takayama *et al.*, 1989; Nou *et al.*, 1991; Kusaba and Nishio 1999;), *Brassica napus* (allotetraploid: *B. oleracea* x *B. rapa*) (Goring and Rothstein, 1992; Goring *et al.*, 1992a; 1992b; 1993; Hiscock *et al.*, 1995a) and to a lesser extent in *Raphanus sativus* (Lewis, 1988; Okazaki and Hinata, 1984; Sakamoto *et al.*, 1998), *Raphanus raphanistrum* (Sampson, 1967) and *Arabidopsis lyrata* (Schierup *et al.*, 2001; Mable *et al.*, 2003). Identification of SSI in Asteraceae (Little *et al.*, 1940; Gerstel, 1950; Gerstel and Riner, 1950; Crowe, 1954; Howlett *et al.*, 1975; Brennan, *et al.*, 2002; Hiscock, 2000a; 2000a; Hiscock *et al.*, 2003), Convolvulaceae (Kowyama *et al.*, 1980, 1994; 1995) and Caryophyllaceae (Lundqvist, 1979, 1990, 1994, 1995) has broadened research into sporophytic self-incompatibility, however the *Brassica* model remains the paradigm for sporophytic systems, and forms the basis of the foregoing discussion.

In *Brassica*, the sporophytic incompatibility reaction occurs at the stigma surface, after recognition of self phenotype (Heslop-Harrison *et al.*, 1975). The pellicle is specific to papillae of dry stigmas and consists of hydrated proteins produced by secretions of papillar cells during stigma maturation (Heslop-Harrison, 1975). The pellicle may play a role in the adhesion of the pollen grain to the stigma and, due to its proteinaceous nature, is proposed as the site of pollen recognition (Heslop-Harrison *et al.*, 1975; Stead *et al.*, 1979, 1980). Pollen of SSI species is characteristically trinucleate at maturation and possesses a pollen tryphine coat that contains molecules important for the pollen-stigma interaction (Heslop-Harrison *et al.*, 1973). The pollen genotype is

haploid, but due to deposition of tapetal remains onto the surface of the developing pollen grain, the genetic control of the phenotype is diploid and carries both S-allele specificities of the sporophytic pollen donor plant (Heslop-Harrison, 1975; Stephenson *et al.*, 1998). In contrast, non-tapetal constituents of the pollen are gametophytically determined, with some evidence suggesting that the gametophyte also contributes to the SI phenotype through the mixing of pollen-derived S-allele products in the locular fluid during microsporogenesis (Heslop-Harrison *et al.*, 1973). Thus SSI is an essentially diploid-diploid recognition system in contrast to the haploid-diploid recognition system of GSI (Mather, 1944). Recognition of compatible pollen leads to the extrusion and adhesion of the pollen-coat onto the pellicle at the apical and sub-apical region of the stigma papillae (Dickinson, 1995; Heslop-Harrison *et al.*, 1975; Nasrallah and Nasrallah, 1989; Stead *et al.* 1980). Enhanced esterase activity at the stigma surface accompanies the binding of the pollen to the stigma and subsequent hydration of the pollen grain is achieved by absorption of water from the stigma (Heslop-Harrison and Heslop-Harrison, 1975b; Sarker *et al.*, 1988). These events are rapid, occurring 10-15 minutes after pollen-stigma contact (Dickinson and Lewis, 1973a, 1973b; Elleman and Dickinson, 1994; Kandasamy *et al.*, 1993). Germination is followed by penetration by pollen tubes of the pellicle-cuticle layer, followed by basipetal growth within the papillar cell wall (Dickinson and Lewis, 1973a, 1973b; Ellemen *et al.*, 1988, 1992). Tubes enter the stigma via the middle lamella at the base of the stigma papillae and proceed to the ovary through the intercellular spaces of the stylar transmitting tissue (Ellemen *et al.*, 1992). Incompatible pollen either fails to hydrate or germinates to produce short stunted pollen tubes that may pierce the cuticle but do not penetrate the subcuticular pectin-cellulose wall layer (Kanno and Hinata, 1969). Inhibition of self-pollen is rapid, occurring within 45-60 minutes of pollination, and is accompanied by depositions of callose in the tips of pollen tubes and in stigma papillae at the pollen-stigma interface (Cabrillac *et al.* 2001; Dickinson, 1995; Heslop-Harrison *et al.*, 1975).

In SSI systems that exhibit independent action of S-alleles, as in the Caryophyllaceae, rejection occurs when one or both of the S-alleles in the pollen phenotype match either of the S-alleles in the phenotype of the pistil (Franklin *et al.*, 1992, 1995). However, in species of *Brassica*, dominance interactions may occur between S-alleles in the pollen and the stigma, and have the effect of reducing cross incompatibility (Thompson and Taylor, 1966a; Stevens and Kay, 1989). Dominance relationships between *Brassica* S-alleles are complex, non-linear, and different in pollen and stigma (Figure 1.13). In *Brassica*, co-dominance of S-alleles commonly occurs in the stigmas, with dominance

relationships being more prevalent in pollen than stigma (Figure 1.13; Kemp and Doughty, 2003). S-alleles in Asteraceae and Convolvulaceae also exhibit non-linear dominance relationships, with dominance interactions of pollen S-alleles being different to those in the stigma (Kowiyama *et al* 1994; Little *et al.* 1940; Hiscock, 2000a; 2000b; Figure 1.13). In *Senecio squalidus* almost 90% of S-alleles in a particular population expressed dominant relationships, with fewer than 3% of S-alleles exhibiting codominant interactions (Brennan *et al.* 2002). Interestingly, all S-alleles so far identified in the one-locus S-gene sporophytic system in *Cerastium arvensae* in the Caryophyllaceae, exhibit only codominance (Lewis, 1994). The 25 S-alleles identified in *Corylus avellana* (Corylaceae) reflect the situation observed in *Brassica*, as these S-alleles exhibit codominance in the pistil, but codominance and dominance interactions in the pollen. However in contrast to *Brassica*, dominant S-alleles in *C. avellana*, exhibit a linear hierarchy of increasing dominance, consisting of 8 levels of S-allele dominance. Level 1, identified as S-1, contains the most recessive S-alleles and level S-8 the most dominant, such that S-1 [S₄], < S-2 [S₂₃] ,< S-3 [S₉, S₁₁, S₂₂, S₂₆], < S-4 [S₁₉], < S-5 [S₂, S₂₅], < S-6 [S₁, S₅, S₇, S₁₀, S₁₂, S₁₄, S₁₅, S₁₆, S₁₇, S₁₈, S₂₀, S₂₁, S₂₄], < S-7 [S₆], < S-8 [S₃, S₈] (where <, means recessive to, S, indicates recessive alleles, and S-alleles at the same S-level are codominant) (Mehlenbacher and Thompson 1988; Mehlenbacher, 1997). Interestingly, in *C. avellana* the majority of dominant S-alleles are codominant to each other, whereas there is significant hierarchy between recessive alleles (Mehlenbacher, 1997). In *Brassica*, the molecular control of dominance has been shown to be different in stigma and pollen. Among S receptor kinase (*SRK*) alleles, the female component of *Brassica* and *Arabidopsis* SI, see below), no differences were observed between stigma transcript expression patterns of dominant and recessive alleles in heterozygotes, or when *SRK*-alleles are combined in co-dominant combinations. Dominance relationships in the stigma are not therefore, a consequence of differential rates of transcription, and must be determined post transcriptionally by modification of the activity, or level of the *SRK* protein (Hatakeyama *et al.*, 2001), or S antisense RNA silencing (Ansaldi *et al.*, 2000; Terryn and Rouzé, 2000). In contrast, dominance relationships between the S-locus cysteine rich (*SCR*) alleles, pollen-expressed determinant of SI in *Brassica* and *Arabidopsis lyrata*, are controlled at the level of transcription, with the presence of dominant *SCR* alleles inhibiting transcription of recessive *SCR* alleles (Shiba *et al.*, 2002; Kakizaki, *et al.*, 2003).

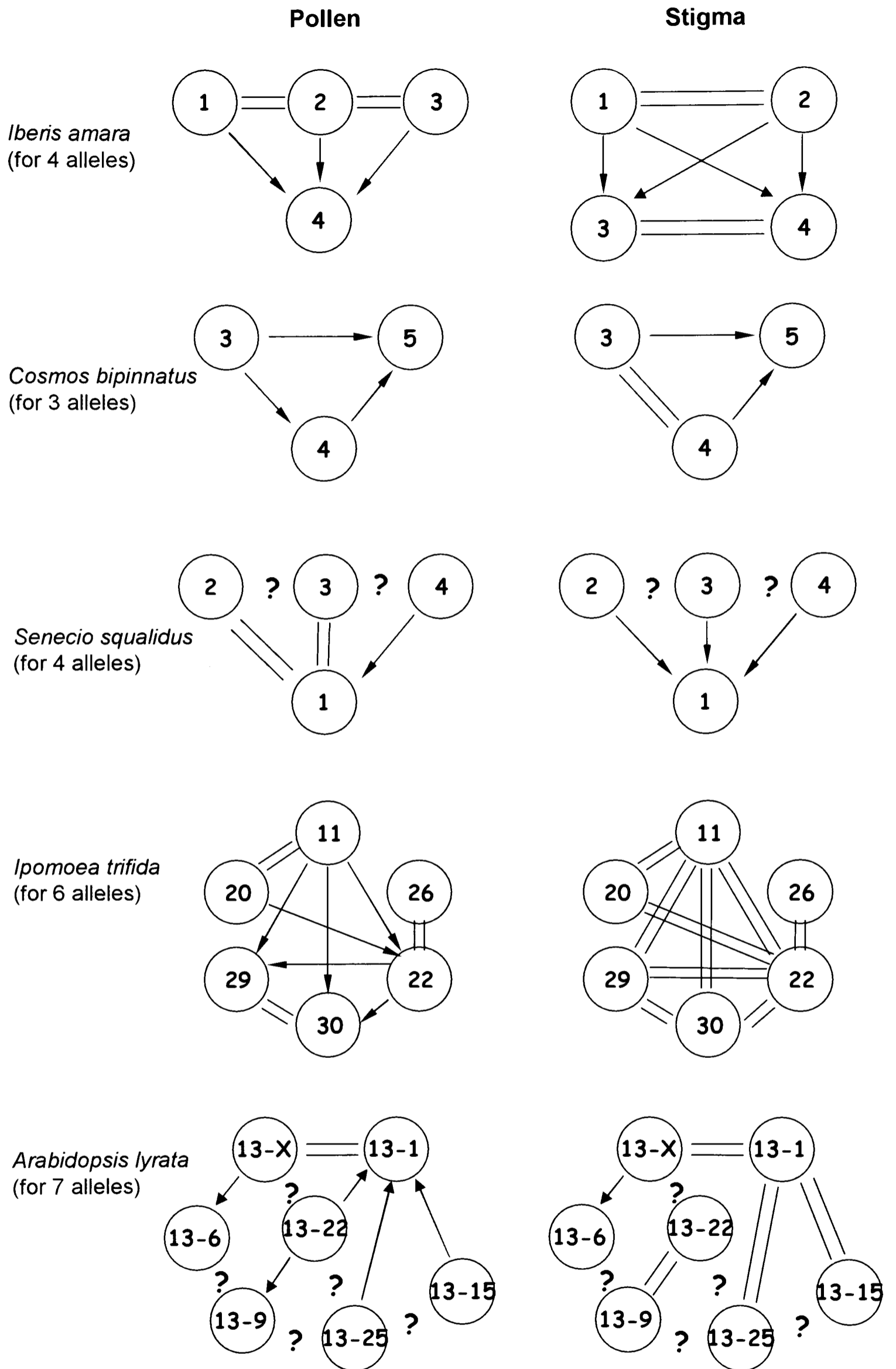


Figure 1.13 Dominance interactions of some S-alleles in the pollen and stigma of *Iberis amara* (Bateman 1954), *Cosmos bipinnatus* (Little, et al. 1940), *Ipomoea trifida* (Kowiyama et al., 1994; 2000); *Arabidopsis lyrata* (Mable et al., 2003) and *Senecio squalidus* (Hiscock, 2000b)
Key: \longrightarrow , dominant; \equiv , codominant.; ?, dominance relationship undefined.

1.5.5- Identifying SSI in plants

Patterns of incompatible and compatible groups in diallel crosses between progeny of controlled pollinations are used to identify gametophytic and sporophytic incompatibility systems (Mackay, 1977). In the gametophytic system, which always exhibits independent action of S-alleles in pollen and stigma, cross pollinated individuals that share one S-allele e.g. $S_1S_2 \times S_1S_3$, and those that do not i.e. $S_1S_1 \times S_2S_2$ are both compatible. However, at the light microscope level, these two cross-pollinations can be distinguished by a differential growth of pollen tubes in the pistil. Pollinations between individuals with one shared allele germinate 50% incompatible pollen tubes, i.e. from S_1 pollen, and 50% compatible pollen tubes, i.e. from S_3 pollen (or S_2 pollen in the reciprocal $S_1S_3 \times S_1S_2$ cross), revealing the semi-compatibility of parental genotypes. By contrast pollinations between $S_1S_1 \times S_2S_2$ individuals germinate 100% compatible pollen tubes. Thus in GSI, a 1:1 segregation of compatible and incompatible pollen tubes in a pistil identifies semi-compatibility, and indicates that the participants in the cross share an S-allele.

In the sporophytic system, the cross $S_1S_2 \times S_1S_3$ may produce many different compatibility patterns, with reciprocal differences in compatibility being characteristic of SSI. These reciprocal differences are a consequence of the complex dominance and codominance relationships that exist between S-alleles in pollen and pistil (Lewis, 1994). In the above example if S_2 and S_3 were dominant to S_1 in the pollen, but codominant to S_1 in the stigma, then the cross $S_1S_2 \times S_1S_3$ would result in 100% reciprocal compatibility. However, if S_1 , S_2 and S_3 were codominant in pollen and stigma then $S_1S_2 \times S_1S_3$ would exhibit 100% reciprocal incompatibility. The same cross would produce reciprocal differences, if in the pollen S_2 were dominant to S_1 but codominant with S_3 , and all S-alleles were codominant in the stigma. Dominance interactions of S-alleles mean it is not always possible to discern, without prior knowledge of S-allele specificities, whether participants in a cross share an S-allele. Furthermore, some sporophytic systems contain a gametophytic genetic component which appears to be responsible for the 5-35% of exceptional crossing results observed regularly in the sporophytic systems of the Brassicaceae; [*Brassica campestris* (Zuberi and Lewis, 1988), *Raphanus sativus* (Lewis *et al.*, 1988), *Sinapis arvensis* (Ford and Kay, 1985)], Caryophyllaceae; [*Cerastium arvensis*, *stellaria holostea* (Lunqvist, 1990, 1994, 1995)] and Asteraceae [*Crepis foetida* (Hughes and Babcock, 1950), *Parthenium argentum* (Gerstel, 1950) *Cosmos bipinnatus* (Crowe, 1954) and *Senecio squalidus* (Hiscock, 2000a, 2000b; Brennan *et al.*, 2002)]. These

exceptional crossing results are observed most often as compatible (+), or semi-compatible (\pm) reactions within groups predicted to be 100% cross-incompatible (Lewis, 1994; Hiscock, 2000b). A second gametophytic 'G'-gene has been invoked to explain these exceptional crossing results, and a new paradigm of incompatibility, the gametophytic-sporophytic (G-S) incompatibility system, has emerged (Lewis *et al.*, 1988; Zuberi and Lewis, 1988). In species of Brassicaceae, G is diallelic, and linked loosely to the S locus (Lewis, 1994; Hiscock, 2000b) and G and S genes are complementary, so that incompatibility within the G-S system is achieved only when G and S-alleles are matched in pollen and stigma. Compatible unmatched combinations of S preclude the expression of matched G genotypes, and vice versa (Lewis, 1994, Table 1.4). To further complicate the compatibility reactions of the G-S system, the G genotype is expressed in some S-matched genotypes, but not others, with expression of G in *Brassica rapa* (syn. *campestris*) and *Raphanus sativus* confined predominantly to those S-alleles high in the dominance series (Lewis, 1994). According to Lewis (1994), a cryptic gametophytic system is indicated whenever compatible and incompatible pollen grains are found on cross-pollinated stigmas of SSI species, including crosses between different plants of the same S genotype, but are completely absent in self pollinations (Lewis, 1994). In Asteraceae species, the presence of a gametophytic system is observed on stigmas as a clear segregation of compatible (+) empty pollen grains with long tubes, and incompatible (-) ungerminated pollen grains, and may additionally include the presence of P-type incompatible pollen tubes (Table 1.4, see below) (Lewis, 1994).

Table 1.4 – Comparison of the genotype and phenotype of the G-S incompatibility reaction in Brassicaceae and Asteraceae

Incompatibility genes		Incompatibility reaction		
S	G	Brassicaceae	Asteraceae	
M	M	-	-	
M	UM	+	+	or P
UM	M	+	+	or P
UM	UM	+	+	or P

Table 1.4 Amended version of Table 1 from Lewis, 1994.

Key: M, matched; UM, unmatched; -, full inhibition of pollen at surface of stigma papilla; +, no inhibition of pollen or pollen tube; P, P-type pollen tubes that penetrate stigma papillae at their bases, but are inhibited in the cellular tissue of the pistil

1.5.6 – SSI molecules in *Brassica*: structure and function

In *Brassica*, SI is controlled by the combined action of two genes located at the S locus (for sterility locus) (Luu *et al.*, 2001b). The two SI genes, SRK (for S-receptor kinase)

and ⁵*SCR* (for S-locus cysteine-rich protein, also known as SP11 (for S locus protein 11) determine the SI response in the stigma and pollen respectively (Schopfer *et al.*, 1999; Takasaki *et al.* 1999, 2000; Takayama *et al.*, 2000a, 2000b; Kachroo *et al.* 2001, 2002; Shiba *et al.*, 2001; Nasrallah *et al.* 2002). A third S-locus linked gene, *SLG* (for S-locus glycoprotein) enhances the activity or stability of *SRK* but is not essential to the SI response in *Brassica* (Luu *et al.* 1999; Suzuki *et al.* 1999; Nasrallah *et al.* 2002). These three genes co-segregate with self-incompatible phenotypes and the expression of *SLG* and *SRK* in stigma papillae corresponds with the onset of self-incompatibility (Nasrallah *et al.*, 1985b; Kandasamy *et al.*, 1990; Boyes and Nasrallah, 1993; Delorme *et al.*, 1995; Stein *et al.*, 1996; Schopfer *et al.*, 1999; Nasrallah *et al.* 2002). *SLG* is the smaller of the two stigma S genes (1.3 kb). It is an intronless gene that encodes a ~57-kDa secreted glycoprotein of ~435 amino acids localised to the stigma-papillar cell wall (Nasrallah *et al.*, 1985a, 1987, 1988; Kandasamy *et al.* 1989; Trick and Flavell, 1989; Goring *et al.*, 1992a, 1992b). *SRK*, the female determinant of SI, is 3.0 kb in length and consists of 7 exons (Figure 1.14). *SRK* encodes a serine/threonine receptor protein kinase of ~857 amino acids (~120 kDa), composed of three domains; an extracellular receptor domain that shares a high level of sequence identity with *SLG*, a transmembrane (TM) domain, and a cytoplasmic catalytic domain that has serine/threonine protein-kinase activity (Nasrallah *et al.* 1987, 1991; Stein *et al.* 1991; Goring and Rothstein 1992; Kusaba *et al.* 1997). In *Brassica*, *SLG* and *SRK* are separated by 20-80 kilobases and behave as a unified component forming an S-locus gene complex (Figure 3.2). As a result of this unification, *Brassica* *SLG* and *SRK* alleles are referred to as S haplotypes (Boyes and Nasrallah, 1993; Nasrallah and Nasrallah 1993). However, since the identification of the male determinants of SSI and S-RNase-mediated GSI, the term haplotype is now used to describe the variants of the S-locus in terms of these male and female determinants, and the term allele is used to describe variants of an S-locus gene (Kao and Tsukamoto, 2004). *SLG* and the *SRK* S domain of corresponding haplotypes share between 75-99% sequence identity (Hiscock *et al.*, 2003)

On the basis of sequence homology, *SLG* genes can be divided into two categories: class-I genes and class-II genes (Kusaba *et al.*, 1997; Nasrallah *et al.*, 1991;

⁵ *SCR*, the male determinant of SI in *Brassicaceae* was isolated and identified in the *Brassica oleracea* S₆ and S₁₃ haplotypes by Schopfer *et al.* (1999). *SP11* the male determinant of SI was isolated from *Brassica rapa* (syn *campestris*) S₂₈ haplotype by Takasaki *et al.* (2000). *SCR* and *SP11* identify the same molecule. *SCR* is used to identify *Brassica* male SI gene in this research

Thompson and Taylor 1966b). Class-II genes are always recessive to class-I genes in the pollen, with class-I genes exhibiting a strong SI response on the stigma surface producing an average of 0 to <10 pollen tubes per self-pollinated stigma while, class-II SLGs exhibit a weakened SI response with 10-30 pollen tubes developing per self-pollinated stigma (Nasrallah and Nasrallah, 1993). Class-I *Brassica* SLGs are intronless, but class-II SLGs have an intron near the 3' end (Tanitkajana *et al.*, 1993; Hatakeyama *et al.*, 1998). Within class-I SLGs and class-II SLGs there is 80-98% nucleotide sequence conservation. However, sequence conservation between class-I and class-II S genes drops to ~65%, with the characteristic class-I conserved nucleotide region at the 3' terminus, being absent in class-II genes, (Nasrallah *et al.*, 1991; Dickinson, *et al.*, 1992; Hinata *et al.*, 1995; Kusaba *et al.*, 1997;). This 3'-terminus conserved region can be distinguished at the protein level by binding of a class I-specific monoclonal antibody raised against *Brassica oleracea* SLG₆ glycoprotein (the glycoprotein produced by the *Brassica oleracea* S₆ haplotype). This class-I specific antibody has since identified two distinct classes of SLG genes in *Raphanus sativus* and *Brassica rapa* (Nasrallah and Nasrallah 1993; Nasrallah *et al.*, 1991; Sakamoto *et al.*, 1998). Class-II SLGs in *Brassica oleracea* are represented by the S₂, S₅, and S₁₅ haplotypes (Kemp and Doughty, 2003); in *B. rapa* (*syn. campestris*) by S₂₉, S₄₀, S₄₄ and S₆₀ haplotypes (Nishio *et al.* 1996; Hatakeyama *et al.*, 1998; Shiba *et al.* 2002) and by S₉, S₁₀, S₁₁, S₁₃ and S₁₆ alleles in *Raphanus sativus* (Sakamoto, *et al.* 1998).

A fourth *Brassica* S gene, the S-locus related 1 gene (*SLR1*) is also expressed in the *Brassica* stigma at the onset of anthesis (Lalonde *et al.* 1989), however, since *SLR1* is not linked to the S-locus it cannot be involved in SI directly and is thought to have a possibly role in adhesion of the pollen to the *Brassica* stigma (Luu *et al.* 1997).

The *SCR* gene contains two exons of 110 bp and 300 bp separated by a large intron region of between 0.75-4.1 kb (Nasrallah *et al.* 2002). *SCR* encodes a cysteine-rich primary protein of 74-77 amino acids with the first 24-26 residues constituting the hydrophobic signal sequence. The mature secreted SCR protein is a small (6-8 kDa) basic (isoelectric point [pI] = 8.1-8.4) highly polymorphic polypeptide that exhibits conservation in only 11 out of ~50 amino acids. Eight of these conserved residues are cysteines involved in intramolecular disulphide bonds (Takayama *et al.*, 2001) *SCR* is expressed gametophytically in the microspores and also sporophytically in the cells of the tapetum (Schopfer *et al.* 1999). Exclusive expression of *SCR* in tapetal tissue is

characteristic of class-II *Brassica* haplotypes, whereas class-I haplotypes express SCR in the gametophyte and tapetal tissue (Shiba *et al.*, 2002; Takayama *et al.*, 2000b). In the mature pollen grain, SCR is located on the surface of the pollen grain in the highly lipidic pollen coat and is known to bind SRK (Stephenson, *et al.*, 1997; Kachroo *et al.*, 2001; Takayama *et al.*, 2001). SCR belongs to a family of small basic cysteine-rich pollen coat proteins (PCPs) known as the PCP A class family which, with the exception of SCR, interact with SLG (Hiscock *et al.*, 1995b; Stanchev *et al.*, 1996; Doughty *et al.*, 1998; 2000). The *Brassica* S-locus spans ~15-500 kb and may contain as many as 17 genes (Hiscock and McInnes, 2003). However, the self-incompatibility components of the S-locus constitute a tightly linked genetic unit encompassing *SRK*, *SCR* and *SLG* and 9 other S-locus linked genes (Suzuki *et al.*, 2000; Nasrallah *et al.* 2002; Figure 1.14)

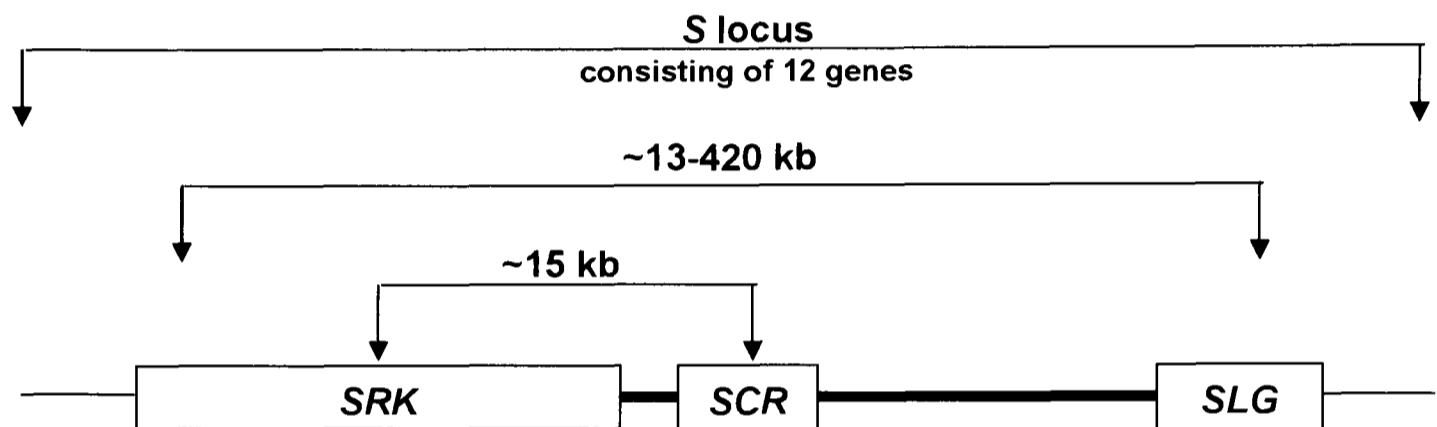


Figure 1.14 Schematic representation of the SI component, SRK, SCR and SLG, of the S locus.

The S-locus contains 12 genes including *SRK*, *SCR*, *SLG*; *SLA* (S-locus anther); *SLL1* (S-locus linked gene1), *SLL2*, *SAE1* (S-locus anther expressed gene 1); *SP4* (S-locus protein 4) and *SP7*. Polymorphism at the S-locus is evidenced by the variation in the order of S-locus genes and in the recorded distances between *SLG* and *SRK* in different *Brassica* haplotypes; e.g. ~13 kb in Bra-S⁹; ~20 kb in Bra-S⁸; ~25 kb in Bna-S⁹¹⁰; ~55 kb in Bol-S¹³; ~130 kb in Bol-S¹⁸; ~170 kb in Bol-S³; ~230 kb in Bol-S¹⁴; ~266 kb in Bol-S²; ~330 kb in Bol-S⁶; ~380 kb in Bol-S²⁰ and ~420 kb in Bol-S¹⁶. The *B. rapa* S-locus is smaller and less variable than the *B. oleracea* S-locus with several large genomic fragments being inserted into the *B. oleracea* S locus since differentiation of *Brassica* S-alleles. (Fig. 1.13 compiled from data in Boyes and Nasrallah, 1993; Nasrallah and Nasrallah 1993; Schierup *et al.*, 1997; Schopfer *et al.* 1999; Suzuki *et al.*, 2000a; Watanabe *et al.*, 2000; Nasrallah *et al.* 2002). **Key:** Bol = *Brassica oleracea*; Bra = *B. rapa*, Bna = *B. napus*)

1.5.7 - *Brassica* S-receptor kinase (SRK) and the SRK S domain

The S receptor kinase gene (*SRK*) was first mapped to the S locus in stigmas of *Brassica oleracea* and *Brassica rapa* (*syn. campestris*) (Sato, *et al.*, 1991; Stein *et al.*, 1991; Goring and Rothstein, 1992). The *SRK* gene consists of seven exons and six introns, with exons being arranged into distinct functional domains (Nasrallah and Nasrallah, 1993). Exon 1 of *SRK* encodes an extracellular glycosylated protein composed of 438 amino-acid residues (Stein *et al.*, 1991). It is known as the S-domain, or more accurately as the SLG-like domain, as it expresses a polypeptide of

406 residues (1-406) that shares between ~75-99% sequence homology with corresponding SLG proteins (Nasrallah and Nasrallah 1993; Stein *et al.*, 1991; Suzuki *et al.*, 1997). The S-domain is preceded by a hydrophobic putative signal sequence (-32 to -1) that has ~70% sequence homology to signal sequences of corresponding SLGs (Stein *et al.*, 1991).

Features characteristic of all S-domains are the PTDT-box within the conserved sequence WQSFDXPTDTΦL (where X represents a non-conserved amino acid; and Φ represents an aliphatic amino acid, i.e. G, A, V, L and I) located at residues 116-132 [*~146–162*]⁶, two conserved potential N-glycosylation sites at residues ~88-90 [*~130-132*] and ~357 [*~389*], and 12 positionally-conserved cysteine residues, CX₅-CX₅-CX₇-CX-CX₂₀-CX₇-CX₂₉-CX₃-CX₃-CX-CX₁₄-C (where X = any amino acid) – the Cys domain - at residues ~260-390 [*~290-400*] (Stein *et al.*, 1991; Nasrallah and Nasrallah, 1993; Torii and Clark, 2000). Variations in the pattern of the Cys domain are generally associated with the spacing between the 5th and 6th, and between the 7th and 8th cysteine residues. For example, in SLR2 (for S locus related 2) sequences and *Brassica oleracea* SLG14, the 7th cysteine is replaced by glycine resulting in a Cys domain containing 11 cysteine residues, while in plant receptor kinases SFR3, ZmPK1 and OsPK10 the distance from the 5th to 6th cysteines is 13, 15 and 17 residues respectively, and cysteines 7 and 8 are separated by 33 residues instead of the 29 or 30 residues characteristic of SLG/SRK and SLR1 S domains respectively (Figure 1.15) (Walker and Zang, 1990; Pastuglia *et al.* 1997a; 1997b; 2002). A diagnostic feature of SLR1 (for S locus related 1) sequences is the presence of 30 residues (instead of 29) between cysteines 7 to 8 (Lalonde *et al.*, 1989).

Aside from the characteristic features of S-domains, considerable sequence divergence exists between S-domain containing S proteins. For example, the S-domains of *Brassica* SRKs, are 60% identical to the S-domain of ARK1 of *Arabidopsis thaliana* but only 23% identical to ZmPK1 S-domain of *Zea mays*; whereas S-domains of RLK1 (for Receptor-Like Kinase 1) and RLK4 RLK1 (for Receptor-Like Kinase 4) of *Arabidopsis thaliana* show only 25% sequence identity with *Brassica* SRK S-domains

⁶ Italicised numbers inside square brackets e.g. [*206-417*] denote the residue number of a primary protein sequence. In S-domain primary proteins the first ~30 residues constitute the signal sequence which does not appear in the mature protein sequence. In general, primary protein sequences are used throughout the thesis. Whenever a mature protein sequence is discussed, both numbering systems are cited with the residue number for the mature protein written first followed by the residue number for the primary protein written in *italics* and enclosed by square brackets

and 22% identity with ZmPK1 (Walker 1994). This sequence divergence and the differences in gene expression of S-domain RLKs probably reflect the different roles these putative receptors play in cellular signalling (Walker 1994). Since the majority of S-domain RLKs are expressed in vegetative tissue and a few in vegetative and reproductive tissue, it is clear that S-domain RLKs so far identified in families outside the Brassicaceae have functions unrelated to self-incompatibility (Table 1.5) (Hiscock and McInnis, 2003). SRK and IRK1 are exceptional S-proteins, as they are the only S-domain RLKs expressed solely in reproductive tissue (Table 1.5).

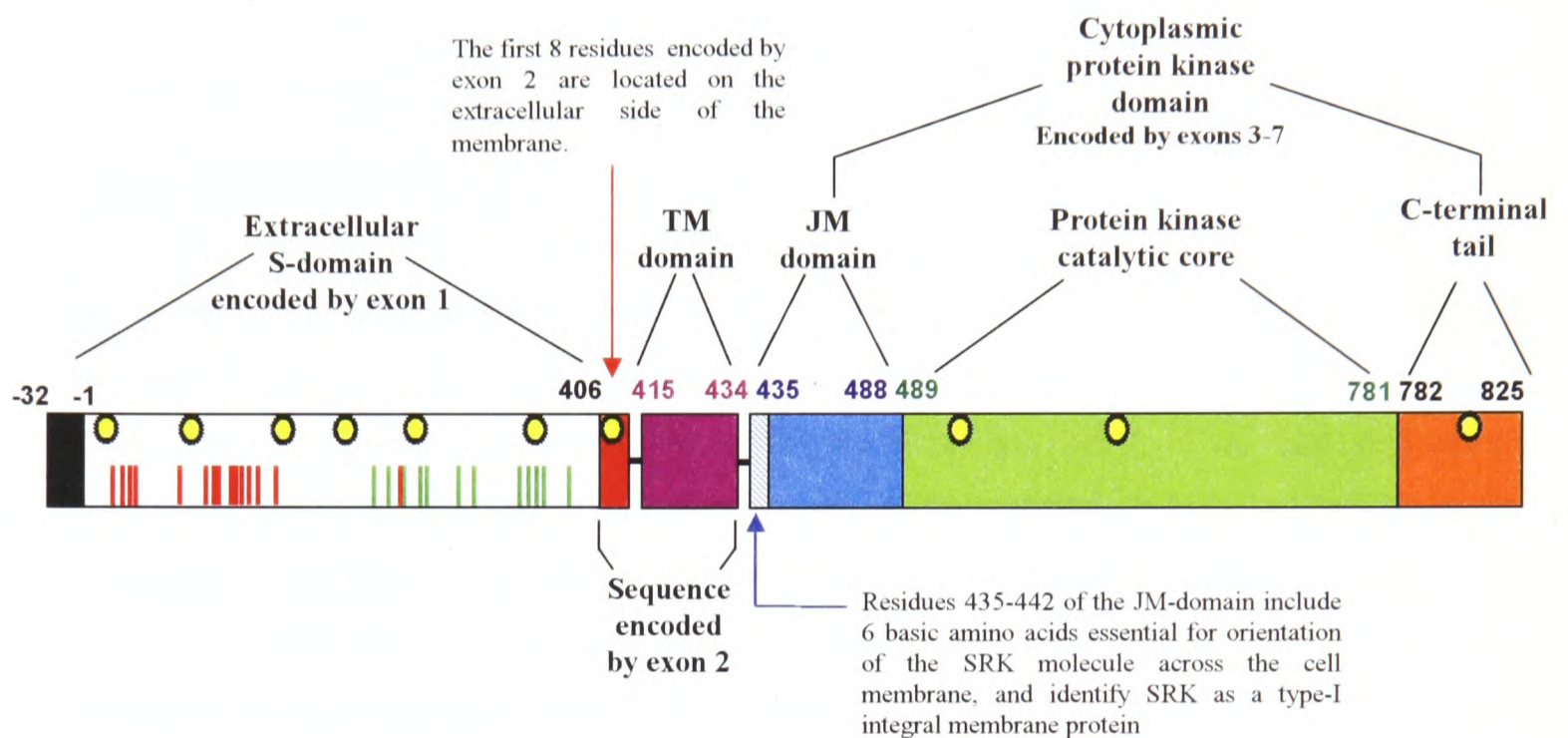


Figure 1.15 Generalised structure of *Brassica oleracea* SRK6.

The SRK S-domain is encoded for by exon 1. Exon 2 encodes 8 extracellular residues and the transmembrane (TM) domain, while exons 3-7 encode the cytoplasmic protein kinase domain and includes the juxtamembrane (JM) domain. Horizontal bars in the figure separate the extracellular, transmembrane and cytoplasmic domains. The black box represents the signal sequence. The 12 conserved cysteine residues of the Cys-domain, represented as green bars, are situated at (Cys 1) **267 [299]**; (Cys 2) **273 [305]**; (Cys 3) **279 [311]**; (Cys 4) **287 [319]**; (Cys 5) **289 [321]**; (Cys 6) **310 [342]**; (Cys 7) **318 [350]**; (Cys 8) **348 [380]**; (Cys 9) **352 [384]**; (Cys 10) **356 [388]**; (Cys 11) **358 [390]**; (Cys 12) **373 [405]**. (Numbers in square brackets represent the position of cysteine residues in the primary protein calculated from the first methionine residue. The un-bracketed numbers indicate the cysteine position in the mature protein). Cysteine residues are spaced according to the pattern CX₅-CX₅-CX₇-CX-CX_n-CX₇-CX_n-CX₃-CX₃-CX-CX₁₄-C (where X = any amino acid, and n represents various numbers). The 15 conserved S-domain residues are represented by red bars at residues: **20, 25, (28-29), 85, 123, (125 – 126), (129 – 133), 163 and 274**. *B. oleracea* SRK6 has 10 potential N-linked glycosylation sites (yellow stars). Seven of the sites at; **15 [47], 88 [130], 164 [196], 228 [260], 282 [314], 357 [389]** and **410 [442]** are located in the extracellular domain, two sites at: **495** and **574** are situated in the catalytic core of the kinase domain and one site **809** in the C-terminal tail. The glycosylation sites at residues **88 [130]** and **357 [389]** are conserved in the majority of SRK-S-domains and all SLG proteins. (Figure. 1.15 constructed using data obtained from Stein *et al.*, 1994, Walker, 1994).

In the *Brassica* SRK gene, the exon encoding the SRK-S-domain is separated from the exon-encoding second domain by the largest intron, consisting of 896 base pairs, (see Figure 1.15). The SRK-S-domain and the first 8 residues encoded by exon 2 are located extracellularly, with the remaining part of exon 2 encoding a 20-residue helical

transmembrane domain, 415-434 [447-466] (Stein *et al.*, 1991; Figure 1.15) The hydrophobic transmembrane domain (TM) is enclosed at its C-terminus by six basic amino acids (Walker 1994). These basic amino acids, situated in the N-terminus of the juxtamembrane (JM) domain, serve as a 'stop-transfer' signal and ensure correct orientation of the SRK molecule in the cell membrane, so that the amino-end of the transmembrane domain is situated in the extracellular space, and the carboxy-end is positioned on the cytoplasmic face of the cell membrane, thus identifying SRK as a type-I integral membrane protein (Stein *et al.*, 1991; Walker, 1994). Exons 3 to 7 encode a 391-residue cytoplasmic protein kinase domain comprising residues 435-825 [467-857] and containing a protein kinase catalytic core extending from residues 489 to 781 [511 to 813], flanked by a 54-residue juxtamembrane domain (435-488 [467-520]) at the N-terminus and a 44-residue C-terminal tail, (782-825 [814-857]) (Stein *et al.*, 1991; Goring and Rothstein 1992; Trick and Heizmann, 1992; Nasrallah and Nasrallah 1993; Stein and Nasrallah 1993; Walker, 1994). Evidence from animal cell receptor tyrosine kinases suggest the juxtamembrane domain and the C-terminal tail might play a regulatory role in SRK enzymes (Walker, 1994). The high degree of homology between the SRK S-domain and corresponding SLGs within *Brassica* haplotypes indicates coevolution of the two S-locus genes (Walker, 1994). The additional discovery of S-locus-encoded intermediary SRK and SLG molecules, suggests that *SLG* arose from *SRK* by partial or complete duplication, followed by deletions of various introns and exons (Tantikanjana *et al.*, 1993).

The SRK kinase domain contains the 12 conserved sub-domains that include invariant and nearly invariant amino acid residues characteristic of all protein kinases (Stein *et al.*, 1991; Stone and Walker, 1995). These conserved regions are important in catalysis and in the maintenance of the three-dimensional structure of the kinase domain (Stone and Walker, 1995). Specificity of protein kinases resides either at serine/threonine, tyrosine or histidine residues, and correlates with consensus sequences within catalytic subdomains VIb and VIII. The amino acid sequences in SRK subdomains VIb (DLKVSN) and VIII (GTYGYMSPE) more closely match the consensus sequences found in animal serine/threonine kinase subdomains VI (DLKPEN) and VIII (GTPXYIAPE), than the corresponding subdomains in tyrosine kinases-VI (DLAARN) and VIII (FPIKWMAPE) - indicating that SRK has serine/threonine activity (Stein *et al.*, 1991; Walker, 1994; Délorme *et al.*, 1995; Stone and Walker 1995). Serine/threonine kinase activity has been demonstrated by

heterologous expression in bacterial cells, confirming that SRK is indeed a serine/threonine kinase (Goring and Rothstein, 1992; Stein and Nasrallah, 1993).

1.5.8 - Plant receptor-like kinases (RLKs)

Protein kinases catalyse the reversible transfer of the γ -phosphate from ATP to amino-acid side chains. They are involved in many aspects of cellular regulation and a number of cell-cell recognition systems (Stone and Walker 1995). Phosphorylation is the most common type of protein modification and is the principal mechanism employed by eukaryotes to regulate protein activity and function (Hunter, 1998). The structure of the SRK molecule suggests it functions as a receptor protein kinase (RPK) as it has the three components, (i) an extracellular domain, (ii) a transmembrane domain, and (iii) protein kinase domain observed in all receptor kinase molecules. The extracellular domain is hypothesised to function in the recognition and binding of the SCR ligand, while the transmembrane and juxtamembrane domains respectively anchor and orientate the protein in the membrane, and the protein kinase domain transduces extracellular signals (Braun *et al.*, 1997).

A growing number of transmembrane receptor-like kinase (RLK) molecules have been identified in plants, and constitutes a family of some 100 members known as the plant receptor-like kinase gene family (plant RLK gene family), with kinase specificity of RLKs associated with serine/threonine residues (Braun and Walker 1996; Braun *et al.*, 1997; Shiu and Bleecker, 2001). Plant receptor-like kinases (RLKs) are all transmembrane proteins that show structural similarity to cell surface receptor protein kinases (RPKs) of animal eukaryote cells, and were named receptor-like kinases (RLKs) to reflect this similarity (Walker, 1993; Braun and Walker, 1996). Receptor protein kinases are found exclusively in metazoans where they are associated with intercellular communication (Hunter, 1998; Cock, *et al.* 2002). In animal cells, specificity of receptor kinases is associated with tyrosine residues and only rarely with serine/threonine residues (Lindberg, 1992). Recent phylogenetic analysis of kinase domains reveals that animal serine/threonine receptor kinases, Raf kinases, plant RLKs and the animal receptor tyrosine kinases share a common origin and constitute a distinct eukaryote serine/threonine/tyrosine kinase superfamily (ePK) (Hunter, 1998; Shiu and Bleecker, 2001; 2003). Within the ePK superfamily, plant RLKs and non-receptor (i.e. cytoplasmic) *Drosophila* Pelle kinases and Pelle-related cytoplasmic kinases form a distinct RLK/Pelle gene family (Shiu and Bleecker, 2001, 2003).

In animal RPKs, a ligand binding to the extracellular domain brings about an increase in the catalytic activity of the cytoplasmic kinase domain via autophosphorylation of specific tyrosine residues, known as RPTKs (receptor protein tyrosine kinases) or serine/threonine residues of RPSKs (receptor protein serine/threonine kinases) (Stone and Walker, 1995; Braun and Walker, 1996; Cock, *et al.*, 2002). Phosphorylation of a specific tyrosine (or serine/threonine) residue transforms the residue into a binding site for a specific substrate molecule of the receptor kinase, and leads to the activation of specific biochemical pathways (Hunter, 1998). Receptor kinases can bind to more than one substrate, leading to the activation of multiple pathways, and can bring about the amplification of the initial signal by phosphorylating secondary molecules at several phosphorylation sites (Hunter, 1998). Many animal RPKs have prominent roles in initiation and transduction of extracellular signals and for some pathways their functions are well described (Fantl *et al.*, 1993; Daum *et al.*, 1994; Marshall, 1994, 1995). Signalling events in plants, however, are less well understood.

The discovery of the *ZmPK1* transmembrane receptor-like protein kinase in *Zea mays* (Walker and Zang, 1990) and the subsequent identification of RLKs in other plant species have opened up the exciting possibility of plant cell-cell signalling systems analogous to those in animal cells (Walker, 1993; Braun *et al.*, 1997; Table 1.5). The newly described CLAVATA⁷ system of *Arabidopsis thaliana*, which regulates the balance between cell proliferation and differentiation at the shoot meristem, and the identification of SCR as the male determinant of SI in *Brassica* and the ligand of SRK, offer two model systems with which to pursue an understanding of plant receptor signalling systems (Stone, *et al.*, 1998; Trotochaud *et al.*, 1999, 2000; Brand *et al.*, 2000; Takayama *et al.*, 2000a).

Based on the structural motifs in their extracellular domains (ectodomains) more than 21 classes of RLKs have been identified (Walker, 1993; Torii, 2000; Cock and McCormick 2001; Pastuglia *et al.*, 2002; Navarro-Gochicoa *et al.*, 2003), mostly deriving their names from the recognised RPK classes. Some classes of RLKs such as TNFR and PR5 consist of one or two members only, and others such as CrRLK1 and RFLK3 contain RLKs that share no homology to known motifs (Walker, 1993; Torii, 2000; Table 1.5). The majority, including the best-described RLKs, consist of several members and occur in six RLK classes. These are RLK classes: (i) S-domain, (ii) leucine-rich repeat (LRR) (iii) epidermal growth factor (EGF) (iv) tumor necrosis factor

⁷ See appendix 1 – Names, descriptions and abbreviations of RLKs, RTKs and associated molecules.

receptor (TNFR) (v) lectin-like, (vi) pathogenesis related-5 (PR5) and (vi) Lysin motif (LysM) (see Table 1.5). Members of the S-domain class of *RLKs* encode extracellular domains that have sequence homology characteristic of S-locus glycoproteins and so contain a Cys domain, a PTDT-box and two conserved glycosylation sites (Torii and Clark, 2000; Table 1.5, Figure 1.15). S-domain proteins appear to be universally present in plants, with nothing close to them recorded in fungi or animals. The leucine-rich repeat (LRR) *RLKs* have extracellular domains containing tandem repeats of conserved leucine residues (Torri and Clark, 2000). The numbers of repeated LRRs present within an extracellular domain vary from 2 to 24 and may additionally be associated with other protein domains (Cock and McCormick, 2001). LRRs occur in proteins associated with protein-protein interactions in organisms as diverse as yeasts, flies, humans and plants (Walker, 1994; Braun and Walker, 1996; Torri and Clark, 2000). The role of LRR *RLKs* in plant development is evidenced by *CLAVATA1*, *ERECTA*, *BRI1*, *OstMK1* and *PRK1*, while *FLS2* and *Xa21* implicate LRR *RLKs* in defence and disease resistance (Table 1.4). The EGF-class of *RLKs* includes the wall-associated receptor kinases, *WAKs*1-5 and *PRO25*, a receptor that interacts with light-harvesting chlorophyll proteins (LHCP) in *Arabidopsis thaliana* (Kohorn *et al.*, 1992; He and Kohorn, 1998). The repeat motif similar to that in EGF is characterised by a conserved arrangement, in the extracellular domains, of six cysteine residues: $X_4\text{-}\underline{C}X_{(2-7)}\text{-}\underline{C}X_{(1-4)}\text{-G/AX-}\underline{C}X_{(1-13)}\text{-}t\text{taX-}\underline{C}X\text{-}\underline{C}X_2\text{-GaX}_{(1-6)}\text{-GX}_2\text{-}\underline{C}X$, where X is any amino acid, the number in brackets represents variable number of X (any amino acid) residues, and a and t are aromatic and non-hydrophobic residues respectively (Campbell and Bork, 1993). EGF-like repeats have been identified in the extracellular regions of animal receptor molecules where they are known to play a role in protein-protein interactions associated with diverse functions such as blood clotting, neural development and cell adhesion (Rebay *et al.*, 2002). In animal systems there may be 30-40 EGF-like repeats in a receptor kinase, with subsets of only two or three repeats being necessary for ligand-binding interactions and activation of receptor signalling (Rebay *et al.*, 1991). The remaining EGF repeats may possibly aid orientation of the ligand in the formation of an active ligand-receptor complex. The TNFR-like repeat class of *RLKs* has the CR4 (CRINKLY4) protein as its sole member (Torii and Clark, 2000). In animal TNFR proteins, the generalised pattern of the second TNFR-like cysteine-rich repeat motif consists of six conserved cysteines, with the characteristic spacing of $\underline{C}X_{(11-15)}\text{-}\underline{C}X_2\text{-}\underline{C}X_3\text{-}\underline{C}X_{(9-11)}\text{-}\underline{C}X_7\text{-}\underline{C}X$ (Ward *et al.*, 1995). The CR4 extracellular domain contains a single 26-amino acid motif, $\underline{C}X_7\text{-}\underline{C}X_2\text{-}\underline{C}X_3\text{-}\underline{C}X_9\text{-}\underline{C}X_7$ that has strong similarity to the second cysteine-rich repeat, $\underline{C}X_{14}\text{-}\underline{C}X_2\text{-}\underline{C}X_3\text{-}\underline{C}X_9\text{-}\underline{C}X_7$ of mammalian TNFR (Becraft, *et al.*, 1996), but additionally contains seven copies of a 39-amino acid repeat that is

distantly related to RCC1 (regulator of chromosome condensation 1), a guanine-nucleotide-exchange factor protein that increases the dissociation of Ran-bound GDP (Renault *et al.*, 1998). The molecular model of the RCC1-like domains of the CR4 extracellular region shows homology to the RCC1 family of 7-bladed propeller proteins. Aside from being a guanine-nucleotide exchange factor for the nuclear Ras homologue Ran, RCC1 also binds to DNA via a protein-protein complex, and thus the C4 ectodomain may be involved in protein-protein interactions (Renault *et al.*, 1998; McCarty and Chory, 2000). Lectin-like RLKs (LecRKs) have extracellular domains that show homology to carbohydrate-binding proteins characteristic of the legume lectin and lectin-like proteins, that are characterised by having at least one non-catalytic carbohydrate-binding domain (Nishiguchi *et al.*, 2002; Torii and Clark, 2000). LecRKs have been identified in *Arabidopsis thaliana* (Brassicaceae), *Medicago truncatula* (Fabaceae) and *Poplar nigra* (Salicaceae) (Hervé *et al.*, 1996; Nishiguchi *et al.*, 2002; Navarro-Gochicoa *et al.*, 2003) and are thought to be involved in recognition and transduction of oligosaccharide signals, small hydrophobic hormones (auxins or cytokinins) or complex glycans (Navarro-Gochicoa *et al.*, 2003). Pathogenesis-related (PR) RLKs have extracellular domains that show similarity to pathogenesis related 5 (PR5) proteins that are produced by plant resistance genes induced by pathogen attack (Torii and Clark, 2000). At present this class of RLKs has only the *Arabidopsis thaliana* PR5-like receptor kinase (PR5K) as its sole member (Wang *et al.*, 1996). The LysM-like RLKs are represented by NFR1 (for Nod factor receptor 1) and NFR5 (Madsen *et al.* 2003). Lysin motifs were first identified in bacterial lysins and are present in many cell wall hydrolases of various bacteria and bacteriophages (Steen *et al.*, 2003). LysM-containing proteins are implicated in peptidoglycan-binding, chitin-binding and cell-wall binding interactions (Radutolu *et al.*, 2003; Steen *et al.*, 2003). NFR1 and NFR5 which contain two and three LysM repeats respectively enable *Lotus japonicus* to recognise its bacterial microsymbiont *Mesorhizobium loti* possibly through the perception of specific lipochito-oligosaccharide Nod-factor signals secreted by rhizobia (Radutolu *et al.*, 2003).

Novel RLKs such as *Brassica napus* PERK1 and those RLKs that show no homology in their extracellular domains to any known protein motifs may simply be the first examples of their class of RLK. As more plant genomes are sequenced, other members belonging to such classes may be revealed. For example, PERK1 (for Proline Extensin-like Receptor Kinase 1) has a proline-rich (41% proline) ectodomain containing one Ser(Pro)₄ pentapeptide and seven Ser(Pro)₂₋₃ tri- and tetrapeptide sequences characteristic of the extensin and extensin-like domains found in many

classes of protein belonging to the hydroxyproline-rich glycoprotein (HRGP) family of plant cell wall-associated proteins (Cassab, 1998; Silva and Goring 2002). Using the predicted PERK1 amino acid sequence of *Brassica napus* a BLASTP search identified 14 *Arabidopsis thaliana* genes encoding proline-rich extensin-like ectodomains, including *AtPERK1* (for *Arabidopsis thaliana* PERK1) an orthologue of PERK1 (Silva and Goring, 2002). Likewise, Stracke *et al.* (2002) identified the pea homologue of the *Lotus japonicus* SYMRK, which is itself a homologue of NORK, by using stretches of SYMRK sequence conservation (Table 1.5). Interspecific and intergeneric leap-frogging from known to unknown related molecules, via conserved domains/sequences, will no doubt reveal the presence of orthologous and/or paralogous receptor molecules in other plant species.

Although an increasing number of RLKs with related ectodomains have been identified, the putative ligands that bind these ectodomains have proved hard to track down, and nothing is known about ligand binding sites, or how binding between ligand and RLK ectodomains is achieved. RLK ligands identified to date are small highly polymorphic peptides i.e. CLV3 (CLAVATA1), SCR (SRK), systemin (SR160/tBR11); flagellin (FLS2), or steroids i.e. brassinolide (BR11) (Schumacher and Chory, 2000; Matsubayashi, 2003). If RLK-ligand binding sites of known ligand-receptor complexes could be identified it might aid identification of corresponding ectodomain binding sites in RLKs with as yet unidentified ligands leading perhaps to the identification of these partner molecules.

Table 1.5 Classification, expression and specificity of plant receptor-like kinases (RLKs).

RLK Class	Species	RLK Gene Product	Site of Tissue Expression	Specific Location	Function	Protein Kinase Specificity	Reference
EGF (Epidermal Growth Factor-like repeats)	<i>Arabidopsis thaliana</i> ^(SC)	PRO25	Vegetative	light-grown leaf tissue possibly in the thylakoid membrane of chloroplasts	Undefined interaction with LHCP, possibly involved in LHCP biogenesis	serine/threonine	Kohorn <i>et al.</i> , 1992.
		WAK1	Vegetative	leaves and stems	Defence mechanism against pathogens, (WAK1 induced by salicylic acid, jasmonic acid, ethylene, and <i>Alternaria brassicicola</i>)	serine/threonine	He <i>et al.</i> , 1996; He and Kohorn, 1998; Park <i>et al.</i> , 2001; Verica and He, 2002.
		WAK2					
		WAK3					
		WAK4					
		WAK5					
Lectin (lectin-like)	<i>Arabidopsis thaliana</i> ^(SC)	LecRK1	Vegetative	weakly expressed in stems; leaves; flowers; siliques; roots.	Putative role in the perception of oligosaccharide-mediated signal transduction	serine/threonine	Hervé <i>et al.</i> , 1996.
		MtLecRK1;1	Vegetative	roots (8-day old nodules)	Possibly legume-rhizobia symbiosis	serine/threonine	Navarro-Gochicoa <i>et al.</i> , 2003.
	MtLecRK7;1	roots					
	MtLecRK7;2	roots, [stems]					
	MtLecRK7;3	roots, leaves, [stems]					
<i>Poplar nigra</i> var. <i>italica</i>	PnLPK	Vegetative	roots, matureleaves calli [traces in stems and apical buds]	Signal transduction associated with wounding response	serine/threonine	Nishiguchi <i>et al.</i> 2002.	

• Key: ^(SC) = self-compatible, ^(SSI) = self-incompatible; --- = information not known; data in square brackets = very low levels of expression in these tissues.

Table 1.5. continued.

RLK Class	Species	RLK Gene Product	Site of Tissue Expression	Specific Location	Function	Protein Kinase Specificity	Reference
LRR (Leucine-Rich Repeat)	<i>Arabidopsis thaliana</i> ^(SC)	<i>AtSERK1</i>	Vegetative	developing ovules and embryos	Enhances embryogenic competence	serine/threonine	Hecht, <i>et al.</i> , 2001.
		<i>BAK1</i>	Vegetative	ubiquitous in seedlings	Growth regulation	serine/threonine	Li, <i>et al.</i> , 2002, Nam, and Li, 2002.
		<i>BR11</i>	Vegetative	ubiquitous in seedlings	Growth regulation	serine/threonine	Li and Chory, 1997. Schumacher and Chory, 2000. Li <i>et al.</i> , 2001.
		<i>CLV1</i>	Vegetative	shoot & floral meristem	Meristem cell fate	serine/threonine	Clark <i>et al.</i> , 1997; Stone <i>et al.</i> , 1998; Jeong <i>et al.</i> , 1999; Trotochaud <i>et al.</i> , 1999; Brand <i>et al.</i> , 2000; Torii, 2000.
		<i>ERECTA</i>	Vegetative	young flower buds; inflorescence meristem; flowers; siliques [stems; rosette leaves; cauline leaves]	Specifies organ shape	serine/threonine	Tori <i>et al.</i> , 1996.
		<i>FLS2</i>	Vegetative	root; stems; flowers; leaves.	Defence-response growth inhibition	serine/threonine	Gomez-Gomez <i>et al.</i> , 1999; Gomez-Gomez and Boller, 2000; Gomez-Gomez <i>et al.</i> , 2001.
		<i>HAESA</i> (formerly <i>RLK5</i>)	Vegetative	abscission zones at base of sepals, petals and stamens; [base of pedicels]	Floral abscission	serine/threonine	Horn and Walker, 1994; Jinn <i>et al.</i> , 2000.
		<i>LRR-PK</i>	Vegetative	etiolated cotyledons; roots (in these organs only if not subjected to light)	Early steps in light-signal transduction	serine/threonine	Decken and Kaldenhof, 1997.

Table 1.5 continued.

RLK Class	Species	RLK Gene Product	Site of Tissue Expression	Specific Location	Function	Protein Kinase Specificity	References	
LRR (Leucine-Rich Repeat)	<i>Arabidopsis thaliana</i> ^(SC)	MRLK	Vegetative	shoot and root apical meristems	Putative role in the transition from vegetative to flowering stage	---	Fujita <i>et al.</i> , 2003.	
		RKF1	Reproductive	Stamens	---	serine/threonine	Takahashi <i>et al.</i> , 1998.	
			RPK1	Vegetative	flowers; stems; leaves; roots (Induced by osmotic stress)	Putative role in signal transduction pathway of the plant hormone abscisic acid	serine/threonine	Hong <i>et al.</i> , 1997.
			TMK1	Vegetative Reproductive	ubiquitous	---	serine/threonine	Chang <i>et al.</i> , 1992.
	<i>Capsella rubella</i>	BRII	---	---	---	serine/threonine	Li, 2003.	
	<i>Daucus carota</i>	SERK	Vegetative	somatic embryo	Embryogenic potential of somatic cells	serine/threonine	Schmidt <i>et al.</i> , 1997.	
	<i>Glycine max</i>	GmNARK1	Vegetative	shoots and innoculated roots	Controls autoregulation of nodulation	serine/threonine	Searle <i>et al.</i> , 2003.	
			BRII	---	---	---	serine/threonine	Li, 2003.
	<i>Lotus japonicus</i>	HARI	Vegetative	roots, nodules, cotyledons, stems, leaves	Autoregulation of homeostasis to maintain non-symbiotic and	serine/threonine	Krusell <i>et al.</i> , 2002. Nishimura <i>et al.</i> , 2002.	
			SYMRK	Vegetative	---	Early signal transduction between NF perception and activation of LB gene.	---	Stracke <i>et al.</i> , 2002.

Table 1.5. continued.

RLK Class	Species	RLK Gene Product	Site of Tissue Expression	Specific Location	Function	Protein Kinase Specificity	References
LRR (Leucine-Rich Repeat)	<i>Lycopersicon esculentum</i>	tBRI1 (SR160 homologue)	Vegetative	----	Plant growth and development	Putative serine/threonine	Montoya <i>et al.</i> , 2002.
		LePRK1 LePRK2	Reproductive	pollen-tube plasma membrane	Pollen-pistil recognition	serine/threonine	Muschietti <i>et al.</i> 1998.
	<i>Lycopersicon peruvianum</i>	SR160 (tBRI1 homologue)	Vegetative	----	Receptor for the palnt polypeptide wound signal systemin	serine/threonine	Scheer and Ryan Jr., 2002.
	<i>Medicago sativa</i>	NORK	---	---	Putative early perception and transduction of Nod factor signal	---	Endre, <i>et al.</i> , 2002.
	<i>Medicago truncatula</i>	NORK	---	---	Putative early perception and transduction of Nod factor signal	---	Endre, <i>et al.</i> , 2002.
	<i>Oryza sativa</i> ^(SC)	OsBRI1	Vegetative	shoot apices, [roots, leaf sheath, developed flower]	Internode elongation, and leaf development	Putative serine/threonine	Yamamuro <i>et al.</i> , 2000.
		OsTMK	Vegetative	stem internodes particularly in regions of cell division and elongation.	Gibberellin-induced; stem-elongation	Primarily threonine	van der Knaap <i>et al.</i> , 1996.
		Xa21	Vegetative	leaves	Developmentally regulated resistance to the <i>Xanthomonas oryzae</i> pv. <i>oryzae</i> race 6 (Xoo)	serine/threonine	Song <i>et al.</i> , 1995b; Wang <i>et al.</i> , 1998.
		Xa26	Vegetative	constitutive expression in leaves from very early seedling stage to adult stage	Non developmentally-regulated resistance to the <i>Xanthomonas oryzae</i> pv. <i>oryzae</i> race 6 (Xoo)	serine/threonine	Sun <i>et al.</i> , 2004.

Table 1.5. continued.

RLK Class	Species	RLK Gene Product	Site of Tissue Expression	Specific Location	Function	Protein Kinase Specificity	References
LRR (Leucine-Rich Repeat)	<i>Petunia inflata</i>	PRK1	Reproductive	pollen	Pollen development	serine/threonine & tyrosine	Mu et al., 1994; Lee et al., 1996.
		PsBRI1	Vegetative	shoot internodes, petioles, tendrils, roots, pods, [seeds]	Plant growth and development: putative cell elongation, xylem differentiation, and stress tolerance	serine/threonine	Nomura et al., 2003.
	<i>Pisium sativum</i>	SYM29	Vegetative	roots, nodules, leaves	Autoregulation of nodulation	serine/threonine	Krusell et al., 2002; Nishimura et al., 2002.
		SYMRK	Vegetative	---	Early signal transduction between NF perception and activation of LB gene	---	Stracke et al., 2002.
		LTK1 LTK2 LTK3	Vegetative	endosperm	Putative seed development and maturation.	serine/threonine	Li and Wurtzel, 1998.
LysM (Lysin Motif)	<i>Lotus japonicus</i>	NFR1	Vegetative	uninoculated roots	Control of endosymbiosis with nitrogen-fixing bacterial microsymbiont <i>Mesorhizobium loti</i>	serine/threonine but with motifs VII and VIII strongly modified or absent	Radutolu et al., 2003.
		NFR5	Vegetative	uninoculated roots			Madsen et al., 2003.
PR (pathogenesis related)	<i>Arabidopsis thaliana</i> ^(SC)	PR5K	Vegetative	inflorescence stems, roots; (rosette leaves and siliques)	Putative receptor for pathogenic signal molecules	serine/threonine	Wang et al., 1996.

Table 1.5. continued.

RLK Class	Species	RLK Gene Product	Site of Tissue Expression	Specific Location	Function	Protein Kinase Specificity	References	
S-domain (SLG-like)	<i>Arabidopsis lyrata</i> ^(SSI)	SRK	Reproductive	stigma papillar cell wall	Self-incompatibility	serine/threonine	Schierup <i>et al.</i> , 2001.	
		ARK1	Vegetative	leaves; [floral buds]	Cell expansion	serine/threonine	Tobias <i>et al.</i> , 1992; Tobias and Nasrallah, 1996; Ohtake <i>et al.</i> , 2000; Pastuglia <i>et al.</i> , 2002.	
	<i>Arabidopsis thaliana</i> ^(SC)	ARK2	Vegetative [Reproductive]	cotyledon, leaves; sepals; [styles]	---	---	serine/threonine	Dwyer <i>et al.</i> , 1994.
		ARK3	Vegetative	Root-hypocotyl boundary; base of lateral roots; axillary buds; flower pedicels.	Cell-growth; plant defence; wound induced	---	serine/threonine	Dwyer <i>et al.</i> , 1994; Ohtake <i>et al.</i> , 2000; Pastuglia <i>et al.</i> , 2002.
		RLK1	Vegetative	rosettes of stems & leaves	---	---	serine/threonine	Walker, 1993.
		RLK4	Vegetative	root-hypocotyl boundary; [rosettes of stems & leaves]	---	---	serine/threonine	
	<i>Brassica napus</i> ^(SSI)	SRK	Reproductive	stigma papillar cell wall	Self-incompatibility	---	serine/threonine	Goring and Rothstein, 1992.
		SFR1		[leaves; roots; stigmas]	Plant defence	---		
		SFR2	Vegetative [Reproductive]	Anther & stigmas of flower buds; leaves; [seeds]	Plant defence & wound induced	---	serine/threonine	Pastuglia <i>et al.</i> , 1997, 2002.
	<i>Brassica oleracea</i> ^(SSI)	SFR3		roots; [leaves]	---	---		
		SRK	Reproductive	stigma papillar cell wall	Self-incompatibility	---	serine/threonine	Stein <i>et al.</i> , 1991, 1993, 1996; Tantikanjana <i>et al.</i> , 1993.
		BcRK1	Vegetative Reproductive	leaves; flower buds; stigmas	ARK1-like (cell growth)	---	---	Suzuki <i>et al.</i> , 1997.
	<i>Brassica rapa</i> ^(SSI)	BcRK3		---	---	---		
		BcRK6		---	---	---		
		SRK	Reproductive	stigma papillar cell wall	Self-incompatibility	---	serine/threonine	Yamakawa <i>et al.</i> , 1995.
	<i>Ipomoea trifida</i> ^(SSI)	IRK1	Reproductive	stigmas and anthers	---	---	Koyama <i>et al.</i> , 1996.	
	<i>Lotus japonicus</i>	SRK	---	---	---	---	NCBI accessions; BAC41328, BAC41329 & BAC41330	
	<i>Senecio squalidus</i>	SSRLK1 -3	Vegetative Reproductive	---	---	---	Hiscock <i>et al.</i> , 2003 Tabah <i>et al.</i> , 2004.	

Table 1.5. continued.

RLK Class	Species	RLK Gene Product	Site of Tissue Expression	Specific Location	Function	Protein Kinase Specificity	References
S-domain (SLG-like)	<i>Oryza sativa</i> ^(SC)	OsPK10	Vegetative	ubiquitous, upregulated by light	---	serine/threonine	Zhao <i>et al.</i> , 1994.
		RLK11	---	---	---	---	Lei <i>et al.</i> , 2002.
	<i>Zea mays</i> ^(SC)	KIK1	Vegetative	etiolated seedlings & husks	---	serine/threonine	Braun <i>et al.</i> , 1997.
TNFR (Tumour Necrosis Factor Receptor-like repeats)	<i>Arabidopsis thaliana</i> ^(SC)	ZmPK1	Vegetative	roots & shoots of seedlings; silks	---	serine/threonine	Walker and Zang, 1990.
		CR4 CRINKLY4	Vegetative	L1 cells in all apical meristems and young organ primordia, developing ovule integuments [root meristemes]	L1 cell layer integrity required for the correct cell organisation in ovule integuments and sepal boundaries	---	Gifford <i>et al.</i> , 2003.
	<i>Zea mays</i> ^(SC)	CR4 CRINKLY4	Vegetative	Shoot apical meristem, young leaf primordia	Leaf epidermis; aleurone differentiation	serine/threonine	Becraft <i>et al.</i> , 1996. Becraft <i>et al.</i> , 2001.
	<i>Nicotiana tabacum</i>	CHRK1	Vegetative	apical domain of embryos, leaf primordia, young leaves, floral organs	Signal transduction regulating plant development and cytokinin homeostasis	---	Kim <i>et al.</i> , 2003.
Proline-rich extensin-like receptor kinases	<i>Brassica napus</i> Westar	PERK1	Vegetative [Reproductive]	stem, petal, leaf [pistil, anther, root]	Possible role in the early general perception and response to a wound and/or pathogen stimulus	serine/threonine	Silva and Goring, 2002.
	<i>Triticum aestivum</i>	WLRK	Vegetative	leaves of seedlings; flag leaves; [culm and spikelets]	Putative role in recognition of a pathogen (<i>Puccinia recondita</i> f. sp. <i>tritici</i>)	serine/threonine	Feuillet <i>et al.</i> , 1997, 1998.
Extracellular domain with 12 invariant cysteines CX ₁ -CX ₁₂ -CX ₍₁₁₋₁₆₎ -CX-CX ₍₉₋₁₁₎ [*] CX ₍₉₎ [*] -CX ₍₆₋₄₄₎ [*] -CX _(16;18) -CX ₍₂₃₎ [*] CX _n -CX ₂ -C	<i>Arabidopsis thaliana</i>	RKF2	---	---	---	serine/threonine	Takahashi <i>et al.</i> , 1998.
	<i>Arabidopsis thaliana</i>	RKF3	---	---	---	serine/threonine	Takahashi <i>et al.</i> , 1998.
No specific pattern identified	<i>Catharanthus roseus</i>	CrRLK1	---	---	---	---	Schulze-Muth <i>et al.</i> , 1996.

1.5.9 - Molecular mechanism of SI in *Brassica*

In *Brassica*, the interaction between S-receptor kinase (SRK) and S-cysteine-rich protein (SCR) is the minimum interaction required for initiation of an SI response (Takayama *et al.*, 2001). Conclusive evidence as to how these two molecules bring about the rejection of self-pollen has still to be produced. A consensus is gathering around the hypothesis that SCR diffuses through the extracellular matrix, produced by contact of self-pollen with stigmas, and binds to an active SRK-receptor complex (Giranton *et al.*, 2000). The binding of SCR to the SRK-receptor complex initiates the *Brassica* SI reaction. Variations observed in SI interactions of some *Brassica* haplotypes are attributed to differences in the molecular constituents of the SRK-receptor complex, the regulation of downstream events and the differing requirements of S-haplotypes for SI-enhancing accessory molecules (Kemp and Doughty, 2003). It is not clear whether the *Brassica* SI system controls the rejection reaction directly through a specific SI mechanism, or indirectly by interfering with pre-existing mechanisms of pollination. Differences in the timing of SI could be explained in terms of the SI reaction impinging on different stages of the pollen-stigma interaction, such as pollen adhesion, hydration, germination and pollen tube penetration. Likewise, the triggering of a pre-existing interspecific incompatibility mechanism may also lead to the production of molecules capable of causing pollen rejection (Lewis and Crowe, 1958; Hiscock and Dickinson 1993; Dickinson, 1995).

In unpollinated stigmas of some *Brassica* haplotypes, SRK molecules form non-covalently bonded complexes with each other (i.e. not involving disulphide bonds) (Giranton, *et al.*, 2000). In the *B. oleracea* S₃ haplotype, unpollinated stigmas contain two S complexes, one of 161 kDa, thought to be a heterodimer of SRK₃-SLG₃ or SRK₃-eSRK₃ (eSRK₃ is an S₃-specific truncated variant of SRK containing only the S-domain region), and one of 233 kDa, representing a putative SRK₃-SRK₃ homodimer (Giranton *et al.*, 2000). In the *B. rapa* S₈ haplotype, SCR₈ binds to a putative receptor dimer of SRK₈ and SLG₈, forming an SCR-SRK-SLG complex (Giranton, *et al.*, 2000; Takayama *et al.*, 2000b). Indeed, *in vivo* experiments demonstrate that SCR₈ is capable of binding both SLG₈ and SRK₈ to form 2 protein complexes: SCR₈-SRK₈ and SCR₈-SLG₈, and data suggest that SLG₈ is integral to the binding of SCR₈ to the putative S₈-receptor complex (Takayama *et al.*, 2000b). These observations show similarities to the *A. thaliana* CLAVATA complex, in which CLV1 (see Table 1.5) also occurs as two protein complexes *in vivo* (Trotochaud *et al.*, 1999, 2000). The smaller ~185 kDa complex is thought to represent an inactive disulphide-linked heterodimer of CLV1 and CLV2, and the larger ~450 kDa complex is hypothesised to be the active

CLV complex that incorporates the ~185 kDa heterodimer plus the CLV3 ligand, with the latter being essential to the assembly of the active complex (Stone, *et al.*, 1998; Trotochaud *et al.*, 1999, 2000; Brand *et al.*, 2000). The ~450 kDa complex also contains, KAPP (kinase-associated protein phosphatase) and Rop (a Rho/Rac-GTP related protein), with ligand stimulation possibly transduced via Rop proteins (Trotochaud *et al.*, 1999, 2000). *Arabidopsis thaliana* offers a second example of receptor kinase complex formation in the WAK1 (wall-associated protein kinase 1) signalling system. WAK1, an EGF-RLK, forms a ~500-kDa receptor complex that incorporates AtGRP-3, a glycine-rich protein of ~48 kDa and KAPP. Binding of AtGRP-3 with the cell-wall domain of WAK1 is essential for the stability of this complex (Park *et al.*, 2001). In the absence of AtGRP-3, WAK1 protein occurs mostly as an inactive 78-kDa molecule. The presence of AtGRP-3 induces the production of 100-kDa active WAK1 protein that is then able to associate into a ~500-kDa complex with AtGRP-3 and KAPP (Park *et al.*, 2001). This WAK1-AtGRP-3-KAPP complex may represent the active complex in a salicylic acid signalling pathway, related to pathogenesis (He, *et al.*, 1998; Park *et al.*, 2001). Receptor-complex formation also occurs in the animal serine/threonine kinase transmembrane receptors $T\beta$ RI and $T\beta$ RII, which must first associate to form a stable complex before being able to be activated by the ligand TGF- β (transforming growth factor- β). As with the CLV3 ligand of the CLAVATA system, the TGF- β ligand is required for the formation of the active $T\beta$ R-receptor complex (Wrana *et al.*, 1994; Wells *et al.*, 1999). Interestingly, TGF- β ligands, which like SCR are small basic cysteine-rich peptides, constitute a large superfamily of molecules identified as cystine knot growth factors that are found from insects to mammals, where they are important modulators of development and the immune response (Schlunegger and Grütter, 1993).

There is not enough evidence to speculate as to the relative activities of the 161-kDa and 233-kDa SRK₃ dimers, or whether SLG₃ participates in this complex. However, there is evidence to suggest that SLG is important to the stabilization of SRK proteins, as suppression of SLG in certain *Brassica* haplotypes is associated with the accumulation of aberrant high-molecular mass aggregates of SRK (Dixit, *et al.*, 2000). This observation also has parallels with the CLAVATA system, where CLV2 is required for the stability of CLV1 complexes (Jeong *et al.*, 1999). SLG may also have additional functions associated with the translation of SRK, since *Brassica* mutants that express low levels of SLG do not accumulate SRK proteins in stigma cells despite the presence of normal levels of SRK transcript (Dixit, *et al.*, 2000). A role for SLG as a

molecular shuttle has also been suggested (Kemp and Doughty, 2003). This latter function is based on the various abilities of membrane-associated SLG, i.e. SLG in the putative SLG-SRK dimer, and soluble SLG to bind SCR (Dixit *et al.*, 2000; Kachroo *et al.*, 2001; Takayama *et al.*, 2001). The differential binding ability of soluble and membrane-bound SLG was observed in the *Brassica rapa* S_8 -haplotype, with soluble SLG exhibiting low affinity for SCR, while membrane-associated SLG (i.e. SLG complexed with SRK) bound SCR with high affinity (Takayama *et al.*, 2001). These data indicate that SLG and SRK may form a high-affinity receptor complex for the SCR ligand. Once again, parallels can be drawn with the TGF- β signalling system, where the membrane-anchored T β RIII receptor binds TGF- β ligand and enhances TGF- β binding to the T β RII transmembrane receptor molecule in the T β RI and T β RII receptor complex (López-Casillas *et al.*, 1994). The soluble form of T β RIII inhibits binding of TGF- β to its receptor, and so distortions in the balance between soluble and membrane-bound versions of T β RIII receptor molecules are capable of modulating T β R-mediated signalling (López-Casillas *et al.*, 1993; 1994). A second analogy between T β RIII and SLG is apparent, in that certain animal cells are TGF- β -responsive in the absence of membrane-bound T β RIII indicating that T β RIII-mediated presentation of the TGF- β ligand to the T β RII receptor complex is either not required in these cells, or is achieved by other means or molecules (López-Casillas *et al.*, 1993a, 1993b). This latter observation has similarities with the *Brassica oleracea* S_{18^-} , S_{24^-} and S_{60^-} haplotypes which all show normal SI even though S_{18^-} and S_{60^-} haplotypes do not produce functional SLG proteins, and the S_{24} S locus does not contain SLG (Suzuki *et al.*, 2000b). It is clear that *Brassica* haplotypes show variation in ligand binding as evidence by the *Brassica oleracea* S_6 -haplotype, where the interaction of SRK and SCR appears independent of any additional components at the stigma surface (Kachroo *et al.*, 2001). Such variations have precedence in animal receptor systems and do not preclude a generalised mechanism of SI across haplotypes, with accompanying augmentations occurring in specific haplotypes.

1.5.10 - SI signal transduction and SRK substrate molecules

To understand the signalling response of SRK it will be necessary to identify which proteins are phosphorylation targets for the activated SRK molecule and by what means the SI signalling pathway is regulated. For receptor tyrosine kinases (RTKs) in animals, a number of substrate molecules have been identified. Some of these substrates are enzymes, but others fall into the category of adaptor proteins, docking proteins and structural proteins (Hunter, 1998). In animal systems, an activated

receptor tyrosine kinase may autophosphorylate on many tyrosine sites. These phosphorylated tyrosine residues (P.Tyr) are able to bind a subset of proteins that contain specific binding domains such as SH2 (Src homology 2), PTB (phosphotyrosine binding) and PH (pleckstrin homology) domains (Hunter, 1998; Appendix 1). The PDGF β (platelet-derived growth factor- β) receptor protein tyrosine kinase (RTPK) is able to bind up to 8 different SH2-containing proteins (van der Geer *et al.*, 1994). In another example, the PDGF β RTK known as CSF-1 (for colony stimulating factor 1), which controls the proliferation and maturation of myeloid cells into macrophages, contains four major tyrosine phosphorylation sites; Tyr 697, Tyr 706, Tyr 721 and Tyr 807 that are crucial for appropriate response to CSF-1 ligand binding (van der Geer and Hunter 1993). Autophosphorylation sites of Tyr 697, Tyr 706 and Tyr 721 bind specific proteins each of which activates distinct signalling pathways concerned with proliferation and differentiation of myeloid cells (van der Geer and Hunter 1993). However, binding at Tyr 807 is required for maximal ligand-stimulated activity of the PDGF β RTK, and mutations at this site compromised all CSF-1 receptor-mediated responses (van der Geer and Hunter 1993). In other cases, multiple autophosphorylation sites within RTK molecules have been shown to be redundant, with the multiple sites possibly serving as mechanisms for amplifying the response to ligand binding (Hunter, 1998). It is clear from these examples of animal receptor-mediated signalling pathways, that the net outcome of receptor-kinase signalling probably involves integration and co-operation between signalling pathways initiated by different autophosphorylation sites of a receptor kinase molecule. The complexity of animal systems may well be reflected in plant RLK signalling, and it may be that the kinase interaction (KI) domain of kinase-associated protein phosphatases (KAPP), ARC1 (for Armadillo repeat containing protein 1) and thioredoxin *h*-like 1 and 2 (THL 1 and 2), that are known to interact with plant RLKs, mediate a complex SI signalling pathway (Braun *et al.*, 1997; Gu *et al.*, 1998; Stone *et al.*, 1999; van der Knaap, 1999).

A fundamental requirement of all receptor kinase systems is the strict regulation of receptor kinase activity so as to avoid spontaneous activation of signalling. Recent evidence indicates that SRK may be held in an inactive state by the actions of two thioredoxin-*h*-like proteins, THL1 and THL2 (Bower *et al.*, 1996; Cabrillac *et al.*, 2001). THL1 and THL2 prevent the constitutive activation of the SI-signalling cascade by interacting, in a phosphorylation-independent manner, with the SRK kinase domain and inhibiting autophosphorylation at specific serine residues (Bower *et al.*, 1996; Cabrillac *et al.*, 2001). Neither molecule is haplotype-specific, but each has different

expression patterns. *THL2* is expressed at high levels in the stigma, whereas *THL1* occurs in stems, leaves, petals, pollen as well as stigmas, albeit at lower levels than *THL2* (Bower *et al.*, 1996; Cabrillac *et al.*, 2001). *In vitro*, thioredoxin inhibition of *Brassica* SRK₃ was shown to be negated by the addition of S₃ pollen coat proteins (Cabrillac *et al.*, 2001). Whether this antagonistic reversible relationship between thioredoxin-inhibited SRK and SCR actually takes place *in planta* has yet to be determined. Goring and coworkers induced low-level constitutive SI rejection in the normally self-compatible *Brassica napus* cv. Westar, by generating transgenic plants that expressed antisense *THL1/2* (Haffani *et al.*, 2004). In mammalian cells, thioredoxins are known to inhibit specific kinases *in vitro* and *in vivo*. A well-described example is the physiological inhibition by thioredoxin of apoptosis signal-regulating kinase 1 (ASK1) (Saitoh, *et al.*, 1998). Expression of thioredoxin negatively regulates ASK1 kinase activity resulting in the inhibition of subsequent ASK1-dependent apoptosis, while inhibition of thioredoxin results in activation of endogenous ASK1.

The characteristic CGPC active site of thioredoxins is altered to CPPC in most members of the thioredoxin-*h* family, including in *THL1* and *THL2* (Mazzurco *et al.*, 2001). In both CGPC and CPPC active sites, the two external cysteine residues are essential for redox activity. However, it appears that only those members of the thioredoxin-*h* family that possess the CPPC active site are able to interact with SRKs, while those with the CGPC motif cannot (Mazzurco *et al.*, 2001). A conserved cysteine residue, Cys⁴⁶⁵, located within the last six residues of the SRK transmembrane domain, is essential for the interaction with *THL1* or *THL2*, as its deletion or substitution by serine is enough to abolish SRK interaction with *THL1* and *THL2* (Mazzurco *et al.*, 2001). Alternatively, when a cysteine is introduced at this position into SFR1 (for S gene Family Receptor Kinase 1, see Table 6.1), which does not normally interact with *THL1* and *THL2*, it gains the ability to interact with both thioredoxin-*h* molecules (Mazzurco *et al.*, 2001). Cys⁴⁶⁵ is required also in the target of the two *Arabidopsis* thioredoxin-*h* proteins TRX3 and TRX4, which also have CPPC active sites. Cys⁴⁶⁵ is present in all SRK molecules, but not in non-SRK S-domain-receptor kinases and may therefore be the specific residue controlling inhibition of SRK (Mazzurco *et al.*, 2001). Thioredoxins function mostly as protein disulphide oxidoreductases, down regulating the activity of proteins via the reduction of disulphide bonds (Holmgren, 1995). It therefore seems likely that Cys⁴⁶⁵ is involved in disulphide bonding, and that *THL1* and *THL2* may inhibit the formation of active SRK dimers/complexes by interfering with the molecular configuration in a localised part of the SRK molecule.

Kinase-associated protein phosphatase (KAPP) was initially identified in *Arabidopsis thaliana* (AtKAPP) but has since been identified in a growing number of monocot and dicot species (Smith and Walker, 1996; Li *et al.*, 1999). KAPPs interact specifically with RLKs and are thought to be key components in signal perception and transduction (Li *et al.*, 1999). The kinase interaction (KI) domain of KAPPs has been shown to interact in a phosphorylation-dependent manner with the catalytic domains of HAESA (RLK5) and CLV1 in *Arabidopsis thaliana* (Stone *et al.*, 1998), OsTMK of *Oryza sativa* (van der Knaap *et al.*, 1999) and KIK1 (KI interacting Kinase 1) in *Zea mays* (Braun *et al.*, 1997). Furthermore, the maize and *Arabidopsis* KAPP-KI domains have been shown to bind the catalytic domains of TMK1 and RLK4 of *Arabidopsis thaliana* (Chang *et al.*, 1992; Walker, 1993), and *Brassica* SRK-A14 (Glavin *et al.*, 1994), but not those of Xa21 of rice (van der Knaap *et al.*, 1999) and ZmPK1 or CRINKLY4 of maize (Becraft *et al.*, 1996; Braun *et al.*, 1997). The *Arabidopsis* KAPP-KI domain also interacts with WAK1 (Park *et al.*, 2001), FLS2 (Gómez-Gómez *et al.*, 2001) SERK1 (Shah *et al.*, 2002), BRI1 and BAK1 (Lee *et al.*, 2003), and the KI domain of OsKAPP (*Oryza sativa* KAPP) is phosphorylated by HAESA (RLK5) (van der Knaap *et al.*, 1999). These data suggest that KAPP-mediated signalling is highly conserved across dicot and monocot species, and probably functions in a multiple of signalling pathways in plants (Stone *et al.*, 1998; van der Knapp, *et al.*, 1999). However, the differing interaction affinities of the various KAPP and RLK molecules, suggest KAPP molecules have retained some level of specificity. Recently, a *Brassica oleracea* KAPP has been identified, and been shown to interact with, and dephosphorylate phosphorylated SRK (pSRK), and in turn become phosphorylated by SRK (Vanoosthuysse *et al.*, 2003).

KAPP molecules are type 2C protein phosphatases (PP2C) (Braun *et al.*, 1997). They are composed of three domains: a potential N-terminal type-I membrane anchor, a centrally-located KI domain, spanning amino acids 98-336, and a carboxyl-terminal type 2C (PP2C) catalytic domain, encompassing 119-amino-acid region, from residues 180 to 298, which constitutes the minimal KI domain (Lee *et al.*, 2003; van der Knaap *et al.*, 1999). Contained within these 119 amino acids is a forkhead-associated (FHA) domain (Lee *et al.*, 2003). Aside from plant KAPPs, which are FHA-containing proteins not located in the nucleus, FHA-containing proteins are nuclear proteins that influence transcription (Hoffmann and Bucher, 1995; Lee *et al.*, 2003). The KAPP-FHA motifs are 55-75 residues long with conserved glycine, arginine, serine, histidine and

asparagine residues that are essential for binding of the KI-FHA motif with the catalytic domain of phosphorylated RLKs (Lee *et al.*, 2003). Although no definitive role for KAPP KI domains has been established in any RLK-signalling pathway, Braun *et al.*, (1997) hypothesise a role for KI domains analogous to that of SH2 and PTB domains of animal RTKs (Appendix 1); however, KI domains bind via phosphoserines (P.Ser) and/or phosphothreonines (P.Thr) (and probably other additional residues) in ligand-activated RLKs, rather than phosphotyrosines (Lee *et al.*, 2003). SH2 and PTB domains are found in many different animal proteins where they are coupled to other domains such as protein kinases, protein phosphatases or protein-protein interaction domains (Braun *et al.*, 1997; Hunter, 1998). In the CLAVATA signalling system KAPP negatively regulates CLV1 through PP2C phosphatase activity *in vitro*, but how this is achieved *in planta* is not understood (Lee *et al.*, 2003; Stone *et al.*, 1998). Recently, the phospho-protein Bc-NDPK III (for *Brassica campestris* nucleoside diphosphate kinase III) was shown to be phosphorylated by SRK at specific serine residues (Matsushita *et al.*, 2002), suggesting that this phospho-protein also plays a role in the SI-phosphorylation cascade through its association with SRK.

The only molecules shown to have a definite role in the downstream SRK-signalling pathway is the Arm-repeat-containing protein 1 (ARC1) (Gu *et al.*, 1998; Stone *et al.*, 1999; Appendix 1) and *M* locus protein kinase (MLPK) (Murase *et al.*, 2004; Appendix 1). ARC1 is a positive regulator of the *Brassica* self-incompatibility system as the removal or down-regulation of ARC1 leads to the reduction or breakdown of *Brassica* SI (Stone *et al.*, 1999, 2003). ARC1 is a modular protein of 661 amino acids expressed specifically in *Brassica* stigmas and shown to interact with the kinase domain of *Brassica* SRKs in a phosphorylation-dependent manner, but not with kinase domains of *Arabidopsis* RLK4 (an S-domain RLK) or RLK5 (an LRR-RLK) (Gu *et al.*, 1998; Kim *et al.*, 2003). ARC1 binds to the kinase domain of phosphorylated SRK (pSRK) through an Arm-repeat region, at residues 277-582, located in the C-terminal half of the ARC1 molecule and is in turn phosphorylated by SRK (Gu *et al.*, 1998; Kim *et al.*, 2003). ARC1 also reacts with the kinase domain of *Brassica* SFR kinases suggesting its interactions may not be specific to SI receptor kinases, or that molecules with similar Arm-repeats interact with SFR kinases (Gu *et al.*, 1998; Mazzurco *et al.*, 2001).

ARC1 is a class-II plant U-box (PUB) protein (Azevedo *et al.*, 2001). Class-II PUBs are characterised by having a U-box (for UFD2-homology domain box. Appendix 1) and five potential Arm-repeats in their C termini, with each Arm-repeat containing a 42-residue leucine-rich motif (Stone *et al.*, 2003). The U-box is a highly conserved domain

containing ~70 amino acids that was first identified in the yeast UFD2 (for ubiquitin fusion degradation 2) protein and is known to be present in some 40 plant proteins (Azevedo *et al.*, 2001). The ARC1 U-box is located at residues 183-247 approximately 30 residues upstream from the start of the Arm-repeat region (Azevedo *et al.*, 2001; Kim *et al.*, 2003). In addition to the Arm-repeat-SRK binding site and the U-box, ARC1 also contains two putative protein-binding sites in the form of a Leu zipper domain, and a coiled-coil domain, and three topogenic signals in the form of a single nuclear location signal (NLS), and two nuclear export signals (NESs) that are located within the ARC1 U-box (Stone *et al.*, 2003). These seven components are hypothesised to participate in an ARC1-mediated self-incompatibility response, with the U-box and its two associated NESs being crucial for SI-mediated signalling (Stone *et al.*, 2003). The U-box is a degenerate version of the RING-finger domain and functions in a similar manner by forming E3-ligase complexes (see below) that mediate ubiquitination of protein substrates (Aravind and Koonin, 2000; Azevedo *et al.*, 2001). Ubiquitination involves the use of small (~76 residue) highly conserved ubiquitin proteins as tags to target proteins for proteasome degradation (Hershko and Ciechanover, 1998; Aravind and Koonin, 2000; Conaway *et al.*, 2002). There are five distinct eukaryote ubiquitin systems each using different ubiquitin-like proteins, ubiquitin-conjugating enzymes, and targeting different substrates (Wilkinson, 1999). A common chemistry in all ubiquitin systems is the covalent conjugation of a repetitive chain of ubiquitin molecules to lysines in a target protein, through a multi-step, multi-enzyme coordinated cascade (Conaway *et al.*, 2002). Conjugation of a ubiquitin molecule includes three stages; (i) adenylation by an activating enzyme designated E1 (ubiquitin-activating enzyme), (ii) transfer, as a thiol ester, to a conjugating enzyme designated E2 (ubiquitin-conjugating enzyme), and (iii) attachment to a target protein by a ligase designated E3 (ubiquitin ligase) (Wilkinson, 1999; Kao and Tsukamoto, 2004). ARC1 has been identified as an E3 ubiquitin-ligase that ubiquitinates proteins via its U-box (Stone *et al.*, 2003; Moon *et al.*, 2004).

The detailed work of Stone *et al.* (2003) led them to the following hypothesis on the action of ARC1 in the *Brassica* SI response. When SRK is inactive, ARC1 can be found in the nucleus courtesy of its NLS, but is located predominantly in the cytosol due to the presence of its two NESs and the XPO nuclear export pathway. On ligand binding, SRK becomes phosphorylated. pSRK then mediates phosphorylation of ARC1 causing the targeting function of NLS to be inhibited. This results in the relocalisation of ARC1 from the cytosol to 26S proteasomes at the cytosolic face of the endoplasmic reticulum (ER). A functioning U-box containing both NESs is essential for

pSRK-activated relocation of ARC1 to the ER. Since ARC1 has E3 ubiquitin-ligase activity, it is envisaged that ARC1 first ubiquitinates its substrates via its U-box and then carries these ubiquitinated molecules to the proteasome for degradation. The Leu zipper and the coiled-coil protein-protein-interaction domains may facilitate binding of substrate molecules while ARC1 associates via its U-box motif with the E2 thiol-ester-conjugating enzyme. A large number of ubiquitinated proteins have been detected after self-incompatible pollinations suggesting that pSRK-activated ARC1 targets more than one substrate for ubiquitination. Self-incompatibility is contingent on the degradation of these ARC1 substrates (Stone *et al.*, 2003). Since the discovery of ARC1 and its putative function in SI, PUBs have been identified in other plants. Kim *et al* (2003) identified the class-II PUB, *NtPUB4* (for *Nicotiana tabacum* PUB4) in tobacco that interacts specifically via its Arm-repeats with CHRK1. Fujita *et al* (2003) isolated a MADS-box protein, AGL24 (for Agamous-like 24) that appears to be a substrate of MRLK, and demonstrated that MRLK-signalling induces the translocation of AGL24 from the cytoplasm to the nucleus in a phosphorylation-dependent manner.

It is interesting to note that the rejection reaction in SSI and RNase-mediated GSI, incorporate 26S ubiquitination of target proteins albeit through different molecules, and also that ARC1 and SLF, an F-box protein are E3 ligases. Ubiquitination may well prove to be a fundamental component of other SI system such as in the Papaveraceae.

A second molecule, *M* locus protein kinase (MLPK), also positively regulates *Brassica* SI through down-stream mediation of SRK signalling (Murase *et al.*, 2004). The *Brassica M* locus constitutes a 50-kb region of the *Brassica* genome consisting of 12 putative open reading frames (ORFs) A to L, and segregates independently of the *Brassica S* locus (Goring and Walker, 2004). *MPLK* is an eight-exon, seven-intron gene located at ORF-G of the *M* locus, and predicts a 404-residue receptor-like cytoplasmic kinase (RLCK) that has no apparent signal sequence or transmembrane domain. The deduced protein starts with the myristoylation motif Met-Gly-XXX-Ser/Thr(Arg) [MGXXXS/T(R)], followed by a 30-residue serine-rich domain and a large kinase domain composed of 11 subdomains (Murase *et al.*, 2004). *MPLK* is expressed predominantly in the stigma, where it is localised to the plasma membrane of cells via its myristoylation motif (McCabe and Berthiaume, 1999; Murase *et al.*, 2004). Like SRK, its expression increases with the onset of self-incompatibility and reaches a maximum one day before anthesis. *MLPK* exhibits autophosphorylation at specific serine and threonine residues, with a single arginine substitution of the highly

conserved Gly¹⁹⁴ in kinase subdomain VIa sufficient to remove MLPK autophosphorylation, and to result in the loss of MLPK kinase activity and MPLK protein expression (Murase *et al.*, 2004).

The hypothesis proposed by Stone *et al* (2003) offers a model to explain the role of ARC1 in SI signalling, but the hypothesis does not suggest a role for the interaction of KAPP and/or THL1 and THL2 with SRK, or how MLPK and ARC1 interact in the SRK signalling cascade. Vansoosthyse *et al.*, (2003) suggest that THL1 and THL2, which interact with SRK in a phosphorylation-independent manner, inhibit SRK in its basal state and KAPP, which interacts with pSRK may function to down-regulate activated SRK. Vansoosthyse *et al.*, (2003) identified two proteins, calmodulin and SNX1 (for sorting nexin 1) that interact with SRK in a phosphorylation-independent manner suggesting that these proteins play a general role in signal transduction, but are not specific to SI signalling.

The targets of ARC1 ubiquitination have not been identified. They could be the different molecules required for the successful germination, penetration and growth of pollen tubes, or transcription factors that regulate genes expressing proteins specific for successful pollination. It is also possible for ubiquitin-dependent proteolysis to activate transcription factors, such as occurs in the Toll-like receptor (TLR)-stimulated NF κ B (for nuclear factor *kappa* B) pathway that is responsible for the activation of many genes concerned with the regulation of the human immune system (Wilkinson, 1999; Imler and Hoffmann, 2001). In this pathway, I κ B (for inhibitory *k*B protein) inhibits the action of the transcription factor NF κ B by binding it in the inactive complex I κ B-NF κ B. Activation of the transcription factor is achieved through ubiquitin-dependent proteolysis, in which a kinase phosphorylates two specific serines on I κ B causing it to dissociate from the inactive I κ B-NF κ B complex. The dissociated I κ B is ubiquitinated and degraded, while the liberated NF κ B molecule is transported to the nucleus where it activates a large number of genes (Wilkinson, 1999; Imler and Hofman, 2001). Interestingly, MLPK is a receptor-like cytoplasmic kinase related most closely to the *Drosophila* Pelle receptor-like cytoplasmic kinase (Shiu and Bleecker, 2001, 2003). Pelle acts downstream of the *Drosophila* Toll receptor to activate both dorsoventral patterning in the *Drosophila* embryo and the anti-fungal response in larvae and adults. Pelle is a death-domain-containing protein, and interacts through this domain with other death-domain proteins to form a Toll receptor-adaptor complex. Ligand activation of the Toll receptor in adult *Drosophila* triggers Pelle-mediated phosphorylation of the inhibitory protein Cactus. Cactus is complexed with the

transcription factor DIF (for Dorsal-related immune factor). Phosphorylated Cactus dissociates from this complex and is degraded by the proteasome. The liberated DIF is then translocated to the nucleus where it induces synthesis of the anti-fungal peptide drosomycin.

MLPK and ARC1 may function similarly to Pelle in *Brassica* SI signalling, by forming an SRK-ARC1-MLPK adaptor complex (Imler and Hofman, 2001). It has been suggested that MLPK and pSRK form an SRK-MLPK signalling complex that when phosphorylated, leads to the activation of a kinase partner and the establishment of binding sites for downstream signaling components (Goring and Walker, 2004). However, following the Pelle scenario described above, ligand activation of the *Brassica* SRK receptor domain could trigger SRK-MLPK-mediated phosphorylation and dissociation of an inhibitory protein complexed to a transcription factor. Phosphorylation of this inhibitory protein may target it for ARC1-mediated proteasome 26S degradation, while the liberated transcription factor translocates to the nucleus and activates genes that bring about the *Brassica* SI response.

It is becoming apparent that ligand-activated RLK signalling pathways may be as complicated as their animal analogues, and like their animal counterparts, RLKs probably phosphorylate a set of substrate molecules at several phosphoserine and/or phosphothreonine residues. Models from animal systems predict the participation of modular proteins containing from one to several specific binding domains that interact with specific regions of the receptor kinase domain. Identification of the various domains of ARC1 supports these predictions and it is likely that other SRK substrates will show similar sophistication. These multiple interaction sites may initiate several SI-specific signalling pathways that co-operatively bring about a self-incompatibility response, or they may serve to interact with other non-SI specific biochemical pathways that indirectly bring about an SI response, as appears is the case with ARC1 (Stone *et al.*, 2003). Future progress in the understanding of the SI signalling pathway is contingent on identification of further downstream components of SRK signalling, and from examination of signalling cascades from other plant receptor kinase systems.

1.6. – Ecology of Mexico: a general overview

1.6.1 – Physical geography of Mexico

In Mexico, the major ecological barriers to species distribution are the various massive mountain ranges, the Gulf of California and the northern desert regions (Figures 1.15 and 1.16). The Sierra Madre Occidental and Sierra Madre Oriental mountain ranges

run north-south along the western and eastern coasts of Mexico respectively. The Sierra Madre Occidental is approximately 500 kilometres wide and has an average elevation of 3000 metres and a maximum height of 4340 metres. It runs from Rio Grande de Santiago, in the state of Jalisco, north through the Mexican states of Sonora and Chihuahua, and into southern Texas, USA. Its western slopes traverse 100 to 400 kilometres through rugged canyons and narrow ridges as they descend to the Pacific coastal plain, and receive more rainfall and have milder winters than the slopes on its eastern side. The eastern side of the Sierra Madre Occidental rises sharply to an average altitude of ~4000 metres forming an ecological barrier that separates the west coast from the rest of Mexico (Figure 1.16, maps A and B). The Sierra Madre Oriental is a narrower shorter less-elevated mountain range, approximately 300 kilometres wide, with an average elevation of 2100 metres and a maximum height of 3960 metres. It forms the eastern escarpment of the Mexican Plateau and runs parallel to the Gulf of Mexico for about 1100 kilometres through the states of Coahuila, Tamaulipas, Nuevo León, San Luis Potosí, Queretaro and Guanajuato. It is the southern most extension of the Rocky Mountains of Canada and the USA (Figure 1.17, maps A and B). Its northeastern slopes have a humid temperate climate, with its wettest climates supporting vegetation of cloud forests. Its western slopes are drier with a more sub-humid temperate climate (Figure 1.17). The Sierra Madre Sur in the south traverses most of the states of Guerrero and Oaxaca. It has a complex geology and diverse topography and an altitude that ranges from 100 to 3500 metres. The climate at its highest elevations ranges from temperate to sub-humid, with heavy summer rains. Its continental and Pacific slopes are steep and covered with oak forests ranging in altitude from 1900 to 2500 metres, cloud forests at 2300 metres, and pine-oak forests and pine forests at altitudes between 2400 and 2500 metres (Rzedowski 1978; Ferrusquía-Villafranca, 1993; Figures 1.15-1.16). The Cordillera Neovolcánica (the Transvolcanic Belt), the most populated, urbanised and industrialised region of Mexico, runs west to east across the entire country at the latitude of Mexico City (17°30'-20°25'N). The middle section of the Transvolcanic Belt is ~100 km wide and ~650 km long and contains 13 of the highest peaks in Mexico, the highest being Pico de Orizaba or Citlaltépetl (~5700 m), Popocatepetl (5452 m), Ixtaccíhuatl (5286 m) and Nevado de Toluca or Zinantécatl (4392 m) (Ferrusquía-Villafranca, 1993).



Figure 1.16 Generalised plan of Mexico - showing the distribution of desert, grassland, forest and mountain environments. The main mountain regions are; the Transvolcanic Mountain Belt, which links the Sierra Madre Occidental and Sierra Madre Oriental; the Macizo (massive) de Oaxaca (1), which links the Sierra Madre Sur with the Transvolcanic Belt; the Sierra Madre de Chiapas (2) and the Sierra de San Cristóbal (3) in the south; and the Sierra de Juárez and San Pedro Mártir in Baja California (4). The Balsas Basin (or Depression) (5), which lies on the southside of the Transvolcanic Belt runs west to east across a vast, relatively flat, terrain at an average height of 1000 metres, but also has valleys that descend to 200 metres and a few scattered mountain peaks at 2000 metres. The climate of the Balsas Basin is sub-humid tropical with annual precipitation of <1200 mm and severe dry seasons of up to 8 months. Its topography and climate acts as an ecological buffer zone separating the mountain flora of the Transvolcanic Belt from that of the Sierra Madre Sur. Two of the largest inland water ecoregions of Mexico, the Lago de Chapala and the smaller Lago de Cuitzeo lie between the Transvolcanic Belt and the southern end of the Sierra Madre Occidental. The Sierra Madre Occidental, Oriental and the Transvolcanic Belt create the western, eastern and southern escarpments of the Central Plateau respectively. Geologically, the Central Plateau is a continuation of the Basin and Range region of the U.S., and consists of a series of basins separated by small scattered mountain ranges (Figure 1.17, map A). The Buried Ranges of north-west Mexico are an extension of the Basin and Range region of Arizona (USA), but have become buried by westward outwashes of debris from Sierra Madre Occidental) (Ferrusquía-Villafranca, 1993). The northern dry zone consisting of the Sonoran and Chihuahuan Deserts is separated into two distinct climatic regions by the northern extension of the Sierra Madre Occidental. On the west, the Sonoran Desert extends northwards into the southern part of Arizona and part of California, and also into the Baja California peninsula, while the Chihuahuan Desert on the east extends into the extreme west of Texas and part of New Mexico. The Chihuahuan Desert is part of the northern extension of Central Plateau. It has a high average elevation of ~2000 m. and as a result, experiences cool winters with periodic frosts. (NB, only the Mexican parts of the Sonoran and Chihuahuan deserts, and the Mexican part of the Sierra Madre Occidental are highlighted in the figure. (Figure 1.16 amended from © maps.com)

The Transvolcanic Belt (TVB) is bordered on its northern side by a series of high basins and on the south the land drops sharply to the sub-humid tropical Balsas Depression, dominated by lowland deciduous forests of *Bursera* and *Ipomoea* species, with some cacti in its semi-arid regions (Figures 1.15; 1.16 map A and 1.17 map A). The Macizo de Oaxaca (Oaxaca Massive) runs north-south from the eastern end of the TVB to the eastern end of the Sierra Madre Sur and includes the Sierra Madre de Oaxaca, and the Sierra Norte de Oaxaca Mountains (Figure 1.16 and 1.16; map A). heavily mineralised area in Mexico and one of the great mining zones of the world (Ferrusquía-Villafranca, 1993).

The mountain ranges of Mexico create an ecological conduit, with the Oaxaca Massive linking the Sierra Madre Sur to the TVB, and the latter linking the Sierra Madres Occidental, Oriental and the Central Mexican Plateau (Figure 1.16 and 1.16; map A). The Mexican Central Plateau has an average elevation of ~2000 metres and extends southward from the U.S.A. through the Chihuahuan desert as far as the latitude of Mexico City (17°30'-20°25'N). It is the most

The Baja California peninsula and the northern states of Sonora, Chihuahua and eastern Coahuila constitute the main desert region of Mexico. The northern desert region of mainland Mexico is divided by the Sierra Madre Occidental into two climatically-distinct areas. On the western divide is the dry Sonoran Desert and on the east, the less dry Chihuahuan Desert (Figure 1.17). Over half the territory of Mexico is more than 900 metres above sea level, with only 35% of the land surface below 500 m. These lowland regions are located chiefly along the Gulf coastal plains of the states of Tamaulipas, Veracruz and Tabasco, and in the Yucatan peninsula (Rzedowski, 1978; Heckadon, 1992; Ferrusquía-Villafranca, 1993; Figure 1.18 maps A and B). Mexico has few navigable rivers, but has several large lakes associated with the valleys of mountain ranges on the western side of the country. Most of the rivers of Mexico are short and run from mountain ranges to the coast (Ferrusquía-Villafranca, 1993). Mexico's geology can be divided into five physical regions. (1) Baja California and the Buried Ranges of north-west Mexico; (2) the Central Plateau and the bordering Sierra Madre Occidental and Oriental; (3) the Gulf Coast Plain and Yucatán Peninsula; (4) the Trans-Mexican Volcanic Belt (Transvolcanic Belt) and (5) the Highlands of Southern Mexico (Figure 1.17)



Figure 1.17 – Physical maps of Mexico. Map A - topology of Mexico, map B – main geological regions of Mexico

Most parts of Mexico experience two seasons; the wet season from June to September and the dry season from October to May, although May and October can also be moist. Mexico shows great variation in precipitation, with some regions experiencing <50 mm average annual precipitation (aap) with no wet season, as occurs in parts of Baja California, while parts of Tabasco and Chiapas experience annual rainfall exceeding 5500 mm with no dry season (Rzedowski, 1973; Lot *et al.*, 1993). Dry climates occur in the north and in the Baja California peninsula that has 200 -500 mm aap, with a lower precipitation in the western Sonoran Desert (200-250 mm) than in the eastern Cihuahuan Desert (300-500 mm) (Rzedowski, 1973; Figure 1.18, map A). Humid environments start from south-east of San Luis Potosí and extend through most of the territory of the states of Veracruz and Tabasco to the Yucatán Peninsula, and include northern Chiapas and parts of Oaxaca, Puebla and Hidalgo (Figure 1.18, map A; Figure 1.1). In these states abundant annual rainfall of 4000 mm are associated with the south-eastern slopes of the Sierra Madre Oriental and the hills north of Oaxaca and Chiapas (Rzedowski, 1973; Figure 1.18, map A). Temperate climates are confined to the mountain ranges of the three Sierra Madres, the Transvolcanic Belt, the Macizo de Oaxaca and mountains of the Central American Mountain chain (Figures 1.15; 1.17, map A; 1.18). The distribution of annual rainfall varies greatly across Mexico. On the Atlantic slopes and in large areas of northern Mexico, between ~5% and 20% of the annual precipitation falls as “winter” rainfall during the dry season (October-May), while the Pacific coastal region from Sinaloa to Chiapas is completely dry throughout November to April (García 1973; Turner and Nesom, 1993).

Average annual temperatures in Mexico are determined by altitude. Higher annual temperatures are associated with lowland coastal regions and cooler temperatures occur inland, at higher altitudes (Figure 1.18, map B). The average temperature for Mexico ranges from 10–28°C, although sub-zero temperatures of -6°C occur on the summits of the highest mountains. In contrast, the low-lying regions of the Yucatan peninsula and the southern pacific coastal zones maintain high constant annual temperatures between 28-30°C (García, 1973; Figure 1.18, map B). Mexico exhibits great variations in climate (Figure 1.18, map A). The climatic diversity of Mexico is determined by its great size (2 million km²), altitude range (0-5000 m), considerable north-south extension, and its latitudinal location traversing the Tropic of Cancer. In addition, the narrowness of its continental mass means the Pacific and Atlantic Oceans influence considerably the Mexican climate (Heckadon, 1992). The Tropic of Cancer not only marks the intersection of the neoarctic and neotropical

biogeographical regions, but also aligns approximately with the transitional strip of Mexico that separates the semi-arid climates governed by anticyclone high pressures in the north, from the humid and semi-humid climates of the south that are influenced predominantly by cyclones and trade winds from the north and east (García, 1973; Turner and Nesom, 1993). Except for Sonora and most of Baja California, the Atlantic and Pacific coasts of Mexico are in the pathway of tropical cyclones. The cyclones originate on the high seas from June to October and generate hurricane-type winds that cause destruction to coastal areas and windward mountain slopes. Cyclones are important also as they carry great quantities of moisture, which precipitate over vast areas of inland Mexico (García, 1973).

Mexico is divided into six zonal habitats based on the distribution of vegetation and climate (Rzedowski 1973, 1978; Toledo and Ordóñez, 1993; Toledo, 1995; Figure 1.18, map A and Figure 1.19). The six natural Mexican terrestrial habitats, defined by climate, biogeography, ecology and vegetation are; (1) humid (and warm) tropical, (2) sub-humid (and warm) tropical, (3) humid temperate, (4) sub-humid temperate, (5) arid/semi-arid and (6) alpine (Figure 1.18 map A). In addition to the six terrestrial zonal habitats, a seventh wetland zone, of aquatic and sub-aquatic flora, should be included. These wetland zones include interior (or continental) bodies of water such as rivers, lakes, inland swamps, and coastal waters such as lagoons and tidal swamps (Lankford, 1977; Scott and Carbonell, 1986; Lot *et al.*, 1993; Figure 1.19). In broad terms, arid scrubland and semi-arid temperate grassland predominate in northern Mexico, with humid and sub-humid tropical forest along the coastal plains of the Gulf of Mexico and the Yucatan peninsula. The mountain regions of Mexico are characterised by pine and evergreen oak forests interspersed with grassland. At higher altitudes, brushwood vegetation composed mainly of shrubs and small trees, gives way to alpine habitats of the high mountain peaks composed of high altitude grasses known as zacatonales or páramos (Rzedowski 1973, 1978; Toledo and Ordóñez, 1993; Toledo, 1995; Figure 1.18, map A and Figure 1.19).

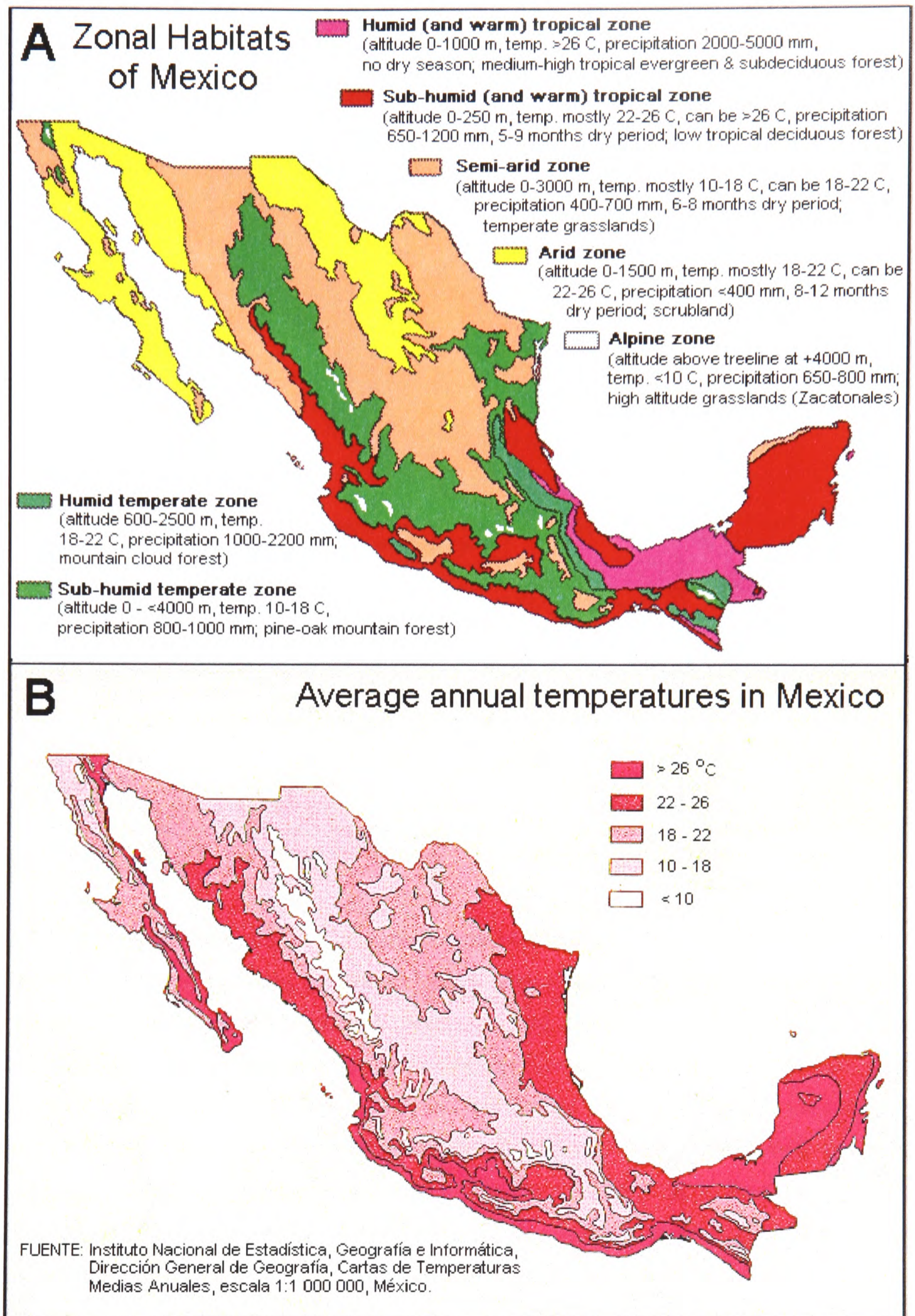


Figure 1.18 - Climate Maps of Mexico
Map A – Zonal Habitat of Mexico. **Map B** – Average annual temperatures in Mexico (°C.)
 (Scale = 1:1 000 000)

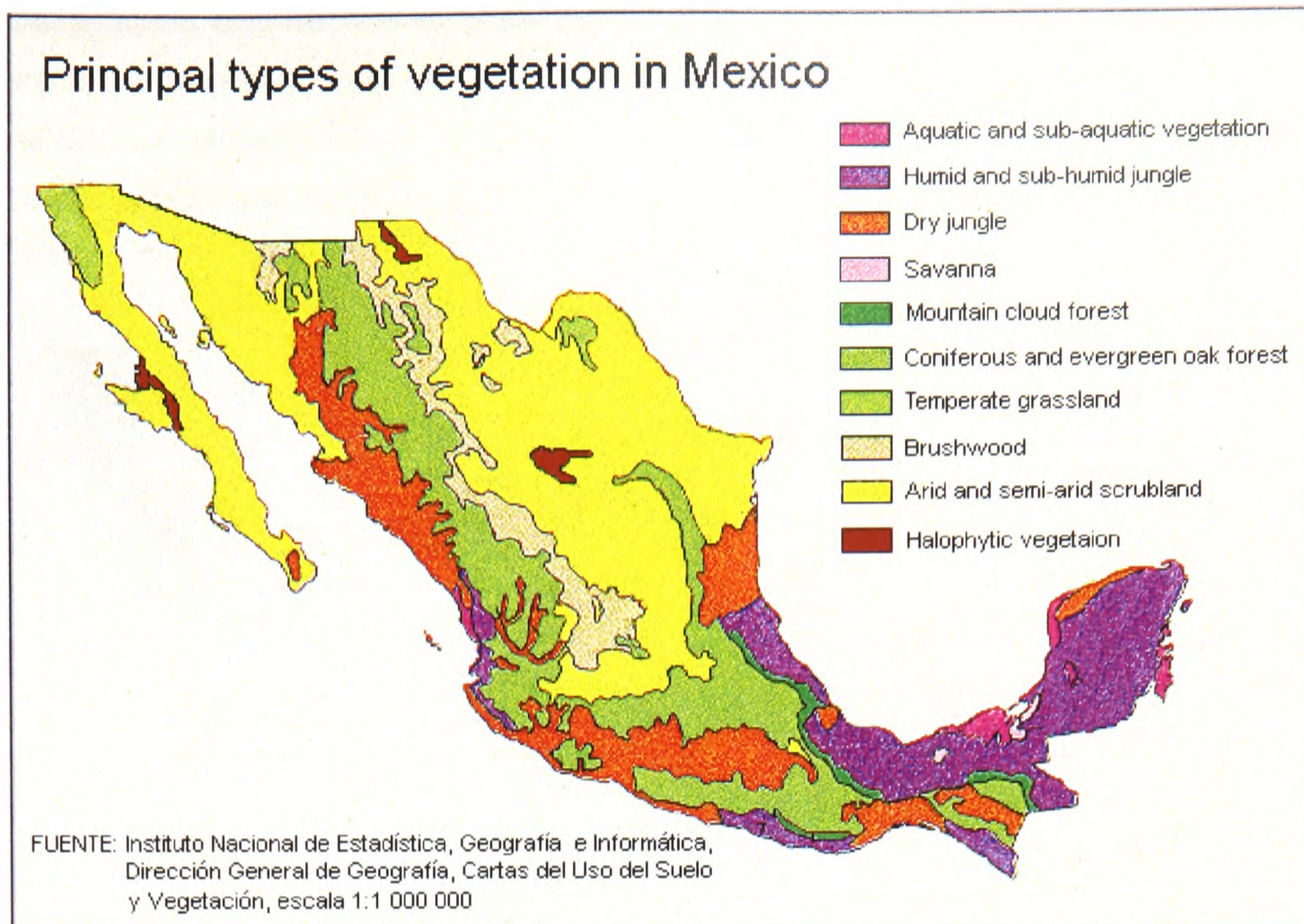


Figure 1.19 – Map of the principal types of vegetation in Mexico

Dry climates predominate in the north of Mexico and support tropical thorn forest typical of dry jungle and scrubland of arid/semi-arid environments. The humid climates along the eastern coast and in the Yucatan peninsula allow the growth of wet jungle vegetation consisting of high tropical evergreen forest to moderately high semi-evergreen forest, and medium-high tropical subdeciduous forest to low tropical deciduous forest. The mountain ranges are covered predominantly with pine-evergreen oak forest and grassland, with brushwood environments of shrubs and small trees occurring at higher altitudes on the eastern peaks of the Sierra Madre Occidental. The humid temperate vegetation of mountain cloud forest is restricted to a narrow inland area of south eastern Mexico that traverses the states of Puebla, Veracruz, and Oaxaca. Savanna environments in Mexico are rare and restricted to three small areas in the south west tip of Chiapas and the costal enclave in Campeche. The alpine zone of high altitude grasslands that occurs on the peaks of the 12 highest mountains at +4000 metres are not shown in this map)

1.6.2 – Floristic richness and megadiversity of Mexico

The flora of Mexico is rich, and ranks fourth after Brazil, Columbia and China as the country with the highest number of vascular plant species (Mittermeier, 1988; Dirzo and Gómez, 1996). The National Council of the Floras of Mexico, a consortium of 40 Mexican institutions created in 1975, is responsible for producing an inventory of Mexican flora, which presently consists of 20 regional floras, 2,100 000 botanical specimens and numerous checklists and florulas (Gentry, 1978; Rzedowski, 1991; Toledo and Ordóñez, 1993; Toledo and Sosa, 1993; Figure 1.20). The floristic knowledge of Mexico is still incomplete, as many isolated environments have yet to be surveyed (Figure 1.20). Estimates of the entire flora of Mexico range from 19, 500 (Dirzo and Gómez, 1996), through 22, 000 (Rzedowski, 1993) and 26, 000 (Gómez-Pompa *et al.*, 1994) to 30, 000 (Toledo, 1995) species of vascular plants, with six plant families constituting almost 40% of this flora (Table 1.6). Of these six families, the Asteraceae, Poaceae and Cactaceae predominate in north and central Mexico, the

Orchidaceae and Rubiaceae show greater diversity in the south, while the Fabaceae are found in greater abundance in the warmer wetter regions particularly in the sub-humid tropical Balsas Basin (Williams, 1956; Scott and Carbonell, 1986; Toledo, 1985; Toledo and Sosa, 1993; Turner and Nesom, 1993; Valdés-Reyna and Cabral-Cordero, 1993).

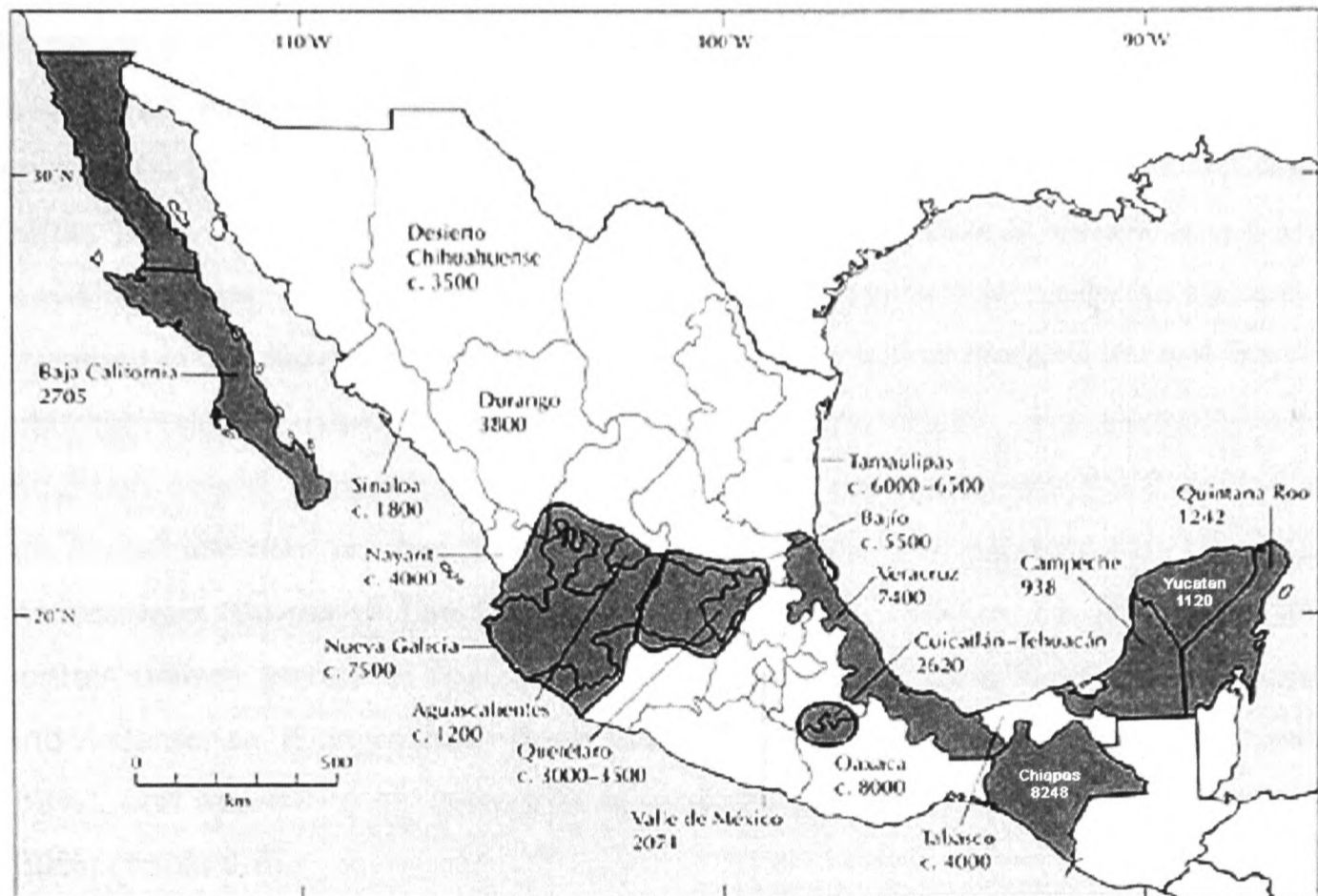


Figure 1.20 – Map showing floristic diversity in the 20 main floristic treatments of Mexico. (© World Wide Fund for Nature 1997). Chiapas, Oaxaca and Veracruz are the states with the highest concentrations of species. A significantly lower number of species occur on the Yucatán Peninsula, which traverses the states of Yucatán, Quintana Roo and Campeche. The shaded areas represent the specific floristic macro-regions of Baja California, Nueva Galicia, Veracruz; Cuicatlán, Chiapas and Yucatan (Rzedowski, 1993; Centres of Plant Diversity website 2004: The Americas)

Table 1.6. Best-represented plant families in Mexico

Family	Number of genera	Number of species
Asteraceae (Compositae)	314	2400
Fabaceae (Leguminosae)	130	1800
Poaceae (Gramineae)	170	950
Orchidaceae	140	920
Cactaceae	70	900
Rubiaceae	80	510
Total	904	7480
Total number of vascular plants in Mexico	2410	20 000 - 30 000

(Source: Centres of Plant Diversity website 2004: The Americas; Williams, 1956; Scott and Carbonell, 1986; Toledo, 1985; Toledo and Sosa, 1993; Turner and Nesom, 1993; Valdés-Reyna and Cabral-Cordero, 1993. Number of genera and species are approximations)

The Mexican flora contains a large number of endemics, with Mexican angiosperms exhibiting 12% endemism at the genus level (283 genera) and 50-60% at the species level (~10 000-18 000 species) (Ramamoorthy and Lorence, 1987; Rzedowski, 1993). Endemic species of flowering plants are found in greater abundance in the sub-humid temperate areas (70% endemism), arid and semi-arid areas (60% endemism) and to a lesser degree in sub-humid tropical areas (40% endemism) and humid temperate areas (30% endemism), while the humid tropical lowlands have a relatively low level of endemism (5% endemism) (Rzedowski, 1991; Centres of Plant Diversity Website, 2004; Table 1.7). Consequently, endemism is highest among shrubs and perennial terrestrial herbs, and lowest in lianas and aquatic plants, with endemic genera more prevalent in the drier climatic regions of the northern half of the country and the Pacific mountain slopes, than in the wetter regions in the south, and along the Atlantic mountain slopes (Rzedowski, 1991). All Mexican sub-humid mountain environments are floristically rich, but the Sierra Madre Occidental, Sierra Madre Sur, the TVB and the southern Sierras of San Cristóbal and Madre de Chiapas are especially rich and contain unique groups of species (Styles, 1993; Figure 1.20). Cactaceae, Rubiaceae and Asteraceae (Compositae) have the highest average level of species endemism (69%), and approximately twice that of Orchidaceae (35%) and Poaceae (Gramineae) (30%) (Table 1.8).

Table 1.7. Plant diversity and endemism versus ecological zones of Mexico

Ecological zone	Number of species	Number of endemic species	Percentage endemic species
1. Humid tropical	5000	250	5
2. Su-bhumid tropical	6000	2400	40
3. Humid temperate	3000	900	30
4. Sub-humid temperate	7000	4900	70
5. Arid/Semi-arid	6000	3600	60
6. Alpine	(included in others)		---
7. Aquatic	1000	150	15
Others (including Alpine, halophytic etc)	2000	400	20

(Source: Toledo *et al.*, 1989; Centres of Plant Diversity website 2004: The Americas).

Table 1.8. Approximate percentage of Mexican endemism in some families of flowering plants

Family	Genera (%)	Species (%)
Cactaceae	36	72
Rubiaceae	14	69
Asteraceae (Compositae)	14	66
Orchidaceae	8	35
Poaceae (Gramineae)	6	30
Malvaceae	5	48
Fabaceae (Leguminosae)	2	52
Burseraceae	20	89
Bignoniaceae	0	1
Hernandiaceae	0	0
Taxaceae	0	100
Lacandoniaceae	100	100

(Source: Rzedowski, 1991)

“Biological diversity of a region is a consequence of factors that promote the appearance of novel phenotypes, facilitate the accumulation of these phenotypes, and operate over a significant period of geological time” (Graham, 1993). The biodiversity and high level of endemism in Mexico may be explained by the existence of several distinctive and large ecological islands and also to its geological history. Mexico existed as a peninsula of North America during most of the Tertiary period, 65 to 1.6 million years ago (mya.), until ~4 to 2 mya when the formation of the Isthmus of Panama joined North and South America (Graham, 1993). During the 60 million years in which Mexico was a peninsula, it experienced severe variations in climate, in contrast to the more constant climatic conditions that prevailed in the wider parts of the North American continent, creating a diversity of climatically distinct habitats able to promote and support novel phenotypes. During the warm climates that occurred between the Paleocene epoch (~65 to 58 mya.) and early Miocene epoch (~24 to 5 mya.), as South America drew closer to North America, Mexico experienced progressive introductions of tropical biota from the south (Graham, 1993). Later, as global temperatures dropped during the mid-Miocene to Pleistocene (1.6 to 0.01 mya.), Mexico received repeated influxes of temperate biota from the north, and so the megadiversity of Mexico has been created from influxes of biota from northern and southern biogeographical regions (Graham, 1993)

The most influential geological factor shaping the megadiversity of Mexico has been the uplifting of the Transvolcanic Mountain Belt (TVB), one of the most important biogeographical areas of Mexico (Graham, 1993). The TVB began to rise in the early Tertiary period (~65 mya), but experienced its most extensive period of elevation and

deformation during volcanic activity of the last 1.6 million years, creating a complex of altitudinal microhabitats. The Sierra Madre Oriental and Sierra Madre Occidental have also aided Mexico's megadiversity, as these mountain ranges are known to have supported a variety of plant communities since late Cretaceous/early Paleocene (Graham, 1993). The north-south orientation of the two mountain ranges creates contrasting conditions on coastal- and continental-facing slopes, and both mountain ranges have acted as conduits for the migration and speciation of northern temperate biota.

The megadiversity of the Mexican flora and fauna, and the high level of endemism identify this region as a place of origin and/or development of a great number of plant groups (Rzedowski 1993). For example, the Cactaceae are of South American origin, but show greatest diversity in Mexico (Rzedowski 1993). The Asteraceae has more genera and species in Mexico than any other country, and this number includes more than 40 endemic genera (Turner and Nesom 1993). The grasses (Poaceae), Cucurbitaceae, Fabaceae (Leguminosae), Fouquieriaceae, Onagraceae, Rhamnaceae, Scrophulariaceae, Gesneriaceae and Rubiaceae contain many examples of genera whose diversity is concentrated almost entirely in Mexico (Rzedowski 1993; Stebbins 1975). Furthermore, many crop plants have their origins in Mexico, and a large portion of the gene belt that encircles the world, between the Tropics of Cancer and Capricorn, is located in Mexico. These data, and the radiation in mammals, birds and several reptiles suggest Mexico is a place of origin for many plant and animal groups, and identifies it also as an active centre of speciation (Ramamoorthy *et al.*, 1993). Mexico is unique not only for its diverse topography and climate, but also as a megadiversity country and a centre of agricultural origin that occupies a large region of the World's gene belt (Ramamoorthy *et al.*, 1993).

1.6.3 – Loss of biodiversity in Mexico

Loss of biodiversity in Mexico has occurred principally through deforestation. Over the past 200 years, forests have been lost to cattle ranching (pasture), agriculture, mining, timber extraction, urban expansion and road building, and has led to a present total annual deforestation rate of 1.5% (Masera *et al.*, 1997; Tables 1.9 and 1.10). Much of the forest region of Mexico, and in particular the temperate mountain forests in which atrosanguinate-type *Cosmos* species grow, was destroyed during 19th and 20th centuries. Logging of the pine-oak forests of Sierra Madre Occidental started in the 1880s and proceeded continuously until late into the 20th century, so that only 0.61% of the original pine-oak forest of this region now remains (Lammertink *et al.* 1997). The

pine-oak forest of the Transvolcanic Belt has suffered similar levels of destruction with only ~3.5% of the original forest remaining (Challenger, 1998). In addition, almost half the population of Mexico lives in the states encompassed by the Transvolcanic Belt, and the pine-oak forests of this region has consequently suffered losses due to a combination of land clearance and pollution from large urban conurbations (Toledo *et al.* 1989). The gentler terrain of the Sierra Madre Oriental has experienced centuries of logging and cultivation, resulting in almost totally elimination of its native pine-oak forests. Nearly half the coniferous and broad-leaved temperate forest of Mexico was removed by fire, the usual method being the traditional practice of burning down the lower stratum of the forest to provide pasture land for cattle (Rzedowski, 1988; Table 1.10). It is this practice that has been the most significant threat to pine-oak forest with ~80% of fire loss in these ecoregions due to this method of land clearance (Rzedowski, 1988).

Table 1.9. Deforestation rate by forest type

Forest type	Estimated area (km²)	Deforestation km²/yr)	Deforestation rate (%/yr)
Temperate coniferous	169 000	1630	0.96
Temperate broadleaved	88 000	820	0.93
Tropical evergreen	97 000	2370	2.44
Tropical deciduous	161 000	3220	2.00
Total	515 000	8040	1.56

(Source: Centres of Plant Diversity website 2004 after Masera, *et al.*, 1997).

Table 1.10. Types of forest and causes of deforestation (%)

Forest type	Causes of Deforestation versus Percentage Annual Deforestation				
	Pasture	Agriculture	Timber extraction	Fire	Other*
Temperate coniferous	28	16	5	49	3
Temperate broadleaved	28	17	5	47	3
Tropical evergreen	58	10	2	22	7
Tropical deciduous	57	14	5	7	16
All forests	49	13	4	24	10

(Source: Centres of Plant Diversity website 2004 after Masera, *et al.*, 1997. *Others includes erosion, road building, urban development etc).

1.6.4 - Summary

The floristic richness of Mexico and its high level of endemism is a consequence of its unique topological and climatic factors, and its access to temperate and tropical biota (Graham, 1993). However, the biodiversity of Mexico has been reduced dramatically through deforestation and pollution from industry and large conurbations.

CHAPTER 2. – The story of *Cosmos atrosanguineus*

2.1 *Cosmos atrosanguineus* in the natural environment

Cosmos atrosanguineus was introduced to Britain in 1861 via seed sent from Mexico, by an unknown source, to William Thompson of Ipswich, later of Thompson and Morgan Seed Merchants (Hooker, 1861; Brickell and Sharman, 1986). In 1861, Thompson sent a few seeds from these plants to Sir William Jackson Hooker (1785-1865), Director at the Royal Botanic Gardens, Kew, where they were raised for the purpose of identification (Stapf, 1929; Hooker, 1861). Hooker, erring on the side of caution, identified the Thompson specimens as a variety of *Cosmos diversifolius* and named it *Cosmos diversifolius* var. *atrosanguineus* “rather than encumber the system with new but doubtful species” (Stapf, 1929; Hooker, 1861). Hooker compared his living specimens of *C. atrosanguineus* with botanical drawings of *C. diversifolius*, basing his identification on flower size and the presence of simply pinnate foliage (Hooker, 1861). As Hooker lacked living material of *C. diversifolius*, he was not able to compare the important diagnostic features of the achenes (Stapf, 1929). Earlier the previous year, Eduard Ortgies (1829-1916), Head Gardener of the Botanical Gardens, Zurich, received seed under the name *Dahlia zimapani* collected by Benedict Roezl in Zimapan, a town in the Mexican State of Hidalgo (Ortgies in Regel, 1861; Stapf, 1929; Appendix 2.1a-c). On examination of 6 plants raised from this seed, Ortgies disagreed emphatically with Hooker’s identification and considered the Mexican specimens to be a new species. Ortgies was better placed to make this judgement than Hooker as he compared his Mexican specimens with living specimens of *C. diversifolius* emphasising the persistence of dark-red flower colour throughout disk and ray florets as a distinctive feature. This claim has been supported by others since (Voss, 1894; Purpus in Stapf, 1929; Sherff, 1932; Sherff and Alexander, 1955). Ortgies named his new species *atrosanguineus* in recognition of its distinctive blood-red flowers. However, he erroneously placed it in the genus *Bidens*, naming it *Bidens atrosanguineus*, detailing his reasons as the presence of free phyllaries (involucre bracts), awnless paleae (flower bracts), permanent achenes and simple pinnate leaves (Ortgies in Regel, 1861). Andreas Voss (1894) was the first to identify Hooker’s and Ortgies’ specimens as *Cosmos atrosanguineus*. Thus the accepted nomenclature for the species is:

***Cosmos atrosanguineus* (Hook.) A. Voss in Vilmorin,
Blumengärtnerei ed. 3. 1 : 485. 1894**

Cosmos diversifolius var. *atrosanguineus* Hook. in Curtis, Bot. Mag. **87**: pl. 5227. (January) 1861. (Figure 2.1)

Bidens atrosanguineus Ortg. in Regel, Gartenflora 10: 406. pl. 347. (December) 1861.

Dahlia zimapani Roezl.; Ortg. in Regel, Gartenflora 10: 406. 1861 (Nom. Inval.).



Figure 2.1 – *Cosmos atrosanguineus*. Reproduction of plate 5227 in *Curtis's Botanical Magazine Vol. 87*, (1861). Described as *Cosmos diversifolius* var. *atrosanguineus* Hook. Now classified as *Cosmos atrosanguineus* (Hook) A. Voss in *Vilmorin's Blumengartnerei* ed. 3. 1; 485 (1894)

Collections of natural *C. atrosanguineus* populations are confined to east and central Mexico from San Luis Potosí south-eastward to Hidalgo (Sherff and Alexander, 1955; Figure 2.2). It flowers from August to November in Mexico and from May to September in England (Sherff, 1932; Brickell and Sharman, 1986, Table 1.1). The collection record of wild *C. atrosanguineus* is limited. Roezl collected the first wild specimen in the late 1850s, and the second and last wild collection recorded by E. Parry and C.C Palmer was in 1878 (Sherff, 1932; Sherff and Alexander, 1955; Appendix 2.1a-c). It exists today only as a cultivated species.



Figure 2.2. Distribution map of *Cosmos atrosanguineus* in Mexico
Cosmos atrosanguineus wild collected specimens are confined to two distinct areas (red spots) near the town of Zimapan in the state of Hidalgo (17) circa 1858, and near the town of San Luis Potosí (11) in the state of San Luis Potos in 1878. (See Figure 1.1 for key to names of Mexican states)

2.2 - Horticultural Importance of *Cosmos atrosanguineus*

Cosmos atrosanguineus has high horticultural value as a garden species and cut flowers due to its attractively-coloured blooms. In 1938, it was bestowed an Award of Merit by the Royal Horticultural Society (Brickell and Sharman, 1986). Its inability to set seed requires investment in labour-intensive vegetative-propagation procedures, where shoots are removed from rootstocks and rooted individually as softwood cuttings (Brickell and Sharman, 1986). The success of this procedure ranges between 40-60% aggravating the commercial costs of production. However, it was the development of this propagation technique in the 1970s that rescued the species' disappearance from cultivation, such that *C. atrosanguineus* is now offered by a few specialist nurseries (Brickell and Sharman, 1986)



Plate 2.1. A single inflorescence of *Cosmos atrosanguineus* Inflorescence measuring 40 mm across extended rays. The 8 velvety atrosanguinate sterile ligulate rays enclose a central inflorescence of 30-40 hermaphrodite disk florets. The outer whorl of disk florets only are open in this specimen, and have protruding stigmas and anthers capped with copious amounts of bright yellow pollen. (Photo: Sarah Lewendon)

2.3 - The emergence of *Cosmos atrosanguineus* as a cultivated species

It is not clear precisely when *Cosmos atrosanguineus* disappeared from the wild. Evidently it existed in the region of Hidalgo (Zimapan) in the late 1850s when Roezli collected his seed (Appendix 2.1a-c). Sherff records a voucher of a wild specimen of *C. atrosanguineus* at the United States National Museum, collected by E. Palmer and C.C Parry at Alvarez in the State of San Luis Potosí between September and October 1878. The remaining four vouchers examined by Sherff were from cultivated sources (Sherff, 1932). Vouchers examined for this study in the Herbarium at the Royal Botanic Gardens, Kew (RBG Kew) and the Royal Botanic Gardens, Edinburgh (RBG Edinburgh) revealed only one *C. atrosanguineus* of wild origin collected by the 1878 Palmer-Parry field expedition. The remaining 7 vouchers dating from 1861 to 1998 are of cultivated origin, with no seed material present in any voucher. Interestingly, the National Herbarium of Mexico at National Autonomous University of Mexico (UNAM) has no wild or cultivated vouchers of *C. atrosanguineus*. The herbaria record for other Mexican *Cosmos* species used in this study contrast starkly with that of *C. atrosanguineus*. *C. bipinnatus* for example, has 33 wild and no cultivated vouchers (collection period 1833-1984), while the herbarium record of *C. carvifolius* consists of 14 wild vouchers (collection period 1836-1984). *C. diversifolius* consists of 13 wild vouchers and one cultivated voucher (collection period 1837-1984), and *C. sulphureus*, 54 wild and 2 cultivated vouchers, (collection period 1841-1984) (Sherff,

1932; McVaugh, 1984). The limited number of wild *C. atrosanguineus* vouchers has led some to conclude that *C. atrosanguineus* had a limited temporal range and habitat (Wilkinson *et al.*, 1998; Ortega-Larrocea *et al.*, 1997). The date of the last wild collected *C. atrosanguineus* specimen in 1878 coincides with the development of the copper-mining industry in the states of Hidalgo and San Luis Potosí, which destroyed much of the natural environment. The mining industry and subsequent urbanisation of these areas most probably eradicated populations of *C. atrosanguineus* from this environment (Ortega-Larrocea *et al.*, 1997)

The disproportionate representation of cultivated specimens within herbaria has called into question the wild status of *C. atrosanguineus*, leading some to suggest that it is an escaped hybrid of cultivated origin (Wilkinson *et al.*, 1998). It is also conceivable that *C. atrosanguineus* is a natural hybrid, that was establishing itself in the Hidalgo and San Luis Potosí region at the onset of the copper mining industry (Ortega-Larrocea *et al.*, 1997). Encroachment from industry and subsequent urbanisation may have checked the distribution of this putative new *Cosmos* hybrid, leading eventually to the destruction of its habitat. In this scenario, the two wild collections in 1861 and 1878 may represent the surviving gene pool of *Cosmos atrosanguineus*. An examination of *Cosmos* chromosomes may shed light on the hybrid status of *C. atrosanguineus*, and confirm whether it is a plant of recent or ancient hybridization. A third possibility is that *C. atrosanguineus*, with its striking inflorescence, has been the victim of overzealous plant collecting. Benedict Roezl, who first collected this species, was a prodigious collector of plants and sent tons of rare plants to Europe from his travels in the Americas, may have unwittingly contributed to the demise of *C. atrosanguineus* as a wild species (Appendix 2.1a -c).

2.4 - *Cosmos atrosanguineus*: a possible self-incompatible clone

The genetic base of European cultivars of *C. atrosanguineus* appears to be narrow, possibly from 1 original source plant (Ortgies in Regel, 1861; Sherff, 1932; Wilkinson *et al.*, 1998, 2003). Ortgies is known to have raised 200 plants from the seed sent to him by Roezl (Ortgies in Regel, 1861). It is not known how many plants were raised from Thompson's Mexican seed, but Thompson's seed source in Mexico is believed to have been from Roezl, which means the Ortgies and Hooker *C. atrosanguineus* plants were probably from the same wild locality (Sherff, 1932).

The earliest available Thompson's seed catalogue dates from 1885 and offers seed of *C. atrosanguineus*, sold under Hooker's name of *Cosmos diversifolius atrosanguineus*,

and described as a half-hardy annual with dark purple flowers (Appendix 2.2 and 2.3a-b). Thompson's ability to purvey seed of this species suggests a viable stock of seed-producing plants. The low seed price, 4 *d.* (4 old English pennies) indicates an ample supply as a limited or failing seed source would surely be priced more highly and advertised as a rare commodity, although the number of seeds per pack would give a better indication of its value and scarcity (Appendix 2.3b). No illustrations of listed species are contained in the Thompson catalogue, so the plant named as *Cosmos diversifolius atrosanguineus* cannot be verified by picture. However, the use of Hooker's nomenclature 24 years after Thompson sent Hooker seed for verification, supposes a direct connection between Thompson's 1885 seed and Hooker's 1861 identification. If one assumes the seed offered in Thompson's catalogue is the progeny of plant material from which Hooker made his identification, it is highly probable that the seed listed in the Thompson 1885 catalogue as *Cosmos diversifolius atrosanguineus* is that of *C. atrosanguineus* (Hook.) Voss, and is probably derived from the original Roezl collection. In Thompson and Morgan's 1942 seed catalogue, *C. atrosanguineus* is advertised as "*Cosmos diversifolius atrosanguineus*, 'King of the Blacks' a Black Dahlia (dark purple)" (Appendix 2.5b), but after 1942 it disappeared from the Thompson and Morgan catalogue and has not been offered since. Privations of World War II may have contributed to its loss from their offer (Appendix 2.4a.). The two hundred *C. atrosanguineus* plants raised from seed by Ortgies and the *C. atrosanguineus* seed offered in Thompson's seed catalogues demonstrate the existence in Europe between 1861 and 1942 of seed-producing plants of *C. atrosanguineus*. This latter point is supported by evidence from the Thompson and Morgan's 1902 catalogue, which includes a selected form of *Cosmos diversifolius atrosanguineus*, suggesting that breeding and selection of different forms of *Cosmos atrosanguineus* was taking place at this time (Appendix 2.4). The original Hooker/Thompson *C. atrosanguineus* accession sent to the Royal Botanic Gardens, Kew in 1861 appears to have died out before the late 1960s (Appendix 2.6a-b). Its inability to set seed and difficulties in vegetative propagation are reasons proffered for its demise. During the same period, and presumably for the same reasons, *Cosmos atrosanguineus* also disappeared from commercial cultivation. Kew's material was replenished in 1977 with non-seed plant material sent from America by Le Roy Davidson (RBG, Kew Accession No. 1977-3447 DAVI⁸) (Appendix 2.6b). In the early 1980s, Fred Larkby, at the Royal Botanic Gardens, Kew, working on the 1977-3447 DAVI accession discovered an effective method of propagating the species (Brickell

⁸ The original source of Le Roy Davidson's plants is not known. Attempts to find out this information from Mr Le Roy Davidson were not successful (Appendix 2.6a-b).

and Sharman, 1986; Appendix 2.4). Since the early 1980s, all commercial specimens of *C. atrosanguineus* in the UK appear to have been generated from the 1977-3447 DAVI accession or a clonal relative using Fred Larkby's propagation method, and thus plants in European horticulture are seemingly clones of this accession. Genetic-fingerprinting research (AFLP) carried out at the Royal Botanic Gardens, Kew supports this view, as AFLP investigations of various European sources of *C. atrosanguineus* exhibited no genetic variation (Wilkinson, *et al.* 1998).

2.5 - Summary

The inability of *C. atrosanguineus* to set seed may be explained in terms of its strong self-incompatibility and narrow genetic base. Low numbers of self-incompatibility alleles (S-alleles) in a population increase cross-incompatibility (Hiscock *et al.*, 2003). The loss of individuals from cultivated populations allied to the unavailability of wild genetically-diverse plant sources has narrowed the gene pool of cultivated individuals of *C. atrosanguineus* to a level where S-allele numbers are too few to produce cross-compatible genotypes, and may account for the demise of the species in Britain prior to the 1970s. For this to have occurred, the genetic diversity of plants at RBG Kew and in commercial cultivation must have been reduced to genets that shared one, but more probably both S-alleles, thus preventing the germination of pollen and the formation of seed.

CHAPTER 3 – *Cosmos* floral biology

3.1 - Introduction

The genus *Cosmos* has been studied in relation to its self-incompatibility system (Crowe, 1954; Howlett *et al.*, 1975; Elleman *et al.*, 1992), pollen structure, (Dickinson and Potter, 1976, 1979; Pacini, 1996a, 1996b), chemistry (Howlett *et al.*, 1973; Saito, 1976; Batesmith, 1980; Inazu and Mato; 1992; Akisha, *et al.*, 1996; Konarev, *et al.*, 2002), growth and development (Molder and Owens; 1972, 1973; Saha *et al.*, 1985), photoperiodism (Madsen, 1947; Zimmer, 1988; Linville, 1995; Bae *et al.*, 1998; Kanellos and Pearson, 2000;) horticultural competence (Linville, 1995; Starman, *et al.*, 1995; Redman *et al.*, 2002) and cytology (Table 1.2), with the majority of these studies concentrated on the type species *Cosmos bipinnatus*. Knox *et al.*, (1970), provided a brief description of *Cosmos* floral biology, but this was limited to observations of meiotic prophase within the anthers. Pacini (1994, 1996a, 1996b), described aspects of *Cosmos* floral biology associated with development and dissipation of the tapetum, but ontogeny after tapetal dissipation was not discussed. For such a large and taxonomically recalcitrant tribe, and with the exception of *Helianthus annuus* (Horner, 1977; Horner and Pearson, 1978), surprisingly few species of Heliantheae have been investigated ontogenetically. *Cosmos* floral developmental has not previously been investigated, and so before embarking on the cytology and pollination biology, a survey of the developmental stages of *Cosmos* disk florets was undertaken. This survey aims to contribute to the understanding of floral ontogeny in *Cosmos* and to identify developmental stages that will aid investigations of *Cosmos* cytology and pollination biology.

3.2 - Materials and Methods

3.2.1 – Light microscopy (LM)

For light microscopy (LM) and ambient scanning electron microscopy (SEM), *Cosmos* inflorescences were fixed in FAA (formalin-acetic acid) for five days and transferred to 70% ethanol. Preparation for wax embedding was completed in an ultra-processor (LKB 2189-050) at 25 °C using Protocol 1 (Appendix 3.1). Inflorescences were embedded in Paraplast and serially sectioned at 20 µm on a Reichert Jung 2040 rotary microtome. Sections were stained in safranin and Alcian blue using Protocol 2 (Appendix 3.2): Stained sections were mounted in DPX (Aldrich), and examined using normal bright-field optics on a Leitz Diaplan photomicroscope, and photographed using a Leica digital camera

3.2.2 – CryoSEM and Ambient SEM

For CryoSEM, fresh plant material was frozen in liquid nitrogen in the freezing/slush chamber of a Stereoscan 240 SEM (Cambridge Instruments). Frozen specimens were transferred to the cryo-chamber of the SEM at -188°C and then viewed in the main SEM chamber at -188°C and 5 kv to check condition of specimens. Specimens were then sublimated at -81°C to dissipate ice crystals, returned to -188°C , passed back to the cryo-chamber and sputter coated for 8-12 minutes at -188°C . Specimens were returned for viewing to the main SEM chamber at -188°C , and photographed at 12-18 kv .

For Ambient SEM, fixed plant material was dissected in 70% alcohol, transferred through an alcohol series at 25°C using Protocol 3 (Appendix 3.3), critical point dried (CPD) (Balzers 030 Critical Point Dryer) and sputter coated for 6 minutes (Emscope Sputter Coater SC500A). Specimens were viewed and photographed at 12-18 kv on a Stereoscan 240 SEM (Cambridge Instruments).

3.2.3 – Semi-thin resin sections (stRS)

Semi-thin sections of *Cosmos* anther tubes and stigmas were prepared using an ultra-processor. Fixation, dehydration and infiltration were achieved using Protocol 4 (Appendix 3.4) Specimens were transferred individually into hemi-hyperbola BEEM capsules containing 100% resin and polymerised between $58-60^{\circ}\text{C}$ at 440 mmHg for 20 hours. Resin blocks were left to harden for a minimum of 24 hours before sectioning. Semi-thin sections of $0.5\ \mu\text{m}$ were cut on an ultratome (LKB Bromma Ultratome Nova), placed on a glass slide, dried on a 90°C hot plate and stained in toluidine blue-O (0.5% toluidine blue in 0.1M phosphate buffer, pH 7.0) for 2 minutes. Sections were mounted in DPX (Aldrich), examined using normal bright-field optics of a Leitz Diaplan photomicroscope, and photographed using a Leica digital camera.

3.2.4 - Light Macroscopy (LMac)

Light macroscopy (LMac) specimens were prepared using fresh plant material and examined using a Wild Photomakroskop M400 (Wild Heerbrugg). Material was photographed using a Leica digital camera.

3.3 – Results and Discussion

3.3.1 - *Cosmos* floral morphology

The mature *Cosmos* capitulum is composed of two whorls of green-coloured involucre bracts, a single whorl of 8 sterile ligulate ray florets often rose, violet or purple in colour but rarely orange sulphureus or whitish, and 30-60 hermaphrodite central disk florets, with the colour of disk florets being taxonomically significant (Chapter 1, Plates 1.3-1-5; Chapter 2, Plate 2.1; Figure 2.1). Each disk floret is subtended on its abaxial side by a single membranous bract that extends above and arches over each floret and is the main feature distinguishing the Heliantheae from all species of Helenieae and Eupatorieae (Karis and Ryding, 1994). (Plate 3.1, A and B).

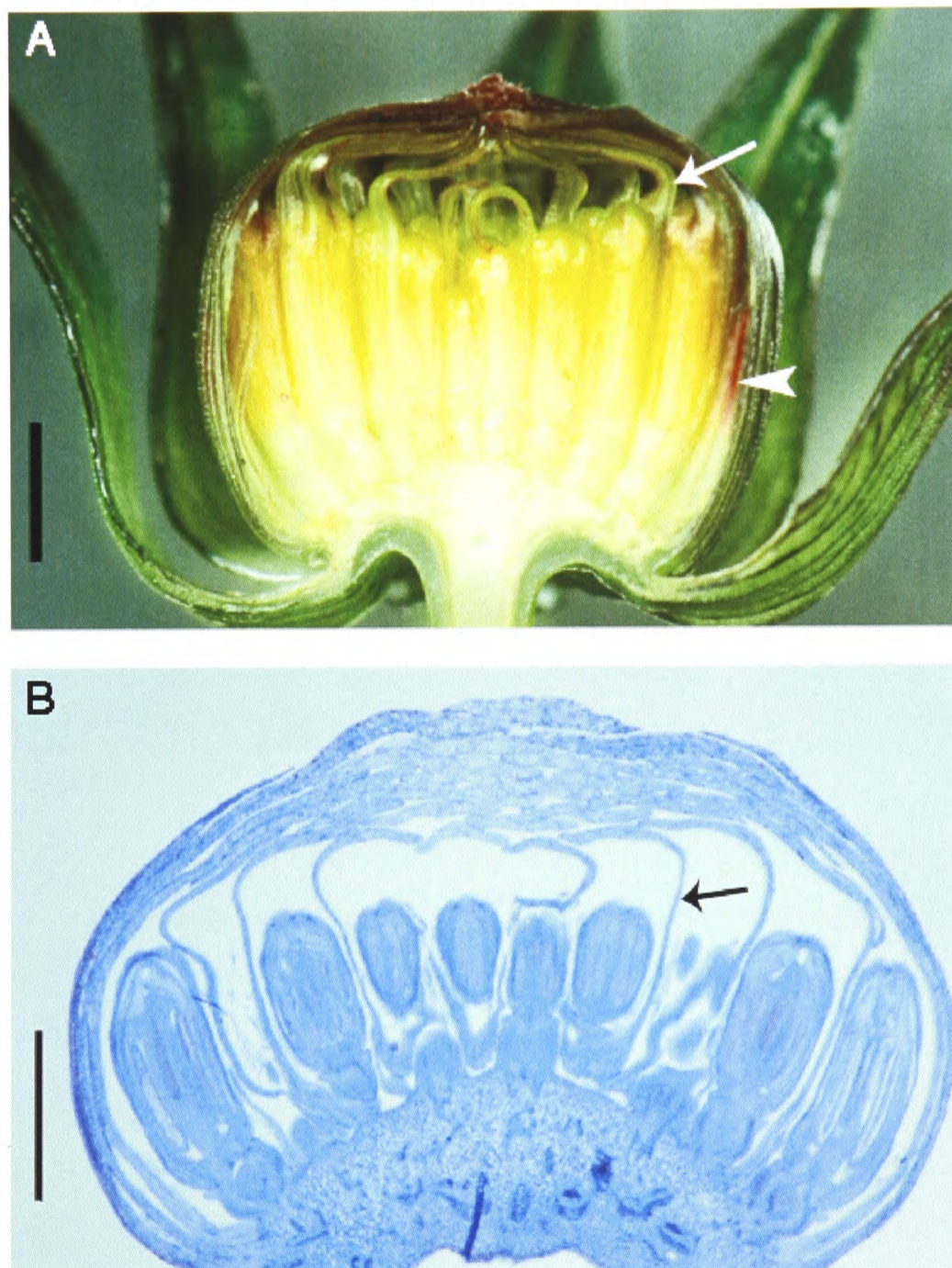


Plate 3.1 - *Cosmos atrosanguineus* stage-1 capitulum

A, Half section of *C. atrosanguineus* capitulum 7 mm in height. (Height/vertical axis calculated from the bract-peduncle junction to the apex of closed capitulum). The first whorl of involucre bracts is open, with the second whorl closed around the elongating ligulate rays and disk florets. A single membranous bract (palae) extends above each disk floret on its abaxial side (arrow). Disk florets develop centripetally, so that younger (smaller) florets are located at the centre and older florets at the periphery. The secondary atrosanguinate colouration is apparent in the ligule of a ray floret on the right side of the inflorescence and in the tip of the adjacent disk floret (arrowheads) (Scale bar = 2 mm). Preparation method, LMac.

B, LS of *C. atrosanguineus* capitulum 3.5 mm in height, containing disk florets at very early stages of development. Both whorls of involucre bracts are closed tightly around disk florets, and each disk floret is subtended by a single bract on its abaxial side (arrow). Ligulate ray florets are not developed at this stage. (Scale bar = 1 mm). Preparation method, LM. (LM bright field).

The hermaphrodite disk florets consist of five 2-3 toothed petals fused to form a tubular corolla that encases the androecium and gynoecium (Plate 3.2, C). The five anthers are held together by a tough thin outer translucent membrane (Plate 3.5, C and F) and form a narrow anther tube that encompasses a single style consisting of two style-branches (Plate 3.2, B and C).

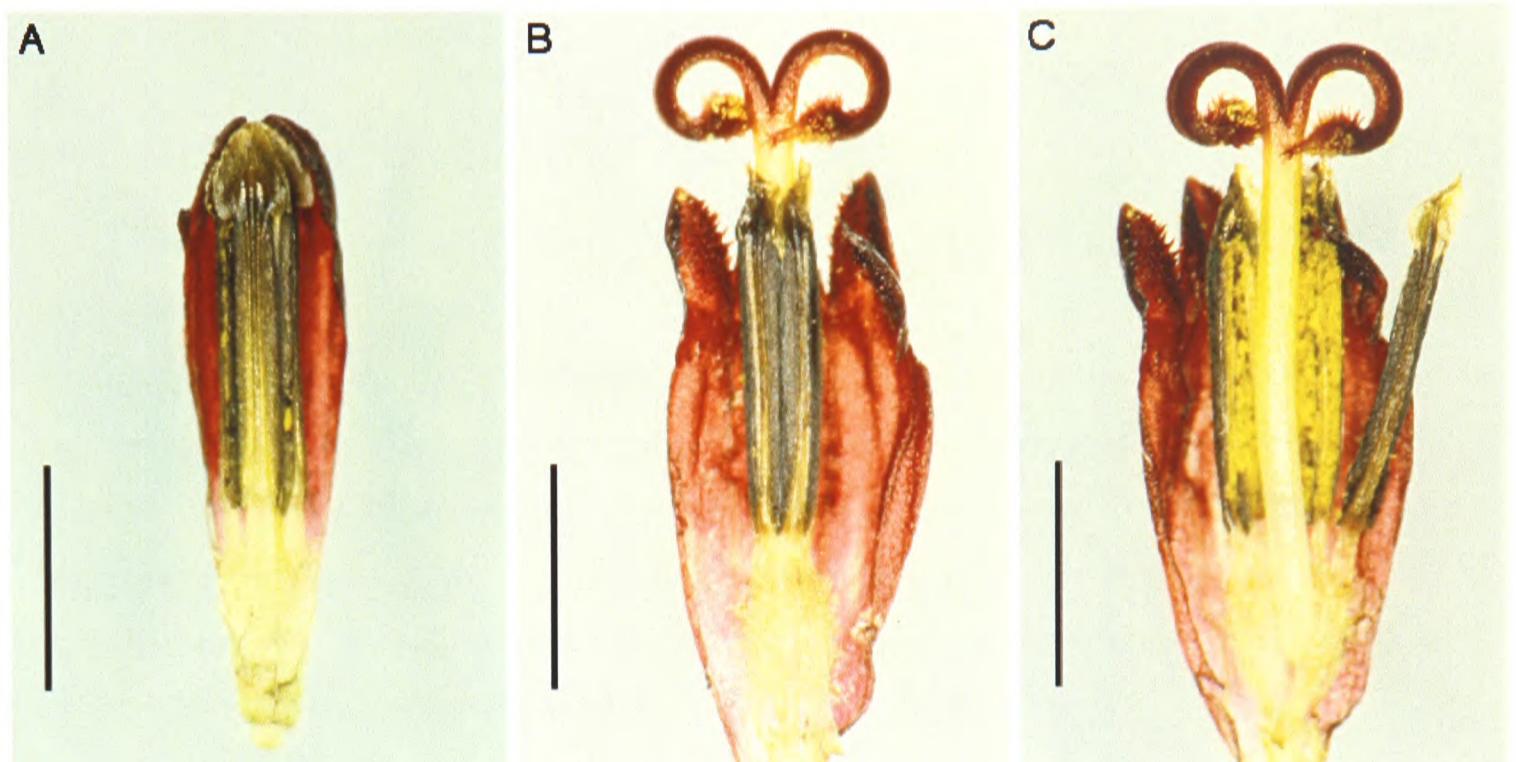


Plate 3.2 – *Cosmos atrosanguineus* disk florets

Disk florets with half corolla tube removed to reveal internal structures. **A** – disk floret pre-anthesis, showing anther tube with dark brown epidermis contained within corolla tube. The five bisporangiate anthers are joined together by a thin translucent membrane forming a connate anther tube. **B** and **C** – mature disk florets post anthesis, with fully emerged reflexed bilobed stigmas. Note the deposition of pollen on the long apical papillae at stigma tips. Prior to anthesis, the two style branches are appressed against each other within the anther tube. As they grow through the anther tube their tips collect pollen grains from the dehiscent anthers, and are presented to insect pollinators at anthesis. Short papillae on the adaxial stigma surface run from the base of stigma tips to the stigma-style junction and are the pollen receptive region of the stigma (**Plate 3.2**). **C** – shows a mature disk floret with anther tube opened to reveal dehiscent anthers. (Scale bars = 2 mm). LMac preparation.

Style branches are papillate, with long non-pollen receptive papillae at the stigma apices, and shorter pollen-receptive papillae on the lateral and adaxial surfaces (Plate 3.2 and 3.3). The stigma/style develops within the anther tube, exists through it vertically at anthesis with pollen presenter lobes arching away from each other to form a fully reflexed bi-lobed stigma at maturity (Plate 3.2, A-C). The long apical non-receptive stigma papillae collect pollen from the dehiscent anthers as they grow up and out of the anther tube, and present them to insect pollinators at anthesis. Each disk floret contains a single inferior ovary with a single ovule (Plate 3.1, B). Achenes are linear, fusiform and characteristically carbonised with their apices tipped with 2-8 usually persistent bristles that are commonly retrorsely barbed (Sherff, 1932; Sherff and Alexander, 1955; McVaugh, 1984).

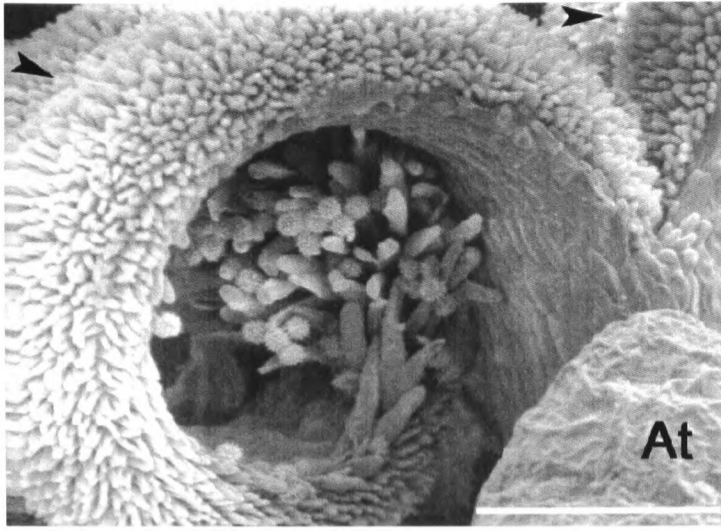


Plate 3.3 - *Cosmos atrosanguineus* fully reflexed stigma lobe

The stigma tip, with its long apical papillae, is curled under the stigma lobe. Pollen collects on the long apical papillae as they emerge through the anther tube, **At**. The short papillae, on the adaxial and lateral surfaces of the stigma, are separated by a region of flat stigma cells that form a groove down the centre of each stigma lobe (arrow heads) (Ambient SEM, mag. = 77.4x. Scale bar = 500 μ m).

3.3.2 -Comparison of disk-floret development in *Cosmos atrosanguineus* and *C. bipinnatus*

Cosmos disk florets can be divided into three distinct stages on the basis of; (i) the corolla (open or closed), (ii) petal colouration, (iv) colour and texture of anther wall, (v) number of anther-wall layers (vi) anther structure (undehisced-tetrasporangiate; undehisced-bisporangiate, or dehisced), (vi) structure of tapetum, (vii) type of sporogenous tissue, (viii) location of stigma (enclosed or emerged) and (ix) orientation of emerged stigma (lobes appressed, arched, or fully reflexed).

(i) Stage-1 florets

Stage-1 disk florets are found in closed inflorescence buds that have a height of ~7 mm or less (Plate 3.3, A-B). Stage-1 disk florets range in height from 1.0 - 3.5 mm and 0.7 - 3.5 mm in *C. atrosanguineus* and *C. bipinnatus* respectively and their corolla tubes are closed (pre-anthesis) (Plate 3.4, A and D). Although the relative height of stage-1 florets is approximately the same for both *Cosmos* species, the diameter of *C. atrosanguineus* stage-1 florets is much greater than that of *C. bipinnatus*. This feature is more clearly observed in transverse section (TS) (Plate 3.5, A and D), with *C. atrosanguineus* early stage-1 florets having an average diameter of 550-600 μ m, while the equivalent stage-1 *C. bipinnatus* florets average 450-500 μ m in diameter. Early stage-1 *C. atrosanguineus* florets have cream coloured tubes and yellow tips, while early stage-1 florets of *C. bipinnatus* have cream coloured tubes with green tips (Plate 3.4, A and D). The cream-coloured appearance of stage-1 corollas is caused by the underlying cream colour of the anther tube passing through the translucent non-pigmented petals. In *C. atrosanguineus* late stage-1 disk florets, yellow pigmentation of petals occurs and the corolla becomes uniformly yellow in colour. In very late stage-1 florets the characteristic atrosanguinate pigmentation appears at the tips of the yellow corollas (Plate 3.4, A). In early stage-1 *C.-bipinnatus* florets, the corolla tips are bright green and the corolla tube is translucent (unpigmented) and thus corollas

appear white in colour due to the colour of underlying anthers. Throughout the early, mid and late stage-1 florets of *C. bipinnatus* corolla tips remain green, and corolla tubes are unpigmented and translucent. However, the walls of the underlying anthers begin to turn brown and impart a light brown colouration to the main body of *C. bipinnatus* late stage-1 disk florets. *C. atrosanguineus* disk florets possess a distinctive pair of barbs at their bases that is not present in the disk florets of *C. bipinnatus*. The barbs are vestigial in stage-1 florets (Plate 3.4A) but become long and prominent by late stage-2 florets after completion of atrosanguinate petal colouration (Plate 3.4, B)

Anthers of *Cosmos* stage-1 florets are characteristically tetrasporangiate, with sporangia in each theca separated by several layers of parenchyma cells (Plate 3.5, A and D). Early and mid stage-1 anthers are cream coloured and have a soft moist texture, as a result of the high water content of anther epidermal cells (Esau, 1977) (The term 'soft' refers to the suppleness of anthers when manipulated with a dissecting needle). In late stage-1 anthers, epidermal cells dehydrate, and dark-brown material is deposited in the cytoplasm (Plate 3.5, B and E). Initial deposition occurs in epidermal cells closest to the filament bundle in the abaxial surface of tetrasporangiate anthers, but eventually spreads to the inner cells on the adaxial surface in bisporangiate anthers of stage-2 disk florets (Plate 4, B and E). As *Cosmos* disk florets enter into stage-2, the wall separating sporangia in each pollen sac are thin and ready to break down, and petals begin their final phase of colouration.

(ii) Stage-2 florets

Stage-2 disk florets are closed (pre-anthesis) and range in height from >3.5 – 8.5 mm and >3.5 – 5.0 mm in *C. atrosanguineus* and *C. bipinnatus* respectively (Plate 3.4, B and E). In *C. atrosanguineus*, the second atrosanguinate-stage of petal colouration begins in early stage-2 disc florets and is completed by the development of late stage-2 florets, by which time the corolla becomes wholly dark purple (Plate 3.4, B). Petal colouration in *C. bipinnatus* begins in early stage-2 disc florets and is completed by the development of late stage-2 florets, but only the top part of the corolla takes on the characteristic yellow colour, the main body of the corolla tube remains unpigmented and translucent (Plate 3.4, E). *C. atrosanguineus* appears to go through two stages of petal colouration, starting with an initial yellow colouration in stage-1 florets, followed by a second atrosanguinate colouration in stage-2 florets (Plate 3.4, A and B), whereas *C. bipinnatus* experiences only one phase of petal colouration that begins and ends within stage-2 florets (Plate 3.4, E). The barbs subtending *C. atrosanguineus*

disk florets lengthen considerably, and become dark-purple by the development of late stage-2 florets.

The anthers of stage-2 *Cosmos* disk florets are bisporangiate, and become brown in colour due to the accumulation of dark-brown material in the cytoplasm of the anther epidermal cells (Plate 3.5, B and E). Late stage-2 anthers have a tough brittle texture due to dehydration of the anther locule, epidermis and endothecium. By the end of late stage-2 disk floret development, many anthers are dehisced and the style lengthens rapidly collecting pollen on the tips of the stigmas as it pushes through the dehisced anthers.

(iii) Stage-3 florets

Stage-3 disk florets are open (anthesis) and range in height from >8.5 –11 mm and >5.0 - 8.0 mm in *C. atrosanguineus* and *C. bipinnatus* respectively (Plate 3.4 C and F). In early stage-3 florets of *C. atrosanguineus* and *C. bipinnatus*, the dark-brown anther tube emerges from inside the corolla (Plate 3.6,A). Initially, the stigma lobes are appressed tightly within the emerging connate anthers, preventing autopollination of the immature stigma, (Howell *et al.*, 1993), but later, the tip of the stigma protrudes through the anther tube creating a three-tiered floral arrangement of stigma, anther and corolla (Plate 3.4, C and F). Eventually, as the style branches push further through the anther tube, they separate to form a V-shaped structure, with stigma tips pointing vertically and the adaxial stigma surfaces facing, but not touching each other, (Plate 3.7). In the early mid stage-3 floret (Plate 3.7), the V-shaped stigma lobes gradually separate and arch away from each other so that the pollen receptive surfaces of each lobe lie perpendicular to the long axis of the floret (Plate 3.6, B). The short pollen-receptive papillae, on the adaxial and lateral surfaces of the stigma are not receptive to pollen at this stage. They become receptive only after the stigma lobes become arched so that the tip of each stigma points down and the greatest surface area of receptive papillae are exposed (Plates 3.4, C and F centre florets). In late stage-3 disk florets, the stigma lobes become fully reflexed and each arm is curled up tightly upon itself, so that stigma tips come into contact with the receptive short papillae on the adaxial and lateral surfaces of stigma lobes. In some self-incompatible Asteraceae (Compositae) species, but not in *Cosmos*, if successful cross pollination has not occurred by this stage, then SI breaks down and the flower is capable of self pollination via deposition of self pollen from the tips of the long apical papillae onto the short receptive papillae of the stigma (Howell *et al.*, 1993).

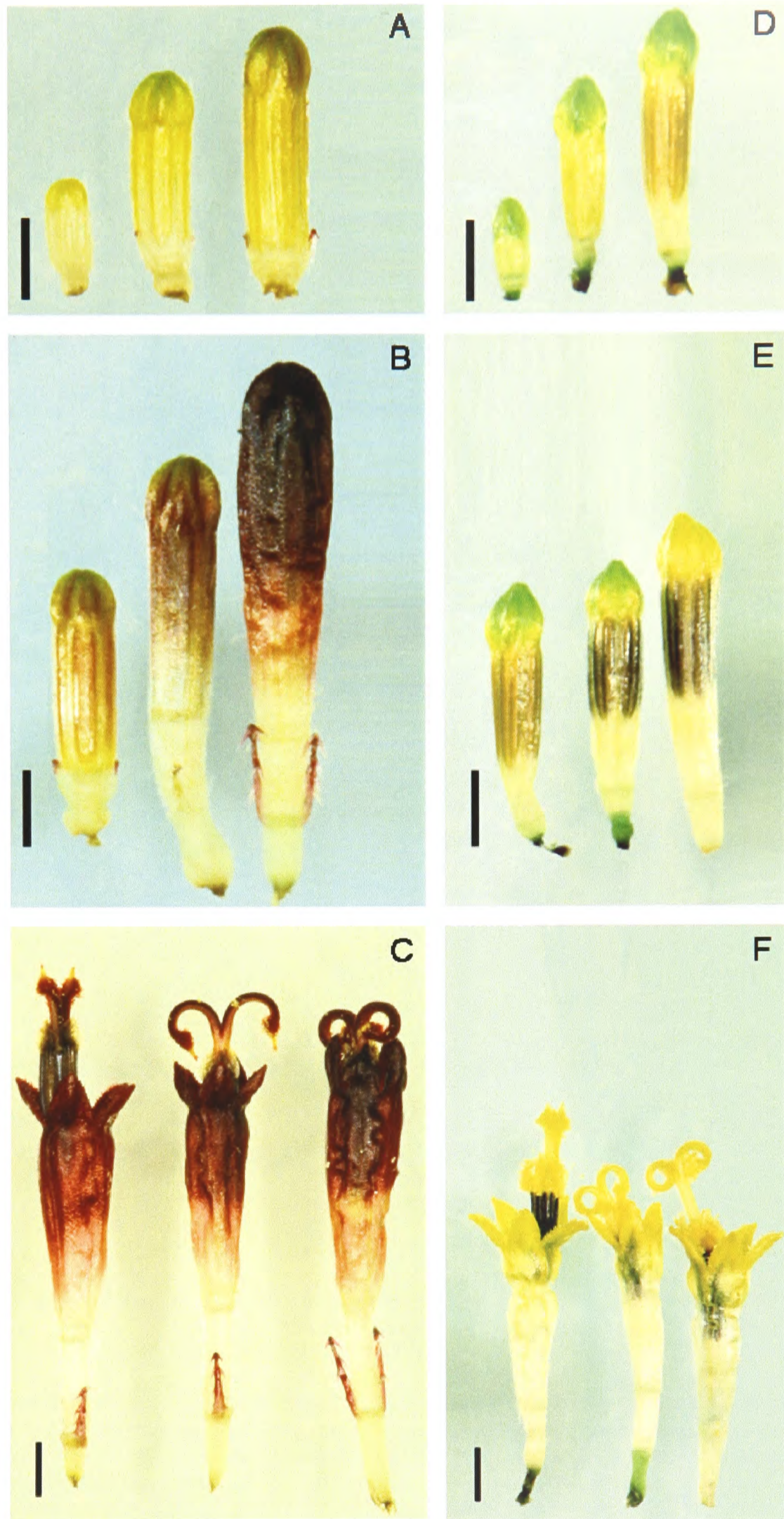


Plate 3.4- Morphological stages in the development of *Cosmos* disk florets

Early, mid and late stage-1, -2 and -3 disk florets of *Cosmos atrosanguineus* (A, B and C) and *C. bipinnatus* (D, E and F). *Cosmos atrosanguineus* and *C. bipinnatus* stage-1 (A & D), stage-2 (B & E) and stage-3 (C & F) are compared. Each of the images A to F contains examples of early-, mid- and late-stage disk florets arranged left to right respectively. (Scale bars = 1 mm). Preparation method, LMac.

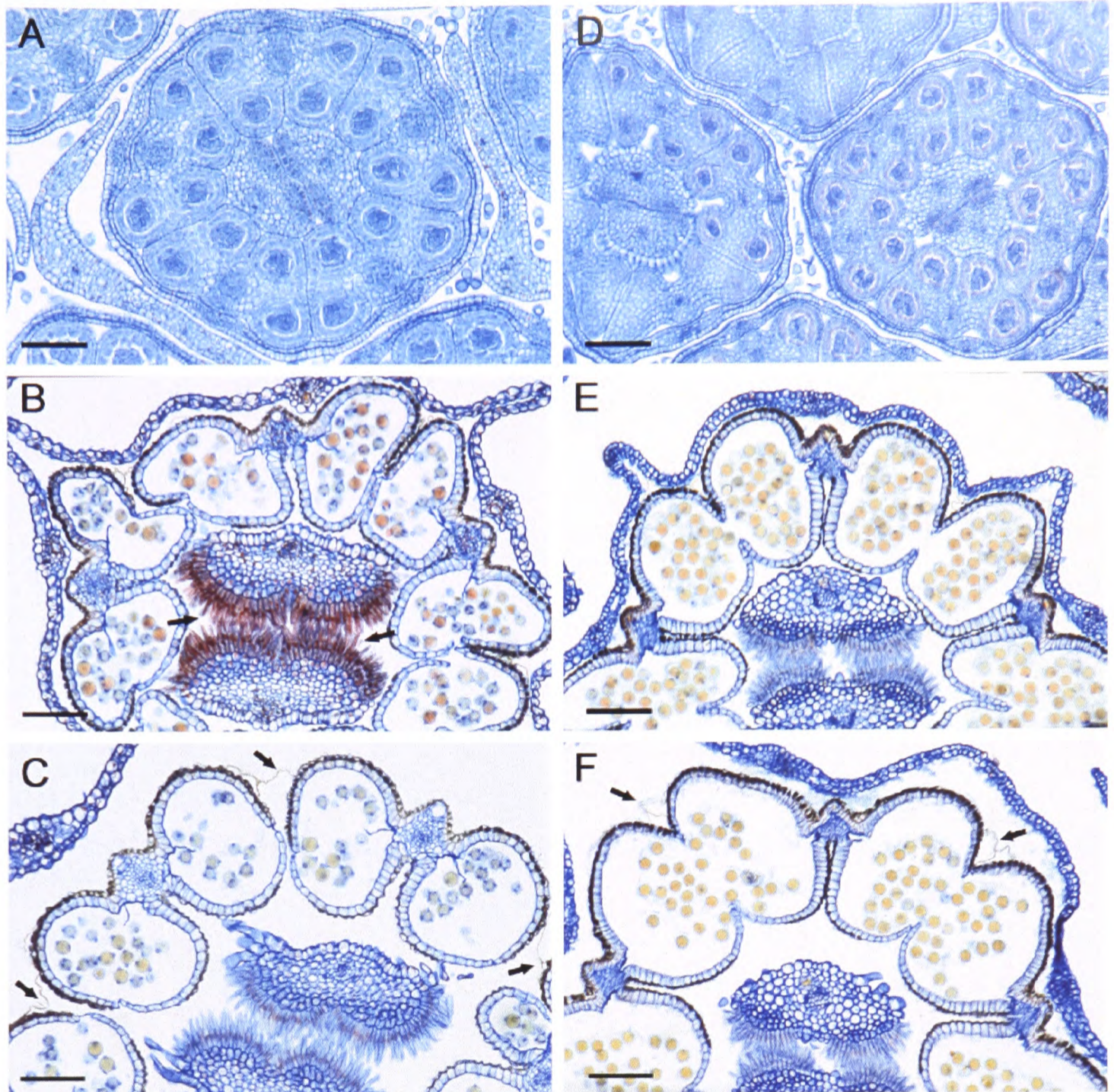


Plate 3.5 – TS stage 1, 2 and 3 disk florets of *C. atrosanguineus* and *C. bipinnatus*
A, B and C, *Cosmos atrosanguineus*. D, E and F, *Cosmos bipinnatus*

A and D – TS early stage-1 disk florets of *C. atrosanguineus* and *C. bipinnatus* respectively showing the greater diameter of *C. atrosanguineus* stage-1 disk florets (diameter = ~580 μm) compared with *C. bipinnatus* (diameter = ~460 μm). *Cosmos* Stage-1 disk florets are closed and have tetrasporangiate anthers. Early stage-1 anthers contain a central sporogenous tissue composed of 4-6 rows of primary-cells, and an anther wall composed of four layers i.e., an inner tapetal layer, a middle layer, an endothecium and the epidermis layers. The disk floret of *C. bipinnatus* in plate 3.5-D is at a slightly later stage of development than the *C. atrosanguineus* disk floret in plate 3.5-A, and so tapetal-cell cytoplasm is more densely staining (red-staining cells), which is characteristic of a maturing peripheral tapetum. The papillar cells, on the adaxial and lateral surface of each stigma lobe are composed of a single layer of small cuboid cells with densely staining nuclei.

B and E – TS mid stage-2 disk florets of *C. atrosanguineus* and *C. bipinnatus* respectively. *Cosmos* Stage-2 disk florets are closed and have bisporangiate anthers with a dark-brown epidermis. In mid stage-2 florets, microspores are binucleate (not visible here), and the tapetal and middle layers are no longer present. Endothelial cells contain primary thickening on inner tangential and both radial walls. The papillar cells on the adaxial and radial stigma surfaces have elongated, and in the case of *C. atrosanguineus* become conspicuously cytoplasmically dense (arrow).

C and F – TS early stage-3 disk florets of *C. atrosanguineus* and *C. bipinnatus* respectively. Stage-3 disk florets are open and their anthers have dehisced. The corolla tube of stage-3 florets has greatly expanded outwards so that it no longer has contact with the anther tube, a feature that facilitates the emergence of the anther tube at anthesis. Stage-3 microspores are trinucleate (not visible here). The stigma papillae have clear cytoplasm and densely-staining nuclei. Note the translucent membrane that encloses and joins the five anthers into a connate structure is clearly visible at this stage (arrows). Scale bars = 100 μm (**A-F** = LM preparation). (LM bright field).



Plate 3.6 – Stage-3 disk florets of *Cosmos atrosanguineus*, showing the distinction between early, mid and late stage-3 disk florets

A - Very early stage-3 floret with anther tube emerging from corolla. The anthers are completely dehisced within the anther tube and the stigmatic lobes are appressed close together within the tube.

B - Mid stage-3 floret showing a partially reflexed stigma. The stigma is not receptive to pollen at this stage, but acts as an organ for secondary pollen presentation. Pollen is presented to insect pollinators on the long apical papillae, with pollen grains being actively loaded onto the apical region of the style as it elongates through the connate of anther tube.

C - Very late stage-3 floret with stigma lobes fully reflexed and exposing the greatest area of the stigma's pollen-receptive surfaces. The stigma lobes in this example have reflexed to their maximum so that the non-receptive stigma tips come into contact with the pollen-receptive surfaces. (Scale bar = 2 mm). Preparation method, LMac.



Plate 3.7 – *Cosmos atrosanguineus* stage-3 disk floret displayed

Mid stage-3 floret with corolla dissected open to show stigma emerging from the connate anther tube. The two stigma lobes move apart from each other as they emerge from the dark-brown connate anther tube. The tips of stigmas consist of long unicellular non-receptive pollen-collecting papillae that form a brush-like structure for presentation of pollen to insect vectors. (Scale bar = 2 mm). Preparation method, LMac.

Anatomical changes within stage-1, -2 and -3 florets accompany changes in morphology, and are described in the anatomical study of microsporogenesis and disk-floret development undertaken below.

3.3.2 - Microsporogenesis and disk floret development in *Cosmos*

Microsporogenesis in *Cosmos atrosanguineus*, *Cosmos bipinnatus* and *Cosmos sulphureus* were investigated using light and scanning-electron microscopy. Floral development in the three *Cosmos* species followed a similar pattern and a generalised description and model of *Cosmos* microsporogenesis was therefore constructed from microscope observations in the three species. This model is discussed below

(i) Early stage-1 – Pre-meiosis

Very early examples of stage-1 anthers have an anther wall composed of four layers, an outer epidermis, an endothecium, a single middle layer and an inner tapetum, that surround a single row of sporogenous cells (Plate 3.8 and Plate 3.9, A). The sporogenous cells undergo mitosis and cytokinesis (Plate 3.9, A-C), resulting in 4-6 rows of microspore mother cells (MMCs) that are appressed tightly against the four-layered anther wall (Plate 3.8, C; Plate 3.9, D). At this stage, microspore mother cells have primary cell walls, and are known to be connected by plasmodesmata to adjacent MMCs and to the uninulceate cells of the tapetum (Plate 3.9, D, Albertsen and Palmer, 1979), but as the anther expands a locular space is formed between the anther-wall layers and the MMCs (Plate 3.8, D). The apical stigma papillae of early stage-1 florets begin to lengthen, but the central papilla cells on the adaxial and lateral stigma surfaces are short, cuboid with large dense nuclei (Plate 3.8, A-B & D). The corolla tube consists of two translucent cell layers (Plate 3.8, A-C; Plate 3.9, B & D).

Prior to meiosis, each MMC begins to secrete a callose (1,3- β -glucan) wall around itself, with callose thickening starting at the cell corners (Plate 3.8, C-D). During callose-wall deposition, the tapetal cells enlarge radially, become cytoplasmically dense, and begin to lose their inner tangential and both radial walls (Plate 3.8, D). Expansion of the tapetum compresses the cells of the middle layer against the endothecium, so that this layer becomes less distinct as the anther expands (Plate 3.8, D). Radial expansion of the anther creates a fluid-filled space that separates the parietal tapetum from the centrally-positioned sporocytes (Plate 3.8, D). A thick callose wall eventually surrounds each MMC and severs plasmodesmatal connections between MMCs and the tapetum, resulting in a physical disjunction between MMCs and tapetum that is bridged by the fluid of the locule (Amela Garcia, *et al.* 2002; Plate 3.8, D).

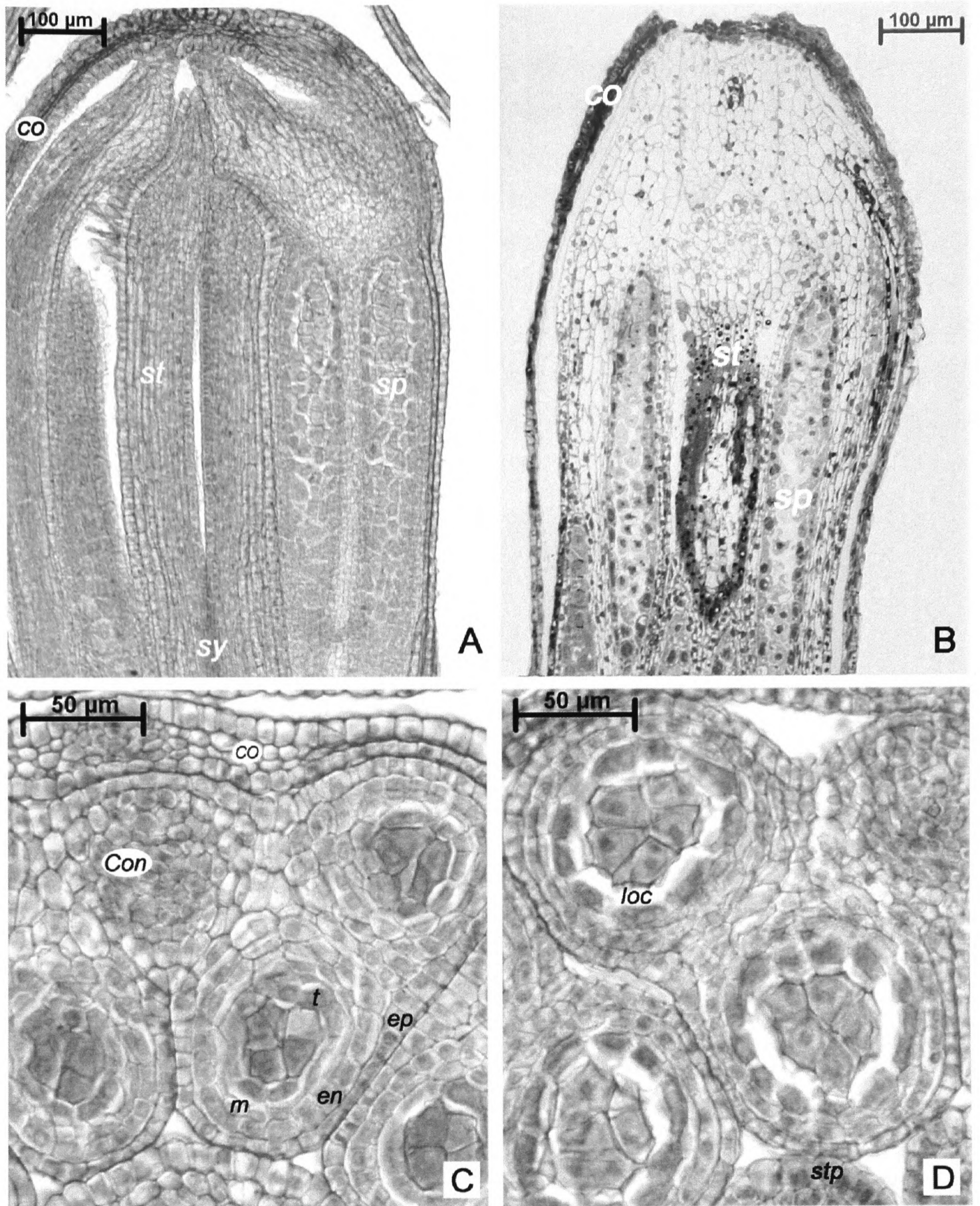


Plate 3.8 – *Cosmos atrosanguineus* early stage-1 disk florets. LS (A), TLS (oblique) (B) and TS (C-D) showing arrangement of stigma (*st*), style (*sy*), microsporangia (*sp*), corolla (*co*) and connective (*con*).

In very early stage-1 florets, the four anther-wall layers are clearly defined as being composed of an outer epidermis (*ep*), an endothecium (*en*), a middle layer (*m*), and a tapetum (*t*) (C-D). In mid to late stage-1 florets, growth of sporogenous tissue and radial expansion of the anther compresses the tapetal layer onto the middle layer, which begins to disintegrate and become less distinct (D, arrowheads). The tapetum assumes a parietal position being separated from the mmcs by the enlarging fluid-filled anther locule (*loc*) (D). The long papillae (*lp*) at the stigma apices elongate throughout the development of stage-1 florets (A-B), but the short papillae (A, arrowheads; D, *stp*), positioned along the adaxial and lateral surface of the stigma, consist of small cuboid-shaped cells with relatively large densely-staining nuclei (A & D). By mid to late stage-1 florets the sporogenous tissue contains 2 rows (B) and 4-6 rows (A & C-D) of mmcs respectively Preparation method: B, stRS; A, C & D, LM (LM bright field).

On completion of callose deposition, the primary cell wall of meiocytes disintegrate, but the cells remain interconnected via large cytoplasmic channels measuring up to 2.5 μm in diameter that traverse the callose walls (Mauseth, 1988). These connections allow cytoplasm and organelles to pass between meiocytes creating a single sporogenous entity known as a syncytium (Shivanna and Johri, 1985). The large cytoplasmic channels reach their maximal development at the zygotene-pachytene period of prophase and disappear completely by the end of anaphase II, when a thick entire callose layer is deposited around each microspore (Shivanna and Johri, 1985; Greyson, 1994). The precise role of the syncytium is not known, but it probably ensures all meiocytes are equally resourced in readiness for meiosis (Shivanna and Johri, 1985).

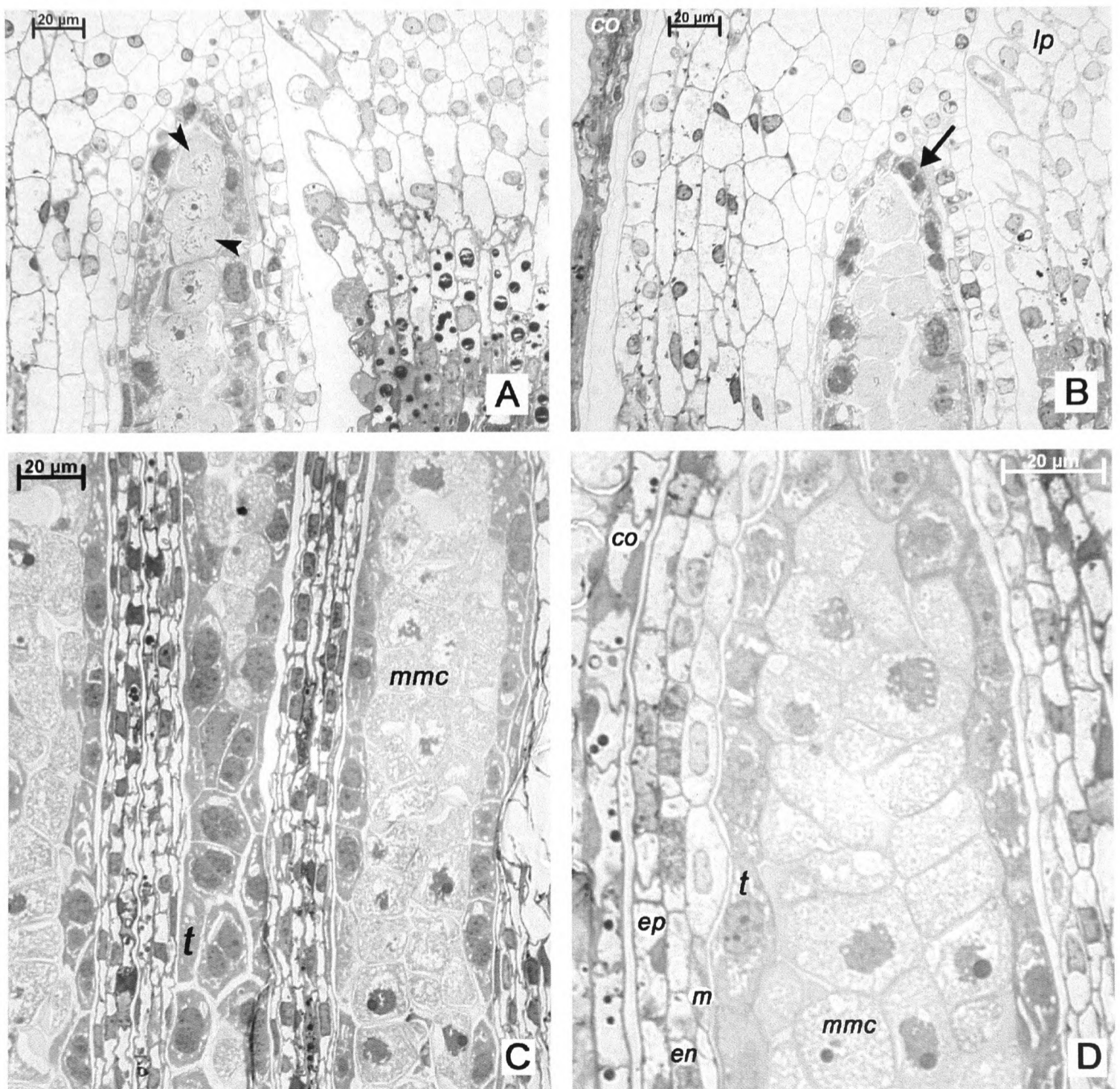


Plate 3.9 – *Cosmos atrosanguineus* LS early stage-1 disk florets

In very early stage-1 florets, the four anther-wall layers are clearly defined as being composed of an outer epidermis (*ep*), an endothecium (*en*), a middle layer (*m*), and a tapetum (*t*) of actively dividing cells (**B, arrow and C**). **A-D**, showing tapetal cells (*t*) with densely-staining cytoplasm and large nuclei. **E-F**, showing the early stage-1 parietal tapetum in direct contact with the MMCs (*mmcs*). **A**, (**arrowheads**) showing sporogenous composed of a single-cell layer of actively dividing cells. **B-D** showing the increase in the sporogenous layer to 2 rows (**B**) and finally 4-6 rows of MMCs (**C-D**). Preparation method for **A-D**, stRS. (LM bright field).

The tapetum, at this stage, is peripheral, cytoplasmically dense, and has a secretory function (Greyson, 1994). The inner tangential and radial tapetal walls appear to become trapped within meiocytes callose walls, and are subsequently ripped away from their cytoplasm as the anther wall expands (Plate 3.10, A-B). Tapeta are categorised as being secretory (or glandular) when they consist of individual cells that remain peripheral to the locule, or amoeboid (or plasmodial) when they invade the locule and deposit their protoplasts directly onto the microspores or pollen grains (Chapman, 1987; Lersten and Curtis, 1990). Asteraceae tapeta are amoeboid, but differ from typical examples as they experience an initial transient parietal-secretory phase that lasts until the formation of free microspores (Rudramuniyappa, 1985; Pacini and Keijzer, 1989; Pacini, 1996a). Some plant species with amoeboid tapeta, have tapetal cell walls composed predominantly of pectin instead of cellulose, and is a factor that may affect their characteristic early breakdown (Shivanna and Johri, 1985; Echlin and Godwin, 1986a; 1986b). Although the pectin content of *Cosmos* tapetal walls is not known, their cell walls breakdown very early before the onset of meiosis (Plate 3.10, A-B). In addition to cell-wall break down, some *Cosmos* tapetal cells undergo karyokinesis during meiosis I and become binucleate, and their cytoplasm become filled with large lipid-containing plastid-like structures, possibly elaioplasts, and small densely-staining lipid-like bodies (Plate 3.10, D & G). The binucleate, densely cytoplasmic condition of the *Cosmos* tapetum indicates high metabolic activity, and is characteristic of the parietal-secretory tapetal phase in *Cosmos* (Pacini, 1996a)

(ii) Mid stage-1 – From meiosis to free microspores

In *Cosmos*, meiosis is more or less synchronous within a sporangium, but each sporangium of an anther may enter meiosis at slightly different times. *Cosmos* meiosis is simultaneous, i.e. both meiotic divisions are completed before cell-wall formation, and results in a tetrahedral arrangement of microspores (Plate 3.10, A-G; Plate 3.11, A-B). In microspores that undergo simultaneous meiosis, cell-wall formation is believed to be centripetal, with walls growing inward from the edges of each cell and meeting at the centre, without prior deposition of cell plates (Dickinson, 1987; Mauseth, 1988). However, light- and electron-microscopy studies of microsporogenesis in *Helianthus annuus* and *Catananche caerulea*, revealed simultaneous cytokinesis of haploid nuclei and cytoplasm followed by the deposition of callose cell plates (Horner and Pearson, 1978; Blackmore and Barnes, 1988). The callose wall appears to be an important framework for deposition of the microspore exine wall, as tetrads released prematurely from their callose walls have abnormal exines and often burst (McCormick, 1993).

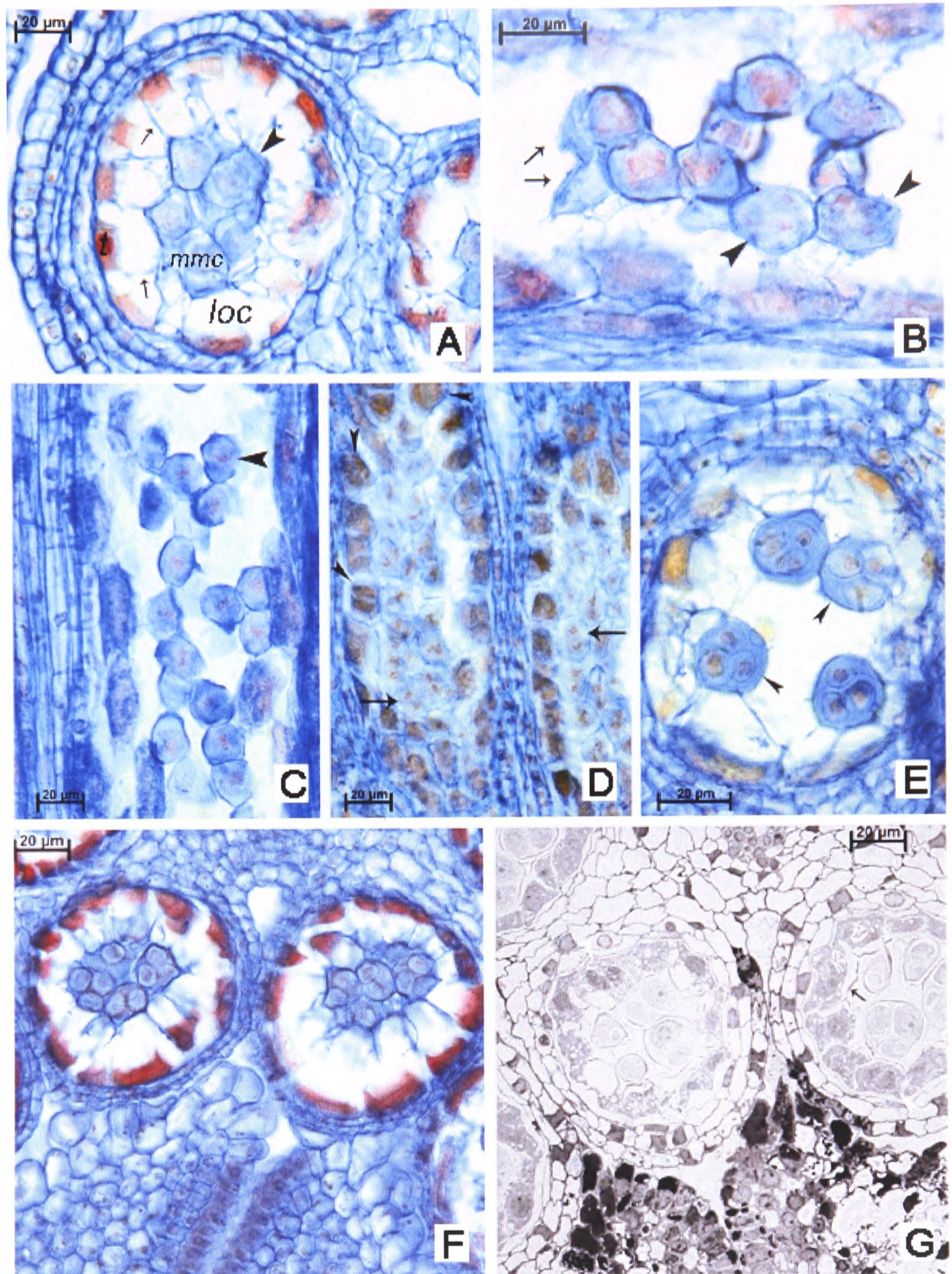


Plate 3.10 – *Cosmos* early to mid stage-1 disk florets LS (C-D) and TS (A, B, E--F). Early stage-1 disk florets (A) and mid stage-1 disk florets (B-G) of *C. atrosanguineus* (A-E & G) and *C. bipinnatus* (F).

A, showing premeiotic MMCs (microspore mother cells) with thick callose walls (arrowhead);

B, MMCs at telophase-II, showing haploid number of chromosomes (not discernable here) located at the four corners of each MMC, before deposition of the callose wall around each haploid microspores

C, MMCs at metaphase-I; showing chromosomes aligned along the equator of the MMCs (arrowhead).

D, MMCs at telophase-I, showing separation of bivalents and migration of chromosome pairs to the poles of MMCs (arrow); and

E, showing a sporangium with four tetrads, each containing four tetrahedrally-arranged haploid microspores (arrowheads)

F, Two inner (adaxial sporangia) from the same anther showing newly formed tetrads with the tapetal inner tangential and radial walls attached to the outer surfaces of the surrounding callose wall.

Expansion of anthers produces a fluid-filled locular space, (*loc*) separating the tapetum (*t*) from MMCs (*mmc*). The parietal tapetum has a secretory function and consists of cells with dense cytoplasm. The inner tangential and radial walls of tapetal cells become trapped within the callose walls of MMCs, and are ripped away from tapetal cytoplasm as the anther wall expands away from the centrally-positioned MMCs, exposing tapetal protoplast to the locular fluid (**arrows in A, B & G**).

During meiosis-I some tapetal cells become binucleate (**D & G**, arrowheads). Meiosis in *Cosmos* is simultaneous resulting in a tetrahedral arrangement of microspores (**E-G**). Preparation method: **A-F**, LM; **G**, stRS. (LM bright field).

In *Cosmos*, the four haploid tetrahedrally-arranged microspores are each encased within a callose wall that forms centripetally, before initiation of the microspore cell wall (Plate 3.10, E-G; Plate 3.11, A-B), indicating that *Helianthus annuus*-type tetrad formation occurs in *Cosmos*, with the surrounding callose wall acting as a framework for cell-wall formation.

The *Cosmos* microspore wall is completed while microspores are attached within tetrads (Plate 3.11, B), so that on separation, the inner contact surfaces of each microspore appears slightly flattened (Plate 3.11, C-D). Although not observable by the methods used in this study, microspore-wall formation in *Cosmos* is initiated by deposition of a primexine cellulose layer between the callose wall and the cell membrane in all areas of the microspore except those destined to form apertures (Blackmore and Barnes, 1985). As the microspore expands, small rod-shaped columellae (bacula) appear in the primexine layer (Shivanna and Johri, 1985; Fitzgerald and Knox, 1995). In *Cosmos*, bases of baculae expand laterally and contact bases of adjacent baculae to form a foot layer, while the tops of baculae expand similarly to form an echinate roof layer or tectum (Howlett *et al.*, 1973, 1975; Horner and Pearson, 1978; Blackmore and Barnes, 1985). The columellae form an absorbent scaffold-like layer onto which sporopollenin precursors are deposited and polymerise to create an extremely resistant non-oxidative outer exine layer, the sexine (or ectexine) (Mauseth, 1988; Piffanelli *et al.*, 1998; Wang *et al.*, 2003).

Sporopollenin is formed from acyl lipid and phenylpropanoid precursors and is synthesised initially by the microspore, as the tetrad callose wall appears impermeable to materials of the locular fluid (Piffanelli *et al.* 1998), although certain data indicate that some tapetally-derived sporopollenin precursors may diffuse through the callose wall (Heslop-Harrison, 1968; Mascarenhas, 1975; Greyson, 1994). Before dissolution of the microspore callose wall is completed, a smooth uniform layer of microspore-derived sporopollenin is laid down between the sexine layer and the microspore cytoplasm, forming the inner exine layer, the nexine (or endexine) (Mauseth, 1988). Although initial sporopollenin deposition may be derived from the microspore, expression during exine deposition of lipid biosynthesis genes and genes that control the activity of phenylpropanoids, identifies the tapetum as the major site of sporopollenin production, with the microspore contributing only a small proportion of sporopollenin to the exine (Piffanelli *et al.* 1998).

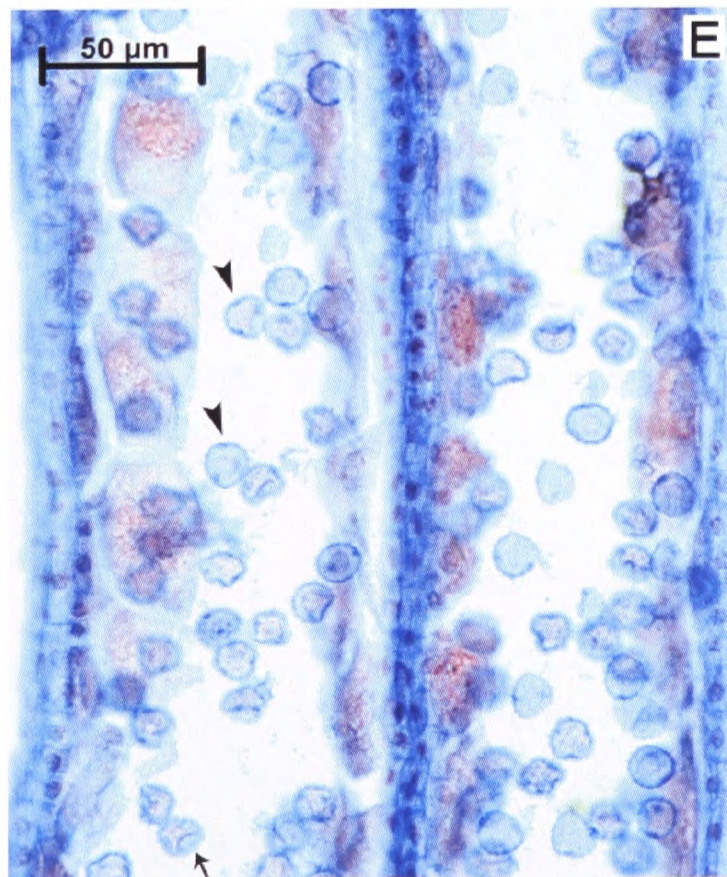
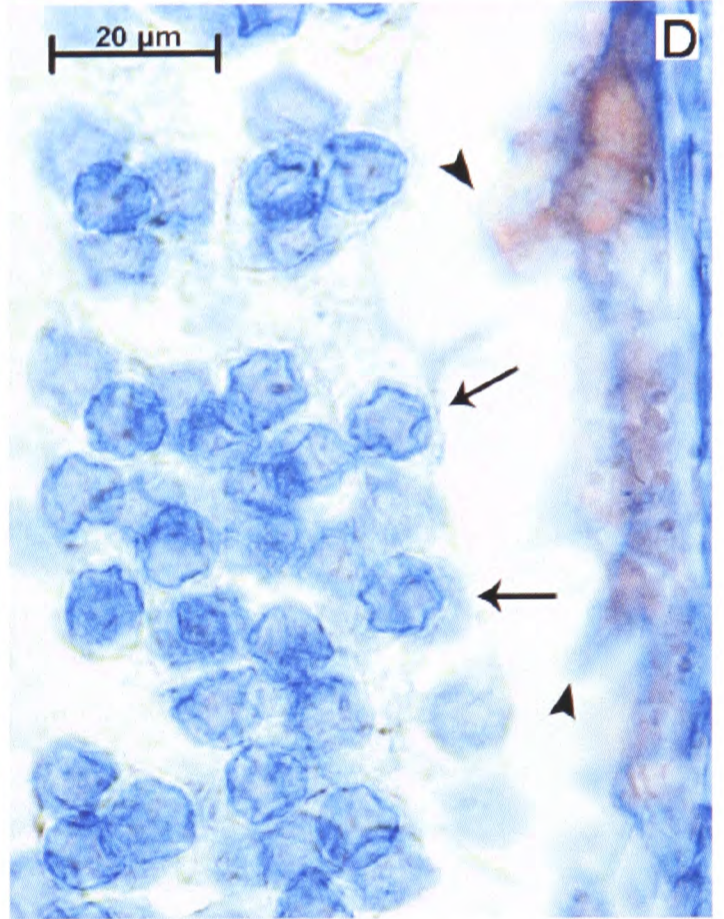
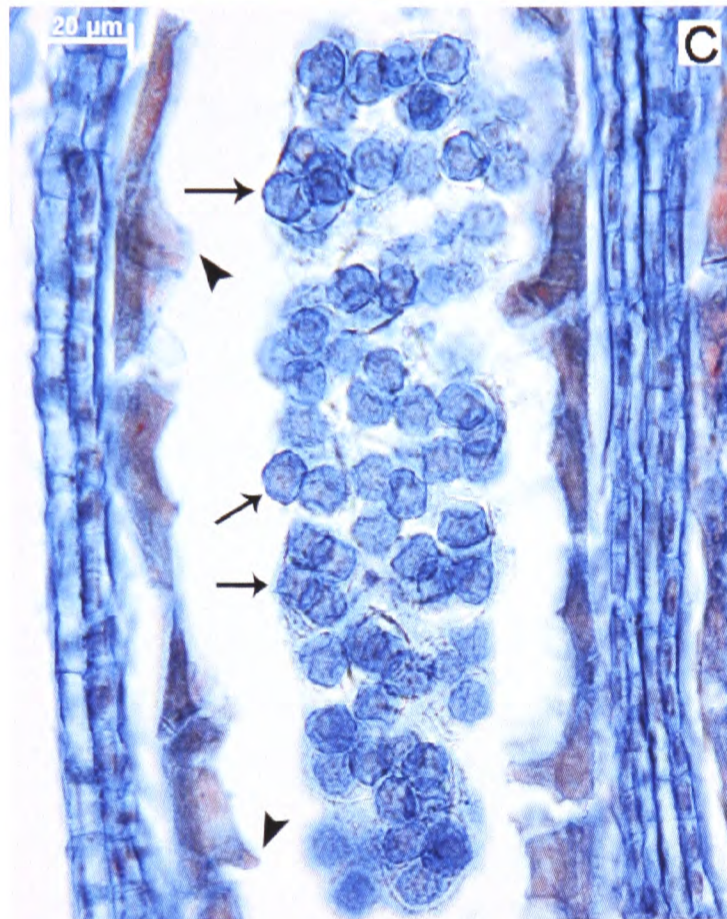
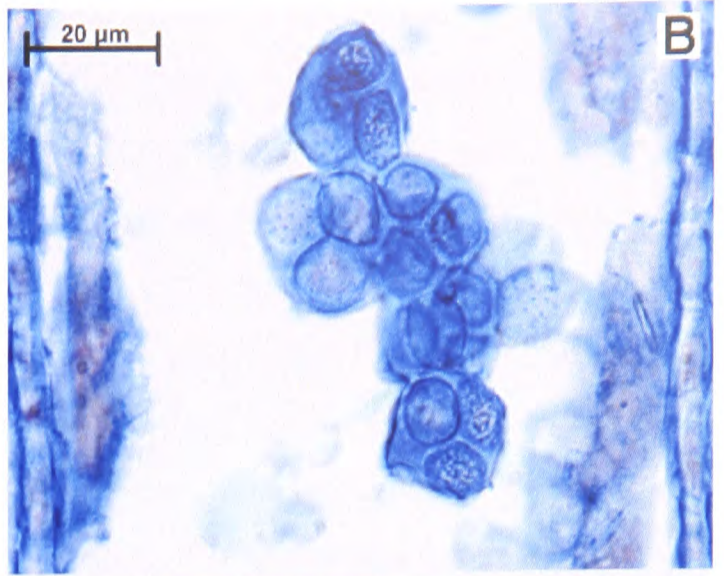
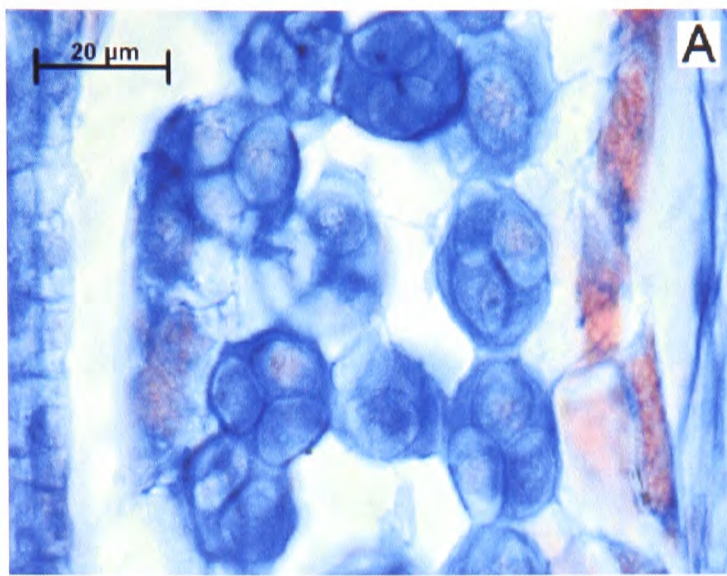


Plate 3.11 - *Cosmos atrosanguineus* LS mid stage-1 anthers

Meiosis in *Cosmos* is simultaneous, resulting in a tetrahedral arrangement of microspores (A). Tetrads adhere to each other by their callose walls (A-C). The echinate microspore wall forms while microspores are attached within tetrads (B), so that on dissolution of the callose wall (C-D), the inner contact surfaces between microspores can be distinguished from outer surfaces by their slightly flattened appearance (C-E, arrows). On release from tetrads the uninucleate microspores expand to a diameter of ~10 µm, become more rounded in shape, with the three colpus regions clearly observable as regions of non-sporopollenin deposition (E, arrowheads). Distinct spaces are evident between adjacent protoplasts of tapetal cells where the primary radial walls used to be (C & E). The tapetal cells begin to expand radially (E), with some cells developing small protoplasmic extensions into the locular space (C-D, arrowheads). Preparation method: A-E, LM. (LM bright field).

During exine formation, the *Cosmos* tapetal cytoplasm becomes densely staining and is metabolically active, most probably in the production of sporopollenin molecules and enzymes (Piffanelli *et al.* 1998; Plate 3.11, A-E). Glucanases, secreted by the parietal tapetum, dissolve the tetrad callose wall, and release microspores into the fluid-filled anther locule (Piffanelli *et al.*, 1998; Plate 3.11, C-E). At tetrad dissolution, *Cosmos* microspores possess thin rudimentary exines with distinct spines, and three coplus regions (Plate 3.11, E). The *Cosmos* anther continues to expand throughout the development of mid stage-1 florets (Plate 3.11, A-E). During this phase, the parenchymous cell layers between sporangia (pollen sacs) of each pollen sac become increasingly compressed, resulting in a reduction in the cell layers separating sporangia (Plate 3.12, C-F).

The corolla tubes of stage-1 florets of *Cosmos bipinnatus* and *C. sulphureus* remain translucent, but in *C. atrosanguineus*, primary yellow petal colouration is initiated. The apical stigma papillae in the three *Cosmos* species continue to lengthen, but the central papillar cells remain small, but appear more rectangular in shape towards the end of this stage, due to an initial expansion in their lengths (Plate 3.10, F-G).

(iii) Late stage-1 – From invasive tapetum to binucleate pollen

The free uninucleate microspores enlarge and become more rounded in shape (Plate 3.11, E). The intine layer has not yet developed and the microspore wall has a double layered exine composed of an echinate sexine, a smooth nexine. The three colpus regions are now more apparent (Plate 3.12, A). The maximal period of sporopollenin production occurs at the free microspore stage, with exine formation completed by the first pollen mitosis (Blackmore and Barnes 1990; Piffanelli, *et al.*, 1998). In *Helianthus annuus*, *Catananche caerulea* and *Tragopogon porrifolius*, the thecal fluid contains tapetally-derived sporopollenin-like material, which becomes deposited onto the free microspores, thickening the microspore wall and elongating the spines (Horner and Pearson, 1978; Blackmore and Barnes, 1987; Barnes and Blackmore, 1988; Piffanelli *et al.*, 1998). It seems likely that the thickening of the *Cosmos* microspore wall observed at the free microspore stage is also due to secretion of tapetal-derived sporopollenin onto the sexine (Plate 3.11, E; Plate 3.12, A).

The onset of tapetal break down in *Cosmos* signals the end of the secretory tapetal phase and the start of the amoeboid phase. At this transition point, protoplasmic processes of the tapetum begin to extrude into the locule (Plate 3.12, A) and the many small vacuoles within the cytoplasm of each free microspore begin to fuse. Initially, at the early vacuolate stage, there is little discernible difference in the shape of the

microspore cytoplasm. However, during the mid- to late-vacuolate stage of microspore development, one large vacuole forms and causes the nucleus and cytoplasm of each *Cosmos* microspore to migrate towards the periphery of the cell (Plate 3.13a, A-C). Increased vacuolation appresses the cytoplasm and nucleus against the nexine layer creating a “signet-ring” shape characteristic of late-vacuolate microspores (Barnes and Blackmore, 1988; Plate 12, E-G; Plate 3.12, A-C; Plate 3.13a A-C; Plate 3.14, A-B, D, E and F). A thin spacer layer is sometimes discernible between sexine and nexine wall layers, and is a region of the microspore wall composed of non-sporopollenin receptive primexine (Horner and Pearson, 1978; Barnes and Blackmore, 1988; Plate 3.13a-b, C). In some vacuolate *Cosmos* microspores, the exine layer collapses inward with the migrating cytoplasm and these pollen grains appear doughnut-shaped from the exterior (Plate 3.13b, C; Plate 3.15, A-B; Plate 3.16 A).

The direction of nuclear migration in vacuolating microspores is not arbitrary, with migration and division of the nucleus being crucial to the subsequent behaviour of the future generative and vegetative cells. In grasses, the nucleus always moves to the side away from the furrow where the future pore will be, and nuclear migration is accompanied by reorganisation of the cytoplasm, with plastids and mitochondria displaced away from the nucleus (Shivanna and Johri, 1985). Although the direction of nuclear migration could not always be determined, *Cosmos* nuclei tended to migrate away from colpus regions, and so in *Cosmos*, as in most taxa, migration of the microspore nucleus is directed away from pores (Shivanna and Johri, 1985). This feature probably affords protection to the nucleus.

The first *Cosmos* pollen mitosis occurs at the late vacuolate ‘signet-ring’ stage and results in a vegetative nucleus and generative nucleus of equal size, positioned adjacent to each other in the compressed cytoplasm (Plate 3.14, F).

In most Asteraceae (Compositae), a transitory callose wall forms around the generative nuclei and a small amount of cytoplasm that attaches the smaller generative cell to the nexine layer of the pollen-grain wall (Blackmore and Barnes, 1988). In *Cosmos*, the generative nucleus, and later the sperm nuclei, have a close association with the vegetative nucleus, being located in close proximity to it throughout pollen-grain development, and this association is particularly close prior to the second pollen mitosis (Plate 3.20 A, E-F; Plate 3.21, D-E). Such associations have been observed in various other species. The pollen grains of alfalfa for example, have more nuclear pores on the surface of the vegetative nucleus adjacent to the generative cell than on the opposite surface, implying communication between the

generative cell and vegetative nuclei (McCormick, 1993). Furthermore, electron-microscope observations show the generative-cell nucleus to have condensed chromatin, and a cytoplasm that contains few mitochondria, and no RNA or protein synthesis. These observations indicate that the generative nucleus, and later the sperm cell nuclei, are transcriptionally inactive (Shivanna and Johri, 1985; McCormick *et al.*, 1991; McCormick, 1993). In contrast, the vegetative nucleus is hydrated, and the cell contains high levels of RNA synthesis, and thus the generative cell may be metabolically dependent on the vegetative cell during this period (Mascarenhas, 1990; McCormick, 1993). The condensed nature of the *Cosmos* generative nucleus and its close association with the vegetative nucleus may reflect such a metabolic dependency (Plate 3.20, F; Plate 3.21, C-E).

In *Cosmos*, after the first pollen mitosis, the vegetative nucleus takes a more central position within the pollen grain, while the generative nucleus assumes a more peripheral location (Plate 3.20 F). As the cytoplasm of the vacuolate pollen grains begin to expand, the first signs of the developing pectocellulosic intine layer are observed. Initially, the intine is laid down over the apertures at the three colpus regions, which are discernible as areas of non-sporopollenin deposition (Plate 3.14, C), but eventually, it spreads out from the colpi and encases the entire microspore membrane, emerging as operculae at the colpi (Plate 3.14 H).

Post pollen mitosis, the binucleate *Cosmos* pollen grain enlarges, the vegetative cell cytoplasm expands fully, the large vacuole disappears, the intine thickens, and the vegetative cell begins to engorge food reserves. Rapid biosynthesis and accumulation of intracellular lipids result in the production of storage oil bodies and the development of a network of membranes in the pollen grain cytoplasm (Piffanelli *et al.*, 1998; Plate 3.13a-b, D; Plate 3.14 E, G-H). Accumulation of lipids and membranes gives the cytoplasm a characteristic 'bubbly' appearance indicative of this phase of rapid lipid biosynthesis (Evans *et al.*, 1992). Pollen-grain lipids are made up mostly of triacylglycerols and phospholipids rich in C₁₈ polyunsaturates, such as linoleic acid (Piffanelli *et al.*, 1998). Since the breakdown of the tapetum and the engorgement of binucleate pollen grains is closely correlated, the majority of engorged soluble carbohydrates, peptides and amino acids are believed to come from the dissipating tapetum, (Shivanna and Johri, 1985; Barnes and Blackmore, 1988). In the early stages of pollen engorgement, the *Cosmos* pollen-grain cytoplasm is less densely stained and the two layers of the exine, and a thick intine layer are clearly identifiable (Plate 3.14, H; Plate 3.20, E-F). At later stages of engorgement, the cytoplasm of the binucleate

Cosmos pollen becomes very densely staining, indicating a high level of metabolic activity (Plate 3.14, H; Plate 3.20, E-F).

Throughout late stage-1, the *Cosmos* tapetum undergoes several important changes. At the early free microspore stage, before microspores become fully rounded in shape, the protoplasts of the parietal tapetum become less cytoplasmically dense, and begin to expand radially into the anther locule (Plate 3.12, A-B). The secretory parietal tapetum now transforms into an invasive amoeboid tapetum. During this phase, the cytoplasm of the early plasmodial tapetum becomes less densely staining, reflecting a reduction in the metabolic activity of the *Cosmos* tapetum as it switches from secretory to amoeboid mode (Plate 3.12, A-G; Forva and Pè, 1992). Initially, the tapetum extends protoplasmic arms into the locular space, while the majority of the protoplasts and tapetal nuclei remain in a peripheral position within the anther (Plate 3.12, A). But eventually, with continued locular invasion, tapetal protoplasts fill the entire locular space and completely engulf the microspores (Plate 3.12, B-G). A periplasmodium does not form prior to tapetal invasion of the locule, as distinct spaces are evident between adjacent protoplasts of tapetal cells where the primary radial walls used to be (Plate 3.10, A-G; Plate 3.11, A-E). However, as invasion of the amoeboid tapetum increases, the tapetal protoplasts appear to fuse, forming a single tapetal syncytium that engulfs the vacuolating microspores (Plate 3.12, B-G; Plate 3.13a, A-C). In some Paraplast-embedded *Cosmos* material, spaces between tapetal protoplasts appear more accentuated than in others, and it may be that the large spaces observed between adjacent tapetal protoplasts in these sections are artefacts (compare Plate 3.11, C and E, with Plate 3.12, A). Resin-embedded material and cryoSEM preparations reveal a more intimate association between adjacent tapetal protoplasts, with fusion of protoplasts occurring at the onset of tapetal invasion (Plate 3.10, G; Plate 3.15, A-H). A conundrum exists concerning the mechanics generating the movement of tapetal protoplasts into the anther locule. Clearly, the *Cosmos* plasmodial fragments are too large and dense for their movement to be the result of Brownian motion or diffusion. It has been suggested that amoeboid tapeta possess functional actin or tubulin cytoskeletons that control their movement, or that dehydration of the locule creates surface tensions capable of drawing tapetal fragments onto pollen grains (Dickinson *et al.*, 2000). In some species of *Gasteria* and *Aloe* (Keijzer 1987; Keijzer and Cresti 1987) the expanding pollen grain is believed to build up a pressure within the anther that presses the disintegrating tapetum onto the pollen grains, with the subsequent transfer of pollen coat materials (see below) being achieved through capillary action. However, these explanations remain speculative, as the actual mechanics governing tapetal movement into the locule have yet to be identified.

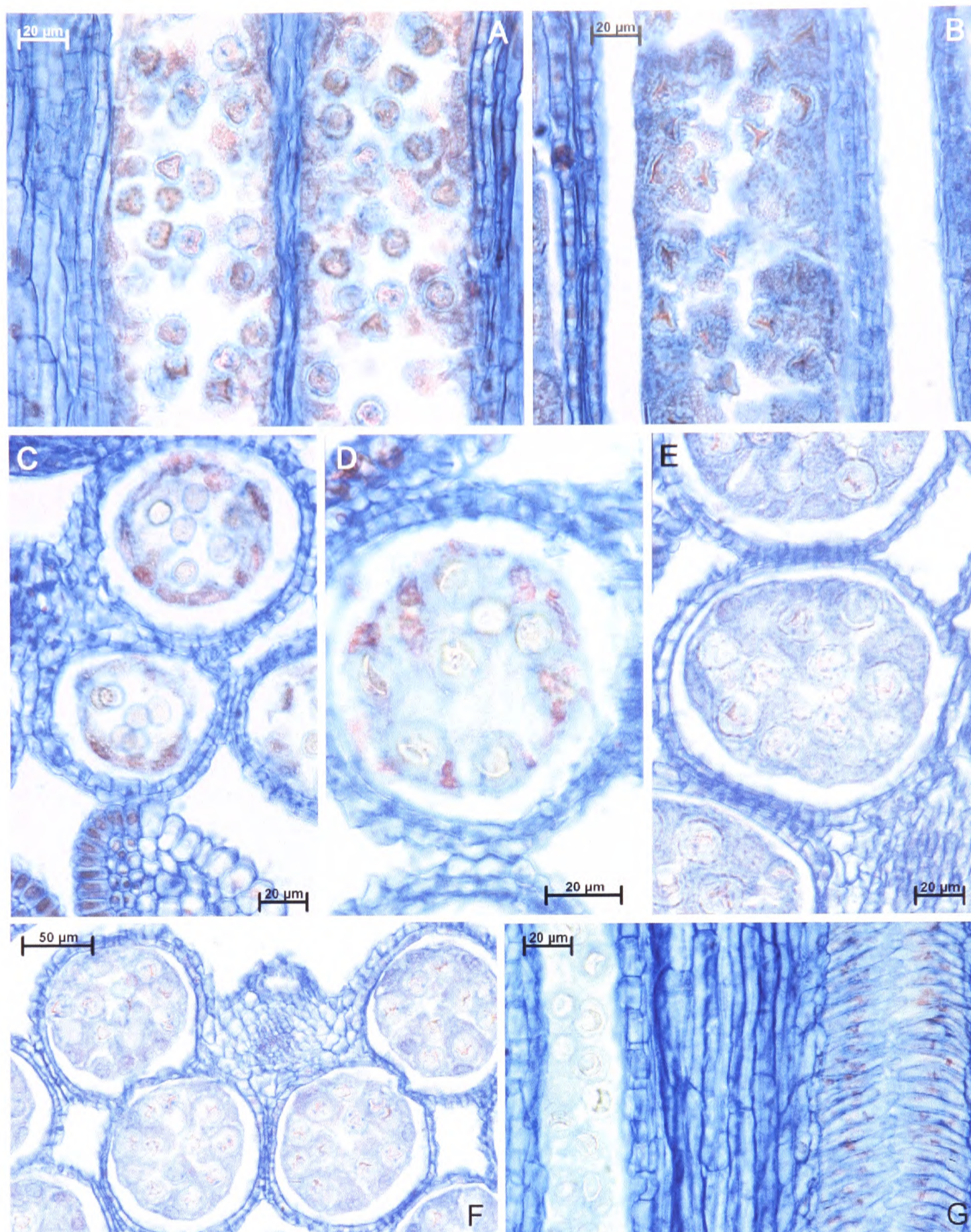


Plate 3.12 – Late stage-1 *Cosmos* disk florets.

Plate shows LS (A, B & G) and TS (C-F) of *C. atrosanguineus*, (A, B, E & F); *C. sulphureus* (C & D) and *C. bipinnatus* (G)

A and C -showing initial stages of tapetal invasion. The free uninucleate microspores are ~10-12 μm in diameter and have thin rudimentary echinate exines and three distinct coplax regions. The microspore intine layer develops at this stage but is visible only in semi-thin sections (See **Plate 3.13**). Tapetal protoplasts become less densely staining and fuse so that the spaces observed between adjacent protoplasts in **Plate 3.11** no longer persist, and a tapetal syncytium is formed. The peritapetal membrane encloses the tapetal syncytium and separates microspores and the plasmodium tapetum from the outer anther wall layers (**B-F**). Microspores at early-vacuolate (**B, D, E & G**) and late-vacuolate (signet-ring) stages (**F**) have become engulfed fully by the syncytial tapetum. The short stigma papillae lengthen from ~15 μm at the early-vacuolate stage (**C**) to ~35 μm by late-vacuolate (signet-ring) stage of microspore development, (**G**). Preparation method: **A-G**, LM. (LM bright field).

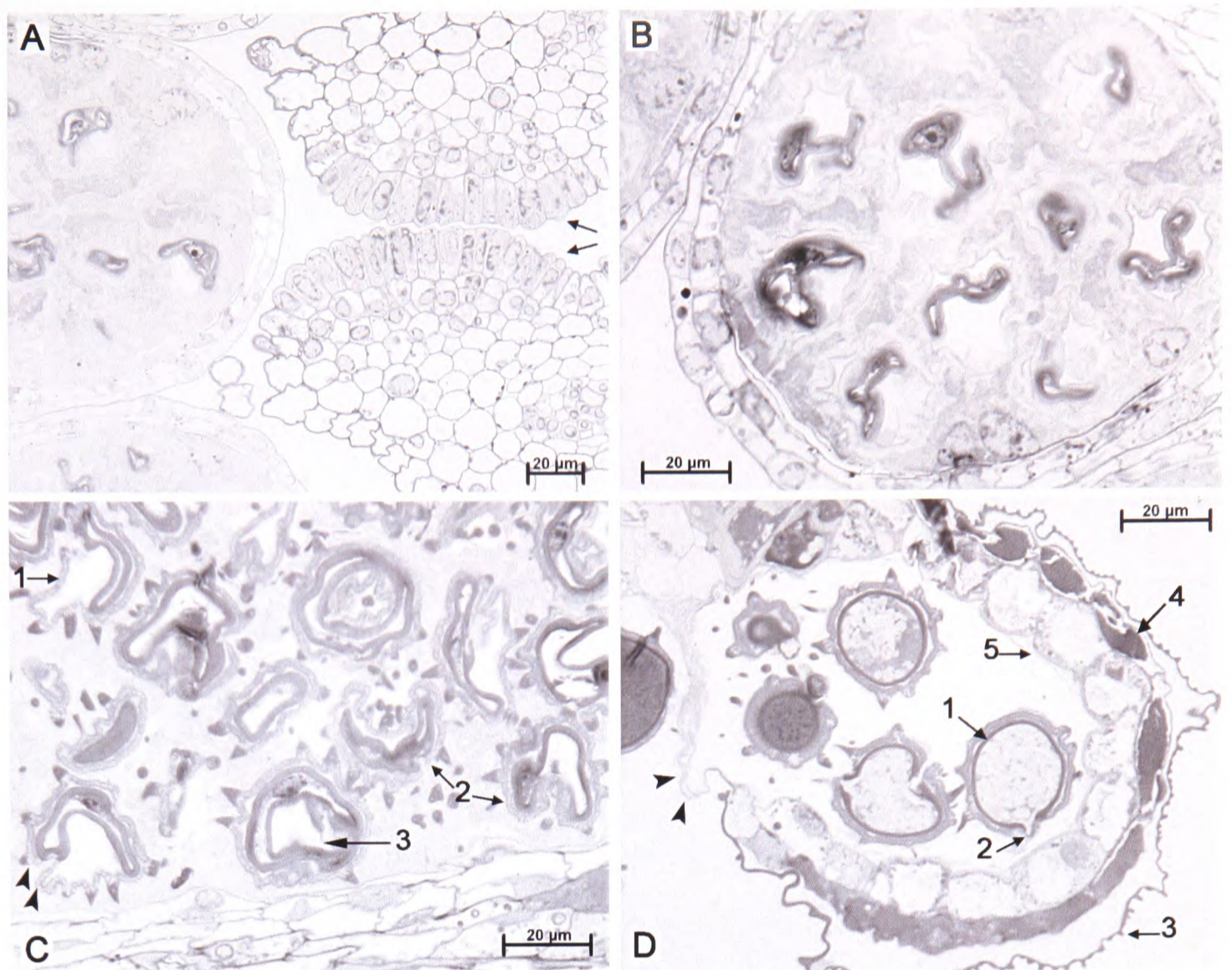


Plate 3.13a – Late stage-1 *Cosmos atrosanguineus* disk florets.

TS (A, B & D) and LS (C) showing anthers and stigma at vacuolate uninucleate microspore stage (A-C) and early binucleate engorging pollen-grain stage (D) Preparation method: A-D, stRS. (LM bright field).

At the late vacuolate stage of microspore development, tapetal protoplasts fuse to form a plasmodial syncytium, which invades the entire locular space and completely engulfs the vacuolating microspores (A-C). Vacuolation of microspores results in the formation of one large vacuole, creating a "signet-ring" shaped appearance of the cytoplasm (C, **arrow 3**), that pushes the cytoplasm and nucleus up against the nexine layer of the microspore (A-C). A thin faint spacer layer of non-sporopollenin receptive primexine is discernible between sexine and nexine wall layers (C, **arrowheads**). In some of the vacuolate microspores, the preparation method has caused the exine layer (C, **arrow 1**) to collapse slightly with the migrating cytoplasm (C, **arrow 2**). The first pollen mitosis occurs at the late vacuolate 'signet-ring' stage, after which the large vacuole disappears, as the cytoplasm of the binucleate pollen grain expands, and the binucleate pollen begins to engorge large amounts of lipidic substances, giving the pollen cytoplasm a bubbly appearance (D). Pollen grains increase in size to ~20 µm diameter, and the tapetal plasmodium clears from the locular space as it becomes deposited on the pollen exine to form the thick tryphine pollen coat (D). The intine layer develops after expansion of the cytoplasm but before pollen engorgement. The pectocellulose intine layer appears first at the regions of the three colpi, but eventually spreads to form a continuous layer around the cell membrane (D, **arrow 1**), emerging as operculae at each colpus (D, **arrow 2**). The cell layers separating the two pollen sacs within each theca disintegrate and exist as a single thin layer of compressed cell remnants (D, **arrowheads**). A tough thin translucent membrane encloses the outer surface of the five anthers joining them into a connate anther tube (D, **arrow 3**). By early engorgement of pollen grains, the tapetum and the middle layer are no longer present. The anther wall is composed of an epidermis filled with dark-brown inclusions (D, **arrow 4**) and an endothecium composed of large cells with U-shaped thickening on the inner tangential and both radial walls (D, **arrow 5**). The short stigma papillae lengthen throughout the vacuolating microspore stage and their cytoplasm become increasingly dense (A, **arrows**), and appear much denser than the layers of parenchymous cells beneath (A).

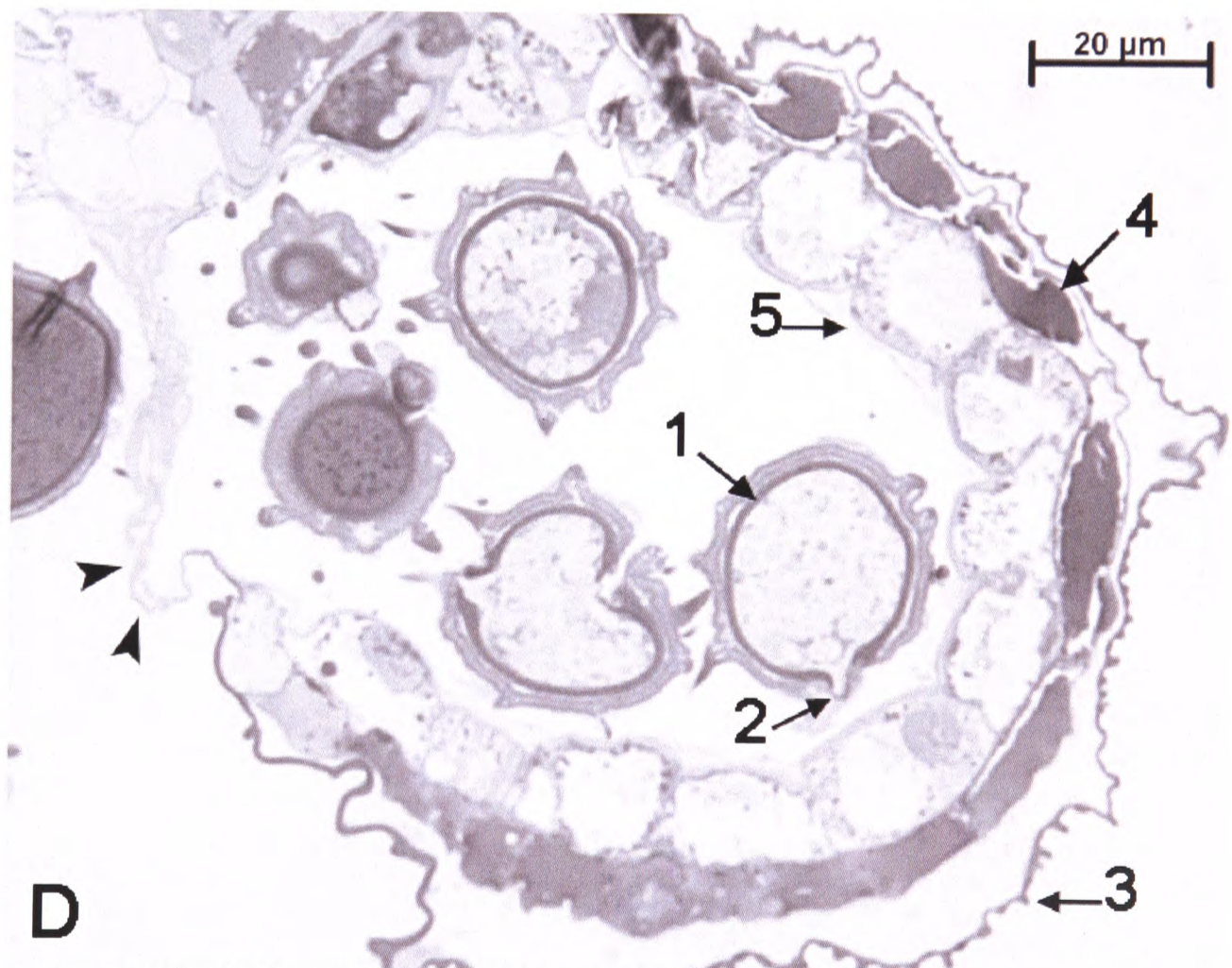
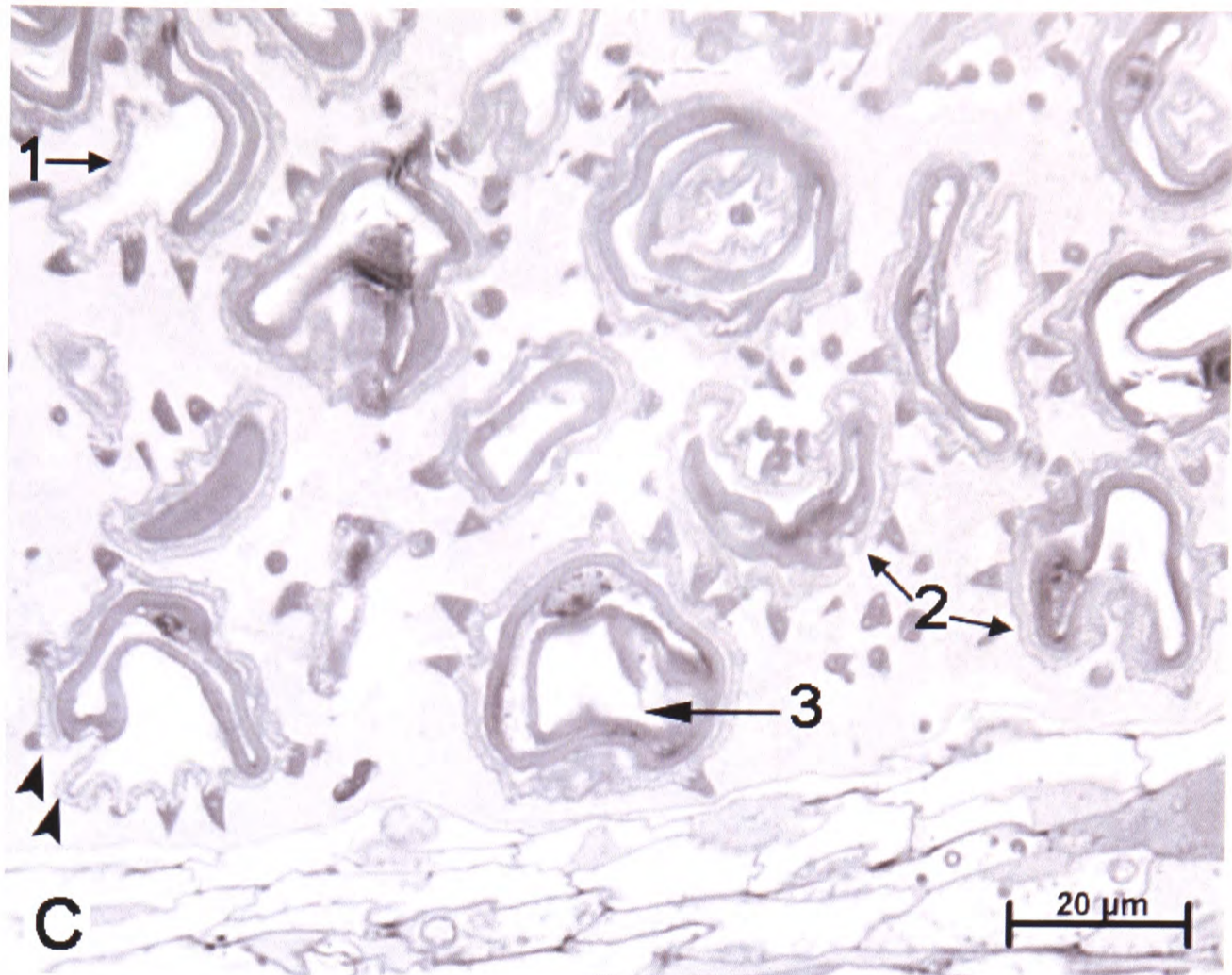


Plate 3.13b – Enlarged Images of C and D from 3.13a showing detail of pollen wall layers in late stage-1 *Cosmos atrosanguineus* disk florets

C, - arrow 1, exine layer; arrow 2, preparation artefact resulting in the collapse of exine layer; arrow 3, single large vacuole pushes cytoplasm and nucleus up against the nexine layer of the microspore, creating the characteristic signet-ring-shaped cytoplasm.

D – arrow 1, pectocellulose intine layer; arrow 2, operculae; arrow 3, thin translucent membrane that encloses and joins the five anthers into a connate anther tube; arrow 4, anther epidermal cell filled with dark-brown coloured material; arrow 5, endothelial cell showing characteristic U-shaped primary wall thickenings on the inner tangential and both radial walls. Preparation method, stRS. (LM bright field).

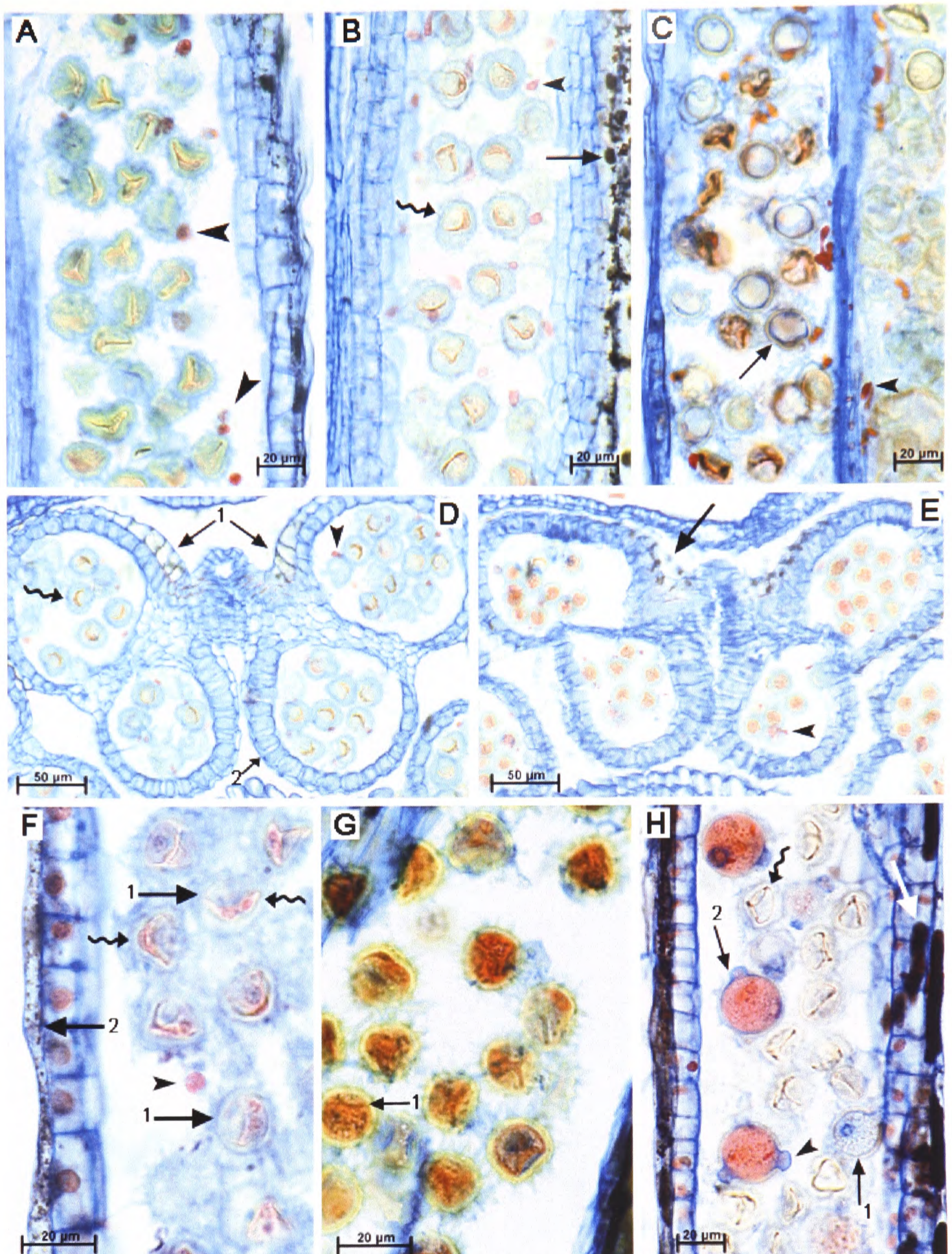


Plate 3.14 – Late stage-1 *Cosmos* anthers. LS (A-C & F-H) and TS (D-E)

C. atrosanguineus (A & H), *C. bipinnatus* (B, & D-F) and *C. sulphureus* (C & G)

B, D, F & H; (fluted arrows). –signet-ring-shaped microspore caused by the vacuolation of the cytoplasm.

A to F – showing less-densely staining tapetal plasmodium, beginning to clear from the anther locule and becoming deposited as a thick layer of tryphine pollen coat on the surface of vacuolate microspores..

A-F (arrowheads) - large densely-staining spherical bodies, ~5 μm in diameter, appear initially within the tapetum and become deposited on the surface of the pollen grains at the later stages of tapetal dissipation..

F (arrows-1) – binucleate pollen grains. The first pollen mitosis takes place within late vacuolate microspores and produces generative and vegetative nuclei of similar sizes that lie next to each other in the collapsed cytoplasm

C, E, G & H - the cytoplasm of the binucleate pollen grain expands rapidly

C (arrow) - the pectocellulose intine layer is initiated from the three colpus regions, and eventually spreads out to surround the entire cell membrane, protruding as operculae at each colpus (**arrowhead**).

G & H (arrow-1) - bubbly appearance of the pollen grain cytoplasm is caused by engorgement of the cytoplasm by vast amounts of lipidic material.

H (arrow 2) –binucleate fully engorged pollen grains, expanded to their full diameter, with densely-staining cytoplasm

D (arrow-1), B, & E (arrows), F (arrow-2) - dark brown material accumulates initially in the cytoplasm of epidermal cells on the abaxial anther surface but eventually occurs in all epidermal cells, **H, (white arrow)**.

D (arrow-2) - the endothecium, consisting of large cells with characteristic U-shaped thickenings

Preparation method: for A-H, LM. (LM bright field).

Between early- to mid-vacuolation of microspores, a peritapetal membrane (Shivanna and Johri, 1985) or culture sac (Heslop-Harrison, 1969) of sporopollenin is formed on the outer surface of the *Cosmos* tapetum, adjacent to the inner tangential walls of the middle layer (Plate 3.16, B-F). The function of this membrane is not known, but it may restrict the free movement of materials into and out of the microspore mass and allow a period of gametophytic isolation during pollen-grain development (Shivanna and Johri, 1985; Pacini). A peritapetal membrane has been observed in *Brassica*, but not in *Lilium*, which exhibits GSI, and hence the peritapetal boundary layer may be a characteristic of SSI species, possibly serving a role in the separation of gametophytic from sporophytic anther tissue, allowing a period of gametophytic activity to prevail in the anther (Bell, 1995). The *Cosmos* peritapetal membrane remains throughout tapetal deposition (Plate 3.16, A-F). Initially, the membrane is appressed against the cells of the middle layer (Plate 3.16, B, D) but eventually, as the middle layer disintegrates, it becomes separated from the outer wall layers, and exists as an independent structure that isolates pollen grains from the sporophytically-derived layers of the anther wall (Plate 3.16, C, E; Plate 3.18, A, C). The dissipating *Cosmos* tapetum contains large densely-staining spherical bodies approximately 5-8 μm in size (Plate 3.14, A-F). Initially, the densely-staining bodies appear at the periphery of the locule, but become associated with the surface of the pollen grains as the locule dehydrates and the plasmodium dissipates (Plate 3.14, E-F; Plate 3.16, D-F). Densely-staining bodies occur in all three *Cosmos* species, and have a spherical shape in *Cosmos atrosanguineus* and *C. bipinnatus*, but are spherical to rod-shaped in *C. sulphureus* (Plate 3.14, A-F). The *Cosmos* spherical bodies, although a product of the tapetum, are not orbicles (Ubisch bodies), since orbicles are a characteristic of secretory tapeta and are found only exceptionally in amoeboid tapeta (Echlin and Godwin, 1968a; Greyson, 1994; Furness and Rudall, 1998; Vinckier and Smets, 2003). In addition, the average size (5-8 μm) of the *Cosmos* spherical bodies is much larger than the 0.2-2.0 μm recorded for most tapetal orbicles (Vinckier and Smets, 2003; Wang *et al.*, 2003). In *Brassica* species, after the first pollen mitosis, tapetal cells accumulate elaioplasts and large cytoplasmic lipid bodies (Hernández-Pinzón *et al.*, 1999). *Brassica* elaioplasts are small structures of $\sim 1 \mu\text{m}$ or less, whereas *Brassica* tapetal cytoplasmic lipid bodies are 1-5 μm in size (Piffanelli *et al.*, 1998). The size-range of the *Cosmos* spherical bodies would indicate that they are cytoplasmic lipid bodies similar to those observed in *Brassica*. The *Brassica* cytoplasmic bodies are derived from tapetal endoplasmic reticulum (ER) (Robert *et al.*, 1994), and have an internal fibrous proteinaceous network composed of full-length oleosin-like proteins encoded by a

large gene family expressed exclusively in the tapetum (Robert *et al.*, 1994; Ferreira *et al.*, 1997; Piffanelli *et al.*, 1998). Safranin is known to stain lignin and nucleic acids red (Conn and Lillie, 1977). Since lignin does not occur in tapeta, the intense red-staining of the *Cosmos* spherical bodies suggests these structures contain nucleic acid, possibly RNA, identifying them as possible sites of gene expression (Plate 3.14, A-C). The *Brassica* full-length oleosin-like precursors have a hydrophobic oleosin-like domain near the N-terminus and a highly polar C-terminal domain (Murphy and Ross, 1998). Upon locular invasion by the tapetal plasmodium, the cytoplasmic lipid bodies contain full-length oleosin-like proteins, however, after their attachment to the exine wall, cleavage of proteins occurs close to the junction of the oleosin-like domain and the C-terminal domain, leaving the highly polar C-terminal domain as the main proteinaceous component of the pollen coat (Wang *et al.*, 1997; Piffanelli *et al.*, 1998). The functions of these protein-coat oleosin-like proteins have not been identified, but the *Cosmos* spherical bodies may be a production site of full-length oleosin-like proteins.

At the late vacuolate (signet-ring) stage of microspore development, the tapetal plasmodium completely engulfs the *Cosmos* microspores, with tapetal fragments deposited on and within the interstices of the pollen exine, to form a chemically-complex, lipoidal pollen coat (Piffanelli, *et al.*, 1998; Plate 3.15; C-H; Plate 3.16, A, E-F). A pollen coat comprised predominantly of plastid-derived lipids, carotenoids and other pigmented compounds is referred to as pollenkit, and one formed from a complex matrix of intact organelles, produced by the partial degeneration of the tapetum is known as tryphine pollen coat, (Dickinson, 1973; Pacini, 1997; Dickinson *et al.*, 2000). The *Cosmos* pollen coat appears to be a tryphine coat, as it results from the partial degradation of the tapetal protoplasts. The pollen coat in *Cosmos* forms a ~0.5- μm thick patterned layer and is laid down as fragments of dehydrating tapetum (Plate 3.17, A-C). The methods used in this study do not offer any information as to the chemical composition of the *Cosmos* pollen coat, but in *Brassica*, the tryphine coat constitutes between 10-15% of pollen-grain mass, and is comprised of layers of lipid, proteins, glucoconjugates, as well as carotenoid and flavanoid pigments (Piffanelli *et al.*, 1998). The major lipid components are non-polar esters of medium to long-chain saturated fatty acids that maintain the semi-solid matrix, which holds proteins and other substances within the pollen coat (Piffanelli *et al.*, 1998). A small amount of very long chain wax esters is also present within the pollen coat and appear, in some cases, to be important for pollen-grain fertility (Piffanelli *et al.*, 1998). In the male-sterile

eceriferum (*cer*) class of *Arabidopsis* mutants, for example, disruption in very-long chain acyl lipid synthesis pathways interferes with the pollen coat structure (Preuss *et al.*, 1993; Aarts *et al.*, 1995). Likewise, the abnormal pollen-epidermis interactions of the *Arabidopsis fiddlehead-1* mutant may be a consequence of alterations in its extracellular very-long chain lipids (Lolle *et al.*, 1997). The major protein components of tryphine coats are hydrolytic enzymes such as esterases, acid phosphatases, amylase, ribonucleases, pollen-allergy proteins and oleosin-like proteins thought to participate in pollen adhesion and in stabilization of the pollen coat during dehydration and rehydration (Knox *et al.*, 1970; Knox and Heslop-Harrison 1971; Knox, 1973; Vithanage, and Knox, 1977, 1979; Vithanage *et al.*, 1982; Grote and Fromme, 1984; Detchepare *et al.*, 1989; Lavithis and Bhalla, 1995; Ross and Murphy, 1996; Ruitter *et al.*, 1997). Aquaporins, dehydrins and proteins involved in pollen-stigma signalling such as SCR and the gametophytically-expressed PCPAs are also located in the pollen coat (Hiscock *et al.*, 1995a, 1995b; Stephenson *et al.*, 1997; Doughty *et al.*, 1993, 1998; Piffanelli *et al.*, 1998; Dickinson *et al.*, 2000). Aside from pollen coat proteins, the intine regions at the colpi contain microspore-derived proteins, which means the proteins contained within the operculae and the tips of emerging pollen tubes are gametophytic in origin (Shivana and Johri, 1985). For example, cutinase, which is responsible for the degradation of the stigmatic cuticle, is an intine protein (Hiscock, *et al.*, 1994). Thus the pollen-coat function in pollen dispersal, pollen adhesion and pollen-stigma recognition is under the control of gametophytically- and sporophytically-derived molecules carried on the surface and interstices of the pollen grain.

The *Cosmos* pollen coat is not deposited evenly over the entire surface of the grain, but is laid down in large uneven clumps, predominantly on the tectum between the spines, and only later becomes evenly distributed over the exine surface (Plate 3.17, A). The mechanism that ensures the even distribution of pollen coat is not understood. In *Cosmos*, fibrillar tapetal material becomes attached to the exine surface and appears to anchor the developing pollen coat onto the exine surface (Plate 3.17, C). Similar material in *Raphanus* (Dickinson and Lewis, 1973a, 1973b; Pacini, 1990), *Brassica* (Elleman and Dickinson, 1990), *Arabidopsis* (Owen and Makaroff, 1995), *Lilium* (Heslop-Harrison, 1968) and *Olea* (Pacini and Juniper, 1979), identified as tapetally-derived proteinaceous fibrils, also appeared to anchor tapetal debris, in a predetermined, manner onto the exine surface (Gaude and Dumas, 1984). In Asteraceae, the pollen coat is known to permeate spaces within the sexine, and

between the nexine and sexine via an active adhesive process (Dickinson *et al.*, 2000). Observations of the formation of the *Cosmos* pollen coat indicate a well-ordered deposition of tapetal fragments, leading to an even distribution of tryphine coat that is anchored by tapetal fibrils to the exine surface (Plate 3.17, B-C, E-F). The completed *Cosmos* pollen coat, like the coats observed in *Brassica* and Asteraceae, has a heterogeneous appearance, with uniform material over the spines, a fibrillar less-dense material covering the perforations, and a granulo-fibrillar layer covering the tectum (Rowley *et al.*, 1981; Dickinson and Elleman, 1985; Elleman and Dickinson, 1986; Rowley, 1990) Plate 3.17, F). The heterogeneous structure of *Brassica* and *Cosmos* pollen coats probably reflects the variety of processes that these structures perform from the time of anther dehiscence to pollen germination. As deposition of the pollen coat is completed and the spherical bodies are absorbed completely onto the pollen grains, the peritapetal membrane dehydrates onto the mass of dehydrating pollen grains, wrapping them in a final layer of pollen coat (Plate 3.17, D; Plate 3.18, C). In *Brassica* and *Arabidopsis*, a clearly defined layer called the coating superficial layer (CSL) forms on the outer surface of the pollen coat and can, with certain treatments, be detached from the pollen coat surface (Gaude and Dumas, 1984; Elleman and Dickinson, 1986). The dissipation of the *Cosmos* peritapetal membrane over the pollen-grain mass may represent the laying down of a *Cosmos* CSL (Plate 3.18, C). Deposition of the peritapetal membrane occurs while anthers are tetrasporangiate, so that the orientation of the two pollen sacs is discernible after dehiscence of the bisporangiate anthers (Plate 3.18, A, C, D).

In late stage-1 anthers, dark-brown material, possibly tannins (Esau, 1977), begins to accumulate in the cytoplasm of epidermal cells (Plate 3.12, D; Plate 3.14, B, D-E, F, H). Deposition of the dark-brown material is initiated in the epidermal cells on the adaxial surface of tetrasporangiate anthers (Plate 3.14, D-E), but is observed, to a lesser degree, in the epidermal cells of the abaxial anther surface, by the time the anther becomes bisporangiate (Plate 3.19, A-E). Deposition of the dark-brown material corresponds with a change in texture of the epidermal cells, which now form a tough, dry, rigid outer layer.

Stage-1 disk florets contain stigmas at the pre-secretory period of cell-growth (Knox, 1984). The apical stigma papillae in the three *Cosmos* species lengthen considerably throughout the stage-1 florets, but papillar cells on the adaxial and lateral surfaces begin lengthening in late stage-1 florets.

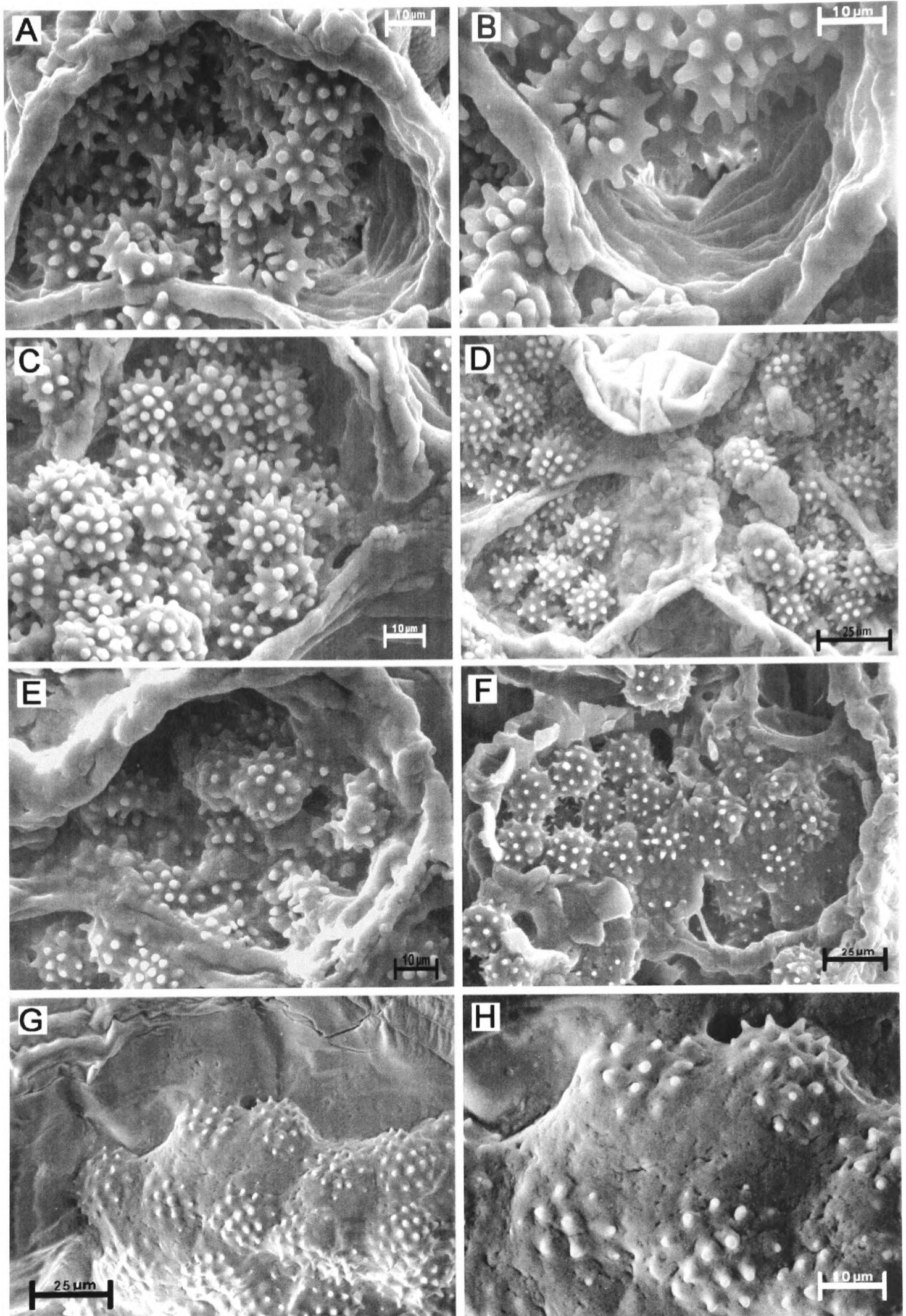


Plate 3.15 – Late stage-1 *Cosmos sulphureus* anthers, TS (A-F) and LS (G-H). (CryoSEM)
 A-B. showing anthers with a parietal secretory tapetum and vacuolate microspores ~10 μm in diameter. The anther locule is clear, tapetal protoplasts are intact, the tapetum has a regular structure, and its cells have not yet fused into a tapetal syncytium. Microspores consist of a thin exine layer, short spines (A-C). Some microspores have collapsed as a result of cell vacuolation (A-B). The regular structure of the tapetal layer becomes disrupted as protoplasmic extensions from the tapetum begin to invade the locular space (C-D). The invasion of the locule by the tapetum marks the transition from a parietal to an amoeboid tapetum (C-F). As invasion of the amoeboid tapetum increases, tapetal protoplasts fuse to form a single tapetal syncytium that fills the locular space and engulfs the vacuolating microspores (F-H).

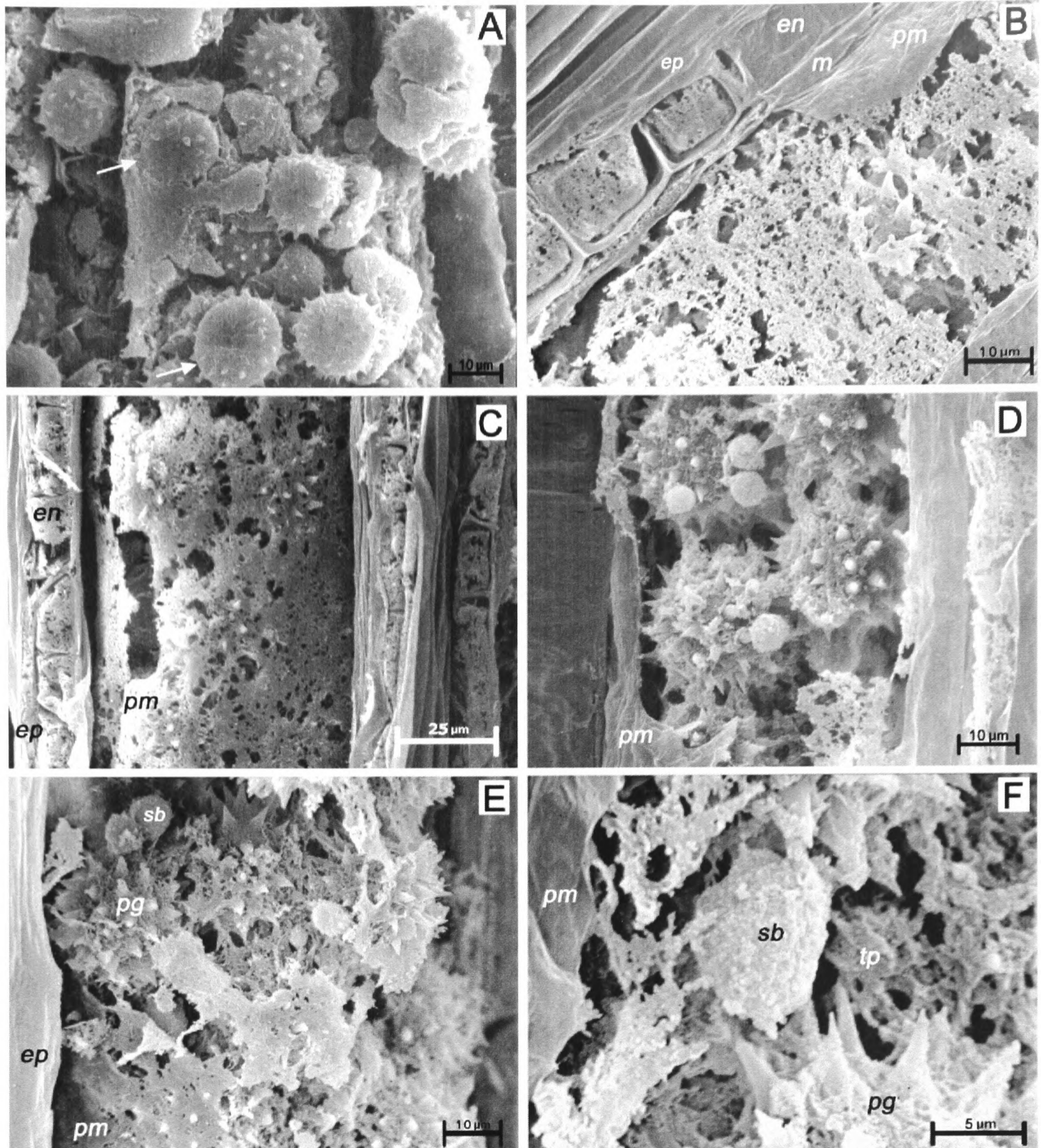


Plate 3.16 – LS Late stage-1 *Cosmos atrosanguineus* anthers (Preparation method: **A-F**, ambient SEM)

The tapetal syncytium completely engulfs the vacuolating microspores (**A**) with tapetal debris deposited on the pollen-grain surface (**pg**) and within the interstices of the exine layer (**B-F**). Some of the vacuolate microspores collapse slightly as a consequence of cell vacuolation producing doughnut-shaped microspores (**A**, white arrows). A peritapetal membrane (**pm**) is formed on the outer surface of the tapetum, adjacent to the inner tangential walls of the middle layer (**m**) (**B**). To the inside of the peritapetal membrane, the tapetal plasmodium (**tp**) fills the locular space, and engulfs the pollen grains. Eventually, as the locule dehydrates, the tapetal plasmodium becomes deposited on the enlarging pollen grains to form a tryphine pollen-coat (**D-F**). Towards the latter stages of tapetal dissolution, large spherical bodies (**sb**) appear within the dissipating tapetal plasmodium (**tp**) and become attached to the outer surface of the engorging pollen grains (**pg**) (**E-F**). The peritapetal membrane dehydrates, becomes separated from the outer anther-wall layers, collapses into the locule and wraps itself around the pollen-grain mass (**A-C** and **E**). Expansion of the anther compresses the middle layer (**m**) against the endothecium (**en**) (**B**), causing the middle layer to disintegrate (**C**). By the latter stage of pollen engorgement, the anther wall is composed of two layers; the large-celled endothecium (**en**) and an epidermis of narrow crumpled cells (**ep**) (**C**). The cells of the endothecium (**en**) begin to lay down their characteristic U-shaped primary cell-wall thickening at this stage (**B**).

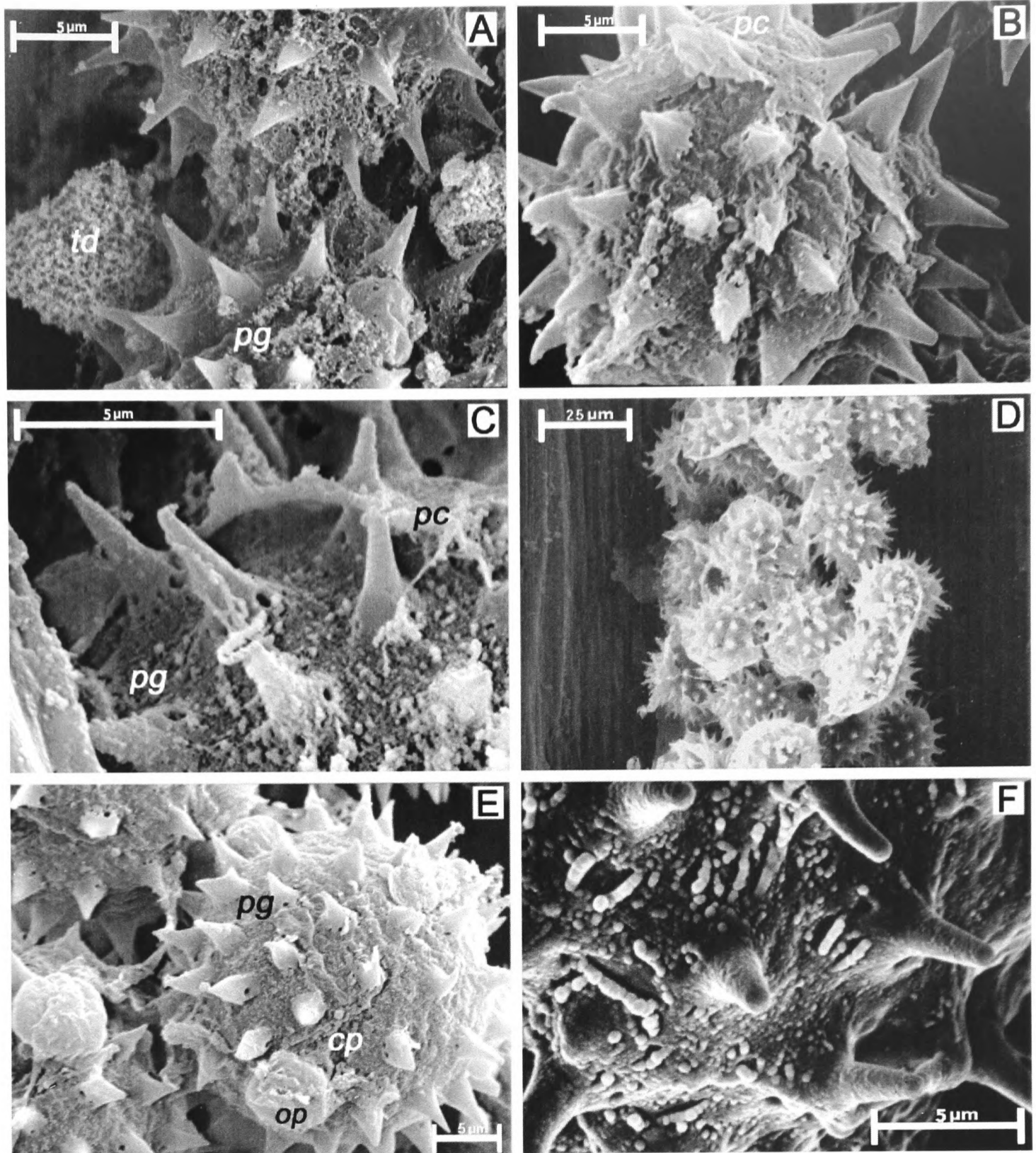


Plate 3.17 – Early stage-2 *Cosmos* pollen grains, showing deposition of pollen coat. *C. atrosanguineus* (B & E); *C. bipinnatus* (A & C-D) and *C. sulphureus* (F) (Preparation method: A-E, ambient SEM; F, CryoSEM.)

The mature *Cosmos* pollen grain is echinate, tricolpate and has a tectate-perforate exine layer, with operculae (*op*) protruding from each colpus (*cp*) (A-C & E.). The main perforations of the tectum are located at the base of the spines (C). Tapetal debris (*td*), formed from the dissipating tapetal plasmodium, is deposited onto the surface of the *Cosmos* pollen grain (*pg*) (A). Continued deposition of tapetal material leads to the formation of a thick (0.5-0.7 μm) tryphine pollen coat (*pc*) (B-C). The peritapetal membrane dehydrates and collapses onto the inner mass of pollen grains wrapping them in a final layer of pollen coat (D). On completion of pollen-coat deposition, the anther locule is free of tapetal material, and the pollen grains within each locule are wrapped together within the dehydrated peritapetal membrane (D). The *Cosmos* pollen coat has a complex architecture, forming a smooth continuous surface over the spines, but a more patterned fibrillar perforated surface over the body of the grain (F). Perforations in the pollen coat correspond to the positions of tectate perforations at the bases of the spines in the underlying exine (B, C and F).

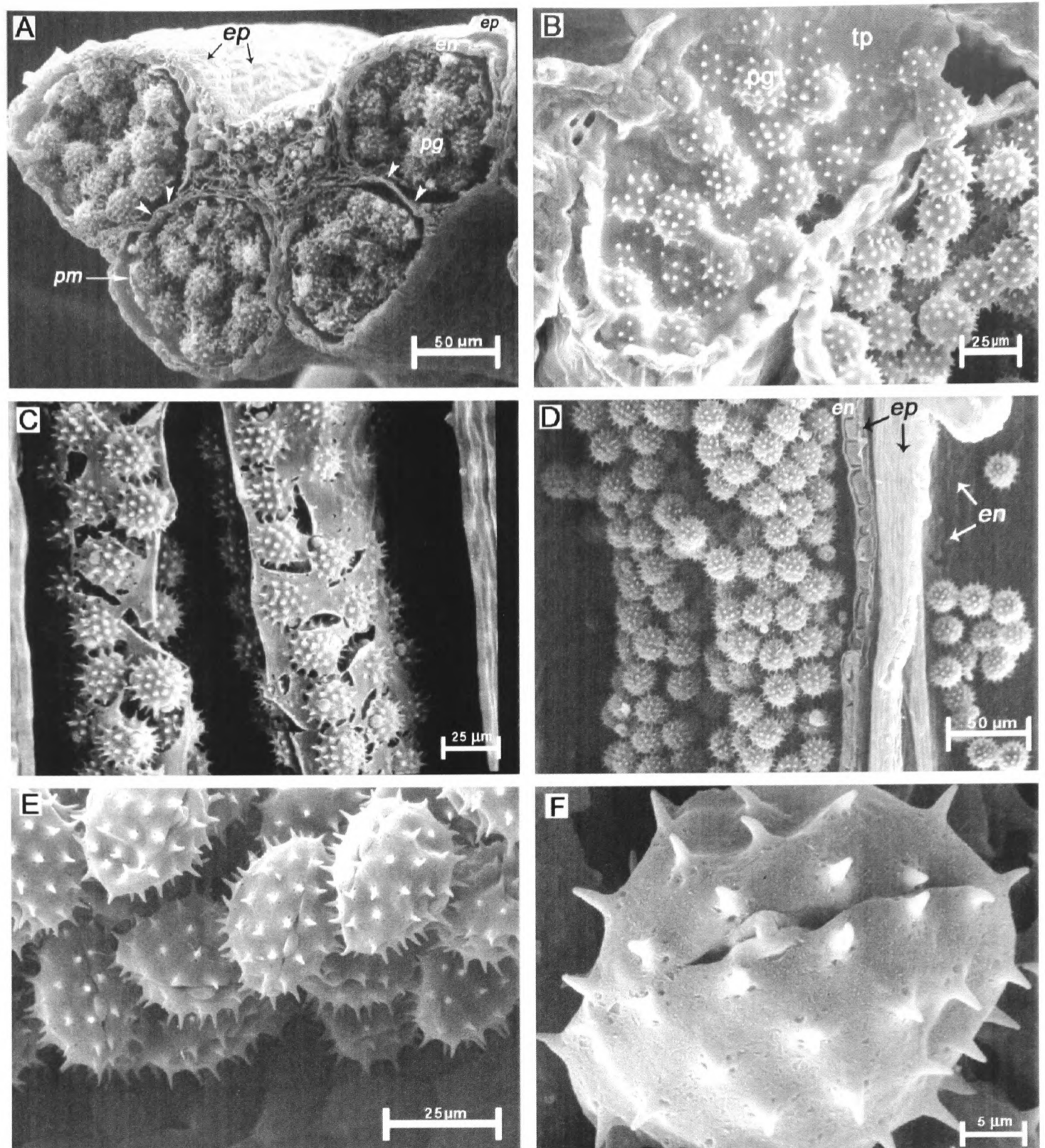


Plate 3.18 – Stage-1 and stage-2 *Cosmos* anthers. TS (A-B) and LS (C-D)

C. bipinnatus (A, C & D) and *C. sulphureus* (B, E & F) (Preparation method: A, C & D, ambient SEM; B, E & F, CryoSEMs)

In late stage-1 florets, a peritapetal membrane (*pm*) encloses the pollen grains (*pg*) of each pollen sac, and separates the central gametophytic sporogenous tissue from the sporophytic outer anther-wall layers (A). The peritapetal membrane breaks down and becomes wrapped around pollen grains while anthers are tetrasporangiate, so that the orientation of the two pollen sacs within a theca is discernable after anther dehiscence (A, C & D). Microspore development within a pollen sac is synchronous, but there may be small differences in the development of microspores within, or between anthers (B, & Plate 3.14, C). On the breakdown of the peritapetal membrane, the anther wall consists of two layers, the large-celled endothecium (*en*) and an epidermis (*ep*) composed of narrow crumpled cells (A & D). The parenchyma cell layers between sporangia (pollen sacs) become increasingly compressed and begin to disintegrate, resulting in a reduction in the cell barrier that separates the two pollen sacs of a theca (A, **arrowheads**). When this layer ruptures, the *Cosmos* anther becomes bisporangiate and the disk floret enters stage-2 period of development. In stage-2 anthers, the tapetal material clears from the dehydrating anther locule (C-E), so that by the time of anther dehiscence the locule is dry and completely free of tapetal debris (C-D). The mature echinate pollen grains are trinucleate, have three colpi with protruding operculae, and are clumped together by means of their sticky pollen coats (D & E),

(iv) Early stage-2 – From engorging pollen grains to second pollen mitosis

As the engorging *Cosmos* pollen grains become cytoplasmically dense, the tissue separating each sporangium in a theca disintegrates to create a bisporangiate anther, which signals the onset of stage-2 floret development (Plate 3.19, C-E; Plate 3.20, A-F). In early stage-2 disk florets, the anthers contain cytoplasmically-dense, fully-engorged pollen grains within dehydrated locules free of plasmodial tapetum (Plate 3.19, B-E; Plate 3.20, A-F). At this stage, the less-densely-staining vegetative nucleus is positioned at the centre of the pollen grain, and the densely-staining generative nucleus remains in a peripheral position attached to the intine layer of the pollen wall (Plate 3.19 E, Plate 3.20, F).

Towards the end of early stage-2 florets, the pollen coat thins and becomes evenly distributed over the pollen grain, the cytoplasm appears less dense and loses its bubbly appearance, and the spherical bodies are less prominent (Plate 3.19 A-E, Plate 3.20, A-F). The *Cosmos* pollen grain is now fully engorged and is ready to enter the second pollen mitosis. Prior to the second mitotic division, the generative nucleus moves to the centre of the vegetative-cell cytoplasm and locates itself adjacent to the vegetative nucleus (Shivanna and Johri, 1985; Blackmore and Barnes, 1988; Greyson, 1994; Plate 3.20, E-F).

In the binucleate *Cosmos* pollen grain, the generative and vegetative nuclei are of similar size but can be distinguished from each other, as the condensed generative nucleus stains more densely than the vegetative nucleus (Plate 3.20, E-F; Plate 3.21, A-B). The second *Cosmos* pollen mitosis results in two small circular generative nuclei that lie adjacent to each other and close to the vegetative nucleus in the centre of the *Cosmos* pollen grain (Plate 3.21, C-E).

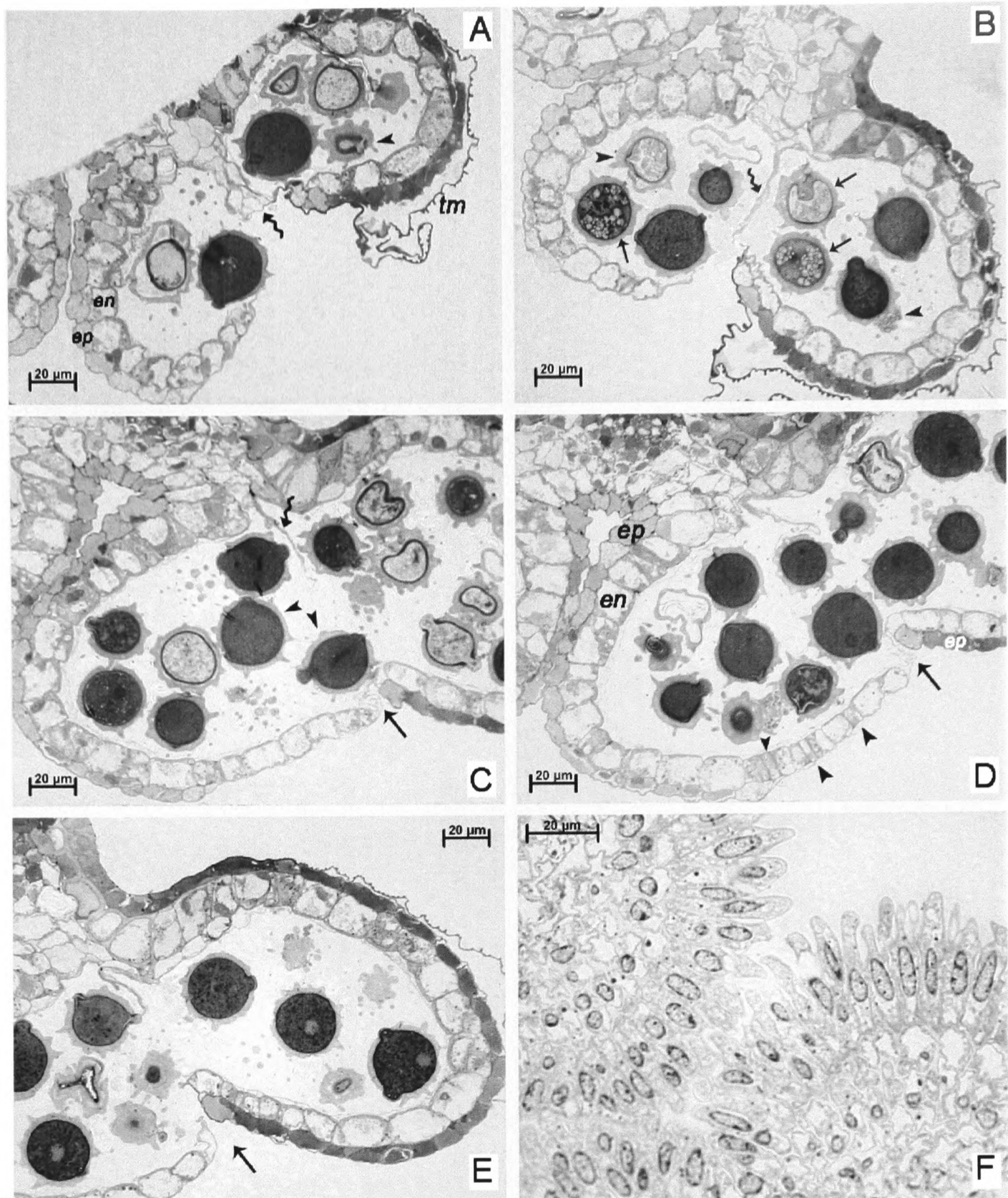


Plate 3.19 – TS *Cosmos atrosanguineus* disk florets, showing the transition from tetrasporangiate stage-1 to bisporangiate stage-2 anthers.

In late stage-1 disk florets, the anther wall consists of two layers the epidermis (*ep*) and the endothecium (*en*) (**A-E**). The epidermal cells progressively accumulate a tough dark material in their cytoplasm (A-E). The rigid epidermal layer thins and darkens as the anther expands with the epidermal cells on the abaxial anther surface accumulating more densely-staining material than those on the inner surface (A-E). The translucent membrane (*tm*) surrounds and adheres to the outer sporangia of each anther and joins them into a single connate anther tube (A, B and E). The cells of the endothecium are large and have primary U-shaped or striated thickenings on their inner tangential and radial walls (A-E). The binucleate pollen grains engorge food materials and expand (B straight arrows). At the early stages of pollen engorgement, the pollen coat is thick and clumpy (A-B, arrowheads), but as pollen grains expand, the pollen coat thins and becomes more evenly distributed on the surface of the pollen grain (C arrowheads, & D-E). The cytoplasm of engorging pollen grains become increasingly densely staining as they expand and accumulate materials (A-D). The cell layers separating the sporangia of each theca break down, so that by the early stages of pollen engorgement, it is a thin single layer of disintegrating cells (A-B, fluted arrows). In later stages, this single layer of cells ruptures, resulting in the formation of bisporangiate anthers (C-D, fluted arrows, & E). Dehiscence of anthers occurs when the thin membrane at the anther stoma (C-D, straight arrows) ruptures (E, straight arrows), allowing the anther walls to open. (F). Preparation method: A-F, stRS. (LM bright field)

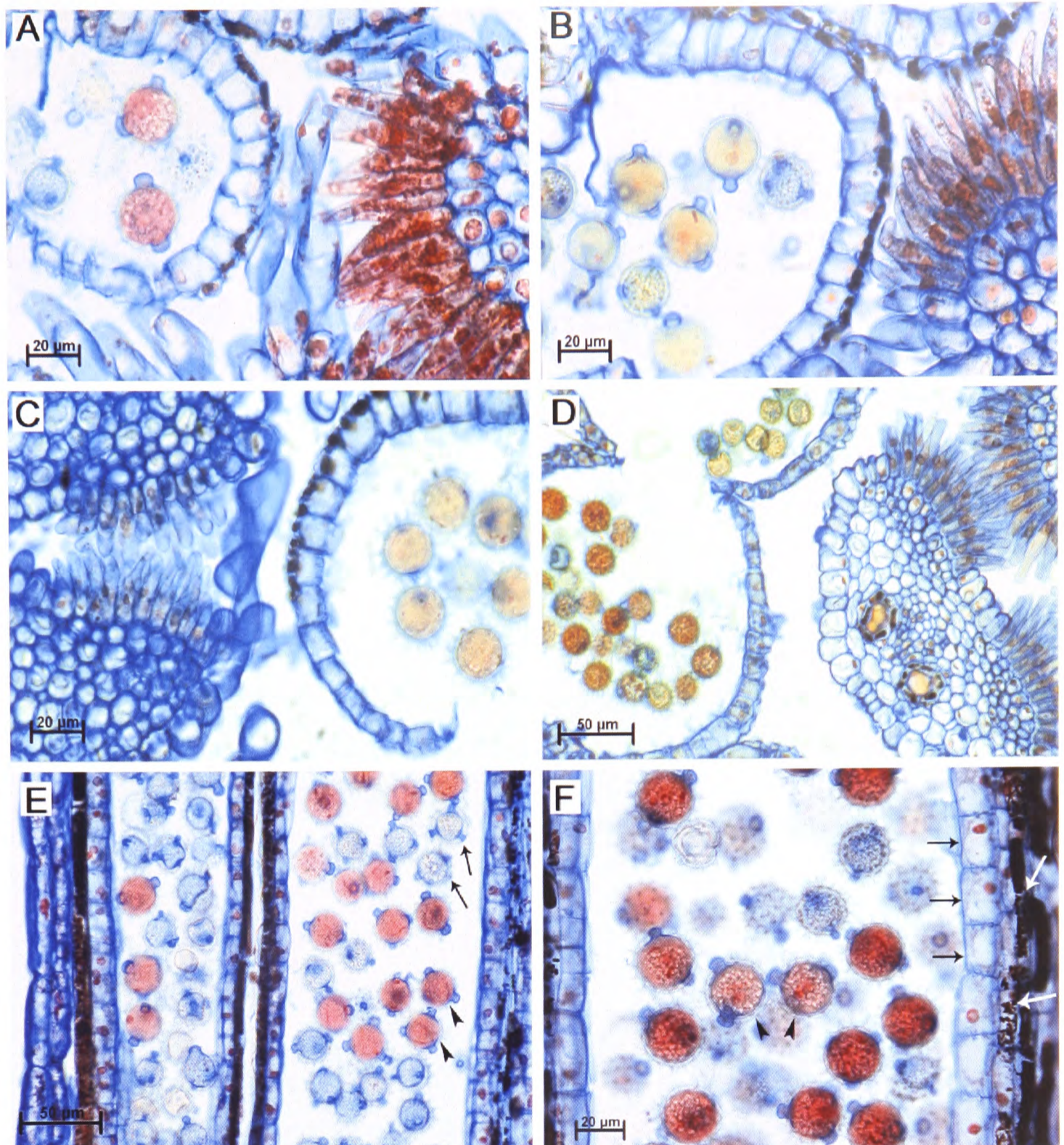


Plate 3.20 – Early and Mid-stage-2 *Cosmos* anthers. TS (A-D) and LS (E-F)
C. atrosanguineus (A-B & E-F); *C. bipinnatus* (C) and *C. sulphureus* (D)

Throughout the period of *Cosmos* pollen engorgement, the short stigma-papillae remain cytoplasmically dense (A-D), and particularly those of *C. atrosanguineus*, which stain intensely red with Alcian blue/safranin staining (A-B). As anthers dehisce and pollen grains undergo second mitosis, the intensity of the red stain in the papillar-cell cytoplasm of the three *Cosmos* species lessens (compare A with B).

E, early stages (arrows) and late stages (arrowheads) of pollen engorgement in early stage-2 disk florets, showing cytoplasmic expansion, intine development and the difference in the cytoplasmic density of early-engorging (arrows) and late-engorging (arrowheads) pollen grains.

F, predominantly late stages of pollen engorgement in mid stage-2 disk florets, showing cytoplasmically-dense binucleate pollen grains with prominent operculae. The cytoplasm of the two central pollen grains (arrowheads) are less dense, and so the vegetative and generative nuclei can be observed more clearly lying next to each other in preparation for the second pollen mitosis

E and F showing the accretion of the dark-brown material in the epidermal cell cytoplasm (F, white arrows), and the U-shaped primary thickening within the endothelial cells (F, black arrows). Preparation method: A-F, wax sections

(v) Mid to Late stage-2 – Anther dehiscence

Mid to late stage-2 anthers are characterised by the movement of the two generative nuclei to opposite poles of the pollen grain (Plate 3.21, E). After the second pollen mitosis, generative nuclei transform into two worm-like structures positioned either side of the centrally placed vegetative nucleus (Plate 3.21, F). The two worm-like structures continue to lengthen as they migrate to the poles of the cell, while the vegetative nucleus condenses to form a ring-like structure in the centre of the pollen grain cytoplasm (Plate 3.21, F).

The mature trinucleate *Cosmos* pollen is now ready for dispersal and is shed inside the late stage-2 *Cosmos* anther before the disk florets open. Anther dehiscence is facilitated by the structure of the remaining two anther wall-layers. The *Cosmos* anther epidermis forms a tough outer layer composed of cells filled with solid brown-staining material. Expansion of the anther causes the inflexible, rigid epidermal cells to become stretched over the large cells of the endothecium, resulting in a thin compressed outer layer (Plate 3.19, E; Plate 3.21, A-B). The cells of the endothecium contain characteristic U-shaped primary thickenings along their inner tangential and radial walls (Plate 3.13a-b D; Plate 3.19, A-E). In the adaxial half of each *Cosmos* sporangium, the first four endothelial cells adjacent to the stomium are not covered by an epidermis and so a weakening is created in the anther wall at this point, which facilitates the rupture of the stomium (Plate 3.19, D). The U-shaped thickening in endothelial cell walls also facilitate anther dehiscence, as dehydration in these cells causes the outer tangential walls to shrink at a faster rate than the thicker radial and inner tangential walls creating a tension in the endothecium that pulls apart the adaxial and abaxial sections of each sporangium (Manning, 1996). Dehydration, shrinkage and accompanying tensile forces eventually cause the anther to rupture along the line of weakness at the stomium, exposing the pollen grains to the stigma (Plate 3.19, E).

The mature pollen grains are collected on the long apical papillae for presentation to insect vectors. Endothelial thickenings develop only towards the latter stages of pollen development, when the tapetum has dissipated and the anther dehydrates (Plate 3.13a-b D). A product within the tapetum has been shown to inhibit the primary-wall thickening of endothelial cells and this inhibition is removed only after breakdown and dissipation of the tapetum (Shivanna and Johri, 1985). The tapetum therefore controls the timing of anther dehiscence, through its inhibition of endothelial-wall thickening

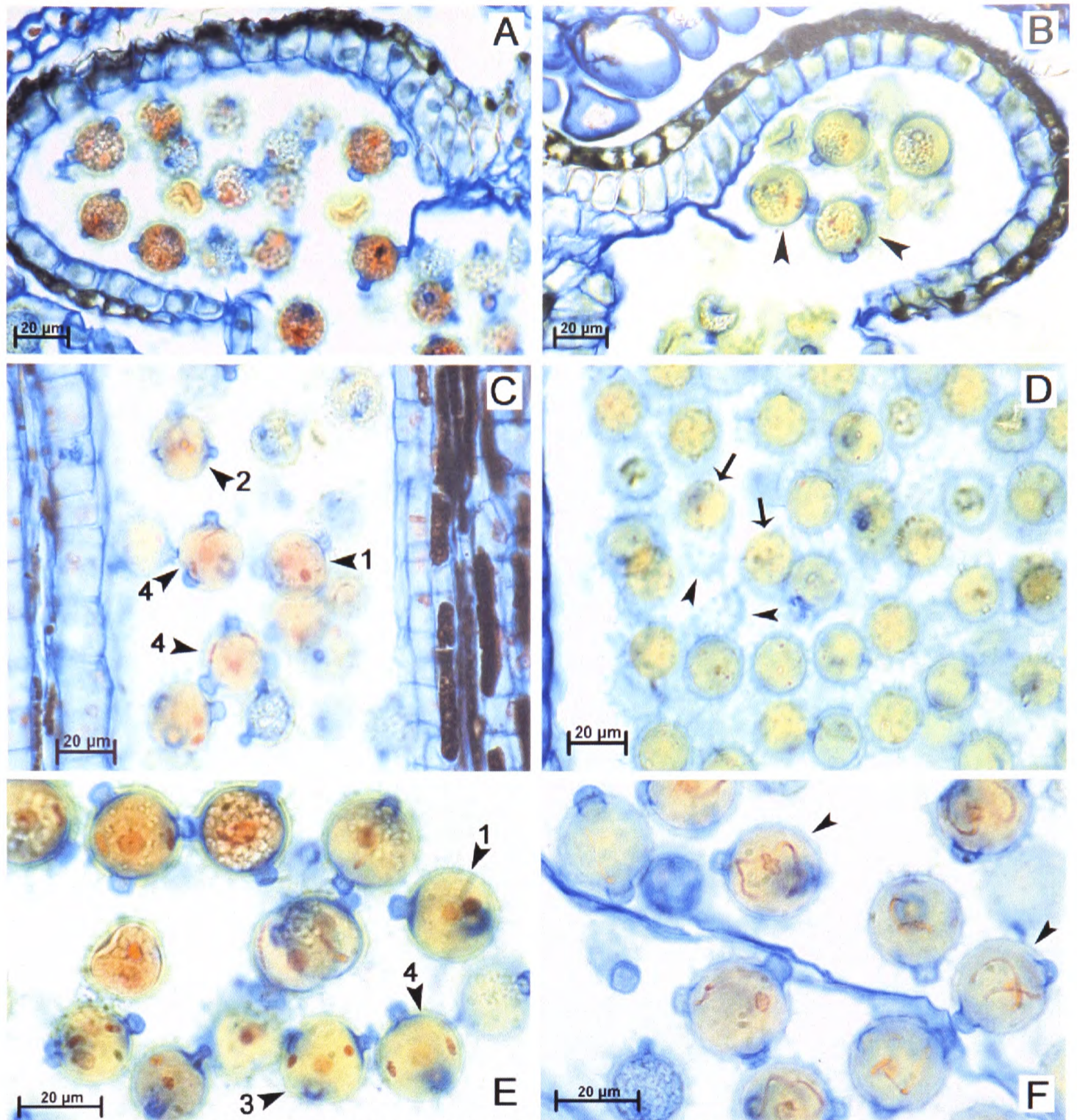


Plate 3.21 – Late stage-2 *Cosmos* anthers, TS (A-B and E-F) and LS (C-D)
C. atrosanguineus (A-C & E-F) and *C. bipinnatus* (D)

(Preparation method: A-F, LM. (LM bright field).

Binucleate, late engorging pollen grains (A) and early trinucleate pollen grains (B, arrowheads) within undehisced anthers. C-E, showing stages before and after the second pollen mitosis. Shortly before the second pollen mitosis, the similar-sized vegetative and generative nuclei lie next to each other in the centre of the pollen grain (C & E, arrowhead 1 & D, arrows). The diffuse vegetative nucleus can be distinguished from the more-densely staining generative nucleus (C, arrowhead 1). The second mitotic division results in a trinucleate pollen grain consisting of two small circular generative nuclei lying adjacent to each other and close to the single large vegetative nucleus in the centre of the pollen-grain (C, arrowhead 2). The vegetative nucleus remains in a central position within the cytoplasm, while each generative nucleus moves to opposite poles of the pollen grain (E, arrowhead 3). Here they begin to elongate to form two worm-like structures (C & E, arrowheads 4). In mature trinucleate *Cosmos* pollen, the two worm-like generative nuclei are located at the periphery of the pollen-grain cytoplasm, and the circular-shaped vegetative nucleus is located at the centre (F, arrowheads). In D, the preparation method has caused the disruption and removal of the pollen coat from some of the pollen grains (arrowheads).

In Asteraceae, stigmatic papillar cells enter a period of extrusion, characterised by the deposition of extracellular stigmatic layers (Knox, 1984). In *Cosmos*, this extrusion period starts in late stage-2 stigmas and is completed by the development of mid stage-3 florets, prior to the onset of stigma receptivity (Knox, 1984). The pellicle, the outermost stigmatic layer, is one of the secretory layers deposited throughout this extrusion period. The Asteraceae pellicle, like that of *Brassica*, is hydrophilic, and likewise is digested by proteinase, but not lipase, and possesses intense non-specific

esterase activity, but exhibits no other enzymic properties (Mattsson *et al.*, 1974; Heslop-Harrison, 1992a). Esterase activity of the pellicle appears first in the bud and increases throughout floral maturation and anthesis (Heslop-Harrison, 1975). Plant pellicle proteins are synthesized in microbodies in the cytoplasm of papillar cells and are then discharged at the plasma membrane, where they diffuse through the pectocellulosic part of the cell wall, and the cuticle, to form a hydrated secretory aggregate on the stigma surface (Heslop-Harrison and Heslop-Harrison, 1975a; Heslop-Harrison *et al.*, 1975; Knox, 1984; Ciampolini and Cresti, 1998; Furuyama and Dzelzkalns, 1999; Hiscock *et al.*, 2002).

The period of extrusion in the *Cosmos* stigma is characterised by a high level of metabolic activity in the short papillar cells located on the adaxial and lateral stigma surface. Densely-staining secretory-type vesicles appear at nuclear and plasma membranes and within the cortical cytoplasm (Plate 3.13-A). Copious secretions are also observed at the plasma membrane of underlying the *Cosmos* stigma cells (Plate 3.20 A-B; Plate 3.25, A). The intensity of staining in the short papillar cells is greater in *C. atrosanguineus* than in the other two *Cosmos* species indicating that the papillar cells of *C. atrosanguineus* are particularly active (Plate 3.20, A-D).

Cosmos has a solid stigma-style, with the cells underlying the papillate epidermis constituting the transmitting tissue. In keeping with solid-styled systems, the cells of the *Cosmos* transmitting tissue are arranged loosely and separated by large intercellular spaces filled with copious amounts of extracellular matrix (Gupta *et al.*, 1998; Plate 3.19, F; Plate 3.25, A). The metabolic activity of the transmitting tissue increases throughout the development of mid to late stage-2 florets with the glandular activity of the *Cosmos* stigma peaking in early stage-3 florets, but is completed before the development of late stage-3 stigmas. (Plate 3.25, G-H). The densely-staining vesicles observed throughout stage-2 and early-to-mid stage-3 stigmas may represent the synthesis and secretion of pellicle proteins and/or other extracellular stigmatic layers. Studies on the *Senecio* stigma showed a small quantity of secreted material occurring at the base of the stigma papillae. Although the secretions observed in *Senecio* are far less copious than those observed in wet stigmas characterised by the Solanaceae and Liliaceae, its secretory character, and those of other Asteraceae stigmas, shows distinctive differences to those of dry tryphine coats, exemplified by the Brassicaceae, which produce no surface secretions other than the pellicle (Ellemen *et al.*, 1992; Hiscock *et al.*, 2002). Furthermore, the stigmatic secretions in Asteraceae contain lipid, carbohydrate and protein, which are secretory components associated with wet stigmas. These findings have led some to question the 'dry'

categorization of the Asteraceae stigma, and propose that wet-dry intermediate properties of the Asteraceae stigma are more appropriately described as 'semidry' (Ellemen *et al.*, 1992; Hiscock *et al.*, 2002). Since key components of the SSI pollen-stigma interaction are thought to reside in stigma secretions (Mattsson *et al.*, 1974; Ellemen *et al.*, 1992; Hiscock *et al.*, 2002), the densely-staining vesicles observed throughout the stage-2 and early to mid stage-3 *Cosmos* stigma, possibly contain molecules involved in the *Cosmos* self-incompatibility reaction.

(vi) Early to Mid Stage-3 – Emergence of anther tube from corolla and separation of stigma lobes

Stage-3 disk-floret development begins at anthesis, with early, mid and late stage-3 disk florets defined according to the orientation of the emerging stigma. In early stage-3 disk florets, the tip of the stigma and the anther tube protrude through the corolla creating a three-tiered floral arrangement of stigma, anther and corolla (Plate 3.22, A). Mid stage-3 disk florets are characterised by the separation of stigma, initially forming a V-shaped structure but with subsequent lateral extension stigma lobes become orientated parallel to the horizontal (Plate 3.22, C; Plate 5.3, D-F). Late stage-3 stigmas are fully reflexed (Plate 3.23, A-B; Plate 3.25, B).

The *Cosmos* stigma has three distinct types of epidermal cell. Long unicellular papillate epidermal cells occur at the apex of the stigma (Plate 3.22, C, E-F; Plate 3.23, A-B). Short unicellular papillate epidermal cells are located on the adaxial and lateral surfaces of the stigma, and run from the sub-apical region of the stigma to the stigma-lobe junction (Plate 3.22, C-D; Plate 3.23, A-B). Flat epidermal cells create a narrow flattened groove, "the stigmatic groove" (Tandon *et al.*, 2001) along the central axis of the adaxial stigma surface, and also form a triangular-shaped platform at the stigma apex (Plate 3.22, C-F; Plate 3.23, A). The long-papillate and flat stigma-epidermal cells are not receptive to pollen, but constitute the region of the stigma specialised for secondary presentation of pollen (reviewed in Chapter 5). In this role, the long papillae present pollen to insect vectors, and the triangular platform of flat epidermal cells acts as an insect landing platform. The short stigma papillae constitute the pollen-receptive region of the stigma and become receptive only when stigma lobes have reflexed (reviewed in Chapter 5).

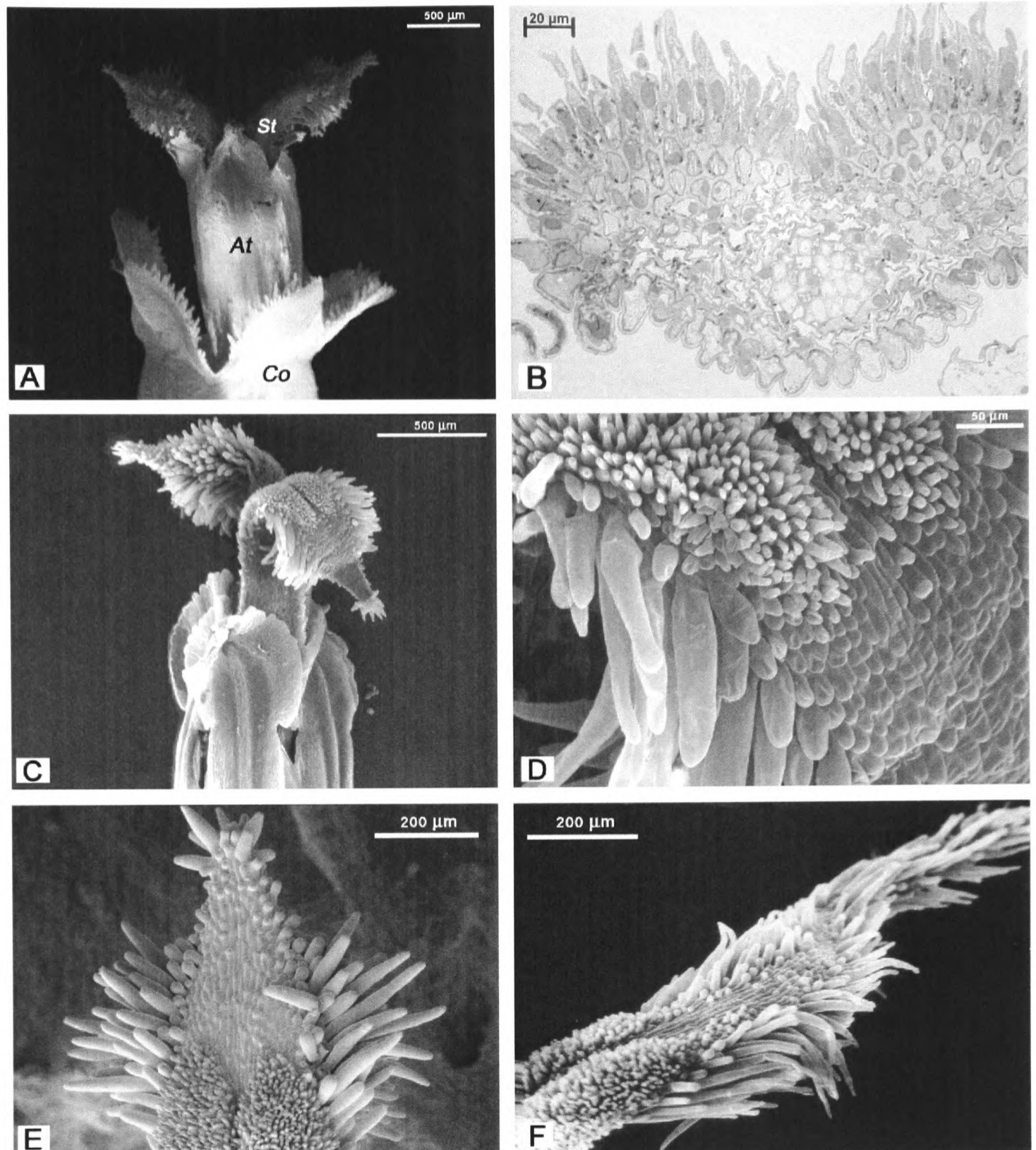


Plate 3.22 - *Cosmos* early to mid stage-3 stigmas

A-to E - *C. atrosanguineus* early to mid stage-3 stigmas. **F - *C. sulphureus*** mid stage-3 stigma (Preparation method: **A, C, D** and **F** ambient SEM; **E**, CryoSEM; **B**, semithin resin section). The *Cosmos* stigma is semi-dry and papillate (**C-F**). Early and mid stage-3 stigmas undergo a rapid period of synthesis, with the papillar cells and the cells of the underlying stigma tissue containing many densely-staining cytoplasmic vesicles (**B**). The intercellular spaces of stigma cells are filled with an extracellular matrix, secreted into the intercellular spaces and onto the surface stigma cells during the period of extrusion (**B**).

The *Cosmos* pellicle covers the cuticle, and together these two layers form a cohesive composite layer referred to as the pellicle-cuticle (Ciampolini and Cresti, 1998). The angiosperm cuticle is made up of short radially-directed rodlets composed of soluble and polymerised aliphatic lipids separated by fluid-conducting channels that allow water to flow from the papillar cytoplasm to the pellicle (Heslop-Harrison and Heslop-Harrison, 1975a; Jeffree, 1996).

When a plant is well hydrated, a fully expanded cuticle results because the fluid-conducting channels between rodlets are filled, and rodlets are held apart from each

other by the water mass. In this situation, stigma papillae are firm, and the outer surface of the papillae is smooth (Plate 3.23, C-D; Plate 3.24, A-B; 3.25, E-F). When a plant becomes dehydrated, fluid is lost from cuticular channels, and cuticular rodlets are subsequently drawn together and concertina on each other creating a corrugated effect on the stigma surface (Plate 3.24, C-D). Severe dehydration may cause stigma papillae to shrink away completely from the pellicle-cuticle layer, revealing it to be a continuous glove-like layer covering the upper two-thirds of papillar cells (Plate 3.24; Plate 3.25, C-D). Since the *Cosmos* pellicle-cuticle layer does not continue to the base of each papillae, no pellicle cuticle layer exists at the junction of the papillar-cell bases and the cells of the stigmatic tissue (Plate 3.25, E-F). The pellicle-cuticle layer of different papillae may become fused along their lengths and/or at their tips (Plate 3.23, D-F; Plate 3.24, A-B; Plate 3.25, A, E-F). Since the photographic plates exhibiting this characteristic are taken from specimens prepared by CryoSEM, the fusion points observed between adjacent papillae are unlikely to be preparation artefacts. It is possible that the fusion of adjacent papillae are the result of adhesion of pellicles of adjacent papillar cells, and may be caused by an excess accumulation of this proteinaceous layer on the stigma surface (Plate 3.23, E-F; Plate 3.25, C-D). It is interesting that adhesion of papillae often occurs between papillae apices, which is the papillar region that most commonly contacts the pollen (Plate 3.23, E-F; Plate 3.24, A-B), and it may be that the stigma extrudes excess proteinaceous material to the part of the papilla most likely to contact the pollen. In general, *Cosmos* papillae become more closely appressed toward their bases (Plate 3.24, A-B) where the cuticle is known to disappear (Hiscock *et al.*, 2002). TEM observations in *Senecio*, revealed these basal regions to be the site of greatest extracellular secretion that contained many cytoplasmic vesicles apparently engaged in the active secretion of material into the cell wall (Hiscock *et al.*, 2002).

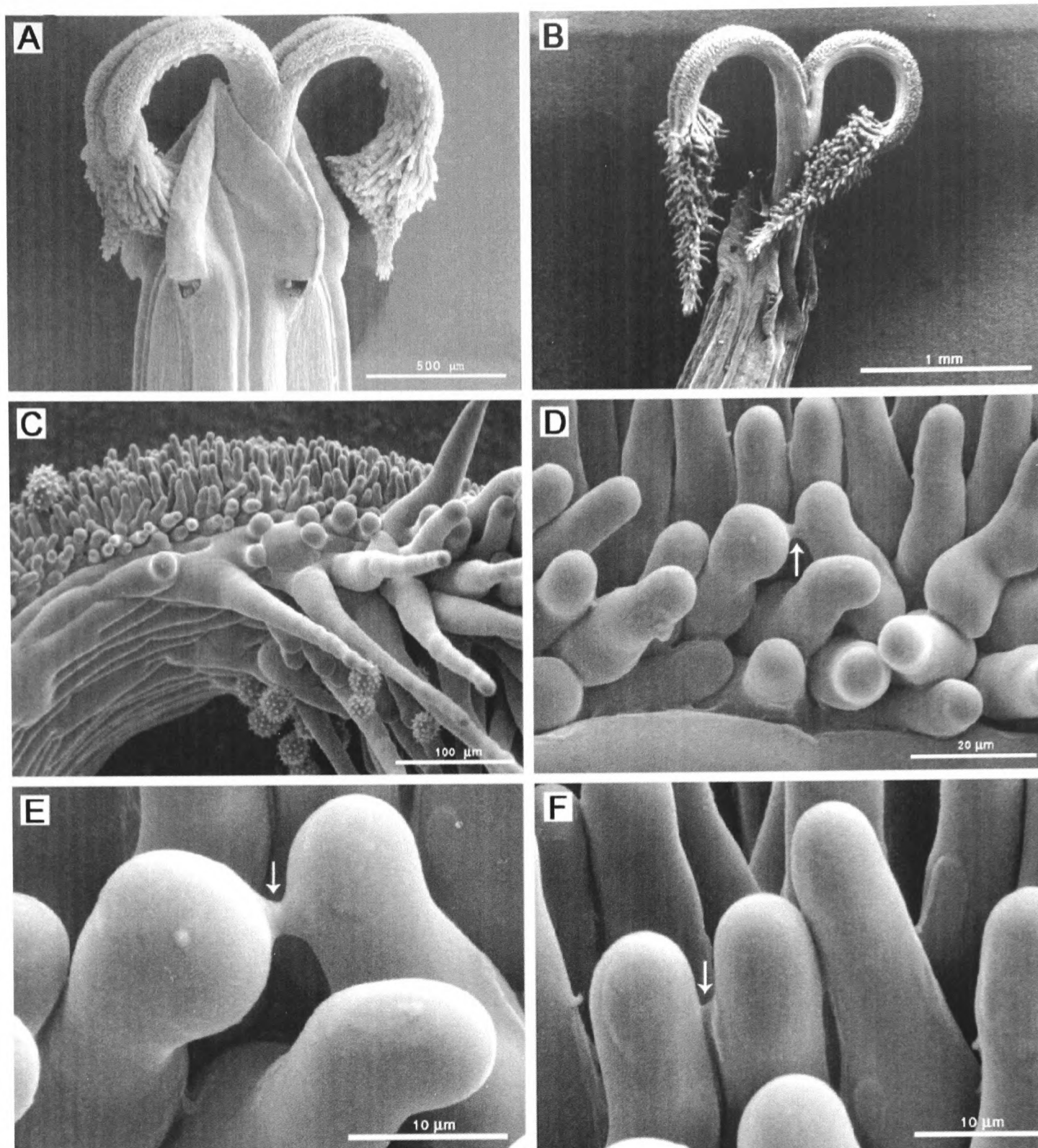


Plate 3.23 – Morphology of stage-3 *Cosmos* stigma

A – *Cosmos bipinnatus*, late stage-3 stigma emerging from anther tube (Ambient SEM).

B to F – *Cosmos sulphureus* late stage-3 stigma (CryoSEM).

B, showing stigma emerging from anther tube; **C** – single stigma lobe showing arrangement and structure of long and short papillae; **D to F** - short stigma papillae, showing attachment of adjacent papilla via fusion of their pellicle-cuticle layers.(arrows)

The *Cosmos* pellicle-cuticle layer is thicker in the long non-pollen receptive papillae at the stigma apex, than in the shorter receptive papillae (Plate 3.25, G-H; Plate 5.6, B, H, I). This feature was noticed also in the cuticles of *Vicia* which showed varying levels of autofertility depending on the thickness of cuticles. In *Vicia* as in *Cosmos*, thin cuticles occur over the short receptive papillae and thick cuticles over the long less-receptive papillae (Heslop-Harrison, 1992a).

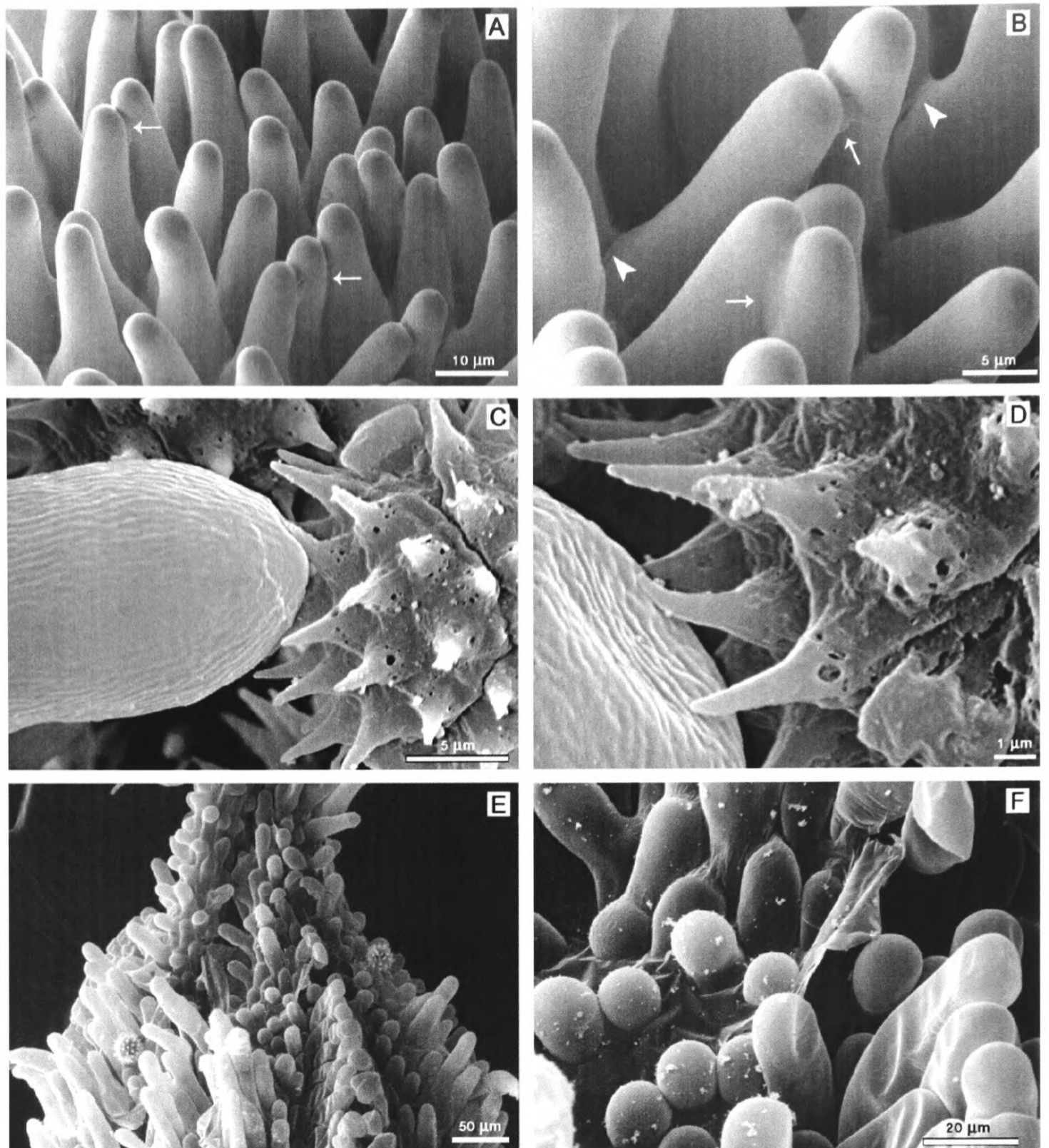


Plate 3.24 – Morphology of stage-3 *Cosmos* stigma

A and B – *Cosmos atosanguineus*, short receptive papillae of a late stage-3 stigma (CryoSEM), showing many papillae attached to each other via fusion of their pellicle-cuticle layer (arrows). The greatest area of fussion between papillae occurs towards the bases of papillae (arrowheads).

C and D – *C. bipinnatus* showing short receptive papillae of a late stage-3 stigma with self pollen grains (Ambient SEM). The ambient SEM preparation method dehydrates specimens. In dehydrated specimens, water is removed from the fluid-conducting channels that exist between the radially-directed rodlets of the cuticle, causing the cuticle to collapse at these points, so that rodlets concertina onto each other, creating a corrugated effect over the surface of the stigma. In non-dehydrated CryoSEM specimens, the cuticular spaces are filled with water so that the cuticle is expanded and appears smooth (**Plate 3.23, C-F; Plate 3.25, E-F**).

E and F – *C. atosanguineus* showing the apical region of a very early stage-3 stigma before separation of stigma lobes (Ambient SEM). Rapid dehydration of these specimens has caused papillar cells to shrink away from pellicle-cuticle layer, revealing this layer to be a continuous glove-like covering that lies over the papillar cells.

In accordance with the stigma classification system of Heslop-Harrison and Shivanna (1977), the *Cosmos* stigma is a Group IIB(i)-type stigma, described as dry, papillate and unicellular (DPU) (Heslop-Harrison, 1992a), but is now more accurately defiend as a semidry papillate unicellular stigma (Hiscock *et al.*, 2002). The early, non-pollen

receptive *Cosmos* stage-3 stigma functions as an organ of secondary pollen presentation. Secondary pollen presentation is “*the developmental relocation of pollen from anthers onto another floral organ which then functions as the pollen presenting organ for pollination*” (Howell *et al.*, 1993). Possession of a secondary pollination mechanism gives a plant a selective advantage as it maximises the chances of vector-mediated pollen dispersal to receptive flowers. Nine different types of secondary pollen presentation mechanisms have been identified (Howell *et al.*, 1993). The Asteraceae are classified as ‘terminal stylar presenters with active pollen placement’, because pollen is presented on the terminal part of a modified style, and is actively loaded onto the style apices as it elongates through the anther tube (Howell *et al.*, 1993). This type of presentation occurs also in the Calyceraceae and Lobeliaceae, and was observed in all three *Cosmos* species in this study. The corolla of *Cosmos* stage-3 florets expands radially away from the anther tube, allowing space for the anther tube to elongate up and through the corolla in preparation for anthesis (Plate 3.5, C and F; Plate 3.6). Similarly, radial expansion of the anther creates space for anther dehiscence and allows room for passage of the elongating style/stigma (Plate 3.22, A).

In *Cosmos*, only the tough thin translucent membrane that encapsulates each anther tube, holds the anthers together at this stage (Plate 3.5, C and F). Occasionally, *Cosmos* stigmas emerge without collecting copious amounts of pollen. This may be a consequence of the physical dynamics within an anther tube, such as the corolla not expanding enough for the dehisced anthers to open out fully, or due to the stigma emerging before full anther dehiscence. In general, only a few stigmas of this type occur per *Cosmos* capitulum and they tend to be associated with those disk florets located at the centre of the capitulum. These central florets open later than the outer florets, and as a consequence, may have less room in which to expand. Ordinarily, anthers of stage-3 *Cosmos* disk florets are completely dehisced, and the copious amounts of pollen are deposited on the long apical stigma papillae (Plate 3.1, B-C and Plate 3.2).

(vii) Late Stage-3 – From arched to fully reflexed stigmas.

The Asteraceae stigma is known to become receptive only when stigma lobes have become arched and the maximum surface area of the receptive short papillae become exposed (reviewed in Chapter 5; Plate 3.23, A-B). By late stage-3 disk-floret development, the cytoplasm of the short stigma papillae clear of densely-staining material, and a thin pellicle-cuticle layer covers the cuticle (Plate 3.25 G-H)

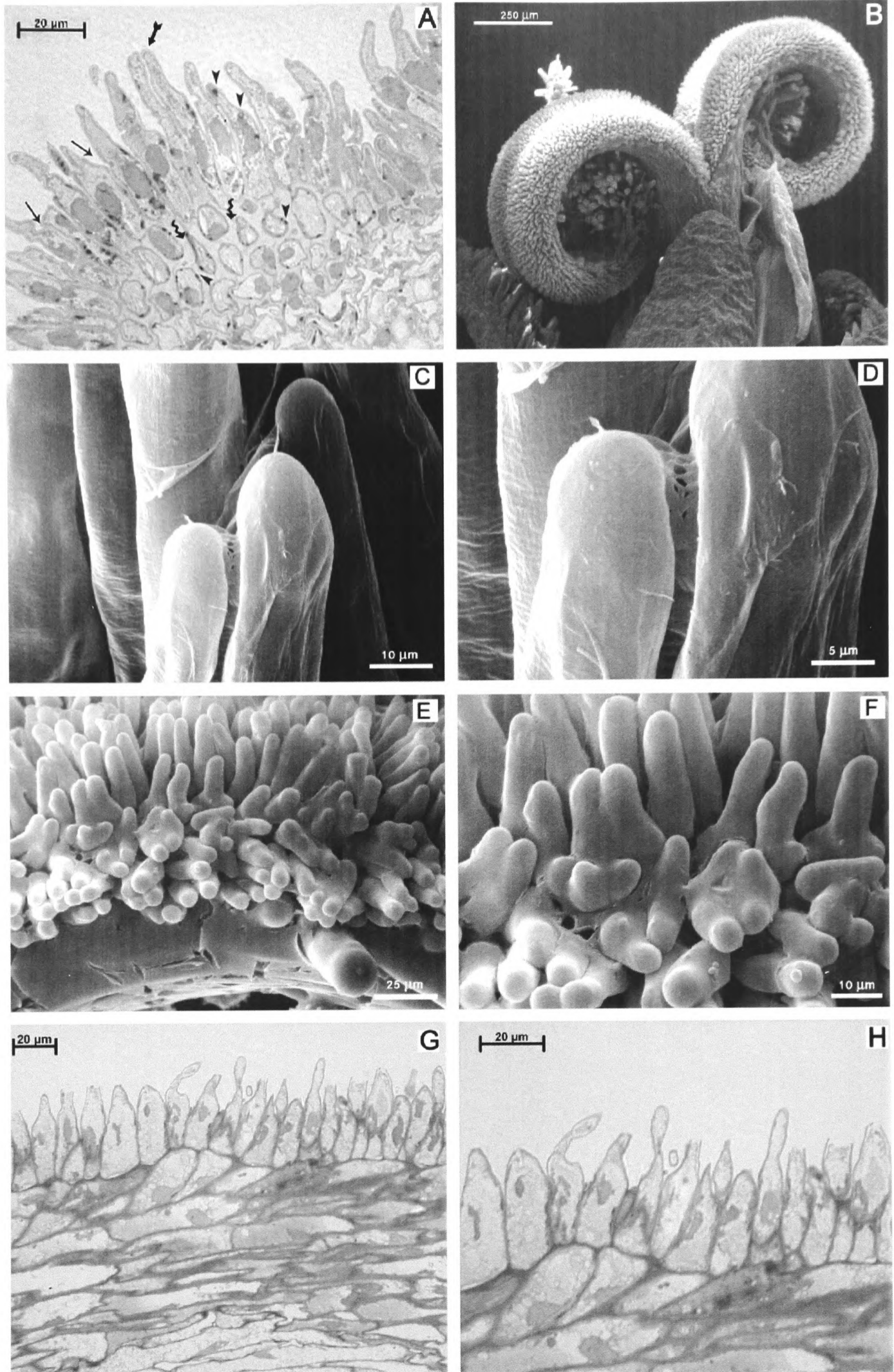


Plate 3.25 –Cosmos stigma papillae showing pellicle-cuticle layer

A (stRS & LM bright field) – TS early stage-3 stigma of *C. atrosanguineus* showing discharge of the contents of densely-staining cytoplasmic vesicles onto stigma surface (arrowheads). Note the pellicle-cuticle layer overlying the papillar cells (arrows). The pellicle-cuticle layer of two adjacent papillae has fused (feathered arrow). The intercellular spaces of underlying stigma cells are filled with an extracellular matrix (fluted arrow). **B** (Cryo SEM). – late stage-3 stigma of *C. atrosanguineus* showing fully reflexed stigma lobes exposing the greatest surface area of receptive short papillae **C and D** (Ambient SEM) – *Cosmos atrosanguineus* late stage-3 stigmas showing long papillae in which the pellicle-cuticle layer has lifted away from the dehydrated stigma papillae. **E and F** (CryoSEM) – *C. sulphureus* late stage-3 stigmas, showing papillae covered by a continuous smooth hydrated pellicle-cuticle layer. The pellicle-cuticle layer covers the upper portions of papillae, but does not continue to the bases of papillar cells **G and H**- LS late stage 3 of *C. atrosanguineus* stigmas, showing papillae and underlying stigma cells with clear cytoplasm that are free of densely-staining vesicles (stRS & LM bright field)

3.3.3 - Conclusion

Microsporogenesis in *Cosmos atrosanguineus*, *C. bipinnatus* and *C. sulphureus* appears to show no morphological aberrations, with no differences observed in the structural development of *C. atrosanguineus* pollen, and that of *C. bipinnatus*, or *C. sulphureus* that could account for the failure of this species to germinate viable pollen. The *Cosmos* pollen coat has a complex structure and its method of deposition has characteristics in common with those of *Raphanus* and *Arabidopsis*. However, the methods used, in this chapter, were not able to discount aberrations in the pollen-coat biochemistry as a cause of pollen failure in *C. atrosanguineus*.

CHAPTER 4 – Cytological Investigations in *Cosmos*

4.1 -Introduction

Cosmos atrosanguineus has been characterised as a self-incompatible tetraploid (Lawrence, 1930). Records from commercial nurseries indicate the existence in cultivation of seed-producing *C. atrosanguineus* individuals between the years of 1890 and 1942 (Appendix 2.2-2.5b). Thereafter, *C. atrosanguineus* has not been known to produce seed. Polyploidization radically transforms plant genomes, throwing them into a period of genomic shock (Pikaard, 2001). One of the many consequences accompanying polyploidization is an often-observed reduction in the fertility and seed production of neopolyploids with a tendency, in some taxa, towards the formation of apomicts (Mastenbroek *et al.*, 1982; Levin, 1983; Ramsey and Schemske, 2000). The reduction in fertility of polyploids is attributed to an increase in the formation of unbalanced gametes (Heslop-Harrison, 1992c). Multivalent formation during meiosis can lead to irregularities at anaphase-I that produce numerically unbalanced gametes, and consequently, autopolyploid genomes with their tendency towards multivalent formation often exhibit greater reductions in fertility than allopolyploids (Mastenbroek *et al.*, 1982). The degree of genomic shock and the subsequent level of genomic rearrangement depend also on the relatedness of parent genomes. The stress in allopolyploid genomes is perceived to be far greater than that encountered by autopolyploids, and results in more dynamic and rapid genomic alterations with loss of fertility as a possible consequence (Song, *et al.*, 1995a; Comai, *et al.*, 2000; Ozkan, *et al.*, 2001; Shaked *et al.*, 2001; Shan *et al.*, 2003).

The purpose of this chapter is to survey the cytology of *C. atrosanguineus*. The survey is by no means extensive or statistically complete, but provides data for the purpose of discussing the possible cytological factors impinging on the fertility of the species. The work assesses, (i) polyploid type (autoploid or allopolyploid), (ii) chromosome associations at diakinesis/metaphase I, (iii) presence of anaphase-I bridges and/or laggards, (iv) meiotic indexes and (v) pollen viability, to ascertain cytological factors that may contribute to the loss of seed production in extant *C. atrosanguineus* accessions. The C-DNA content of *C. atrosanguineus*, *C. bipinnatus* and *C. sulphureus* was obtained from the Plant DNA C-values Database (Release 2.0) (Bennett and Leitch 1995; 1997; 2003) and is included to aid in the assessment of ploidy level in the three *Cosmos* species. Finally, pollen grain number and pollen volume of *Cosmos* species are compared.

4.1.1 - Pollen viability: a discussion of methods

Pollen viability is a measure of male fertility (Kearns and Inouye, 1993). The reproductive ability of a species depends on the viability of its gametes. Since the viability of ovules is difficult to assay, plant fertility is most often evaluated through an assessment of pollen viability (Leduc *et al.*, 1990). Pollen viability is the ability of pollen to germinate, produce a pollen tube and fertilise a viable ovum (Mayer and Gottsberger, 2000). The length of time during which pollen remains viable after dehiscence depends on the species (Stanley and Linskens, 1974; Shivanna and Johri, 1985), the size of pollen population (Brewbaker and Majumder, 1961), the time of dehiscence, the season (Thomson *et al.* 1994; Kumar *et al.*, 1995; Stone *et al.*, 1995; Tangmitcharoen, and Owens, 1997), the age of plant (Aizen and Rovere, 1995), the environmental conditions (La Porta and Roselli, 1991; Thomson *et al.*, 1994; Stone *et al.*, 1995) and the nucleate state of pollen at dehiscence (Brewbaker, 1967; Mayer and Gottsberger, 2000). Decreases in pollen viability are associated with aged plants or pollen, low pollen populations, environmental stress, high temperatures, long exposure to sunshine, low relative humidity and vice versa. In general, binucleate pollen shows greater longevity than trinucleate pollen, which is relatively short lived, from 20 minutes in some grasses, to 2 days, and viability is highest in the mornings, 2 to 8 hours after dehiscence (Shivanna and Johri, 1985; Stanley and Linskens, 1974; Khatum and Flowers, 1995).

In *Cosmos*, pollen is shed in the trinucleate state, and as with most Asteraceae species, the viability of *Cosmos* pollen is short-lived and adversely affected by high temperatures, with a 50% loss of viability occurring within two hours of dehiscence at 30°C (Hoekstra and Buinsma, 1975). This *Cosmos* viability window ranges from 1 to 2 days with optimum viability occurring 4 to 6 hours after dehiscence (Brewbaker and Majumder, 1961; Brewbaker, 1967; Stanley and Linskens, 1974; Hoekstra and Buinsma, 1975; Shivanna and Johri, 1985; Kearns and Inouye, 1993).

Several methods have been devised to measure the viability of pollen (King, 1960; Alexander, 1969; Heslop-Harrison and Heslop-Harrison, 1970; Stanley and Linskens, 1974; Shivanna and Johri, 1985; Dafni, 1992; Shivanna and Rangaswamy, 1992; Kearns and Inouye, 1993; Khatum and Flowers 1995; Mayer and Gottsberger, 2000; Rodriguez-Riano and Dafni, 2000). Direct measurements involve scoring germinated pollen grains and/or seed set after deposition of pollen on receptive stigmas (Stanley and Linskens, 1974; Shivanna and Johri, 1985; Mayer and Gottsberger, 2000). Since

Cosmos atrosanguineus is a sporophytic self-incompatible species not known to produce seed, and its reputed clonal origins preclude *in vivo* pollen germination, such methods are inappropriate for this species. Alternatively, pollen viability can be measured *in vitro* by scoring pollen germination in an artificial germination medium (Shivanna and Rangaswamy, 1992). *In vitro* germination is not a reliable measure of pollen viability since the inability of pollen to germinate *in vitro* is often related to factors other than viability (Stanley and Linskens, 1974; Shivanna and Johri, 1985). Furthermore, trinucleate pollen in general, and Asteraceae pollen in particular, is notoriously difficult to germinate *in vitro* (Brewbaker and Kwack, 1963; Shivanna and Heslop-Harrison, 1981; Leduc *et al.*, 1990) In spite of past evidence, attempts were made, without success, to germinate *Cosmos* pollen *in vitro* using a variety of media, (McIlvaine, 1921; Brewbaker and Kwack, 1963; Coleman and Goff, 1985; Leduc *et al.*, 1990).

Indirect methods for assessing pollen viability rely on correlating the colour of dyes with certain physiological or physical characteristics indicative of pollen viability. Physical characteristics rely on the adsorption of dyes to a specific cell constituent of mature viable pollen (Stanley and Linskens, 1974). Nuclear dyes such as acetocarmine and vital stains such as Alexander's stain, and aniline blue in lactophenol (ALS) have been used to differentiate viable 'stained' pollen from non-viable 'unstained' pollen (Alexander, 1969; 1980; Stanley and Linskens, 1974). Physiological characteristics of viability rely on identifying the activity of specific pollen enzymes and are observed as rapid changes in pollen colour (Rodriguez-Riano and Dafni, 2000). Viability tests such as Baker's procedure (Dafni, 1992) and tetrazolium salts such as MTT (2,5-diphenyl tetrazolium bromide) and TTC (2,3,5-triphenyl tetrazolium chloride), detect the presence of dehydrogenase and peroxidase activity (Khatum and Flowers 1995; Norton, 1996). The X-Gal-test detects the activity of β -galactosidase (Singh *et al.*, 1985; Trognitz, 1991), p-phenylenediamine detects peroxidases (Rodriguez-Riano and Dafni, 2000) and FDA (fluorescein diacetate) detects esterase activity and cell membrane integrity (Heslop-Harrison and Heslop-Harrison, 1970; Heslop-Harrison and Shivanna, 1984).

On the balance of evidence (Shivanna and Johri, 1985; Kearns and Inouye, 1993; Thomson *et al.*, 1994; Stone *et al.*, 1995; Mayer and Gottsberger, 2000; Rodriguez-Riano and Dafni, 2000) and for ease of use (La Porta and Roselli, 1991), the fluorescein diacetate (FDA) was the method adopted here to assess the viability of *Cosmos* pollen (Heslop-Harrison and Heslop-Harrison, 1970). FDA assesses two

properties of a pollen grain; (i) the integrity of its plasma membrane and (ii) esterase activity in the cytoplasm (Mayer and Gottsberger, 2000). Both properties are considered to be indicative of viable pollen. In brief, fluorescein diacetate (FDA) enters the pollen grain and is hydrolysed by esterases in the cytoplasm of the vegetative cell resulting in the release of fluorescein. The non-polar FDA substrate is believed to pass through the plasma membrane of the pollen grain at a rate that is more rapid than the passing out of the liberated polar fluorescein. Accumulation of fluorescein in the vegetative cell makes the pollen grain fluoresce a bright greenish-yellow under appropriate UV light/filters (Heslop-Harrison and Heslop-Harrison, 1970). Greenish-yellow fluorescence implies pollen viability, as intact plasma membranes and esterase activity are considered to be prerequisites for functioning pollen.

Shivanna *et al.* (1991) noticed that FDA scores were often higher than the actual *in vivo* seed-producing performance of pollen (Mayer and Gottsberger, 2000; La Porta and Roselli, 1991). In response to these observations they proposed that FDA-determined pollen viability measures a pollen grain's eventual ability to germinate but not its seed-siring ability. They described the latter as pollen vigour, and defined this as a measure of pollen's ability to sustain pollen tube growth through the biochemical environment of the stigma until fertilization (Shivanna *et al.* 1991; Thomson *et al.*, 1994). Viability and vigour together constitute overall pollen competence (Thomson *et al.*, 1994). When this more restricted definition of pollen viability is invoked, FDA-determined pollen viability correlates favourably with *in vivo* germination of pollen on plant stigmas (Shivanna *et al.*, 1991). FDA can produce false negatives. A pollen grain can fail the FDA test if it lacks esterase activity, or if the permeability of its membrane becomes disrupted. The most common disrupter of membrane permeability in pollen is desiccation. On pollen hydration, membrane permeability is restored and the pollen grain gives a positive FDA (Thomson *et al.*, 1994). Pollen drying is the most likely cause of FDA false negatives. The problem may be alleviated by allowing pollen grains to equilibrate in a humid atmosphere before FDA testing (Heslop-Harrison and Shivanna, 1984; Shivanna and Johri, 1985).

In addition to assessing pollen viability, an estimation of pollen-grain number per disk floret was undertaken for *Cosmos atrosanguineus*, *C. bipinnatus* and *C. sulphureus*. The pollen viability multiplied by the number of pollen grains per disk floret gives the number of viable pollen produced per disk floret.

4.2 - Materials and Methods

4.2.1 - Chromosome Counts: mitosis in root tip cells

Between the months of May and July rapidly-growing roots-tips were removed from potted plants and collected in distilled water. Root-tips were pretreated in either a saturated solution of 1-bromonaphthalene (ABN) at 4°C for 26 hours, or 1% paradichlorobenzene (PDB) solution at 22°C for 5 hours, or 2 mM 8-hydroxyquinoline solution (OQ) at 22°C for 5 hours, and then fixed in a freshly-prepared solution of 3:1 ethanol: acetic acid. The material was hydrolysed in 1 M HCl at 60°C for 8½ minutes and stained in 3 ml of Feulgen for 30 minutes. Slides were prepared by removing meristems from stained material and macerating them in a drop of 2% aceto-orcein before applying a coverslip and squashing. Where material was available, somatic chromosome counts were confirmed from 10 well-spread metaphase cells from roots selected randomly from five individuals of each accession.

4.2.2 - Chromosome Counts: meiosis in pollen mother cells (PMCs)

In the mornings of the months of April and May, suitably-sized disk florets (early to mid stage-1 florets, as described in Chapter 3) were removed from an inflorescence and the anther tube dissected away from petals and stigma. The anther tube was opened out, placed adaxial-side down on a microscope slide and a drop of 2% aceto-orcein stain was placed to the side of the anther tube. Pollen mother cells were released into the aceto-orcein stain by moving the anther tube into the stain and pressing the anthers gently with a dissecting needle in a single action to optimise the fixation of the pollen mother cells by the stain. Debris was removed from the preparation, a coverslip applied and pressed gently but firmly between blotting paper to spread and flatten cells. Meiosis counts and chromosome pairing configurations at diakinesis-metaphase I were analysed only in microsporocytes that had well-spread chromosomes.

4.2.3 - Meiotic index

The meiotic indexes for accessions of *Cosmos atrosanguineus* and *C. bipinnatus* were calculated using the method of Love (1949), as described in Boff and Schifino-Wittmann (2003). In this method, the presence of four equal-sized cells within a tetrad indicates normal meiosis. Any tetrad formation deviating from this prescribed norm reflects abnormal meiosis. The meiotic index is expressed as a percentage of normal tetrads, i.e. (number of normal tetrads ÷ total number of tetrads) x100. A meiotic index of 90% or higher indicates meiotically stable plants. Meiotic indexes for *C. atrosanguineus* and *C. bipinnatus* accessions were calculated from permanized slides of pollen mother cells prepared as described in these methods. Tetrads in two *C.*

atrosanguineus accessions (1997 6334 and 1999 3819) and one *C. bipinnatus* accession (1996 582) were observed. Where material was available, several plants from each of the accessions were observed in the calculation of meiotic index. Tetrads were counted under the x40 objective of a Zeiss microscope. In addition to observations of tetrads, anaphase-I and telophase-I cells from the two *C. atrosanguineus* accessions and the single *C. bipinnatus* accession were examined for the presence of laggards, bridges and aberrant chromosome orientations. Where material was available several plants from each accession were observed. Thus a combination of meiotic index and observations of chromosome disjunction at anaphase-I and telophase-I provide the evidence upon which the stability of meiosis and gamete formation can be assessed. Permanent slides of anaphase-I chromosomes and tetrads were photographed under a 100x oil immersion objective using a Zeiss Photomicroscope III and Ilford Pan F (plus 50) film (Ilford Imaging, Cheshire, UK). Data pertaining to anaphase-I, and tetrad photomicrographs were entered into the Cytology Database administered by the Cytogenetics Section of the Jodrell Laboratory at the Royal Botanic Gardens, Kew. Film negatives are held in the Cytogenetics Section of the Jodrell Laboratory at the Royal Botanic Gardens, Kew.

4.2.4 - Permanizing Slides

Permanent slides were made by freezing with liquid nitrogen, removing coverslips, dehydrating in absolute alcohol, double mounting in a drop of euparal and drying in a 45°C-oven for 2-4 weeks. Microscope slides used for this research have been donated to the Cytology Slide Collection of the Jodrell Laboratory at the Royal Botanic Gardens, Kew. Photomicrographs were taken under 100x oil immersion objective using a Zeiss Photomicroscope III and Ilford Pan F (plus 50) film. Data pertaining to photomicrographs were entered into the Cytology Database as described above (Table 4.1)

4.2.5 - Preparation of karyotypes

Photomicrographs of good somatic metaphase chromosomes from *C. atrosanguineus*, *C. carvifolius* and *C. sulphureus* were enlarged three times using a photocopier. Due to the small size of *C. bipinnatus* chromosomes, the photomicrograph used to karyotype this species was enlarged 3½ times. Individual chromosomes were cut out from enlarged photocopies and apparently homologous chromosomes were matched up and stuck on white card in order of decreasing length using centromeres as the point of alignment, with the shorter of the two chromosome arms at the top. Chromosomes were traced in pencil, inked, scanned into the computer and an idiogram made from scanned images using Photoshop 7 software.

Morphological classification of chromosomes followed the methods of Naranjo *et al.*, (1983), wherein chromosomes are defined according to centromere position as: *M*, median point; *m*, median region; *sm*, submedian region; *st*, subterminal region; *t*, terminal region, and *T*, terminal point. Centromeres occurring at intermediate positions between two categories are classified as *m-sm*, *sm-st* or *st-t*. Very long secondary constrictions, the nucleolar organising regions (NORs), were ignored when classifying a chromosome, with only the length of the satellite being taken into account.

Table 4.1. *Cosmos* plant material and photomicrographs used in cytology investigation

Cosmos species	RBG, Kew Acc No.	RBG, Kew Cytology No.	RBG, Kew Cytology Slide Collection No.	RBG, Kew Cytology Photo. Ref. No.
<i>C. atrosanguineus</i>	1997 6334	98-69	46	98-15-03
			73	02-01-35
	1999 3819	01-163	31x	02-01-11
			38x	02-06-04
<i>C. bipinnatus</i>	1996 582	98-86	32	98-13-03
		98-57	6M	01-14-05
		98-66	14M	No photo taken
		98-81	20M	No photo taken
<i>C. carvifolius</i>	1999 383	98-136	65	98-15-24
<i>C. sulphureus</i>	1996 980	98-49	47	98-12-36
	No data	61-881	188	01-14-10

4.2.6 - Idiograms of chromosomes at diakinesis-metaphase I

Idiograms were constructed from scanned images of photomicrographs taken of pollen mother cells at diakinesis-metaphase I, drawn using Photoshop 7 software.

4.2.7 - Fluorescein diacetate (FDA) determination of pollen viability

A stock solution of fluorescein diacetate (FDA) (Sigma Chemicals) was prepared by dissolving 2 mg/ml in acetone and was stored at -20°C . A working solution was prepared freshly by adding 1-5 drops (drop by drop) of FDA stock solution to 10 ml of freshly-made 0.5 M sucrose solution until it turned a light milky colour. *Cosmos* plants were placed in a humidity chamber at 90% humidity for 1 hour before pollen was collected for viability testing to enable membrane recovery of the dehydrated trinucleate pollen and to prevent false-negative results⁹. A 10 μl drop of FDA-sucrose

⁹Due to technical problems with the humidity controls of the humidity chambers at RBG, Kew, it was not possible to obtain high humidity environments prior to pollen viability counts.

solution was placed on a 22 x 22 mm coverslip and pollen from a single dehisced anther tube was touched onto the surface of the droplet and left for 10 minutes in a Petri dish lined with wet filter paper. The coverslip was picked up onto a clean microscope slide and examined under the x10 objective of a Leitz Diaplan microscope under UV illumination. Anther tubes from four disk florets per inflorescence were selected, and five inflorescences were sampled per plant. Ten plants were assessed for *Cosmos atrosanguineus* and *C. bipinnatus*, and four plants for *C. sulphureus*. Where plant material was available, different accessions were tested for each species. Pollen viability percentages were recorded by first counting the number of grains under white light and then switching to the fluorescent light to score grains with golden-yellow fluorescence as viable pollen grains. Pollen viability was calculated as; the number of fluorescent pollen grains ÷ total number of pollen grains x100. Fresh pollen was collected in the mornings between the hours of 8 a.m. and 12 noon during the months of July for *Cosmos atrosanguineus* and *C. bipinnatus*, and the months of November and April for *C. sulphureus*. Pollen was collected from anthers that had dehisced within 4-8 hours prior to time of collection.

4.2.8 - Estimating pollen-grain numbers per disk floret

Estimations of pollen grain number for *Cosmos atrosanguineus* and *C. bipinnatus* accessions were made for healthy plants during the 3-10th August 2001 and for accessions of *C. sulphureus*, between 28-30th April 2002. A mid stage-2 anther (just prior to dehiscence) was dissected from an anther tube and transferred to a calibrated tube/vial where it was squashed into a 900 µl droplet of 70% ethanol containing 3 drops of 0.5% aniline blue and 4 drops of detergent. The forceps used to squash the anther were rinsed carefully in the droplet to prevent loss of pollen material. The pollen solution was made up to 1 ml with the same ethanol/dye/detergent solution and vortexed for 1½ minutes. Pollen grains from five separate 4-µl samples of each 1-ml vortexed solution were counted under the x10 objective of a light microscope using a haemocytometer. Pollen-grain numbers were estimated from five disk florets per inflorescence, and from two inflorescences per plant. Estimations were undertaken for three *Cosmos atrosanguineus* accessions and one accession each for *C. bipinnatus* and *C. sulphureus*. The total number of pollen grains produced per disk floret was calculated by taking the average number of grains in fifty 4-µl samples of anther solution, multiplied by 1250 (arrived at by multiplying the dilution factor [x250], by the number of anthers per disk floret [x5],

4.2.9 - Calculating pollen-grain size

Pollen grains from ripe anthers of *Cosmos* inflorescences fixed in FAA (Formalin Acetic-Alcohol) and stored in 70% ethanol, as described in the Methods section of Chapter 3, were measured under the x100 oil immersion lens of a light microscope. Mature anthers were dissected from late stage-2 disk florets and squashed in 70% ethanol. Anther debris was removed and a cover slip applied. The main body of echinate *Cosmos* pollen (not including spines) was measured. Polar and equatorial diameters were measured of 50 pollen grains taken from an assortment of individuals and accessions.

4.2.10 - Statistical methods

Statistical analyses of data collected on pollen viability, pollen-grain number per disk floret, and pollen size were undertaken using MINITAB statistical software version 13.32 (MINITAB, 2000^a; 2000^b). All data were first submitted to an Anderson-Darling test for normality of distribution, and the 0.05 significance level was used in all analyses. Observations of difference were analysed using one-way analysis of variance (ANOVA) in samples exhibiting normal distribution and the Kruskal-Wallis, and/or Mann-Whitney-*U* test for non-normally distributed data. Spearman-rank-order correlation (r_s) was used to test data for association of variables.

4.3 – Results and Discussion

4.3.1 - Introduction

Photographs and karyotypes of mitosis chromosomes of *Cosmos atrosanguineus*, *C. bipinnatus*, *C. carvifolius* and *C. sulphureus* are displayed in Figures 4.1 to 4.9. Photographs and idiograms of PMCs at diakinesis-metaphase-I, for *C. atrosanguineus*, *C. bipinnatus* and *C. sulphureus* are presented in Figures 4.10 to 4.13. Meiotic indexes and chromosome observations at anaphase-I for *C. atrosanguineus* and *C. bipinnatus* are presented in Table 4.4. Chromosome associations at diakinesis for *C. atrosanguineus*, *C. bipinnatus* and *C. sulphureus* are displayed in Table 4.5. Chromosome lengths were calculated for each *Cosmos* karyotype and scale bars are included to aid comparison of chromosome/karyotype sizes in the four *Cosmos* species. These data are summarised in Table 4.2. Results of pollen viabilities for *C. atrosanguineus*, *C. bipinnatus* and *C. sulphureus* are presented in Tables 4.6-4.9. Tables 4.10 and 4.11 contain the data for pollen grain number per disk floret and pollen size for selected accessions of *C. atrosanguineus*, *C. bipinnatus* and *C. sulphureus* respectively

A note of caution must be raised regarding chromosome measurements undertaken in this chapter. Chromosome preparation techniques are known to introduce variability in chromosome size (Stebbins, 1971; Sybenga, 1992). Contraction of chromosomes at mitosis is not uniform between cells and rates of contraction differ as a result of slight differences in the stage of mitosis blocked by treatments (Sybenga, 1992). In addition, contraction rates within a cell, between homologues, and even between chromatids of the same chromosome may vary (Sybenga, 1992). The squashing process also introduces variability, as it sometimes causes chromosomes to become stretched irregularly, introducing slight differences in size both between and within cells (Sybenga, 1992). In a statistically-valid comparison of chromosomes, variations in chromosome sizes introduced by preparation techniques are compensated by making repeat measurements from 40-50 cells of the same individual, and where material is available, from several plants of each accession (Stebbins, 1971; Sybenga, 1992). A precise quantitative analysis of *Cosmos* chromosome size, although invaluable in some contexts, is not the purpose of this chapter. The comparison of *Cosmos* karyotypes seeks to identify the chromosome number, ploidy level and the range of karyotypes within the genus. As such, measurements of individual chromosomes are included here as a non-statistical corollary in a rudimentary comparison of karyotypes. They offer a general overview of the sizes of the four *Cosmos* karyotypes relative to each other, but provide no significant data regarding the mean or range in chromosome size within species. Likewise, chromosome associations at meiosis should be verified by observations of a statistically-valid number of cells. In the case of *Cosmos bipinnatus* and *C. sulphureus* this was achieved, but in *C. atrosanguineus* it was difficult to 'catch' cells at meiosis and to obtain clear spreads of chromosome associations. Hence, conclusions presented in this study of chromosome associations in *C. atrosanguineus* are rudimentary and will require further assessment of a greater number of meiosis sporocytes in a broader range of *C. atrosanguineus* accessions before statistically valid conclusion can be drawn.

4.3.2 - Karyotypes of *Cosmos* mitosis (root-tip) chromosomes

(i) *Cosmos atrosanguineus*

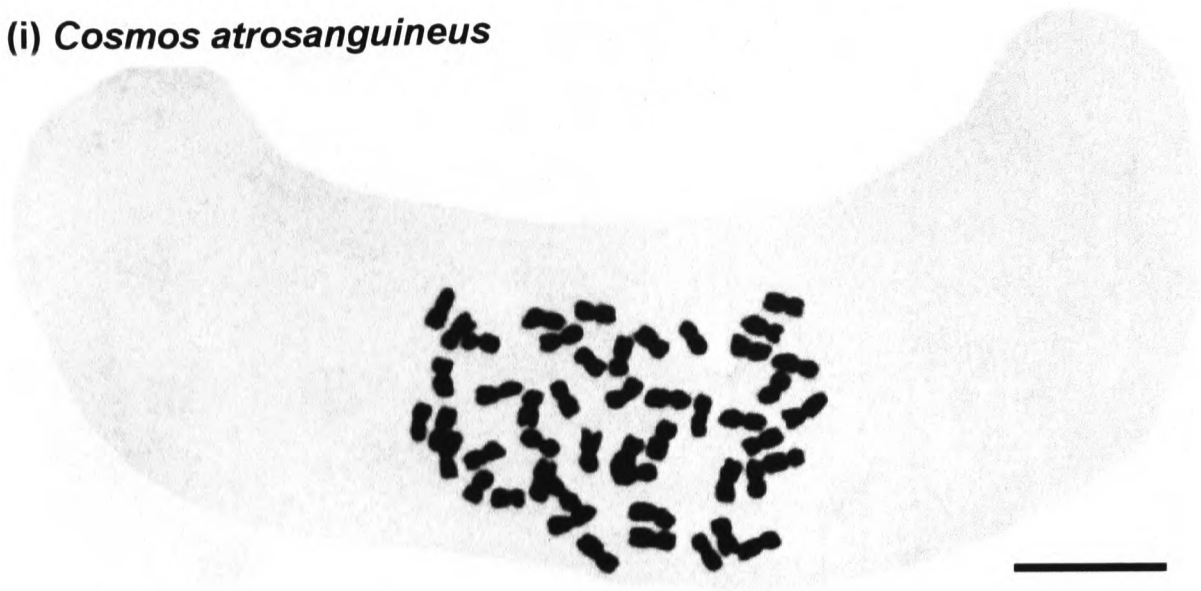


Figure 4.1. Somatic (root) cell showing chromosomes of *Cosmos atrosanguineus* (98-69) [slide No. 73]. $2n = 4x = 48$. Pre-treatment: ABN at 4°C for 26 hrs. Scale bar = 10 μm



Figure 4.2.

Somatic (root) cell showing chromosomes of *Cosmos atrosanguineus* (98-82) [slide No. 46]. Root material pretreated in ABN at 4°C for 25 hrs. Reducing the pre-treatment time by one hour produced chromosomes that were less condensed than in Figure 4.1 and better for karyotyping (See Figure 4.3 below for karyotype of this chromosomes spread). Scale bar = 10 μm .

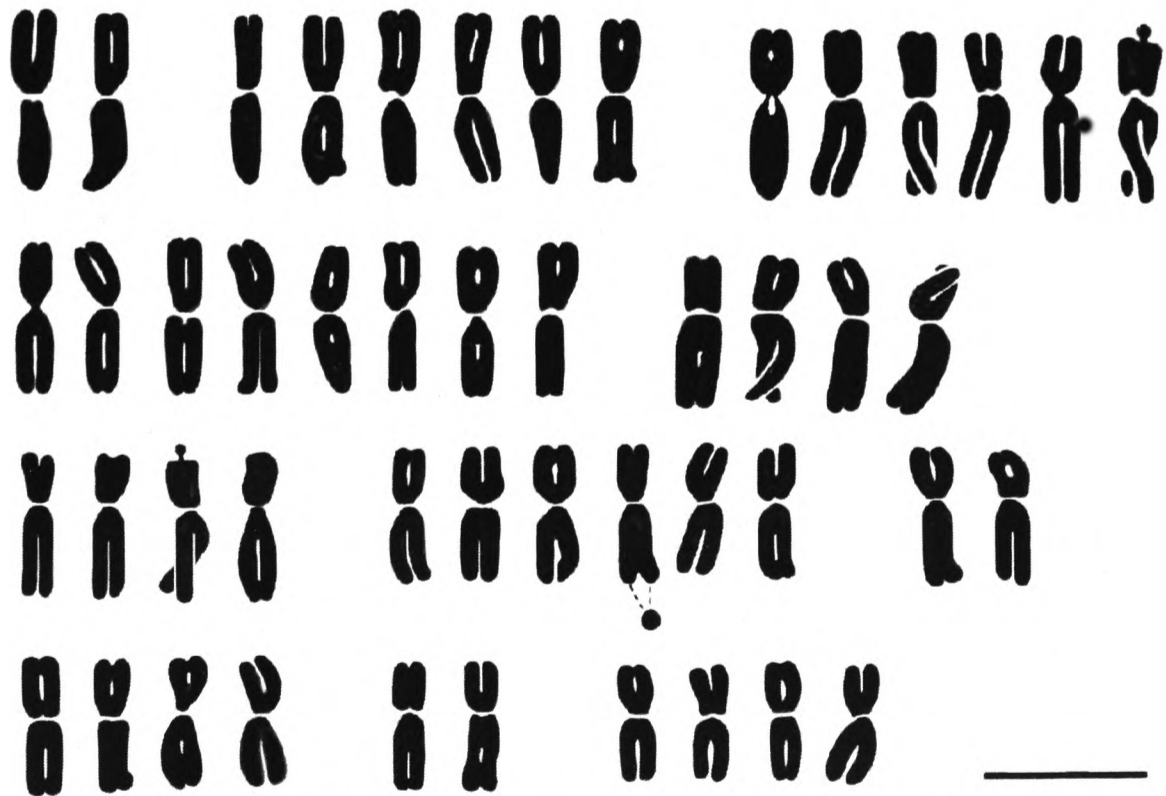


Figure 4.3. Karyotype drawing of *Cosmos atrosanguineus* (98-82) $2n = 4x = 48$. Morphological description of chromosomes (from left to right and top to bottom). **Row 1:** Chromosomes 1-2, *M* (5.7 μm); Chromosomes 3-8, *m* (5.4 μm); Chromosomes 9-14, *m-sm* (5.4 μm). **Row 2:** Chromosomes 15-22, *m* (4.6 μm); Chromosomes 23-26, *m-sm* (4.6 μm). **Row 3:** Chromosomes 27-30, *sm* (4.3 μm); Chromosomes 31-36, *m* (4.3 μm); Chromosomes 37-38, *m-sm* (4.3 μm). **Row 4:** Chromosomes 39-42, *m* (4.3 μm); Chromosomes 43-44, *m-sm* (4.0 μm); Chromosomes 45-48, *m* (3.6 μm). Scale bar = 5 μm .

(ii) *Cosmos bipinnatus*

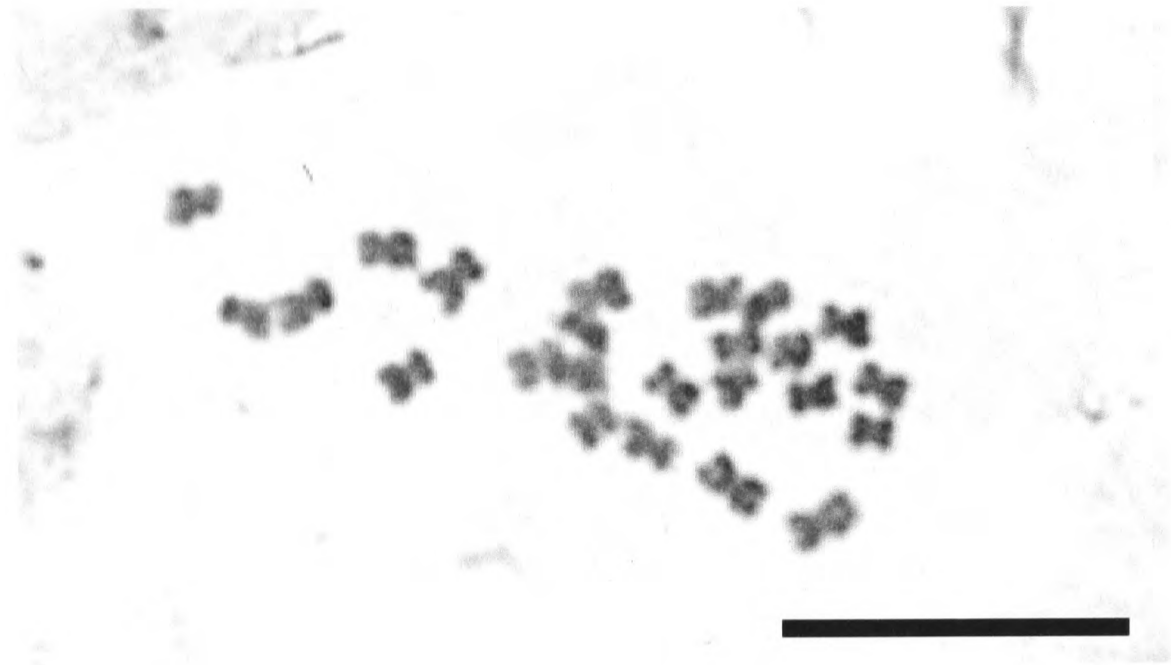


Figure 4.4, Somatic (root) cell showing chromosomes of *Cosmos bipinnatus* (98-86) [slide No. 32], $2n = 2x = 24$. Pre-treatment: PDB at 22°C for 5 hrs. Scale bar = 10 μm

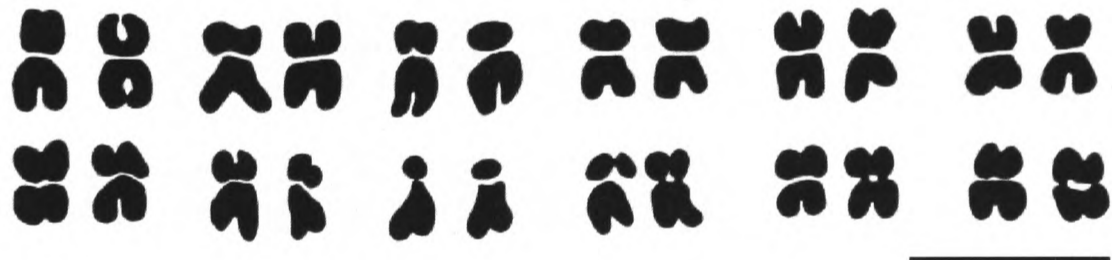


Figure 4.5, Karyotype drawing of *Cosmos bipinnatus* (98-86) [slide No. 32]. $2n = 2x = 24$. Morphological description of chromosomes (from left to right and top to bottom). **Row 1:** Pair 1, *M* (2.1 μm); Pair 2, *m* (1.9 μm); Pair 3, *sm* (1.9 μm); Pair 4, *m* (1.7 μm); Pair 5, *m* (1.7 μm); Pair 6, *M* (1.5 μm). **Row 2:** Pair 7, *M* (1.5 μm); Pair 8, *sm* (1.5 μm); Pair 9, *st* (1.5 μm); Pair 10, *sm* (1.5 μm); Pair 11, *M* (1.2 μm); Pair 12, *m* (1.2 μm). Scale bar = 4 μm .

(iii) *Cosmos carvifolius*



Figure 4.6. Somatic (root) cell showing chromosomes of *Cosmos carvifolius* (98-136) slide No. 65], $2n = 2x = 22$. Pre-treatment: ABN at 4°C for 26 hrs. Scale bar = 10 μm

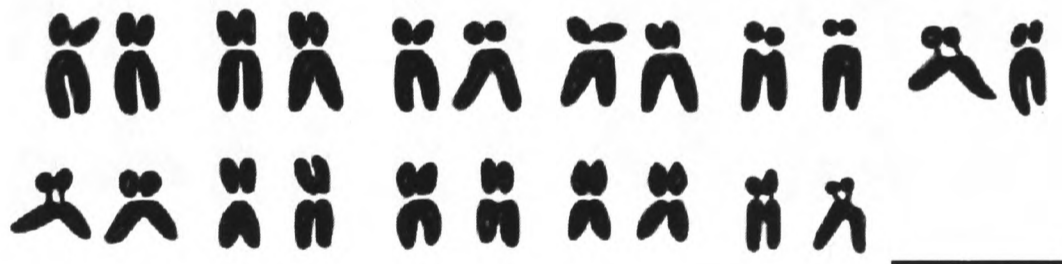


Figure 4.7. Karyotype drawing of *Cosmos carvifolius* (98-136) [slide No. 65]. $2n = 2x = 22$. Morphological description of chromosomes (from left to right and top to bottom). **Row 1:** Pair 1, *st* (3.2 μm); Pair 2, *st* (3.0 μm); Pair 3, *st* (2.6 μm); Pair 4, *st* (2.6 μm); Pair 5, *st* (2.6 μm); Pair 6, *sm-st* (2.6 μm). **Row 2:** Pair 7, *sm* (2.6 μm); Pair 8, *m* (2.7 μm); Pair 9, *m* (2.3 μm); Pair 10, *m* (2.3 μm); Pair 11, *sm* (2.1 μm). Scale bar = 5 μm .

(iv) *Cosmos sulphureus*

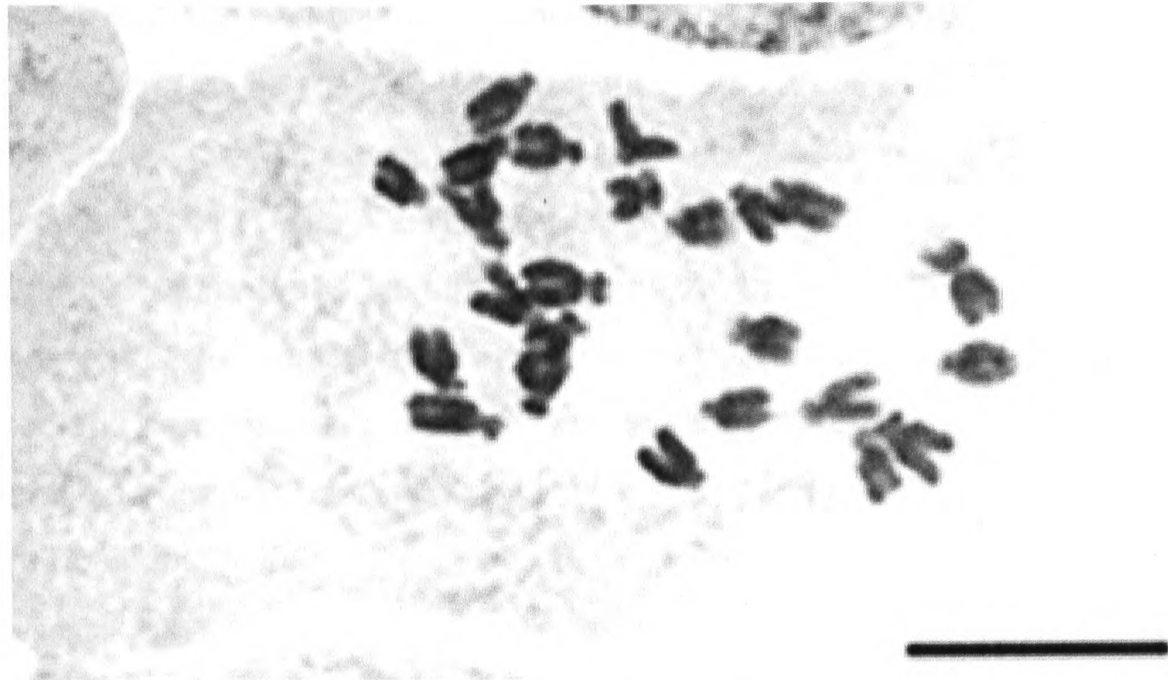


Figure 4.8. Somatic (root) cell showing chromosomes of *Cosmos sulphureus* (98-49) [slide No. 47], $2n = 2x = 24$. Pre-treatment: OQ at 22°C for 6 hrs. Scale bar = 10 μm

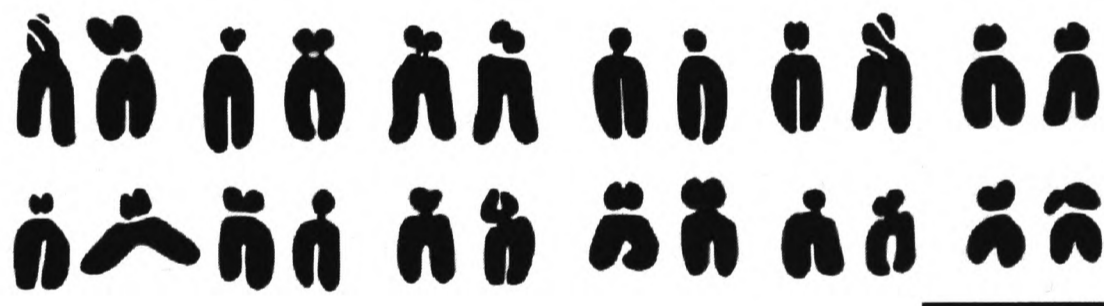


Figure 4.9. Karyotype drawing of *Cosmos sulphureus* (98-49) [slide No. 47]. $2n = 2x = 24$. (Morphological description of chromosomes (from left to right and top to bottom). **Row 1:** Pair 1, *sm* (3.9 μm); Pair 2, *st* (3.6 μm); Pair 3, *sm-st* (3.6 μm); Pair 4, *st* (3.1 μm); Pair 5, *sm-st* (3.1 μm); Pair 6, *sm-st* (2.8 μm). **Row 2:** Pair 7, *st* (2.5 μm); Pair 8, *sm-st* (2.5 μm); Pair 9, *sm-st* (2.5 μm); Pair 10, *sm* (2.5 μm); Pair 11, *sm-st* (2.5 μm); Pair 12, *sm* (2.2 μm). Scale bar = 5 μm .

The karyotype of the *C. bipinnatus* (1996 582) accessions is characterised as having 24 chromosomes, 4M (*median point*), 4m (*median region*), 3sm (*submedian region*), 1st (*subterminal region*) pairs (Table 4.2, and Figure 4.3), which agrees essentially with previously-published *C. bipinnatus* karyotypes of 8m and 4sm pairs (Ohri *et al.*, 1988). A published karyotype of *C. sulphureus* is given as 24 chromosomes with 6sm and 6st pairs (Ohri *et al.*, 1988), whereas the *C. sulphureus* (1996 980) accession used in this study is described slightly more distinctly as having 24 chromosomes with 3sm, 6sm-st, 3st pairs (Table 4.2 and Figure 4.9). In general, the karyotypes of the *C. bipinnatus* and *C. sulphureus* accessions identified in this study agree with published data, and reveal *C. bipinnatus* to have mainly metacentric chromosomes with median to sub-median centromere positions (*m to sm*), and *C. sulphureus* to have predominantly acrocentric chromosomes with sub-median to sub-terminal (*sm to st*) centromere positions.

Cosmos atrosanguineus and *C. carvifolius* have not been karyotyped previously. Figures 4.1 to 4.3 show a *C. atrosanguineus* karyotype of 48 predominantly metacentric chromosomes with median to sub-median centromere positions, and a *C. carvifolius* karyotype of 22 predominantly acrocentric chromosomes with sub-median to sub-terminal centromere positions (Table 4.2)

Evidence from chromosome numbers, karyotypes and C-DNA values (Table 4.3) identify *C. atrosanguineus* as an allotetraploid species (Bennett and Leitch 1995; 1997; 2003). The allopolyploid origin of the *C. atrosanguineus* is indicated by the morphological grouping of chromosomes into three pairs of putative homologues (Figure 4.3; chromosomes 1-2, 37-38 and 43-44) and three sets of 6 homologous/homoeologous chromosomes (Figure 4.3; chromosomes 3-8, 9-14 and 31-36). An autopolyploid would have chromosomes grouped in fours.

The lack of a bimodal size distribution in the *C. atrosanguineus* karyotype suggests its diploid progenitors had morphologically similar, same-sized karyotypes, or that the *C. atrosanguineus* genome has undergone extensive chromosomal rearrangement since polyploidization, resulting in a predominantly metacentric karyotype. *Cosmos carvifolius* and *C. sulphureus* have probably not contributed to the formation of polyploid *C. atrosanguineus* in the natural environment, since neither of these species is known to occur in the area of San Luis Potosí or Hidalgo, which are the only known locations of wild *C. atrosanguineus*' populations (Figures 1.2, 1.3 and 2.1). The distribution of *C. bipinnatus* does encompass these two areas, but the chromosome

number, morphology and size of *C. bipinnatus*, and those of *C. carvifolius* and *C. sulphureus* exclude these species as progenitors of *C. atrosanguineus*. For example, *Cosmos bipinnatus* has a karyotype consisting of 24 essentially metacentric chromosomes, but its chromosomes are ~3 times smaller than those in *C. atrosanguineus* and its C-DNA content ~5 times less, (Table 4.3). On this evidence, it is unlikely to have contributed to the polyploid genome of tetraploid *C. atrosanguineus*. In contrast, *Cosmos sulphureus* has 24 chromosomes that are similar in size to those of *C. atrosanguineus* and contains approximately half the amount of its C-DNA. However, its acrocentric-sub-telocentric karyotype and geographical distribution at low altitudes militate against it being a putative parent of *C. atrosanguineus*. Likewise, *Cosmos carvifolius* with its 22 chromosomes seems an unlikely parent of a 48-chromosome polyploid. A progenitor *Cosmos* species of 22 chromosomes presupposes allopolyploidization with a *Cosmos* species having 26 chromosomes, which, aside from the published count for *C. juxtlahuacensis* Panero & Villaseñor ($2n = 26$ [13 II]) (Strother and Panero, 2001) is a chromosome number not found in the genus (Stuessy, 1977; Robinson *et al.*, 1981). In addition, its predominantly acrocentric-sub-telocentric chromosomes are on average only half the size of *C. atrosanguineus* chromosomes (Table 4.2).

Table 4.2 Summary of cytological investigations on four *Cosmos* species

<i>Cosmos</i> species	Kew Acc No.	Cytology No.	Treatment for mitosis (°C/hrs)	Sporophyte chromosomes (2n)			Treatment for meiosis	Gametophyte chromosomes (n)	
				(2n)	Karyotype morphology (homologues)	Approximate size range of chromosomes (µm)		(n)	Chromosome associations
<i>C. atrosanguineus</i>	1997 6334	98-69	ABN 4/26	48	(M = 1), (m = 14), (m-sm = 7), (sm = 2)	5.5-3.5	2% aceto- orcein	24	4 IV, 16 II
	1999 3819	01-163	ABN 4/26	48	(M = 1), (m = 14), (m-sm = 7), (sm = 2)	5.5-3.5		24	3 IV, 18 II
<i>C. bipinnatus</i>	1996 582	98-93	PDB	24	(M = 4), (m = 4), (sm = 3), (st = 1)	2.0-1.0		12	12 II
		98-57	22/5						
<i>C. carvifolius</i>	1999 383	98-136	ABN 4/26	22	(m = 3), (sm = 2), (sm-st = 1), (st = 5),	3.0-2.0		No data	---
<i>C. sulphureus</i>	1996 980	98-49	OQ 22/5	24	(sm = 3), (sm-st = 6), (st = 3),	4.0-2.0		12	12 II

Key: II, bivalent and IV, quadrivalents

Table 4.3 C-DNA values of four *Cosmos* species

Entry No.	Species	2n	Ploidy (x)	DNA amount (pg)		
				1C	2C	4C
280	<i>Cosmos bipinnatus</i>	24	2	1.5	3.1	6.2
281	<i>Cosmos sulphureus</i>	24	2	3.0	6.0	12.0
297a	<i>Cosmos atrosanguineus</i>	48	4	7.3	14.7	29.4

Table compiled from the Plant DNA C-values Database (Release 2.0) (Bennett and Leitch 1995; 1997; 2003)

4.3.3 - Idiograms of chromosomes at diakinesis-metaphase I

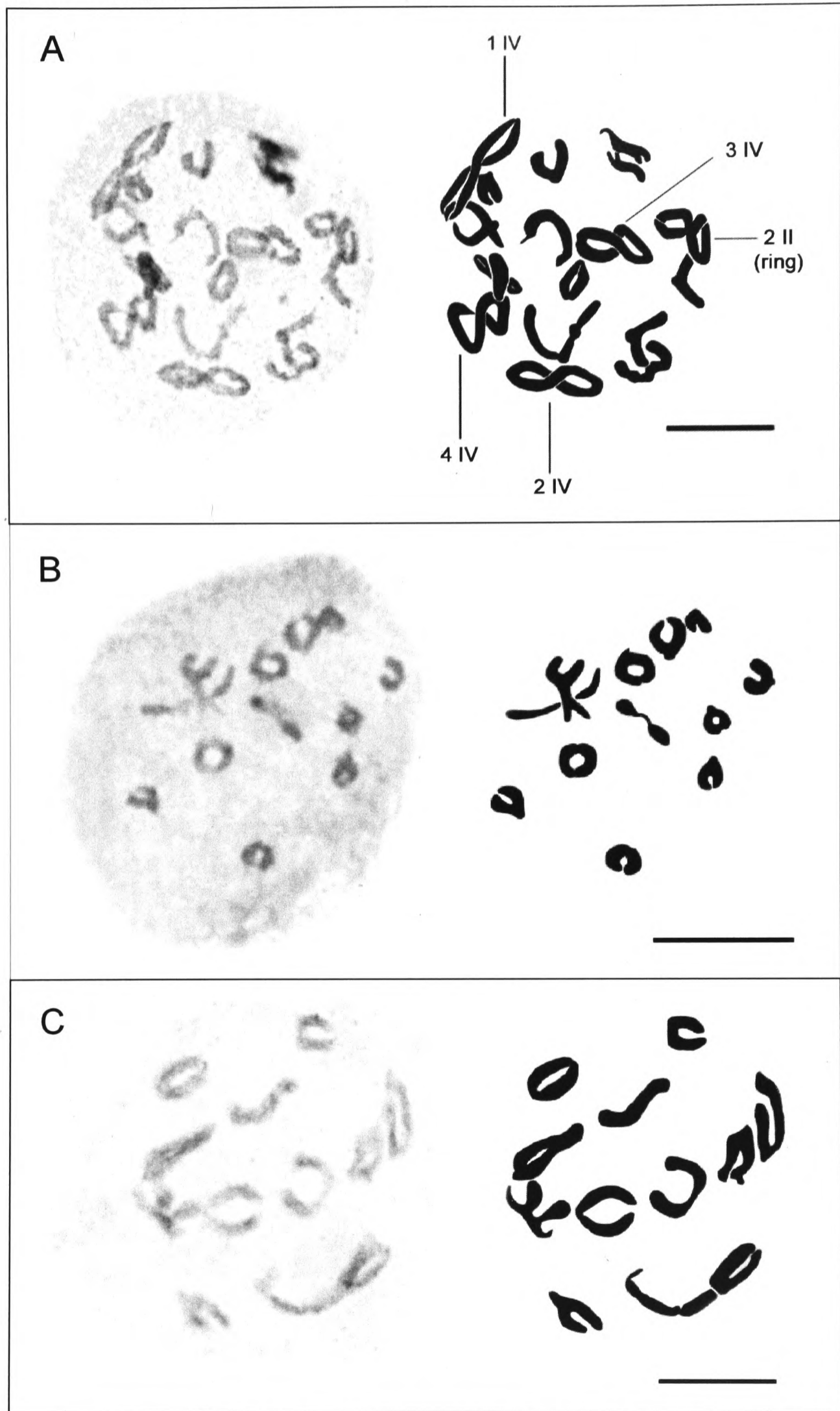


Figure 4.10. *Cosmos* chromosomes at diakinesis-metaphase-I with associated drawing. Pollen mother cells squashed in 2% aceto-orcein. **A**, *Cosmos atrosanguineus* (Kew accession no. 1999-3819; Cytology No. 01-163; Slide 38x), with 4 figure-of-eight quadrivalents identified as in **Figure 4.11** over page. **B**, *Cosmos bipinnatus* (Kew accession no. 1996-582; Cytology No. 98-57; Slide 6M). **C**, *Cosmos sulphureus* (Cytology No. 61-881; Slide 188). Scale bars = 10 μ m.

(i) *Cosmos atrosanguineus*

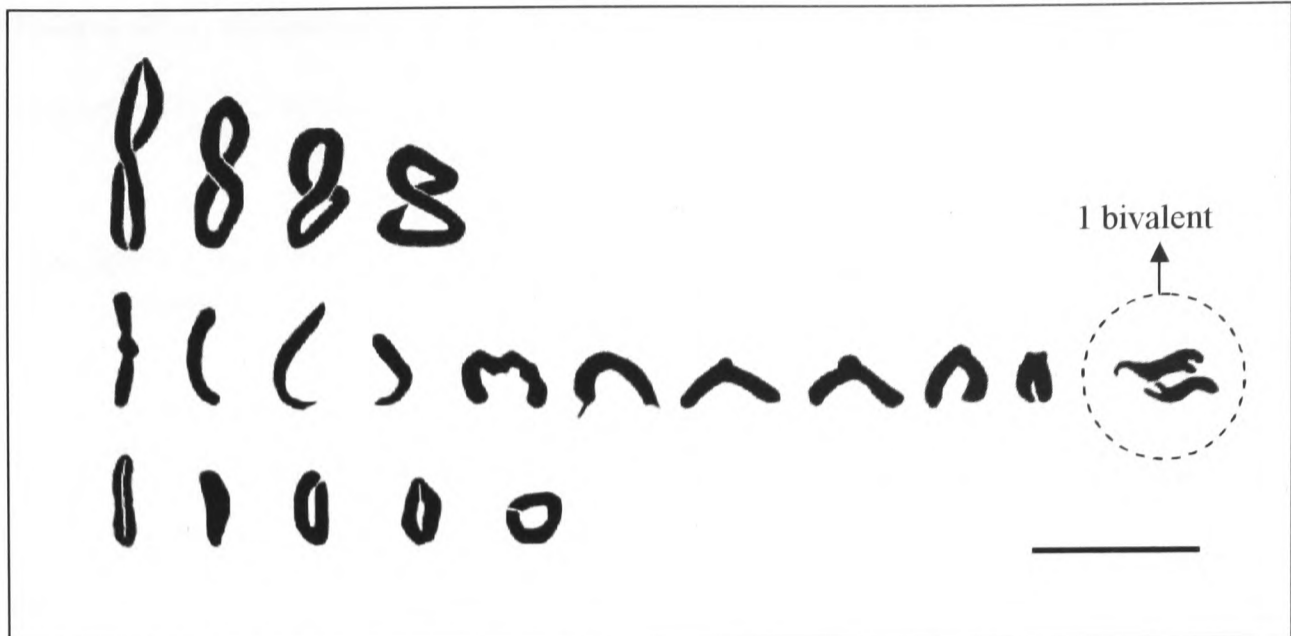


Figure 4.11. Idiogram of *Cosmos atrosanguineus* chromosomes at diakinesis-metaphase I, showing 4 figure-of-eight quadrivalents and 16 bivalents (11 rod bivalents indicating single chiasma, and 5 ring bivalents, indicating 2 terminal chiasmata. The four figure-of-eight quadrivalents represent, from left to right, quadrivalents (IV); 1, 2, 3 and 4 in Figure 4.10A. (Scale bar = 10 μ m)

(ii) *Cosmos bipinnatus*

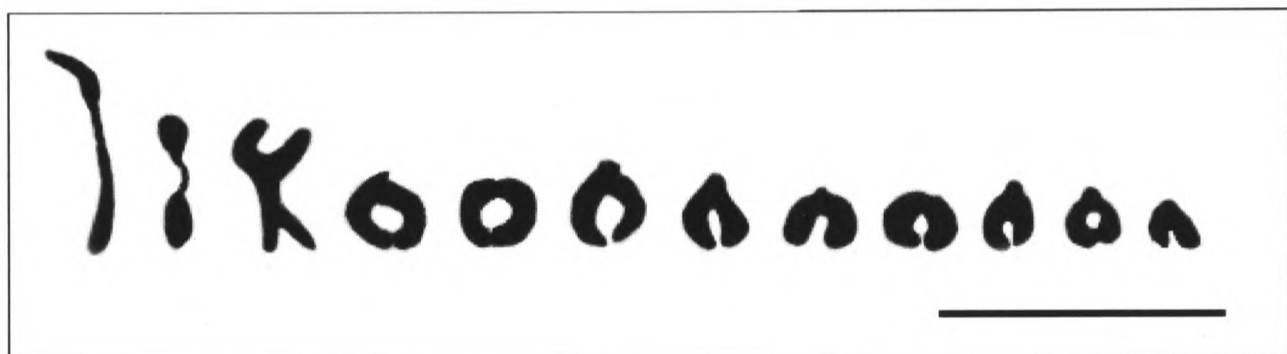


Figure 4.12. Idiogram of *Cosmos bipinnatus* chromosomes at diakinesis-metaphase I, showing 12 bivalents (2 ring bivalents and 10 rod bivalents. (Scale bar = 10 μ m)

(iii) *Cosmos sulphureus*

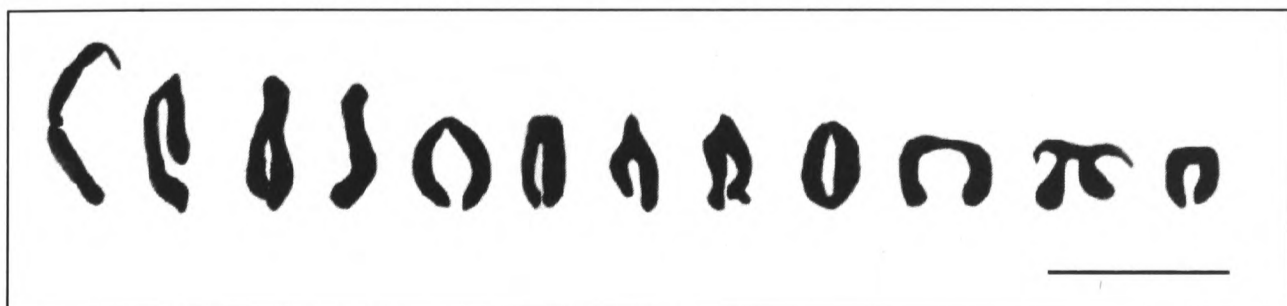


Figure 4.13. Idiogram of *Cosmos sulphureus* chromosomes at diakinesis-metaphase I, showing 12 bivalents (11 rod bivalents and 1 ring bivalent. (Scale bar = 10 μ m)

Table 4.4 – Numbers of normal tetrads, anaphase-I laggards and bridges observed in accessions of *C. atrosanguineus* and *C. bipinnatus*

<i>Cosmos</i> species, accession & plant	Meiotic index			Anaphase-I			
	Total number. of tetrads	Number of normal tetrads	Meiotic Index (%)	Total number. of anaphase cells	Number of cells with laggards or bridges	Number of cells with perpendicular spindle orientation at telophase I	Percentage cells with abnormal disjunction
<i>C. atrosanguineus</i> 1997 6334							
Plant 98-69	246	244	99.2	63	0	2	3.17
Plant 98-92	307	303	99.0	28	0	0	0.00
<i>C. atrosanguineus</i> 1999 3819							
Plant 01-162	202	202	100.0	46	0	3	6.52
Plant 01-163	368	363	98.6	57	0	2	3.51
<i>C. bipinnatus</i> 1996 582							
Plant 98-44	148	148	100.0	237	0	0	0
Plant 98-66	307	305	99.3	217	0	0	0

Table 4.5 Chromosome associations at diakinesis in three *Cosmos* species

<i>Cosmos</i> species	Kew Acc. No.	Cytology No.	Slide No.	Chromosome associations	No. of Cells	Frequency of chromosome association in cells observed (%)
<i>C. atrosanguineus</i>	1999 3819	01-163	38x	4 IV + 16 II	3	75
			31x	4 IV + 16 II		
			31x	4 IV + 16 II		
			31x	3 IV + 18 II	1	25
<i>C. bipinnatus</i>	1996 582	98-57	6M	12 II	50	100
		98-66	14M	12 II		
		98-81	20M	12 II		
<i>C. sulphureus</i>	---	61-881	188	12 II	50	100

Photographs and idiograms of chromosome associations at diakinesis-metaphase-I for *Cosmos atrosanguineus*, *C. bipinnatus* and *C. sulphureus* are displayed in Figures 4.10 to 4.13. *Cosmos bipinnatus* and *C. sulphureus* show regular bivalent formation and normal meiosis as expected for diploid non-hybrid species. The *C. atrosanguineus* karyotype consists of 16 bivalents and four figure-of-eight quadrivalents. The presence of quadrivalents might be expected to cause some irregularities in the formation of *C. atrosanguineus* gametes. However, the high meiotic index (mi = 98-100%) and the lack of observed anomalies at anaphase-I and telophase-I indicate normal meiosis and balanced gamete formation, with no discernible difference observed in the meiotic stability of *C. atrosanguineus* (mi = 98-100%) and *C. bipinnatus* (mi = 98-100%)

(Tables 4.2 and 4.4). Increased frequency of quadrivalents with zig-zag ring or zig-zag chain configurations is known to enhance the chance of equal distribution of chromosomes at anaphase I and may explain observed increases in fertility in some polyploid species (Mastenbroek *et al.*, 1982). *Cosmos atrosanguineus*, through its four zig-zag figure-of-eight quadrivalents may have regulated meiosis positively towards the formation of euploid gametes by the adjustment of its chromosome orientation.

The low number of quadrivalents and the absence of binomial distribution of quadrivalents in meiocytes suggest that *C. atrosanguineus* is a stable secondary segmental allotetraploid of recent origin (Sybenga, 1996; Boff and Schifino-Wittman, 2003). The recent origin is supported by its C-DNA values being 2½ to 5 times greater than in known diploid *Cosmos* species, and its segmental allopolyploidy is evidenced by the consistent presence of low numbers of quadrivalents in meiocytes. Boff and Schifino-Wittman (2003) found that the DNA contents of tetraploid *Leucaena confertiflora* and tetraploid *L. pallida* were twice the amount recorded for diploids of the species, and suggested that this feature allied to the low frequency of quadrivalents observed in these tetraploid species is evidence of their recent polyploidization. The supposition being that as neopolyploids, tetraploid *L. confertiflora* and *L. pallida* have not had the requisite time to undergo the processes of genome-size reduction and bivalent-formation associated with more ancient 'diploidized' polyploids. *Cosmos atrosanguineus*, with its relatively large genome size and low quadrivalent frequency may well reflect the state of a recently-evolved segmental allopolyploid undergoing diploidization. Whether a stabilized secondary segmental allopolyploid, or a segmental allopolyploid in transition to diploid stability, the evidence from this study identifies *C. atrosanguineus* as an allotetraploid species.

4.3.4 Pollen viability in three *Cosmos* species

Table 4.6 - Pollen-viability: *Cosmos atrosanguineus*

Data recorded between: 24-30 July (2001)

Inflorescence	Mag	Filter	Pollen count (Number of fluorescent pollen grains ÷ total number of pollen number grains)																					
			A					B					C					D					E	
Disk floret			1	2	3	4	5	6	7	8	9	10	11	12	13	14	15	16	17	18	19	20	% viability	
1999 3819 (plant 1)	X10	2	2/11	1/12	4/8	3/8	2/6	2/5	6/15	2/7	1/9	2/8	2/12	3/11	6/27	8/21	7/22	11/42	6/13	2/10	2/13	4/21	27.74	
1999 3819 (plant 2)			2/18	1/8	1/6	3/20	2/6	1/6	5/15	1/16	4/14	3/15	1/12	1/8	2/9	1/8	3/14	4/15	1/6	1/16	2/10	4/19	18.41	
1999 3819 (plant 3)			8/38	20/39	4/9	5/21	5/11	2/7	6/16	3/9	2/8	4/10	3/18	5/15	3/19	7/24	7/37	12/27	9/43	13/51	15/41	19/40	32.54	
1999 3819 (plant 4)			7/18	3/17	5/11	4/15	1/10	8/19	10/25	10/29	2/14	4/14	9/12	3/12	2/10	2/16	4/9	4/13	1/6	2/7	2/5	2/6	30.82	
1999 2254 (plant 5)			3/13	3/12	2/6	6/16	6/39	4/33	13/35	14/69	9/30	9/44	4/52	15/72	3/31	2/24	7/41	7/33	2/11	3/10	1/6	2/6	21.80	
1999 2254 (plant 6)			5/10	15/20	12/25	12/23	14/27	10/32	13/38	14/34	10/25	19/37	21/37	25/38	17/36	5/21	14/33	8/23	7/16	6/12	4/15	8/14	45.97	
1999 2254 (plant 7)			3/19	4/14	1/7	2/5	2/4	3/8	2/9	3/9	2/8	2/5	2/12	2/9	10/20	4/23	1/5	3/8	1/6	1/5	3/12	3/10	28.76	
1997 6334 (plant 8)			1/4	2/12	9/20	8/22	2/9	2/7	4/13	4/9	6/28	2/6	4/6	3/11	5/16	2/9	14/49	9/39	3/8	3/10	5/17	2/12	31.13	
1997 6334 (plant 9)			7/32	9/23	3/14	6/14	5/13	12/39	5/19	8/22	4/13	4/16	3/13	5/16	7/20	4/23	4/14	3/19	3/9	2/8	3/10	2/12	28.80	
1997 6334 (plant 10)			11/24	12/31	13/29	10/23	3/12	4/11	3/16	11/27	14/34	9/25	10/28	18/40	17/45	8/48	6/17	6/25	5/21	6/20	8/14	4/16	34.50	
																						Mean	30.00	
																						Standard deviation	7.40	

Table 4.7 - Pollen-viability: *Cosmos bipinnatus* 1996 582

Data recorded between: 17-23 July (2001)

Inflorescence		Pollen count (Number of fluorescent pollen grains ÷ total number of pollen number grains)																						
		A					B					C					D					E		
Disk floret	MagFilte	1	2	3	4	5	6	7	8	9	10	11	12	13	14	15	16	17	18	19	20	% viability		
Plant 1	x10	3/18	6/24	5/18	5/23	6/16	9/30	10/28	6/28	13/48	7/25	2/10	4/19	4/15	9/27	8/27	2/12	9/31	2/10	3/39	5/42	24.34		
Plant 2		9/41	13/41	7/12	9/14	11/25	9/26	9/18	9/25	7/17	7/15	7/27	14/24	8/17	10/28	32/56	31/62	10/47	20/50	10/34	18/52	42.43		
Plant 3		7/35	5/24	4/27	2/25	13/47	15/37	13/34	15/40	14/44	11/52	12/61	8/54	5/41	8/43	6/33	9/46	9/36	11/39	6/19	2/25	22.97		
Plant 4		4/15	5/14	6/14	5/17	13/30	31/34	14/33	14/22	11/32	12/24	7/12	13/24	4/11	6/18	13/31	7/14	7/20	4/16	7/13	12/30	45.31		
Plant 5		14/31	8/19	4/18	7/11	10/18	12/17	13/26	12/16	12/23	13/20	5/32	7/13	9/32	6/21	15/21	9/22	11/27	6/22	4/19	4/23	44.28		
Plant 6		12/46	18/53	29/62	17/52	5/19	11/35	17/55	14/65	13/40	7/29	11/31	3/14	4/16	9/20	8/20	3/16	6/11	3/8	6/18	11/21	33.88		
Plant 7		4/7	4/25	7/34	3/12	9/38	7/15	7/16	6/9	5/19	7/21	9/11	9/13	12/21	37/51	18/36	15/22	19/30	42/50	19/26	21/36	51.56		
Plant 8		12/16	12/21	12/38	17/25	21/30	3/8	26/44	22/41	6/10	12/27	6/9	9/19	17/30	19/26	6/15	9/25	2/7	7/16	15/25	11/22	51.76		
Plant 9		13/25	10/28	21/34	14/27	7/12	16/21	12/16	14/20	11/18	15/25	15/26	8/13	7/18	6/21	7/13	7/29	8/14	6/15	14/22	4/10	53.44		
Plant 10		13/22	7/25	7/12	3/7	7/18	15/33	14/27	9/18	10/22	11/18	11/23	4/8	5/14	3/7	18/31	23/42	9/16	9/13	4/7	10/27	48.99		
		Mean																				42.00		
		Standard deviation																				11.17		

Table 4.8 - Pollen-viability: *Cosmos sulphureus* 1996 980 (Late Autumn)

Inflorescence		Pollen count (Number of fluorescent pollen grains ÷ total number of pollen number grains)																				Mean Standard deviation		
		A					B					C					D							E
Disk floret	Mag	1	2	3	4	5	6	7	8	9	10	11	12	13	14	15	16	17	18	19	20	% viability		
Plant 1	X10	4/13	2/13	4/10	1/5	2/9	6/15	3/18	3/8	7/18	3/11	4/15	3/7	3/9	4/7	6/11	6/17	4/8	6/28	7/22	4/15	33.43		
Plant 2		6/19	3/8	4/20	7/18	5/14	8/17	6/13	7/19	9/22	4/19	4/8	3/9	5/12	3/12	4/11	5/12	6/14	4/11	5/18	8/21	36.70		
Plant 3		4/15	5/28	7/17	7/23	6/26	14/16	5/17	4/16	4/13	3/9	5/12	1/5	8/23	10/28	7/29	8/22	6/16	3/8	7/12	5/14	35.80		
Plant 4		2/11	3/7	4/16	4/13	7/25	8/20	11/27	10/31	1/6	4/7	3/8	3/9	2/11	5/16	5/13	1/8	4/11	2/13	9/22	5/15	32.14		

Data recorded on: 11 November (2000)

Table 4.9 - Pollen-viability: *Cosmos sulphureus* 1996 980 (Spring)

Inflorescence		Pollen count (Number of fluorescent pollen grains ÷ total number of pollen number grains)																				Mean Standard deviation		
		A					B					C					D							E
Disk floret	Mag	1	2	3	4	5	6	7	8	9	10	11	12	13	14	15	16	17	18	19	20	% viability		
Plant 5	X10	10/14	7/12	15/17	23/26	5/8	4/7	14/20	15/17	29/38	29/44	17/30	22/28	7/12	10/14	14/22	9/13	18/27	29/36	16/20	15/19	71.52		
Plant 6		9/13	9/11	13/15	7/12	19/28	14/19	14/18	21/30	38/53	15/30	29/62	17/52	23/34	34/42	15/17	11/16	37/46	22/25	15/37	18/25	68.62		
Plant 7		15/19	12/18	35/42	36/44	15/25	19/23	19/28	9/15	9/13	7/15	16/27	23/29	13/21	20/27	16/22	14/23	25/29	31/39	18/20	16/19	71.91		
Plant 8		26/29	29/41	20/27	29/38	24/33	17/25	19/33	34/42	17/18	12/14	8/10	8/12	14/25	15/18	9/16	14/19	22/29	7/17	6/11	5/9	69.66		

Data recorded between: 25-26 April (2001)

Pollen viability, pollen number per disk floret and pollen size in *Cosmos atrosanguineus*, *C. bipinnatus* and *C. sulphureus* do not show normal distribution (Appendix 4.1.1 – 4.1.5; $p = < 0.05$), and so Kruskal-Wallis was used to compare three or more populations, and Mann-Whitney U was used to compare two populations, and as a *post hoc* test for Kruskal-Wallis (Dytham, 2003).

There is a significant difference in the pollen viability of the three *Cosmos* species (Table 4.6-4.9; Figure 4.24; Appendix 4.2, Box 1, $p = < 0.05$ \therefore reject 1H_0), with the viability of *C. bipinnatus* (~42%) being significantly higher than that of *C. atrosanguineus* (~30%) and *C. sulphureus* (Autumn) (~34%) (Appendix 4.2, Box 2, $p = < 0.05$ \therefore reject 2H_0), and *C. sulphureus* (Spring) having the highest pollen viability (~71%) (Appendix 4.2, Boxes 3-7, $p = < 0.05$ \therefore reject 3H_0 - 7H_0 ; Figure 4.14). There is weak statistical support suggesting that pollen viability in the three *C. atrosanguineus* accessions is different (Appendix 4.2, Box 8, $p = 0.49$ \therefore reject 8H_0), however the majority of this difference occurs between accessions 1999 2254 (~32%) and 1997 6334 (~31%) (Appendix 4.2, Box 9, $p = > 0.05$ \therefore cannot reject 9H_0 , however see Box 10, $p = 0.02$ \therefore reject $^{10}H_0$), and thus, with such a small survey of *C.-atrosanguineus* accessions it might be questioned whether any meaningful difference exists in the viability of these accessions (Appendix 3.2, Box 8 –11).

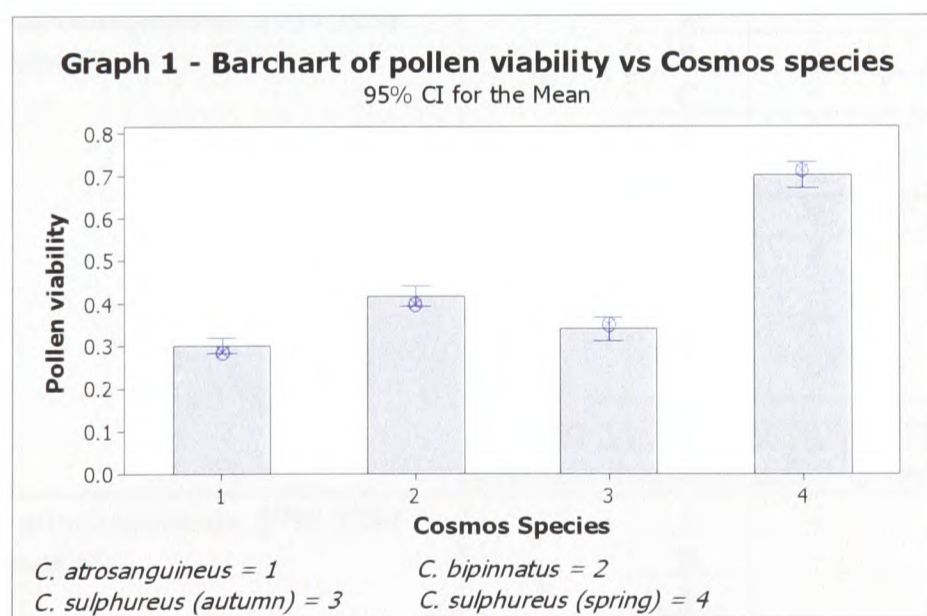


Figure 4.14 – Bar chart showing pollen viability of three *Cosmos* species
Pollen viability of *Cosmos atrosanguineus*, *C. bipinnatus*, *C. sulphureus* (autumn) and *C. sulphureus* (spring) compared as a bar chart (Graph 1)

4.3.5 - Pollen-grain number in three *Cosmos* species

Table 4.10. *Cosmos* pollen-grain numbers per 4- μ l sample of vortexed anther solution

<i>Cosmos</i> Species, accession & plant	Inflore- scence	Disk floret	Number of pollen grains per 4- μ l sample				
			Sample 1	Sample 2	Sample 3	Sample 4	Sample 5
<i>C. atrosanguineus</i> 1999 3819 (Plant 2)	1	A	5	6	5	7	6
		B	6	4	7	3	6
		C	5	6	6	6	7
		D	7	8	6	8	6
		E	6	4	6	5	6
	2	A	6	5	5	6	5
		B	5	7	6	4	6
		C	6	7	6	7	5
		D	4	6	7	5	6
		E	6	5	6	6	5
	Average number of pollen grains per 4 μ l sample					5.78	
	Average number of pollen grains per disk floret					7225.00	
<i>C. atrosanguineus</i> 1999 3819 (Plant 3)	1	A	3	6	3	4	6
		B	6	6	7	6	6
		C	9	7	6	6	8
		D	6	6	4	6	5
		E	7	6	5	5	6
	2	A	4	6	6	8	5
		B	5	6	6	6	6
		C	6	5	4	6	3
		D	5	6	7	6	6
		E	7	6	5	6	7
	Average number of pollen grains per 4 μ l sample					5.76	
	Average number of pollen grains per disk floret					7200.00	
<i>C. atrosanguineus</i> 1999 3819 (Plant 2 and Plant 3 combined)	Average number of pollen grains per 4 μ l sample					5.77	
	Average number of pollen grains per disk floret					7213.00	
<i>C. atrosanguineus</i> 1999 2254 (plant 5)	1	A	3	6	7	4	7
		B	5	6	5	6	5
		C	6	8	6	3	6
		D	5	4	6	6	4
		E	6	7	5	4	5
	2	A	6	7	6	7	5
		B	4	6	4	5	6
		C	8	6	7	6	3
		D	6	5	4	6	5
		E	7	7	6	8	6
	Average number of pollen grains per 4 μ l					5.64	
	Average number of pollen grains per disk					7050.00	
<i>C. atrosanguineus</i> 1999 2254 (plant 6)	1	A	3	6	7	6	5
		B	5	6	6	5	5
		C	6	5	6	4	6
		D	5	6	6	7	6
		E	8	6	7	8	7
	2	A	3	5	5	6	7
		B	6	6	4	5	6
		C	5	4	6	6	7
		D	6	6	6	5	6
		E	3	5	7	6	4
	Average number of pollen grains per 4 μ l					5.64	
	Average number of pollen grains per disk					7050.00	
<i>C. atrosanguineus</i> 1999 2254 (Plant 5 and Plant 6 combined)	Average number of pollen grains per 4 μ l					5.64	
	Average number of pollen grains per disk					7050.00	

Table 4.10. continued

<i>Cosmos</i> Species & accession	Inflorescence	Disk floret	Number of pollen grains per 4- μ l sample				
			Sample 1	Sample 2	Sample 3	Sample 4	Sample 5
<i>C. atrosanguineus</i> 1997 6334 (Plant 9)	1	A	6	5	8	5	6
		B	6	7	4	7	6
		C	3	6	5	6	5
		D	6	6	7	6	5
		E	6	5	6	5	6
	2	A	6	6	5	7	3
		B	6	7	6	4	6
		C	4	6	5	6	6
		D	5	3	5	5	5
		E	6	6	7	6	6
Average number of pollen grains per 4 μ l sample					5.66		
Average number of pollen grains per disk floret					7075.00		
<i>C. atrosanguineus</i> 1997 6334 (Plant 10)	1	A	5	6	5	6	7
		B	6	5	5	3	6
		C	5	4	3	5	5
		D	5	7	6	6	6
		E	6	7	4	6	7
	2	A	8	6	6	5	6
		B	7	5	6	5	4
		C	5	5	3	6	6
		D	5	5	6	7	6
		E	6	6	8	6	5
Average number of pollen grains per 4 μ l					5.58		
Average number of pollen grains per disk					6975.00		
<i>C. atrosanguineus</i> 1997 6334 (Plant 9 and Plant 10 combined)	Average number of pollen grains per 4 μ l					5.62	
	Average number of pollen grains per disk					7025.00	
<i>C. atrosanguineus</i> (all accessions combined i.e. plants 2, 4, 5, 6, 9 & 10)	Average number of pollen grains per 4 μ l					5.68	
	Average number of pollen grains per disk					7100.00	
<i>C. bipinnatus</i> 1996 582 (Plant 3)	1	A	7	6	5	6	6
		B	5	7	8	8	7
		C	5	4	3	5	6
		D	7	8	7	8	5
		E	10	7	6	9	9
	2	A	7	5	6	5	7
		B	9	7	8	7	8
		C	8	6	6	7	8
D		4	6	5	6	5	
E		8	7	9	7	8	
Average number of pollen grains per 4 μ l sample					6.66		
Average number of pollen grains per disk floret					8325.00		
<i>C. bipinnatus</i> 1996 582 (Plant 8)	1	A	3	4	5	5	3
		B	5	6	7	6	7
		C	7	8	6	6	9
		D	6	5	6	7	7
		E	7	8	9	8	9
	2	A	9	8	8	7	9
		B	4	5	5	5	6
		C	7	8	7	7	8
		D	6	7	5	7	6
		E	6	6	7	7	5
Average number of pollen grains per 4 μ l sample					6.48		
Average number of pollen grains per disk floret					8100.00		
<i>C. bipinnatus</i> 1996 582 (Plant 3 and Plant 8 combined)	Average number of pollen grains per 4 μ l sample					6.57	
	Average number of pollen grains per disk floret					8213.00	

Table 4.10. continued

<i>Cosmos</i> Species & accession	Inflorescence	Disk floret	Number of pollen grains per 4- μ l sample				
			Sample 1	Sample 2	Sample 3	Sample 4	Sample 5
<i>C. sulphureus</i> (Spring) 1996 980 (Plant 6)	1	A	3	5	5	5	6
		B	6	5	6	7	7
		C	7	4	6	7	6
		D	5	3	6	6	7
		E	6	5	6	7	6
	2	A	4	5	5	4	6
		B	5	6	6	6	7
		C	7	6	5	5	4
		D	6	7	5	8	5
		E	7	6	6	7	6
	Average number of pollen grains per 4 μ l sample					5.72	
	Average number of pollen grains per disk floret					7150.00	
<i>C. sulphureus</i> (Spring) 1996 980 (Plant 7)	1	A	8	5	5	6	6
		B	6	7	5	7	6
		C	5	3	5	4	4
		D	7	6	6	8	7
		E	6	7	7	6	6
	2	A	5	7	6	6	7
		B	3	3	5	3	4
		C	8	7	7	6	8
		D	5	5	6	6	6
		E	5	6	6	5	7
	Average number of pollen grains per 4 μ l sample					5.82	
	Average number of pollen grains per disk floret					7275.00	
<i>C. sulphureus</i> (Spring) 1996 980 (Plant 6 and Plant 7 combined)	Average number of pollen grains per 4 μ l sample					5.77	
	Average number of pollen grains per disk floret					7213.00	

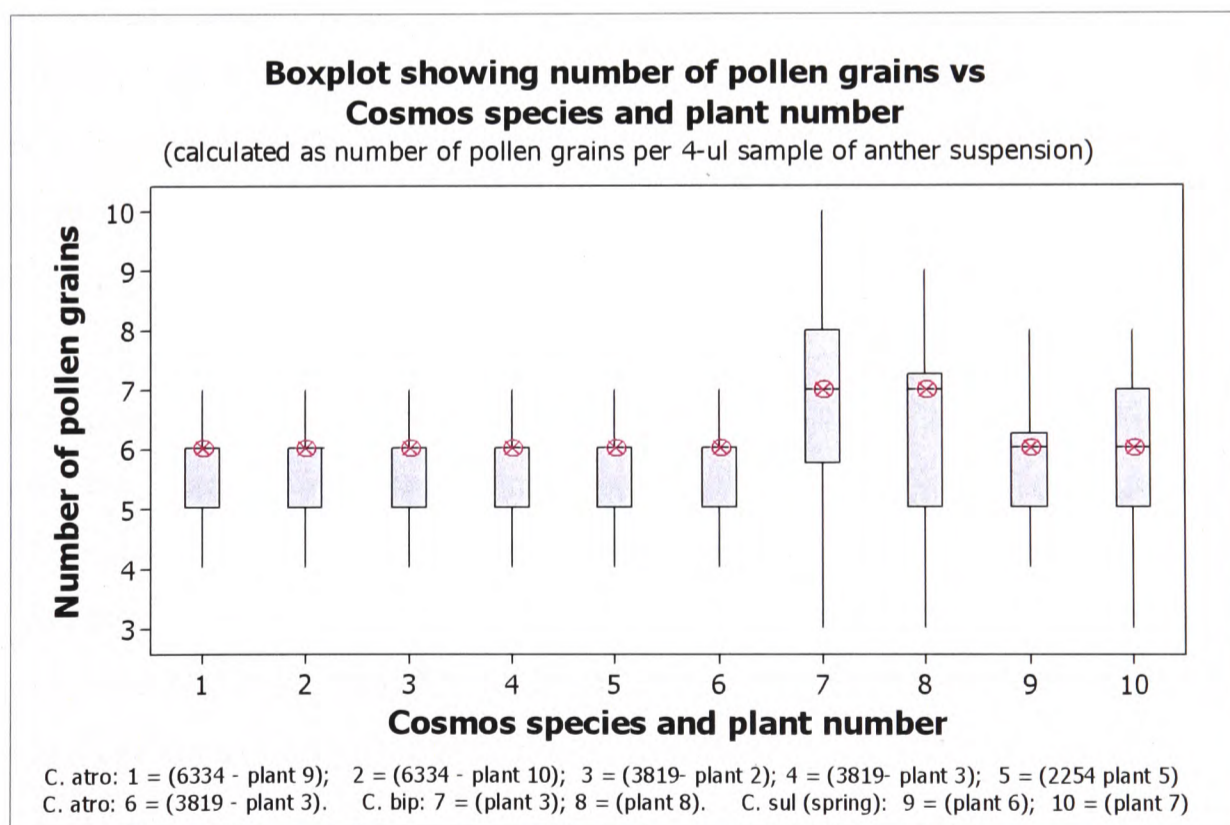


Figure 4.15 – Boxplot comparing number of pollen grains produced in three *Cosmos* species

Pollen grain numbers calculated per 4- μ l sample of anther suspension in *Cosmos* species and *Cosmos* accessions i.e. *C. atrosanguineus* 1977-6334 plants 9 & 10, *C. atrosanguineus* 1999-3819 *C. atrosanguineus* plants 2 and 3, 1999-2254 plants 5 and 6; *C. bipinnatus* 1996 582 plants 2 & 8; and *C. sulphureus* (spring) plants 9 & 10.

Cosmos bipinnatus produces significantly more pollen grains (~8200) per disk floret than *C. atrosanguineus* (~7100) and *C. sulphureus* (~7000), with the two latter species showing no significant difference in the number of pollen grains produced by their disk florets (Appendix 4.2, Box 12-13 & 15, $p = <0.05$ ∴ reject $^{12}H_0$, $^{13}H_0$ & $^{15}H_0$; Box 14, $p = 0.38$ ∴ cannot reject $^{14}H_0$; Figure 4.15). No significant difference was observed in pollen-grain numbers produced by *C. atrosanguineus* accessions 1997 6334 (~7025), 1999 3819 (~7213) and 1999 2254 (~7050) (Appendix 4.2, Box 16, $p = 0.63$ ∴ cannot reject $^{16}H_0$).

4.3.6 – Analysis of pollen viability and pollen-grain number

Plants 2 and 3 of *C. atrosanguineus* accession 1999 3819, plants 5 and 6 of *C. atrosanguineus* accession 1999 2254 and plants 9 and 10 *C. atrosanguineus* accession 1997 6334 represent individuals that exhibited the highest and lowest extremes of pollen viability for *C. atrosanguineus* populations. The three *C. atrosanguineus* accessions were chosen primarily to assess the number of pollen grains produced by disk florets, and secondly, to ascertain whether there is an association between pollen viability and pollen grain number. For the same reasons, plants 3 and 8 of *C. bipinnatus* 1996 582, and plants 6 and 7 of *C. sulphureus* (Spring) 1996 980 were selected for assessment of pollen-grain number. No difference was observed in the pollen grain numbers produced by individuals that exhibited the highest and lowest extremes of pollen viability for each *Cosmos* accession ((Appendix 4.2, Box 17-21, $p = >0.05$ ∴ cannot reject $^{17}H_0$ to $^{21}H_0$) and there was no significant association between pollen viability and pollen number in these the three *Cosmos* species (Box 22, $r_s = -0.02$, $p = 0.77$ ∴ cannot reject $^{22}H_0$.)

Cosmos species have predominantly spherical pollen (mean polar/equatorial (P/E) ratio = 1.0) with the occasional appearance in pollen grain samples of slightly prolate pollen (mean P/E ratio = >1.0) (Table 4.10). Since some of the pollen grains measured were weakly prolate, a single diameter could not be used to represent pollen size. Instead, pollen volumes for each species were used to compare sizes of pollen grains. The volume of *Cosmos* pollen was calculated using the standard formulae.

For spherical pollen:

$$V = \frac{4}{3}\pi r^3$$

For prolate pollen:

$$V = \frac{4}{3}\pi abc$$

Where, a is the length of the *semimajor* (polar) axis, b is the length of the *semiminor* (equatorial) axis, and c is the length of the *semimean* axis, which in this case is the same as the length of the *semiminor* (equatorial) axis

4.3.7 – Pollen-grain size in three *Cosmos* species

Table 4.11 Size of mature pollen grains in three *Cosmos* species.

Dimensions of <i>Cosmos</i> pollen grains (μm)												
No.	<i>C. atrosanguineus</i>				<i>C. bipinnatus</i>				<i>C. sulphureus</i>			
	P (μm)	E (μ)	Vol. (μm^3)	P/E ratio	P (μm)	E (μm)	Vol. (μm^3)	P/E ratio	P (μ)	E (μ)	Vol. (μm^3)	P/E ratio
1	27.2	27.2	10539.76	1.00	18.2	18.2	3157.46	1.00	24.0	24.0	7240.32	1.00
2	24.3	24.3	7515.24	1.00	21.0	21.0	4850.45	1.00	24.2	24.2	7422.84	1.00
3	23.7	23.7	6972.19	1.00	22.1	22.1	5653.28	1.00	22.2	22.2	5730.37	1.00
4	24.2	24.2	7422.84	1.00	22.6	22.6	6045.74	1.00	21.6	21.6	5278.19	1.00
5	24.2	24.2	7422.84	1.00	22.6	22.6	6045.74	1.00	23.5	23.5	6797.16	1.00
6	24.8	24.8	7988.75	1.00	22.9	22.9	6289.71	1.00	23.0	23.0	6372.47	1.00
7	21.9	21.9	5501.19	1.00	21.8	21.8	5426.17	1.00	21.7	21.7	5351.84	1.00
8	23.6	23.6	6884.30	1.00	21.4	21.4	5132.93	1.00	30.6	23.5	8851.79	1.30
9	24.7	24.7	7892.51	1.00	21.8	21.8	5426.17	1.00	27.9	23.5	8070.74	1.19
10	24.9	24.9	8085.78	1.00	22.4	22.4	5886.65	1.00	23.1	23.1	6455.95	1.00
11	27.0	27.0	10308.97	1.00	22.4	22.4	5886.65	1.00	22.3	22.3	5808.16	1.00
12	26.4	26.4	9636.87	1.00	33.6	24.4	10478.33	1.38	23.7	23.7	6972.19	1.00
13	26.5	26.5	9746.79	1.00	21.3	21.3	5061.31	1.00	23.9	23.9	7150.19	1.00
14	26.0	26.0	9205.43	1.00	22.5	22.5	5965.84	1.00	24.2	24.2	7422.84	1.00
15	27.1	27.1	10423.94	1.00	22.0	22.0	5576.89	1.00	23.0	23.0	6372.47	1.00
16	26.5	26.5	9746.79	1.00	22.0	22.0	5576.89	1.00	18.7	18.7	3424.91	1.00
17	23.9	23.9	7150.19	1.00	23.3	23.3	6625.09	1.00	18.9	18.9	3535.98	1.00
18	27.2	27.2	10539.76	1.00	21.1	21.1	4920.07	1.00	19.7	19.7	4004.26	1.00
19	27.4	27.4	10773.97	1.00	19.5	19.5	3883.54	1.00	18.7	18.7	3424.91	1.00
20	27.4	27.4	10773.97	1.00	19.4	19.4	3824.10	1.00	18.8	18.8	3480.15	1.00
21	26.4	26.4	9636.87	1.00	20.0	20.0	4190.00	1.00	19.4	19.4	3824.10	1.00
22	26.9	26.9	10194.85	1.00	22.7	22.7	6126.35	1.00	19.2	19.2	3707.04	1.00
23	25.4	25.4	8582.72	1.00	21.4	21.4	5132.93	1.00	18.4	18.4	3262.70	1.00
24	25.1	25.1	8282.19	1.00	27.1	22.6	7250.36	1.20	30.1	22.0	7631.07	1.37
25	25.1	25.1	8282.19	1.00	22.8	22.8	6207.67	1.00	22.4	22.4	5886.65	1.35
26	23.3	23.3	6625.09	1.00	21.5	21.5	5205.22	1.00	23.6	23.6	6884.30	1.00
27	25.1	25.1	8282.19	1.00	29.0	21.3	6891.77	1.36	20.4	20.4	4446.46	1.00
28	25.1	25.1	8282.19	1.00	29.0	21.5	7021.80	1.35	20.9	20.9	4781.49	1.00
29	25.1	25.1	8282.19	1.00	20.7	20.7	4645.53	1.00	28.3	20.4	6169.08	1.39
30	27.9	27.9	11374.61	1.00	21.6	21.6	5278.19	1.00	21.3	21.3	5061.31	1.00
31	28.5	28.5	12124.35	1.00	21.3	21.3	5061.31	1.00	20.3	20.3	4381.39	1.00
32	27.4	25.4	9259.58	1.07	24.3	24.3	7515.24	1.00	22.6	22.6	6045.74	1.00
33	27.2	25.2	9047.81	1.07	24.6	24.6	7797.03	1.00	20.8	20.8	4713.18	1.00
34	25.9	25.9	9099.62	1.00	24.0	24.0	7240.32	1.00	21.6	21.6	5278.19	1.00
35	26.3	26.3	9527.77	1.00	23.8	23.8	7060.82	1.00	20.2	20.2	4316.96	1.00
36	26.9	26.9	10194.85	1.00	22.2	22.2	5730.37	1.00	21.5	21.5	5205.22	1.00
37	27.0	27.0	10308.97	1.00	23.3	23.3	6625.09	1.00	21.5	21.5	5205.22	1.00
38	24.5	24.5	7702.33	1.00	23.4	23.4	6710.76	1.00	28.4	21.5	6876.52	1.32
39	25.3	25.3	8481.75	1.00	23.4	23.4	6710.76	1.00	31.9	23.9	9544.65	1.33
40	25.6	25.6	8787.07	1.00	30.4	22.5	8061.43	1.35	23.3	23.3	6625.09	1.00
41	25.8	25.8	8994.63	1.00	21.7	21.7	5351.84	1.00	30.0	23.0	8312.86	1.30
42	25.5	25.5	8684.50	1.00	22.3	22.3	5808.16	1.00	20.2	20.2	4316.96	1.00
43	27.7	27.7	11131.75	1.00	23.0	23.0	6372.47	1.00	33.8	25.3	11332.64	1.33
44	27.6	27.6	11011.62	1.00	22.8	22.8	6207.67	1.00	21.3	21.3	5061.31	1.00
45	27.5	27.5	10892.36	1.00	22.7	22.7	6126.35	1.00	20.7	20.7	4645.53	1.00
46	24.8	24.8	7988.75	1.00	20.4	20.4	4446.46	1.00	18.4	18.4	3262.70	1.00
47	24.9	24.9	8085.78	1.00	21.6	21.6	5278.19	1.00	19.2	19.2	3707.04	1.00
48	25.6	25.6	8787.07	1.00	22.8	22.8	6207.67	1.00	19.4	19.4	3824.10	1.00
49	25.1	25.1	8282.19	1.00	20.5	20.5	4512.17	1.00	20.0	20.0	4190.00	1.00
50	25.3	25.3	8481.75	1.00	20.7	20.7	4645.53	1.00	18.7	18.7	3424.91	1.00
Mean	25.7	25.6	8984.63	1.00	22.7	22.0	5862.65	1.03	22.6	21.4	5621.84	1.06
SDev	1.40	1.37	1400.00	0.01	2.77	1.31	1200.00	0.10	3.79	1.89	1800.00	0.13

Key: P, polar diameter, E, Equatorial diameter; Vol., Volume of pollen grain.

Cosmos atrosanguineus has significantly larger pollen ($\sim 9000 \mu\text{m}^3$) than *C. bipinnatus* ($\sim 5900 \mu\text{m}^3$) and *C. sulphureus* ($\sim 5600 \mu\text{m}^3$) with the latter two species showing no significant difference in the size (volume) of their pollen grains (Table 4.11; Appendix 4.2, Boxes 23–25, $p = <0.05 \therefore$ reject $^{23}H_0$ to $^{25}H_0$; Box 26, $p = 0.24 \therefore$ cannot reject $^{26}H_0$; Figure 4.16).

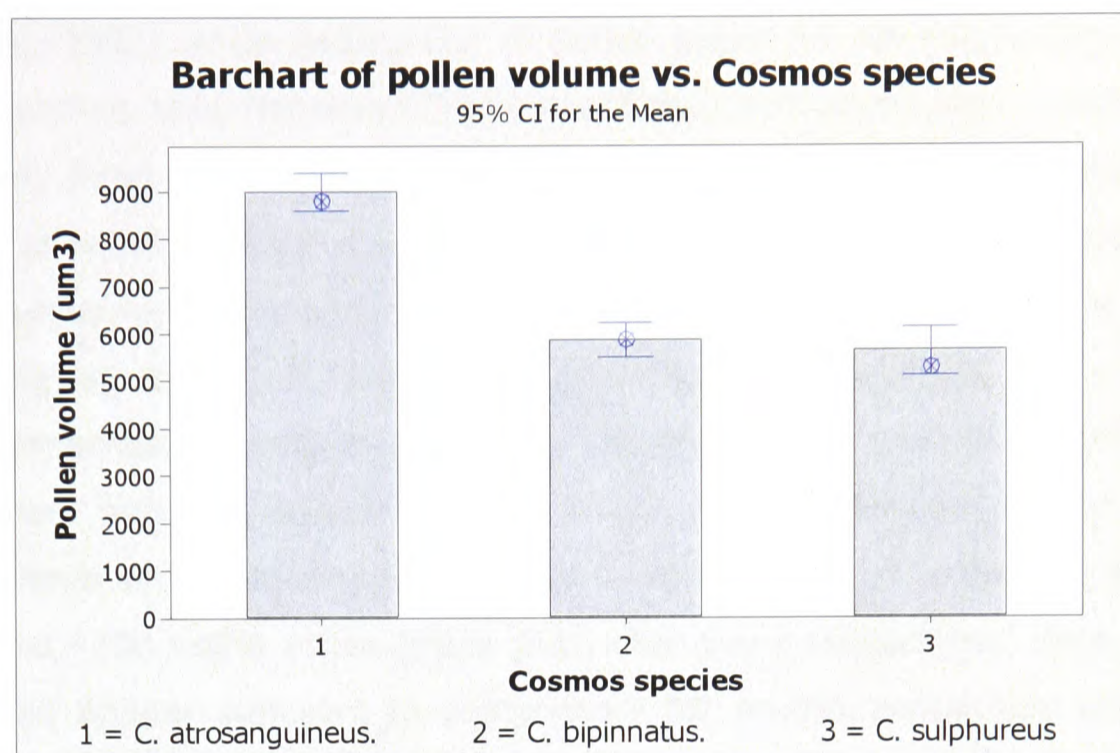


Figure 4.16 – Barchart of pollen volume in *C. atrosanguineus*, *C. bipinnatus* and *C. sulphureus*.

4.3.8 - Summary

Cosmos atrosanguineus and *C. bipinnatus* accessions used in this study exhibited an average pollen viability of $\sim 30\%$ and $\sim 42\%$ respectively and a range in pollen viability of ~ 18 to 46% (*C. atrosanguineus*) and ~ 23 to 53% (*C. bipinnatus*). Although relatively low, these pollen viability scores are compensated by the abundance of pollen produced per disk floret, averaging ~ 7000 and ~ 8000 grains respectively for *C. atrosanguineus* and *C. bipinnatus*, and by the fact that one successful pollination only is required to fertilise the single ovule of each disk floret. From an ecological perspective, a measure of the number of viable pollen grains per viable ovule would be a more meaningful indicator of pollen production than the number of viable pollen grains per disk floret (Stanley and Linskens, 1974). Pollen viabilities of 93% for *C. bipinnatus* and 92 - 97% for *C. sulphureus* have previously been reported using acetocarmine-staining techniques (Mathew and Mathew, 1988; Husaini and Iwo, 1990). The viability for *C. bipinnatus* accessions used in this study is considerably lower than these reports. However, due to technical faults with humidity chambers, it was not possible for *C. atrosanguineus* and *C. bipinnatus* plants to be exposed to high humidity conditions before assessment of their pollen viability. As a result these data

may include false negative results related to pollen desiccation. My view is that these viability scores probably reflect a slight under-estimation for the two species, since problems in methodology have caused under-estimation of FDA-determined pollen viability in previous studies (Abdul-Baki, 1992; Thomson *et al.*, 1994; Mayer and Gottsberger, 2000). For example, reduced fluorescence intensity due to prolonged exposure to UV light while scoring has resulted in underestimations of pollen viability (Abdul-Baki, 1992), while desiccation of pollen grains on hot sunny days has been known to produce false negative FDA scores (Mayer and Gottsberger, 2000; Thomson *et al.*, 1994). Even if these low viability percentages are accepted as representing the true state of pollen viability in *C. atrosanguineus* and *C. bipinnatus* accessions, the average number of viable pollen grains produced per disk floret for each species is considerable, at ~2100 and ~3400 viable pollen grains respectively. Using these data and a conservative hypothetical ovule viability of 20 percent, which equates approximately with the lowest *Cosmos* pollen viability recorded in this study, *C. atrosanguineus* and *C. bipinnatus* accessions were capable of producing an average of ~400 and ~700 viable pollen grains per viable ovule respectively. Such a quantity which would appear sufficient to compensate for environmental loss (Stanley and Linskens, 1974). Additional evidence from *Senecio squalidus* (subtribe: Asteroideae; tribe: Senecioneae), suggests that the pollen viability reported for *Cosmos* in this study may not be such an underestimation, since FDA-determined pollen viabilities for *S. squalidus* range from ~16 to 53% with a mean of ~30% (Hiscock, 2000b).

Cosmos sulphureus (1999 980) showed an average pollen viability of ~70% in Spring (April) and ~35% in late Autumn (November). These pollen viability percentages are considerably lower than those previously reported for the species (Husaini and Iwo, 1990; Mathew and Mathew, 1988). The low autumn viability may be the result of environmental factors, as these plants fell prey to Red Spider mite during October 2000 and had to be sprayed before viability readings were taken. In December 2000, after a second infestation of Red Spider mite, *C. sulphureus* plants 1-4 were destroyed and new stock plants (5-8) of the 1996 980 accession were grown under glass with temperature and humidity controls for a further assessment of pollen viability in April 2001. These healthy plants exhibited an improved pollen viability of 70% and produced ~5000 viable pollen grains per disk floret. This increased viability may be a consequence of the higher humidity environment in which these plants were grown.

The pollen-grain volume of *C. atrosanguineus* accessions used in this study was significantly larger than the pollen volume recorded for the two diploid species, having

an average of ~35% and ~38% greater pollen volume than *C. bipinnatus* and *C. sulphureus* respectively. (Appendix 4.2, Box 23-26, $^{18}\text{H}_0$ to $^{21}\text{H}_0$). This observation agrees with the gigas characteristics associated with polyploids, where increased size of stomatal cells and pollen-grains are frequently used to infer ploidy level (Stanley and Linskens, 1974; Otto and Whitton, 2000). In contrast, results of pollen grain numbers produced by the three *Cosmos* species showed that significantly more pollen grains were produced per disk floret by *C. bipinnatus* (~8200), while no significant difference existed in the number of pollen grains produced between the disk florets of *C. atrosanguineus* (~7100) and *C. sulphureus*. (~7200). That *Cosmos bipinnatus* produces more pollen grains than *C. atrosanguineus* follows expectations, and is a consequence of limitations in the packing volume within anthers, so that polyploids with their larger pollen volume tend to pack fewer pollen grains per anther than their diploid relatives (Stanley and Linskens, 1974). However, the similarity in pollen grain number between *C. atrosanguineus* and *C. sulphureus* was not expected. That *C. sulphureus* produced as few pollen grains as *C. atrosanguineus* may be species-specific or a consequence of variable environmental conditions. *Cosmos sulphureus* has smaller flowers (2-4 cm) than *C. bipinnatus* (4-8 cm) and *C. atrosanguineus* (4-6 cm) (McVaugh, 1984; Sherff, 1932; Sherff and Alexander, 1955), and so the lower pollen-grain number may be a consequence of the smaller flower size. However, the size of a flower tends to affect pollen size and not pollen number, as a reduction in the number of pollen grains would have negative consequences for survival, by reducing an individual's chances of successful pollinations (Stanley and Linskens, 1974). Light exposure positively affects pollen number, with more pollen produced in flowers that experience increased light exposure. Stanley and Linskens (1974) demonstrated that pollen formation is directly dependent on light exposure, with greater amounts of pollen produced in flowers that have been exposed to longer periods of light. *C. sulphureus* accessions used in this study appeared to be short-day plants and thus the reduced exposure to light during the growing period of this species may affect the pollen grain number. A problem existed throughout this study in using *C. sulphureus* as a comparative species: whereas *C. atrosanguineus* and *C. bipinnatus* were grown in the open, side by side, under the same environmental conditions, *Cosmos sulphureus* accessions were grown under glass and flowered in late Autumn or early Spring, having experienced very different growing conditions as a consequence. Although the later and earlier flowering times of *C. sulphureus* aided the logistics of the research, differences in environmental factors always had to be considered when comparing data from this species with those from *C. atrosanguineus* and *C. bipinnatus*. It is therefore difficult to draw any meaningful conclusions when comparing

data generated by *C. sulphureus* with those of the other two *Cosmos* species. It would be more informative if *Cosmos* pollen data were collected from diploid and tetraploid examples of the same species grown under the same environmental conditions. In the absence of such material, comparisons are more valid when drawn from species having the same growing/flowering times and the same environmental requirements, as was the case for *C. atrosanguineus* and *C. bipinnatus*.

4.3.9 - Conclusion

The cytology shows *C. atrosanguineus* to be a true polyploid species capable of producing chromosomally-balanced male gametes and viable pollen. Meiosis in the pollen mother cells appears normal, with no discernible cytological incongruencies or aberrations that could contribute to the present inability of *C. atrosanguineus* accessions to set seed. Meiosis in the megaspore mother cells was not investigated, so it is not possible to conclude what contribution the female side makes to this inability. From the results of this study, the inability of *C. atrosanguineus* pollen to germinate on cross-pollinated stigmas would appear to be a consequence of factors other than its pollen cytology or viability

Cosmos atrosanguineus is probably a segmental allopolyploid of recent origin. Its allotetraploid karyotype appears to have been the result of polyploidization between two distinct *Cosmos* genomes, possibly having similar chromosome morphology and size. These conclusions raise questions as to the identity of the progenitor species and the time of the polyploidization event. The latter may be identified through a calculation of coalescent times of duplicated-gene sequences as pioneered by Gaut and Doebley (1997), and as such is outside the scope of this thesis. The former question, regarding possible parental progenitor species, is discussed below

4.3.10 - Possible progenitor species of *Cosmos atrosanguineus*

The size, morphology and/or C-DNA content of *C. bipinnatus*, *C. carvifolius* and *C. sulphureus* karyotypes and the natural distribution of these species exclude them as putative diploid progenitors of *C. atrosanguineus*. *Cosmos bipinnatus* is known to occur in Hidalgo, but populations of *C. carvifolius* or *C. sulphureus* have their distributions further to the west, with neither having distributions that include the regions of Hidalgo or San Luis Potosí (Figures 1.1-1.3). None of these species is known to produce natural polyploids (Table 1.2), with *C. bipinnatus* and *C. carvifolius* tending towards weedy habits (Plates 1 and 2), which is atypical for polyploids (Stebbins, 1950; Sherff and Alexander, 1955; McVaugh, 1984;). The more likely

progenitor species of *C. atrosanguineus* are probably to be found in the tuber-producing, dark-sanguineous ligulate perennial *Cosmos* species of the section *Discopoda*, such as *C. concolor* Sherff, *C. jaliscensis* Sherff, *C. modestus* Sherff, *C. montanus* Sherff, *C. purpureus* D.C. and *C. scabiosoides* H.B.K. (hereafter referred to as atrosanguinate *Cosmos* species), and those non-atrosanguinate *Discopoda* species restricted to the States of San Luis Potosí, and Hidalgo, such as *C. diversifolius* Otto ex Knowles & Westc. and *C. palmerii* var. *odontophyllus* Sherff (Sherff, 1932; Sherff and Alexander, 1955; Melchert, 1968; McVaugh, 1984; Figures 4.19, A). *C. mattfeldii*, a perennial atrosanguinate *Cosmos* of section 3 - Mesinenia, also requires inclusion in the search for progenitors of *C. atrosanguineus*

Cosmos concolor, *C. jaliscensis*, *C. modestus*, *C. montanus*, *C. purpureus*, and *C. scabiosoides* all have inflorescences composed of 8 sterile purplish-black ligulate florets subtended on long peduncles. These six species are differentiated from each other and from *C. atrosanguineus* by minor differences in foliar habit and the colour of disk corollas (Sherff, 1937; McVaugh, 1984). *C. concolor*, which has the rare feature of wholly purple disk corollas characteristic of *C. atrosanguineus*, is the most similar to *C. atrosanguineus*, being distinguished from it only by its smaller compound leaves, 3-5 cm long compared with 7-13 cm of *C. atrosanguineus* (Sherff and Alexander, 1955). *C. montanus* and *C. modestus* also have smaller leaves (4-7 cm and 6-7 cm long respectively) than *C. atrosanguineus* but differ further by having wholly yellow disk corollas (McVaugh, 1984). *C. jaliscensis* closely resembles *C. atrosanguineus* but has a more branching habit and more flower heads per peduncle. Its disk corollas vary from being almost wholly yellow with purple-tipped lobes to almost wholly deep purple (McVaugh, 1984). *C. scabiosoides* is a large, tall (70-130 cm) species that includes several varieties and forms with gigas characteristics. All forms of *C. scabiosoides* are distinguished from *C. atrosanguineus* by having yellow disk corollas with purple-tipped lobes (Sherff, 1932; Sherff and Alexander, 1955; McVaugh, 1984). *Cosmos purpureus* occurs as two varieties in the wild, *C. purpureus* var. *purpureus* and *C. purpureus* var. *bicolor*. *C. purpureus* var. *purpureus* has wholly purple disk corollas characteristic of *C. atrosanguineus* but is much taller, at 1.0 - 2.5 metres, than *C. atrosanguineus* (0.4 - 0.6 m.) and has bipinnified, hairy, slightly wrinkled glandular leaves. *C. purpureus* var. *bicolor* can be distinguished from *C. purpureus* var. *purpureus* by the colour of its disk florets, which have wholly yellow corollas except for the dark purple corolla-teeth (Sherff and Alexander, 1955; McVaugh, 1984). *C. mattfeldii*, is a member of section 3 – Mesinenia, but unlike other members of this section, it has atrosanguinate ligules and wholly purple disk corollas characteristic of *C. atrosanguineus*. *C. mattfeldii*, is

similar in height (0.5 m) to *C. atrosanguineus*, but differs in having simple leaves and producing fewer heads, (2-3) per plant.



Figure 4.17. Distribution in Mexico of *Cosmos scabiosoides*

C. scabiosoides has a wide distribution from the west to east coast of central Mexico (green shading) in the states of N. Nayarit (12), S.E. Jalisco (13), southern Zacatecas (10), S.E. Michoacan (20), Mexico (21), Morelos (22), Puebla (25) Vera Cruz (18), Oaxaca (27) and Chiapas (28) (See Figure 1.1 for key to the names of Mexican states). (Map of Mexico amended from © pickatrail.com).

Cosmos scabiosoides is the atrosanguinate *Cosmos* that has the broadest distribution in Mexico (Figure 4.17), and its flowering time in Mexico, August to November, mirrors exactly that of *C. atrosanguineus* (Table 4.12). *C. scabiosoides* is distributed from the west to east coast of central Mexico in the north of Nayarit (12), south east Jalisco (13), southern Zacatecas (10), south east Michoacan (20), Mexico (21), Morelos (22), Puebla (25) Vera Cruz (18), Oaxaca (27) and Chiapas (28) (Figure 4.17). It is found at altitudes of 2000-2400 metres, on hillsides and grassy openings of oak-grassland and pine-oak forest (McVaugh, 1984). Although it is not known to occur in the Central Plateau states of Hidalgo and San Luis Potosí, its distribution in the state of Mexico and north east Jalisco bring it into close proximity to the two recorded sites of wild *C. atrosanguineus* populations. Populations of *C. scabiosoides* are known to occur in the Sierra Madre Occidental of north-east Jalisco and south-west Zacatecas, in the Transvolcanic mountain belt of north east Michoacan, and in the mountainous regions of Veracruz and Chiapas. However, it is not found in the south or west of Jalisco or Michoacan, or in any part of the states of Guerrero, Oaxaca, or the southern slopes of the Chiapas mountains. It would appear from this distribution pattern that the Transvolcanic Mountain Belt, which dissects Jalisco, and Michoacan, and separates

the southern states of Guerrero and Oaxaca from the northern states of Mexico, has impeded the southward spread of this species. *Cosmos scabiosoides* is not known to occur in humid or sub-humid tropical regions and thus its eastward progression into the wetlands of Tabasco and the Yucatan peninsula is impeded by the warm wet habitats that prevail in these areas.



Figure 4.18 - Distribution in Mexico of *Cosmos jaliscensis*.

C. jaliscensis is endemic to the state of Jalisco (13) in the Sierra de la Campana region, north west of Los Volcanes (green shading) (See Figure 1.1 for key to the names of Mexican states). (Map of Mexico amended from © pickatrail.com)

Cosmos jaliscensis flowers in October (Table 4.12), and is endemic to the state of Jalisco (13) where it is restricted to the Sierra de la Campana region, north-west of Los Volcanes in the Transvolcanic Belt (Villaseñor, 1991; 1994; Figure 4.18). It grows on steep slopes and valleys within open pine-oak forest at altitudes of 1800 metres (Table 4.12). The growing region of *C. jaliscensis* is separated from sites of known *C. atrosanguineus* populations by 350-400 kilometres of mountainous terrain that includes the highest mountain ranges of the Sierra Madre Occidental (Figures 1.5-1.6 and 4.18). *C. jaliscensis* is therefore unlikely to be a progenitor of *C. atrosanguineus* (Figures 4.18), however, its location in Jalisco occurs within the growing region of *C. scabiosoides* and so it is possible that *C. jaliscensis* hybridised with *C. scabiosoides* and/or a putative progenitor of *C. atrosanguineus* and may therefore share part of its genome with *C. atrosanguineus* and/or *C. scabiosoides*

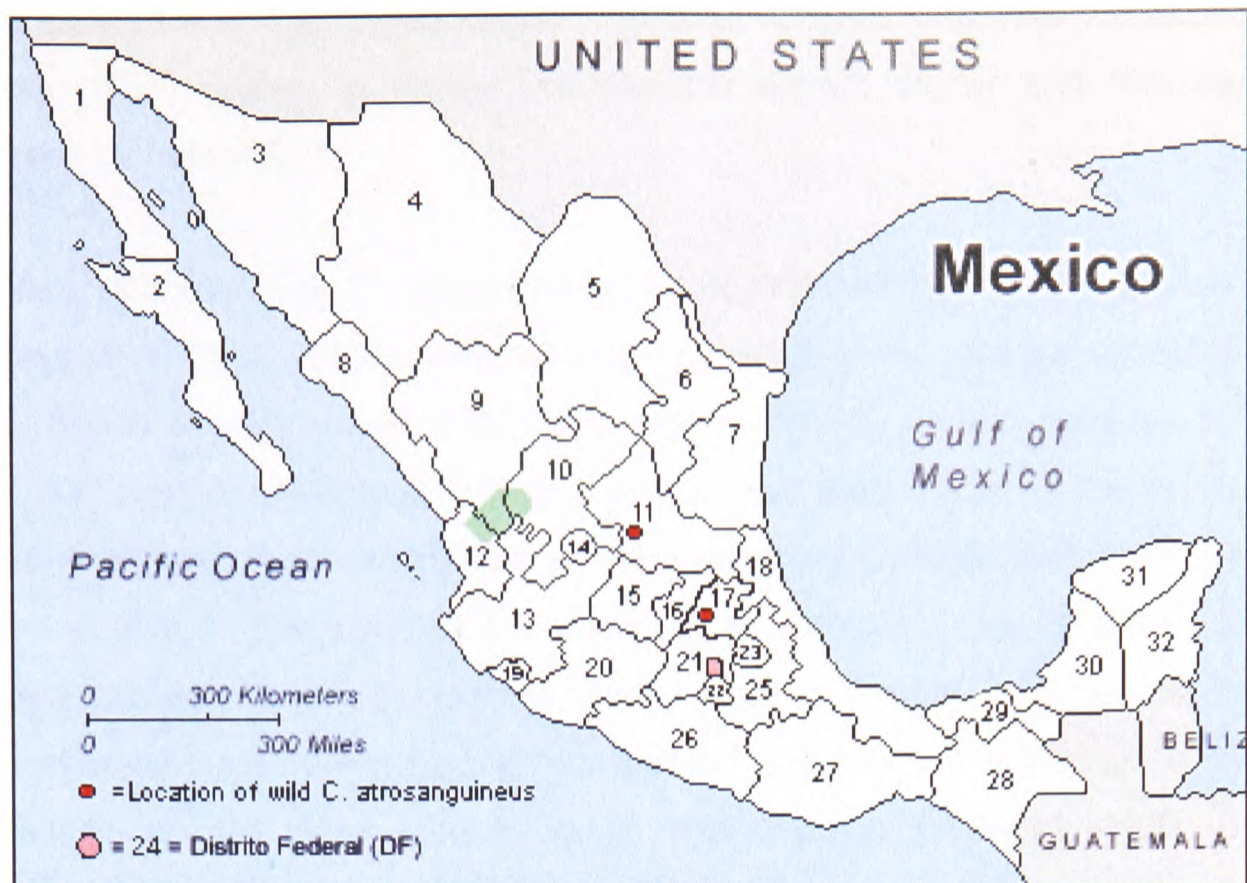


Figure 4.19. Distribution in Mexico of *Cosmos montanus*.



Figure 4.20. Distribution in Mexico of *Cosmos concolor*.

The distribution *C. montanus* and *C. concolor* is restricted to the southern part of Durango (9), south-western Zacatecas (10) and north-eastern Nayarit (12). (See Figure 1.1 for key to the names of Mexican states). (Map of Mexico amended from © pickatrail.com)

Cosmos concolor and *C. montanus* flower from July to September, and August to September respectively (Table 4.12). The herbarium record of *C. concolor* and *C. montanus* is limited to a few wild collections made by Joseph Nelson Rose (1862-1928) between 16th-18th August 1897. The two species are known to occur in the high ridge-and-canyon country in a small region of Mexico where the southern part of Durango (9), south-western Zacatecas (10) and north-eastern Nayarit (12) meet

(Figures 4.19 and 4.20). This region, hereafter referred to as the 'Huasemote-Santa-Teresa (HST) region, is almost inaccessible except by air and has been poorly explored by botanists.

Cosmos concolor and *C. montanus* occur at high altitude in the Sierra Madre at approximately 2000-2500 metres amongst pine-oak forest and oak-grassland (Sherff, 1932; Sherff and Alexander, 1955; McVaugh, 1984). *C. scabiosoides* is also known to grow in this region (McVaugh, 1984). It may be that the isolation of the HST region has provided a haven for the speciation of atrosanguinate *Cosmos* species and may prove to be a source of other cytotypes and species of atrosanguinate *Cosmos*. However, its isolated location and its distance from sites of known wild populations of *C. atrosanguineus* mean that any atrosanguinate *Cosmos* species endemic to HST are unlikely to be the direct progenitors *C. atrosanguineus* (Sherff, 1932; Sherff and Alexander, 1955; McVaugh, 1984). Since *C. scabiosoides* also grows in this area, *C. concolor* and *C. montanus* may be participants, or the progeny of hybridisation events that involved *C. scabiosoides* and/or the putative progenitors of *C. atrosanguineus*.



Figure 4.21 - Distribution in Mexico of *Cosmos purpureus* var. *purpureus*. Distribution in Guerrero (26) Mexico (21), Morelos (22), Tlaxcala (23), Puebla (25) and Veracruz (18) (green shading). (See Figure 1.1 for key to the names of Mexican states). (Map of Mexico amended from © pickatrail.com)

Varieties of *Cosmos purpureus* flower from September to October, and have a distribution from Guerrero (26) north-eastwards to the states of Mexico (21), Morelos (22), Tlaxcala (23), Puebla (25) and Veracruz (18) (Figure 4.21; Table 4.12). The herbarium record shows it was first collected in October 1827 by J.L. Berlandier on the

western slopes of the Cordillera de Guchilaque near Cuernavaca (Morelos) and last collected in 1910 in the state of Veracruz. *C. purpureus* grows at an altitude of 2000-2500 metres on mountain slopes. Its geographical distribution brings it close to the Hildago collection-site of *C. atrosanguineus* and also encompasses the growing region of *C. scabiosoides* and *C. diversifolius* (Sherff, 1932; Sherff and Alexander, 1955).

Cosmos modestus (section-4, Discopoda) and *C. mattfeldii* (section-3, Mesinenia) have a limited herbarium record. *C. modestus* is known to occur in Mexico at an altitude of 2500 metres in the pine-oak forests of the Macizco de Oaxaca (Oaxaca Massive) in the state of Oaxaca (27). Its probable flowering period is September to October (Sherff, 1937; Table 4.12). The distribution of *C. mattfeldii* is known from only one poorly recorded collection "in clay soil" at an altitude of 900 metres, in southern Mexico, on September 21 1898, probably in the state of Michoacan (20) or Guerrero (26) (Sherff, 1934)

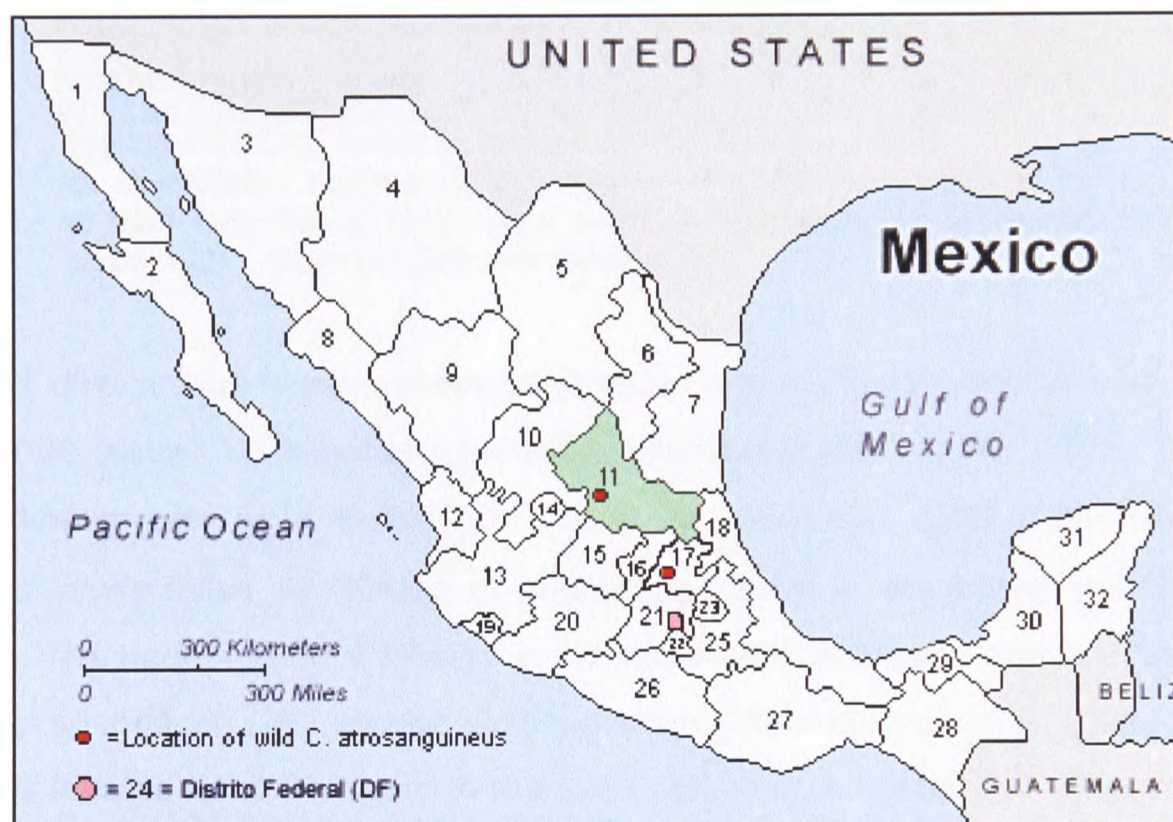


Figure 4.22 Distribution in Mexico of *Cosmos palmerii* var *odontophyllus* is restricted to the state of San Luis Potosí (11)

Of the *Cosmos* species localised to San Luis Potosí (11), only *C. diversifolius* and *C. palmerii* var. *odontophyllus* appear as possible parents. They are perennial species similar in habit to *C. atrosanguineus*, but possess violet to lilac coloured ligulate florets and wholly yellow disk corollas. *C. palmerii* var. *odontophyllus* flowers from September to October at altitudes, 2000-2500 metres, in mountain regions, where it can be found in grasslands or grassy openings of dry pine-oak forest (Table 4.12). The ploidy level of *C. palmerii* var. *odontophyllus* has not been assessed but *C. palmerii* is tetraploid ($2n = 4x = 48$). Although, the geographical distribution of *C. palmerii* var. *odontophyllus* encompasses none of the growing regions of extant atrosanguinate Discopoda

Cosmos species (Figure 4.22), its putative chromosome number and ploidy level ($2n = 4x = 48$), identify it as a possible progenitor species.



Figure 4.23 Distribution in Mexico of *Cosmos diversifolius*
C. diversifolius has two distinct regions of distribution, north, in the state of San Luis Potosí (11) and a south in the states of Michoacan (20), Mexico (21), Guerrero (26) and Oaxaca (27),

Cosmos diversifolius flowers between October and November growing at altitudes of 1900-2000 metres on hillsides covered in pine-oak forest (Sherff, 1932; Table 4.12), and is known only as a diploid ($2n = 2x = 24$) (Melchert, 1968). The distribution of *Cosmos diversifolius* in Mexico is interesting, as it is separated into two distinct regions. The larger region is located in the south west of Mexico and encompasses the states of Michoacan (20), Mexico (21), Guerrero (26) and Oaxaca (27), and the smaller region is located north-eastward in the state of San Luis Potosí (11) (Figure 4.23). The two regions are separated by a 150-200-kilometre strip of land, encompassing the states of Guanajuato (15), Queretaro (16) and Hidalgo (17), where *C. diversifolius* is not known (Figure 4.23). The absence of *C. diversifolius* populations from these intervening states is odd, since there are few major ecological barriers in the high plateau region of Mexico in which these states are located. Its absence from the record could be the result of selective plant collecting, but is more probably a reflection of the rapid rate of habitat destruction that has occurred in these states during the 17th to 20th centuries. It is possible, that prior to the industrialisation and urbanisation of this region, the distribution of *C. diversifolius* encompassed one or all of these intervening states, uniting the San Luis Potosí populations with the populations in the south west. If this were the case, then *C. diversifolius* would be the only Discopoda *Cosmos*

species with a distribution that links known populations of the atrosanguinate *Cosmos* species *C. atrosanguineus*, *C. purpureus* and *C. scabiosoides*.

Table 4.12 - Flowering times in Mexico of thirteen *Cosmos* species

<i>Cosmos species</i>	Jan	Feb	Mar	Apr	May	Jun	Jul	Aug	Sept	Oct	Nov	Dec
<i>C. atrosanguineus</i>								1800 - 2500				
<i>C. concolor</i>								1000 - 2000				
<i>C. jaliscensis</i>										1800		
<i>C. mattfeldii</i>									900			
<i>C. modestus</i>									2500			
<i>C. montanus</i>								2000-2500				
<i>C. purpureus</i>									2000-2500			
<i>C. scabiosoides</i>								2000 - 2400				
<i>C. diversifolius</i>										1900-2000		
<i>C. palmerii</i> var. <i>odontophyllus</i>									2000-2500			
<i>C. bipinnatus</i>									2000 - 2500			
<i>C. carvifolius</i>										1000 - 2000		
<i>C. sulphureus</i>								450 - 1000				

Key: orange bars, atrosanguinate *Cosmos* species of the section Discopoda; lilac bars, non-atrosanguinate *Cosmos* species of the section Discopoda; blue bar, non-Discopoda, atrosanguinate *Cosmos* species; green bars, non-Discopoda, non-atrosanguinate *Cosmos* species. Numbers inside bars signify the altitude at which *Cosmos* species occur in Mexico.

The six atrosanguinate *Cosmos* perennials of the Discopoda section, *C. concolor*, *C. jaliscensis*, *C. modestus*, *C. montanus*, *C. purpureus* and *C. scabiosoides*, flower contemporaneously with *C. atrosanguineus* and are endemic to sub-humid temperate pine-oak mountain habitats at altitudes between 1800-2500 metres (Table 4.12). The Mexican sub-humid-temperate mountain ecological zones support a particularly diverse and abundant flora that includes herbaceous plants, shrubs and trees, and many endemics (Table 1.7). Examples of this mountain diversity are evident in *Pinus* ~48 species (Pinaceae), *Quercus* ~135 species (Fagaceae), *Sedum* ~60 species (Crassulaceae), *Eryngium* ~50 species (Apiaceae or Umbelliferae), *Salvia* ~300 species (Lamiaceae), *Castilleja* ~50 species (Scrophulariaceae), *Eupatorium* ~220 species (Asteraceae), *Senecio* ~180 species (Asteraceae), *Stevia* ~70 species (Asteraceae) and *Muhlenbergia* ~100 species (Poaceae) that thrive in sub-humid temperate ecological zones (Ramamoorthy 1984; Nixon, 1993, Ramamoorthy and Elliott 1993; Styles, 1993). Mountain temperate regions are also important centres for

the evolution of native Mexican weeds, and species of Asteraceae such as *Bidens* and *Cosmos* are actively evolving endemic weedy ectotypes in these eco-regions (Plates 1.1 and 1.2). Variations in precipitation and topography give rise to a variety of pine-oak mountain environments and produce complex microhabitats capable of supporting high levels of endemism (Table 1.7). In the high plateau regions (3000-4000 m) of more moist sub-humid temperate forest (800-1200 mm aap), large pine species such as *P. hartwegii* and *P. culminicola* predominate at the timberline and represent an ecological transition zone between the pine-oak forests of the lower altitudes (1500-2500 m), and the high-altitude grasslands (zacatonales) above the treeline (+4000 m) (Styles, 1993). In drier sub-humid temperate habitats (700-800 mm aap – average annual precipitation), lower temperate vegetation (1500-2500 m) forms a mixture of pine-oak forest and tropical thorn forests and the ecological transition between these lower mixed forests and the higher arid zacatonales is occupied by oak-grassland, not pine (Rzedowski 1978). The herbarium records of the six atrosanguinate *Cosmos* species identify their habitats as pine-oak forest or oak-grassland (Sherff, 1932; Sherff and Alexander, 1955; McVaugh, 1984), suggesting that these species prefer sub-humid temperate habitats towards the drier end of the precipitation range at 800-1000 mm aap, which are known to promote endemism and speciation.

Of the six atrosanguinate *Cosmos* species in the section *Discopoda*, *C. scabiosoides* ($2n = 4x = 48$), *C. jaliscensis* and *C. concolor* (both $2n = 6x = 72$), are known to form polyploids (Melchert, 1968; Table 1.2). *Cosmos scabiosoides* is the most-widely distributed species of the group and is the only atrosanguinate *Cosmos* occurring close to known localities of *C. atrosanguineus* in San Luis Potosí and Zimapan in the Central Plateau region of Mexico. Its distribution also includes known locations of *C. concolor*, and *C. montanus* on the eastern slopes of the Sierra Madre Occidental, *C. jaliscensis* and *C. modestus* in the Transvolcanic belt, and *C. purpureus* in the Central Plateau (Figure 4.24). Diploid and tetraploid populations of *Cosmos scabiosoides* occur together, proving that the genome of this species is capable of polyploidization and successful competition in the natural environment (Melchert, 1968; Table 1.2). Although, more detail regarding the type of polyploidy and chromosome morphology needs to be ascertained, the possibility exists that either diploid *C. scabiosoides* ($2n = 2x = 24$) or its tetraploid form ($2n = 4x = 48$) could have served as a progenitor species of allotetraploid *C. atrosanguineus* ($2n = 4x = 48$). If diploid *C. scabiosoides* were one of the putative parents, then the other progenitor species should also be diploid with a somatic number of 24 chromosomes. *C. montanus* ($2n = 2x = 24$) and *C. purpureus* ($2n = 2x = 24$) are the only other diploid atrosanguinate *Cosmos* species with this

chromosome number. Both species are known to grow at high altitudes, within the distribution range of *C. scabiosoides*, and each conceivably could have been a partner in a hypothetical hybridisation-polyploidization event with diploid *C. scabiosoides*. It is possible also for tetraploid *C. scabiosoides* to have been a progenitor of *C. atrosanguineus* through hybridization with the non-reduced gametes from either *C. montanus*, or *C. purpureus*. Pollination experiments and the karyotyping of these species would verify this prediction, and thus the cytology and reproductive biology of diploid and tetraploid *C. scabiosoides*, *C. montanus* and *C. purpureus* should be investigated as possible progenitors of *C. atrosanguineus*. In contrast, the hexaploids *Cosmos jaliscensis* and *C. concolor* ($2n = 6x = 72$) seem unlikely candidates as progenitor species, due to their high ploidy levels and limited geographical distribution in Jalisco and the southern extremes of Durango/Zacatecas respectively (Sherff, 1932; Sherff and Alexander, 1955; Melchert, 1968; McVaugh, 1984). Nevertheless, it is conceivable that a *C. atrosanguineus* allotetraploid arose by the union of euploid $3x$ gametes of a hexaploid species, and those of a closely-related diploid species producing an allotetraploid with an $A^1A^1A^1A^2$ genome. The *Cosmos atrosanguineus* karyotype described in this study, with its pairings of 6 and 8 putative homoeologues does not preclude this possibility. However, for this to have occurred, a very close genetic and spatial relationship must have existed between the participant hexaploid and diploid genomes. Hexaploid populations of *C. concolor* ($2n = 6x = 72$) and diploid populations of *C. montanus* ($2n = 2x = 24$) grow in the same isolated HST region and may represent the parent genotypes in this hypothetical hybridization event. However, the isolated habitat in which this hybridization would have occurred makes it difficult to explain how the resultant allotetraploid managed the 300-600-kilometre migration from the mountains of the HST ridge-canyon region to the states of Hidalgo and San Luis Potosí in the central Mexican plateau. Furthermore, if *C. concolor* and *C. montanus* were the progenitor species of *C. atrosanguineus*, populations of the latter might be expected to have been present in this eco-region when J.N. Rose made his 1897 collection of *C. concolor* and *C. montanus*, since the two wild collections of *C. atrosanguineus* in Hidalgo (1860) and San Luis Potosí (1878) had been made prior to this date. Alternatively, *Cosmos scabiosoides*, with its diploid and tetraploid forms and its distribution throughout the growing regions of *C. concolor* and *C. jaliscensis*, and close to those of *C. atrosanguineus*, could have served as the diploid progenitor in a hypothetical hybridization with the hexaploid *C. jaliscensis* or *C. concolor*. Morphologically, *C. jaliscensis* shows greater similarity to diploid and tetraploid *C. scabiosoides* than it does to its fellow hexaploid *C. concolor*, suggesting a close relationship between *C. jaliscensis* and *C. scabiosoides* that may have permitted

hybridization between the species (Melchert, 1968). Pollination experiments and an examination of the *C. jaliscensis* and *C. concolor* karyotypes should confirm the relative relationship of these two species to each other and to *C. scabiosoides* and/or *C. atrosanguineus*.

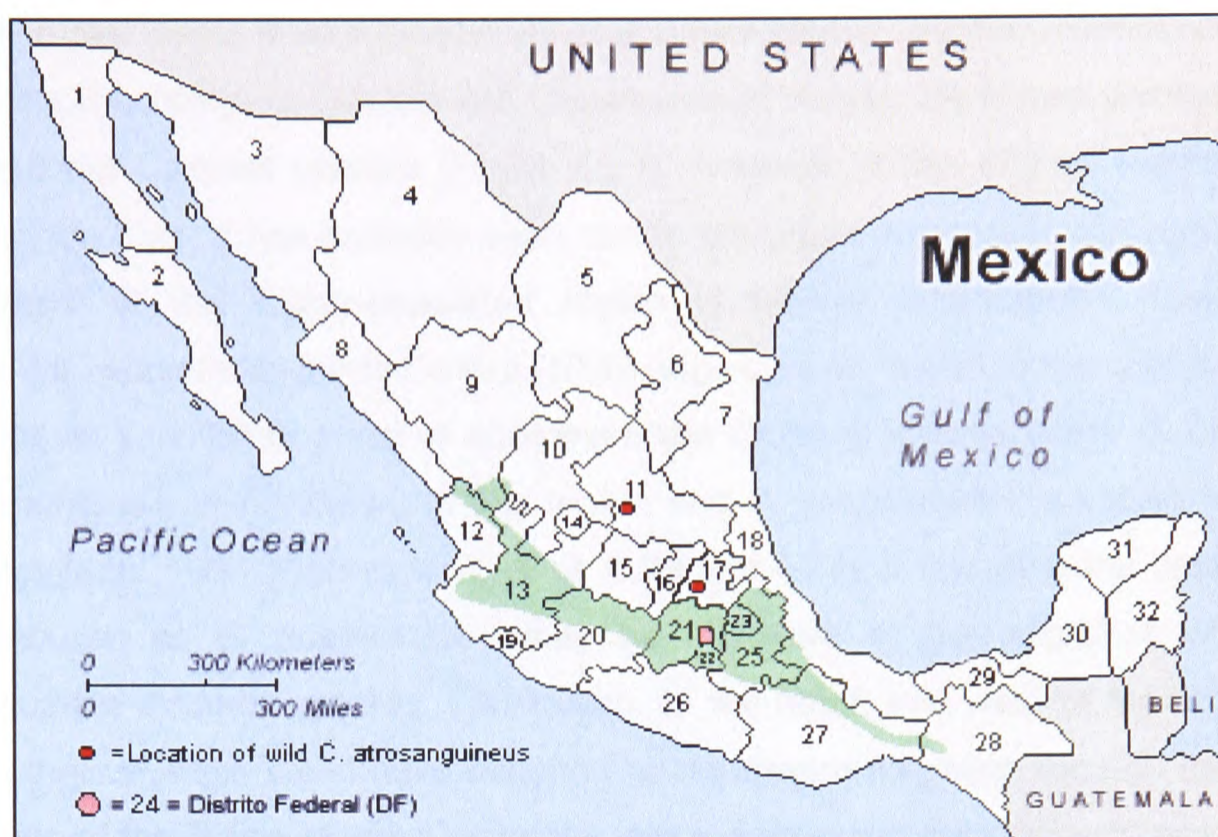


Figure 4.24 – Map showing the known Mexican distribution of the atrosanguinate-type *Cosmos* species; *Cosmos atrosanguineus*; *C. scabiosoides*; *C. concolor*, *C. mattfeldii*, *C. modestus*, *C. montanus* and *C. purpureus* (See Figure 1.1 for key to the names of Mexican states. Map of Mexico amended from © pickatrail.com).

4.3.11 - Possible centre of origin of atrosanguinate *Cosmos* species

Atrosanguinate *Cosmos* species are endemic to pine-oak-forest mountain regions that form a patchwork of habitat islands along ridges, valleys and mountain slopes at altitudes of 1500 to 3300 metres. The unique climatic and topological factors that prevail within these pine-oak-forest islands have encouraged the evolution of specific ecotypes and species. Except for *C. scabiosoides*, populations of atrosanguinate *Cosmos* species occur in restricted localities, and so it is difficult to determine the possible centre of origin for these species, and with the high level of pine-oak deforestation that has occurred in Mexico during the past 100 years, it is possible that this environment no longer exists. However, the TVB (Transvolcanic Belt) possesses the ecological factors appropriate for the emergence and spread of endemic species, as it forms an important ecological corridor connecting the Sierra Madre Occidental and Sierra Madre Oriental (Rzedowski, 1978). In addition, the diverse altitudes and the high levels of volcanic activity of the TVB have created a unique landscape of microhabitats that are conducive to radiation and speciation of taxa, and are responsible for the high level of biodiversity characteristic of the region (Challenger, 1998). The TVB is a known centre of diversity for the genera *Quercus* and *Pinus*, and

for the family Asteraceae, with 370 species of the Asteraceae endemic to this region (Turner and Nesom 1993). The Sierra de Manantlan, located in the western regions of the TVB, is a particular centre of diversification for the Malvaceae, and Asteraceae (Fryxell, 1988; Turner and Nesom, 1993). Migration north-west and north-east, from the TVB to the Sierra Madre Occidental and Sierra Madre Oriental respectively, and south to the mountains of Oaxaca and Chiapas could explain the known distribution of atrosanguinate *Cosmos* species (Figure 4.24). However, if this original habitat were located in the TVB, it has probably been lost to the urban expansion and agricultural development of this highly-populated region of Mexico. Alternatively, one could propose the Huasemote-Santa-Teresa (HST) ridge-canyon region in the Sierra Madre Occidental as a centre of origin of atrosanguinate *Cosmos* species, since *C. concolor* and *C. montanus*, are endemic to this region and *C. scabiosoides* is known to grow there (McVaugh, 1984; Figures 4.17; 4.19, 4.20 and 4.24). If this were the case, then the distribution of *C. scabiosoides* may be indicative of the migration of other atrosanguinate *Cosmos* species. Distribution, to the south and west of Mexico, from this hypothetical origin could have occurred by southward migration through the pine-oak forests of the Sierra Madre Occidental, eastwards along the northern face of the TVB, (or the high basins that border the northern slopes of the TVB), and south via the Macizo de Oaxaca and the Sierra Madre Sur to the mountain regions of Chiapas. The reciprocal migration is also possible. If a putative atrosanguinate-type hybrid did migrate via the pine-oak forest eco-region of the HST region, or the TVB, then the specific microhabitats encountered in this migration could have facilitated the adaptive radiation of this hybrid, resulting in the creation of the novel atrosanguinate phenotypes and ploidy levels characterised by *C. atrosanguineus*, *C. concolor*, *C. jaliscensis*, *C. modestus*, *C. montanus*, *C. purpureus*, and *C. scabiosoides*. The present fragmented and narrow distribution of atrosanguinate *Cosmos* species is probably a consequence of the fragmentation of pine-oak forests so that these species exist only in a few isolated mountain regions.

In my opinion, the best hypothesis for the origin of atrosanguinate *Cosmos* species is the Transvolcanic belt (TVB) region. The dry temperate habitats (800-1000 mm aap) that predominate in this region is the habitat most often associated with the growth and success of atrosanguinate *Cosmos*, and is the habitat that promotes speciation in general. Furthermore, the atrosanguinate *Cosmos* species appear to be of recent origin, and the most recent and influential factor that has contributed to speciation and the megadiversity of Mexico has been the uplifting of the TVB, which experienced its most extensive period of elevation during the last 1.6 million years.

CHAPTER 5 – Pollen-stigma interactions in *Cosmos*

5.1 – Introduction

5.1.1 - Pollen–stigma interactions in sporophytic self-incompatible species: the *Brassica* model

The SSI pollen-stigma interaction has been described most completely for the *Brassicaceae*, *Raphanus sativus* and *R. raphanistrum* (Ockendon, 1972; Dickinson and Lewis, 1973a, 1973b; Ockendon and Gates, 1975; Hill and Lord, 1987). In compatible crosses of *Brassica* and *Raphanus*, growth of pollen tubes occurs in approximately 70% of the pollen grains that adhere to the stigma. Compatible grains become attached to the apical and sub-apical regions of stigma papillae, at non-colpal regions, by fusion of the outermost protein-lipidic tryphine layer of the pollen grain, with the outermost proteinaceous pellicle layer of the stigma, forming an adhesive foot that anchors the pollen grain onto the papilla (Elleman *et al.*, 1988; 1992; Elleman and Dickinson, 1994). The adhesive foot forms at the contact point of pollen and stigma, and is created from outpourings of stigma surface material and the tryphine pollen coat. The adhesive foot facilitates the hydration of the pollen grain, serving as a conduit for water absorption from the stigma (Roberts *et al.*, 1984a; Elleman and Dickinson, 1994). Within 30 – 45 minutes a single pollen tube emerges from one of the three colpi. The *Raphanus* pollen-tube wall consists of three layers: a callosic inner layer, lying immediately adjacent to the cytoplasm, which is surrounded by a fibrillar pecto-cellulosic cell-wall layer that is continuous with the intine, and an outer protein-lipidic electron-opaque layer continuous with the tryphine. As the pollen tube develops, the outer layer becomes increasingly fibrillar and, on contact with the papilla surface, fuses with the papillar pellicle. Subsequent growth of compatible tubes is unidirectional and occurs within the pellicle-cuticle layer, so that all tubes on a compatible stigma are orientated downward towards the bases of papillae (Dickinson and Lewis, 1973a, 1973b). During the basipetal growth of compatible pollen tubes, the three pollen tube layers are maintained, with continuous fusion occurring between the outermost fibrillar pollen-tube layer and the stigma pellicle-cuticle (Dickinson and Lewis, 1973a, 1973b). In incompatible *Raphanus* pollinations, the majority of pollen grains fail to form a foot layer and do not adhere to stigmatic surface, so these pollen grains are removed easily from the stigma surface. Approximately 40% of incompatible *Raphanus* pollen grains do germinate a three-layered pollen tube, as occurs in compatible pollen, but in the majority of cases these pollen tubes fail to penetrate the stigmatic pellicle and cease growth 1-2 hours after germination.

5.1.2 - Pollen-stigma Interactions in SSI species: the Asteraceae model

The pollen-stigma interactions of the Brassicaceae described above is the model for the sporophytic self-incompatibility response. Pollen-stigma Interactions observed in species of Asteraceae show differences from the *Brassica* model, and give further insight into the complexity and diversity of SSI. In the Asteraceae species *Parthenium hysterocarpus*, *P. argentatum* (Gerstel and Riner, 1950; Lewis, 1994) and *Senecio squalidus* (Hiscock, 2000a; 2000b), four categories of pollen-stigma interaction, one compatible and three incompatible, have been identified. In compatible interactions, an adhesive foot layer forms between the pollen coat and stigma pellicle, resulting in hydration of the pollen grain. Compatible pollen tubes grow downward along the side of papillar cells within the pellicle-cuticle layer, and do not penetrate the stigma tissue (Roberts *et al*, 1984a and 1984b): penetration of the stigma occurs at the base of the papillar cells where no cuticle is present. Compatible pollen tubes enter the stigmatic tissue via the middle lamella and continue to grow downward between stigma cells towards the conducting tissue (Gerstel and Riner, 1950). A short distance after stigma penetration, after reaching the conducting tissue, compatible pollen tubes make a 90° turn and follow a path parallel to the long axis of the stigma, turning downwards into the style and onwards into the ovary, where fertilization of the ovule takes place (Hiscock, 2000b). The contents of compatible pollen grains are emptied into pollen tubes shortly after tube germination, and as a consequence, compatible pollen grains are devoid of stainable material by the time pollen tubes penetrate the stigma (Lewis, 1994). The, 90°-bend observed after penetration of the stigma is characteristic of compatible pollen tubes, and is never observed in those occasional incompatible pollen tubes that penetrate the stigma (Gerstel and Riner, 1950; Hiscock, 2000b).

Of the three incompatible categories of pollen-stigma interaction observed in Asteraceae, category-1 type incompatibility is the most profound, as pollen development is arrested before germination of the pollen grain, with many grains failing to adhere to the stigma. The majority of Asteraceae incompatible pollen-stigma interactions fall into this category and it may be that many of the category-1 type incompatible pollen grains also include non-viable pollen (Gerstel, 1950; Gerstel and Riner, 1950; Lewis, 1994; Hiscock, 2000b). In the second, smaller category-2 type incompatibility reaction, incompatible pollen grains germinate to produce short stunted pollen tubes that do not normally penetrate the stigma surface. Growth of these incompatible pollen tubes is arrested shortly after germination, at or near the apices of stigma papillae, and is accompanied by characteristic depositions of callose in pollen tubes and in adjacent papillar cells. These incompatible pollen grains retain their

contents and fluoresce brightly when stained with aniline blue (Lewis, 1994). The category-3 type incompatible pollen-stigma interaction occurs less frequently, but is observed regularly in species of Asteraceae. Pollen grains exhibiting this type of incompatibility germinate pollen tubes that follow the same path as compatible pollen tubes up until penetration of the stigma, after which the pollen-tube tips become swollen, fill with callose, and cease growth. The category-3 type incompatibility reaction may be accompanied by deposition of callose in the stigma cells surrounding the aborted pollen tube, but is not always observed (Hiscock 2000b). Lewis (1994) designated pollen exhibiting a category-3 type incompatibility interaction as *P*-type pollen, as it was identified first in *Parthenium hysterocarpus* and *P. argentatum* where it occurred in matched *S*-incompatible combinations as well as in unmatched compatible combinations of *S*-alleles. In *S. squalidus*, *P*-type pollen is associated predominantly with anomalous semi-compatible crosses, revealing an incompatibility similar to the stylar incompatibility reaction in GSI, and is thought to reflect the action of a cryptic *Senecio G*-gene (Hiscock, 2000a). For Lewis (1994), the genetic basis of the *P*-type reaction is substantiated by the observation that *P*-type reaction occur between individuals with *S*-matched and *S*-unmatched alleles, but never in self-pollinations, and that *P*-type pollen segregates clearly from incompatible and compatible pollen on the same stigma, after cross-pollination. These three Asteraceae incompatible reactions, may be viewed as representing variations in the timing of the incompatibility response, with the *P*-type reaction revealing a late sporophytic or gametophytic incompatibility reaction akin to the GSI stylar incompatibility reaction (Pandey, 1958; Lewis, 1994; Hiscock, 2000b). Sarker *et al.* (1988) revealed an incompatible reaction in the cellular tissue of the *Brassica* pistil, after observing *P*-type pollen on self-pollinated *B. oleracea* stigmas treated with a protein inhibitor. Thus in SSI species of Asteraceae and Brassicaceae, it is possible for an incompatibility reaction to occur at the pollen-stigma interface, and within the cellular tissue of the pistil (Lewis, 1994).

Brassica flowers become self-incompatible just before anthesis, when SRK molecules in the stigma reach maximal levels of expression. Before this period, the *Brassica* stigma is unable to distinguish self-pollen from cross pollen (Hiscock and McInnes, 2003). Selfed bud-pollinations are therefore possible, and have been used to produce *S*-homozygous *Brassica* lines, with some 80-100 *Brassica* SI haplotypes characterised to date (Franklin *et al.*, 1995). In *Senecio squalidus*, the morphology of disk and ray florets militates against bud pollination, and 'forced' selfings are achieved instead by treating stigmas with dilute saline solution 2-3 hours prior to pollination, and thus full

diallele crosses have been possible, revealing an estimate of six S-alleles for a single *S. squalidus* (Oxford) population (Hiscock, 2000a, 2000b; Brennan, *et al.* 2002).

A further augmentation to SI is the often observed phenomenon of pseudo self-compatibility (PSC), which produces anomalous crossing results in selfed individuals, such that some selfed plants set a small amount of seed (Larsen, 1983; Dana and Ascher, 1986a, 1986b; Reinartz and Les, 1994; Levin, 1996; Nilesen *et al.*, 2003). In *Senecio squalidus*, PSC individuals produce 3-5 seeds per capitulum on selfing compared to 20-60 seeds produced on outcrossing (Hiscock, 2000a, 2000b; Brennan 2002). Genetic PSC is believed to be under the control of modifier loci that are unlinked to the S-locus (Pandey, 1960; 1967). These modifier loci affect the activity of genes at the S-locus by suppressing the expression of S-alleles and enhancing SC, PSC or S-phenotypes that differ from those predicted by the S-genotype. The concomitant reduction in the SI response of PSC individuals is characterised by the so called 'leaky' SI observed in self-pollinations of class-II *Brassicaceae* and in *Senecio squalidus* (Levin, 1996; Hiscock, 2000a, 2000b). In *S. squalidus*, the stigmas of PSC genotypes lose partial or total ability to discriminate pollen S-specificities, so that as female parents they are compatible with all other individuals. In contrast, the pollen of these PSC individuals retain their S-specific expression, indicating that, in the case of *S. squalidus*, S-modifier loci of PSC phenotypes affect only the female component of SI (Hiscock, 2000b). The presence of S-modifier loci provides variation to the sporophytic incompatibility system that offers a selective advantage should the balance between SI and SC be detrimentally disturbed, as may occur in the case of populations bottlenecks or colonisation events (Levin, 1996; Brennan *et al.*, 2002). In such a scenario, a decrease in the number of S-alleles would increase the instance of SI, such that the fecundity of PSC individuals would outweigh the detrimental effects of homozygosity, increasing their selective advantage and leading to the possible breakdown of SI (Levin, 1996). The documented breakdown of SI in *Aster furcatus* (Asteraceae) and the partial SSI of *Scaligeria affinis* (Asteraceae) are believed to be a consequence of reduced S-alleles caused by a decline in population size and the favouring of PSC phenotypes (Reinartz and Les, 1994; Nielsen *et al.*, 2003). The many accounts of successful colonisation by SI Asteraceae species may be explained by the flexibility of the Asteraceae SSI system, which permits biparental breeding and occasional selfing while favouring heterozygosity and outbreeding (Estes and Thorp, 1975; Reinartz and Les, 1994; Luijten, *et al.*, 1996; Maddox *et al.*, 1996; Young *et al.*, 2000). The survival of small temporarily isolated populations are particularly

advantaged by this type of flexibility, as it allows a degree of inbreeding, without the loss of SSI (Larsen, 1983).

SSI systems are more complex than systems of GSI, with the sporophytic system often being augmented by additional mechanisms such as dominance interaction of S-alleles, cryptic G-genes and S-modifier loci. These augmentations increase the mating potential of individuals with shared S-alleles, by reducing cross-incompatibility and increasing SC phenotypes (Hiscock, 2000a; 2000b; Brennan *et al.*, 2002). In summary, the extra level of complexity of SSI bestows a selective advantage to individuals, particularly when these individuals experience a radical reduction in population size.

In this chapter, fluorescent microscopy (FM) and scanning electron microscopy (SEM) are used to investigate: (i) the *Cosmos* pollen-stigma interaction in stage-1, stage-2 and stage-3 disk florets, (ii) the receptivity of the *Cosmos* stigma in early, mid- and late stage-3 disk florets, (iii) interspecific reciprocal pollinations between stage-3 disk florets of *Cosmos atrosanguineus* and *C. bipinnatus*, and (iv) compatibility relationships in intraspecific pollinations of *C. atrosanguineus*, *C. bipinnatus* and *C. sulphureus* populations with unknown S-allele specificities.

5.2 - Materials and Methods

5.2.1 - *Cosmos* reproductive biology: cross- and self-pollinations

Cosmos plants were grown in pots and maintained in an insect-proof glasshouse at 15-20°C under natural light conditions. Controlled pollinations were carried out in July and August 2001 for *C. bipinnatus* and *C. atrosanguineus*, and in November 2000 for *C. sulphureus*. *Cosmos* plants with capitula consisting of mid to late stage-2 disk florets were labelled, and their capitula enclosed in large polythene bags of pore size 0.2 mm. When ~50% of disk florets had reached the late stage-3 phase of development, intraspecific cross-pollinations, and self-pollinations were carried out by gently dabbing stigmas of late stage-3 disk florets with the tips of early to mid stage-3 disk florets that were presenting copious amounts of pollen. Pollinated capitula were placed inside porous tissue pollination bags (10 cm x 10 cm), secured with a light-weight plastic clip and left for up to 12 hours. Pollinated stigmas were then removed and squashed in a drop of decolourised aniline blue in 50% glycerol (Linskens and Esser, 1957) and observed using a Leitz Diaplan microscope under UV illumination. For each pollination, five disk florets were tested per capitulum and three separate capitula were pollinated per individual plant. To minimise environmental factors, pollinations for a specific cross were carried out over the same time period.

Cross-pollinations were designated as compatible (+) if an average of >20 compatible pollen tubes were produced per stigma, and incompatible if an average of <5 compatible pollen tubes were produced per stigma. Cross-pollinations having an average per stigma of >5 but <20 compatible pollen tubes, and which contained *P*-type pollen (category-3 type pollen) were designated as having inconclusive compatibility and identified as possible semi-compatible (\pm) individuals. Self-pollinations having an average of 0-<2 compatible pollination per stigma were designated as strongly self-incompatible, and those with 2-5 compatible pollinations were designated as having 'leaky' self-incompatibility, and identified as possible PSC individuals. The numbers of compatible (+) and incompatible (-) pollen tubes were recorded for each cross.

5.2.2 - Forced self-pollinations

(i) Saline treatment

Reflexed stigmas of late stage-3 disk florets were dabbed gently with a sable paintbrush soaked in 0.1%, 0.5% and 1.0% NaCl in 0.1% Tween 20 in deionised water. Stigmas were left for 3 hours to dry, and self pollen from early to mid stage-3 disk florets presenting copious amounts of pollen were then applied to stigmas.

(ii) Bud pollinations

While attached to the plant, the stigmas of mid to late stage-1 and -2 disk florets were exposed by making a single incision along a groove of the corolla tube from just above the base to its apex using a Neolus hubbed sterile needle 0.5 x 16 mm (Terumo Europe N.V., Leuven-Belgium). The anther tube was opened similarly by making a single incision along the translucent membrane at a junction between adjacent anthers (Plate 5.1). The appressed lobes of the enclosed stigma were gently prised open using a pair of fine-tipped blunt-ended tweezers. The tips and adaxial surfaces of the exposed stage-1 and -2 stigmas were dabbed gently with self-pollen and cross-pollen from early to mid stage-3 disk florets and left for 4 to 8 hours at 60% humidity. Pollinated stigmas were then removed and squashed in a drop of decolourised aniline blue in 50% glycerol (Linskens and Esser, 1957) and observed using a Leitz Diaplan microscope under UV illumination, or were prepared for CryoSEM and Ambient SEM, and viewed in a Stereoscan 240 SEM (Cambridge Instruments) as described in the Materials and Methods section of Chapter 3.

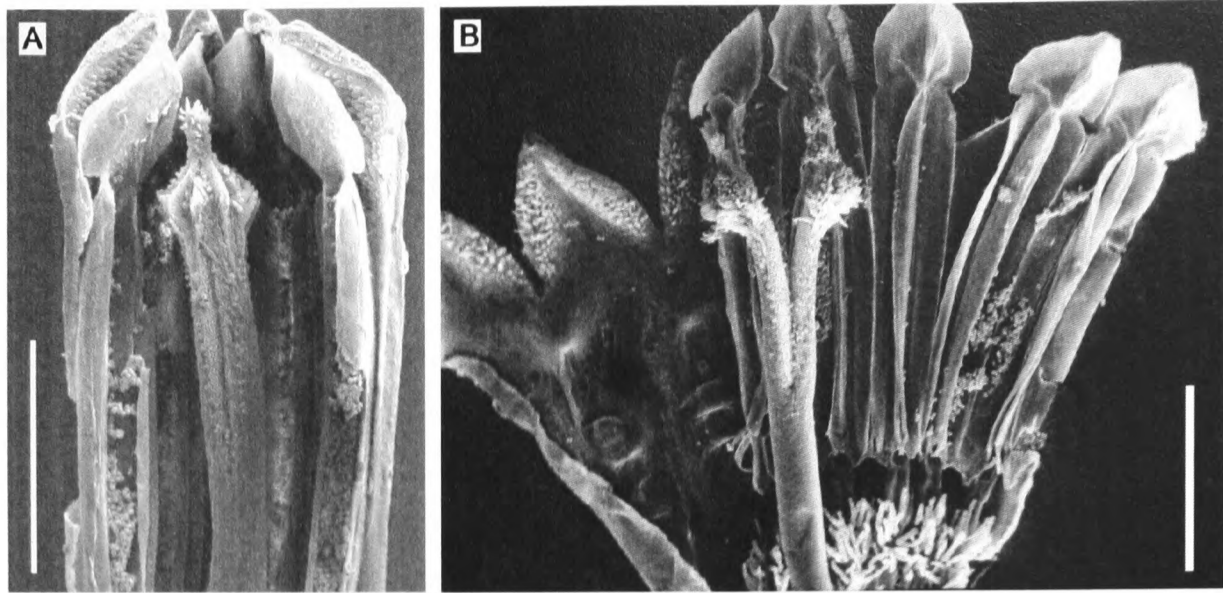


Plate 5.1 - *Cosmos bipinnatus* stage-2 disk florets with corolla and anther tube dissected open to show developing stage-2 stigma

A – Disk floret with corolla and anther tube dissected open to show stigma with lobes appressed together. The pollen sacs in the foreground have had the lower part of their walls removed to reveal anthers that are free of tapetal debris and peritapetal membranes and which contain mature trinucleate pollen. The intact pollen sacs in the background have dehisced and are in the process of depositing their pollen onto the emerging stigma. **B** – Disk floret, at a slightly later stage of development than **A**, showing fully dehiscent anthers. Stigma lobes have been prised open slightly to reveal the short receptive papillae on the adaxial surface of the stigma. Scale bars = 1 mm. Preparation method, Ambient SEM.

5.2.3 - Pollen-stigma Interactions in *Cosmos*

Early, mid and late stage-3 disk florets were pollinated as described above, and left for 30 mins, 1, 2, 4, 8 and 16 hours. Pollinated stigmas were then removed and squashed in a drop of decolourised aniline blue in 50% glycerol (Linskens and Esser, 1957) and observed using a Leitz Diaplan microscope under UV illumination, or were prepared for CryoSEM and Ambient SEM, and observed in a Stereoscan 240 SEM (Cambridge Instruments, as described in Chapter 3 - Materials and Methods).

5.2.4 - Interspecific pollinations between *Cosmos atrosanguineus* and *C. bipinnatus*

Late stage-3 stigmas of *C. atrosanguineus* were pollinated with pollen from early stage-3 disk florets of *C. bipinnatus* as described in section 5.2.1, and left for six hours. The reciprocal cross was also carried out following the same procedure. Pollinated stigmas were then removed and squashed in a drop of decolourised aniline blue in 50% glycerol (Linskens and Esser, 1957) and observed using a Leitz Diaplan microscope under UV illumination.

5.3 - Results

5.3.1 - Forced self-pollinations

(i) Saline treatment

Pre-treatment of all *Cosmos* stigmas with saline solution prior to self-pollination was not successful, as the saline solution caused the *Cosmos* stigma to dehydrate, and to curl up and wither within 20 minutes of application. It may be necessary to use lower

concentrations of saline solution in order to prevent damage to stigmas. However, it may be that the *Cosmos* stigma is not tolerant of salt, and that this method is not appropriate for this genus of Asteraceae.

(ii) Bud pollinations

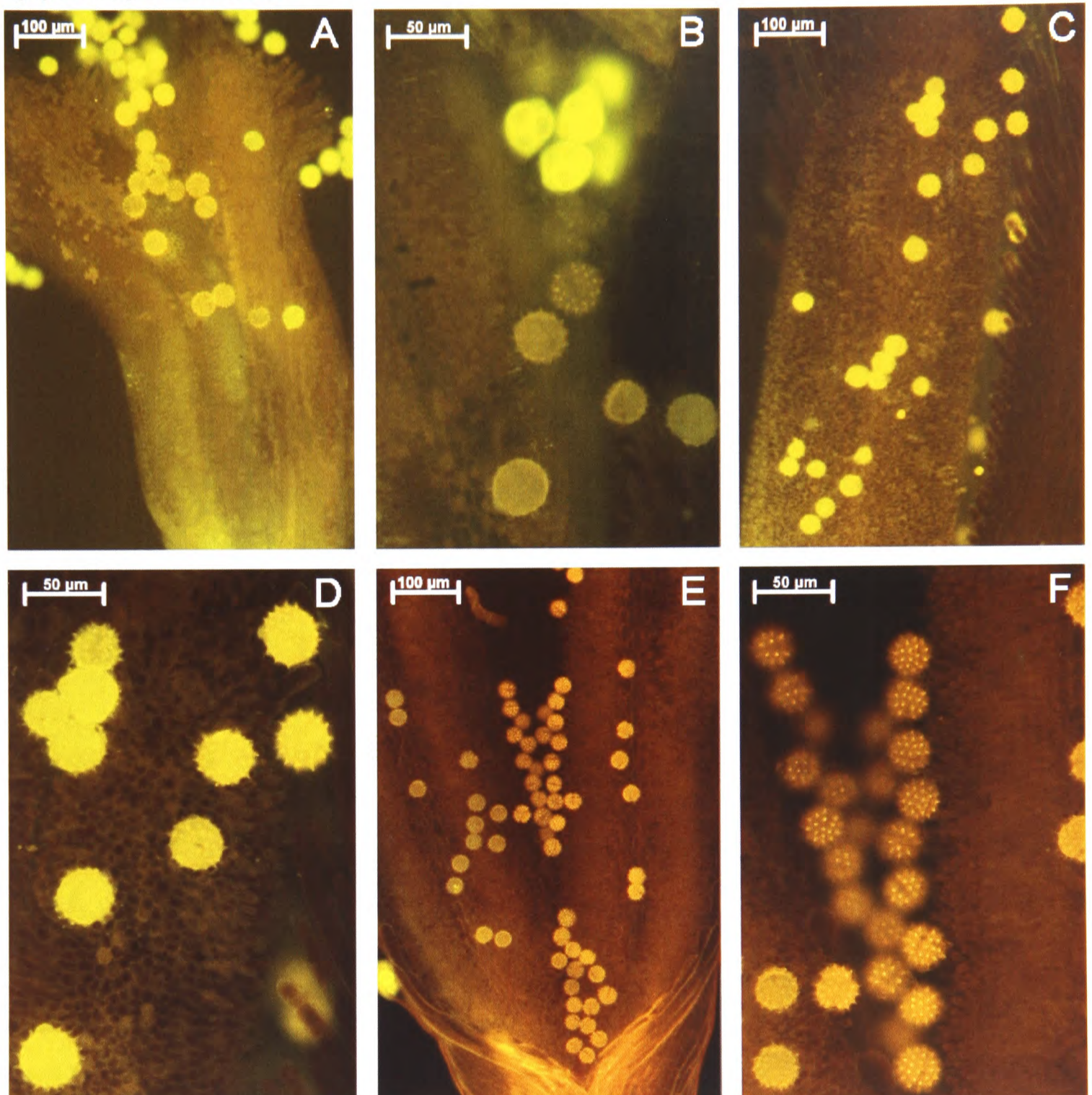


Plate 5.2 - *Cosmos* selfed bud pollinations

A & B – *C. atrosanguineus*, stage-1 stigma x stage-3 pollen. Tetrads from the stage-1 disk floret have escaped from their anthers during the dissecting open of the anther tube, allowing comparison of tetrads with mature self-pollen taken from a stage-3 disk floret of the same inflorescence. **C & D** – *C. atrosanguineus*, stage-2 stigma x stage-3 pollen, showing a category-1 type incompatibility response. **E & F** – *C. bipinnatus*, stage-2 stigma x stage-3 pollen, showing a category-1 type incompatibility response and the tricolpate structure of the mature pollen

Stage-1 and stage-2 *Cosmos* stigmas were not receptive to self-pollen, and a category-1 type incompatibility reaction occurred in selfed buds of all three *Cosmos* species, with no germination of pollen tubes observed in these bud pollinations. The majority of the self-pollen failed to adhere to stage-1 or stage-2 stigmas, or collected in the stigmatic groove, or at the stigma-style junction (Plate 5.2, E-F).

5.3.2 - Stigma receptivity in *Cosmos*

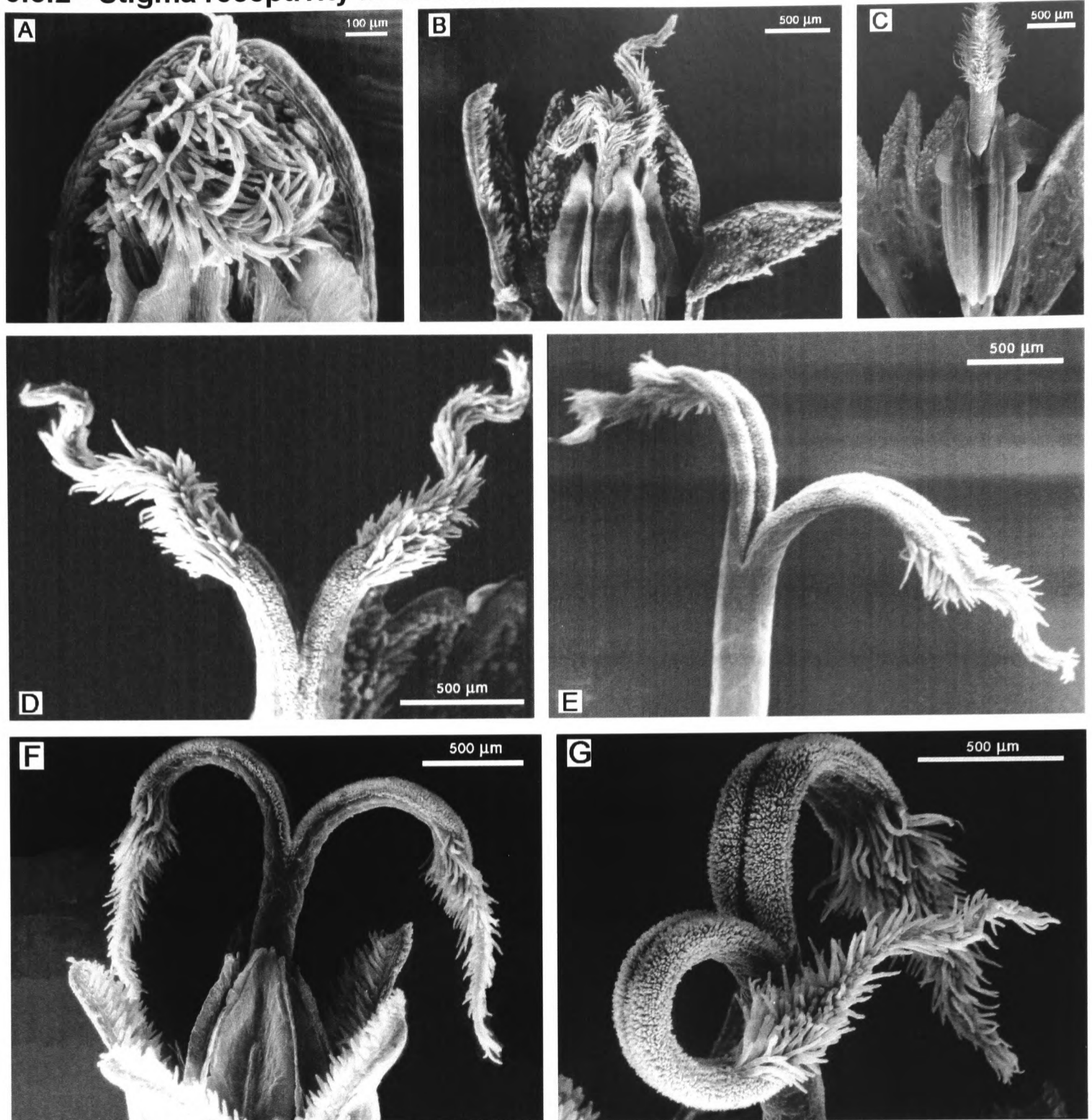


Plate 5.3 – *Cosmos sulphureus* stage-3 disk floret, showing stages in the development of the receptive stigma. (CryoSEM)

A-to C - early stage-3 disk florets with corolla dissected open to reveal anther tube and emerging stigma; **D and E** - mid stage-3 stigmas; **F and G** - late stage-3 stigmas. Note the absence of pollen on the *Cosmos sulphureus* stigmas. This is because the anthers in these florets have not dehisced prior to the emergence of stigmas as normally happens. Although not a common occurrence, this anomaly was only observed when *Cosmos* plants were grown in damp, high humidity conditions. The specimens used in this plate were collected after a weekend spraying regime for red spider mite at the glasshouses at the Royal Botanic Gardens, Kew. As a consequence, ventilators to glasshouses were closed for a 12-hour period after spraying, and these *Cosmos sulphureus* plants experienced high humidity conditions that prevented dehiscence of their anthers. This researcher took advantage of this artefact, so as to obtain clean "pollen free" stigmas that clearly demonstrated the different stages of stigma emergence in stage-3 disk florets.

The development of *Cosmos* stage-3 disk florets begins with the emergence of the stigma from the anther tube and corolla at anthesis (Plate 5.3, A-B). Early stage-3 florets are characterised by having stigma lobes appressed at their adaxial surfaces, shielding the short stigma papillae as the stigma passes through the anther tube and exserts the corolla (Plate 5.3, C). Consequently, only the long non-receptive stigma papillae are exposed in the early stage-3 floret. The stigma at this stage functions as an organ of secondary pollen presentation. Mid stage-3 stigmas are characterised by the separation of stigma lobes. Initially, lobes separate to form a V-shape (Plate 5.3, C), but eventually spread out parallel to the horizontal (Plate 5.3, E).

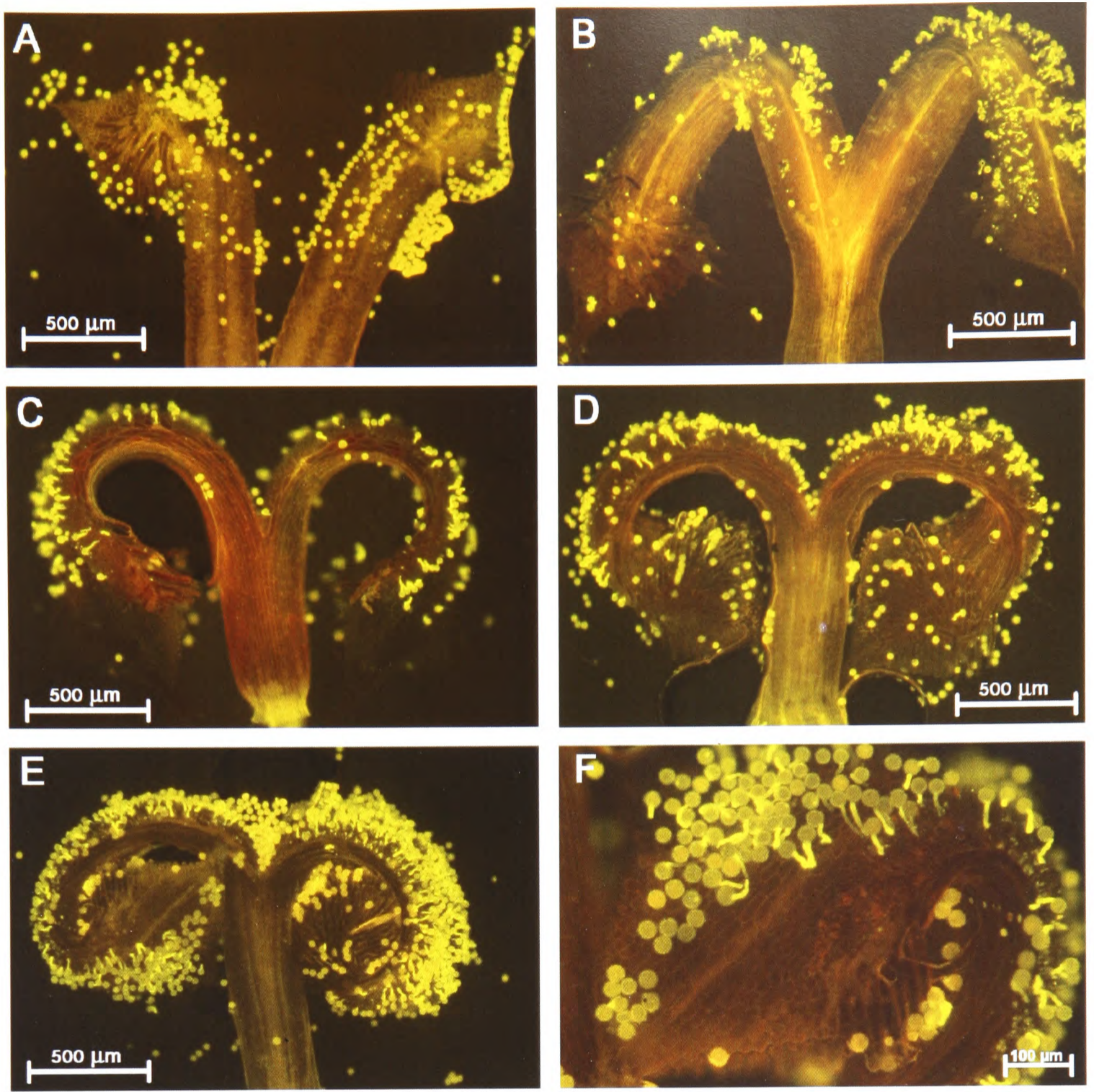


Plate 5.4 – Cross-compatible pollinations of *Cosmos bipinnatus* showing the onset of stigma receptivity from mid to late stage-3 stigmas.

The early and mid-stage-3 *Cosmos* stigmas are not receptive to pollen (Plate 5.4, A), with stigma receptivity occurring in the short papillae of late stage-3 florets only after stigma lobes have become arched (Plate 5.3, F-G; Plate 5.4, B-F). Initially, receptivity of the *Cosmos* stigma appears as stigma lobes begin to arch downward (Plate 5.4, B), but reaches a maximum in the fully reflexed stigma, when exposure of the short papillae is at its greatest (Plate 5.4, C-F). Occasionally, long papillar cells that lie close to the short receptive papillae may form an adhesive foot layer with *Cosmos* pollen (Plate 5.9, B-D). Cross-pollination of early or mid-stage-3 *Cosmos* stigmas results in a category-1 type incompatibility reaction (Plates 5.6 and 5.7), whereas cross-pollinated late stage-3 stigmas produce compatible pollen tubes (Plate 5.4, E) and/or category-1, -2 or -3 type incompatible pollen depending on the S-alleles of the individuals crossed (Plates 5.10 to 5.12). In compatible crosses, between 20-40% of the pollen grains that adhere to the stigma germinate to produce compatible pollen tubes, which equates with *Cosmos* pollen viability (Chapter 4)

5.3.3 – The *Cosmos* pollen-stigma interaction

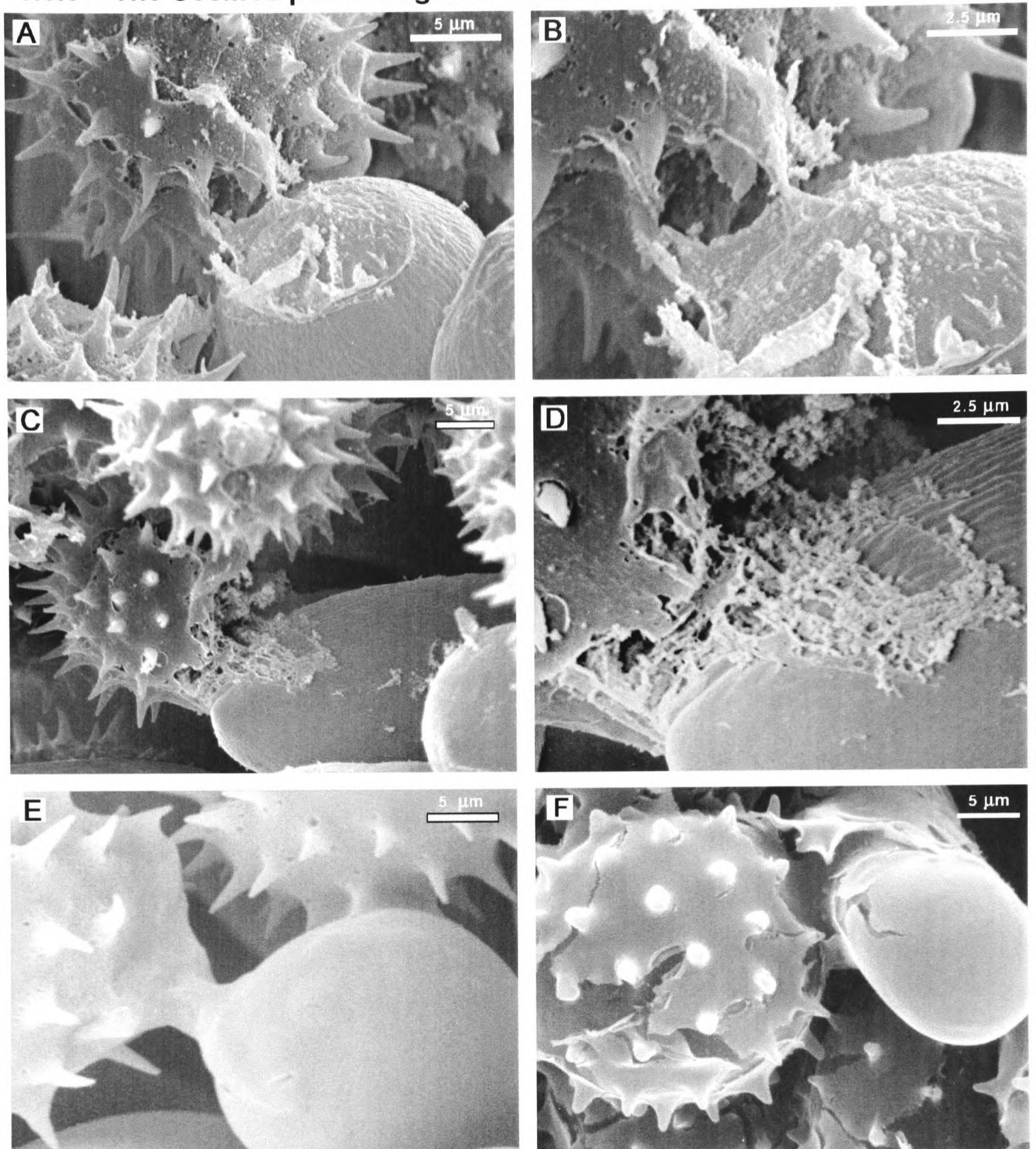


Plate 5.5 – *Cosmos* pollen-stigma interaction, observed on short stigma papillae, 15 to 45 minutes after cross-pollination (ambient humidity). A-to D- *Cosmos bipinnatus* (ambient SEM); E- *C. bipinnatus* (CryoSEM); F- *C. sulphureus* (CryoSEM).

The pollen-stigma interaction in *Cosmos* begins with an outpouring of the tryphine pollen coat onto the apical region of stigma papillae (Plate 5.5, A-B). The stigma pellicle subsequently blisters, lifts away from the underlying cuticle and fuses with the tryphine coat to form an adhesive foot layer (Plate 5.5, C-F). The cuticle does not appear to be involved in the initial interaction between the *Cosmos* pollen and stigma, as its characteristic patterning remains intact and undisturbed during fusion of tryphine and pellicle (Plate 5.5, C-D). However later, during the formation of the adhesive foot layer, the cuticle does appear to fuse with the tryphine coat (Plate 5.5 E-F). In

specimens prepared using CryoSEM, the hydrated properties of membranes are better maintained, so that the blistering of the pellicle and the cohesive nature of the foot layer can be observed more distinctly than specimens prepared for ambient SEM (Plate 5.5, cf. E with C-D). In some CryoSEM preparations, fracturing of the surface layers reveals the fusion-interface between the pollen grain and the stigma (Plate 5.5, F). Within the first hour of cross-pollinations, it is not possible to distinguish compatible pollen from category-3 type incompatible pollen, as compatible *Cosmos* pollen, and incompatible category-3 type *Cosmos* pollen both initiate an adhesive foot and germinate pollen tubes. However, approximately 6-8 hours after pollination category-3 type incompatible pollen tubes cease growth.

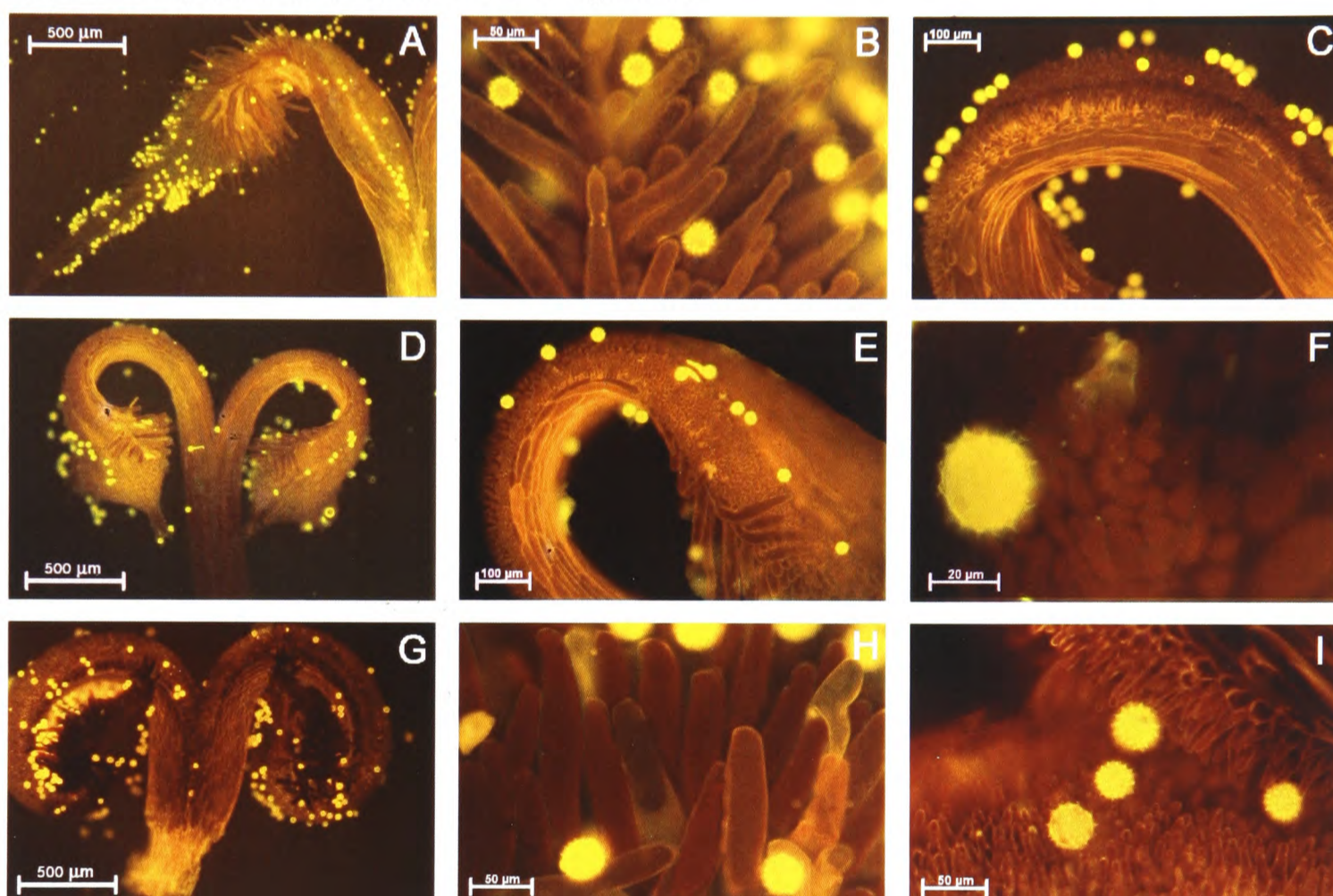


Plate 5.6 – Self pollinated *Cosmos* stigmas showing category-1 type incompatibility, 4 hours after pollination (Fresh material pollinated in ambient humidity, stained in aniline blue and observed in UV illumination. **A to C** – *Cosmos sulphureus* Sul-1 x Sul-1 (see pollination results). **D to F** – *Cosmos bipinnatus*; Bip-3 x Bp-3 (see pollination results, Tables 5.2a-e). **G to I** – *Cosmos atrosanguineus* Atro-4 x Atro-4 (see pollination results, Tables 5.6a-e).

Self-pollinated *Cosmos* stigmas exhibit a category-1 type pollen-stigma interaction, which is characterised by little or no out-pouring of pollen coat and no formation of an adhesive foot (Plate 5.7, A-E). Consequently, the majority of self-pollen does not adhere to the stigma, and is removed easily from the short stigma papillae by gentle movements or when washed with aqueous solutions (Plate 5.6, A, C-F & I; Plate 5.7, A-D). The majority of self-pollen is located within the long apical papillae for presentation to insects (Plate 5.6, A-B, D & H-G; Plate 5.7, A, E-G), or along the stigmatic groove formed by the flat stigma-epidermal cells (Plate 5.6, A, C & E). Very occasionally, self-pollen may germinate tubes, but their tubes cease growth when 1 to

2 pollen grains in length, and they do not form an adhesive association with papillae or initiate a callosic response (Plate 5.6, D-E; Plate 5.7, B-D.). In high humidity environments, self-pollen can be induced to release their pollen coats onto the stigma, but there is no reciprocal blistering of the pellicle, or formation of an adhesive foot (Plate 5.7, F-G), although some hydrated self pollen may adhere to the pellicle via their hydrated pollen coats (Plate 5.7, A., F-G; Elleman *et al.*, 1992).

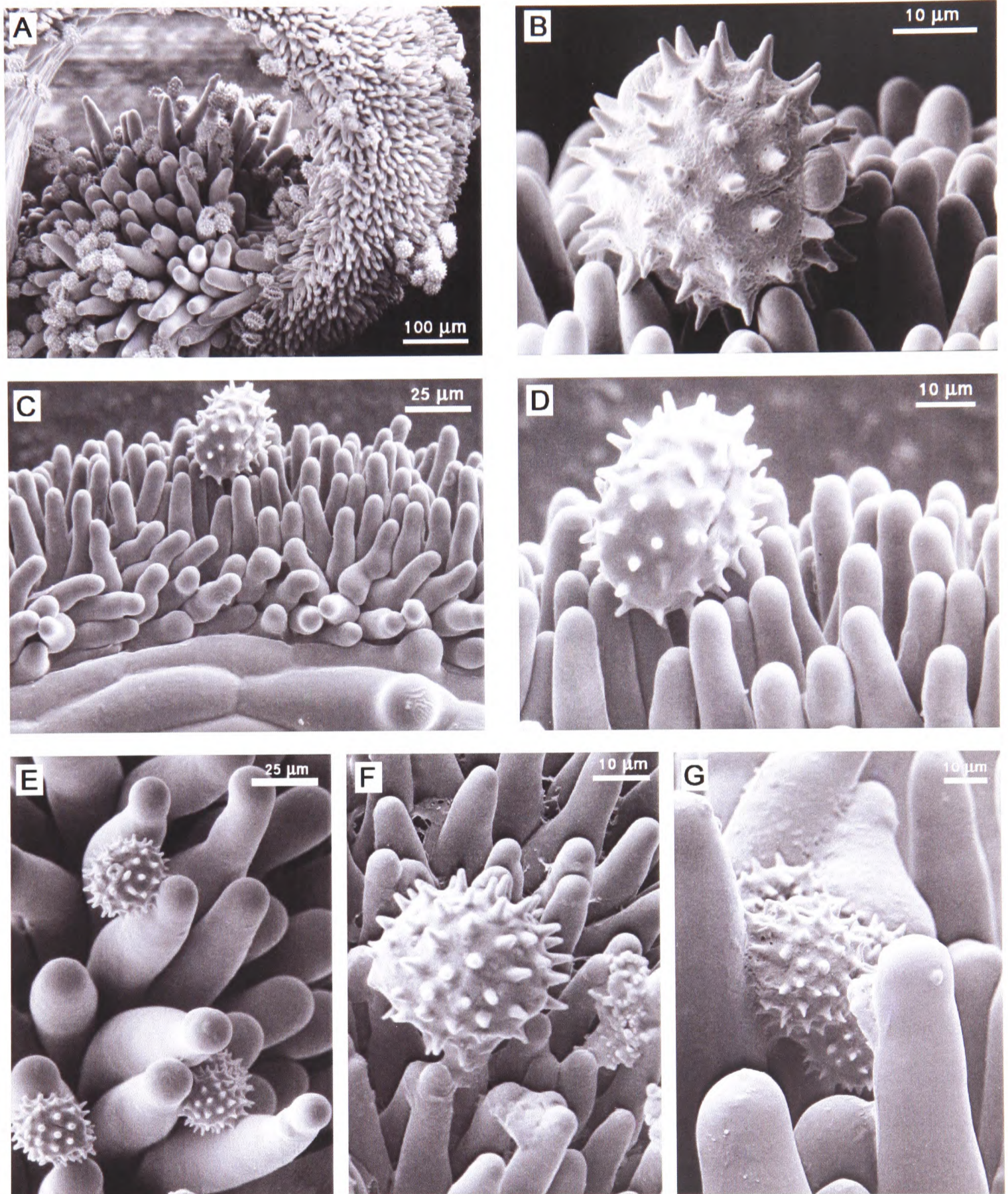


Plate 5.7– Self-pollinated *Cosmos* stigmas, exhibiting a category-1 type incompatibility reaction, observed 4 hours after pollination (Preparation technique, CryoSEM).

A – *Cosmos atrosanguineus* (ambient humidity); **B** - detail of **A**, showing self-pollen grain on short stigma papillae. **C** - *C. sulphureus* (ambient humidity); **D** - detail of **C** showing self pollen grain on short stigma papillae. **E** - *C. sulphureus* (ambient humidity) self-pollen grains on long apical stigma papillae. **F** & **G** – *C. atrosanguineus* (70%+ humidity) showing hydrated self-pollen grains on short (**F**) and long papillae (**G**) in plants that have been induced by the high humidity environment to deposit their pollen coat onto stigma papillae ((**E-G**))

Plates 5.8 to 5.10 illustrate the development of pollen grains in cross-pollinated *Cosmos* stigmas. In general, *Cosmos* cross-incompatible pollen exhibits a category-1 type incompatibility reaction. In strongly cross-incompatible pairings, almost all pollen exhibits a category-1 type pollen-stigma interaction (Plate 5.10 H), while in less-strongly cross incompatible pairings, between ~10-30% of incompatible pollen grains exhibits a category-2 type incompatibility reaction. *Cosmos* category-2 type pollen does not form an adhesive foot layer with stigma papillae prior to germination although fibrillar extensions, (Plate 5.9, F) produced from the outer-wall layer of the pollen tube may become attached to the stigma surface. However, contact is not reciprocated by the stigma, and there is no blistering of the pellicle layer or subsequent fusion of the pollen and stigma surface layers (Plate 5.9, E-F). The *Cosmos* Category-2-type incompatible pollen germinates a short pollen tube that ceases growth when 1 to 4 pollen grains in length. The tips of these stunted incompatible pollen tubes often contain plugs of callose and may swell, creating a club-shaped appearance at the ends of tubes (Plate 5.10, E, C, F & I). In some, but not all, cross-incompatible *Cosmos* pairings deposition of callose in papillar cells adjacent to pollen tubes occurs (Plate 10, E-G). Since category-2 incompatible pollen tubes are not held in physical contact with the papillar surface, the lengthening of their pollen tubes tends to lift pollen grains away from the surface of the stigma (Plate 5.8, E-F; Plate 5.9, E, G-H; and Plate 5.10, A-C). Category-2 type pollen grains do not pass their contents into pollen tubes and so fluoresce brightly when stained with aniline blue (Plate 5.10, G & I). Furthermore, category-2 pollen tubes often develop haphazardly on the stigma, with some tubes growing horizontally across the tops of papillae, others vertically away from papillae, and a few cyclically around the grain (Plate 5.8, D; Plate 5.10, D; Plate 5.11, A-B). When category-2 pollen tubes do grow downwards into papillae this often occurs after a period of haphazard horizontal growth so that pollen tubes have twists and kinks at the point where direction of growth changed (Plate 5.10, E-G & I). Severe bends, kinks, or twists at the base of pollen tubes prior to downward growth are characteristic of category-2 type pollen, and this growth habit can be used to distinguish category-2 type pollen from category-3 type pollen in the early stages of pollen-tube development, as the category-3 pollen tubes invariably grow straight downwards against the sides of stigma papillae, without any prolonged prior period of horizontal growth.

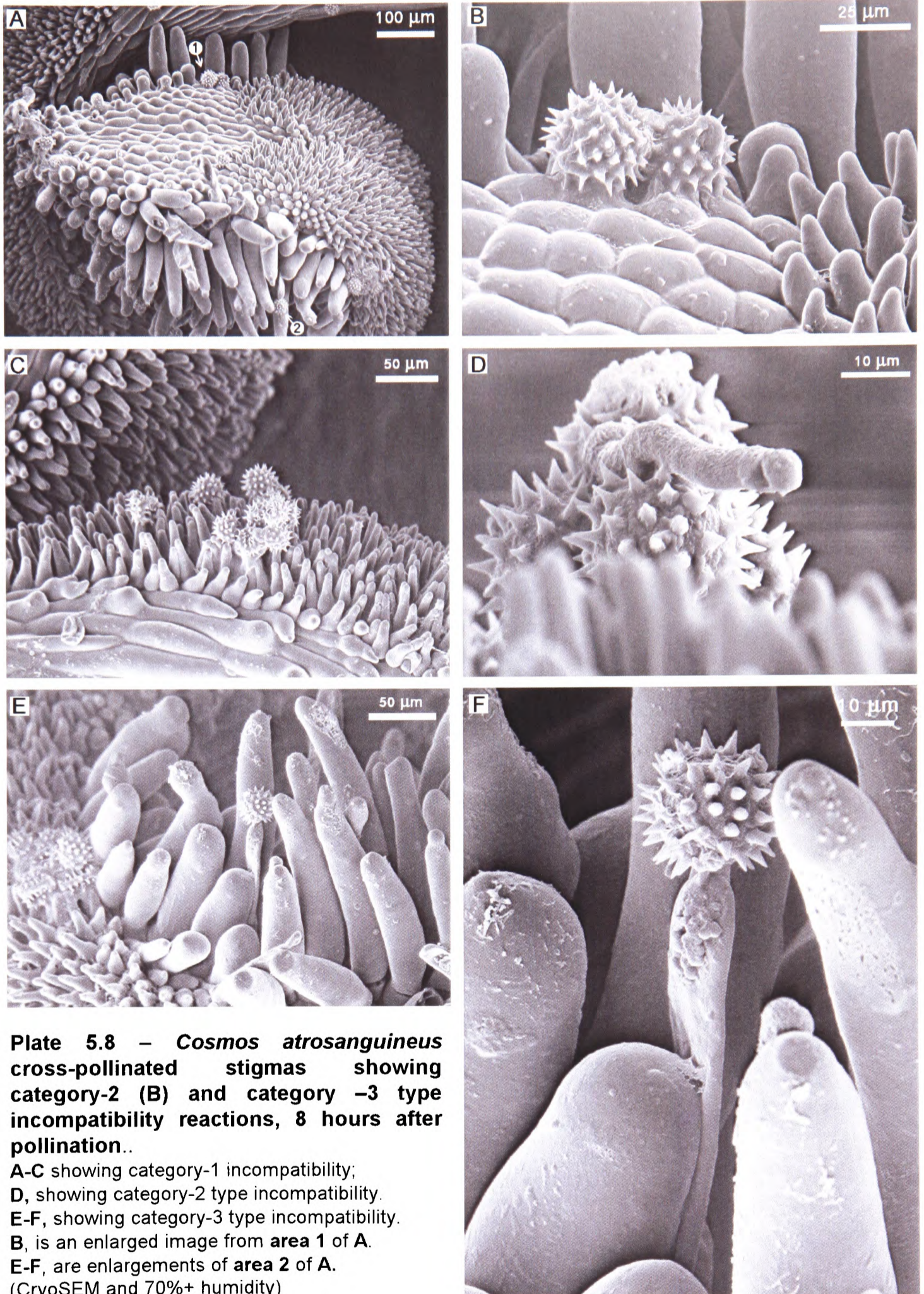


Plate 5.8 – *Cosmos atrosanguineus* cross-pollinated stigmas showing category-2 (B) and category –3 type incompatibility reactions, 8 hours after pollination..

A-C showing category-1 incompatibility;
 D, showing category-2 type incompatibility.
 E-F, showing category-3 type incompatibility.
 B, is an enlarged image from area 1 of A.
 E-F, are enlargements of area 2 of A.
 (CryoSEM and 70%+ humidity)

Plate 5.9 (overpage) – Cross-pollinated *Cosmos* stigmas (Preparation technique, CryoSEM)
 A, – *C. sulphureus* cross-pollinated incompatible stigma; B, - enlargement of area 1 from A showing the formation of adhesive foot at the sub-apical region of a long stigma papilla. C & D - enlargement of area 2 from A showing the formation of adhesive foot at the base of a long stigma papilla. E-H.- *C. bipinnatus* cross-pollinated incompatible stigmas showing category-1 and category-2 type incompatible pollen.

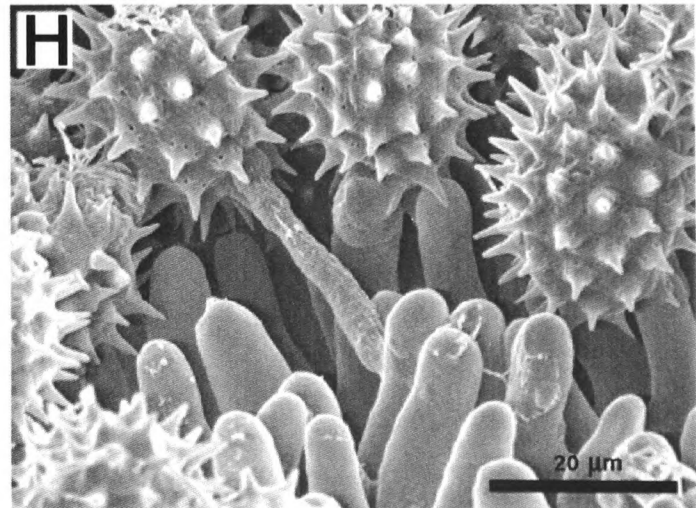
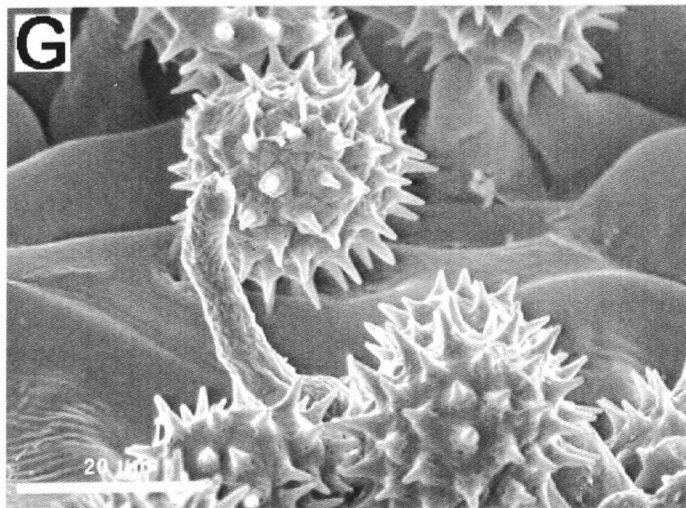
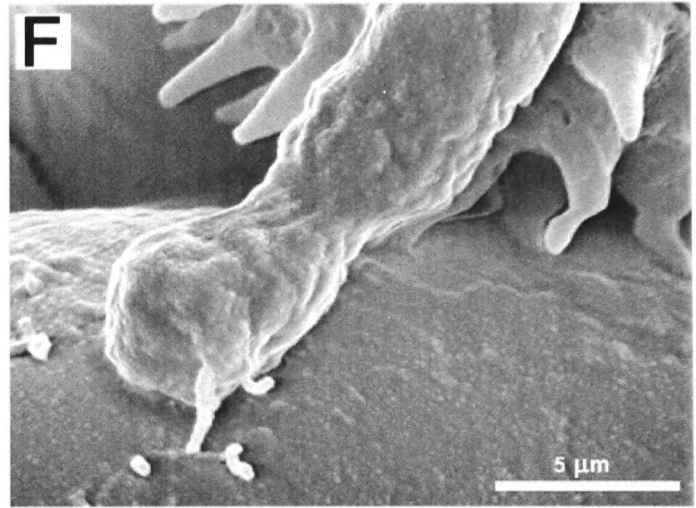
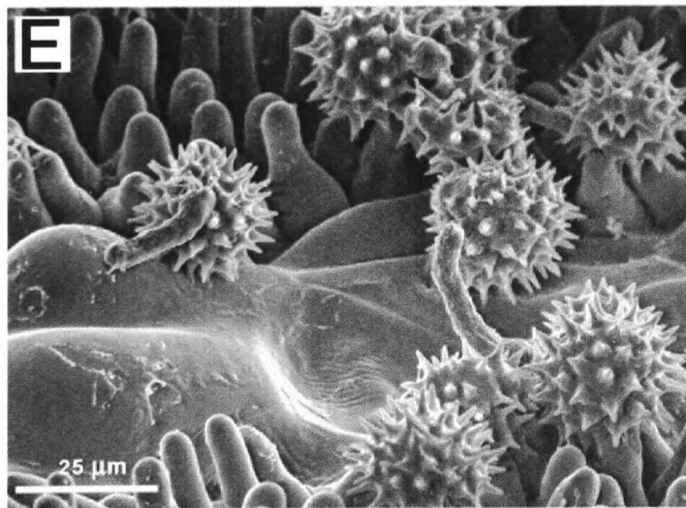
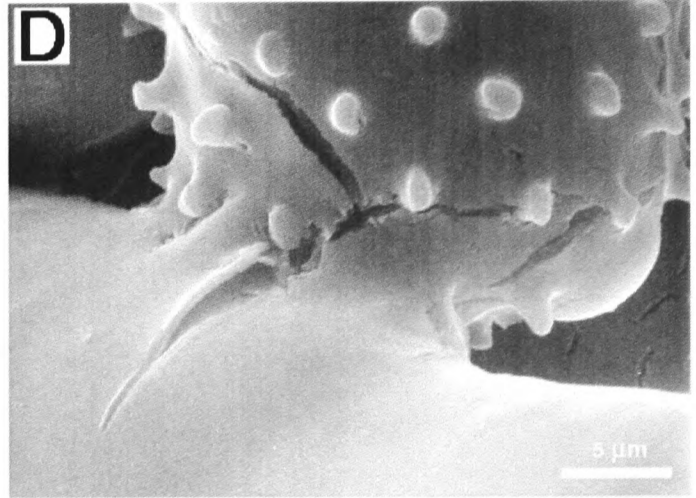
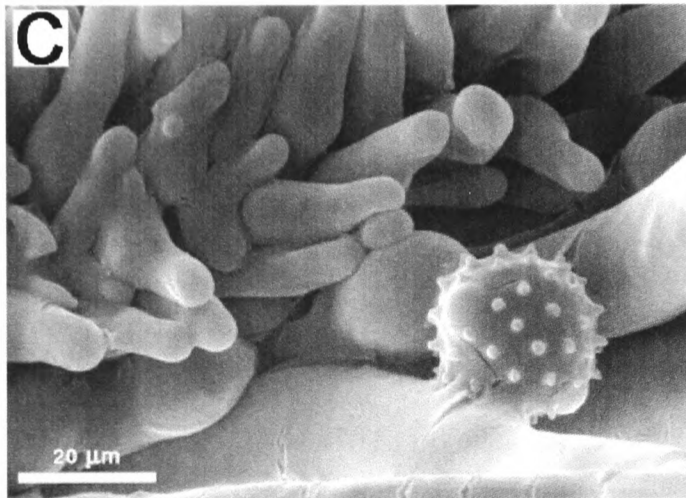
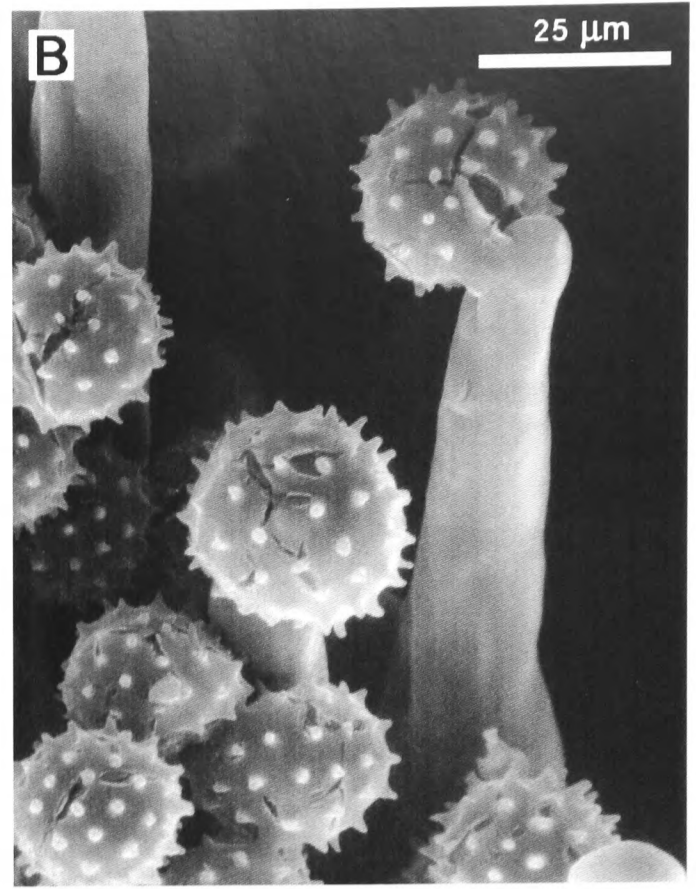
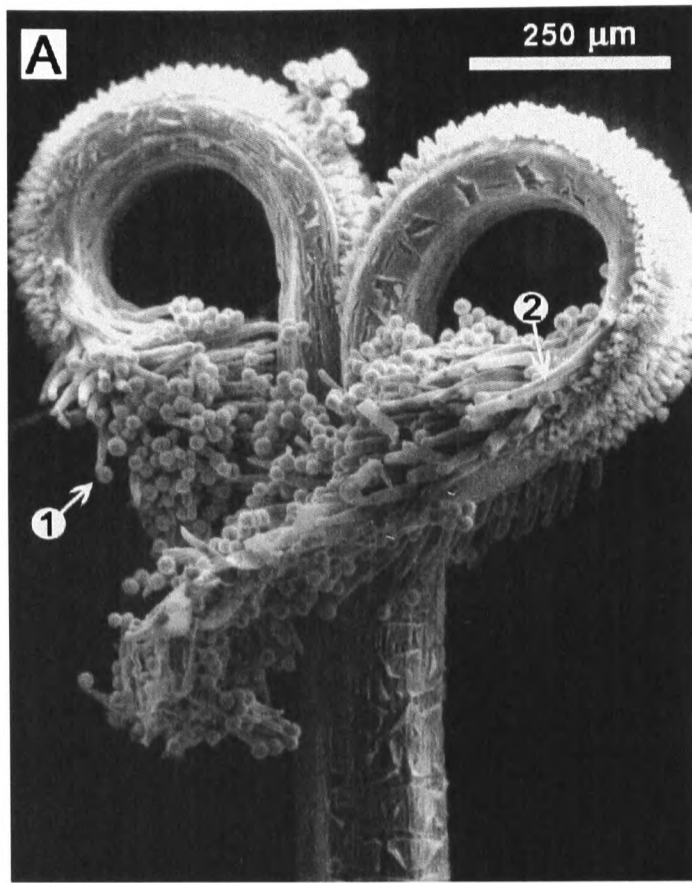


Plate 5.9 – Cross-pollinated *Cosmos* stigmas (for descriptions see bottom of previous page)

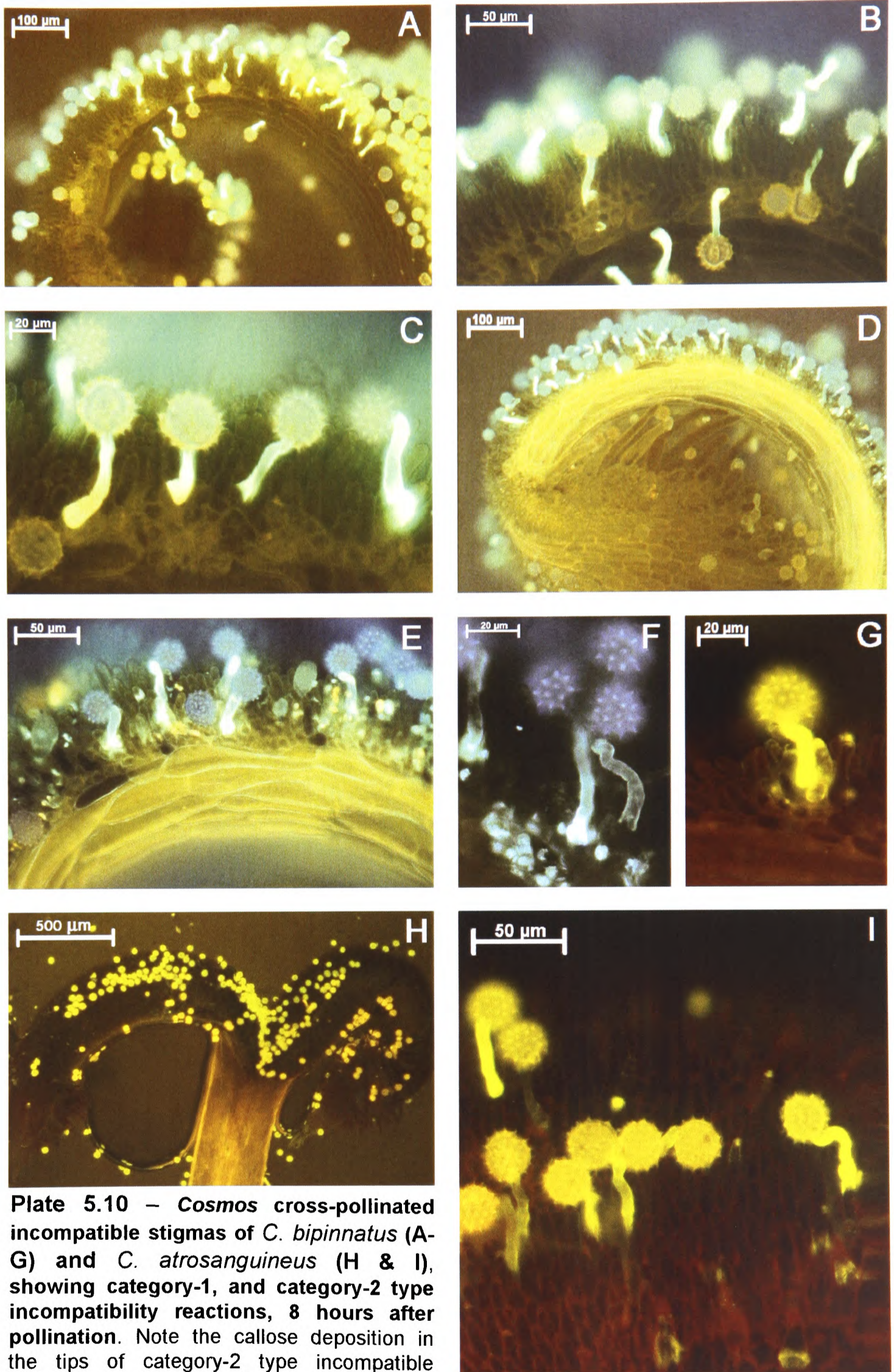


Plate 5.10 – *Cosmos* cross-pollinated incompatible stigmas of *C. bipinnatus* (A-G) and *C. atrosanguineus* (H & I), showing category-1, and category-2 type incompatibility reactions, 8 hours after pollination. Note the callose deposition in the tips of category-2 type incompatible pollen and associated stigma papillae (E-G). This is characteristic of category-2 type incompatibility (CryoSEM and 70%+ humidity).

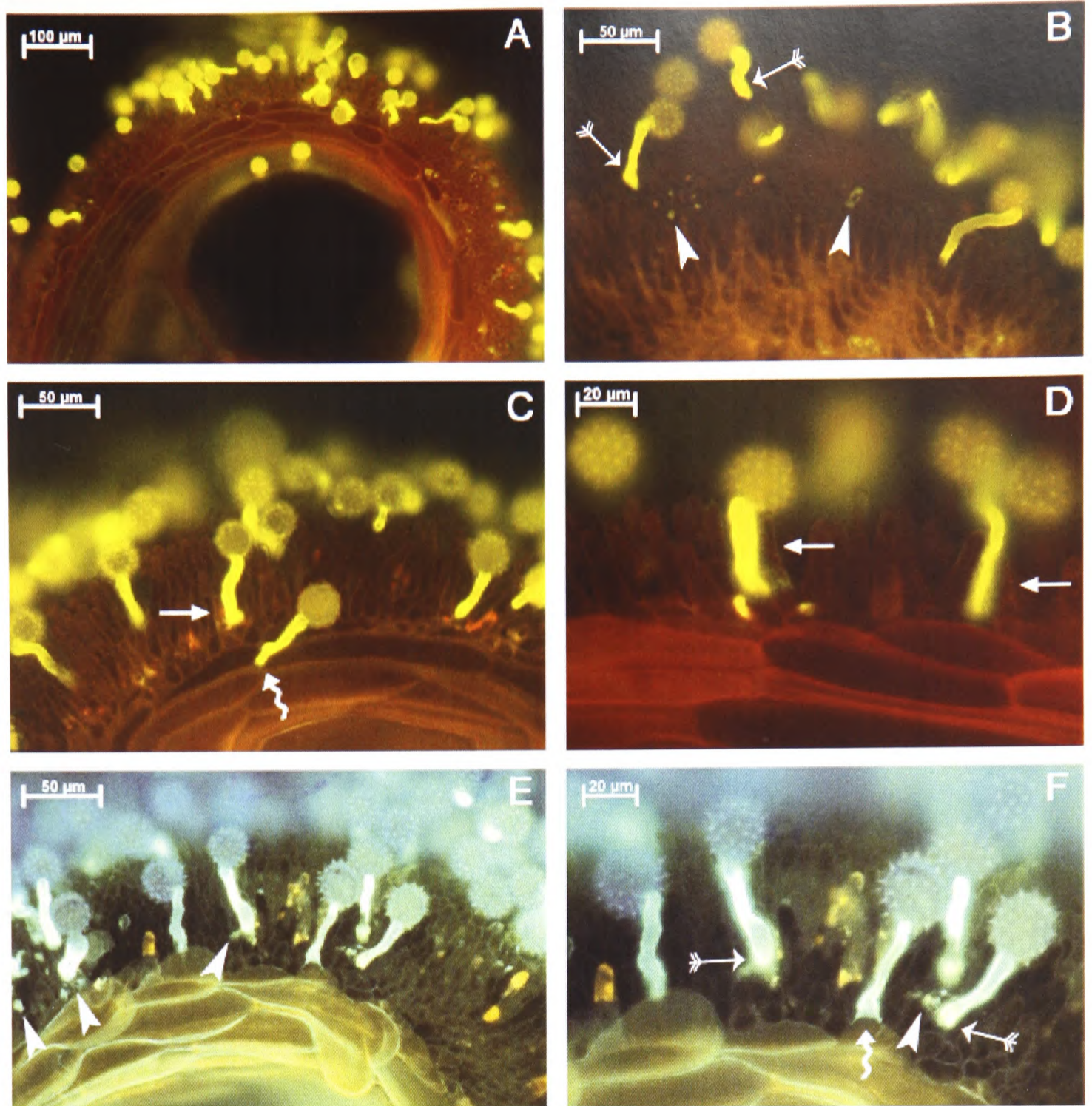


Plate 5.11 – *Cosmos* cross pollinated stigmas, 8 hours after pollination, comparing category-2 and category-3 type incompatibility reactions in *Cosmos*. A-B, *Cosmos sulphureus*; C-F, *Cosmos bipinnatus*. Note the close affinity that one surface of the *P*-type pollen forms with the adjacent surface of the papilla (C-D, arrows). *P*-type pollen tubes enter the stigma at the base of papilla and then cease growth (C & F, fluted arrows) Note the deposition of callose in some papillae (B & E, arrowheads), and the swelling and deposition of callose in the tips of category-2 type pollen tubes (B & F, feathered arrows).

In *Cosmos* category-3 type incompatible pollen, (also known as *P*-type pollen), the tryphine coat and stigma pellicle form an adhesive foot layer, and a pollen tube subsequently germinates and grows straight downwards along the length of the papilla (Plate 5.11, C-D). The pollen-tube surface adjacent to the papilla maintains physical contact with the pellicle-cuticle layer of the papillae, and appears to form a fusion interface between pollen-tube and papilla that directs the growth of the pollen tube downwards into the stigma tissue (Plate 5.11, D-F). *Cosmos P*-type pollen tubes appear to enter the stigma at the base of the papillar cells and pass into the stigma tissue via the middle lamella (Plate 5.11, C & F fluted arrows). Shortly thereafter they cease growth. Cessation of *P*-type pollen tubes may be accompanied by the deposition of callose in the tips of pollen tubes and adjacent papillae, and/or by swelling of pollen-tube tips (Plate 5.12).

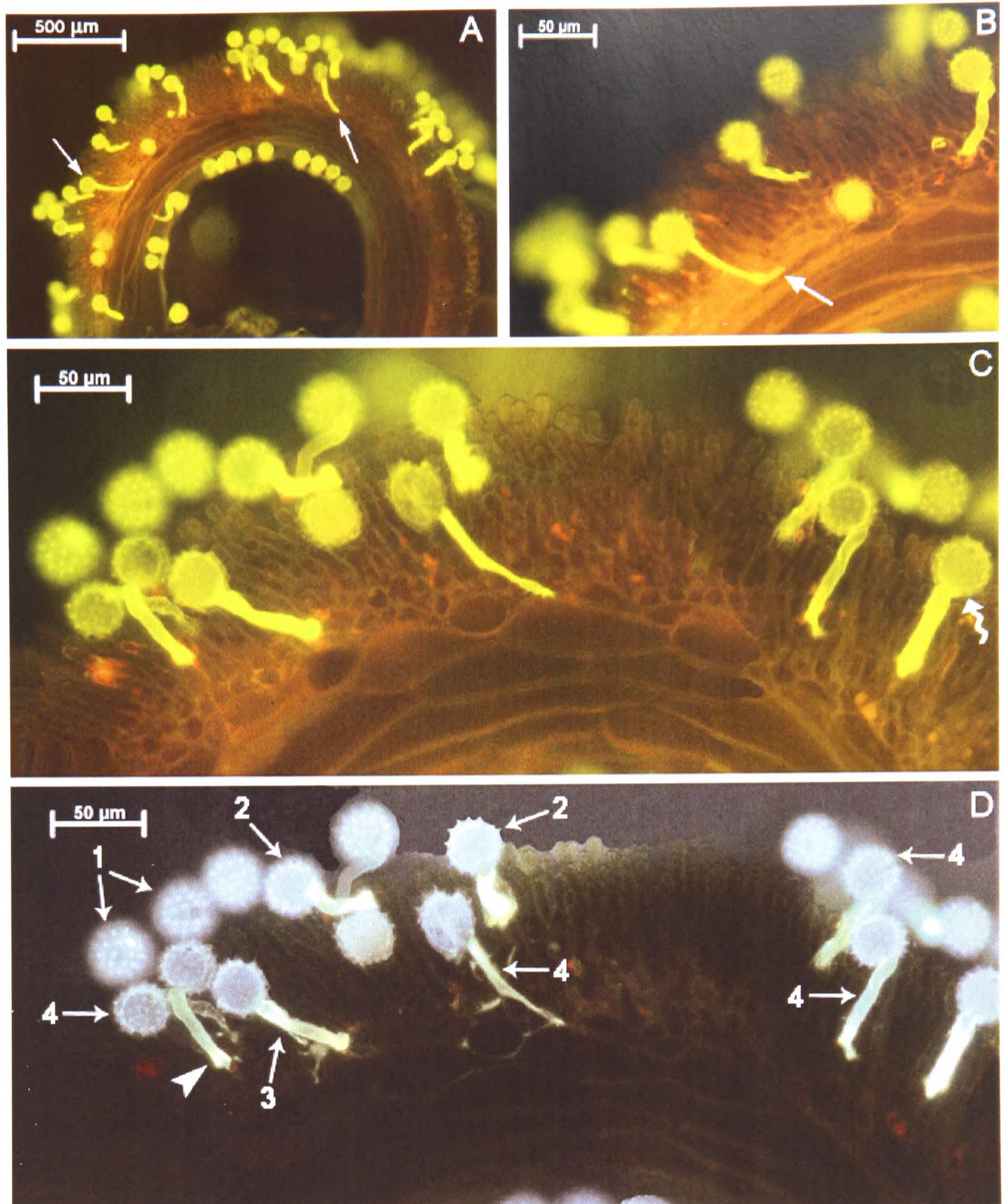


Plate 5.12 – *Cosmos bipinnatus* stage-3 cross-pollinated stigmas 8 hours after pollination showing segregation of incompatible and compatible pollen tubes on stigmas

A, stigma lobe showing segregation of incompatible category-1, -2 and *P*-type pollen and compatible pollen in the semi-compatible pollination, [Bip 3 x Bip 4] (Table 5.1c), showing the characteristic 90° bend observed in compatible *Cosmos* pollen tubes after penetration of stigma (**arrows**). **B**, enlarged region from **A** showing detail of a compatible pollen tube (**arrow**). **C & D**, enlarged region from **A**, observed with yellow and blue filters respectively. In **D**, note the presence of category-1 pollen (arrow 1), category-2 pollen (arrow 2), *P* type pollen (arrow 3) and compatible pollen (arrows 4), segregating on the same stigma. *P*-type pollen (arrow 3) has emptied the contents of its grain into the pollen tube and these contents are beginning to pass down the tube, but growth in this pollen tube has already ceased as its tip is swollen and plugged with callose. The *P*-type pollen tube to its left (arrowhead) also has a swollen and callosed tip, and both *P*-type pollen tubes have instigated a mild callose reaction in adjacent papillae. The pollen grains of category-1 and category-2 type incompatible pollen (arrows 1 and 2) retain their contents and their grains fluoresce brightly. Compatible pollen (arrows 4) and some *P*-type pollen (arrow 3 and arrowhead), pass the contents of their grain into the tube just before the tube penetrates the stigma. Consequently their pollen grains are empty and do not fluoresce brightly. These features are observed more effectively with the yellow filter. *P*-type pollen can only be distinguished from compatible pollen after penetration of the stigma, when compatible tubes make a characteristic 90° turn towards the style, whereas *P*-type pollen tubes cease growth soon after stigma penetration. In addition, compatible pollen tubes tend to be thinner and less heavily callosed (**D**, **arrows 4**) than incompatible *P*-type tubes which generally have thicker more heavily callosed pollen-tube walls (**C**, **fluted arrow**).

Compatible *Cosmos* pollen shows identical development to *Cosmos P*-type pollen until penetration of the stigma at the base of the papilla. At this point *P*-type pollen tubes abort, whereas compatible pollen tubes continue growth within the middle lamella of stigma cells and, a short distance after entering the stigmatic tissue, make a 90° turn towards the style (Plate 5.12 A-D). *P*-type pollen tubes never reach this point and their pollen tubes remain straight with swollen and callosed tips (Plate 5.12 A-B). Compatible pollen grains and the majority of *P*-type pollen grains empty their contents into the pollen tubes just prior to pollen-tube penetration of the stigma and so their grains are empty and do not fluoresce brightly with aniline blue staining and UV illumination. A distinction can be made between compatible and *P*-type pollen because as the compatible pollen tube makes its 90° turn the pollen-grain material has already travelled down the tube and passed into the apical regions of the tube embedded in the stigma (Plate 5.12, C-D). The contents of *P*-type pollen grains may enter the pollen tube as the tube penetrates the stigma, but shortly thereafter *P*-type pollen tubes cease growth and their tips become swollen and plugged with callose (Plate 5.12, C-D).

The segregation of incompatible, compatible and *P*-type pollen on cross-pollinated stigmas implies the presence of a cryptic *Cosmos* gametophytic gene (*G*). *G*-alleles are expressed later in the SI reaction than sporophytic *S*-alleles, and so the *G*-incompatibility reaction occurs not at the stigma surface, but in the stigmatic tissue, which is where the growth of *P*-type incompatible tubes is arrested.

5.3.4 - Interspecific pollinations: *C. atrosanguineus* x *C. bipinnatus*

In low humidity environments, placing stage-3 pollen of one *Cosmos* species on to the stigma of another results in category-1 type incompatibility reaction with an occasional accompaniment of long spindly category-2 type pollen tubes (Plate 5.13, A, B and E). In higher humidity environments, a greater number of pollen grains can be induced to germinate pollen tubes, but these tubes do not interact with the stigma papillae, and are thin or emaciated, and grow haphazardly until depletion of resources inhibits their growth (Plate 5.13, A-E). In the main, *C. bipinnatus* pollen germinate tubes more readily on *C. atrosanguineus* stigma than vice versa (Plate 5.13, A-C), although the majority of interspecific *Cosmos* pollinations results in a category-1 type incompatibility reaction, the majority of which, i.e 50% to 80%, probably constitutes non-viable pollen.

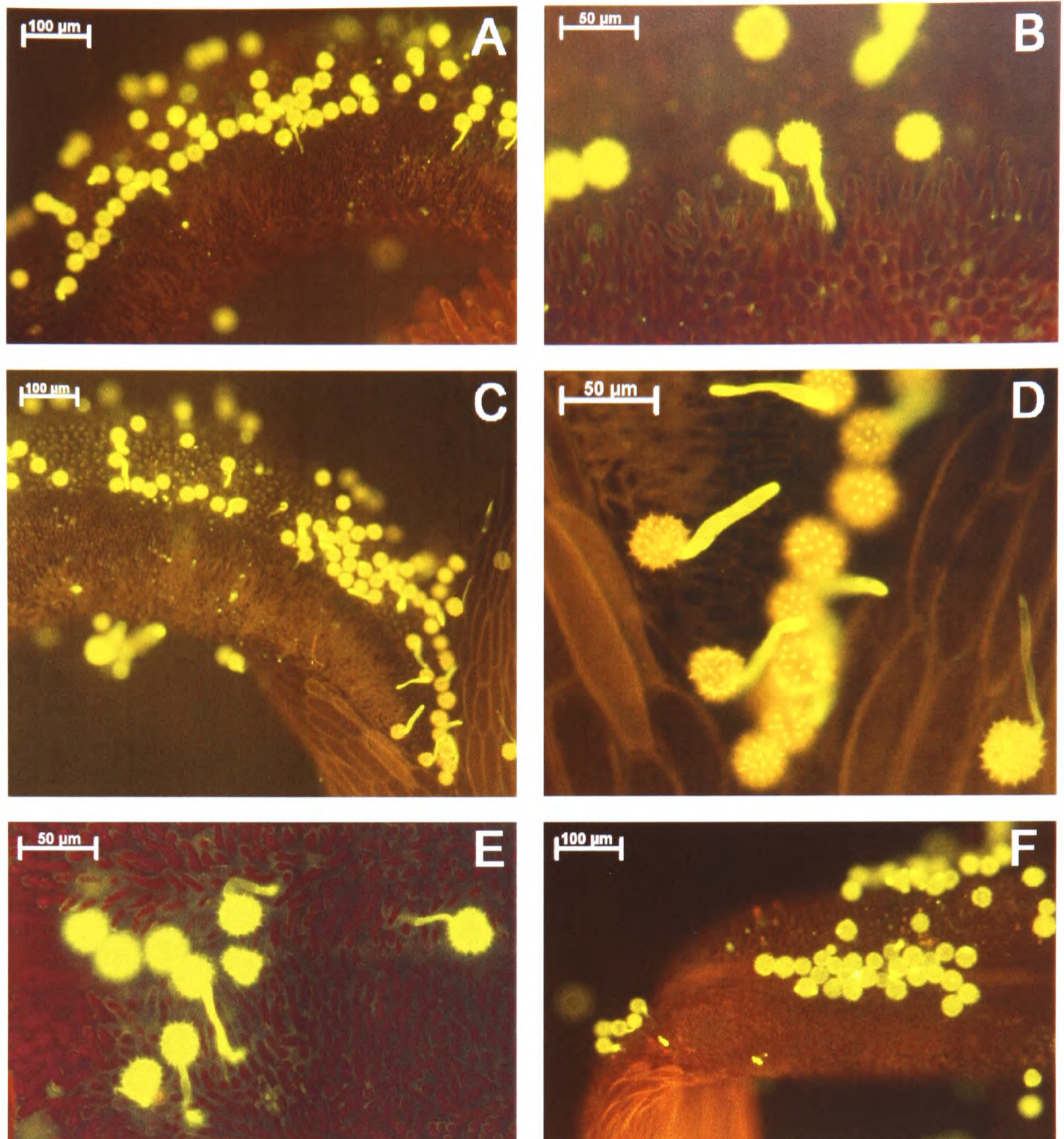


Plate 5.13 Interspecific pollinations between of *Cosmos atrosanguineus* and *C. bipinnatus* carried out in high humidity environment

A to D, *C. atrosanguineus* stage-3 stigma x *C. bipinnatus* stage-3 pollen, four hours after pollination; and E, *C. atrosanguineus* stage-2 stigma x *C. bipinnatus* stage-3 pollen, four hours after pollination, F, *C. bipinnatus* stage-3 stigma x *C. atrosanguineus* stage-3 pollen, four hours after pollination.

5.3.5 - Pollination experiments in populations of *Cosmos atrosanguineus*, *C. bipinnatus* and *C. sulphureus*

Compatibility relationships in five *Cosmos bipinnatus*, five *C. atrosanguineus* and four *C. sulphureus* individuals of unknown S-allele specificities were analysed by counting the number of incompatible i.e. category-2 pollen tubes and compatible pollen tubes germinating on 15 stigmas of each cross (Tables 5.1; 5.2 and 5.3). Data from Chapter 4 (Tables 4.6-4.9) indicate that ~50% to ~80% of category-1 type incompatible pollen

may actually represent non-viable grains. Since category-1 type incompatible pollen, i.e incompatible pollen that neither adheres to the stigma papillae, nor germinates a pollen tube (but whose grains may become mechanically trapped on or within stigma papillae), cannot be distinguished from non-viable pollen by the methods used in this study, its numbers were not recorded. Only category-2 type incompatible pollen, i.e pollen that germinates stunted pollen tubes, and compatible pollen were recorded. Consequently, a *Cosmos* individual recorded as having 0 compatible and 0 incompatible pollen tubes, as occurs in all pollinations of *Cosmos atrosanguineus* (Tables 5.3a-e), would have been observed with only category-1 type pollen on its stigma. However, these category-1 type pollen were not recorded as they probably represent non-viable pollen. A *Cosmos* individual recorded as having 0 compatible and 5 incompatible pollen tubes, would have been observed with five category-2 type pollen tubes on its stigma, but may also have had many category-1 type pollen grains (or non-viable pollen grains) on its stigma. Pollinated stigmas observed with no pollen on their stigmas were not included in the results as it was not possible to ascertain whether the pollen grains from these stigmas had been washed off during the staining process or were the result of pollination error.

Table 5.1a – POLL-01 *Cosmos bipinnatus* (1995 582) Bip 1 x Bip 1 to 5.

Female Parent ♀	Male parent ♂									
	Bip 1		Bip 2		Bip 3		Bip 4		Bip 5	
	C	ϕ	C	ϕ	C	ϕ	C	ϕ	C	ϕ
1	1	4	35	4	0	4	66	5	8	15
2	0	4	49	3	0	1	106	3	6	19
3	0	3	35	4	0	3	32	2	3	15
4	0	2	31	3	1	3	27	3	5	20
5	0	0	28	2	1	2	22	3	3	11
6	0	0	26	1	0	0	74	2	2	7
7	0	0	19	2	0	0	46	5	4	15
8	1	1	35	2	0	3	50	7	1	4
9	0	4	48	1	0	3	31	7	4	11
10	0	0	25	3	0	5	53	8	0	2
11	0	1	44	3	0	0	76	4	3	14
12	0	5	51	1	0	0	65	6	0	5
13	0	2	41	2	0	1	34	8	3	16
14	1	2	29	2	0	2	58	2	0	12
15	1	3	53	1	0	3	63	3	2	8
Total	4	31	549	34	2	30	803	68	44	174
Mean	0.27	2.07	36.60	2.27	0.13	2.00	53.53	4.53	2.93	11.60
Standard deviation	0.46	1.71	10.56	1.03	0.35	1.60	22.67	2.20	2.28	5.44
Mode	0	0	35	2	0	3	N/A	3	3	15
Median	0	2	35	2	0	2	53	4	3	12
Compatibility status	-		+		-		+		-	

Key: C = number of compatible pollen tubes per stigma; ϕ = number of category-2 type incompatible pollen tubes per stigma. +, compatible; -, incompatible; ± inconclusive compatibility; N/A, not applicable. Self-pollinations are highlighted grey.

Table 5.1b – POLL-01 *C. bipinnatus* (1995 582) Bip 2 x Bip 1 to 5

Female Parent ♀	Male parent ♂									
	Bip 1		Bip 2		Bip 3		Bip 4		Bip 5	
	C	ϕ	C	ϕ	C	ϕ	C	ϕ	C	ϕ
1	5	1	1	0	2	0	2	3	7	2
2	1	2	2	3	1	0	19	3	8	0
3	5	0	2	6	3	0	36	4	18	6
4	2	0	0	3	6	1	9	1	6	0
5	1	3	0	2	3	0	6	3	6	0
6	2	0	0	0	5	5	28	4	5	2
7	3	0	0	0	1	2	14	4	12	12
8	3	0	0	0	7	2	11	2	24	13
9	5	5	0	1	7	1	26	5	21	1
10	10	1	0	2	4	1	10	4	4	1
11	0	0	1	2	9	4	7	2	6	2
12	6	5	0	2	1	4	9	3	13	4
13	2	1	0	1	2	1	6	1	7	9
14	5	3	0	0	5	3	5	1	5	11
15	7	1	0	0	6	0	4	0	11	3
Total	57	22	6	22	62	24	192	40	153	66
Mean	3.80	1.47	0.40	1.47	4.13	1.60	12.8	2.67	10.2	4.40
Standard deviation	2.68	1.77	0.74	1.68	2.53	1.68	10.0	1.45	6.27	4.63
Mode	5	0	0	0	1	0	9	3, 4	6	2
Median	3	1	0	1	4	1	9	3	7	2
Compatibility status	-		-		-		±		±	

Table 5.1c – POLL-01 *C. bipinnatus* (1995 582) Bip 3 x Bip 1 to 5

Female Parent ♀	Male parent ♂									
	Bip 1		Bip 2		Bip 3		Bip 4		Bip 5	
	C	ϕ	C	ϕ	C	ϕ	C	ϕ	C	ϕ
1	0	0	4	10	0	0	4	1	13	4
2	9	1	21	0	0	0	3	0	10	25
3	4	3	5	2	0	6	5	3	21	21
4	2	0	9	2	0	3	7	5	12	7
5	1	5	27	1	0	0	7	2	7	9
6	6	3	30	1	0	2	12	1	5	0
7	1	3	13	3	0	0	7	2	15	13
8	2	1	22	4	0	4	4	0	6	1
9	3	3	8	2	0	0	17	6	7	0
10	2	4	7	1	0	0	10	2	11	6
11	3	1	2	1	0	4	6	1	4	4
12	3	0	5	2	0	0	33	10	11	7
13	2	3	24	2	0	0	11	3	4	0
14	1	2	6	1	0	1	9	4	5	2
15	2	2	3	1	0	0	5	2	8	5
Total	41	31	186	33	0	20	140	42	139	104
Mean	2.73	2.07	12.40	2.20	0.00	1.33	9.33	2.80	9.27	6.93
Standard deviation	2.25	1.53	9.64	2.37	0.00	1.99	7.52	2.62	4.73	7.52
Mode	2	3	5	1	0	0	7	2	7	0
Median	2	2	8	2	0	0	7	2	8	5
Compatibility status	-		±		-		±		±	

Table 5.1d – POLL-01 *C. bipinnatus* (1995 582) Bip 4 x Bip 1 to 5

Female Parent ♀	Male parent ♂									
	Bip 1		Bip 2		Bip 3		Bip 4		Bip 5	
	C	ϕ	C	ϕ	C	ϕ	C	ϕ	C	ϕ
1	0	5	9	5	7	3	1	6	5	0
2	0	5	8	4	0	2	2	11	2	0
3	0	2	3	5	0	4	0	0	6	0
4	0	0	8	5	8	10	0	4	7	2
5	0	0	5	2	1	3	0	5	7	3
6	1	4	0	0	6	2	0	4	11	13
7	3	1	3	1	11	11	0	2	1	3
8	2	3	1	0	3	5	0	2	0	1
9	1	5	5	3	3	1	2	1	0	6
10	0	1	3	1	0	2	0	0	0	0
11	2	4	3	1	4	3	0	1	0	0
12	2	4	0	1	3	2	0	0	0	1
13	1	1	0	2	0	2	1	1	1	6
14	2	4	1	5	5	3	0	1	0	3
15	2	3	7	1	0	3	0	4	4	0
Total	16	42	56	36	51	56	6	42	44	38
Mean	1.07	2.80	3.73	2.40	3.40	3.73	0.40	2.80	2.93	2.53
Standard deviation	1.03	1.82	3.13	1.92	3.44	2.91	0.74	2.98	3.51	3.56
Mode	0	4	3	1	0	3	0	1	0	0
Median	1	3	3	2	3	3	0	2	1	1
Compatibility status	-		-		-		-		-	

Table 5.1e – POLL-01 *C. bipinnatus* (1995 582) Bip 5 x Bip 1 to 5

Female Parent ♀	Male parent ♂									
	Bip 1		Bip 2		Bip 3		Bip 4		Bip 5	
	C	ϕ	C	ϕ	C	ϕ	C	ϕ	C	ϕ
1	25	3	3	0	3	0	0	0	0	0
2	8	3	32	2	3	10	2	2	0	0
3	12	9	3	1	5	2	0	1	0	0
4	10	1	5	3	0	1	0	0	0	0
5	11	5	21	5	3	5	0	0	0	0
6	30	3	24	3	6	5	0	0	0	0
7	34	4	14	1	2	5	0	0	0	0
8	13	3	11	3	4	3	1	1	0	0
9	13	7	15	6	1	3	0	0	0	1
10	9	5	4	0	3	13	0	0	0	0
11	22	4	5	3	11	0	0	0	0	0
12	19	2	6	1	1	7	0	0	0	2
13	24	7	19	3	3	4	0	0	0	0
14	14	4	13	2	8	6	0	0	0	0
15	12	3	11	1	2	5	0	1	0	0
Total	256	63	186	34	55	69	3	5	0	3
Mean	17.0	4.20	12.40	2.27	3.67	4.60	0.20	0.33	0.00	0.20
Standard deviation	8.11	2.11	8.65	1.71	2.87	3.54	0.56	0.62	0.00	0.56
Mode	12	3	3	3	3	5	0	0	0	0
Median	13	4	11	2	3	5	0	0	0	0
Compatibility status	±		±		-		-		-	

Table 5.2 – Compatibility relationships of POLL-01 *Cosmos bipinnatus* (1995 582) Bip 1 to 5

<i>Cosmos bipinnatus</i> individual		Male Plant				
		Bip 1	Bip 2	Bip 3	Bip 4	Bip 5
Female Plant	Bip 1	—	+	—	+	—
	Bip 2	—	—	—	±	±
	Bip 3	—	±	—	±	±
	Bip 4	—	—	—	—	—
	Bip 5	±	±	—	—	—

Self-pollinations are shaded light grey

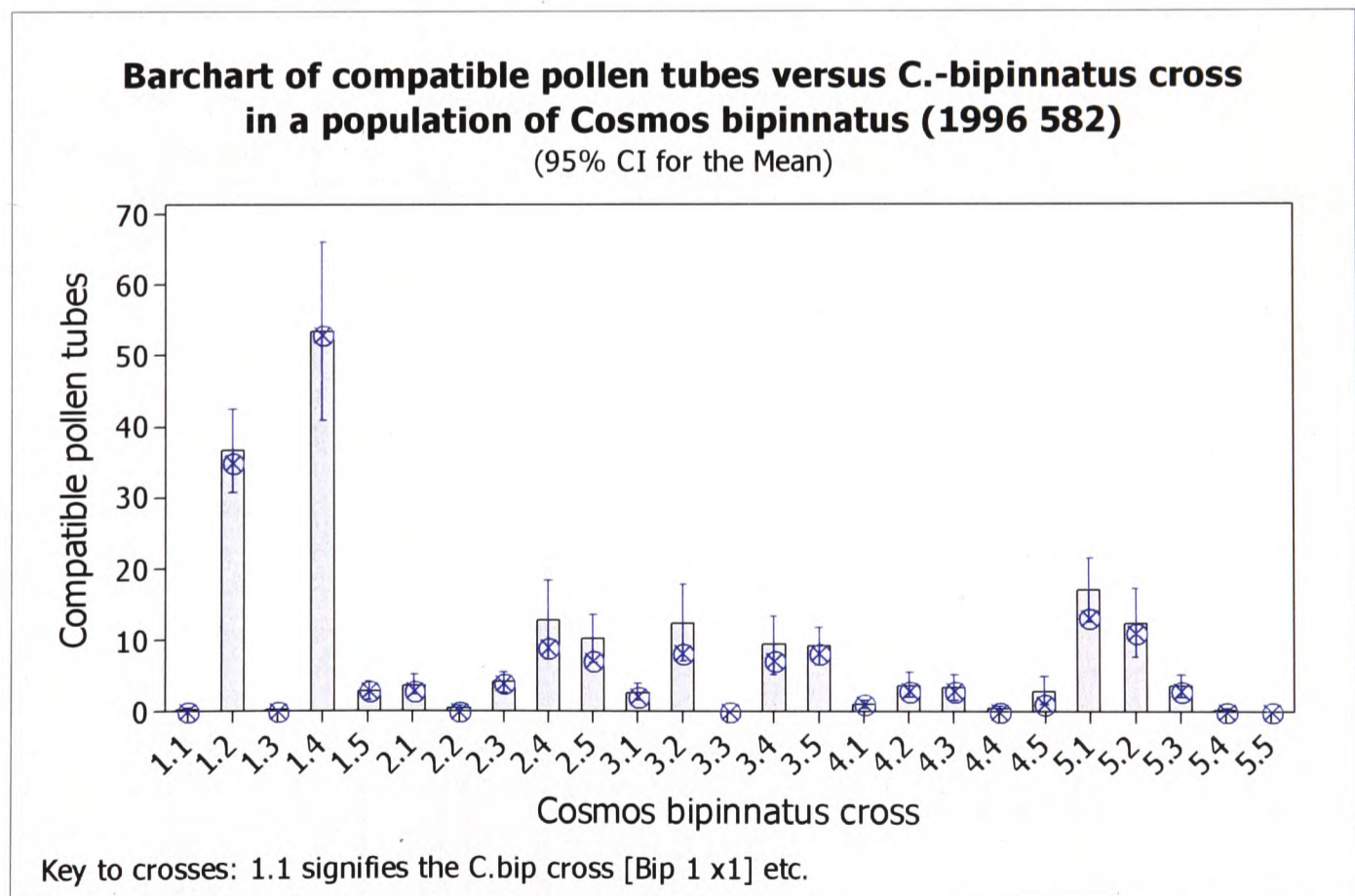


Figure 5.1 – Barchart of compatible pollen tubes produced in all *Cosmos bipinnatus* crosses in pollination experiment POLL-01.
Barchart constructed from data in Tables 5.1a-e

Table 5.3a – POLL-01 *Cosmos atosanguineus* (1999 3819) Atro 1 x Atro 1 to 5.

Female Parent ♀	Male parent ♂									
	Atro 1		Atro 2		Atro 3		Atro 4		Atro 5	
	C	ϕ	C	ϕ	C	ϕ	C	ϕ	C	ϕ
1	0	0	0	0	0	0	0	0	0	0
2	0	0	0	0	0	0	0	0	0	0
3	0	0	0	0	0	0	0	0	0	0
4	0	0	0	0	0	0	0	1	0	0
5	0	0	0	0	0	0	0	0	0	0
6	0	0	0	0	0	0	0	0	0	0
7	0	0	0	0	0	0	0	0	0	0
8	0	0	0	0	0	0	0	0	0	0
9	0	0	0	0	0	0	0	0	0	0
10	0	0	0	0	0	1	0	0	0	0
11	0	0	0	0	0	0	0	1	0	0
12	0	0	0	0	0	0	0	0	0	0
13	0	0	0	0	0	0	0	0	0	0
14	0	0	0	0	0	0	0	0	0	0
15	0	0	0	0	0	0	0	0	0	0
Total	0	0	0	0	0	1	0	2	0	0
Mean	0.00	0.00	0.00	0.00	0.07	0.00	0.00	0.13	0.00	0.00
Standard deviation	0.00	0.00	0.00	0.00	0.00	0.26	0.00	0.35	0.00	0.00
Mode	0	0	0	0	0	0	0	0	0	0
Median	0	0	0	0	0	0	0	0	0	0
Compatibility status	-		-		-		-		-	

Table 5.3b – POLL-01 *C. atosanguineus* (1999 3819) .Atro 2 x Atro 1 to 5

Female Parent ♀	Male parent ♂									
	Atro 1		Atro 2		Atro 3		Atro 4		Atro 5	
	C	ϕ	C	ϕ	C	ϕ	C	ϕ	C	ϕ
1	0	3	0	0	0	1	0	1	0	0
2	0	0	0	0	0	0	0	0	0	0
3	0	1	0	0	0	0	0	0	0	0
4	0	0	0	0	0	3	0	0	0	1
5	0	0	0	0	0	0	0	0	0	0
6	0	0	0	0	0	0	0	0	0	0
7	0	1	0	0	0	0	0	0	0	1
8	0	0	0	0	0	1	0	0	0	2
9	0	0	0	0	0	0	0	0	0	0
10	0	0	0	0	0	0	0	0	0	0
11	0	0	0	0	0	1	0	0	0	0
12	0	1	0	0	0	2	0	1	0	0
13	0	0	0	0	0	0	0	0	0	0
14	0	0	0	0	0	0	0	0	0	0
15	0	0	0	0	0	0	0	0	0	0
Total	0	6	0	0	0	8	0	2	0	4
Mean	0.00	0.40	0.00	0.00	0.00	0.53	0.00	0.13	0.00	0.27
Standard deviation	0.00	0.83	0.00	0.00	0.00	0.92	0.00	0.35	0.00	0.59
Mode	0	0	0	0	0	0	0	0	0	0
Median	0	0	0	0	0	0	0	0	0	0

Compatibility status	-	-	-	-	-
----------------------	---	---	---	---	---

Table 5.3c – POLL-01 *C. atrosanguineus* (1999 3819) Atro 3 x Atro 1 to 5

Female Parent ♀	Male parent ♂									
	Atro 1		Atro 2		Atro 3		Atro 4		Atro 5	
	C	ϕ	C	ϕ	C	ϕ	C	ϕ	C	ϕ
Atro 3 (1999 3819)										
1	0	0	0	0	0	0	0	0	0	0
2	0	0	0	0	0	0	0	0	0	0
3	0	0	0	0	0	0	0	0	0	0
4	0	0	0	0	0	0	0	0	0	0
5	0	0	0	0	0	0	0	0	0	0
6	0	0	0	0	0	0	0	0	0	0
7	0	0	0	0	0	0	0	0	0	2
8	0	0	0	0	0	0	0	0	0	1
9	0	0	0	0	0	0	0	0	0	0
10	0	0	0	0	0	0	0	0	0	0
11	0	0	0	0	0	0	0	0	0	0
12	0	0	0	0	0	0	0	0	0	0
13	0	0	0	0	0	0	0	0	0	0
14	0	0	0	1	0	0	0	0	0	0
15	0	0	0	0	0	0	0	0	0	0
Total	0	0	0	1	0	0	0	0	0	3
Mean	0.00	0.00	0.00	0.07	0.00	0.00	0.00	0.00	0.00	0.20
Standard deviation	0.00	0.00	0.00	0.26	0.00	0.00	0.00	0.00	0.00	0.56
Mode	0	0	0	0	0	0	0	0	0	0
Median	0	0	0	0	0	0	0	0	0	0
Compatibility status	-	-	-	-	-	-	-	-	-	-

Table 5.3d – POLL-01 *C. atrosanguineus* (1999 2254) Atro 4 x Atro 1 to 5

Female Parent ♀	Male parent ♂									
	Atro 1		Atro 2		Atro 3		Atro 4		Atro 5	
	C	ϕ	C	ϕ	C	ϕ	C	ϕ	C	ϕ
Atro 4 (1999 2254)										
1	0	1	0	1	0	0	0	0	0	0
2	0	0	0	1	0	0	0	0	0	0
3	0	0	0	0	0	0	0	0	0	0
4	0	0	0	0	0	0	0	0	0	0
5	0	0	0	0	0	0	0	0	0	0
6	0	1	0	0	0	0	0	0	0	0
7	0	0	0	0	0	0	0	0	0	0
8	0	0	0	0	0	0	0	0	0	0
9	0	0	0	0	0	0	0	0	0	0
10	0	0	0	0	0	0	0	0	0	0
11	0	0	0	0	0	0	0	0	0	1
12	0	0	0	0	0	0	0	0	0	0
13	0	0	0	0	0	0	0	0	0	0
14	0	0	0	0	0	0	0	0	0	0
15	0	0	0	0	0	0	0	0	0	0
Total	0	2	0	2	0	0	0	0	0	1
Mean	0.00	0.13	0.00	0.13	0.00	0.00	0.00	0.00	0.00	0.07
Standard deviation	0.00	0.35	0.00	0.35	0.00	0.00	0.00	0.00	0.00	0.26
Mode	0	0	0	0	0	0	0	0	0	0
Median	0	0	0	0	0	0	0	0	0	0
Compatibility status	-	-	-	-	-	-	-	-	-	-

Table 5.3e – POLL-01 *C. atrosanguineus* (1997 6334) Atro 5 x Atro 1 to 5

Female Parent ♀ Atro 5 (1997 6334)	Male parent ♂									
	Atro 1		Atro 2		Atro 3		Atro 4		Atro 5	
	C	ϕ	C	ϕ	C	ϕ	C	ϕ	C	ϕ
1	0	0	0	0	0	0	0	0	0	0
2	0	0	0	0	0	0	0	0	0	0
3	0	1	0	1	0	0	0	0	0	0
4	0	0	0	0	0	0	0	0	0	0
5	0	0	0	0	0	0	0	0	0	0
6	0	0	0	0	0	0	0	0	0	0
7	0	0	0	0	0	0	0	1	0	0
8	0	0	0	0	0	0	0	1	0	0
9	0	1	0	2	0	0	0	0	0	0
10	0	0	0	0	0	0	0	0	0	0
11	0	0	0	0	0	0	0	0	0	0
12	0	0	0	0	0	0	0	0	0	2
13	0	0	0	0	0	0	0	0	0	0
14	0	1	0	0	0	0	0	0	0	0
15	0	0	0	0	0	0	0	0	0	0
Total	0	3	0	3	0	0	0	2	0	2
Mean	0.00	0.20	0.00	0.20	0.00	0.00	0.00	0.13	0.00	0.13
Standard deviation	0.00	0.41	0.00	0.56	0.00	0.00	0.00	0.35	0.00	0.52
Mode	0	0	0	0	0	0	0	0	0	0
Median	0	0	0	0	0	0	0	0	0	0
Compatibility status	—		—		—		—		—	

Table 5.4 – Compatibility relationships of POLL-01 *C. atrosanguineus* Atro 1 to 5

<i>Cosmos atrosanguineus</i> individual + (accession number)		Male Plant				
		Atro 1	Atro 2	Atro 3	Atro 4	Atro 5
Female Plant	Atro 1 (1999 3819)	—	—	—	—	—
	Atro 2 (1999 3819)	—	—	—	—	—
	Atro 3 (1999 3819)	—	—	—	—	—
	Atro 4 (1999 2254)	—	—	—	—	—
	Atro 5 (1997 6334)	—	—	—	—	—

Self-pollinations are shaded light grey

Table 5.5a – POLL-01 *Cosmos sulphureus* (1996 980) Sul 1 x Sul 1 to 4.

Female Parent ♀	Male parent ♂								
	Sul 1	Sul 1		Sul 2		Sul 3		Sul 4	
		C	ϕ	C	ϕ	C	ϕ	C	ϕ
1		0	0	0	0	2	2	1	1
2		1	3	0	0	3	7	2	2
3		0	0	1	1	0	0	0	0
4		0	0	0	0	0	4	0	0
5		0	4	0	0	3	5	1	1
6		0	2	0	0	0	5	0	0
7		0	0	0	0	1	5	0	0
8		0	0	1	3	0	3	0	0
9		0	0	0	0	0	3	0	0
10		1	2	0	0	0	8	0	1
11		0	0	1	2	0	4	0	3
12		0	0	0	0	1	13	0	0
13		0	0	0	0	0	4	0	0
14		0	0	0	0	3	6	2	4
15		0	0	2	1	1	11	0	2
Total		2	11.	5.	7.	14	80	6	14
Mean		0.13	0.73	0.33	0.47	0.93	5.33	0.40	0.93
Standard deviation		0.35	1.33	0.62	0.92	1.22	3.35	0.74	1.28
Mode		0	0	0	0	0	4, 5	0	0
Median		0	0	0	0	0	5	0	0
Compatibility status		-		-		-		-	

Table 5.5b – POLL-01 *C. sulphureus* (1996 980) Sul 2 x Sul 1 to 4

Female Parent ♀	Male parent ♂								
	Sul 2	Sul 1		Sul 2		Sul 3		Sul 4	
		C	ϕ	C	ϕ	C	ϕ	C	ϕ
1		0	0	0	0	0	1	0	1
2		0	3	0	0	0	1	0	0
3		0	0	0	2	0	0	0	0
4		0	0	0	1	0	1	0	0
5		0	0	0	0	0	0	0	0
6		0	3	0	0	0	0	0	1
7		0	0	0	0	0	5	0	0
8		0	0	0	0	0	0	0	0
9		0	4	0	0	0	0	0	0
10		0	1	0	0	0	0	0	0
11		0	0	0	1	0	0	0	0
12		0	2	0	0	0	3	0	0
13		0	1	0	0	0	0	0	0
14		0	0	0	0	0	0	0	0
15		0	0	0	0	0	0	0	2
Total		0	14	0	4	0	11	0	4
Mean		0.00	0.93	0.00	0.27	0.00	0.73	0.00	0.27
Standard deviation		0.00	1.39	0.00	0.59	0.00	1.44	0.00	0.59
Mode		0	0	0	0	0	0	0	0
Median		0	0	0	0	0	0	0	0
Compatibility status		-		-		-		-	

Table 5.5c – POLL-01 *C. sulphureus* (1996 980) Sul 3 x Sul 1 to 5

Female Parent ♀	Male parent ♂									
	Sul 3		Sul 1		Sul 2		Sul 3		Sul 4	
	C	ϕ	C	ϕ	C	ϕ	C	ϕ	C	ϕ
1	22	1	3	0	0	1	0	0		
2	29	1	1	9	0	0	0	0		
3	19	4	0	5	0	0	0	0		
4	20	1	0	3	0	2	0	0		
5	31	3	0	5	0	0	0	0		
6	37	5	0	3	0	2	0	0		
7	25	2	2	11	0	0	0	0		
8	28	4	0	6	0	0	0	0		
9	31	3	0	0	0	1	0	0		
10	27	2	0	0	0	0	0	0		
11	33	3	0	2	0	1	0	2		
12	38	3	3	3	0	0	0	0		
13	23	1	1	3	0	0	0	0		
14	15	2	0	7	0	0	0	1		
15	21	4	0	0	0	0	0	0		
Total	399	39	10	57	0	7	0	3		
Mean	26.60	2.60	0.67	3.80	0.00	0.47	0.00	0.20		
Standard deviation	6.71	1.30	1.11	3.38	0.00	0.74	0.00	0.56		
Mode	27	3	0	0	0	0	0	0		
Median	31	1	0	3	0	0	0	0		
Compatibility status	+		-		-		-			

Table 5.5d – POLL-01 *C. sulphureus* (1996 980) Sul 4 x Sul 1 to 4

Female Parent ♀	Male parent ♂									
	Sul 4		Sul 1		Sul 2		Sul 3		Sul 4	
	C	ϕ	C	ϕ	C	ϕ	C	ϕ	C	ϕ
1	0	0	0	0	6	2	0	3		
2	0	2	0	0	9	3	0	1		
3	0	0	0	2	26	0	0	0		
4	0	0	0	0	7	3	0	0		
5	0	3	0	0	2	7	0	0		
6	0	0	0	0	1	5	0	0		
7	0	0	0	0	7	4	0	1		
8	0	0	0	0	9	2	0	3		
9	0	0	0	0	3	3	0	0		
10	0	0	0	0	14	5	0	0		
11	0	0	0	0	3	13	0	0		
12	0	3	0	0	19	4	0	0		
13	0	1	0	1	0	9	0	2		
14	0	0	0	0	1	4	0	0		
15	0	0	0	3	15	5	0	2		
Total	0	9	0	6	122	69	0	12		
Mean	0.00	0.60	0.00	0.40	8.13	4.60	0.00	0.80		
Standard deviation	0.00	1.12	0.00	0.91	7.49	3.16	0.00	1.15		
Mode	0	0	0	0	9	3	0	0		
Median	0	0	0	0	7	4	0	0		
Compatibility status	-		-		±		-			

Table 5.6. – Compatibility relationships of POLL-01 *C. sulphureus* (1996 980) Sul 1 to 4

<i>Cosmos sulphureus</i> individual		Male Plant			
		Sul 1	Sul 2	Sul 3	Sul 4
Female Plant	Sul 1	—	—	—	—
	Sul 2	—	—	—	—
	Sul 3	+	—	—	—
	Sul 4	—	—	±	—

Self-pollinations are shaded light grey

5.3.6 – Analysis of pollination experiments in *Cosmos*

(i) Introduction

The following analysis of results focuses on the intraspecific pollinations in the two small populations of *C. bipinnatus* and *C. atrosanguineus*. The *C. sulphureus* pollination data were not scrutinised in detail because many of the analyses and conclusions drawn from *C. bipinnatus* and *C. atrosanguineus* pollinations are pertinent to *C. sulphureus* and also because the pollination times of *C. sulphureus* were not concurrent with the other two *Cosmos* species, and were therefore subject to environmental differences.

In pollination experiments discussed hereafter, UV illumination and aniline-blue staining of self-pollinated stigmas appeared as in Plate 5.6, A, C, D-E, G and I. Strong cross-incompatible stigmas appeared as in Plate 5.10, H, and stigmas exhibiting less strong cross-incompatibility appeared as in Plate 5.4, C-D. Stigmas of compatible pollinations were as in Plate 5.4, E, and semi-compatible stigmas containing pollen of all four Asteraceae compatibility types, appeared as in Plate 5.12, A-B. Statistical analyses of pollination data is presented in Appendix 5.1 and 5.2. Pollen tube germination in *Cosmos* was not distributed normally and so Kruskal-Wallis and Mann-Whitney were used to analyse pollinations results (Appendix 5.1, Boxes 2a-2b, $p = <0.05 \therefore$ reject $^{1a}H_0 - ^{1b}H_0$). There was great variation in the production of compatible pollen tubes in POLL-01 pollinations (Appendix 5.1, Boxes 2c, $p = <0.05 \therefore$ reject $^{1c}H_0$). Analyses of these data are discussed below.

(ii) - Pollination in five *C. bipinnatus* individuals

The most interesting observation in the pollination results of *C. bipinnatus* is the presence of three compatibility groups, i.e. compatible (+), incompatible (-) and inconclusive (\pm) (Table 5.2). Of the 20 cross-pollination pairs, 11 pairs were incompatible, 7 pairs showed inconclusive compatibility, and 2 pairs were compatible (Table 5.2). The high number of cross-incompatible groups indicate that the five *C. bipinnatus* individuals share a small number of S-alleles (Table 5.2). Selfed *C. bipinnatus* individuals exhibit strong SI, having a (mean)/(mode)/(median) of (0.0)/(0)/(0) compatible pollen tubes respectively per selfed stigma (Tables 5.1a-e). Selfed groups separate into two subgroups depending on the number of compatible pollen tubes produced per stigma (Appendix 5.2, Box 2a, $p = 0.05 \therefore$ weak support for not rejecting $^{2a}H_0$; Box 2b, $p = 0.97 \therefore$ cannot reject $^{2b}H_0$). In the first self-incompatible subgroup, represented by Bip 3 and Bip 5, selfing results in a very strong SI response

with zero compatible pollen tubes germinating on stigmas (Appendix 5.2, Box 2a.). In contrast, some stigmas of the second self-incompatible subgroup, represented by Bip 1, Bip 2 and Bip 4, produce a small but significant number of compatible pollen tubes on selfing (<0.5)/(0)/(0) compatible pollen tubes respectively per selfed stigma, and may represent PSC genotypes.

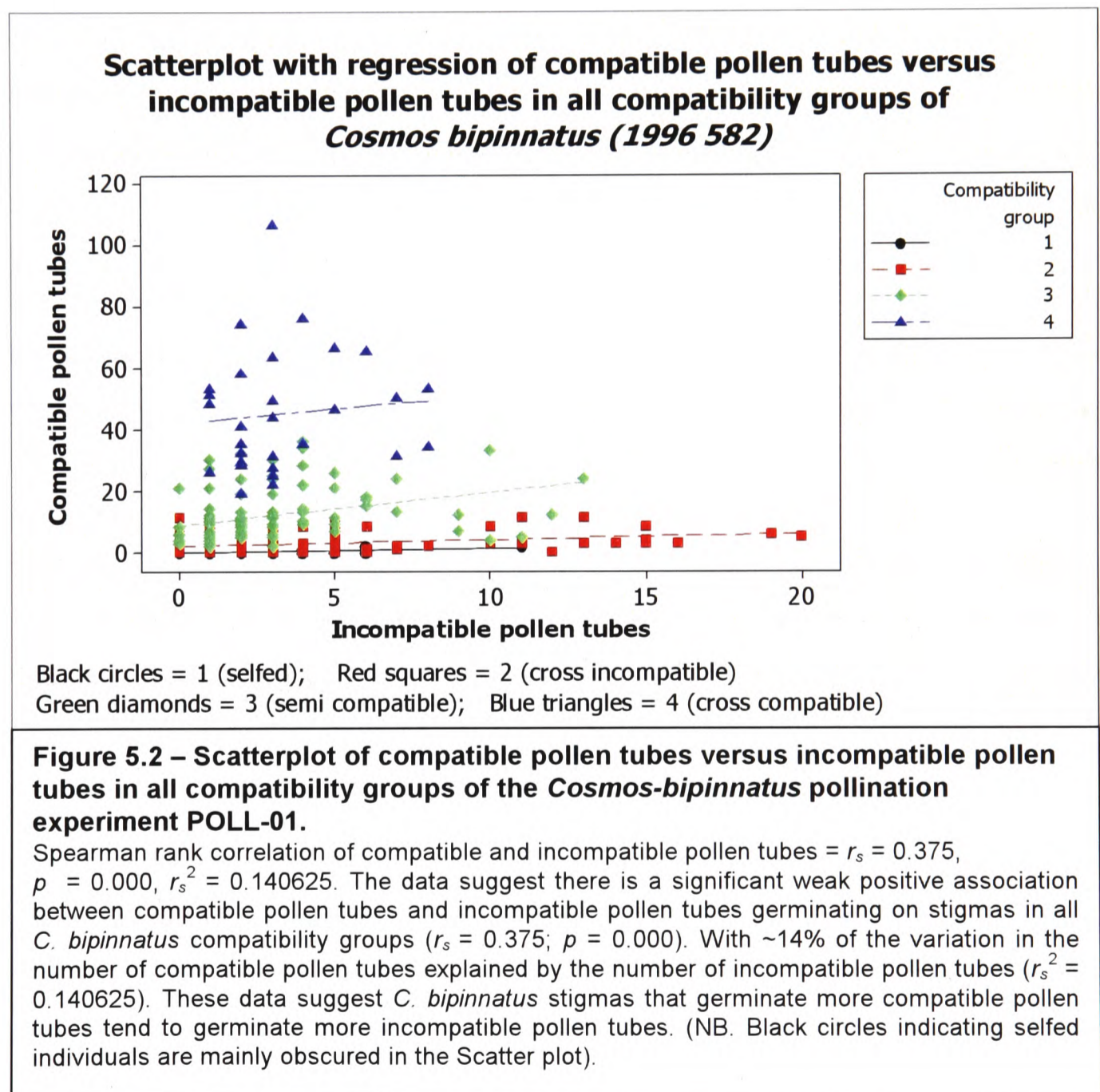
In cross-compatible groups (i.e. non-selfed), the outcrosses [Bip 1 x 3], and [Bip 5 x 4] were the only cross-incompatible pairings to show reciprocal incompatibility (Tables 5.1a-e). They also showed the strongest cross-incompatible reaction in terms of the least number of compatible pollen tubes germinating per stigma with a (mean)/(mode)/(median) = (<0.5)/(0)/(0) respectively (Tables 5.1a-e; Appendix 5.2, Box 3; $p = < 0.05 \therefore$ Reject 3H_0). Incompatibility in these cross pollinations was particularly strong when Bip 1 and Bip 5 were the female partner, with no significant difference observed in the strength of the incompatibility in these two crosses and those of selfed *C. bipinnatus* groups (Appendix 5.2, Box 5, $p = 0.13 \therefore$ cannot reject 5H_0). The reciprocal crosses [Bip 3 x 1] and [Bip 4 x 5], produced a (mean)/(mode)/(median) = (~ 2)/(0)/(1) compatible pollen tubes per stigma, which was significantly more than were produced in selfed groups (Appendix 5.2, Box 3, cf. double underlined crosses). The cross [Bip 4 x 1] also showed strong cross-incompatibility with a (mean)/(mode)/(median) = (~ 2)/(0)/(1) compatible pollen tubes per stigma, but the reciprocal cross [Bip 1 x 4] was fully compatible (Tables 5.1a & 5.1d). These data, and the observation that [Bip 1 x 3], and [Bip 4 x 5] exhibit reciprocal incompatibility suggest that Bip 1 and Bip 3 probably share both S- and G-alleles, and likewise Bip 4 and Bip 5. While Bip 1 and Bip 4, which do not show reciprocal differences in incompatibility, probably share one S- and/or G-allele in common, with dominance interactions occurring between S-alleles (DeMauro, 1993; Reinartz and Les, 1994).

As observed for selfed individuals, *C. bipinnatus* cross-incompatible groups divide into distinct subgroups that identify three strengths of cross incompatibility. Members of the first cross-incompatible subgroup, represented by [Bip 1 x 3] and [Bip 5 x 4], exhibit a very strong cross-incompatible reaction equivalent to that observed in self-incompatible groups, producing a (mean)/(mode)/(median) of (>0.5)/(0)/(0) compatible pollen tubes per stigma respectively (Tables 5.1a-e; Appendix 5.2, Box 5, $p = 0.13 \therefore$ cannot reject 5H_0). In addition, members of subgroup 1 exhibit reciprocal cross-incompatibility, although reciprocal crosses may not exhibit the same strength of cross-incompatibility. Members of the second cross-incompatible subgroup, represented by

the crosses [Bip 4 x 1] and [4 x 5], produce a (mean)/(mode)/(median) of (>1<3)/(0)/(1) compatible pollen tubes per stigma respectively, which is significantly more than in selfed groups (Appendix 5.2, Box 4, $p = <0.05 \therefore$ reject 4H_0), but significantly fewer than in members of the third cross-incompatible subgroup that produce a (mean)/(mode)/(median) of (~2-4)/(0-5)/(2-4) compatible pollen tubes per stigma (Appendix 5.2, Box 6, $p = <0.05 \therefore$ reject 6H_0 ; Boxes 7-8, $p = >0.05 \therefore$ cannot reject 7H_0 & 8H_0). Subgroup 3 contains the weakly cross-incompatible crosses [Bip 1 x 5], [Bip 2 x 1], [Bip 2 x 3], [Bip 3 x 1], [Bip 4 x 2], [Bip 4 x 3] and [Bip 5 x 3], and is the commonest type of cross-incompatibility observed in *C. bipinnatus*. Members of cross-incompatible subgroups 2 and 3 are reciprocally compatible or semi-compatible. In diploid and tetraploid races of *Rutidosia leptorrhynchoides* (Asteraceae) the likelihood of one-way compatibility and reciprocal incompatibility increased with relatedness of individuals crossed (Young *et al.*, 2000). The high frequency of one-way compatibility and semi-compatibility in this *C.-bipinnatus* population, and the low incidence of reciprocal compatibility, indicates that the five *C.-bipinnatus* individuals used in this study are close relatives and must share at least one S-allele. Unfortunately, seed set for each *C. bipinnatus* pollination was not assessed so it was not possible to confirm whether compatible pollen tubes observed on stigmas actually led to fertilization and seed production. Statistically the difference in the numbers of compatible pollen tubes produced by cross-incompatible subgroup 3 is significant (Appendix 5.2, Box 6, $p = <0.05 \therefore$ reject 6H_0 and Box 8, $p = 0.77 \therefore$ cannot reject 8H_0), and it may be that the occasional production of compatible pollen tubes, in these incompatible groups, creates flexibility in the reproductive biology of *C. bipinnatus* and offers a selective advantage to the species. The molecular control of this process may be the result of interaction of G- and S-alleles, or be the consequence of the action of modifier loci, akin to the putative PSC modifier loci, that in some way are able to reduce the strength of cross-incompatibility. The semi-compatibility observed in the reciprocal crosses; [Bip 1 x 5], [Bip 2 x 1], [Bip 2 x 3] [Bip 4 x 2] and [Bip 4 x 3] suggest an epistatic interplay of S- and G-alleles is occurring in these crosses: it is conceivable that differential displays in the strength of cross incompatibility observed in this in *C. bipinnatus* population are achieved by G-locus-controlled down regulation of S.

The number of incompatible category-2 type pollen tubes per stigma is not contingent on compatibility group, with considerable variation occurring within and between compatibility groups (Appendix 5.2, Boxes 9-12, $p = <0.05 \therefore$ reject 9H_0 to ${}^{12}H_0$). There was a weak but significant positive association between compatible pollen and incompatible category-2 type pollen tubes germinating on *C. bipinnatus* stigmas

(Appendix 5.2; Boxes 13, 24-25, $r_s = \sim 0.40$, $p = < 0.05$ \therefore reject $^{13}H_0$, $^{24}H_0$ - $^{25}H_0$ and Figure 5.2), indicating that stigmas germinating more compatible pollen tubes tend to germinate more incompatible pollen tubes. This observation most probably reflects the effects of environmental factors such as humidity, temperature and light on the pollen-stigma interaction, as these factors are known to affect stigma competence, pollen viability and pollen-tube growth (Emerson, 1940; Dumas and Gaude, 1981; Dickinson and Elleman, 1985, 1994; La Porta and Roselli, 1991; Thomson *et al.* 1994; Kumar *et al.*, 1995; Stone *et al.*, 1995; Tangmitcharoen and Owens, 1997), and reiterates the necessity for caution when comparing pollination experiments undertaken in differing environmental conditions. As occurred in this study with *Cosmos sulphureus* pollination experiments.



The seven inconclusive crosses [Bip 2 x 4], [Bip 2 x 5], [Bip 3 x 2], [Bip 3 x 4], [Bip 3 x 5], [Bip 5 x 1] and [Bip 5 x 2] germinated significantly lower numbers of compatible pollen per stigma than cross-compatible pollinations, but significantly more compatible pollen tubes than cross-incompatible groups (Appendix 5.2, Boxes 14-15, $p = < 0.05$ \therefore

reject $^{14}H_0 - ^{15}H_0$). The seven members of this inconclusive compatibility group exhibited similar levels of compatibility producing a (mean)(mode)/(median) of (9-17)(3-12)/(7-13) compatible pollen tubes per stigma respectively (Tables 5.1a-e; Appendix 5.2, Boxes 16-17, $p = >0.05 \therefore$ cannot reject $^{16}H_0$ or $^{17}H_0$). These seven inconclusive compatibility pairings were categorised as being semi-compatible, and defined as having an average of >5 but <20 compatible pollen tubes per stigma. *C. bipinnatus* semi-compatible groups were distinguishable from compatible groups by the numbers of *P*-type pollen tubes on their stigmas. Most cross-compatible pollinations do not germinate *P*-type pollen, or germinate them in much fewer numbers than occur on semi-compatible stigmas. On semi-compatible stigmas, compatible pollen and *P*-type pollen segregate in a ratio of $<2:1$ respectively, whereas compatible groups have a ratio of $>20:1$ compatible pollen : *P*-type pollen (Plate 5.12). *P*-type pollen was never observed in self-pollinations, and occurred rarely in cross-incompatible groups. The difference in the ratio of compatible pollen to *P*-type pollen is therefore a useful marker for distinguishing semi-compatible individuals. For example, the semi-compatible cross [Bip 5 x 1] germinated a significantly higher number of compatible pollen tubes per stigma; (i.e. $\sim 12-13$ compatible pollen tubes), than semi-compatible crosses [Bip 2 x 4], [Bip 2 x 5], [Bip 3 x 2], [Bip 3 x 4], [Bip 3 x 5] and [Bip 5 x 2], (i.e. $\sim 7-8$ compatible pollen tubes) Appendix 5.2, Box 16, highlighted data). Initially, [Bip 5 x 1] was identified as being weakly compatible and assigned to the compatible group along with [Bip 1 x 2] and [Bip 1 x 4]. However, the difference in the number of compatible pollen tubes produced in [Bip 5 x 1] and the other two cross-compatible groups was significantly larger than between [Bip 5 x 1] and semi-compatible groups (Appendix 5.2, Boxes 18-21, $p = <0.05 \therefore$ reject $^{18}H_0$ to $^{21}H_0$). On the strength of these data, and the observed $\sim 2:1$ -segregation of compatible and *P*-type Bip-1 pollen on Bip-5 stigmas, [Bip 5 x 1] was re-assigned to the semi-compatible group.

Two cross-compatible groups, [Bip 1 x 2] and [Bip 1 x 4] were identified in the 20 cross pollinations. Both these cross-compatible pairings were reciprocally incompatible, and showed wide differences in the production of compatible pollen tubes with few or no *P*-type pollen tubes observed on stigmas (Appendix 5.2, Box 19, $p = <0.05 \therefore$ reject $^{19}H_0$). As only two cross-compatible pairings were identified, the sample-size for this compatibility group was too small to assess whether the number of compatible pollen tubes produced by [Bip 1 x 2] and [Bip 1 x 4] represents extremes, or norms of cross-compatibility in *C. bipinnatus* (Appendix 5.2, Box 23, $p = <0.05 \therefore$ reject $^{23}H_0$). A larger population size may reveal an overlap in the numbers of compatible pollen tubes produced by weakly compatible individuals and those with

strong semi-compatibility, reflecting a continuum in cross compatibility from weak to strong, as was observed in populations of *Aster furcatus* and *Scalesia affinis* (Reinartz and Les, 1994; Nielsen *et al.*, 2003). If this were the case, then the ratio of compatible and *P*-type pollen tubes may be an important criterion for distinguishing strong semi-compatible pollinations from weak cross-compatible ones. A recommendation from this study would be to record incompatible pollen tubes as two groups that identify *P*-type and category-2 type pollen separately

The identification in *C. bipinnatus* of semi-compatible groups indicates the presence of a cryptic *Cosmos* G-gene. The semi-compatible cross [Bip 2 x 5] was unique, since it was the only semi-compatible cross to show reciprocal semi-compatibility (Tables 5.1a-e and 5.2), whereas all other semi-compatible crosses displayed reciprocal incompatibility. The reciprocal differences observed in semi-compatible, cross-incompatible and cross-compatible groups suggest *S*-alleles in *Cosmos* interact differently in pollen and stigma, and that dominance interaction of *S*-alleles is occurring in this *C.-bipinnatus* population. As observed for self-incompatible and cross-incompatible groups, *C. bipinnatus* appears to exhibit different strengths of semi compatibility and cross compatibility. These differences in the strength of *Cosmos* compatibility could be attributed to differences in microclimate, but may also have a genetic component resulting from the action of *S*-unlinked modifier loci on *S*- and/or *G*-alleles.

(iii) – Estimating possible *S*-allele specificities in five *Cosmos bipinnatus* (1996 582) individuals Bip 1 to Bip 5

Bip 4 stigmas showed the highest level of incompatibility, rejecting pollen from all Bip individuals (Table 5.1d), suggesting that expression of at least one *S*-allele of Bip-4 stigma matches the expression of *S*-alleles in pollen of all other Bip individuals. In contrast, Bip-4 pollen was one of the most successful, producing a compatible or semi-compatible reaction in three out of four cross pollinations, indicating that the activity of *S*-alleles in the pollen is being modified or suppressed (Tables 5.1a-e). Bip-1, Bip-2, Bip-3 and Bip-5 stigmas exhibited cross compatibility with at least one Bip individual, with Bip-1 and Bip-3 stigmas showing the broadest range of compatibility relationships. For example, Bip-1 stigmas were compatible with Bip-2 and Bip-4 pollen, but rejected pollen from Bip-3 and Bip-5, while the Bip-3 stigma was semi-compatible with all cross pollen aside from Bip-1, which it rejected. These data affirm the supposition made above that Bip 1 and Bip 3 probably share both *S*- and *G*-alleles. In contrast, Bip 1 and Bip 3, were the least successful pollen donors, with Bip-3 pollen being rejected by all

Bip stigmas, and Bip-1 pollen being rejected by all but the Bip-5 stigma. These data suggest that expression of S- and/or G-alleles in Bip-3 pollen matches the expression of S- and G-alleles in all Bip stigmas, and that dominance interaction of S-alleles is also occurring in this *C. bipinnatus* population. Apart from the exceptional crosses [Bip 2 x 4], [Bip 3 x 5] and [Bip 5 x 1], all compatibility groups observed in the 25 *C.-bipinnatus* pollinations discussed above can be explained by invoking a minimum of four S-alleles; S_1 , S_2 , S_3 , and S_4 , if: $(S_2 > S_1) = S_3 = S_4$, in the stigma, and $(S_4 > S_1) = S_2 = S_3$ in the pollen¹⁰. The distribution of S-alleles in *C.-bipinnatus* individuals as described in Table 5.6 accords with the compatibility groups recorded in Tables 5.1a-e and supports the suppositions that (i) Bip 1 and Bip 3 share both S- and G-alleles, (ii) Bip 1 to Bip 5 share at least one S-allele (iii) dominance interaction of S-alleles operates in this *C.-bipinnatus* population and (iv) exceptional crossing results are associated with semi-compatible groups.

Table 5.7 - Possible S- and G-alleles in *C. bipinnatus* individuals Bip 1 to Bip 5

<i>C. bipinnatus</i> individual	Possible S-alleles in stigma	Possible S-allele in pollen	Possible G-alleles
Bip 1	$S_1 \underline{S_2}$	$S_1 S_2$	$G_1 G_2$
Bip 2	$S_1 S_3$	$S_1 S_3$	$G_1 G_1$
Bip 3	$S_1 \underline{S_2}$	$S_1 S_2$	$G_1 G_2$
Bip 4	$S_1 S_4$	$S_1 \underline{S_4}$	$G_1 G_2$
Bip 5	$S_2 S_4$	$S_2 S_4$	$G_2 G_2$

Dominant S-alleles are highlighted in bold and underlined

Table 5.8 – Compatibility relationships of POLL-01 *C. bipinnatus* (1995 582) Bip 1 to 5

Possible dominance relationships of S-alleles in stigma (♀) and pollen (♂)			Male Plant (♂)				
			Bip 1	Bip 2	Bip 3	Bip 4	Bip 5
			$S_1 S_2$	$S_1 S_3$	$S_1 S_2$	$S_1 \underline{S_4}$	$S_2 S_4$
Female Plant (♀)	Bip 1	$S_1 \underline{S_2}$	—	+	—	+	—
	Bip 2	$S_1 S_3$	—	—	—	±	±
	Bip 3	$S_1 S_2$	—	±	—	±	(±)
	Bip 4	$S_1 S_4$	—	—	—	—	—
	Bip 5	$S_2 S_4$	(±)	±	—	—	—

Key: Exceptional crosses are in brackets. Dominant S-alleles are in bold and underlined. Compatible crosses +, incompatible crosses, —; semi-compatible crosses, ±; anomalous semi-compatible crosses, (±). Self-pollinations are highlighted light grey.

¹⁰ The symbol, = represents codominance, and > represents dominance.

The S-alleles assigned to Bip 1 - Bip 5 predict full cross compatibility for the five semi-compatible crosses, [Bip 2 x 5], [Bip 3 x 2], [Bip 3 x 4], [Bip 2 x 4] and [Bip 5 x 2] (Table 5.8). Since the ratio of compatible pollen tubes to *P*-type pollen tubes was not recorded systematically in this study, it is not possible to determine whether these semi-compatible crosses represent weak cross-compatible pairings or truly semi-compatible groups. A detailed examination of the germination of compatible pollen tubes and *P*-type pollen may reveal these crosses to be weakly cross compatible, or there may be other components in these crosses that down regulate the compatibility reaction. The important observation in these semi-compatible crosses is the germination of compatible pollen tubes, albeit in lower numbers than expected, indicating that the expression of S-allele specificities is being down regulated, but not contravened. In contrast, the anomalous semi-compatible crosses [Bip 3 x 5] and [Bip 5 x 1] do contradict their assigned S-allele specificities, since the genetics predicts cross-incompatibility for these two crosses (Tables 5.5 and 5.6). Anomalous results, particularly compatible (+) or semi-compatible (\pm) reactions within groups predicted to be 100% cross incompatible, have been observed previously in self-incompatible species of Asteraceae, and are thought to be a consequence of the action of an Asteraceae G-gene (Table 1.4; Hughes and Babcock, 1950; Gerstel, 1950; Crowe, 1954; Hiscock 2000a, 2000b; Brennan *et al.*, 2002).

If, as in *Brassica*, the putative *Cosmos* G-gene is diallelic, and complementary to S, then only when G- and S-alleles in the pollen match G- and S-alleles in the stigma will complete incompatibility be achieved, with unmatched combinations of G precluding the expression of matched S-genotypes. The anomalous semi-compatible cross [Bip 5 x 1] could thus be explained by the G-specificities described in Table 5.7. In the case of the cross [Bip 5_(S2S4-G2G2) x Bip 1_(S1S2-G1G2)], which is predicted from its S-alleles to be incompatible, Bip-1_(S1S2-G1) pollen would germinate compatible pollen tubes on Bip 5_(S1S4-G2G2) stigmas because G-alleles in stigma and pollen are unmatched. However, Bip-1_(S1S2-G2) pollen, carrying the alternative G₂ allele, would be incompatible as they match the G₂ allele in Bip-5_(S2S4-G2G2) stigma. The anomalous semi-compatible phenotype [Bip 5 x 1] may therefore be explained as a consequence of the differential interaction of G₁ and G₂ pollen on the G₂G₂ stigma, and hence incompatible-(G₂) *P*-type pollen tubes, segregate from compatible-(G₁) pollen tubes in the stigmatic tissue. The reciprocal cross, [Bip 1_(S1S2-G1G2) x Bip 5_(S2S4-G2G2)] would be 100% incompatible because all Bip-5 pollen carries the G₂-allele, and so S- and G-alleles are matched in stigma and pollen. The anomalous semi-compatible cross [Bip 3_(S1S2-G1G2) x Bip 5_(S2S4-G2G2)] cannot similarly be explained, as S- and G-alleles are matched and this cross should

therefore be incompatible. Aside from experimental error, this observation is difficult to explain with respect to S- and G-specificities ascribed to Bip 4 and Bip 5 in Table 5.7, and shows the importance of supporting pollen-tube germination data with seed set data. The results of the [Bip 3 x 5] cross show a second anomaly in that a greater number of incompatible type-2 pollen was recorded for this anomalous semi-compatible cross (i.e. mean ~7 type-2 pollen) compared with the other anomalous semi-compatible cross [Bip 5 x 1] (i.e. mean ~4 type-2 pollen). It may be that the putative *Cosmos* G-gene exhibits varying strengths of expression depending on the S-allele genetic background.

The G-alleles in Table 5.7 help to explain the exceptional cross [Bip 5 x 1], however they contradict the compatibility observed in the four cross-incompatible groups; [Bip 2 x 1], [Bip 2 x 3], [Bip 5 x 3] and [Bip 5 x 4]. In these S-matched cross-incompatible groups, G-alleles are unmatched, and so, according to Lewis (1994) (Table 1.4), their phenotypes should be semi-compatible or cross-compatible. In *Brassica*, the G-genotype is known to be expressed in some S-matched genotypes, particularly those high in the dominance series, but not others, and it may be that these four cross-incompatible groups contain such an S-matched genetic background (Lewis, 1994). If so, then for the hypothetical S- and G-alleles ascribed to this *C. bipinnatus* population, the S-matched genotypes [S₁S₂ x S₁S₃], [S₁S₂ x S₂S₄] and [S₁S₄ x S₂S₄] may be unaffected by expression of unmatched G-genotypes. This feature appears to reside in the interplay between specific S-allele combinations, as the unmatched G-genotype in the S-matched genotype [S₁S₃ x S₁S₄] is semi compatible, as occurs in the cross [Bip 2 x 4]. The dominance relationships of S-alleles have not been categorised for any extant *C. bipinnatus* population. However, should such work be undertaken, it would be interesting to note whether expression of unmatched G-alleles in *Cosmos* is associated with specific S-allele combinations, such as those high in the dominance series, as occurs in *Brassica* and *Raphanus* (Lewis, 1994).

The data from *C. atrosanguineus* pollinations contrast sharply with those from *C. bipinnatus*. In the small *C. atrosanguineus* population, Atro1 to Atro 5 produced only cross incompatible groups, and all Atro cross pollinations exhibited strong incompatibility, with no difference observed in the reaction of crossed and selfed individuals. These data suggest that S- and G-alleles are matched in the five *C. atrosanguineus* individuals, that PSC modifier loci are not expressed in these five individuals and that this *C. atrosanguines* population is made up of clones.

5.4 – Discussion

5.4.1 - Introduction

Since S-allele specificities were not known for the three *Cosmos* populations, the various allelic interactions and compatibility groups cannot be quantified accurately. However, observations of pollinated stigmas, and compatibility pairs have identified some generalities about *Cosmos* SI. *Cosmos* appears to have a gametophytic-sporophytic (G-S) SI system and exhibits dominance interaction of S-alleles. Evidence of PSC was observed in some stigmas of selfed *C. bipinnatus* individuals, but was not observed in selfed individuals of *C. atrosanguineus*. The strong incompatibility observed in *C. atrosanguineus* is probably due to the clonal status of cultivated individuals allied to an inability of the species to override SI. In several Asteraceae species, loss of S-alleles due to founder effects, genetic drift and/or the selective collection of alleles, all of which have probably occurred in *C. atrosanguineus*, can lead to the breakdown of SI (Reinartz and Les, 1994; Nielsen *et al.*, 2003). This breakdown is controlled by genes, unrelated, but epistatic to the S-locus, which express self-compatibility factors capable of weakening or suppressing SI (Thompson and Taylor, 1966a; Ronald and Ascher, 1975). In small populations, genetic drift adversely reduces allelic richness. Models for single-locus SSI suggest that a maximum of four S-alleles requires a population of 32 individuals, while 16 individuals would be incapable of maintaining critical S-allele numbers (DeMauro, 1993; Reinartz and Les, 1994). Polyploidy is also associated with the breakdown of SI particularly for individuals with GSI (Nielsen, *et al.* 2003). However, for SSI species, and Asteraceae in particular, very low rates of SI-breakdown are observed in diploids and tetraploids (Nielsen, *et al.* 2000; Young *et al.* 2000). Artificial populations of *Tragopogon* hinted at higher rates of selfing in tetraploid *T. mirus* (*T. dubius* x *T. porifolius*) than diploid *T. dubius*, however wild populations of the same species showed significantly higher rates of outcrossing in the tetraploid than the diploid (Cook and Soltis, 1999; 2000). High out-crossing rates were also observed in natural populations of *Scalesia divisa*, an Asteraceae of the Galápagos Islands that has undergone several founder events (Nielsen, *et al.* 2000). In contrast, polyploid *Scalesia affinis*, which is also a successful founder species of the Galápagos Islands, exhibits “partially active self-incompatibility” (Nielsen, *et al.* 2003), (or conversely, strong pseudo-self compatibility) in which selfed individuals produce considerably fewer achenes than outcrosses, and have stigmas that remain receptive for longer. In addition, differential strengths of self-compatibility were observed across the population, with some individuals producing no achenes per capitulum on selfing while others produced as many as 30 (Nielsen, *et al.* 2003). Similar observations have been made for natural Asteraceae populations of

Pyrrhopappus carolinianus, *Aster furcatus*, *Arnica montana*, *Centaurea solstitialis* and *Rutidosia leptorrhynchoides* (Estes and Thorp, 1975; Reinartz and Les, 1994; Luijten, *et al.*, 1996; Maddox *et al.*, 1996; Young *et al.*, 2000 respectively). The success of *Scalesia affinis* as a founder species is attributed to its transformation from a fully self-incompatible to a partially self-incompatible species (Nielsen, *et al.* 2003). It is suggested that, either the number of individuals in the original founder *S. affinis* population were too few to produce viable numbers of S-alleles, or genetic drift reduced S-alleles to non-viable levels. In such a population, selection for PSC or SC phenotypes, capable of producing viable seed would be an advantage, and so partially self-incompatible individuals would be favoured as they increase fecundity. SI in *S. affinis* has not totally dissolved, and it appears that this species retains the best of both worlds, with selfing producing significantly fewer viable seeds than outcrossing, and strongly self-incompatible individuals remaining in the population. However, like vegetative reproduction, PSC/partial self-incompatibility in *S. affinis* may allow time for mutation effects to produce a sufficient number of S-alleles to permit sexual reproduction (Reinartz and Les, 1994; Young *et al.*, 2000; Nielsen, *et al.* 2003). The data from *C. bipinnatus* pollination experiments in this study, albeit a small population, reflect the compatibility behaviour in *Scalesia affinis* and other Asteraceae species where differential levels of PSC have been identified (Reinartz and Les, 1994; Hiscock *et al.*, 2000a; Young *et al.*, 2000; Nielsen, *et al.* 2003). However, in *Cosmos atrosanguineus*, PSC was never observed. According to the hypothesis presented here, the two known sites of wild *C. atrosanguineus* populations in Mexico are suggested to represent neotetraploid founder populations that have undergone a reduction in S-allele numbers. Since seed was collected from both these populations, S-allele numbers were clearly sufficient to sustain sexual reproduction in these wild populations. However as European progeny from this Mexican seed were lost, S-allele numbers may have fallen below viable levels. The effects of inbreeding depression may have compounded this situation, as lower seed/ovule ratios are known to occur in Asteraceae species after only one or two generations of inbreeding (DeMauro, 1993; Nielsen *et al.*, 2003). Since PSC or partial self-incompatibility was never observed in *C. atrosanguineus* accessions, existing genets probably represent self-incompatible individuals in which PSC modifier loci are not present or not expressed. The selection pressure on this species is so great that even weakly PSC individuals would surely be promoted. It may be that the *C. atrosanguineus* genome never contained PSC-modifier loci, or its PSC genets have been lost from extant European populations. A similar scenario was recorded for Illinois (US) populations of *Hymenoxys acaulis* var. *glabra* (Asteraceae), the Lakeside Daisy. Like *C. atrosanguineus*, *H. acaulis* is a herbaceous

perennial that persists through the winter and spreads vegetatively by rhizomes. The species exhibits SSI and produces normal viable pollen. However by the late 1970s industrial development reduced Illinois populations to 30 clones, all of which were incapable of producing seed. By the 1970s, the last Illinois Lake daisy population effectively became extinct, with the persistence of the population due solely to vegetative growth (DeMauro, 1993). Recovery protocols were developed for this population by introducing S-allelic variability from related but heterogenic *H. acaulis* populations from Ohio. Since neither wild nor heterogenic populations of *C. atrosanguineus* exist, its recovery and conservation in Mexico will require different methods that rely on chemical and/or molecular suppression of *Cosmos* SI.

5.4.2 – Interspecific pollinations between *C. atrosanguineus* x *C. bipinnatus*

Interspecific pollinations between *Cosmos bipinnatus* and *C. atrosanguineus* generally result in a category-1 type incompatibility reaction. However, category-2 type cross pollen tubes were observed on stigmas of both *Cosmos* species, with *C. bipinnatus* germinating pollen tubes more readily on *C. atrosanguineus* stigma than vice versa. These results indicate that the pollen-stigma reaction in *Cosmos* is specific and accord with the results from similar work undertaken in *Arabidopsis* (Zinkl, *et al.* 1999). Both species of *Cosmos* germinated pollen tubes more readily when placed on stigmas in higher humidity environments (70%) than in ambient humidity, indicating the importance of pollen hydration in the germination of *Cosmos* pollen. The observation from cross pollination experiments (5.3a-e) and these interspecific pollinations show that *C. atrosanguineus* has the capacity to germinate an occasional category-2 incompatible pollen tube, and on rare occasions to produced emaciated *P*-type pollen (Plate 5.9), when placed in high humidity environments. Even on selfing, high humidity environments encourage the release of the *Cosmos* pollen coat onto stigma papillae (Plate 5.7, F-G) a feature that was observed in *Arabidopsis* also (Zinkl, *et al.*, 1999). It appears, that if the ambient humidity is high enough, then germination of *Cosmos* pollen may occur without direct uptake of water from the stigma. However, these high-humidity-induced pollen tubes are thin and weak, and grow haphazardly on the stigma. They cease growth when tubes are between 1-5 pollen grains in length and pollen food reserves become depleted. The observations indicate that *C. atrosanguineus* pollen is capable of germination. It also reveals the crucial role the stigma plays in maintaining the integrity of the pollen, as only when communication between pollen and stigma is maintained throughout the pollen's passage to the ovary, can the growth of the pollen be sustained. In category-1 and category-2 incompatible pollen this communication is never initiated, or ceases early, before penetration of the stigma,

whereas communication in *P*-type pollen is maintained until stigma penetration, but ceases thereafter. These data identify the *Cosmos* stigma as the main resourcer of the *Cosmos* pollen tube in its passage through the conducting tissue.

5.4.3 – Pollen-stigma interactions in *Cosmos*

The interactions of the *Cosmos* pollen and stigma show features characteristic of the pollen-stigma interaction observed in other species of Asteraceae, with category-1 and category-2 incompatibility being the most prevalent, and *P*-type pollen being associated with exceptional semi-compatible groups (Gerstel and Riner, 1950; Lewis, 1994; Hiscock, 2000). The 90° bend observed in compatible *Cosmos* pollen tubes accords with observations from pollination studies in other species of Asteraceae such as *Senecio squalidus* (Hiscock, 2000a; Hiscock *et al.*, 2002) and species of *Parthenium* (Lewis, 1994). The directional growth and maintenance of the *Cosmos* pollen tube on its journey to the stigma is crucial to successful fertilization and may be under long-range control of genes in the stigma, as has been observed in *Arabidopsis* (Hülkamp *et al.*, 1995). The *Cosmos* pollen stigma-interaction appears to occur initially between the pollen coat and the stigma pellicle, and brings about the formation of an adhesive foot layer that facilitates pollen hydration. However, in *Arabidopsis thaliana* it has been shown that the initial binding of pollen and stigma is independent of the extracellular pollen coat, and the *Arabidopsis* pollen-adhesion molecules are thought to reside in the exine, not in the tryphine pollen coat, and are lipophilic in nature (Zinkl, *et al.*, 1999). Observations of fibrillar processes extending from the outer surface of *Cosmos* pollen tubes, suggest pollen-adhesion molecules in *Cosmos* may also be lipophilic and similarly located to the exine.

5.4.4 - Conclusion

The interaction of pollen and stigma in *Cosmos* is characteristic of Asteraceae species, consisting of four categories of pollen-stigma interaction and exhibiting anomalous crossing results. There is strong evidence that a G-S self-incompatibility system operates in *Cosmos* and that dominance interaction of S-alleles is prevalent in the genus. PSC appears to operate in *C. bipinnatus*, but was not observed in *C. atrosanguineus*. Bud pollinations and application of saline solution to stigmas were unable to override SI.

CHAPTER 6 - In search of the Cosmos SI gene

6.1 – Introduction

6.1.1 - The S-domain multigene family

S receptor kinase (*SRK*) and S-locus glycoprotein (*SLG*) are members of the complex S-domain multigene family (Table 6.1), which includes *SRK*, the *Brassica* female SI gene, and non-SI S-locus linked genes such as *SLG*, *BcRK1* (Suzuki *et al.* 1997), *BcRL1* and *BcSL1* (Kai *et al.* 2001). A third category of S-genes includes *SLR1* (Lalonde *et al.* 1989), *NS₁* (Isogai *et al.* 1987, 1988, 1991), *AtS1* (Dwyer *et al.*, 1992) *SLR2* (Boyes *et al.* 1991), and *SLR3* (Cock *et al.* 1995) that are independent of the S-locus, and as such cannot be involved in SI directly. However, the expression pattern of *SLR1*, in the stigma at the onset of anthesis, indicates a role in the pollination process probably associated with pollen adhesion (Luu *et al.* 1997). Another group of non-S-locus linked S-family genes *SFR1*, *SFR2*, *ARK 1* and *ARK3* have dual functions in plant development and plant response to wounding and/or bacterial infection, which postulates a link between development and disease-resistance signalling pathways (Pastuglia *et al.*, 1997, 2002). The functions of the remaining non-S-locus S-genes are unknown, or inferred from sequence similarity to other S-genes. The functions of the S-locus linked genes *SRK* and *SLG* have been determined empirically. *SRK* is essential for self-incompatibility in *Brassica* species while *SLG* appears to participate in pollen-stigma adhesion and may also act as a facilitator to *SRK* by a process that has yet to be identified (Luu *et al.* 1997; Takasaki *et al.* 2000)

Table 6.1 S-domain genes: abbreviations, names and plant origin

Gene Name	Gene Name	Plant Source
<i>AtS1</i>	<i>Arabidopsis thaliana self-incompatibility locus</i>	<i>Arabidopsis thaliana</i>
<i>ARK1</i>	<i>Arabidopsis</i> receptor kinase 1	
<i>ARK2</i>	<i>Arabidopsis</i> receptor kinase 2	
<i>ARK3</i>	<i>Arabidopsis</i> receptor kinase 3	

Table 6.1 continued

Gene Name	Gene Name	Plant Source
<i>BcRK1</i>	<i>Brassica campestris</i> receptor kinase 1	<i>Brassica rapa</i> syn. <i>campestris</i> (S9 haplotype)
<i>BcRL3</i> (<i>BcRK3</i>)	<i>Brassica campestris</i> receptor kinase 3	
<i>BcRK5</i>	<i>Brassica campestris</i> receptor kinase 5	
<i>BcRK6</i>	<i>Brassica campestris</i> receptor kinase 6	
<i>BcRL1</i>	<i>Brassica campestris</i> receptor-like 1 (pseudogene)	
<i>BcRL2</i>	<i>Brassica campestris</i> receptor-like 2 (pseudogene)	
<i>BcSL1</i>	<i>Brassica campestris</i> SLG-like 1 (pseudogene)	
<i>BcSL10</i>	<i>Brassica campestris</i> SLG-like 10	
<i>EP1</i>	<i>Epidermal 1 glycoprotein</i>	<i>A. thaliana</i> , <i>Daucus carota</i>
<i>ISG1</i>	<i>Ipomoea</i> secreted glycoprotein 1	<i>Ipomoea trifida</i>
<i>ISG2</i>	<i>Ipomoea</i> secreted glycoprotein 2	
<i>ISG3</i>	<i>Ipomoea</i> secreted glycoprotein 3	
<i>IRK1</i>	<i>Ipomoea</i> receptor kinase 1	
<i>IRK2</i>	<i>Ipomoea</i> receptor kinase 2 (possible pseudogene)	
<i>KIK1</i>	Kinase-interacting domain interacting kinase	<i>Zea mays</i>
<i>NS1</i>	Non-specific S-glycoprotein 1 (SLR1 homologue)	<i>Brassica rapa</i> (syn. <i>campestris</i>)
<i>NS2</i> (<i>SLR1-2</i>)	Non-specific S-glycoprotein 2 (SLR1 homologue)	
<i>NS3</i>	Non-specific S-glycoprotein 3 (SLR1 homologue)	
<i>OsPK10</i>	<i>Oryza sativa</i> protein kinase 10	<i>Oryza sativa</i>
<i>RLK1</i>	<i>Arabidopsis</i> receptor like kinase 1	<i>Arabidopsis thaliana</i>
<i>RLK4</i>	<i>Arabidopsis</i> receptor like kinase 4	

Table 6.1 continued

Gene Name	Gene Name	Plant Source
<i>SFR1</i>	S-gene family receptor kinase 1	<i>Brassica oleracea</i> var. <i>acephala</i> (S3 haplotype)
<i>SFR2</i>	S-gene family receptor kinase 2	
<i>SFR3</i>	S-gene family receptor kinase 3	
<i>SFR2-9</i>	S-gene family receptor kinase 2-9	<i>Brassica rapa</i> (syn. <i>campestris</i>) (S9 haplotype)
<i>SLG</i>	S-locus glycoprotein	Numerous <i>Brassicaceae</i>
<i>SLR1</i>	S-locus related 1 glycoprotein	Numerous <i>Brassicaceae</i>
<i>SLR2</i>	S-locus related 2 glycoprotein	Numerous <i>Brassicaceae</i>
<i>SLR3-1</i>	S-locus related 3-1 glycoprotein	<i>Brassica oleracea</i> self compatible (Sc) S-locus
<i>SLR3-2</i>	S-locus related 3-2 glycoprotein	<i>Brassica oleracea</i> (S29 haplotype)
<i>SRK</i>	S-receptor kinase	<i>Arabidopsis lyrata</i> , <i>Brassica oleracea</i> , <i>B. napus</i> , <i>B. rapa</i> , <i>Lotus japonicus</i> .
<i>SSRLK1</i>	<i>Senecio</i> S-receptor-like kinase 1	<i>Senecio squalidus</i>
<i>SSRLK2</i>	<i>Senecio</i> S-receptor-like kinase 1	
<i>SSRLK3</i>	<i>Senecio</i> S-receptor-like kinase 1	
<i>ZmPK1</i>	<i>Zea mays</i> protein kinase 1	<i>Zea mays</i>

6.1.2 - S-gene and S-domain morphology

The *Brassica SRK* and *SLG* genes are highly polymorphic and have many alleles. One hundred alleles have been identified in *Brassica rapa* (syn. *campestris*) and ~70-80 in *B. oleracea* (Ockendon, 1974, 1982; Hinata, *et al.*, 1993; Ruffio-Châble *et al.*, 1997; 1999; Sakamoto *et al.*, 1998). Contrastingly, the *SLR1* gene is monomorphic, exhibiting 99% intraspecific nucleotide-sequence similarity in *Brassica* haplotypes (Lalonde *et al.*, 1989). The polymorphism in the nucleotide sequence of *SLG* and the

receptor-encoding region of *SRK* is reflected in the amino acid sequence where it is used as a diagnostic to distinguish SI molecules from other S-domain proteins (Nishio *et al.*, 1997; Sakamoto *et al.* 1998; Schierup *et al.* 2001).

Sequence variability of *SLG* and *SRK* S-domains is restricted to three specific regions. The first region, identified as hypervariable region I (HvI) occurs from residues 173-188 [203-218]. Hypervariable region II (HvII) is located from amino acids 238-274 [268-305], and hypervariable region III (HvIII) encompasses residues 296-310 [326-440] (Fig.1) (Kusaba *et al.* 1997). Nasrallah and co-workers identified alternating regions of conservation and variability, designated A, B, C and D, in *Brassica oleracea* *SLG6*, *SLG13* and *SLG14* (Nasrallah *et al.* 1987). Region A, residues 1-182 [30-211], and region C, residues 275-378 [305-409], show approximately 80% residue conservation between haplotypes, with 144 out of 181 amino acid residues perfectly conserved in region A, and 83 of 103 residues conserved in region C. The highest sequence variability occurs in region B (182-274) [212-304] where only 39 of the 93 residues are perfectly conserved. This region contains HvII, which contributes considerably to this variability. Region D consists of 28 residues (379-405) [409-435] that are conserved in 13 amino-acid positions.

SLR1 also has alternating regions of conservation and variability that correspond roughly with those of *SLG* but contains differences that distinguish it from *SLG* (Fig 6.2). These include a lower level of sequence conservation in the carboxyl end of the molecule, fewer *N*-glycosylation sites and the presence of 30 residues between cysteines 7 and 8, as opposed to the 29 residues present in *SLG* S-domains. The most distinguishing feature of *SLR1* is a lack of polymorphism. *SLR1* molecules show no variability between haplotypes while *SLGs* exhibit between 20-30 percent intraspecific variability (Lalonde *et al.* 1989; Nasrallah *et al.* 1987).

6.1.3 - Diagnostic features of the S-domain

The presence of a PTDT-box, a Cys domain and potential *N*-glycosylation sites in an amino acid sequence identifies an S-protein. In addition to these diagnostic S-domain features, putative SI molecules should also possess specific sites of hypervariability, and intraspecific polymorphism in nucleotide and protein sequences (Nasrallah *et al.* 1987; Saupe and Glass., 1997)

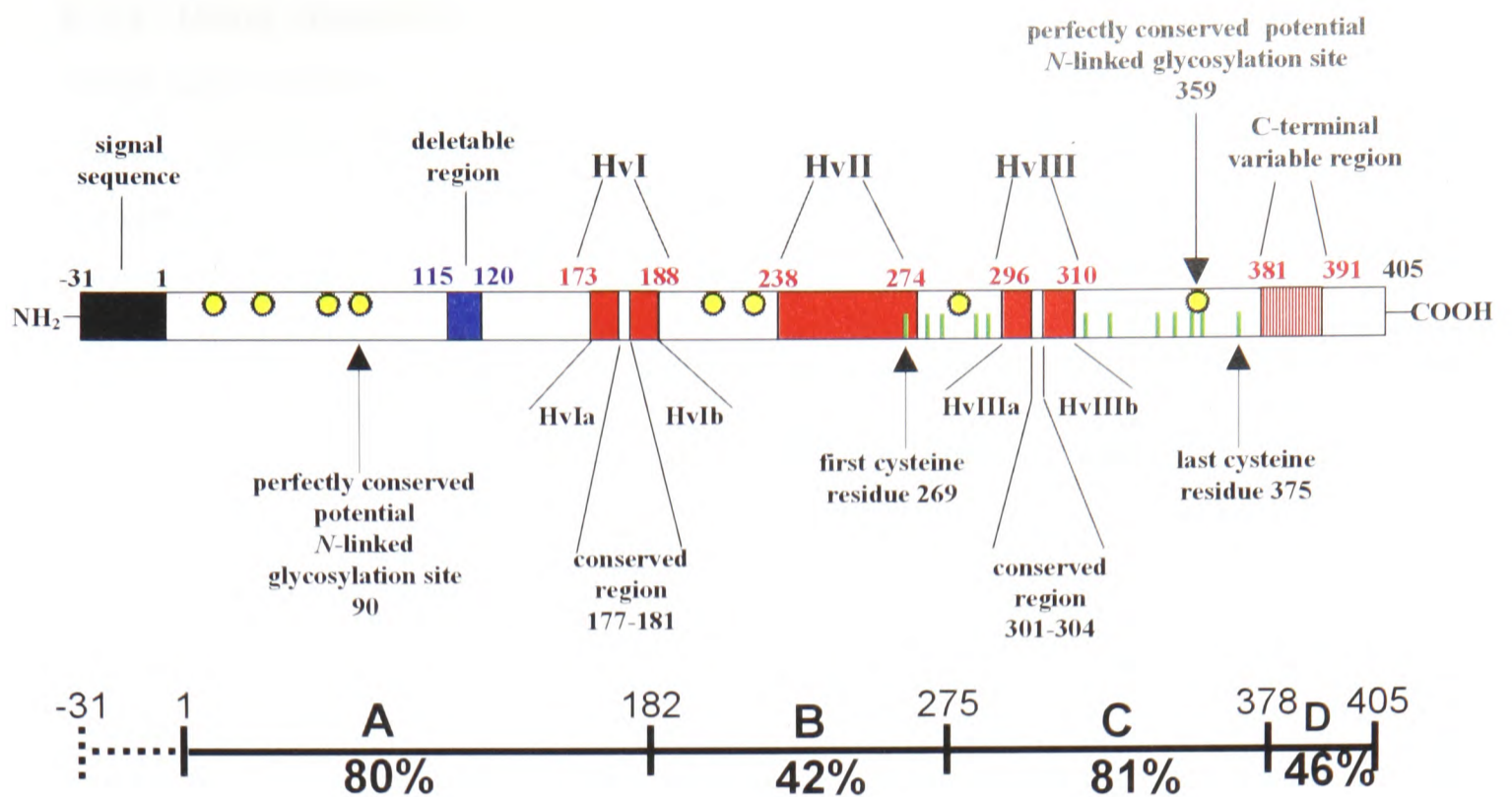


Figure 6.1. Generalised structure of *Brassica oleracea* SLG6. SLG cDNAs encode a primary protein composed of two domains; a signal-sequence domain of 31 residues and a 405-residue domain that corresponds to the secreted glycoprotein. The 12 conserved cysteine residues are represented as green bars: cysteine (1) **269 [300]**; (2) **275 [306]**; (3) **281 [312]**; (4) **289 [320]**; (5) **291 [322]**; (6) **312 [343]**; (7) **320 [351]**; (8) **350 [381]**; (9) **354 [385]**; (10) **358 [389]**; (11) **360 [391]**; (12) **375 [406]** constitute the Cys-domain. The 12 conserved cysteine residues (11 perfectly conserved and one almost conserved) are exactly spaced according to the pattern: (cys 1) +6 residues = (cys 2) +6 residues = (cys 3) +8 residues = (cys 4) +2 residues = (cys 5) +21 residues = (cys 6) +8 residues = (cys 7) +30 residues = (cys 8) +4 residues = (cys 9) +4 residues = (cys 10) +2 residues = (cys 11) +15 residues = (cys 12). *Brassica oleracea* SLG6 has 8 potential *N*-linked glycosylation sites (yellow stars) at; **15, 33, 83, 90, 214, 230, 284** and **359**. The two perfectly conserved potential *N*-glycosylation sites are located at **90 [120]** and **359 [389]**. The black filled box, the blue filled box and the red filled boxes represent the signal sequence, the deletable region and the three hypervariable regions respectively. The striped red box represents the C-terminal variable region encoded by synonymous nucleotide substitutions. The scale bar below the figure identifies the alternating conserved and variable regions A, B, C and D which show approximately 80%, 42%, 81% and 46% amino acid sequence conservation respectively in *Brassica* S-domains (Fig. 6.1. constructed from data contained in Kusaba *et al.*, 1997; Nasrallah *et al.*, 1987 and SLG6 protein sequence Genbank accession CAA68375).

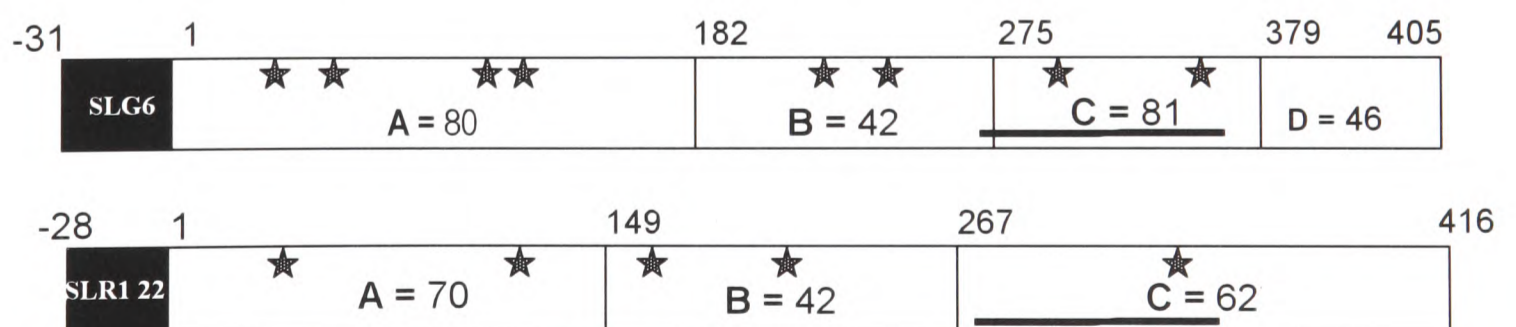


Figure 6.2. Schematic structure comparing *Brassica oleracea* SLG6 and SLR1-22 S-proteins. The black box, stars, black line and white boxes represent respectively the signal peptide, the *N*-glycosylation sites, the cys domain and regions A, B, C and D of alternating sequence conservation and variability. The numbers in the white boxes correspond to the percentage conservation. SLR1 has 5 potential *N*-glycosylation sites at **15, 97, 152, 215,** and **368**, but does not have the variable D region at the carboxyl end of the molecule. Fig. 2 constructed from data in Lalonde *et al.* 1989, and Nasrallah *et al.*, 1987)

6.1.4 - Using sequence conservation to isolate S-genes

There are presently more than one hundred nucleotide sequences of *Brassica* S-genes. Alignment of these sequences has revealed areas of conserved nucleotide sequence. Researchers have used these conserved regions to design pairs of *Brassica* S-primers that have successfully amplified S-gene sequences from species of *Brassica* and other genera of Brassicaceae (Nasrallah *et al.*, 1987; Trick and Flavell, 1989; Chen & Nasrallah, 1990; Dwyer *et al.*, 1991; Brace *et al.*, 1993; Dzelzkains *et al.*, 1993; Nishio *et al.*, 1994; Watanabe *et al.*, 1994; Yamakawa *et al.*, 1994; Delorme *et al.*, 1995; Nishio *et al.*, 1996; Sakamoto *et al.*, 1998; Stein *et al.*, 1996; Cabrillac *et al.*, 1999; Charlesworth *et al.*, 2000; Kusaba *et al.*, 2000; Miege *et al.*, 2001). Attempts at using the conserved *Brassica* nucleotide regions to design primer combinations capable of amplifying S-sequences from species outside the Brassicaceae have not met with success. The reason for this lack of success is the degeneracy of the genetic code. S-molecules encoded by S-genes from species outside the Brassicaceae are assumed to be similar to *Brassica* S-molecules, but the degenerate nature of the genetic code means these molecules are probably encoded by nucleotide sequences that vary considerably from those in *Brassica*. One way to overcome the problem of nucleotide degeneracy is to design primers from conserved regions of the amino-acid sequence. The three successful attempts at isolating S-gene sequences from non-Brassicaceae species used this method.

In 1990, Walker and Zang isolated and identified *ZmPK1* from *Zea mays* (Poaceae). *ZmPK1* encodes an S-domain serine/threonine protein kinase that is expressed in roots and shoots of seedlings (Table 1.4). Its function is unknown but its expression in the vegetative tissue rules it out as a gene concerned with pollination or SI. The same technique was used to identify the S-gene sequences ISG1, ISG2, ISG3, IRK1 and IRK2 in *Ipomoea trifida* (Convolvulaceae) (Kowyama *et al.*, 1995). Recently, Hiscock *et al.* (2003) designed degenerate primers using the same conserved S-domain regions employed by Kowyama to isolate the three non-S-linked *Senecio* S-receptor-like kinase cDNAs; SSRLK1, SSRLK2 and SSRLK3. In all three cases, mixtures consisting of a high numbers of degenerate primers were required in order to amplify putative S-sequences. Walker and Zang, for example used as downstream primers a mixture of sixty-four 17 unit oligomers (17-mer) corresponding to all possible RNA sequences encoding the conserved amino acid sequence Asp-Leu-Lys-Pro-Glu-Asn (DLKPEN) from catalytic subdomain VI of the protein kinase molecule. Similarly, for their upstream primer they used a mixture of 128 26-mer oligonucleotides corresponding to all the possible complementary RNA sequences encoding the conserved amino acid sequence Gly-Thr-Pro-Glu-Thr-Ile-Ala-Pro-Glu (GTPXYIAPE) from catalytic subdomain

VIII. The conserved amino-acid sequences in subdomain VI and VIII are characteristic of serine/threonine protein kinases and consequently the use of primers based on such ubiquitous sequences resulted in PCR amplification of many non-specific, non-S-domain sequences. The amplified sequences thus required further processing. This was achieved by more stringent amplification of appropriate-sized PCR products, followed by cloning and sequencing. Clones containing specific diagnostic sequences were selected as hybridisation probes to screen a *Zea mays* root cDNA library (Walker and Zang, 1990). Screening of 300 000 independent recombinants identified 2 clones of 1,700 and 2,700 base pairs from which nested deletions were constructed and sequenced.

In the case of *Ipomoea trifida*, Kowyama *et al.*, (1995) used as downstream primers a mixture of 512 23-mer oligonucleotides corresponding to all the possible RNA sequences encoded by the conserved amino acid sequence; Phe-Asp-Tyr-Pro-Thr-Asp-Thr (FDYPTDT), from the N-terminus of *Brassica* S-domains. The upstream primer mixture consisted of 1536 18-mer oligonucleotides corresponding to all the possible complementary RNA sequences encoded by Gly-Thr-Gly-Cys-Val-Ile (GTGCVI), located at the carboxyl end of *Brassica* S-domains. Once again, PCR amplification produced many non-specific fragments, which required further processing. Unlike Kowyama *et al.*, (1995), Hiscock *et al.*, (2003) having no success using the FDYPTDT conserved amino acid region, used instead the conserved GCVIWT (Gly-Cys-Val-Ile-Trp-Thr), at the C-terminal end of *Brassica* S-domains, for construction of downstream degenerate primers, and the conserved kinase domain Pro-Lys-Ile-Ser-Asp-Phe-Gly (PKISDFG), for upstream primers, to isolate three S-domain sequences from *Senecio squalidus* (Tabah *et al.*, 2004).

This chapter describes a simple method of obtaining S-gene sequences from species of Brassicaceae and Asteraceae using pairs of universal S-domain-specific primers in conjunction with PCR and direct cycle sequencing. It is envisaged that these PCR-generated S-gene sequences may include the putative *Cosmos* SI gene. The S-domain sequences obtained were used to construct an S-domain matrix from which Neighbour-Joining (NJ) distance trees were produced and analysed

6.2 - Materials and methods

6.2.1 - Plant material

The *Brassica oleracea* inbred lines homozygous for S_2 , S_3 , S_5 , S_6 , S_9 , S_{13} , S_{15} S_{29} self-incompatibility haplotypes and *Arabidopsis thaliana* Colombia ecotype were obtained

as silica gel-dried material from HRI–Wellesbourne, UK courtesy of Rosemary McClenaghan. The genetic background of haplotypes is as follows: S_2 , various cultivars and crosses: S_3 , *acephala*; S_5 , *acephala* x *alboglabra*; S_6 , *acephala*; S_9 , *acephala*; S_{13} , *acephala* x *gemmifera*; S_{15} , *acephala* x *gemmifera*; S_{29} , various cultivars and crosses. *Cosmos* species and *Centaurea cyanus* were obtained as fresh material from the Living Collections Department (LCD) Royal Botanic Gardens, Kew. *Cosmos atrosanguineus* Sherff 5010 was supplied by the Herbarium, Royal Botanic Gardens, Kew courtesy of Dr. N. Hind. Fresh material of *Conyza* species, *Diplotaxis tenuifolia*, *Picris echioides* and *Senecio* species was collected wild in West and North London (Table 6.2).

Table 6.2 Plant material

	Species	Accession No.*	Origin	Coll. Date	Voucher	DNA Bank No.**
1	<i>Arabidopsis thaliana</i> (L.) Heynh.	HRI - W	Columbia	NA	NA	NA
2	<i>Brassica oleracea</i> L. (Haplotype S_2)	DJ-2024	UK	NA	NA	NA
3	<i>Brassica oleracea</i> L. (Haplotype S_3)	DJ-8189	UK	NA	NA	NA
4	<i>Brassica oleracea</i> L. (Haplotype S_5)	DJ-4078/1	UK	NA	NA	NA
5	<i>Brassica oleracea</i> L. (Haplotype S_6)	DJ-4080	UK	NA	NA	NA
6	<i>Brassica oleracea</i> L. (Haplotype S_9)	DJ-8153	UK	NA	NA	NA
7	<i>Brassica oleracea</i> L. (Haplotype S_{13})	DJ-4099	UK	NA	NA	NA
8	<i>Brassica oleracea</i> L. (Haplotype S_{15})	DJ-4049	UK	NA	NA	NA
9	<i>Brassica oleracea</i> L. (Haplotype S_{29})	DJ-2025	UK	NA	NA	NA
10	<i>Centaurea cyanus</i> L.	2002 1446	UK	2002	pending	pending
11	<i>Conyza canadensis</i> (L.) Cronquist	2002 3497	UK Intrd. (N.A)	2002	sn K	18976
12	<i>Conyza sumatrensis</i> (Retz.) E. Walker	2002 3499	UK Intrd. (S.A)	2002	sn K	18977
13	<i>Cosmos atrosanguineus</i> (Hook.) A. Voss	1999 2254	Mexico	1998	sn K	18986
14	<i>Cosmos atrosanguineus</i> (Hook.) A. Voss	1999 3819	Mexico	1977	Chase 629 K	629
15	<i>Cosmos atrosanguineus</i> (Hook.) A. Voss	1997 6334	Mexico	1979	Chase 628 K	628
16	<i>Cosmos atrosanguineus</i> (Hook.) A. Voss	Sherff 5010	Mexico	1929	Sherff 5010 K	18978
17	<i>Cosmos bipinnatus</i> Cav.	1996 582	Mexico	1995	sn K	18979
18	<i>Cosmos carvifolius</i> Benth.	1999 383	Mexico	1994	sn K	18980
19	<i>Cosmos sulphureus</i> Cav.	1996 980	Mexico	1990	sn K	18981
20	<i>Diplotaxis tenuifolia</i> (L.) DC.	2002 3495	UK	2002	sn K	18982
21	<i>Picris echioides</i> L.	2002 3494	UK Intrd. (S.E)	2001	sn K	18983
22	<i>Senecio squalidus</i> L.	2002 3493	UK Intrd. (S.E)	2001	sn K	18984
23	<i>Senecio vulgaris</i> L.	2002 3492	UK	2001	sn K	18985

**Brassica* accession numbers after Brace *et al.*, 1993; Accessions numbers of Asteraceae/Compositae taxa and *Diplotaxis tenuifolia* assigned by the Royal Botanic Gardens, Kew. ** DNA Bank No. refers to the DNA Bank and Database of the Molecular Systematics Section, Jodrell Laboratory, Royal Botanic Gardens, Kew. Key to abbreviations: Coll, collection; Intrd, introduced; K, Herbarium of the Royal Botanic Gardens Kew; (NA), North America; (SA), South America; (SE), South Europe; HRI-W, Horticultural Research International Wellesbourne

6.2.2 - Primers

Seventeen degenerate primers, nine forward primers (2a, 2b, 5a, 5b, 5c, 5f, 5h, 6a, and Xc), and eight reverse primers (Xb, 6a, 6b, 9a, 9b, 9c, 9d and 10b) were designed using the Omega® 2.0 Bioinformatics Software package (Accelrys inc. Cambridge, UK) and were synthesised by MWG-Biotech. Fifteen primer pairs were used to amplify varying-sized S-domain fragments from Asteraceae and Brassicaceae species (Table 6.3).

Primer pairs 8, 9 and 10 are predicted to amplify three similar large fragments of ~1000 nucleotides each, each encoding ~350 amino-acid residues. These fragments represent approximately 82 percent of the translatable S-domain region. Primer pairs 1 and 2 are predicted to amplify two similar ~500-nucleotide fragments towards the 5'-prime end (5' end) of the S-gene, encoding ~150 to 170 amino acids. The translated sequences of primer pairs 1 and 2 should contain the conserved N-glycosylation site at residue ~90 [~120] characteristic of S-domain proteins. Primer pairs 4 5 6 (5f+9d) 7, 12, 13 and 15 are predicted to amplify a ~700-800 nucleotide sequence towards the 3' end of S-genes and should encode ~250 amino acids. The encoded sequences generated by primer pairs 4, 5, 6, 7 12, 13 and 15 are predicted to include the Cys domain and the second conserved N-glycosylation site at residue ~359 [~389]. Primers 5c, 5f, 6a and 6b were designed as internal primers so that specific S-fragments generated by primer pairs 1 and 2 are predicted to overlap by ~250 bases with specific S-fragments generated by primer pairs 4, 5, 6, 7, 12, 13 and 15 (Table 6.3). Primer pairs 11 and 14 are class-II specific primer pairs predicted to amplify ~200 and ~650 nucleotides respectively from class-II type S-genes. Sequences generated by primer pair 11 are predicted to encode ~70 amino acids and sequences generated by primer pair 14 are predicted to encode a ~200 amino-acid sequence and should contain the diagnostically informative Cys domain and the conserved potential N-glycosylation site at residue 389.

Five-prime-end fragments, produced by primer pairs 1 and 2, and 3'-end fragments, produced by primer pairs 4, 5, 6, 7, 12, 13 and 15, are predicted to share a ~200-nucleotide overlap and to produce a 1000-nucleotide contiguous sequence concurrent with sequences 8, 9 and 10. In this research, sequences generated by primer pairs 1 and 2 are termed 5'-end Compositae primer set (CosPS) sequences, and those generated by primer pairs 3, 4, 5, 6, 7 12, 13 and 15 are referred to as 3'-end CosPS sequences. Sequences generated by primer pairs 8, 9 and 10 are identified as wholepiece CosPS sequences.

Table 6.3 Primer Pairs

Primer pair No.	Primer pairs	Predicted size of PCR-fragment (bases)	Predicted location of PCR-fragment (bases)	Percentage of full-length S-gene sequence amplified (%)	Predicted size of longest ORF (residues)
<u>1</u>	2a+6a	~500	5'-end	~40	~150
<u>2</u>	2b+6b	~500	5'-end	~40	~170
<u>3</u>	6a+9b	~500	3'-end	~40	~200
<u>4</u>	5c+9b	~700	3'-end	~55	~250
<u>5</u>	5f+9c	~700	3'-end	~55	~250
<u>6</u>	5f+9d	~700	3'-end	~55	~250
<u>7</u>	5f+10b	~800	3'-end	~60	~250
<u>8</u>	2a+9b	~1000	wholepiece	~70	~350
<u>9</u>	2b+9d	~1000	wholepiece	~70	~350
<u>10</u>	2b+10b	~1100	wholepiece	~85	~350
<u>11</u>	5h+Xb	~200	3'-end	~15	~50
<u>12</u>	5h+9a	~700	3'-end	~55	~250
<u>13</u>	5h+10b	~800	3'-end	~60	~250
<u>14</u>	Xc+10b	~700	3'-end	~55	~200
<u>15</u>	5a+5b+10b	~800	3'-end	~60	~250

6.2.3 - DNA extraction

Total cellular DNA was extracted at 65°C from 2.0 g of fresh leaf material, 0.3 g of silica gel-dried leaves or 0.1 g of herbarium material in 10 ml of 2 x CTAB (cetyltrimethylammonium bromide) using a modified method of Doyle and Doyle (1987) and incubated for 10-15 minutes at 65°C. The solution was extracted once with equal volumes of SEVAG (chloroform : isoamyl alcohol, 24:1) gently agitated for 30 minutes at room temperature and then spun at 8000 rpm for 10 minutes at 25°C in a Sorvall® Discovery™ 90 Centrifuge. The aqueous, DNA-containing phase (top layer) was transferred into 50 ml capped tubes and precipitated with 2½ times volume -20°C ethanol for fresh and silica gel-dried material, and 2/3 volume -20°C isopropanol for herbarium material. Contents were mixed gently and left to precipitate at -20°C for one week. DNA was pelleted at 3000 rpm for 5 minutes in a Sorvall® Legend RT Centrifuge. The supernatant was discarded, the pellet washed in 3 ml 70% ethanol for 5 minutes and centrifuged at 3000 rpm for 2 minutes. The supernatant was discarded and the pellet left to air dry for 24 hours to ensure evaporation of residual alcohol. Purification of DNA was achieved by caesium chloride/ethidium bromide (CsCl/EtBr) equilibrium density gradient centrifugation. The air-dried pellet was suspended in 3 ml CsCl/EtBr solution (1.55 g/ml⁻¹ at 1%), transferred to 5 ml open-top Sorvall ultracentrifuge tubes and equilibrated to 4.45 ml with CsCl/EtBr solution (1.55 g/ml⁻¹ at 1%). Samples were centrifuged overnight at 45000 rpm and 25°C in a Beckman J2-MC

centrifuge. Under UV light (312 nm), 1.2 μ l DNA was removed from the central fluorescent band and transferred to transparent 4 ml graduated tubes. To remove ethidium bromide, an equal volume of n-butanol was added to DNA samples, mixed by thorough shaking and left to stand for 15 minutes. The lower aqueous DNA-containing layer was transferred to dialysis tubing and washed with constant stirring for 3 hours in double-distilled sterile water (H_2O_{dds}). Samples were concentrated for 40 minutes and dialysed twice more overnight in dialysis buffer (80x TE [pH 8.0] dialysis buffer : H_2O_{dds} , 1:40). Concentration of DNA stock solutions was determined by spectrophotometry using a Shimadzu UV-1201 UV-Vis spectrophotometer.

DNA quality and fragment size range was assessed on ethidium-bromide stained agarose gel. Five microlitres of DNA sample in 5 μ l of loading dye was run on a 1% agarose gel at 80mV for 45 minutes against 5 μ l of standard DNA size markers *EcoR I/Hind III* digests of phage λ DNA (Abgene, Surrey UK).

6.2.4 - PCR amplification

PCR was carried out in a final volume of 50 μ l using standard protocols. Ten microlitres of PCR product was visualised on a 1% agarose gel containing 1% ethidium bromide and run at 100 mV for 25 minutes against 5 μ l of the standard DNA size marker LAMBDA *EcoR I/Hind III* (Abgene, Surrey UK). Products containing single appropriate-sized fragments were cleaned using CONCERT™ Rapid PCR Purification system (Life Technologies, Paisley UK) according to the manufacturer's instructions. The concentration of purified PCR-amplified DNA was determined by spectrophotometry, with an absorbance of 1.0 at 260 nm corresponding to 50 μ g DNA/ml.

Separation of appropriate sized fragments from non-specific bands was achieved either by cloning the purified amplified DNA using the pGEM®-T Easy Vector System I (Promega, Madison, USA), or by gel extraction. For gel extraction, appropriate-sized fragments were excised from gels and used in a second 50 μ l PCR reaction using the PCR protocol previously described but reducing the number of cycles to 15. The amplified DNA was visualised, measured and purified, as described previously in the methods

6.2.5 - Cycle sequencing

Direct cycle sequencing from the cleaned cDNA was achieved using the ABI Prism Big Dye™ Terminator Cycle Sequencing Ready Reaction Kit with AmpliTaq® DNA

Polymerase (ABI, Warrington, Cheshire UK). Cycle sequencing reactions were carried out in a volume of 10 μ l: 1 μ l Big Dye™; 3 μ l sequencing buffer (200 mM Trizma base, 5 mM MgCl₂, pH 9.0); and primer and cDNA template were used according manufactures instructions. The cycle-sequencing protocol was 26 cycles of; 96°C/10 seconds, 50°C/5 seconds, 60°C/4 minutes. Unincorporated dyes were removed from each cycle-sequencing reaction by briefly vortexing in 3M sodium acetate : 100% ethanol (1:25 μ l), placing tubes on ice for 30 minutes and then spinning down for 25 minutes at 13 000 rpm. Reactions were drained, washed in 300 μ l of 70% ethanol, vortexed briefly and spun down at 13 000 rpm for 15 minutes. The latter step was repeated once more, after which tubes were drained and left to air dry overnight. Samples were sequenced on a 3100 Genetic Analyzer Automated Sequencer (ABI, Warrington, Cheshire UK) in accordance with the manufacturer's instructions.

6.2.6 - Sequence editing and analysis

Sequences were edited using the dirty data algorithm of Sequencher™ version 4.1 (Gene Codes Corp. Ann Arbor Michigan, USA). Protein translations and open reading frames were deduced using Gene Runner© version 3.05 (Hastings Software Inc.). Analysis of deduced protein sequences Gene Runner© version 3.05 (Hastings Software Inc.). The Dot plot function of the Omega 2.0 Bioinformatics software was used to make pairwise comparisons of nucleotide sequences. Dot plot parameters were as follows: scoring matrix, Omega 2.0 nucleic acid identity matrix with no ambiguities; window size, 30; hash value, 3; jump value, 1; stringency, 90%. Dot plots were used to compare 5'-end CosPS nucleotide sequences with each other and with wholepiece CosPS-nucleotide sequences. Three prime-end CosPS sequences were analysed similarly against each other and wholepiece CosPS sequences. Dot plots were also used to compare regions of predicted overlap between 5'-end and 3'-end CosPS sequences.

Pairwise alignment percentage identities generated by the Omega 2.0 alignment software were used to identify sequence redundancy within 5'-end, and within 3'-end sequences. Sequences that showed > 85% pairwise similarity were submitted to dot plot analysis. Taxon-specific nucleotide sequences having dot plots with >97% identity were considered to be the same sequence particularly if the percentage difference was restricted to the ends of each sequence. BLASTN (BLAST® - Basic Local Alignment Search Tool for Nucleotides) searches were performed on nucleotide sequences using the default parameters of the NCBI (National Center for Biotechnology Information) BlastN facility (Altschul *et al.*, 1990 and 1997).

Local similarity scores for deduced CosPS protein sequences were calculated using the SSEARCH algorithm (FASTA© program William R. Pearson and the University of Virginia, USA) and the NCBI/Blast NR protein database. The parameters used were: Ktup = 1, BLOSUM50 scoring matrix, gap penalty -12 and gap-extension penalty -4 (Pearson, 1996; Pearson and Lipman, 1988). The PRSS algorithm was used to evaluate the significance of the pairwise similarity scores of each CosPS deduced protein sequence with its highest-scoring similarity sequence in the NCBI/Blast NR protein database. The PRSS comparison used the same parameters as were used to calculate local similarity scores (-12, -4) with 1000 shuffles and the uniform shuffle mode selected (Pearson, 1996; Pearson and Lipman, 1988). Homology was ascribed to CosPS sequences when a search produced related library sequences of comparable length to the sequence that had similarity scores with E values much lower than 0.02, while the highest scoring unrelated sequences had E values not less than 0.5 (Pearson, 1996).

Non-redundant deduced protein sequences of Asteraceae species and *Diplotaxis tenuifolia* were submitted to a search of the Conserved Domain Database and Search Service (v.1.62) of NCBI (Marchler-Bauer *et al.* 2003) with the E value set at 0.01 and the low complexity filter mode selected.

6.2.7 – Tree-building methods

Distance methods were used to investigate relationships of deduced CosPS protein sequences with each other and with a representative sample of S-domain sequences obtained from NCBI Genbank. Protein sequences were aligned using ClustalX 1.81 (Jeanmougin *et al.*, 1998). Pairwise alignment parameters were set with a gap opening penalty = 70.0 and a gap extension penalty = 0.1, and a delay divergent sequences set at 30%. Multiple alignment parameters were set with a gap opening penalty = 50.0, a gap extension penalty = 0.2, and a protein gap = 4. The profile adjustment mode of the ClustalX software was used to align sequences. The ClustalX aligned S-domain matrix was edited in MacClade© (Version 4.03) (W.P. Maddison and D.R. Maddison 2000) and analysed using the mean character difference of the Neighbour-Joining algorithm of PAUP (Swofford, 2002) with random seeding selected. Bootstrap sampling used 1000 repetitions.

6.3 - Results

6.3.1 – Introduction

(i) Assessment of DNA quality

Fresh and silica gel-dried samples produced abundant high molecular weight DNA of ~5000 nucleotides. The DNA of *Cosmos atrosanguineus sherff* 5010 extracted from herbarium material was considerably degraded giving a faint smear with a maximum weight of ~1000 nucleotides. It was predicted that primer pairs 8 (2a+9b), 9 (2b+9d) and 10 (2b+10b) would fail to amplify in this taxon. The results of PCR amplifications support this prediction (Tables 6.4 and 6.5).

(ii) Assessment of amplification and cycle-sequencing reactions

Results of PCR and cycle-sequencing reactions are presented in Table 6.4. Primer pairs 5 and 6 produced identical taxon-specific sequences in *Brassica oleracea* haplotypes, *Cosmos* species and *Senecio vulgaris*. No differences were observed in the quality of sequences produced by each primer pair, and so, for each of the aforementioned taxa, single contiguous sequences were made from the PCR products of primer pair 5 and 6, and are identified as CosPS sequence 5+6 (5f+9c+9d) in Tables 6.4 and 6.5.

In haplotypes of *Brassica oleracea*, primer pair 5 and primer pair 6 produced two different-sized fragments of ~700 and ~500 nucleotides (nt) identified as bands 1 (ba1) and band 2 (ba2) respectively. Primer pair 9 also produced two different-sized fragments bands identified as band 1 (~1000 nt.) and band 2 (~800 nt.)

(iii) Sequence quality

CosPS nucleotide sequences were graded using a 3-star quality rating system, identifying sequences as excellent (3 stars ***), good (2 stars **) or fair (one star *). The data are included in column three of Table 6.5. A sequence was assigned the quality *excellent*, when the forward- and reverse-primer strands formed a contiguous sequence in Sequencher™ version 4.1 with a minimum-match percentage of 95% and a minimum overlap of 200 bases. *Good* quality sequences were produced by contiguous sequences that had a minimum-match percentage of 85% and a minimum overlap of 100 bases. Sequences that had a minimum overlap of 50 bases and minimum-match percentage of 75% were graded as *fair* quality.

(iv) Open Reading Frames (ORFs) and longest length ORFS

Table 6.5 lists and characterises the longest ORFs deduced from CosPS nucleotide sequences generated by primer pairs 1-15 in 23 plant taxa

Table 6.4. Results of amplification and cycle-sequencing reactions in Asteraceae and Brassicaceae species

Nos.	Taxa	Accession Number	Primer Pairs															Total number of sequences
			1	2	3	4	5 + 6	7	8	9	10	11	12	13	14	15		
			2a+6a	2b+6b	6a+9b	5c+9b	5f+9c+9d	5f+10b	2a+9b	2b+9d	2b+10b	5h+Xb	5h+9a	5h+10b	Xc+10b	5a+5b+10b		
1	<i>Arabidopsis thaliana</i>	HRI-W	✓	✓	—	✓	—	—	✓	—	—	—	—	—	—	—	6	
2	<i>Brassica oleracea</i> (S2)	DJ-2024	✓	✓	✗	✗	?	?	?	?	?	?	?	?	?	?	5	
3	<i>Brassica oleracea</i> (S3)	DJ-8189	✓	✓	✓	✓	✓ ²	✓	✓	✓	✓	✓	✓	✓	✓	✓	10	
4	<i>Brassica oleracea</i> (S5)	DJ-4078/1	?	?	✓	✗	✓ ²	✓	✓	✓	✓	✓	?	✓	✓	✓	6	
5	<i>Brassica oleracea</i> (S6)	DJ-4080	✓	✓	✓	✓	✓ ¹ ✓ ²	✓	?	?	✓	✓	✓	✓	✓	✓	12	
6	<i>Brassica oleracea</i> (S9)	DJ-8153	?	✓	✓	✓	?	?	?	?	?	?	?	?	?	?	6	
7	<i>Brassica oleracea</i> (S13)	DJ-4099	✓	✓	✓	✓	✓ ²	✓ ¹ ✓ ²	✓	✓	✓	✓	✓	✓	✓	✓	13	
8	<i>Brassica oleracea</i>	DJ-4049	?	?	✗	✗	✓ ²	?	?	?	?	?	?	?	?	?	7	
9	<i>Brassica oleracea</i>	DJ-2025	?	?	✓	✓	?	?	?	?	?	?	?	?	?	?	7	
10	<i>Centaurea cyanus</i>	2002-1446	✗	✓	✗	?	?	?	?	?	?	?	?	?	?	?	7	
11	<i>Coryza canadensis</i>	2002-3497	✗	?	✗	✗	?	?	?	?	?	?	?	?	?	?	3	
12	<i>Coryza sumatrensis</i>	200-3499	✗	(✓)	✗	✗	?	?	?	?	?	?	?	?	?	?	3	
13	<i>Cosmos atosanguineus</i>	1999-2254	✓	✓	✗	✓	✓	✓	✓	✓	✓	✓	✓	✓	✓	✓	9	
14	<i>Cosmos atosanguineus</i>	1999-3819	✓	✓	✗	✓	✓	✓	?	?	?	?	?	?	?	?	7	
15	<i>Cosmos atosanguineus</i>	1997-6334	✓	✓	✗	✓	✓	✓	?	?	?	?	?	?	?	?	8	
16	<i>Cosmos atosanguineus</i>	Sherff 5010	✓	—	✗	✓	—	—	✗	✗	✗	✗	✗	✗	✗	?	2	
17	<i>Cosmos bipinnatus</i>	1996-582	✓	✓	✗	✓	✓	✓	?	?	?	?	?	?	?	?	8	
18	<i>Cosmos carvifolius</i>	1999-383	✓	✓	✗	✓	✓	✓	?	?	?	?	?	?	?	?	8	
19	<i>Cosmos sulphureus</i>	1996-980	✓	?	✗	✗	✓	?	?	?	?	?	?	?	?	?	3	
20	<i>Diplotaxis tenuifolia</i>	2002-3495	?	?	—	✓	?	?	?	?	?	?	?	?	?	?	4	
21	<i>Picris echioides</i>	2002-3494	✗	✓	—	?	?	?	?	?	?	?	?	?	?	?	3	
22	<i>Senecio squalidus</i>	2002-3493	✗	✓	✗	✗	✓	✗	✗	✗	✗	✗	✗	✗	✗	✗	2	
23	<i>Senecio vulgaris</i>	2002-3492	✗	✓	✗	✓	✓	✗	✗	✗	✗	✗	✗	✗	✗	✗	4	
Total number of sequences			12	16	6	14	13	19	12	7	11	8	3	7	3	12	143	

Key to symbols: ✓ indicates successful amplification and cycle sequencing of an S-domain encoding sequence; ✗ indicates failure of PCR amplification reaction; ? indicates success in amplification but failure in direct cycle sequencing (In the majority of cases, this failure is a consequence of primer pairs amplifying two closely related same-sized fragments); ✓¹ and ✓² identifies successful amplification and cycle sequencing of bands 1 and 2 respectively using primer pairs 5+6, and 9; (✓) indicates successful amplification and cycle sequencing of non-S-domain encoding sequences. — identifies taxa that were not sequenced with a specific primer pair.

6.3.2 - Analysis of Results

(i) PCR amplification and cycle-sequencing reactions

Primer pairs 1-15 produced 143 sequences in the 23 taxa. The least successful taxa were the *Brassica oleracea* S₂ class-II haplotype, *Conyza* species, *Picris echioides*, *Senecio squalidus* and *Cosmos atrosanguineus*-5010. These taxa exhibited high failure rates in amplification, and each taxon generated only two or three sequences out of a possible 15 sequences. The most successful priming occurred in *Brassica oleracea* S₆ and S₁₃ haplotypes producing 12 and 13 sequences respectively. The most successful priming of Asteraceae species occurred in *Cosmos atrosanguineus*, *C. bipinnatus* and *C. carvifolius* producing an average of 8 to 9 sequences (Table 6.4).

Primer pairs 7, 2 and 4 were the most successful, priming in 19, 16 and 14 taxa respectively. Apart from primer pairs 3, 11, 12, and 14, which are specific to *Brassica oleracea*, these degenerate primers work successfully in a range of Asteraceae and Brassicaceae species. Aside from primer pair 2 in *Conyza sumatrensis* that produced a nucleotide sequence related to the *Zea mays* pol polyprotein, and primer pair 8 in *Cosmos atrosanguineus* (accessions 2254, 3819) and *Centaurea cyanus* that produced sequences related to glucan and callose synthase respectively, these degenerate primers primed exclusively S-gene sequences (Table 6.5).

(ii) Control species

Arabidopsis thaliana (tribe: Sisymbrieae), *Brassica oleracea* (tribe: Brassiceae) and *Diplotaxis tenuifolia* (tribe: Brassiceae), were used as control species. The five class-I haplotypes; S₃, S₆, S₉, S₁₃ and S₂₉ amplified with all primers, but showed varying degrees of success with direct sequencing. The class-I haplotypes S₆ and S₁₃ sequenced better with all primers than the class-I haplotypes S₃, S₉ and S₂₉, and all class-I haplotypes amplified and sequenced more successfully than class-II haplotypes; S₂, S₅ and S₁₅. These observations in *Brassica oleracea* suggest primers used in this study are predisposed to class-I S-sequences. This is exemplified by primer pairs 4 and 15 that amplify and sequence in all class-I haplotypes but fail to amplify in the three class-II haplotypes, and is reinforced by primer pairs 11 and 14, which were designed as class-II specific primers, and failed to amplify in class-I *Brassica oleracea* haplotypes, Asteraceae species and *Diplotaxis tenuifolia* (Table 6.4).

Arabidopsis thaliana Colombia ecotype is an important control species. It is a member of the Brassicaceae, but located in a different tribe to *Brassica oleracea*. In contrast to

the cultivated species of *Brassica*, it is a wild species for which the entire genome has been sequenced. Inclusion of *A. thaliana* and *Diplotaxis tenuifolia*, a wild species of the tribe Brassiceae, allows primers to be tested in non-*Brassica* Brassicaceae species. In addition the use of *A. thaliana* allows the accuracy and authenticity of priming to be checked, as any nucleotide sequence produced by primers in this taxon should match directly a sequence in the *A. thaliana* sequence database. The evidence of SSEARCH results in *A. thaliana* and *Brassica oleracea* haplotypes confirms the ability of primers to amplify and generate statistically significant fragments of predicted size that share 98 to 100% identity with specific *A. thaliana* and *B. oleracea* database sequences. Extrapolation from these results supposes that these degenerate primers are priming appropriately in Asteraceae species, and that the sequences they produce in Asteraceae are the product of accurate and sensitive priming.

(iii) Analysis of taxa-specific nucleotide sequences and encoded protein sequences

Analyses of CosPS nucleotide sequences and CosPS deduced protein sequences are summarised in Table 6.5. The first aim of these analyses is to describe the characteristics of each nucleotide sequence and its predicted longest ORF sequence, and to make an assessment of sequence homology using the BLASTN and SSEARCH algorithms. The second aim of the analysis is to identify redundant taxon-specific CosPS sequences.

Table 6.5 Longest ORFs of nucleotide sequences generated by primer pairs 1-15 in species of Asteraceae and Brassicaceae

Taxon Name	Primer pair	Sequence quality	Sequence Length (bases)	Translation Frame	ORF length (AA)	Actual Molecular weight (kD)	Start-stop DNA base number	Start-stop Triplets	Number of S-domain hits in NCBI/Blast NR database having E value < 0.02	Name of Top protein SSEARCH	Name of Top NCBI/Blast Nucleotide Search
<i>Arabidopsis thaliana</i> HRI-W	1	***	425	+1	141	16.179	1-423	Beg-End	~400	<i>Ath</i> ARK1	<i>Ath</i> RK
	2	***	493	+2	164	18.775	2-493	Beg-End	~400	<i>Ath</i> ARK3	<i>Ath</i> ARK3
	4	***	706	+1	235	26.946	1-705	Beg-End	~400	<i>Ath</i> AtS1	<i>Ath</i> AtS1
	7	***	692	+3	230	26.191	3-692	Beg-End	~400	<i>Ath</i> ARK3	<i>Ath</i> ARK3
	8	***	972	+1	324	37.046	1-972	Beg-End	~400	<i>Ath</i> AtS1	<i>Ath</i> AtS1
	10	***	1026	+3	341	38.460	3-1025	Beg-End	~400	<i>Ath</i> ARK3	<i>Ath</i> ARK3
	Contig. 4+8	***	985	+1	328	37.585	1-984	Beg-End	~400	<i>Ath</i> AtS1	<i>Ath</i> AtS1
	Contig. 2+7+10	***	1093	+2	364	41.279	2-1093	Beg-End	~400	<i>Ath</i> ARK3	<i>Ath</i> ARK3

Key to abbreviations in table 9: **Aly**, *Arabidopsis lyrata*; **Ath**, *Arabidopsis thaliana*; **Bol**, *Brassica oleracea*; **Bra**, *B. rapa*; **Bna**, *B. napus*; **Itr**, *Ipomoea trifida*; **Osa**, *Oryza sativa*. Beg-End, (beginning-end) that no start or stop codons were located within amplicon sequence. Contiguous sequences are highlighted in grey, e.g. Contig 4+8 identifies the contiguous sequence, constructed from the two sequences generated by primer pairs 4 and 8.

Table 6.5 continued.

Taxon Name	Primer pair	Sequence quality	Sequence Length (bases)	Translation Frame	ORF length (AA)	Actual Molecular weight (kD)	Start-stop DNA base number	Start-stop Triplets	Number of S-domain hits in NCBI/Blast NR database having E value < 0.02	Name of Top protein SSEARCH	Name of Top NCBI/Blast Nucleotide Search
<i>Brassica oleracea</i> - S ₂ DJ-2024	1	*	397	+1	132	15.001	1-396	Beg-End	~400	<i>Bra</i> BcRK1	<i>Bra</i> <i>BcRL1</i> (pseudogene)
	2	*	382	+3	126	14.147	3-380	Beg-End	~400	<i>Bol</i> SLR2	<i>Bra</i> <i>BcRL3</i> (for BcRK3)
	11	***	215	+1	71	8.361	1-213	Beg-End	~400	<i>Bol</i> SLG5	<i>Bol</i> SRK2k
	12	***	661	+3	132	15.385	3-401	Beg-TAG	10	<i>Bra</i> BcRK1	<i>Bra</i> <i>BcRL1</i> (pseudogene)
				-3	113	12.658	659-318	Beg-TGA	None	None	
14	***	612	+1	204	23.238	1-612	Beg-End	~400	<i>Bol</i> SRK2k	<i>Bol</i> SRK2k	
<i>Brassica oleracea</i> - S ₃ DJ-8189	1	**	418	+2	139	15.540	2-418	Beg-End	~400	<i>Ath</i> ARK1	<i>Bra</i> <i>BcSL1</i> (pseudogene)
	2	**	455	+2	151	17.323	2-454	Beg-End	~400	<i>Bra</i> BcRK3	<i>Bra</i> <i>BcRL3</i> (for BcRK3)
	3	*	482	+1	160	18.425	1-480	Beg-End	~400	<i>Bol</i> SRK3	<i>Bol</i> SLG3
	4	*	665	+1	221	25.525	1-663	Beg-End	~400	<i>Bol</i> SLG3	<i>Bol</i> SLG3
	5+6 (Ba2)	***	579	+3	192	22.341	3-578	Beg-End	~400	<i>Bol</i> SLR3-1	<i>Bol</i> SLR3-1
	7	*	686	+3	228	26.144	3-686	Beg-End	~400	<i>Bol</i> SLG3	<i>Bol</i> SLG3
	8	**	874	+2	291	33.450	2-874	Beg-End	~400	<i>Bol</i> SLG3	<i>Bol</i> SLG3
	12	***	599	+1	199	22.744	2-597	Beg-End	~400	<i>Bra</i> SRK1	<i>Bra</i> BcRK1
	13	**	705	+2	234	26.424	2-703	Beg-End	~400	<i>Bol</i> SLR2	<i>Bol</i> SLR2
	15	***	698	+3	232	26.641	3-698	Beg-End	~400	<i>Bol</i> SLG3	<i>Bol</i> SLG3
	Contig. 3+4+7+8	**	973	+2	324	36.910	2-973	Beg-End	~400	<i>Bol</i> SLG3	<i>Bol</i> SLG3
Contig. 2+13	**	1035	+2	344	38.900	2-1033	Beg-End	~400	<i>Bol</i> SLR2	<i>Bol</i> SLR2	
<i>Brassica oleracea</i> - S ₅ DJ-4078/1	3	*	457	+1	152	16.843	1-456	Beg-End	~400	<i>Bra</i> BcRK1	<i>Bra</i> <i>BcRL1</i> (pseudogene)
	5+6 (Ba2)	***	578	+1	192	22.356	1-576	Beg-End	~400	<i>Bol</i> SLR3-1	<i>Bol</i> SLR3-1
	7	*	452	+2	150	16.435	2-451	Beg-End	~400	<i>Bra</i> SLG40	<i>Bol</i> SRK5
	11	***	216	+2	71	8.361	2-214	Beg-End	~400	<i>Bol</i> SLG5	<i>Bol</i> SRK5
	12	***	637	+2	92	10.490	362-637	ATG-End	~400	<i>Bra</i> SRK1	<i>Bra</i> BcRK1 (for SRK1)
				+3	149	17.161	3-452	Beg-TAG	~400		
14	***	610	+2	203	22.996	2-610	Beg-End	~400	<i>Bol</i> SRK5	<i>Bol</i> SRK5	

Table 6.5 continued.

Taxon Name	Primer pair	Sequence quality	Sequence Length (bases)	Translation Frame	ORF length (AA)	Actual Molecular weight (kD)	Start-stop DNA base number	Start-stop Triplets	Number of S-domain hits in NCBI/Blast NR database having E value < 0.02	Name of Top protein SSEARCH	Name of Top NCBI/Blast Nucleotide Search
<i>Brassica oleracea</i> - S6 DJ-4080	1	*	220	+1	73	8.472	1-219	Beg-End	~400	<i>Bol</i> SFR1	<i>Bra</i> <i>BcSL1</i> (pseudogene)
	2	**	466	+1	155	17.885	1-465	Beg-End	~400	<i>Bra</i> BcRK3	<i>Bra</i> <i>BcRL3</i> (for BcRK3)
	3	***	505	+2	168	19.099	2-505	Beg-End	~400	<i>Bol</i> SLG6	<i>Bol</i> SLG6
	4	***	634	+1	211	24.410	1-633	Beg-End	~400	<i>Bol</i> SLG6	<i>Bol</i> SLG6
	5+6 (Ba1)	*	683	+1	227	26.083	1-681	ATG-End	~400	<i>Bol</i> SLG6	<i>Bol</i> SLG6
	5+6 (Ba2)	***	582	+2	193	22.546	2-580	Beg-End	~400	<i>Bol</i> SLR3-1	<i>Bol</i> SLR3-1
	7	*	560	+2	186	21.952	2-559	Beg-End	~400	<i>Bol</i> SRK6	<i>Bol</i> SRK6
	8	**	972	+1	324	37.181	1-972	Beg-End	~400	<i>Bol</i> SLG6	<i>Bol</i> SLG6
	9 (Ba2)	***	826	+1	275	31.714	1-825	Beg-End	~400	<i>Bol</i> SLR3-1	<i>Bol</i> SLR3-1
	12	***	718	+3	239	27.257	1-717	Beg-End	~400	<i>Bra</i> SRK1	<i>Bra</i> <i>BcRK1</i> (for SRK1)
	13	**	711	+1	237	27.487	1-711	Beg-End	~400	<i>Bra</i> BcRK3	<i>Bra</i> <i>BcRL3</i> (for BcRK3)
	15	***	685	+1	228	26.409	1-684	Beg-End	~400	<i>Bol</i> SRK6	<i>Bol</i> SRK6
	Contig. 5+6+9 (Ba2)	***	854	+1	284	32.926	1-852	Beg-End	~400	<i>Bol</i> SLR3-1	<i>Bol</i> SLR3-1
	Contig. 3+4+8	***	1015	+1	338	38.539	1-1014	Beg-End	~400	<i>Bol</i> SLG6	<i>Bol</i> SLG6
Contig. 2+13	**	1047	+1	349	40.392	1-1047	Beg-End	~400	<i>Bra</i> BcRK3	<i>Bra</i> <i>BcRL3</i> (for BcRK3)	
<i>Brassica oleracea</i> -S9 DJ-8153	2	*	434	+3	144	16.538	3-434	Beg-End	~400	<i>Bra</i> BcRK3	<i>Bra</i> <i>BcRL3</i> (for BcRK3)
	3	**	482	+1	160	18.163	1-480	Beg-End	~400	<i>Bol</i> SLG9	<i>Bol</i> SLG9
	4	**	652	+2	217	24.884	2-652	Beg-End	~400	<i>Bol</i> SLG9	<i>Bol</i> SLG9
	10	**	888	+2	295	33.875	2-886	Beg-End	~400	<i>Bol</i> SLG9	<i>Bol</i> SLG9
	12	***	721	+1	240	27.479	1-720	Beg-End	~400	<i>Bra</i> BcRK1	<i>Bra</i> <i>BcRK1</i>
	15	***	697	+2	232	26.049	2-697	Beg-End	~400	<i>Bol</i> SLG9	<i>Bol</i> SLG9
	Contig. 3+4+10+1 5	**	907	+2	302	34.247	2-907	Beg-End	~400	<i>Bol</i> SLG9	<i>Bol</i> SLG9

Table 6.5 continued.

Taxon Name	Primer pair	Sequence quality	Sequence Length (bases)	Translation Frame	ORF length (AA)	Actual Molecular weight (kD)	Start-stop DNA base number	Start-stop Triplets	Number of S-domain hits in NCBI/Blast NR database having E value < 0.02	Name of Top protein SSEARCH	Name of Top NCBI/Blast Nucleotide Search
<i>Brassica oleracea</i> - S13 DJ-4099	1	***	439	+1	146	16.949	1-438	Beg-End	~400	<i>Bol</i> SLG13	<i>Bol</i> SRK13
	2	**	465	+1	155	17.729	1-465	Beg-End	~400	<i>Bra</i> BcRK3	<i>Bra</i> BcRL3 (for BcRK3)
	3	***	520	+1	173	19.741	1-519	Beg-End	~400	<i>Bol</i> SRK13	<i>Bol</i> SRK13
	4	***	689	+3	229	26.432	1-689	Beg-End	~400	<i>Bol</i> SRK13	<i>Bol</i> SRK13
	5+6 (Ba2)	***	585	+2	194	22.605	2-583	Beg-End	~400	<i>Bol</i> SLR3-1	<i>Bol</i> SLR3-1
	7	*	698	+2	232	26.656	2-697	Beg-End	~400	<i>Bol</i> SLG13	<i>Bol</i> SLG13
	8	***	976	+1	325	37.496	1-975	Beg-End	~400	<i>Bol</i> SRK13	<i>Bol</i> SRK13
	9 (Ba1)	*	958	+3	318	36.715	3-956	Beg-End	~400	<i>Bol</i> SRK13	<i>Bol</i> SRK13
	9 (Ba2)	***	736	+1	245	28.228	1-735	Beg-End	~400	<i>Bol</i> SLR3-1	<i>Bol</i> SLR3-1
	10	**	956	+2	318	36.487	2-955	Beg-End	~400	<i>Bol</i> SRK3	<i>Bol</i> SRK13
	12	***	633	+1	211	24.176	1-633	Beg-End	~400	<i>Bra</i> SRK1	<i>Bra</i> BcRK1
	13	**	654	+1	218	25.097	1-654	Beg-End	~400	<i>Bra</i> BcRK3	<i>Bra</i> BcRL3 (for BcRK3)
	15	***	691	+1	230	26.364	1-690	Beg-End	~400	<i>Bol</i> SLG13	<i>Bol</i> SLG13
	Contig. 7+15	***	706	+1	235	26.777	1-705	Beg-End	~400	<i>Bol</i> SLG13	<i>Bol</i> SLG13
	Contig. 5+6+9 (Ba2)	***	805	+1	268	30.993	1-804	Beg-End	~400	<i>Bol</i> SLR3-1	<i>Bol</i> SLR3-1
Contig. 1+3+4+8+10	***	1021	+1	340	39.047	1-1020	Beg-End	~400	<i>Bol</i> SRK13	<i>Bol</i> SRK13	
Contig. 2+13	**	1038	+1	346	39.683	1-1038	Beg-End	~400	<i>Bra</i> BcRK3	<i>Bra</i> BcRL3 (for BcRK3)	
<i>Brassica oleracea</i> – S15 DJ-4049	5+6 (Ba2)	***	588	-1	196	22.958	588-1	Beg-End	~400	<i>Bol</i> SLR3-1	<i>Bol</i> SLR3-1
	7	*	700	+2	233	26.806	2-700	Beg-End	~400	<i>Bol</i> SRK15	<i>Bol</i> SRK15
	9 (Ba2)	***	772	+2	257	29.846	2-772	Beg-End	~400	<i>Bol</i> SLR3-1	<i>Bol</i> SLR3-1
	11	***	216	+2	71	8.519	2-214	Beg-End	~400	<i>Bol</i> SRK15	<i>Bol</i> SRK15
	12	***	637	+2	92	10.570	362-637	ATG-End	~101	<i>Bra</i> BcRK1	<i>Bra</i> BcRK1
				+3	157	18.071	3-476	Beg-TGA	~101	<i>Bra</i> BcRK1	
	13	**	688	+2	229	25.860	2-688	Beg-End	~400	<i>Bol</i> SRK15	<i>Bol</i> SRK15
	14	***	625	+3	207	23.453	3-623	Beg-End	~400	<i>Bna</i> -SLG type	<i>Bol</i> SLGB (S15)
Contig. 5+6+9 (Ba2)	***	844	+2	281	32.654	2-844	Beg-End	~400	<i>Bol</i> SLR3-1	<i>Bol</i> SLR3-1	

Table 6.5 continued.

Taxon Name	Primer pair	Sequence quality	Sequence Length (bases)	Translation Frame	ORF length (AA)	Actual Molecular weight (kD)	Start-stop DNA base number	Start-stop Triplets	Number of S-domain hits in NCBI/Blast NR database having E value < 0.02	Name of Top protein SSEARCH	Name of Top NCBI/Blast Nucleotide Search
<i>Brassica oleracea</i> - S29 DJ-2025	3	***	549	+2	182	20.661	2-547	Beg-End	~400	<i>Bol</i> SLG29-2	<i>Bol</i> SLG29-2
	4	***	678	+1	226	26.022	1-678	Beg-End	~400	<i>Bol</i> SLG29-2	<i>Bol</i> SLG29-2
	7	*	705	+1	235	26.475	1-705	Beg-End	~200	<i>Bol</i> SLG23	<i>Bol</i> SRK29
	8	***	974	+3	324	37.312	3-974	Beg-End	~400	<i>Bol</i> SLG29-2	<i>Bol</i> SLG29-2
	12	***	635	+3	211	24.166	3-635	Beg-End	~400	<i>Bra</i> BcRK1	<i>Bra</i> BcRK1
	13	**	719	+2	239	27.613	2-718	Beg-End	~400	<i>Bra</i> BcRK3	<i>Bra</i> BcRL3 (for BcRK3)
	15	***	687	+3	228	25.758	3-686	Beg-End	~400	<i>Bol</i> SRK29	<i>Bol</i> SRK29
	Contig. 7+15	***	705	+1	235	26.453	1-705	Beg-End	~200	<i>Bol</i> SLG23	<i>Bol</i> SRK29
	Contig 3+4+8	***	1014	+3	337	38.643	3-1013	Beg-End	~400	<i>Bol</i> SLG29-2	<i>Bol</i> SLGS29-2
<i>Centaurea cyamus</i> 2002-1446	2	***	477	+3	159	17.670	3-476	Beg-End	~350	<i>Itr</i> ISG2	<i>Ciona intestinalis</i>
	7	***	751	+1	250	28.613	1-750	Beg-End	~350	<i>Itr</i> IRK1	<i>Itr</i> IRK1
	8	**	949	+1	315	36.121	1-948	Beg-TGA	None	<i>Osa</i> 1,3 beta glucan synthase	<i>Ath</i> Callose synthase
	9	***	786	+3	262	29.454	3-788	Beg-End	~350	<i>Ath</i> RLK	<i>Ath</i> Callose synthase
	10	***	1035	+2	345	39.357	2-1036	Beg-End	~350	<i>Itr</i> ISG2	<i>Itr</i> IRK1
	13	***	756	+2	252	28.962	2-757	Beg-End	~350	<i>Ath</i> RLK	<i>Ath</i> Chromosome 4
	15	**	765	+3	255	28.792	3-767	Beg-End	~350	<i>Itr</i> ISG1	<i>Homo sapiens</i> Chromosome 12
<i>Conyza canadensis</i> 2002-3497	7	***	756	+3	251	28.333	3-755	Beg-End	~350	<i>Ath</i> RLK	<i>Itr</i> IRK1
	10	***	1001	+1	333	37.135	1-999	Beg-End	~350	<i>Itr</i> ISG3	<i>Bol</i> SRK11
	15	***	721	+1	240	27.220	1-720	Beg-End	~350	<i>Itr</i> ISG3	<i>Itr</i> IRK1
<i>Conyza sumatrensis</i> 2002-3499	2	***	497	-3	165	18.877	497-3	Beg-End	None (~500 Pol polprotein)	<i>Zea mays</i> Pol polprotein	<i>Ath</i> gag pol polyprotein
	10	***	1051	+1	350	39.186	1-1050	Beg-End	~350	<i>Itr</i> ISG3	<i>Bol</i> SRK11
	15	***	690	+3	229	26.053	3-689	Beg-End	~350	<i>Itr</i> ISG3	<i>Homo sapiens</i> Chromosome 18

Table 6.5 continued.

Taxon Name	Primer pair	Sequence quality	Sequence Length (bases)	Translation Frame	ORF length (AA)	Actual Molecular weight (kD)	Start-stop DNA base number	Start-stop Triplets	Number of S-domain hits in NCBI/Blast NR database having E value < 0.02	Name of Top protein SSEARCH	Name of Top NCBI/Blast Nucleotide Search
<i>Cosmos atosanguineus</i> 1999-2254	1+2	***	513	+3	171	19.523	3-512	Beg-End	~350	<i>Itr</i> IRK1	<i>Itr</i> <i>IRK1</i>
	4	***	670	+2	223	25.658	2-670	Beg-End	~350	<i>Ath</i> RLK	<i>Ath</i> At4g30790
	5+6	***	709	+2	236	26.702	2-709	Beg-End	~350	<i>Itr</i> IRK1	<i>Itr</i> <i>IRK1</i>
	7	***	707	+3	235	26.635	3-707	Beg-End	~350	<i>Itr</i> IRK1	<i>Itr</i> <i>IRK1</i>
	8 Cl-1.3.5	***	965	+1	321	36.900	1-963	Beg-End	None (~80)	<i>Ath</i> callose synthase	<i>Osa</i> glucan synthase
	9	***	963	+1	321	36.386	1-963	Beg-End	~350	<i>Itr</i> IRK1	<i>Itr</i> <i>IRK1</i>
	10	***	1040	+2	346	39.113	2-1039	Beg-End	~350	<i>Itr</i> IRK1	<i>Itr</i> <i>IRK1</i>
	15	*	666	+3	221	24.528	3-665	Beg-End	~350	<i>Itr</i> ISG2	<i>Itr</i> <i>IRK1</i>
	Contig. 1+2+5+6 +7+9+10	***	1077	+3	358	40.456	3-1076	Beg-End	~350	<i>Itr</i> IRK1	<i>Itr</i> <i>IRK1</i>
<i>Cosmos atosanguineus</i> 1999-3819	1+2	***	529	+1	176	19.923	1-528	Beg-End	~350	<i>Itr</i> IRK1	<i>Aly</i> srelk10.1B3
	4	***	632	+2	210	24.131	2-631	Beg-End	~350	<i>Itr</i> ISG3	<i>Homo sapiens</i> SEP1 strand exchange protein
	5+6	***	680	+3	226	25.712	3-680	Beg-End	~350	<i>Itr</i> IRK1	<i>Itr</i> <i>IRK1</i>
	7	***	707	+3	235	26.635	3-707	Beg-End	~350	<i>Itr</i> IRK1	<i>Itr</i> <i>IRK1</i>
	8 Cl-1.4.11	***	972	+1	324	37.273	1-972	Beg-End	~80	<i>Ath</i> callose synthase	<i>Osa</i> glucan synthase
	10	***	1044	+1	348	39.270	1-1044	Beg-End	~350	<i>Itr</i> IRK1	<i>Itr</i> <i>IRK1</i>
	Contig. 1+2+5+6 +7+10	***	1069	+1	356	40.199	2-1069	Beg-End	350	<i>Itr</i> IRK1	<i>Itr</i> <i>IRK1</i>
<i>Cosmos atosanguineus</i> 1997-6334	1+2	***	518	+2	172	19.573	2-517	Beg-End	~350	<i>Itr</i> ISG2	<i>Aly</i> srelk10.1B3
	4	***	651	+1	217	24.884	1-651	Beg-End	~350	<i>Ath</i> RLK	<i>Ath</i> <i>RLK</i>
	5+6	***	711	+1	237	26.699	1-711	Beg-End	~350	<i>Itr</i> IRK1	<i>Itr</i> <i>IRK1</i>
	7	***	677	+3	225	25.300	3-677	Beg-End	~350	<i>Itr</i> IRK1	<i>Itr</i> <i>IRK1</i>
	8	***	944	+3	314	35.700	3-944	Beg-End	~350	<i>Itr</i> IRK1	<i>Itr</i> <i>IRK1</i>
	9	***	900	+1	300	33.877	1-900	Beg-End	~350	<i>Itr</i> IRK1	<i>Itr</i> <i>IRK1</i>
	10	***	959	+3	319	36.009	3-959	Beg-End	~350	<i>Itr</i> IRK1	<i>Itr</i> <i>IRK1</i>
	Contig. 1+2+5+6 +7+9+10	***	1048	+2	349	39.353	2-1048	Beg-End	~350	<i>Itr</i> IRK1	<i>Itr</i> <i>IRK1</i>

Table 6.5 continued.

Taxon Name	Primer pair	Sequence quality	Sequence Length (bases)	Translation Frame	ORF length (AA)	Actual Molecular weight (kD)	Start-stop DNA base number	Start-stop Triplets	Number of S-domain hits in NCBI/Blast NR database having E value < 0.02	Name of Top protein SSEARCH	Name of Top NCBI/Blast Nucleotide Search
<i>Cosmos atrosanguineus</i> 5010-Sherff	1	***	505	+3	167	19.029	3-503	Beg-End	~350	<i>Itr</i> IRK1	<i>Itr</i> <i>IRK1</i>
	4	***	668	+1	222	25.587	1-666	Beg-End	~350	<i>Ath</i> RLK	<i>Homo sapiens</i> <i>RP11-120A1</i>
<i>Cosmos bipinnatus</i> 1996-582	1	***	505	+3	167	18.953	3-503	Beg-End	~350	<i>Itr</i> IRK1	<i>Ath</i> <i>RLK</i>
	2	***	385	+3	127	14.722	3-383	Beg-End	~350	<i>Bra</i> BcRK3	<i>Bra</i> <i>BcRL3</i> (for BcRK3)
	4	***	516	+1	172	19.728	1-516	Beg-End	~350	<i>Aly</i> S-related	<i>Homo sapiens</i> <i>SEP1</i> strand exchange
	5+6	***	704	+3	234	26.366	3-704	Beg-End	~350	<i>Itr</i> IRK1	<i>Itr</i> <i>IRK1</i>
	7	***	715	+1	238	26.879	1-714	Beg-End	~350	<i>Itr</i> IRK1	<i>Itr</i> <i>IRK1</i>
	8	***	792	+2	263	30.154	2-790	Beg-End	~350	<i>Itr</i> IRK1	<i>Itr</i> <i>IRK1</i>
	10	***	1003	+1	334	37.565	1-1002	Beg-End	~350	<i>Itr</i> IRK1	<i>Itr</i> <i>IRK1</i>
	15	***	703	+3	233	25.742	3-701	Beg-End	~350	<i>Itr</i> ISG3	<i>Itr</i> <i>IRK1</i>
Contig. 1+5+6+7+ 8+10	***	1080	+3	359	40.610	3-1079	Beg-End	~350	<i>Itr</i> IRK1	<i>Itr</i> <i>IRK1</i>	
<i>Cosmos carvifolius</i> 1999-3819	1+2	***	529	+1	176	19.923	1-528	Beg-End	~350	<i>Itr</i> ISG2	<i>Aly</i> <i>srelk10.1B3</i>
	4	***	524	+1	174	19.947	1-522	Beg-End	~350	<i>Ath</i> RLK	<i>Homo sapiens</i> <i>SEP1</i> strand exchange protein
	5+6	***	673	+1	224	25.513	1-672	Beg-End	~350	<i>Itr</i> IRK1	<i>Itr</i> <i>IRK1</i>
	7	***	723	+1	241	27.346	1-723	Beg-End	~350	<i>Itr</i> IRK1	<i>Itr</i> <i>IRK1</i>
	8 Cl-23	***	975	+1	325	36.752	1-975	Beg-End	~350	<i>Itr</i> IRK1	<i>Itr</i> <i>IRK1</i>
	10	***	989	+3	329	36.954	3-989	Beg-End	~350	<i>Itr</i> IRK1	<i>Itr</i> <i>IRK1</i>
	15	***	764	+2	253	28.043	2-763	Beg-End	~340	<i>Ath</i> RLK	<i>Itr</i> <i>IRK1</i>
Contig. 1+2+5+6+ 7+8+10	***	1083	+1	361	40.873	1-1083	Beg-End	~350	<i>Itr</i> IRK1	<i>Itr</i> <i>IRK1</i>	
<i>Cosmos sulphureus</i> 1996-980	1	***	456	+2	151	16.724	2-454	Beg-End	~350	<i>Itr</i> ISG3	<i>Aly</i> <i>srelk7</i>
	5+6	***	692	+1	230	26.205	1-690	Beg-End	~350	<i>Itr</i> IRK1	<i>Bra</i> <i>NS3</i>
	7	***	749	+2	249	28.122	2-748	Beg-End	~350	<i>Itr</i> IRK1	<i>Bra</i> <i>NS3</i>
	Contig. 5+6+7	***	749	+2	249	28.122	2-748	Beg-End	~350	<i>Itr</i> IRK1	<i>Bra</i> <i>NS3</i>

Table 6.5 continued.

Taxon Name	Primer pair	Sequence quality	Sequence Length (bases)	Translation Frame	ORF length (AA)	Actual Molecular weight (kD)	Start-stop DNA base number	Start-stop Triplets	Number of S-domain hits in NCBI/Blast NR database having E value < 0.02	Name of Top protein SSEARCH	Name of Top NCBI/Blast Nucleotide Search
<i>Diplotaxis tenuifolia</i> 2002-3495	4	***	696	+2	231	26.471	2-694	Beg-End	~350	<i>Bol</i> SLG6	<i>Bol</i> SLG22
	7	**	751	+2	250	28.261	2-751	Beg-End	~350	<i>Bra</i> SLG	<i>Bra</i> SLG26
	13	***	702	+2	233	26.077	3-701	Beg-End	~350	<i>Bol</i> SFR2	<i>Bol</i> ARLK
	15	***	768	+1	256	29.249	1-768	Beg-End	~340	<i>Rsa</i> SLG2	<i>Rsa</i> SLG2
	Contig 7+15	***	771	+1	257	29.471	1-771	Beg-End	~340	<i>Bol</i> SRK6	<i>Bra</i> SLG26
<i>Picris echioides</i> 2002 3494	2	***	529	+3	175	19.425	3-527	Beg-End	~350	<i>Itr</i> ISG3	<i>Homo sapiens</i> clone RP11- 38G5
	7	***	746	+2	248	27.915	2-745	Beg-End	~350	<i>Ath</i> RLK	<i>Homo sapiens</i> Chromosome 21
<i>Senecio squalidus</i> 2002-3493	2	**	404	+2	134	15.045	3-403	Beg-End	~350	<i>Bra</i> BcRK3	<i>Bra</i> BcRL3 (for BcRK3)
	7	***	684	+3	227	26.149	3-683	Beg-End	~350	<i>Ath</i> RLK	<i>Hepatitis B</i> virus strain C-1858
<i>Senecio vulgaris</i> 2002-3492	2	**	432	+3	143	16.301	3-431	Beg-End	~350	<i>Bra</i> BcRK3	<i>Bra</i> BcRL3 (for BcRK3)
	4	***	642	+1	214	24.688	1-642	Beg-End	~350	<i>Itr</i> ISG3	<i>Homo sapiens</i> chromosome 5 clone CTD- 2350L11
	5+6	***	680	+1	171	20.100	1-516	Beg-TAG	~350	<i>Ath</i> ARK3	<i>Homo sapiens</i> chromosome 5 clone CTD- 2350L11
	7	***	713	+2	237	27.416	2-712	Beg-End	~350	<i>Ath</i> RLK	<i>Ath</i> At4g27300 putative receptor protein kinase

Analysis of the 143 CosPS nucleotide sequences generated by primer pairs 1-15 identified twenty-seven 5'-end, eighty-five 3'-end, and twenty-six whole-piece CosPS sequences predicted to encode S-domain molecules (Table 6.4). These 138 S-domain encoding sequences contained redundant sequences. Combining redundant CosPS nucleotide sequences into contiguous sequences resulted in 88 non-redundant S-domain encoding CosPS nucleotide sequences. These 88 non-redundant S-domain encoding CosPS nucleotide sequences are listed and described in Table 6.6.

Table 6.6 List of the 88 distinct CosPS nucleotide sequences generated by Primer Pairs 1-15 in Asteraceae and Brassicaceae

Species	Acc. No.	Seq. No.	Name of Sequence	Sequence Length	
				Bases	Res.
Control sequence 1 <i>Brassica oleracea</i> SLG13	CAA38995	+ve	SLG13 – <i>S</i> -locus secreted glycoprotein from the <i>Brassica oleracea</i> -S13 haplotype	1308	435
Control sequence 2 <i>Ipomoea trifida</i> IRK1	AAC23542	+ve	IRK1 – <i>Ipomoea</i> receptor kinase 1 from <i>Ipomoea trifida</i>	3249	853
<i>Arabidopsis thaliana</i>	HRI - W	1	CosPS–Ath_sequence 1	425	141
		2	CosPS–Ath_contig ¹	985	328
		3	CosPS–Ath_contig ²	1093	364
<i>Brassica oleracea</i> -(S2)	DJ-2024	4	CosPS–Bol-(S2)_sequence 11	215	71
		5	CosPS–Bol-(S2)_sequence 2	382	126
		6	CosPS–Bol-(S2)_sequence 1	397	132
		7	CosPS–Bol-(S2)_sequence 14	612	204
		8	CosPS–Bol-(S2)_sequence 12	661	113 132
<i>Brassica oleracea</i> -(S3)	DJ-8189	9	CosPS–Bol-(S3)_sequence 1	418	139
		10	CosPS–Bol-(S3)_sequence 5+6 (ba 2)	665	192
		11	CosPS–Bol-(S3)_sequence 12	599	199
		12	CosPS–Bol-(S3)_sequence 15	698	232
		13	CosPS–Bol-(S3)_contig. 3+4+7+8	973	324
		14	CosPS–Bol-(S3)_contig. 2+13	1035	344
<i>Brassica oleracea</i> -(S5)	DJ-4078/1	15	CosPS–Bol-(S5)_sequence 11	216	71
		16	CosPS–Bol-(S5)_sequence 7	396	131
		17	CosPS–Bol-(S5)_sequence 3	457	152
		18	CosPS–Bol-(S5)_sequence 5+6 (ba 2)	578	192
		19	CosPS–Bol-(S5)_sequence 12	637	92 149
		20	CosPS–Bol-(S5)_sequence 14	610	203
<i>Brassica oleracea</i> -(S6)	DJ-4080	21	CosPS–Bol-(S6)_sequence 1	220	73
		22	CosPS–Bol-(S6)_sequence 7	560	186
		23	CosPS–Bol-(S6)_sequence 5+6 (ba 1)	683	227
		24	CosPS–Bol-(S6)_sequence 15	684	228
		25	CosPS–Bol-(S6)_sequence 12	718	238
		26	CosPS–Bol-(S6)_contig. 5+6+9 (ba 2)	854	284
		27	CosPS–Bol-(S6)_contig. 3+4+8	1015	338
		28	CosPS–Bol-(S6)_contig. 2+13	1047	349

Acc. No., Accession number; **Seq. No.**, sequence number; **Res**, residues. The prefix, CosPS indicates the sequence was generated using primer pairs described in Table 6. **Bol-(S6)** identifies *B. oleracea* S6 haplotype as the DNA source; **Cen.cyan**, *centaurea cyanus*; **Con.can**, *Conyza canadensis*; **Con.sum**, *Conyza sumatrensis*; **Cos.atr**, *Cosmos atosanguineus*; **Cos.bip**, *C. bipinnatus*; **Cos.car**, *C. carvifolius*; **Cos.sul**, *C. sulphureus*; **Dip.ten**, *Diplotaxis tenuifolia*; **Pic.ech**, *Picris echioides*; **Sen.squ**, *Senecio squalidus*; **Sen.vul**, *S. vulgaris*. The number at the end of the sequence name identifies the specific primer pair or combinations of primer pairs used to amplify the CosPS sequence, and construct the contig.

Table 6.6 continued.

Species	Acc. No.	Seq. No.	Name of CosPS Sequence	Sequence Length	
				Bases	Res.
<i>Brassica oleracea</i> -(S9)	DJ-8153	29	CosPS-Bol-(S9)_sequence 2	434	144
		30	CosPS-Bol-(S9)_sequence 12	721	240
		31	CosPS-Bol-(S9)_contig 3+4+10+15	907	302
<i>Brassica oleracea</i> -(S13)	DJ-4099	32	CosPS-Bol-(S13)_sequence 12	633	211
		33	CosPS-Bol-(S13)_contig 7+15	706	235
		34	CosPS-Bol-(S13)_contig ¹ . 5+6+9 (ba 2)	805	268
		35	CosPS-Bol-(S13)_sequence 9 (ba1)	958	318
		36	CosPS-Bol-(S13)_contig ³ . 1+3+4+8+10	1021	340
		37	CosPS-Bol-(S13)_contig ² . 2+13	1038	346
<i>Brassica oleracea</i> -(S15)	DJ-4049	38	CosPS-Bol_(S15)_sequence 11	216	71
		39	CosPS-Bol_(S15)_sequence 14	625	207
		40	CosPS-Bol_(S15)_sequence 13	688	229
		41	CosPS-Bol_(S15)_sequence 7	700	233
		42	CosPS-Bol_(S15)_sequence 12	637	92 157
		43	CosPS-Bol-(S15)_contig 5+6+9 (ba2)	844	281
<i>Brassica oleracea</i> -(S29)	DJ-2025	44	CosPS-Bol-(S29)_sequence 12	635	211
		45	CosPS-Bol-(S29)_sequence 7+15	705	235
		46	CosPS-Bol-(S29)_sequence 13	719	239
		47	CosPS-Bol-(S29)_contig 3+4+8	1014	337
<i>Centaurea cyanus</i>	2002 1446	48	CosPS-Cen.cyan_sequence 2	481	159
		49	CosPS-Cen.cyan_sequence 7	751	250
		50	CosPS-Cen.cyan_sequence 9	788	262
		51	CosPS-Cen.cyan_sequence 10	1038	345
		52	CosPS-Cen.cyan_sequence 13	757	252
		53	CosPS-Cen.cyan_sequence 15	769	255
<i>Conyza canadensis</i>	2002 3497	54	CosPS-Con.can sequence 7	756	251
		55	CosPS-Con.can sequence 10	1001	333
		56	CosPS-Con.can sequence 15	721	240
<i>Conyza sumatrensis</i>	2002 3499	57	CosPS-Con.sum sequence 10	1051	350
		58	CosPS-Con.sum sequence 15	690	229
<i>Cosmos atrosanguineus</i>	1999 2254	59	CosPS-Cos.atr ⁽²²⁵⁴⁾ -sequence 4	670	223
		60	CosPS-Cos.atr ⁽²²⁵⁴⁾ -sequence 15	666	221
		61	CosPS-Cos.atr ⁽²²⁵⁴⁾ -contig 1+2+5+6+7+9+10	1077	358
<i>Cosmos atrosanguineus</i>	1999 3819	62	CosPS-Cos.atr ⁽³⁸¹⁹⁾ -sequence 4	632	210
		63	CosPS-Cos.atr ⁽³⁸¹⁹⁾ -contig 1+2+5+6+7+10	1069	356

Table 6.6 continued.

Species	Acc. No.	Seq. No.	Name of CosPS Sequence	Sequence Length	
				Bases	Res.
<i>Cosmos atrosanguineus</i>	1997 6334	64	CosPS–Cos.atr ⁽⁶³³⁴⁾ -sequence 4	651	217
		65	CosPS–Cos.atr ⁽⁶³³⁴⁾ -sequence 8	944	314
		66	CosPS–Cos.atr ⁽⁶³³⁴⁾ -contig 1+2+5+6+7+9+10	1048	349
<i>Cosmos atrosanguineus</i>	Sherff 5010	67	CosPS–Cos.atr ⁽⁵⁰¹⁰⁾ -sequence 1	505	167
		68	CosPS–Cos.atr ⁽⁵⁰¹⁰⁾ -sequence 4	668	222
<i>Cosmos bipinnatus</i>	1996 582	69	CosPS–Cos.bip_sequence 2	385	127
		70	CosPS–Cos.bip_sequence 4	516	172
		71	CosPS–Cos.bip_sequence 15	703	233
		72	CosPS–Cos.bip_contig 1+5+6+7+8+10	1080	359
<i>Cosmos carvifolius</i>	1999 383	73	CosPS–Cos.car_sequence 4	524	174
		74	CosPS–Cos.car_sequence 15	764	253
		75	CosPS–Cos.car_contig 1+2+5+6+7+8+10	1083	361
<i>Cosmos sulphureus</i>	1996 980	76	CosPS–Cos.sul_sequence 1	456	151
		77	CosPS–Cos.sul_contig 5+6+7	749	249
<i>Diploaxis tenuifolia</i>	2002 3495	78	CosPS–Dip.ten_sequence 4	696	231
		79	CosPS–Dip.ten_sequence 13	702	233
		80	CosPS–Dip.ten_contig 7+15	771	256
<i>Picris echioides</i>	2002 3494	81	CosPS–Pic.ech_sequence 2	529	175
		82	CosPS–Pic.ech_sequence 7	746	248
<i>Senecio squalidus</i>	2002 3493	83	CosPS–Sen.squ_sequence 2	404	134
		84	CosPS–Sen.squ_sequence 7	684	227
<i>Senecio vulgaris</i>	2002 3492	85	CosPS–Sen.vul_sequence 2	432	134
		86	CosPS–Sen.vul_sequence 4	642	214
		87	CosPS–Sen.vul_contig 5+6	680	171
		88	CosPS–Sen.vul_sequence 7	713	237

6.3.3 - Analysis of encoded *Arabidopsis thaliana* and *Brassica oleracea* CosPS sequences

Priming in *Arabidopsis thaliana* and *Brassica* shows that in these taxa, primer pairs 1-15 identify exclusively S-domain encoding sequences of expected lengths, and prime consistently 5'-end, 3'-end and wholepiece sequences predicted for each primer pair (Table 6.6).

The accuracy of priming was evidenced by the ability of primer pairs to produce *A. thaliana* nucleotide sequences that had zero E-values and aligned with 96-100% identity for their entire lengths with specific *A. thaliana* sequences in the NCBI-NR database. Likewise, in haplotypes of *Brassica oleracea*, primer pairs 1-15, amplified accurately and precisely, identifying haplotype specific S-gene sequences with a high degree of significance. Furthermore, primer pairs 1-15 were able to identify S-sequences in *Brassica oleracea* that had previously only been identified in *Brassica rapa*.

6.3.4 - Analysis of encoded Asteraceae CosPS protein sequences

In addition to BLASTN and BLASTP analyses of Asteraceae and *Diplotaxis tenuifolia* nucleotide and deduced protein sequences (Table 6.5), the predicted CosPS protein sequences for these taxa were assessed for the presence of conserved domains using the Conserved Domain Database and Search Service (CDD) (v.1.62) (Bork and Gobson, 1996; Marchler-Bauer *et al.* 2003). Prior to the CDD search, the conserved domains of 50 full-length representative S-domain sequences from a range of plant taxa were surveyed. The results of this survey are detailed in Table 6.7, and show that S-domain proteins typically contain the six conserved domains: (i) B-lectin CD (smart00108) and (ii) B-lectin CD (cd00028), both consisting of 117 residues located at residues ~30-170 of the primary S-protein.; (iii) Agglutinin CD (pfam01453), 110 residues long, located at residues ~70-200; (iv) S-locus glycoprotein CD (pfam00954), consisting of 138 amino acids and located at residues ~195-350; (v) PAN_AP Apple-like CD (cd00129) and (vi) PAN_AP, divergent subfamily of APPLE CD (smart00473), which are 80 and 79 residues long respectively, and locate to residues ~340-440 of primary S-proteins ((Table 6.7).

The location of these six conserved domains varies slightly in S-proteins. In most primary S-proteins, B-lectin CDs (smart00108 and cd00028) usually occupy residues 35-166 and exhibit 90%-100% alignment between S-proteins (Table 6.7). However, these CD domains may also be found further towards the N-terminus as in *Brassica oleracea* SFR2, SRK11 and SLG5 where they occupy residues 32-155, 30-155 and 29-151 respectively, and in *Lotus japonicus* SRK where they are located between residues 15-135. The Agglutinin CD (pfam01453) shows approximately 100% alignment in S-proteins and typically occurs between residues 68-196. The only exception is *Lotus japonicus* SRK in which the Agglutinin CD is located further upstream at residues 56-162, as is its S-locus glycoprotein CD (pfam00954) positioned at residues 180-315, instead of residues 195-348. In spite of these positional differences its SRK S-domain retains 100% alignment with the S-locus CD. The PAN_AP Apple-like CD (cd00129) and (vi) the PAN_AP, divergent subfamily of APPLE CD (smart00473) show ~100% alignment in most S-proteins, and are located between residues 339-439 (Table 6.7). An interesting observation from analysis of S-protein CD domains is the absence of the S-locus glycoprotein conserved domain in SRK of *Linum usitatissimum*, OsPK10 of and ZmPK1. The qualification of these sequences as S-domain molecules appears to be due to the presence of a Cys domain, their B-lectin (smart00108 and cd00028) and Agglutinin (pfam01453) CDs. A further minor difference occurs in the E values between the S-

locus conserved domains of class-I and class-II S-proteins. Class-II S-domains generally have S-locus CDs with slightly lower significance in their E values at $1e-50$ instead of $1e-59$ found in most class-I S-proteins (Table 6.7).

6.3.5 - Criteria for identifying S-domain CosPS-protein sequences

A candidate CosPS S-domain sequence should include one or all of the six conserved domains at the appropriate location. CosPS proteins predicted from 5'-end CosPS sequences should contain the B-lectin CDs (smart00108 and cd00028), and the Agglutinin CD (pfam01453) and may additionally contain the conserved potential N-glycosylation site at residues ~90 [~120] and the PTDT box at residues 116-132 [~146–162]. Proteins predicted from the 3'-end CosPS nucleotide sequences should, depending on their length, contain the S-locus glycoprotein CD (pfam00954), the PAN_AP Apple-like CD (cd00129), and the PAN_AP divergent subfamily of APPLE CD (smart00473), as well as the PTDT box, the conserved potential N-glycosylation site at residues ~359 [~389], the Cys domain between residues 259-380 [~289-410]. Proteins predicted from wholepiece CosPS sequences and wholepiece-contiguous CosPS sequences should contain all six S-associated conserved domains, the conserved potential N-glycosylation sites at residues ~90 [~120] and ~359 [~389]; the Cys domain, and may additionally include a PTDT box. The *Brassica oleracea* SLG13 full-length protein sequence (Genbank acc. no. CAA38995) was used as the model S-domain sequence against which deduced CosPS protein sequences of Asteraceae species and *Diplotaxis tenuifolia* were compared.

The results of CDD searches are summarised in Table 6.8, and show that primer pairs 1-10, 12-13 and 15 isolate S-domain encoding sequences in Asteraceae that contain appropriately positioned S-associated conserved domains, the conserved potential N-glycosylation sites at residues ~90 [~120] and/or ~359 [~389], and the 12 positionally-conserved cysteine residues of the Cys domain. The S-locus glycoprotein domain of the encoded Asteraceae CosPS protein sequences are located between residues 190-345 and thus equate favourably with the location of S-locus glycoprotein domains previously reported (Table 6.7 & 6.8). Some of the Asteraceae deduced CosPS sequences also include a PTDT box, or a variant thereof. The encoded wholepiece (partial) Asteraceae CosPS sequences have 5-6 potential N-glycosylation sites, which equates favourably with the average 6-7 sites recorded for comparable regions in *Brassica* SLGs and SRK S-domains.

Table 6.7. Location of S-associated conserved domains in fifty full-length S-protein and S-like protein sequences retrieved from database the NCBI-NR (non-redundant) database and aligned using the Genbank CDD sequence comparison facility.

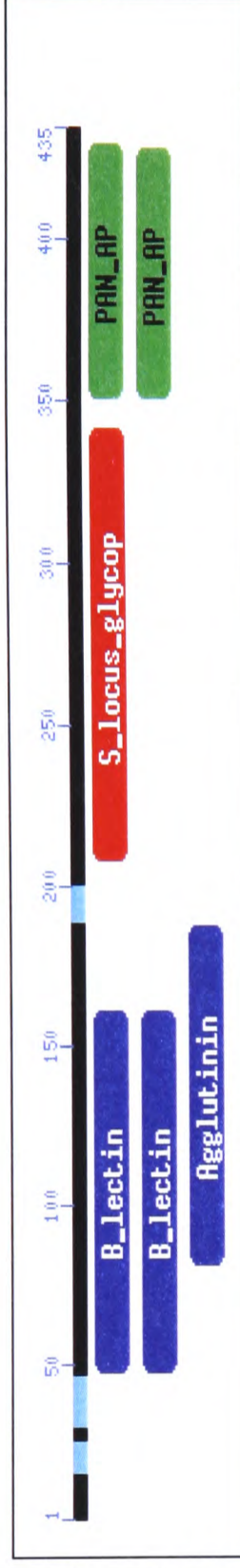
No.	Name S-protein	(smart00108) & (cd00028)	(cd00028)	(pfam00954)	(cd00028)	(smart00473)
		B_lectin (Bulb-type mannose- specific lectin) (L=117)	Agglutinin, Lectin (probable mannose binding (L=110)	S_locus- Glycoprotein (L=138)	PAN_AP, Apple-like (L=80)	PAN_AP, divergent subfamily of APPLE (L=79)
1	<i>Ath</i> -ARK1 (S70769)	35-153	76-179	198-333	342-422	342-421
2	<i>Ath</i> -ARK2 (AAB33486)	36-158	77-185	204-339	348-428	348-427
3	<i>Ath</i> -ARK3 (AAP04019)	37-159	78-185	204-339	349-428	349-427
4	<i>Ath</i> -AtS1 (AAG51043)	47-165	85-192	210-348	357-418	358-418
5	<i>Bna</i> -SLG (JQ2380)	47-162	81-188	207-342	350-431	350-430
6	<i>Bna</i> -SLR1 (S38424)	37-171	91-202	218-345	364-443	364-442
7	<i>Bna</i> -SRK (JQ1677)	42-164	83-191	210-346	354-434	354-433
8	<i>Bol</i> -SFR1 (T14519)	40-163	81-189	208-343	352-432	352-431
9	<i>Bol</i> -SFR2 (T14470)	32-155	73-182	200-335	344-424	344-423
10	<i>Bol</i> -SFR3 (T14520)	36-154	74-182	201-330	340-419	340-419
11	<i>Bol</i> -SLG-Sc (CAA72988)	48-164	83-191	210-344	352-431	352-431
12	<i>Bol</i> -SLG2-b (BAA83745)	48-164	83-191	210-348	356-435	356-435
13	<i>Bol</i> -SLG3 (CAA55949)	46-156	80-183	201-337	345-426	345-425
14	<i>Bol</i> -SLG5 (CAA35963)	29-151	70-178	197-332	341-419	341-419
15	<i>Bol</i> -SLG6 (P07761)	40-162	81-189	207-343	351-431	351-430
16	<i>Bol</i> -SLG9 (BAA21934)	39-149	73-176	195-331	339-419	339-418
17	<i>Bol</i> -SLG13 (CAA38995)	47-162	81-188	207-342	350-430	350-429
18	<i>Bol</i> -SLG15 (CAB41880)	48-164	83-191	210-348	356-435	356-435
19	<i>Bol</i> -SLG20 (BAC24062)	42-157	76-180	203-338	346-428	346-427
20	<i>Bol</i> -SLG29-2 (P22553)	42-161	80-188	206-342	350-430	356-435
21	<i>Bol</i> -SLR1 (AAB23284)	37-164	84-192	211-347	357-436	357-435
22	<i>Bol</i> -SLR2 (B53223)	42-164	86-191	210-345	345-432	345-432
23	<i>Bol</i> -SRK5 (CAB41878)	41-157	76-184	203-341	349-429	349-428
24	<i>Bol</i> -SRK11 (BAC24043)	30-155	74-182	201-337	345-427	345-426
25	<i>Bol</i> -SRK29 (T14471)	41-163	82-190	208-345	353-433	353-432
26	<i>Bol</i> -SRK57 (BAC24056)	35-150	69-177	195-331	339-419	339-418
27	<i>Bol</i> -SRK65 (BAC24060)	31-153	72-180	198-334	342-422	342-421
28	<i>Bra</i> -SLG8 (S14951)	40-162	81-189	207-342	350-430	350-429

Table 6.7 continued.

No.	Gene Name	(smart00108) & (cd00028)	(cd00028)	(pfam00954)	(cd00028)	(smart00473)
		B_lectin Bulb-type mannose-specific lectin (L=117)	Agglutinin, Lectin (probable mannose binding (L=110))	S_locus-Glycoprotein (L=138)	PAN_AP, Apple-like (L=80)	PAN_AP, divergent subfamily of APPLE (L=79)
29	<i>Bra</i> -SLG9 (T14392)	44-153	77-180	199-335	343-424	343-423
30	<i>Bra</i> -SLG12 (JC2250)	47-162	81-189	208-343	351-431	351-430
31	<i>Bra</i> -SLG22 (BAB21000)	40-162	81-189	208-344	352-432	352-431
32	<i>Bra</i> -SLG29 (T14376)	48-164	83-191	210-348	356-435	356-435
33	<i>Bra</i> -SLG40 (BAB20998)	41-157	76-184	203-341	349-428	349-428
34	<i>Bra</i> -SLG41 (BAA21956)	39-155	73-182	200-336	344-425	344-424
35	<i>Bra</i> -SLG44 (BAB20999)	42-157	76-184	203-341	349-428	349-428
36	<i>Bra</i> -SRK29 (BAA31252)	47-163	82-190	209-347	355-434	355-434
37	<i>Bra</i> -BcRK1 (BAA23676)	36-156	77-183	201-336	345-425	345-424
38	<i>Bra</i> -BcRK3 (BAB69682)	47-159	83-186	205-337	X	X
39	<i>Bra</i> -BcRK5 (BAB69683)	27-150	68-177	195-330	339-419	339-418
40	<i>Bra</i> -BcRK6 (BAB69684)	52-166	84-181	212-343	365-439	365-439
41	<i>Bra</i> -BcSL10 (BAB69687)	27-150	68-177	195-232*	---	---
42	<i>Itr</i> -ISG1 (AAA97901)	43-166	84-196	211-346	354-436	354-435
43	<i>Itr</i> -ISG2 (AAA97902)	45-160	77-190	205-340	348-428	348-428
44	<i>Itr</i> -ISG3 (AAA97903)	42-156	75-183	201-335	344-424	344-423
45	<i>Itr</i> -IRK1 (AAC23542)	37-158	78-185	203-338	346-410	346-427
46	<i>Lus</i> -Glycoprotein (AAO15899)	43-160	86-174	X	X	X
47	<i>Lja</i> -SRK (BAC41328)	15-135	56-162	180-315	325-405	325-405
48	<i>Rsa</i> -SLG7 (BAA31731)	47-162	81-189	207-343	351-431	351-430
49	<i>Osa</i> -OsPK10 (AAA33915)	48-164	89-180	X	X	X
50	<i>Zma</i> -ZmPK1 (P17801)	42-160	84-177	X	X	X
Approximate Percentage Alignment and Significance values of Class-I S-domains						
	% align	90-100	~100	~100	~100	~100
	E value	6e-28	4e-25	1e-59	2e-09	2e-08
Approximate Percentage Alignment and Significance values of Class-II S-domains						
	% align	90-100	~100	~100	~100	~99
	E value	3e-25	4e-22	1e-50	2e-07	2e-06

Key to abbreviations: *At*, *Arabidopsis thaliana*; *Bna*, *B. napus*; *Bol*, *B. oleracea*; *Bra*, *Brassica rapa*; *Itr*, *Ipomoea trifida*; *Lus*, *Linum usitatissimum*, *Lja*, *Lotus japonicus*; *Osa*, *Oryza sativa*; *Rsa*, *Raphanus sativus*; *Zma*, *Zea mays*

Table 6.8 Positions of S-domain-associated conserved domains in predicted CosPS protein sequences of Asteraceae species and *Diplotaxis tenuifolia*. Conserved-domain positions are adjusted to their expected positions in predicted full-length CosPS



Seq. No.	Sequence name	Sequence type	Length (aa)	B-lectin domains (smart00108) & (cd00028.) (L=117)	Agglutinin domain (pfam01453.) (L=110)	S-locus glycoprotein domain (pfam00954) (L=138)	PAN_AP Apple-like domain (cd00129) (L=80)	PAN_AP divergent subfamily of APPLE domain (smart00473) (L=79)	Cys domain	N-glycosylation site-120	N-glycosylation site-389	Number of potential N-glycosylation sites	PTDT Box
+ve	<i>Brassica oleracea</i> SLG13	complete	435	47-162	81-188	207-342	350-430	350-429	✓	✓	✓	8	✓
48	CosPS-Cen.cyan-sequence 2	Partial, 5' end	159	✓	✓	---	---	---	---	✗	---	2	(✗)
49	CosPS-Cen.cyan-sequence 7	Partial, 3' end	250	---	---	205-342	✓	✓	✓	---	✓	4	---
50	CosPS-Cen.cyan-sequence 9	Partial, wholepiece	262	✓	✓	206-326	---	---	(✓)	✓	---	5	(✗)
51	CosPS-Cen.cyan-sequence 10	Partial, wholepiece	345	✓	✓	198-335	✓	✓	✓	✓	✓	6	✓
52	CosPS-Cen.cyan-sequence 13	Partial, 3' end	252	---	---	200-335	✓	✓	✓	---	✗	2	---
53	CosPS-Cen.cyan-sequence 15	Partial, 3' end	255	---	---	226-339	✓	✓	✓	---	✓	3	✓
54	CosPS-Con.can-sequence 7	Partial, 3' end	251	---	---	205-339	✓	✓	✓	---	✓	6	---
55	CosPS-Con.can-sequence 10	Partial, wholepiece	333	✓	✓	199-335	✓	✓	✓	✓	✓	5	(✗)
56	CosPS-Con.can-sequence 15	Partial, 3' end	240	---	---	190-324	✓	✓	✓	---	✓	6	---
57	CosPS-Con.sum-sequence 10	Partial, wholepiece	350	✓	✓	200-338	✓	✓	✓	✓	✓	6	(✗)
58	CosPS-Con.sum-sequence 15	Partial, 3' end	229	---	---	189-320	✓	✓	✓	---	✓	5	---

Key to symbols. Three dot lines --- means not applicable, as the primer pair used to generate the CosPS sequence did not primer the region in which the conserved domain or conserved residues are located in *Brassica*. ✓ = present (and in the case of the Cys domain it means that all 12 cysteine residues are present and positionally conserved); ✗ = absent, (✓) = initial part of Cys domain only is present i.e. only the first 4-6 positionally conserved cysteine residues. (✗), indicates that the PTDT box has undergone changes in 1 to 5 residues, but is recognisable as a variant of this conserved region. +ve, indicates the positive control. The illustration at the top of the table shows the location of S-domain-associated conserved domains of *Brassica oleracea* SLG13 and was obtained from the NCBI Conserved Domain Database.

Table 6.8 Positions of S-associated conserved domains in predicted CosPS protein sequences of Asteraceae species and *Diplotaxis tenuifolia*. Conserved-domain positions are adjusted to their expected positions in predicted full-length CosPS protein sequences.

Seq. No.	Sequence name	Sequence type	Length (aa)	B-lectin domains (smart00108) & (cd00028.) (L=117)	Agglutinin domain (pfam01453.) (L=110)	S-locus glycoprotein domain (pfam00954) (L=138)	PAN_AP Apple-like domain (cd00129) (L=80)	PAN_AP, divergent subfamily of APPLE domain (smart00473) (L=79)	Cys domain	N-glycosylation site-120	N-glycosylation site-389	Number of potential N-glycosylation sites	PTDT Box
+ve	<i>Brassica oleracea</i> SLG13	complete	435	47-162	81-188	207-342	350-430	350-429	✓	✓	✓	8	✓
59	CosPS-Cos.atr ⁽²²⁵⁴⁾ sequence 4	Partial, 3' end	223	---	---	201-335	---	---	✓	---	✓	4	---
60	CosPS-Cos.atr ⁽²²⁵⁴⁾ sequence 15	Partial, 3' end	221	---	---	189-327	---	---	✓	---	✓	4	---
61	CosPS-Cos.atr ⁽²²⁵⁴⁾ contig.	Partial, wholepiece	358	✓	✓	211-346	✓	✓	✓	✓	✓	5	✓
62	CosPS-Cos.atr ⁽³⁸¹⁹⁾ sequence 4	Partial, 3' end	210	---	---	188--322	---	---	✓	---	✓	5	---
63	CosPS-Cos.atr ⁽³⁸¹⁹⁾ contig.	Partial, wholepiece	356	✓	✓	204-339	✓	✓	✓	✓	✓	5	✓
64	CosPS-Cos.atr ⁽⁶³³⁴⁾ sequence 4	Partial, 3' end	217	---	---	194-330	---	---	✓	---	✓	5	---
65	CosPS-Cos.atr ⁽⁶³³⁴⁾ sequence 8	Partial, wholepiece	314	✓	✓	193-327	---	---	✓	✓	✓	4	✓
66	CosPS-Cos.atr ⁽⁶³³⁴⁾ contig.	Partial, wholepiece	348	✓	✓	210-345	✓	✓	✓	✓	✓	5	✓
67	CosPS-Cos.atr ⁽⁵⁰¹⁰⁾ sequence 1	Partial, 5' end	167	✓	✓	---	---	---	---	✓	---	---	✓
68	CosPS-Cos.atr ⁽⁵⁰¹⁰⁾ sequence 4	Partial, 3' end	151	---	---	196-330	---	---	(✓)	---	---	5	---
69	CosPS-Cos.bip sequence 2	Partial, 5' end	127	✓	✓	---	---	---	---	✓	---	---	(X)
70	CosPS-Cos.bip sequence 4	Partial, 3' end	172	---	---	163-284	---	---	✓	---	✓	5	---
71	CosPS-Cos.bip sequence 15	Partial, 3' end	233	---	---	191-315	✓	✓	✓	---	✓	5	---
72	CosPS-Cos.bip contig.	Partial, wholepiece	359	✓	✓	211-346	✓	✓	✓	✓	✓	4	✓
73	CosPS-Cos.car sequence 4	Partial, 3' end	174	---	---	162-289	---	---	✓	---	---	4	---
74	CosPS-Cos.car sequence 15	Partial, 3' end	253	---	---	205-329	✓	---	✓	---	✓	3	---
75	CosPS-Cos.car contig	Partial, wholepiece	361	✓	✓	212-347	✓	✓	✓	✓	✓	4	✓

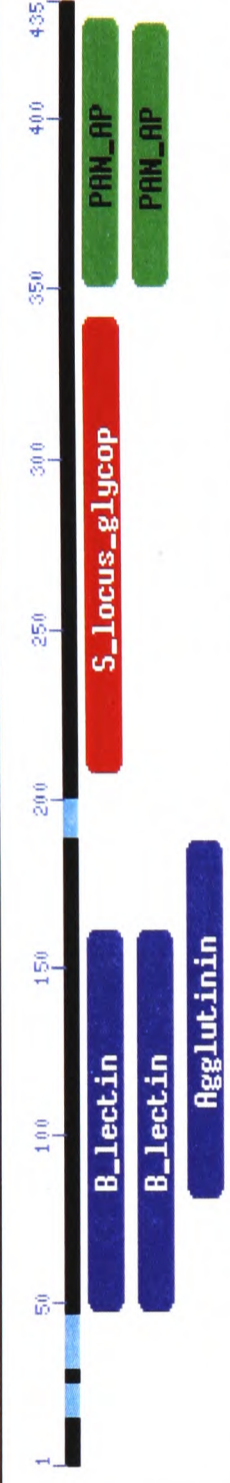
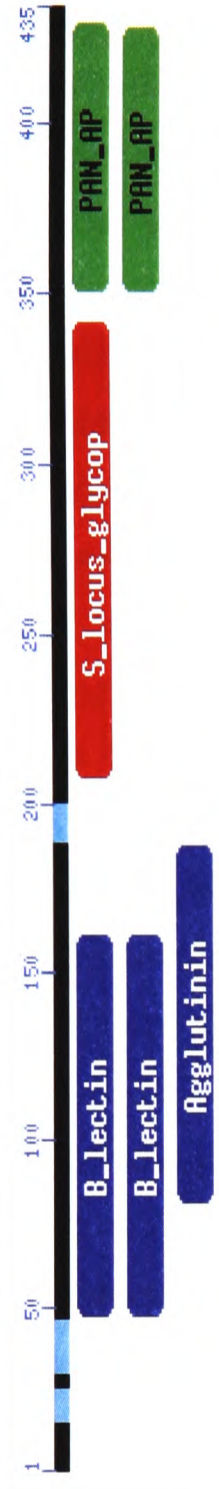


Table 6.8 Positions of S-associated conserved domains in predicted CosPS protein sequences of Asteraceae species and *Diplotaxis tenuifolia*. Conserved-domain positions are adjusted to their expected positions in predicted full-length CosPS protein sequences.

Seq. No.	Sequence name	Sequence type	Length (aa)	B-lectin domains (smart00108) & (cd00028,) (L=117)	Agglutinin domain (pfam01453,) (L=110)	S-locus glycoprotein domain (pfam00954) (L=138)	PAN_AP Apple-like domain (cd00129) (L=80)	PAN_AP, divergent subfamily of APPLE domain (smart00473) (79)	Cys domain	N-glycosylation site-120	N-glycosylation site-389	Number of potential N-glycosylation sites	PTDT Box
+ve	<i>Brassica oleracea</i> SLG13	complete	435	47-162	81-188	207-342	350-430	350-429	✓	✓	✓	8	✓
76	CosPS-Cos.sul_sequence 1	Partial, 5' end	151	✓	✓	---	---	---	---	✓	---	2	✓
77	CosPS-Cos.sul_contig.	Partial, 3' end	249	---	---	206-343	✓	✓	✓	---	✓	3	---
78	CosPS-Dip.ten_sequence 4	Partial, 3' end	231	---	---	203-339	✓	✓	✓	---	✗	3	---
79	CosPS-Dip.ten_sequence 13	Partial, 3' end	233	---	---	185-316	---	---	✓	---	✓	4	---
80	CosPS-Dip.ten_sequence 7+15	Partial, 3' end	256	---	---	206-342	✓	✓	✓	---	✓	4	---
81	CosPS-Pic.ech_sequence 2	Partial, 5' end	175	✓	✓	---	---	---	---	✗	---	3	(✗)
82	CosPS-Pic.ech_sequence 7	Partial, 3' end	248	---	---	201-335	✓	✓	✓	---	✓	4	---
83	CosPS-Sen.squ_sequence 2	Partial, 5' end	134	✓	✓	---	---	---	---	✓	---	2	(✗)
84	CosPS-Sen.squ_sequence 7	Partial, 3' end	227	---	---	196-331	✓	---	✓	---	✓	2	---
85	CosPS-Sen.vul_sequence 2	Partial, 5' end	143	✓	✓	---	---	---	---	✓	---	3	(✗)
86	CosPS-Sen.vul_sequence 4	Partial, 3' end	214	---	---	196-320	---	---	✓	---	✓	5	---
87	CosPS-Sen.vul_sequence 5+6	Partial, 3' end	171	---	---	200-332	---	---	(✓)	---	---	4	---
88	CosPS-Sen.vul_sequence 7	Partial, 3' end	237	---	---	193-327	✓	✓	✓	---	✗	3	---



6.4 - Discussion

6.4.1 - Trends and patterns in priming of CosPS sequences

Sequences 1 to 88 (Table 6.6) represent the S-domain-encoding CosPS sequences generated by primer pairs 1-15. The priming ability of these primers varied in plant species, with some combinations of primer-pair and species generating many CosPS sequences and others very few (Table 6.5). Primer pairs 7, 2 and 4 produced the highest number of S-domain encoding sequences in the 23 taxa, however the quality of sequences produced by these primers varied. In all Brassicaceae species apart from *A. thaliana*, primer pairs 2 and 7 produced sequences with a one-star (fair) or two-star (good) quality rating. This lower-than-excellent sequence quality was caused by double priming of two closely related sequences. In *Brassica oleracea* haplotypes, the two sequences generated by primer pairs 2 or 7 had identical peaks for 85-90% of their respective lengths. However, double peaks occurred in 10-15% of the sequence that compromised editing in these regions. In the main, ambiguous nucleotides were not difficult to edit as a primary sequence with a dominant signal prevailed in most cases. In the case of primer pair 7, which gave the most recalcitrant priming in *Brassicaceae*, editing was sometimes difficult and led to contrasting results. Judicious editing for the primary or secondary sequence resulted in either an *SRK*-related or an *SLG*-related sequence. In *B. oleracea* haplotypes used in this study, primer pair 7 favoured equally the priming of *SRK*- and *SLG*-related sequences, as the dominant signal produced haplotype-specific *SRK* sequences in *S*₅, *S*₆, *S*₁₅ and *S*₂₉ haplotypes, but haplotype-specific *SLG* sequences in *S*₃, *S*₉ and *S*₁₃ haplotypes (Table 6.5). In *S*₂ and *S*₉ haplotypes the forward and reverse strands produced by primer pair 7 could not be edited with confidence due to double priming of two equal-strength signals, while in *Diplotaxis tenuifolia*, primer pair 7 produced a single *SLG*-related sequence of good quality.

In contrast to the situation observed in *Brassica oleracea* haplotypes, priming with primer pair 7 in species of Asteraceae produced almost exclusively excellent-quality sequences throughout predicted lengths. In Asteraceae species, primer pair 7 generated receptor-like-kinase (RLK) related sequences homologous to *IRK1* of *Ipomoea trifida* or serine-threonine receptor-like kinase genes of *A. thaliana* (Table 6.5). It appears from these data that primer pair 7 is capable of priming simultaneously *SRK*- and *SLG*-related sequences in *B. oleracea* but not in species of Asteraceae or *Diplotaxis tenuifolia*, and may be functioning as an S-haplotype diagnostic primer pair, capable of identifying taxa that possess S-haplotype morphology, i.e. an S-locus consisting of *SLG* and *SRK*, from those that do not. This hypothesis could be tested through an assessment of the priming ability of primer pair 7 in the *B. oleracea* *S*₂₄ haplotype and *Arabidopsis lyrata* that have S-loci

devoid of *SLG*. Primer pair 2 generated a dominant signal identified as a *BcRL3* homologue in S_2 , S_3 , S_6 , S_9 , and S_{13} haplotypes, and a secondary weaker signal that was too weak to be edited with confidence. In the class-II haplotypes S_5 , S_{15} and S_{29} , the two signals produced by primer pair 2 were of equal strength and could not therefore be edited by the methods used in this study. Aside from *Senecio squalidus*, *S. vulgaris* and *Cosmos bipinnatus* where primer pair 2 generated good- and excellent-quality sequences identified as *BcRL3* homologues, it either failed to produce a sequence in the remaining species of Asteraceae, or generated S-domain-encoding sequences related to *Ipomoea trifida* S-proteins (Table 6.5).

In general, the primer pairs used in this study generate a greater number of distinct sequences in Brassicaceae than in Asteraceae, however the sequences produced by the latter are of higher quality. In many of the *Brassica oleracea* haplotypes, the low sequence quality is a consequence of double priming of two closely related same-sized S-domain sequences. In the majority of these sequences, the primary dominant sequence is clearly identifiable from the much weaker secondary signal and so sequence editing was not generally compromised. However, it would be preferable, in all circumstances where double priming takes place, to clone out the alternative sequences from the cleaned PCR product with a suitable cloning kit such as the pGEM[®]-T Easy Vector System I (Promega, Madison, USA). If this is done, the non-specificity of primer pairs 2, 7, 5+6 and 9 may prove an asset, since two or more S-domain sequences may be cloned by the use of a single primer pair.

6.4.2 - Homology in CosPS Sequences

(i) *Brassica oleracea* CosPS-sequences 5+6 (band 2) and 9 (band 2) are *SLR3-1* homologue

CosPS nucleotide sequences 5+6(ba2) and 9(ba2) of the *Brassica* haplotypes S_3 , S_5 , S_6 , S_{13} and S_{15} , are *SLR3-1* homologues that show ~98% pairwise sequence identity to each other, and to the *Brassica oleracea* *SLR3-1* (X81833) (Table 6.9a), with the encoded CosPS protein sequences reflecting the same level of sequence identity (Table 6.9b). *SLR3-1* was first isolated from the mutant *B. oleracea* self-compatible locus (Sc-S-locus) and was thought to be specific to this mutant, as it has not previously been isolated from self-incompatible haplotypes (Cock *et al.*, 1995). Evidence from this research indicates *SLR3-1* is a highly conserved monomorphic gene in *B. oleracea* where it probably serves a universal and fundamental function (Tables 6.9a and 6.9b). In species of Asteraceae and

Diplotaxis tenuifolia, primer pairs 5+6 and 9 isolate sequences that are not related to *SLR3-1*, suggesting that the conservation of this gene is specific to *Brassica species*.

Table 6.9a. Pairwise percentage identities of CosPS-nucleotide sequences 5+6(ba2) and 9(ba2) in *Brassica oleracea* haplotypes S_3 , S_5 , S_6 , S_{13} and S_{15} and *Brassica oleracea* *SLR3-1* (X81833)

	<i>Bol</i> -(S_3) CosPS 5+6(ba2)	<i>Bol</i> -(S_5) CosPS 5+6(ba2)	<i>Bol</i> -(S_6) CosPS 5+6+9(ba2)	<i>Bol</i> -(S_{13}) CosPS 5+6+9(ba2)	<i>Bol</i> -(S_{15}) CosPS 5+6+9(ba2)	<i>Brassica oleracea</i> <i>SLR3-1</i> (X81833)
<i>Bol</i> -(S_3) CosPS 5+6(ba2)		99	98	98	99	99
<i>Bol</i> -(S_5) CosPS 5+6(ba2)			98	98	98	98
<i>Bol</i> -(S_6) CosPS 5+6+9(ba2)				99	99	98
<i>Bol</i> -(S_{13}) CosPS 5+6+9(ba2)					99	99
<i>Bol</i> -(S_{15}) CosPS5+6+9(ba2)						99

Table 6.9b. Pairwise percentage identities for deduced protein sequences of CosPS_sequences 5+6(ba2), and CosPS_contigs 5+6+9(ba2) of *Brassica oleracea* haplotypes S_3 , S_5 , S_6 , S_{13} and S_{15} and *Brassica oleracea* *SLR3-1* (CAA57427)

	<i>Bol</i> -(S_3) CosPS 5+6(ba2)	<i>Bol</i> -(S_5) CosPS 5+6(ba2)	<i>Bol</i> -(S_6) CosPS 5+6+9(ba2)	<i>Bol</i> -(S_{13}) CosPS 5+6+9(ba2)	<i>Bol</i> -(S_{15}) CosPS 5+6+9(ba2)	<i>Brassica oleracea</i> <i>SLR3-1</i> (CAA57427)
<i>Bol</i> -(S_3) CosPS5+6(ba2)		99	98	97	98	99
<i>Bol</i> -(S_5) CosPS +6(ba2)			98	98	98	98
<i>Bol</i> -(S_6)CosPS5+6+9(ba2)				99	98	98
<i>Bol</i> -(S_{13}) CosPS5+6+9(ba2)					98	99
<i>Bol</i> -(S_{15}) CosPS5+6+9(ba2)						99

(ii) Primer pair 2 generates *BcRL3* homologues in *Brassica oleracea*, *Cosmos bipinnatus* and two *Senecio* species. Primer pair 13 generates *BcRL3* homologues in *Brassica oleracea* haplotypes

Primer-pair-2 generates sequences in *Brassica oleracea* haplotypes S_2 , S_3 , S_6 , S_9 , S_{13} ; *Cosmos bipinnatus*, *Senecio squalidus* and *S. vulgaris* that identify as *BcRL3* homologues (Table 6.5). In *C. bipinnatus*, primer pair 2 produces an excellent-quality sequence, while in *B. oleracea* haplotypes and the two *Senecio species* double priming of two similar same-sized sequences reduced the sequence quality (Table 6.5). Aside from the CosPS-2 sequence of the S_2 haplotype, which produced an *SLR2* homologue, all *Brassica* and *Senecio* CosPS-2 sequences, produced a dominant signal that identified as *BcRL3* homologues. Similarly, primer-pair-13 identified *BcRL3* homologues in S_6 , S_{13} , and S_{29}

haplotypes, but an *SLR2* homologue in S_3 . Consequently, CosPS sequences 2 and 13 of S_3 , S_6 and S_{13} haplotypes were combined to produce a good-quality contiguous sequence of approximately 1050 nucleotides, designated as CosPS-contig 2+13 (Table 6.5). CosPS-contig 2+13 produced an *SLR2* homologue in the *B. oleracea* S_3 haplotype, but *BcRL3* homologues in S_6 and S_{13} haplotypes. *BcRL3* has been isolated previously only from the *Brassica rapa*- S_9 haplotype (Suzuki *et al.* 1999), and has not, to date, been identified in haplotypes of *B. oleracea*. Considering the 98-99% nucleotide sequence identity that these *B. oleracea* *BcRL3* homologues share with *B. rapa* *BcRL3*, it is surprising that they have not been identified sooner in the *B. oleracea* genome. It may be however, that the putative *B. oleracea* *BcRL3* gene is not expressed and that these *BcRL3* homologues represent pseudogenes. The sequence data would appear to contradict this, as the level of sequence conservation of the *B. oleracea* *BcRL3* homologues is much higher than normally observed for non-expressed pseudogenes, where one would expect a greater accumulation of nucleotide changes, and stop codons. Even more surprising is the level of sequence conservation between *BcRL3*-type homologues in *Senecio squalidus*, *S. vulgaris* and *C. bipinnatus* (Table 6.10a), which exhibit approximately 85~90% nucleotide sequence identity to *B. rapa* *BcRL3*, and ~60-80% identity in predicted protein sequences to the *Brassica rapa* *BcRK3*, the protein expressed by *BcRL3* (Table 6.10b). This level of sequence conservation is extraordinarily high, and very rare for S-gene sequences from disparate plant taxa. For example, S-domain proteins in *Zea mays*, (Poaceae), *Lotus japonicus*, (Fabaceae) *Ipomoea trifida* (Convolvulaceae), *Arabidopsis lyrata* (Brassicaceae, tribe: Sisymbrieae) and *Raphanus sativus* (Brassicaceae, tribe: Brassiceae) show 25%, 41%, 56%, 66% and 85% identity respectively to *Brassica* S-domain proteins, with the percentage identity between *Brassica* and non-*Brassica* S-domain molecules tending to be lower, than between *Brassica* species, (Kowyama *et al.*, 1995; Nishimura *et al.* 2002; Schierup *et al.* 2001; Walker and Zang 1990). Sequence constraint has been observed in RLK kinase domains, where it is considered important for the maintenance of enzymatic function (Hinata *et al.* 1993, 1995). In contrast, SRK receptor domains accumulate high levels of sequence diversity, with diversity generally increasing with increasing distance of plant taxa (Hinata *et al.*, 1995). The high level of intergenic conservation in *BcRL3* homologues suggests a fundamental and essential function for these molecules that is not associated with self and non-self recognition, and suggests also that the same ligand may operate in the stimulation of *BcRL3* homologues in these widely disparate plant genomes.

Table 6.10a. Percentage pairwise nucleotide identities of *BcRL3* homologues generated by CosPS primer pair 2 and 13 in *Brassica oleracea* haplotypes; *S*₂, *S*₃, *S*₆, *S*₉, *S*₁₃; *Cosmos bipinnatus*, *Senecio squalidus* and *Senecio vulgaris*.

	<i>Bol</i> (<i>S</i> ₂) seq. 2	<i>Bol</i> (<i>S</i> ₃) seq. 2+13	<i>Bol</i> (<i>S</i> ₆) seq. 2+13	<i>Bol</i> (<i>S</i> ₉) seq. 2	<i>Bol</i> (<i>S</i> ₁₃) eq. 2+13	<i>Bol</i> (<i>S</i> ₂₉) seq. 13	<i>Cosmos</i> <i>bipinnatus</i> Seq. 2	<i>Senecio</i> <i>squalidus</i> Seq. 2s	<i>Senecio</i> <i>vulgaris</i> Seq. 2	<i>Brassica</i> <i>rapa</i> <i>BcRL3</i> (AB041620)
<i>B. oleracea</i> (<i>S</i> ₂)		74	74	74	73	41	75	75	77	73
<i>B. oleracea</i> (<i>S</i> ₃)			81	88	80	71	85	94	87	81
<i>B. oleracea</i> (<i>S</i> ₆)				92	97	98	86	94	89	88
<i>B. oleracea</i> (<i>S</i> ₉)					91	41	85	85	90	89
<i>B. oleracea</i> (<i>S</i> ₁₃)						95	85	93	89	87
<i>B. oleracea</i> (<i>S</i> ₂₉)							41	42	37	85
<i>Cosmos bipinnatus</i>								88	86	83
<i>Senecio squalidus</i>									83	92
<i>Senecio vulgaris</i>										86

Table 6.10b. Percentage pairwise identities of deduced amino acid sequences of *BcRL3* homologues generated by CosPS primer pair 2 and 13 in *Brassica oleracea* haplotypes; *S*₂, *S*₃, *S*₆, *S*₉, *S*₁₃; *Cosmos bipinnatus*, *Senecio squalidus* and *Senecio vulgaris*.

	<i>Bol</i> (<i>S</i> ₂) seq. 2	<i>Bol</i> (<i>S</i> ₃) seq. 2+13	<i>Bol</i> (<i>S</i> ₆) seq. 2+13	<i>Bol</i> (<i>S</i> ₉) seq. 2	<i>Bol</i> (<i>S</i> ₁₃) eq. 2+13	<i>Bol</i> (<i>S</i> ₂₉) seq. 13	<i>Cosmos</i> <i>bipinnatus</i> Seq. 2	<i>Senecio</i> <i>squalidus</i> Seq. 2	<i>Senecio</i> <i>vulgaris</i> Seq. 2	<i>Brassica rapa</i> <i>BcRK3</i> (BAB69682)
<i>B. oleracea</i> (<i>S</i> ₂)		50	50	49	49	17	50	46	54	48
<i>B. oleracea</i> (<i>S</i> ₃)			68	76	68	53	70	87	72	69
<i>B. oleracea</i> (<i>S</i> ₆)				82	95	95	70	87	75	79
<i>B. oleracea</i> (<i>S</i> ₉)					80	26	70	71	81	77
<i>B. oleracea</i> (<i>S</i> ₁₃)						92	70	85	76	78
<i>B. oleracea</i> (<i>S</i> ₂₉)							18	19	25	71
<i>Cosmos bipinnatus</i>								75	70	65
<i>Senecio squalidus</i>									64	82
<i>Senecio vulgaris</i>										70

The *Brassica oleracea* (*S*₂₉) CosPS-13 sequence is a 3'-end sequence and forms only an ~200 base-pairs overlap with the 5'-end CosPS-2 sequences, and hence the pairwise percentage between these CosPS sequences is considerably reduced.

(iii) Primer pair 12 generates *BcRK1* homologues in *Brassica oleracea*

Primer pair 12 generates *BcRK1* homologues in *B. oleracea* haplotypes *S*₃, *S*₆, *S*₉, *S*₁₃, *S*₁₅ and *S*₂₉ (Table 6.8), but generates a homologue of the *BcRL1* pseudogene, that has sequence similarity to *BcRK1*, in the *B. oleracea* *S*₂ haplotype. The *BcRK1* gene has been isolated previously only from the *Brassica rapa*-*S*₉ haplotype (Suzuki *et al.* 1999). *Brassica oleracea* *BcRK1*-type homologues are highly conserved exhibiting ~90-100% pairwise

identity with each other, and ~88-96% pairwise identity to *B. rapa BcRK1* (Table 6.11a). The same pattern of sequence conservation occurs in the predicted amino acid sequences, with *B. oleracea* haplotypes showing ~90-100% identity between haplotypes, and ~90-95% identity to SRK1, the protein encoded by *BcRK1* (Table 6.11b). A single stop codon in the middle of the CosPS-12 sequences of the *S*₂ and *S*₅ class-II haplotypes prevents a complete open reading frame being achieved for these haplotypes, indicating that primer pair 12 identifies a pseudogene in each of these taxa.

Table 6.11a. Percentage pairwise nucleotide identities of *BcRK1* homologues generated by CosPS primer pair 12 in *Brassica oleracea* haplotypes; *S*₂, *S*₃, *S*₅, *S*₆, *S*₉, *S*₁₃, *S*₁₅ and *S*₂₉

	<i>Bol</i> (<i>S</i> ₂)	<i>Bol</i> (<i>S</i> ₃)	<i>Bol</i> (<i>S</i> ₅)	<i>Bol</i> (<i>S</i> ₆)	<i>Bol</i> (<i>S</i> ₉)	<i>Bol</i> (<i>S</i> ₁₃)	<i>Bol</i> (<i>S</i> ₁₅)	<i>Bol</i> (<i>S</i> ₂₉)	<i>Brassica rapa</i> <i>BcRK1</i> (AB000970)
<i>B. oleracea</i> (<i>S</i> ₂)		92	93	89	89	91	96	88	88
<i>B. oleracea</i> (<i>S</i> ₃)			96	95	95	95	95	95	92
<i>B. oleracea</i> (<i>S</i> ₅)				93	93	94	96	93	91
<i>B. oleracea</i> (<i>S</i> ₆)					96	96	91	100	95
<i>B. oleracea</i> (<i>S</i> ₉)						96	91	97	95
<i>B. oleracea</i> (<i>S</i> ₁₃)							94	95	93
<i>B. oleracea</i> (<i>S</i> ₁₅)								91	89
<i>B. oleracea</i> (<i>S</i> ₂₉)									96

Table 6.11b. Percentage Pairwise Identities of deduced amino acid sequences of *B. rapa BcRK1* homologues generated by CosPS primer pair 12 in *Brassica oleracea* haplotypes; *S*₃, *S*₆, *S*₉, *S*₁₃ and *S*₂₉.

	<i>Bol</i> (<i>S</i> ₃)	<i>Bol</i> (<i>S</i> ₆)	<i>Bol</i> (<i>S</i> ₉)	<i>Bol</i> (<i>S</i> ₁₃)	<i>Bol</i> (<i>S</i> ₂₉)	<i>Brassica rapa</i> SRK1 (BAB69682)
<i>B. oleracea</i> (<i>S</i> ₃)		93	93	93	93	90
<i>B. oleracea</i> (<i>S</i> ₆)			96	94	100	94
<i>B. oleracea</i> (<i>S</i> ₉)				97	97	95
<i>B. oleracea</i> (<i>S</i> ₁₃)					94	92
<i>B. oleracea</i> (<i>S</i> ₂₉)						95

6.4.3 - Pairwise percentage identities of encoded CosPS protein sequences generated by primer pairs 1-15 in Asteraceae and *Diplotaxis tenuifolia*.

Table 6.12 summarises the percentage pairwise identities of the 41 predicted CosPS protein sequences produced by primer pairs 1-15 in Asteraceae species and *Diplotaxis tenuifolia*. The data include the *Brassica oleracea* SLG₁₃ and the *Ipomoea trifida* IRK1 protein sequences as comparative sequences. In general, predicted CosPS protein sequences of Asteraceae species show greater pairwise identity to *Ipomoea* IRK1 (Table

6.12; row Ipo.) than to *Brassica oleracea* SLG13 (Table 6.12; row S13), reflecting the relative close relatedness in the Tree of Life of Convolvulaceae (euasterids I) and Asteraceae (euasterids II) compared with Brassicaceae (eurosids II) (Figure 6.3).

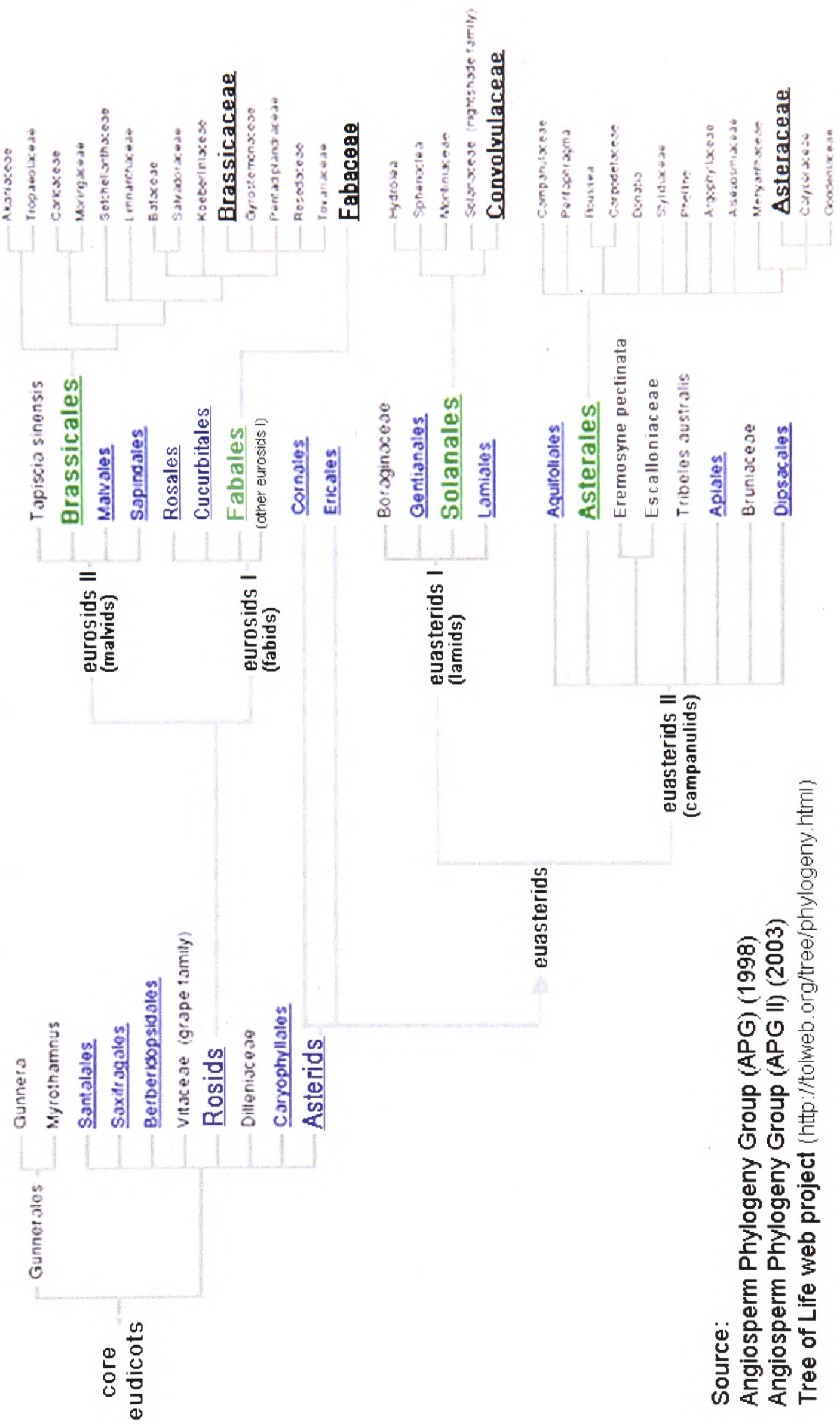
Comparisons of the 41 deduced CosPS protein sequences generated by primer pairs 1-15 in Asteraceae species and *Diploaxis tenuifolia* were undertaken at several levels. Initially, deduced CosPS protein sequences were organised into a matrix and analysed for regions of sequence conservation and variability. No alternating regions of sequence conservation and variability were observed in the encoded CosPS S-domain sequences, with many primer pairs generating monomorphic infrageneric and intraspecific sequences. Regions of hypervariability were not identified in any of the encoded CosPS sequences, and so these sequences do not have molecular characteristics expected for SI molecules. Since, specific haplotypes were not identified for individual Asteraceae species and *Diploaxis tenuifolia*, one cannot be sure that individuals sequenced were distinct genotypes. It is possible that the monomorphic character of certain sequences from the smaller populations of Asteraceae species, such as *Centaurea cyanus* (4 individuals) and *Cosmos carvifolius* (6 individuals) are the result of these individuals being derived from clonal populations. However, in the case of *Cosmos bipinnatus* and *C. sulphureus* this cannot be the case, as the five *C. bipinnatus* and four *C. sulphureus* individuals sequenced by primer pairs 1-15, represent the individuals Bip 1-5 and Sul 1-4 used in the pollination experiments undertaken in Chapter 5. In these pollination experiments, Bip 1 to 5 and Sul 1 to 4 exhibited a range of compatibility relationships that testify to the genetic variability within these two *Cosmos* populations. In conclusion, the pairwise data indicate that S-domain encoding CosPS sequences generated by primer pairs 1-15 are not SI molecules. Kowyama *et al.* (2000) and Hiscock *et al.* (2003), working on SI in Convolvulaceae and Asteraceae respectively, have speculated that self-incompatibility in these two families is probably under the control of genes and molecules unrelated to *Brassica* SRK or SCR, with Hiscock and McInnis (2003) identifying a pair of 35-kDa glycoproteins designated as SSPs (for Stigma S-associated Proteins) as candidate SI molecules in *Senecio squalidus*. The preliminary findings on CosPS sequences undertaken in this chapter tentatively support these speculations and suggest that control of SI in *Cosmos* and Asteraceae is not the same as in *Brassica*.

Table 6.12. Percentage Pairwise Identities of predicted CosPS protein sequences generated by primer pairs 1-15 in Asteraceae species and *Diplotaxis tenuifolia*.

Seq. No.	Centauraea cyanus															Conyza				Coryza				Diplotaxis tenuifolia															Pic. ech.	Sen. Squal.	Senecio vulgaris						
	Ipo															can.		sum.	3819		6334			5010					Cosmos					Diplotaxis													
	48	49	50	51	52	53	54	55	56	57	58	59	60	61	62	63	64	65	66	67	68	69	70	71	72	73	74	75	76	77	78	79	80	81	82	83	84	85				86	87	88			
S13 Brass.	40	32	37	33	42	37	38	31	36	30	37	29	35	22	49	33	49	35	45	49	47	31	56	34	32	50	33	30	50	45	50	40	37	63	36	51	39	39	37								
Ipo	Convul	37	47	35	53	41	44	31	36	30	35	30	36	23	58	35	57	35	54	58	57	35	37	35	29	57	33	32	57	40	59	43	46	49	44	40	37	41	32	42	42	43					
48	49	16	33	37	17	11	15	38	11	38	11	38	11	18	11	33	12	33	15	33	32	11	27	3	10	34	3	15	33	45	16	16	9	19	47	18	28	14	25	8	8	14					
49	50		18	87	36	60	29	30	27	32	26	35	24	52	35	52	35	40	50	20	32	15	34	27	52	33	29	52	15	52	37	36	40	15	36	14	35	12	39	39	37						
50	51			30	17	14	15	30	14	30	15	21	14	35	19	34	18	33	35	38	15	28	16	16	35	16	18	36	35	22	21	13	21	31	18	25	17	25	19	22	16						
51	52				39	61	32	36	30	37	30	37	23	60	36	60	36	55	59	60	35	36	36	30	60	34	33	59	40	57	41	40	43	41	39	37	38	34	38	34	46	41	39				
52	53				31		35	36	35	40	34	38	26	39	38	40	37	30	37	12	37	9	38	30	38	37	37	39	17	40	36	37	38	17	46	10	98	10	30	29	93	93					
53	54						26	29	22	32	22	26	13	56	21	58	24	43	54	17	22	15	26	27	56	25	27	58	11	57	35	32	40	12	33	14	29	14	40	33	32	32					
54	55						45	97	50	91	31	35	32	29	33	31	27	31	12	28	10	26	45	33	27	49	33	16	33	29	27	32	15	41	11	34	9	27	24	34	34	34					
55	56						44	97	44	40	37	37	37	37	37	39	34	37	35	35	29	36	50	36	35	53	37	43	34	35	30	35	40	39	32	38	30	28	23	36	36	36					
56	57								47	91	27	35	30	29	31	28	25	30	8	28	5	26	45	30	27	46	31	10	31	26	27	31	10	39	5	33	5	27	24	33	33	33					
57	58									47	40	38	37	37	38	39	33	36	36	35	29	36	51	36	35	58	37	43	36	35	30	38	40	43	32	39	30	29	24	40	40	40					
58	59									25	36	30	26	30	25	26	30	9	26	6	23	46	29	24	47	31	10	31	26	27	29	11	39	6	33	6	28	25	32	32	32						
59	60									24	37	98	37	98	31	37	13	86	11	98	26	36	97	32	36	18	35	35	28	36	17	39	11	37	11	37	11	32	29	36	36	36					
60	61									21	25	21	24	19	21	6	23	7	23	48	20	22	50	20	9	21	20	23	20	11	25	8	27	9	21	18	26	26	26	26	26	26					
61	62									35	98	35	87	99	99	34	38	37	29	94	35	30	95	41	95	41	95	48	46	50	44	39	34	39	33	57	56	40	40	40	40	40	40				
62	63									35	99	30	35	9	93	4	98	28	34	98	31	35	12	34	33	30	34	33	30	34	11	38	5	38	6	33	29	38	38	38	38	38	38				
63	64									35	87	96	91	34	37	29	93	35	30	94	40	95	40	95	40	95	48	46	51	38	39	33	39	33	57	56	40	40	40	40	40	40	40				
64	65														30	35	11	89	7	98	27	35	98	32	35	15	34	35	29	35	14	40	8	37	9	32	29	36	36	36	36	36	36				
65	66														87	85	27	35	30	26	86	28	25	90	37	73	41	36	40	37	29	35	32	32	51	47	32	32	32	32	32	32	32				
66	67														99	34	38	37	29	94	35	29	95	41	93	48	46	49	43	37	34	39	33	57	56	40	40	40	40	40	40	40	40				
67	68														9	38	2	5	94	2	10	95	41	34	17	8	20	44	11	34	10	33	17	17	9	9	9	9	9	9	9	9	9				
68	69															4	91	27	32	90	31	33	12	32	30	28	32	30	28	32	11	35	5	37	6	33	30	36	36	36	36	36	36				
69	70															4	7	38	4	14	38	32	14	18	3	36	33	10	75	7	7	7	7	7	7	7	7	7	7	7	7	7	7				
70	71																		27	36	96	29	36	3	34	35	31	35	2	38	3	38	4	33	22	38	38	38	38	38	38	38	38				
71	72																		29	27	66	30	9	29	26	27	31	10	33	7	32	7	28	7	28	23	30	30	30	30	30	30	30	30			
72	73																		35	29	94	40	92	48	47	51	43	36	35	37	33	57	57	39	39	39	39	39	39	39	39	39	39	39			
73	74																		29	35	1	33	34	31	34	2	36	3	37	4	32	23	37	37	37	37	37	37	37	37	37	37	37	37			
74	75																			31	16	30	29	27	32	16	40	14	37	13	24	20	37	13	24	20	37	37	37	37	37	37	37	37	37		
75	76																			39	93	48	45	51	44	38	34	38	33	58	56	40	40	40	40	40	40	40	40	40	40	40	40	40	40		
76	77																			15	15	7	19	61	17	32	15	30	7	7	13	13	13	13	13	13	13	13	13	13	13	13	13	13	13		
77	78																											48	47	51	13	38	14	39	12	57	56	40	40	40	40	40	40	40	40	40	
78	79																													46	82	17	36	18	34	22	37	36	34	34	34	34	34	34	34	34	
79	80																														8	34	4	37	8	36	36	37	37	37	37	37	37	37	37	37	
80	81																														18	37	20	35	23	37	38	37	37	37	37	37	37	37	37	37	
81	82																																														
82	83																																														
83	84																																														
84	85																																														
85	86																																														
86	87																																														
87																																															

Key to Table 6.12. The numbers 48-88 relate to the numbered sequences in Table 6.6. [Abbreviations: S13, Brassica oleracea positive control (Brassica oleracea SLG13 Genbank accession number CAA38995); Ipo, Ipomoea trifida positive control (Ipomoea trifida IRK1 Genebank accession number AAC23542); can., canadensis; sum., sumatrensis; sul., sulphureus; Pic. ech., Picris echinoides; Sen. Squal., Senecio squallidus; Dip., Diplotaxis; Pic., Picris; Brass., Brassicaceae; Convul., Convulvaceae]. Light blue highlight = infrageneric sequence identity > 90%; green highlight = intergeneric sequence identity > 70%; yellow highlight = intergeneric sequence identity between 50-70%; grey highlight = interfamilial sequence identity between 45-70%, i.e. encoded CosPS sequences that have between >44% and <71% identity with Ipomoea trifida IRK1 (AAC23542) and Brassica oleracea SLG13 (CAA38995).

Figure 6.3 - A phylogeny of core eudicots emphasising the relationship of Brassicaceae, Fabaceae, Convolvulaceae and Asteraceae



Source:
 Angiosperm Phylogeny Group (APG) (1998)
 Angiosperm Phylogeny Group (APG II) (2003)
 Tree of Life web project (<http://tolweb.org/tree/phylogeny.html>)

6.5 – Analysis of encoded CosPS S-domain sequences

6.5.1 – Introduction

Primer pairs 1-15 were not able to isolate the putative *Cosmos* SI sequence. However they were successful in identifying 88 distinct S-domain encoding sequences in Asteraceae and Brassicaceae. The ubiquity of S-domain proteins within plant genomes is becoming apparent, and it would be interesting to elucidate the molecules to which these encoded CosPS S-domains are attached. Are CosPS S-domains membrane-bound receptor kinases, cytoplasmic receptor kinases, or glycoproteins? And what role do the S-associated conserved domains serve in these molecules? Answers to these questions will no doubt, come from proteomics, but initially such research may be aided by analysis of S-protein relationships using appropriate tree-building methods (Hanks *et al.*, 1988). Three strategies are commonly used for building trees from large subsets of data. These are: (i) the sampling of many taxa using a single gene i.e. one gene in all taxa, such as the plastid *rbcL* sequences across angiosperms, (ii) the combining or 'concatenating' of multiple genes from the same set of species, i.e. genes 1 and 2 in all taxa, such as in a matrix constructed from the protein-coding plastid genes *ndhF* and *rbcL*, and (iii) supertree construction in which a set of trees with at least some taxa in common are used to produce a super tree containing all the taxa found in the original tree (Sanderson and Driskell, 2003).

The S-domain trees produced for this study used a more fragmented strategy as the 23 Brassicaceae and Asteraceae taxa generated 88 non-overlapping paralogous CosPS sequences of variable length. However rigorous a concatenated matrix may be, datasets constructed from multiple genes encounter potential problems. In particular, different evolutionary history of genes arising from recombination, introgression and other processes can mix phylogenetic signals. Furthermore, sequence data for some taxa is not always available and so accuracy may be compromised. In this study, S-gene sequences were generally not orthologous and so phylogeny could not be inferred. With these limitations in mind, the neighbour-joining (NJ) distance method was used to construct a tree of encoded CosPS protein sequences. First, distance relationships of the 41 encoded CosPS protein sequences generated in the 13 Asteraceae taxa and *Diplotaxis tenuifolia* were assessed using *Brassica oleracea* SLG13 and *Ipomoea trifida* IRK1 protein sequences as outgroup proteins. Then, a more extensive analysis was carried out in which the 88 S-domain encoding CosPS sequences isolated by primer pairs 1-10, 12-13 and 15, were analysed in a matrix of 218 S-domains from a diverse and representative range of plant taxa. The results of these analyses are presented in Figures 6.4a-b and 6.5a-b.

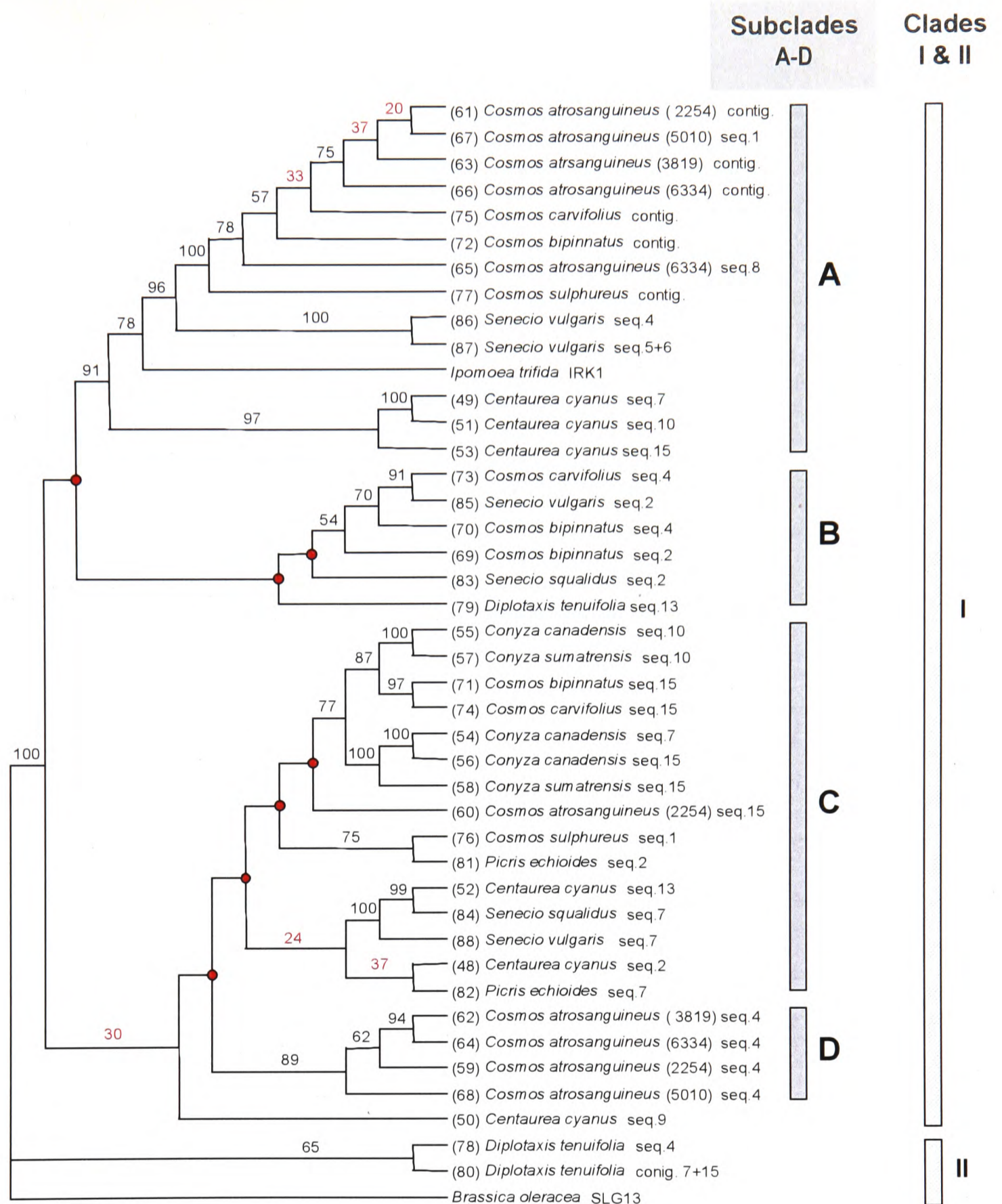


Figure 6.4a A majority-rule NJ Tree comparing distance relationships of the 41 encoded CosPS protein sequences generated by CosPS Primer Pairs 1-10 12-13 and 15 in species of Asteraceae and *Diptotaxis tenuifolia*. Numbers on tree represent the percentage bootstrap support per 1000 replications. Bootstrap percentages of less than 50% and 40% are highlighted in blue and red respectively. Number of taxa = 43; Number of characters = .476 Outgroup members = 2, *Brassica oleracea* SLG13 and *Ipomoea trifida* IRK1. Distance settings: (i) objective function = Minimum Evolution (ME); (ii) negative branch length allowed but set to zero for tree score; (iii) distance measure = mean character difference. Tree score = ME = 6.2587. Red circles indicate nodes that are not supported in the bootstrap tree. Numbers in brackets correspond with the number assigned to encoded CosPS protein sequences in Table 6.6.

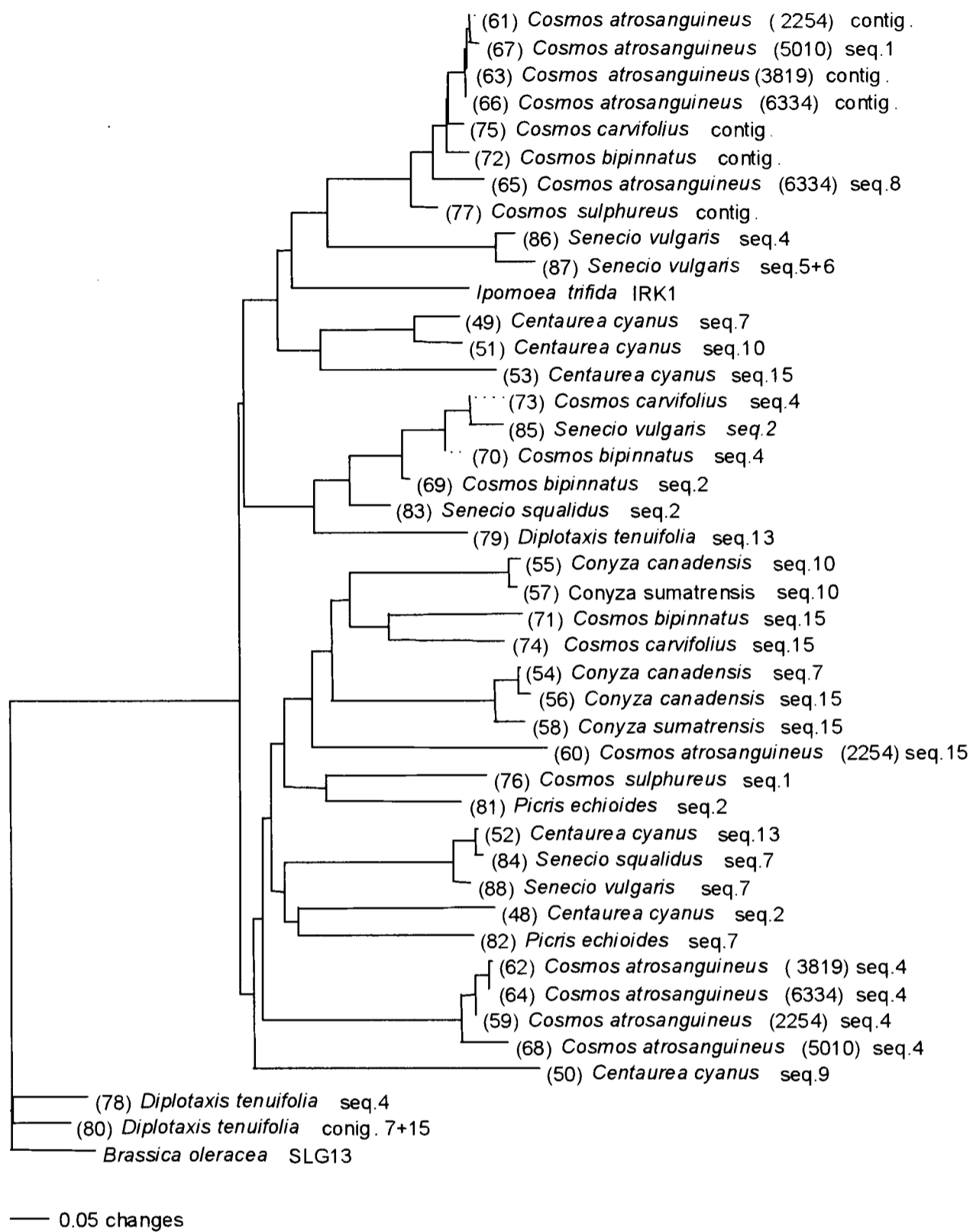


Figure 6.4b Phylogram of Neighbour-Joining (NJ) Tree comparing distance relationships of 41 encoded CosPS protein sequences generated by CosPS Primer Pairs 1-15 in species of Asteraceae and *Diplotaxis tenuifolia*. Numbers in brackets correspond with the number assigned to CosPS protein sequences in Table 6.6.

6.5.2 – Distance relationships of 41 encoded CosPS S-domains of Asteraceae and *Diplotaxis tenuifolia*

Gene families such as the S-domain gene family have members that have experienced complex and varied histories involving varying degrees of duplication, recombination, silencing and concerted evolution, so that the history of the gene family does not reflect the history of the species containing it (Sanderson and Driskell, 2003). Methods/algorithms have been developed whereby species and gene trees may be reconciled or optimised. However, concatenation of S-domain sequences is not an appropriate method for reconstructing species phylogeny, and it must be stressed that the analysis undertaken in this study does not seek to do this. The NJ trees illustrated in Figures 6.4 and 6.5 are S-domain trees constructed from predominantly paralogous S-domain sequences. The aim of the tree-building exercise used in this study is not to describe the phylogeny of S-domains but to examine the relatedness of S-domain sequences and to identify possible orthologues where these become apparent. Reference to species phylogeny is included only where a relationship of S-domains reflects or supports known species phylogeny.

Encoded CosPS sequences from all species of Asteraceae, and CosPS-sequence 13 of *Diplotaxis tenuifolia* form a well supported (100 BP¹¹) distinct clade that is more closely related to IRK1 of *Ipomoea trifida* than to *Brassica oleracea* SLG13 (Figure 6.4a, Clade I). In contrast, the encoded *Diplotaxis tenuifolia* seq.4 and the *Diplotaxis tenuifolia* contig.7+15 sequences form a second outgroup with the *Brassica oleracea* SLG13 sequence (Figure 6.4a, Clade II), and suggests that these two CosPS *Diplotaxis tenuifolia* sequences may be SLG proteins. However, since the separation of the *Diplotaxis tenuifolia* outgroup and *Brassica oleracea* SLG13 outgroup is not resolved in this tree, it is not possible to determine any meaningful relationship between the sequences in these two outgroups. Only that the two deduced S-proteins of *Diplotaxis tenuifolia* and the *Brassica oleracea* SLG13 sequence in clade II are distinctively different from the encoded S-protein sequences in clade I.

The cladal separation of Asteraceae-encoded S-proteins and Convolvulaceae S-proteins from S-proteins of Brassicaceae reflects the position of these three families within the Tree of Life (APG, 1998; APGII, 2003), with Asteraceae and Convolvulaceae ascribed to the euasterids, and Brassicaceae to the more distantly-related eurosids

¹¹ BP, bootstrap percentage

(Figure 6.3). The inclusion of the encoded *D. tenuifolia* CosPS-13 sequence in Clade I is interesting, as the top protein SSEARCH for this sequence was SFR2 of *B. oleracea*, with which it shares 77% sequence identity (E value = $3.2e^{-105}$), whereas the top protein SSEARCH of the *D. tenuifolia* encoded CosPS sequences in clade II, matched with ~80% identity to *Brassica* SLGs (Table 6.5). The location in major clade I of the CosPS-*D. tenuifolia* seq.13 is probably a consequence of its S-domain being more closely related to S-domains of receptor kinase proteins than to those of SLGs. If the latter proves to be a common feature of S-domain sequences, it may be possible to distinguish some S-receptor-like kinases from S-glycoproteins simply from an analysis of their S-domains.

Within clade I, subclade-A forms a distinct group of S-domain-encoding CosPS sequences that includes sequences from *Centaurea*, *Cosmos*, *Senecio* and *Ipomoea*. Subclade-A is the best-resolved and best-supported clade within the tree (91 BP). Its resolution is due, in part, to the fact that the subclade consists predominantly of wholepiece and contiguous CosPS sequences that encode approximately 350 amino acids representing ~80% of the S-domain region. In contrast, subclade-B is comprised of 3'-end and 5'-end CosPS sequences encoding ~150 and ~250 amino acids respectively, and consequently the resolution of this clade is reduced such that its relationship to subclade-A is not supported in the topology of the bootstrap tree. Nevertheless, within subclade-B there is a well-supported relationship between CosPS.4 encoded sequences of *Cosmos carvifolius* and *C. bipinnatus* (91 BP) and the CosPS.2 encoded sequence of *Senecio vulgaris* (70 BP) and moderate support for including the CosPS.2 encoded sequence of *C. bipinnatus* within this group (54 BP). Subclades C and D contain a mixture of encoded 3'-end, 5'-end and whole-piece CosPS sequences. Generally, the terminal branches of each subclade are well supported and reveal some interesting relationships. Encoded CosPS sequences from the same Asteraceae genus are more closely related to each other than to those from other genera of Asteraceae, as occurs with the contiguous *Cosmos* sequences, and the *Centaurea cyanus* sequences in subclade A. However, in certain of the encoded CosPS sequences, there is a stronger intergeneric than intrageneric relationship between sequences, with specific primer pairs generating very different sequences in the various plant taxa. Specific primers clearly prime differently in the 10 Asteraceae species. For example, primer pair 1 and 2 generates CosPS sequences in *C. sulphureus* and *Picris echioides* that encoded S-domains related to ISG3, whereas, in *Cosmos atrosanguineus*, *C. bipinnatus*, *C. carvifolius* and *Centaurea cyanus* they

produced CosPS sequences encoding IRK1- or ISG2-type proteins (Table 6.8). Primer pairs 7 and 13 appear to generate homologous sequences in *Senecio* spp. and *Centaurea cyanus* respectively, and illustrate the contrasting situation, in which different primer pairs identify the identical sequences in different plant taxa (Clade C, sequences 52, 84 and 88 show 99-100 BP). Both scenarios are apparent in primer pair 2, which identifies *BcRL3* homologues in *Senecio squalidus*, *S. vulgaris* and *Cosmos bipinnatus*, but generates ISG2-, ISG3- and IRK1-type encoded sequences in the remaining Asteraceae taxa.

The relationship of the Asteraceae CosPS sequences generally accords with the tribal phylogeny of the family. Tribal relationships discussed in Chapter 1 (Figures 1.5 – 1.10), placed Heliantheae (which includes *Cosmos*), Astereae (*Conyza*) and Senecioneae (*Senecio*) in the Asteroideae subfamily, with these tribes being more closely related to each other than to the Lactuceae (*Picris*) and Cardueae (*Centaurea*) located in the more basal Cichoriodeae subfamily. In the well-resolved subclade-A and the fairly well-resolved subclade-B the relationship of *Cosmos*, *Senecio* and *Centaurea* encoded CosPS sequences reflects the phylogeny of Asteraceae tribes. For example, in subclade-A, CosPS sequences from *Senecio* and *Cosmos* which are members of the Asteroideae subfamily form a well-supported (78 BP) group that is sister to a very well-supported (97 BP) group consisting of CosPS sequences of *Centaurea* which is in the more basal Cichoriodeae subfamily (Figure 6.4a-b). The relationship of these two sister groups has 91% bootstrap support, indicating this to be a robust and significant relationship. In another example, subclade-B forms a weakly-supported group (BP 54) composed of encoded CosPS sequences of *Cosmos* and *Senecio*, which is sister to subclade-A, although this latter relationship is not supported in the topology of the bootstrap tree. A final example appears in the top part of subclade-C, which forms a well-supported group, (BP 77) consisting of *Cosmos* and *Conyza* encoded CosPS sequences. In general, encoded CosPS sequences of *Cosmos*, *Conyza* and *Senecio* show greater relatedness to each other than to the encoded CosPS sequences of *Centaurea* and *Picris*, reflecting the sub-familial split between Asteroideae and Cichoriodeae. The noted exceptions occur between *Centaurea cyanus* seq.13 (52) and *Senecio squalidus* seq.7 (84) (Figure 6.4a, subclade A), and also between *Cosmos sulphureus* seq.1 (76) and *Picris echioides* seq.2 (81) (Figure 6.4a, subclade C). The latter exception is probably a consequence of insufficient data due to the short length of the sequence, but the former exception no doubt reflects the ability of primer pairs 7 and 13 to identify homologous sequences in *Senecio* and *Centaurea*. Subclade D

forms a well-supported group consisting of *C. atrosanguineus* seq.4 encoded S-domains. Surprisingly, the encoded CosPS.4 S-domains of *C. bipinnatus* and *C. carvifolius* do not segregate with those of *C. atrosanguineus*, but with encoded CosPS-2 BcRK3 homologues of *Senecio spp.* and *C. bipinnatus*. The highest pairwise protein hits for *C. bipinnatus* and *C. carvifolius* seq.4 S-domains were an *A. lyrata* S-related sequence and an unspecified *A. thaliana* RLK respectively (Table 6.5), and those of *C. atrosanguineus* seq.4 encoded S-domains showed homology to an unspecified *A. thaliana* RLK. Since homology is transitive, the predicted S-domains of *Cosmos* CosP.4 sequences might be expected to form a distinct well-supported group of *A. thaliana*-like RLKs. The reason that *Cosmos* CosP.4 sequences have segregated into different clades in this NJ tree may be due to the variable lengths of these sequences. The encoded CosPS.4 S-domains of *C. atrosanguineus* accessions range from 210-223 residues in length, whereas those of *C. bipinnatus* and *C. carvifolius* are between 172-174 residues. Furthermore, the small variability that occurs in CosPS.4 sequences occurs in the part of the sequence that is absent in the shorter sequences generated by *C. bipinnatus* and *C. carvifolius*. Alternatively, it is possible that primer pair 4 amplifies different sequences in *C. bipinnatus* and *C. carvifolius* than in *C. atrosanguineus* accessions. The accuracy of a specific portion of a tree is improved by increasing the number of sites and/or the number of species within a matrix, and so the inclusion of a greater number of full-length CosPS sequences from the same set of species would aid resolution of this part of the tree (Sanderson and Driskell, 2003).

6.5.3 - Distance relationships of 88 encoded CosPS S-domains with Brassicaceae, Convolvulaceae and Fabaceae S-domains

The encoded CosPS sequences generated by primer pairs 1-10, 12-13 and 15 were entered into a matrix with representative S-domain sequences obtained from the NCBI-NR database. Table 6.13 gives details of all sequences included in the CosPS S-domain matrix used to construct the NJ tree in Figure 6.5a-b.

Table 6.13a List of NCBI S-domain protein sequences used to construct the Neighbour-Joining (NJ) trees of S-domains illustrated in Figures 6.5a and 6.5b.

Species	Seq. No.	Accession No.	S-protein	Information
<i>Arabidopsis lyrata</i>	1	AAK19321	SRK22	Haplotype <i>S</i> ₂₂ , <i>SRK</i> gene. (311 aa).
	2	AAO16810	S-related kinase 8	<i>S</i> -related kinase 8 gene exon 1, <i>S</i> -like glycoprotein; Aly 8. (326 aa).
	3	AAO16812	S-related kinase 14	<i>S</i> -related kinase 14 gene exon 1, for <i>S</i> -like glycoprotein; Aly14. (204 aa).
	4	BAB40986	SRKa	<i>SRKa</i> gene for <i>S</i> -locus receptor kinase b protein. (847 aa).
	5	BAB40987	SRKb	<i>SRKb</i> gene for <i>S</i> -locus receptor kinase b protein. (853 aa).
	6	AAK19313	SRK3	Haplotype <i>S</i> ₃ , allele 13-3 exon 1. <i>SRK</i> gene for S receptor kinase (320 aa).
	7	AAK19320	SRK9	Haplotype <i>S</i> ₉ , allele 13-9 exon 1. (319 aa).
<i>Arabidopsis thaliana</i> cultivar <i>Columbia</i>	8	AAB21528	SLR1 (AtS1)	<i>AtS1</i> = Self-incompatibility locus. <i>S</i> -locus related protein SLR1 homolog. (439 aa.)
	9	NP_176755	RK (similar to BcRK1)	At1g65790 gene for receptor kinase, putative. Similar to <i>Brassica rapa</i> receptor kinase 1 gene. (843 aa).
	10	NP_193868	RK (similar to SFR2)	At4g21370 gene for receptor kinase, putative. Similar to receptor-like kinase <i>SFR2</i> gene of <i>Brassica oleracea</i> . (844 aa).
	11	AAA32786	ARK1	At1g65790 gene for receptor-like serine/threonine protein kinase ARK1 protein. (843).
	12	AAB33486	ARK2	ARK2 = receptor-like serine/threonine protein kinase ARK2. (850).
	13	NP_193869	ARK3	At4g21380 gene for <i>ARK3</i> receptor-like serine/threonine protein kinase ARK3 protein. (850 aa).

Table 6.13 continued

Species	Seq. No.	Accession No.	S-protein	Information
<i>Arabidopsis thaliana</i> cultivar <i>Columbia</i>	14	AAF23832	RK	Putative receptor kinase gene on chromosome 1. (1162 aa).
	15	NP_172600	RLK	Receptor-like protein kinase, putative; protein encoded by At1g11330 gene on chromosome 1. (840 aa).
	16	NP_176756	RLK	Receptor -like kinase, putative; protein encoded by At1g65800 gene on chromosome 1. (847 aa).
	17	D86247	Protein	Hypothetical protein with S-receptor kinase; protein kinase homology and S-locus-specific glycoprotein homology. (797 aa).
	18	NP_194459	RK (similar to SFR2)	At4g27290 gene for Putative receptor-like kinase similar to SFR2 gene of <i>Brassica oleracea</i> . (772 aa).
	19	NP_201077	RLK1	At5g62710 gene for S-domain receptor-like serine/threonine protein kinase gene for RLK1 protein similar to Sorghum bicolor <i>SbRLK1</i> . (589 aa).
	20	AAK28315	RLK4	<i>RLK4</i> gene = S-domain receptor-like protein kinase 4 gene for serine/threonine protein kinase. (658 aa).
<i>Brassica amplexicaulis</i>	21	BAB97355	SLR1	S-locus related 1 glycoprotein. (419 aa).
<i>Brassica barrelieri</i>	22	BAB97356	SLR1	S-locus related 1 glycoprotein. (419 aa).
<i>Brassica deflexa</i>	23	BAB97357	SLR1	S-locus related 1 glycoprotein. (425 aa).
<i>Brassica erucastrum</i>	24	BAB97358	SLR1	S-locus related 1 glycoprotein. (420 aa).
<i>Brassica insularis</i> subsp. <i>insularis</i>	25	AAF22255	SLR1	S-locus related 1 glycoprotein. (434 aa).
<i>Brassica maurorum</i>	26	BAB97359	SLR1	S-locus related 1 glycoprotein. (422 aa).
<i>Brassica napus</i> strain Westar	27	CAA79608	SLG Type II	S-locus glycoprotein.type II. (445 aa)
	28	CAA81540	SLR1	S-locus related 1 glycoprotein. (444 aa).
	29	CAA79735	SLR1	S-locus related 1 glycoprotein. (446 aa).
	30	AAA70389	SLG-Ws-1	S-locus glycoprotein. (436 aa).

Table 6.13a continued

Species	Seq. No.	Accession No.	S-protein	Information
<i>Brassica napus</i> subsp. <i>napus</i> cultivar Topas 2	31	CAB89186	SLG	<i>S</i> -locus glycoprotein. (437 aa)
	32	S38424	SLR1	<i>S</i> -locus related 1 glycoprotein. (450 aa).
	33	AAA62232	SRK	<i>S</i> -locus receptor kinase. (849 aa).
<i>Brassica nigra</i>	34	BAB97360	SLR1	<i>S</i> -locus related 1 glycoprotein. (419 aa).
<i>Brassica oleracea</i>	35	BAA83745	SLG2-b	Haplotype <i>S</i> _{2-b} , for <i>SLG</i> _{2-b} <i>S</i> -locus glycoprotein. (445 aa).
	36	BAA83746	SRK2-b	Haplotype <i>S</i> _{2-b} , <i>SRK</i> _{2-b} gene for <i>S</i> -locus receptor kinase. (854 aa).
	37	CAC84431	SRK2-d	<i>S</i> -locus receptor kinase, allele <i>SRK2d</i> . (443 aa).
	38	CAC84411	SRK2-k	<i>S</i> -locus receptor kinase, allele <i>SRK2k</i> . (658 aa).
	39	CAA55949	SLG3	Self-incompatible <i>S</i> ₃ haplotype homozygous line for <i>S</i> -locus glycoprotein. (431 aa).
	40	CAA55950	SRK3	Self-incompatible <i>S</i> ₃ haplotype homozygous line for <i>S</i> -locus receptor kinase. (850 aa).
	41	CAA46677	SLG5	Haplotype <i>S</i> ₅ var. <i>italicaxgemmifera</i> , <i>SLG</i> ₅ gene for <i>S</i> -locus glycoprotein. (394 aa).
	42	CAB41878	SRK5	Haplotype <i>S</i> ₅ , <i>SRK</i> ₅ gene for <i>S</i> -locus receptor kinase. (848 aa).
	43	CAA68375	SLSG6	Haplotype <i>S</i> ₆ , <i>SLG</i> ₆ for <i>S</i> -locus glycoprotein. (436 aa).
	44	AAA33000	SRK6	Haplotype <i>S</i> ₆ , <i>SRK</i> ₆ for <i>S</i> -locus receptor kinase. (857 aa).
	45	BAA21934	SLG9	Haplotype <i>S</i> ₉ , <i>SLG</i> ₉ for <i>S</i> -locus glycoprotein. (424 aa).
	46	CAA38995	SLG13	Haplotype <i>S</i> ₁₃ , <i>SLG</i> ₁₃ for <i>S</i> -locus glycoprotein. (435 aa).
	47	BAA83748	SLG13-b	Haplotype <i>S</i> _{13-b} , <i>SLG</i> _{13-b} for <i>S</i> -locus glycoprotein. (435 aa).
	48	BAA83905	SRK13	Haplotype <i>S</i> ₁₃ , <i>SRK</i> ₁₃ exon for <i>S</i> -locus receptor kinase. (854 aa).
	49	BAA83906	SRK13-b	Haplotype <i>S</i> _{13-b} , <i>SRK</i> _{13-b} exon for <i>S</i> -locus receptor kinase. (856 aa).
	50	CAB41880	SLGB (<i>S</i> ₁₅)	Haplotype <i>S</i> ₁₅ , <i>SLGb</i> for <i>S</i> -locus glycoprotein. (445 aa).
	51	CAB41879	SRK15	Haplotype <i>S</i> ₁₅ , <i>SRK</i> ₁₅ for <i>S</i> -locus receptor kinase. (849 aa).
	52	BAA34232	SLG23	Haplotype <i>S</i> ₂₃ , <i>SLG</i> ₂₃ for <i>S</i> -locus glycoprotein. (435 aa).

Table 6.13a continued

Species	Seq. No.	Accession No.	S-protein name	Information
<i>Brassica oleracea</i>	53	BAA34233	srk23	Haplotype S_{23} , SRK_{23} for <i>S</i> -locus receptor kinase. (846 aa).
	54	BAA21938	SLG25	Haplotype S_{25} , SLG_{25} for <i>S</i> -locus glycoprotein. (429 aa).
	55	BAC24047	SRK25	Haplotype S_{25} , SRK_{25} for <i>S</i> -locus receptor kinase. (439 aa).
	56	CAA34254	SLG29-2	Haplotype S_{29-2} SLG_{29-2} for <i>S</i> -locus glycoprotein. (435 aa).
	57	CAA82930	SRK29	Haplotype S_{29} , SRK_{29} for <i>S</i> -locus receptor kinase. (857 aa).
	58	BAB79442	SRK32	Haplotype S_{32} , SRK_{32} for <i>S</i> -locus receptor kinase. (422aa).
	59	CAA73133	ARLK	Haplotype S_{29} , $ARLK$ gene for serine/threonine receptor kinase. (847 aa).
	60	T14519	SFR1	Haplotype S_3 , $SFR1$ = <i>S</i> -gene family receptor kinase gene 1 expressed during the defence response in <i>Brassica oleracea</i> . (849 aa).
	61	CAA67145	SFR2	Haplotype S_3 , $SFR2$ = <i>S</i> -gene family receptor kinase gene 2 expressed during the defence response in <i>Brassica oleracea</i> . (847 aa).
	62	T14520	SFR3	Haplotype S_3 , $SFR3$ = <i>S</i> -gene family receptor kinase gene 3 expressed during the defence response in <i>Brassica oleracea</i> . (841 aa).
	63	AAB23284	SLR1	$SLR1$ gene for <i>S</i> -locus related 1 glycoprotein. (443 aa).
	64	CAA34253	SLR	$SLR1$ (S_{29} haplotype) for <i>S</i> -locus related 1 glycoprotein. (444 aa).
	65	CAC84429	SLR2	Allele (S_2) SLR_{2-2c} for <i>S</i> -locus related 2 glycoprotein. (352 aa).
	66	B53223	SLR2	S_6 haplotype, $SLR2$ gene for <i>S</i> -locus related 2 glycoprotein. (434 aa).
	67	A53223	SLR2	S_2 haplotype, $slr2$ gene for <i>S</i> -locus related 2 glycoprotein. (439 aa).
	68	CAA57427	SLR3-1	S_c <i>S</i> -locus homozygous line. <i>S</i> -locus related 3-1 glycoprotein. (357 aa).
	69	CAA56871	SLR3-2	Haplotype S_3 , <i>S</i> -locus related 3-2 glycoprotein. (384 aa).
	70	CAA72988	SLG- S_c	$SLG-S_c$ gene from <i>Brassica oleracea</i> variety <i>acephala</i> self compatible <i>S</i> -locus. (494 aa).

Table 6.13a continued

Species	Seq. No.	Accession No.	S-protein name	Information
<i>Brassica oxyrrhina</i>	71	BAB97361	SLR1	<i>SLR1</i> gene for <i>S</i> -locus related 1 glycoprotein. (419 aa).
<i>Brassica rapa</i>	72	AAA33002	SLG6	Haplotype <i>S</i> ₆ , <i>slg</i> ₆ for <i>S</i> -locus glycoprotein. (418 aa).
	73	BAA12674	SLG8	Haplotype <i>S</i> ₈ , <i>SLG</i> ₈ for <i>S</i> -locus glycoprotein. (435 aa).
	74	BAA07576	SRK8	Haplotype <i>S</i> ₈ , <i>SRK</i> ₈ for <i>S</i> -locus receptor kinase. (858 aa).
	75	BAA12675	SLG12	Haplotype <i>S</i> ₁₂ , <i>SLG</i> ₁₂ for <i>S</i> -locus glycoprotein. (437 aa).
	76	BAA21947	SLG21	Haplotype <i>S</i> ₂₁ , <i>SLG</i> ₂₁ for <i>S</i> -locus glycoprotein. (431 aa).
	77	BAA21949	SLG26	Haplotype <i>S</i> ₂₆ , <i>SLG</i> ₂₆ for <i>S</i> -locus glycoprotein. (437 aa).
	78	BAC24025	SRK26	Haplotype <i>S</i> ₂₆ , <i>SLG</i> ₂₆ for <i>S</i> -locus receptor kinase. (438 aa).
	79	BAA21950	SLG27	Haplotype <i>S</i> ₂₇ , <i>SLG</i> ₂₇ for <i>S</i> -locus glycoprotein. (428 aa).
	80	BAA31251	SLG29	Haplotype <i>S</i> ₂₉ , <i>SLG</i> ₂₉ for <i>S</i> -locus glycoprotein. (449 aa).
	81	BAB20998	SLG40	Haplotype <i>S</i> ₄₀ , <i>SLG</i> ₄₀ for <i>S</i> -locus glycoprotein. (438 aa).
	82	BAB21956	SLG41	Haplotype <i>S</i> ₄₁ , <i>slg</i> ₄₁ for <i>S</i> -locus glycoprotein. (435 aa).
	83	BAB20999	SLG44	Haplotype <i>S</i> ₄₄ , <i>slg</i> ₄₄ for <i>S</i> -locus glycoprotein. (438 aa).
	84	BAA92837	SRK60	Haplotype <i>S</i> ₆₀ , <i>SRK</i> ₆₀ for <i>S</i> -receptor kinase 60. (859 aa).
	85	BAA82744	SLR1-4	<i>SLR1-4</i> gene for <i>S</i> -locus related 1-4 glycoprotein. (446 aa).
	86	CAA41346	NS1	Haplotype <i>NS1</i> gene for <i>S</i> -locus related 1 glycoprotein homologue. (439 aa).
	87	BAA82743	NS2 (slr1-2)	<i>NS2 (SLR1-2)</i> gene for <i>S</i> -locus related 1 glycoprotein homologue. (446 aa).
	88	BAA32408	NS3	Haplotype <i>S</i> ₁₂ , <i>NS3</i> gene for <i>S</i> -locus related 1 glycoprotein homologue. (446 aa).
	89	BAB69685	SLR2-9A	Haplotype <i>S</i> ₉ , <i>SLR2-9A</i> gene for <i>S</i> -locus related 2-9A. (356 aa).
	90	BAB69686	SLR2-9B	Haplotype <i>S</i> ₉ , <i>SLR 2-9B</i> gene for <i>S</i> -locus related 2-9B. (356 aa).
	91	BAA23676	BcRK1	Haplotype <i>S</i> ₉ , <i>BcRK1</i> gene for <i>S</i> -receptor kinase 1 protein. (847 aa).
92	BAB69682	BcRK3 (BcRL3)	Haplotype <i>S</i> ₉ , <i>BcRK3</i> gene for receptor kinase 3 protein. (847 aa).	

Table 6.13a continued

Species	Seq. No.	Accession No.	S-protein	Information
<i>Brassica rapa</i>	93	BAB69683	BcRK5	Haplotype <i>S</i> ₀ , <i>BcRK5</i> gene for receptor kinase 5 protein. (838 aa)
	94	BAB69684	BcRK6	Haplotype <i>S</i> ₀ , <i>BcRK6</i> gene for receptor kinase 6 protein. (816 aa)
	95	BAB69687	SLG-like 10	Haplotype <i>S</i> ₀ , <i>BcSL10</i> gene for SLG-like 10 protein. (232 aa).
<i>Brassica tournefortii</i>	96	BAB97362	SLR1	<i>SLR1</i> gene for <i>S</i> -locus related 1 glycoprotein. (422 aa).
<i>Brassica villosa</i>	97	BAB97363	SLR1	<i>SLR1</i> gene for <i>S</i> -locus related 1 glycoprotein. (420 aa).
<i>Crambe kralikii</i>	98	BAB97364	SLR1	<i>SLR1</i> gene for <i>S</i> -locus related 1 glycoprotein. (412 aa).
<i>Diplotaxis eruroides</i>	99	BAB97365	SLR1	<i>SLR1</i> gene for <i>S</i> -locus related 1 glycoprotein. (420 aa).
<i>Diplotaxis siifolia</i>	100	BAB97366	SLR1	<i>SLR1</i> gene for <i>S</i> -locus related 1 glycoprotein. (420 aa).
<i>Eruca sativa</i>	101	BAB97367	SLR1	<i>SLR1</i> gene for <i>S</i> -locus related 1 glycoprotein. (419 aa).
<i>Eruca vesicaria</i>	102	BAB97368	SLR1	<i>SLR1</i> gene for <i>S</i> -locus related 1 glycoprotein. (419 aa).
<i>Erucastrum abyssinicum</i>	103	BAB97369	SLR1	<i>SLR1</i> gene for <i>S</i> -locus related 1 glycoprotein. (420 aa).
<i>Erucastrum gallicum</i>	104	BAB97370	SLR1	<i>SLR1</i> gene for <i>S</i> -locus related 1 glycoprotein. (419 aa).
<i>Erysimum cheiri</i>	105	BAA31733	SLR1	<i>SLR1</i> gene for <i>S</i> -locus related 1 glycoprotein. (410 aa).
<i>Hirschfeldia incana</i>	106	AAF22269	SLR-(<i>S</i> 20)	Allele 20, <i>SLR</i> gene for <i>S</i> -locus related glycoprotein. (363 aa).
<i>Ipomoea trifida</i>	107	AAA97901	ISG1	<i>ISG1</i> gene for S-domain like secreted glycoprotein 1. <i>S</i> ₂₂ homozygote stigma tissue. (451 aa).
	108	AAA97902	ISG2	<i>ISG2</i> gene for S-domain like secreted glycoprotein 2. <i>S</i> ₂₂ homozygote stigma tissue. (451 aa).
	109	AAA97903	ISG3	<i>ISG3</i> gene for S-domain like secreted glycoprotein 3. <i>S</i> ₂₂ homozygote stigma tissue. (454 aa).
	110	AAC23542	IRK1	<i>IRK1</i> gene for serine/threonine receptor kinase 1 protein. (853 aa).
	111	AAA97904	IRK2	<i>IRK2</i> gene for serine/threonine receptor kinase 2 protein. <i>S</i> ₂₂ homozygote stigma tissue. (233 aa.)

Table 6.13a continued

Species	Seq. No.	Accession No.	S-protein	Information
<i>Lotus japonicus</i>	112	BAC41328	SRK similar protein	Protein product similar to S-receptor kinase encoded by chromosome 3. (686 aa.)
	113	BAC41329	SRK similar protein	Unnamed protein product similar to S-receptor kinase encoded by chromosome 3. (862 aa.)
	114	BAC41330	SRK similar protein	Protein product similar to S-receptor kinase encoded by chromosome 3 (730 aa.).
<i>Lunaria annua</i>	115	BAB97371	SLR1	<i>SLR1</i> gene for S-locus related 1 glycoprotein. (415 aa).
<i>Moricandia arvensis</i>	116	BAB97372	SLR1	<i>SLR1</i> gene for S-locus related 1 glycoprotein. (416 aa).
<i>Orychophragmus violaceus</i>	117	BAA31732	SLR1	<i>SLR1</i> gene for S-locus related 1 glycoprotein. (417 aa).
<i>Raphanus raphanistrum</i> subsp. <i>raphanistrum</i>	118	AAF22261	SLR1-9	Allele 9. <i>SLR1-9</i> gene for S-locus related glycoprotein. (367 aa).
	119	AAF22260	SLR1-15	Allele 15. <i>SLR1-15</i> gene for S-locus related glycoprotein. (3674aa).
	120	AAF22272	SLR1-23	Allele 23. <i>SLR1-23</i> gene for S-locus related 1 glycoprotein. (364 aa).
	121	AAF22263	SLR-11	Allele 11. <i>SLR1-11</i> gene for S-locus related glycoprotein. (368 aa).
	122	AAF22264	SLR-12	Allele 12. <i>SLR1-12</i> gene for S-locus related glycoprotein. (368 aa).
	123	AAF22265	SLR-13	Allele 13. <i>SLR1-13</i> gene for S-locus related glycoprotein. (364 aa).
<i>Raphanus sativus</i>	124	BAA31727	SLG4	Haplotype S_4 . for S-locus glycoprotein 4. (431 aa).
	125	AAL17679	SLG6	Haplotype S_6 . for S-locus glycoprotein 6. (436 aa).
	126	AAL17681	SLG10	Haplotype S_{10} . for S-locus glycoprotein 10. (438 aa).
	127	BAA31734	SLR1	<i>SLR1</i> gene for S-locus related 1 glycoprotein. (419 aa).
<i>Sinapis alba</i>	128	BAB97373	SLR1	<i>SLR1</i> gene for S-locus related 1 glycoprotein. (420 aa).
<i>Sinapis arvensis</i>	129	BAB97374	SLR1-13	Strain SIN-ARV-13. <i>SLR1-13</i> gene for S-locus related 1 glycoprotein. (420 aa).
	130	AAF22259	SLR1-10	Allele 10, <i>SLR1-10</i> gene for S-locus related 1 glycoprotein. (366 aa).
	131	BAB97375	SLR1-20	Strain SIN-ARV-20. <i>SLR1-20</i> gene for S-locus related 1 glycoprotein. (420 aa).
	132	AAF22266	SLR	Allele 2, <i>SLR</i> gene for S-locus related glycoprotein. (371 aa)

Table 6.13b - List of encoded CosPS sequences, generated by primer pairs 1-15, used to construct the Neighbour-Joining (NJ) trees of S-domains illustrated in Figures 6.5a and 6.5b

Species	HRI –W Acc. No.	Seq. No.	Name of CosPS Sequence	Sequence Length (amino acids)
<i>Arabidopsis thaliana</i>	HRI – W	133	<i>Arabidopsis thaliana</i> seq. 1	141
		134	<i>Arabidopsis thaliana</i> contig-1. (4+8)	328
		135	<i>Arabidopsis thaliana</i> contig-2. (2+7+10)	364
<i>Brassica oleracea</i> –(S2)	DJ-2024	136	<i>Brassica oleracea</i> (S2) seq. 1	132
<i>Brassica oleracea</i> -(S3)	DJ-8189	137	<i>Brassica oleracea</i> (S3) seq. 1	139
		138	<i>Brassica oleracea</i> (S3) seq. 12	199
		139	<i>Brassica oleracea</i> (S3) seq. 15	232
		140	<i>Brassica oleracea</i> (S3) seq. 5+6 (ba2)	192
		141	<i>Brassica oleracea</i> (S3) contig-1 (3+4+7+8)	221
		142	<i>Brassica oleracea</i> (S3) contig (2+13)	344
<i>Brassica oleracea</i> -(S5)	DJ-4078/1	143	<i>Brassica oleracea</i> (S5) seq. 5+6 (ba2)	192
<i>Brassica oleracea</i> -(S6)	DJ-4080	144	<i>Brassica oleracea</i> (S6) seq. 1	73
		145	<i>Brassica oleracea</i> (S6) seq. 5+6 (ba1)	227
		146	<i>Brassica oleracea</i> (S6) seq. 7	186
		147	<i>Brassica oleracea</i> (S6) seq. 12	238
		148	<i>Brassica oleracea</i> (S6) seq. 15	228
		149	<i>Brassica oleracea</i> (S6) contig-1 [5+6+9 (ba2)]	284
		150	<i>Brassica oleracea</i> (S6) contig-2 (3+4+8)	338
		151	<i>Brassica oleracea</i> (S6) contig-(2+13)	349
<i>Brassica oleracea</i> -(S9)	DJ-8153	152	<i>Brassica oleracea</i> (S9) seq. 2	144
		153	<i>Brassica oleracea</i> (S9) seq. 12	240
		154	<i>Brassica oleracea</i> (S9) contig-1 (3+4+10+15)	302
<i>Brassica oleracea</i> -(S13)	DJ-4099	155	<i>Brassica oleracea</i> (S13) contig-(7+15)	235
		156	<i>Brassica oleracea</i> (S13) seq. 9 (ba1)	318
		157	<i>Brassica oleracea</i> (S13) seq. 12	211
		158	<i>Brassica oleracea</i> (S13) contig--1 [5+6+9 (ba2)]	268
		159	<i>Brassica oleracea</i> (S13) contig-2 (1+3+4+8+10)	340
		160	<i>Brassica oleracea</i> (S13) contig. (2+13)	356
<i>Brassica oleracea</i> -(S15)	DJ-4049	161	<i>Brassica oleracea</i> (S15) seq. 7	233
		162	<i>Brassica oleracea</i> (S15) contig-1 [5+6+9 (ba2)]	281
<i>Brassica oleracea</i> -(S29)	DJ-2025	163	<i>Brassica oleracea</i> (S29) contig. (7+15)	235
		164	<i>Brassica oleracea</i> (S29) seq. 12	211
		165	<i>Brassica oleracea</i> (S29) seq. 13	239
		166	<i>Brassica oleracea</i> (S29) contig-2 (3+4+8)	337

Table 6.13b continued. (CosPS sequences generated by primer pairs 1-15)

Species	RBG, Kew Acc. No.	Seq. No.	Name of CosPS Sequence	Sequence Length (amino acids)
<i>Centaurea cyanus</i>	2002 1446	167	<i>Centaurea cyanus</i> seq. 2	159
		168	<i>Centaurea cyanus</i> seq. 7	250
		169	<i>Centaurea cyanus</i> seq. 9	262
		170	<i>Centaurea cyanus</i> seq. 10	345
		171	<i>Centaurea cyanus</i> seq. 13	252
		172	<i>Centaurea cyanus</i> seq. 15	255
<i>Conyza canadensis</i>	2002 3497	173	<i>Conyza canadensis</i> seq. 7	251
		174	<i>Conyza canadensis</i> seq. 10	333
		175	<i>Conyza canadensis</i> seq. 15	240
<i>Conyza sumatrensis</i>	2002 3499	176	<i>Conyza sumatrensis</i> seq. 10	350
		177	<i>Conyza sumatrensis</i> seq. 15	229
<i>Cosmos atrosanguineus</i>	1999 2254	178	<i>Cosmos atrosanguineus</i> ⁽²²⁵⁴⁾ seq. 4	223
		179	<i>Cosmos atrosanguineus</i> ⁽²²⁵⁴⁾ seq. 15	221
		180	<i>Cosmos atrosanguineus</i> ⁽²²⁵⁴⁾ contig.	358
<i>Cosmos atrosanguineus</i>	1999 3819	181	<i>Cosmos atrosanguineus</i> ⁽³⁸¹⁹⁾ seq. 4	210
		182	<i>Cosmos atrosanguineus</i> ⁽³⁸¹⁹⁾ contig.	348
<i>Cosmos atrosanguineus</i>	1997 6334	183	<i>Cosmos atrosanguineus</i> ⁽⁶³³⁴⁾ seq. 4	217
		184	<i>Cosmos atrosanguineus</i> ⁽⁶³³⁴⁾ seq. 8	314
		185	<i>Cosmos atrosanguineus</i> ⁽⁶³³⁴⁾ contig.	349
<i>Cosmos atrosanguineus</i>	Sherff 5010	186	<i>Cosmos atrosanguineus</i> ⁽⁵⁰¹⁰⁾ seq. 1	167
		187	<i>Cosmos atrosanguineus</i> ⁽⁵⁰¹⁰⁾ seq. 4	151
<i>Cosmos bipinnatus</i>	1996 582	188	<i>Cosmos bipinnatus</i> seq. 1	127
		189	<i>Cosmos bipinnatus</i> seq. 4	172
		190	<i>Cosmos bipinnatus</i> seq. 15	233
		191	<i>Cosmos bipinnatus</i> contig.	359
<i>Cosmos carvifolius</i>	1999 383	192	<i>Cosmos carvifolius</i> seq. 4	174
		193	<i>Cosmos carvifolius</i> seq. 15	253
		194	<i>Cosmos carvifolius</i> contig.	361
<i>Cosmos sulphureus</i>	1996 980	195	<i>Cosmos sulphureus</i> seq. 1	151
		196	<i>Cosmos sulphureus</i> contig.	249
<i>Diplotaxis tenuifolia</i>	2002 3495	197	<i>Diplotaxis tenuifolia</i> seq. 4	231
		198	<i>Diplotaxis tenuifolia</i> seq. 13	233
		199	<i>Diplotaxis tenuifolia</i> contig- (7+15)	257

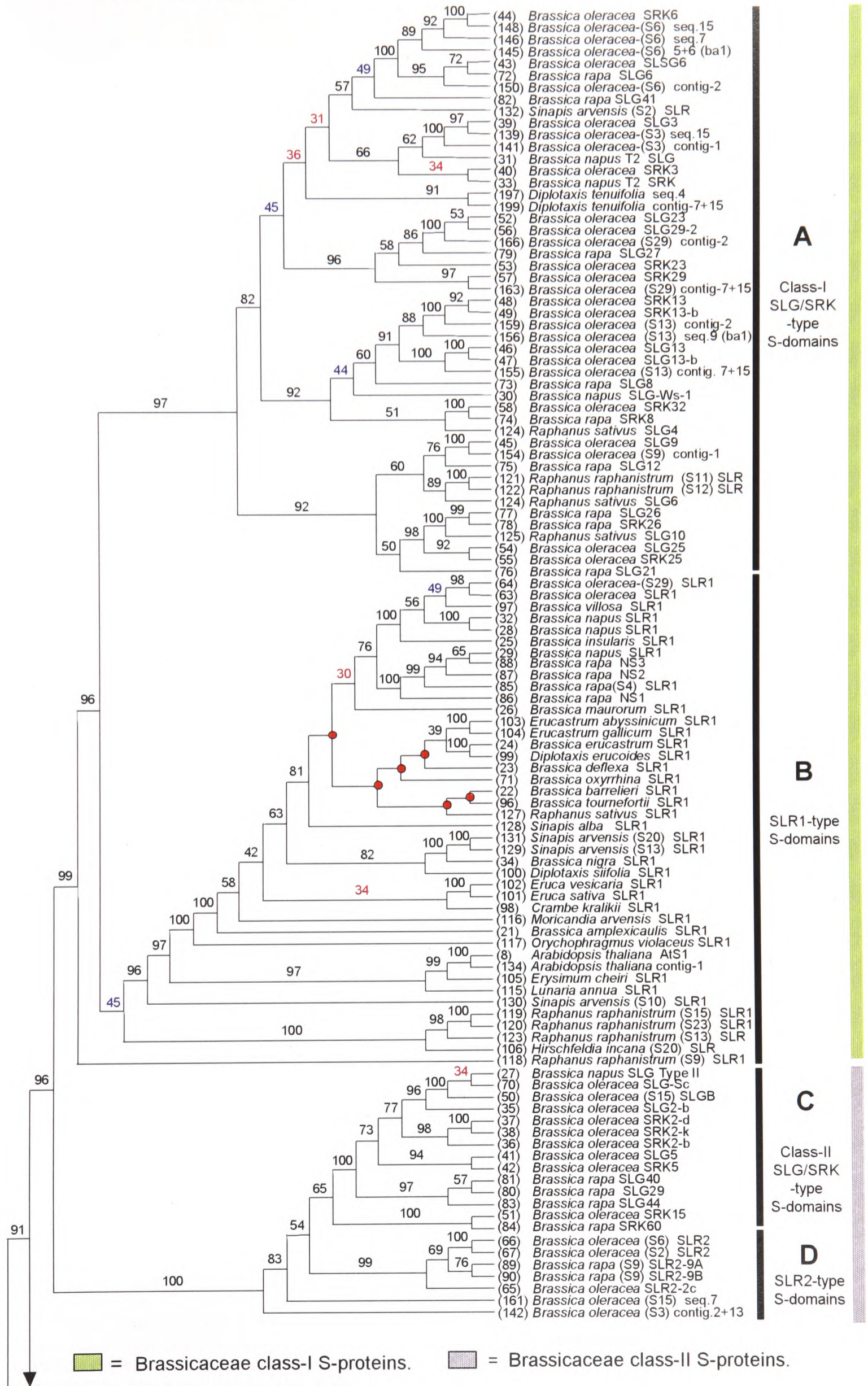
Table 6.13b continued (CosPS sequences generated by primer pairs 1-15)

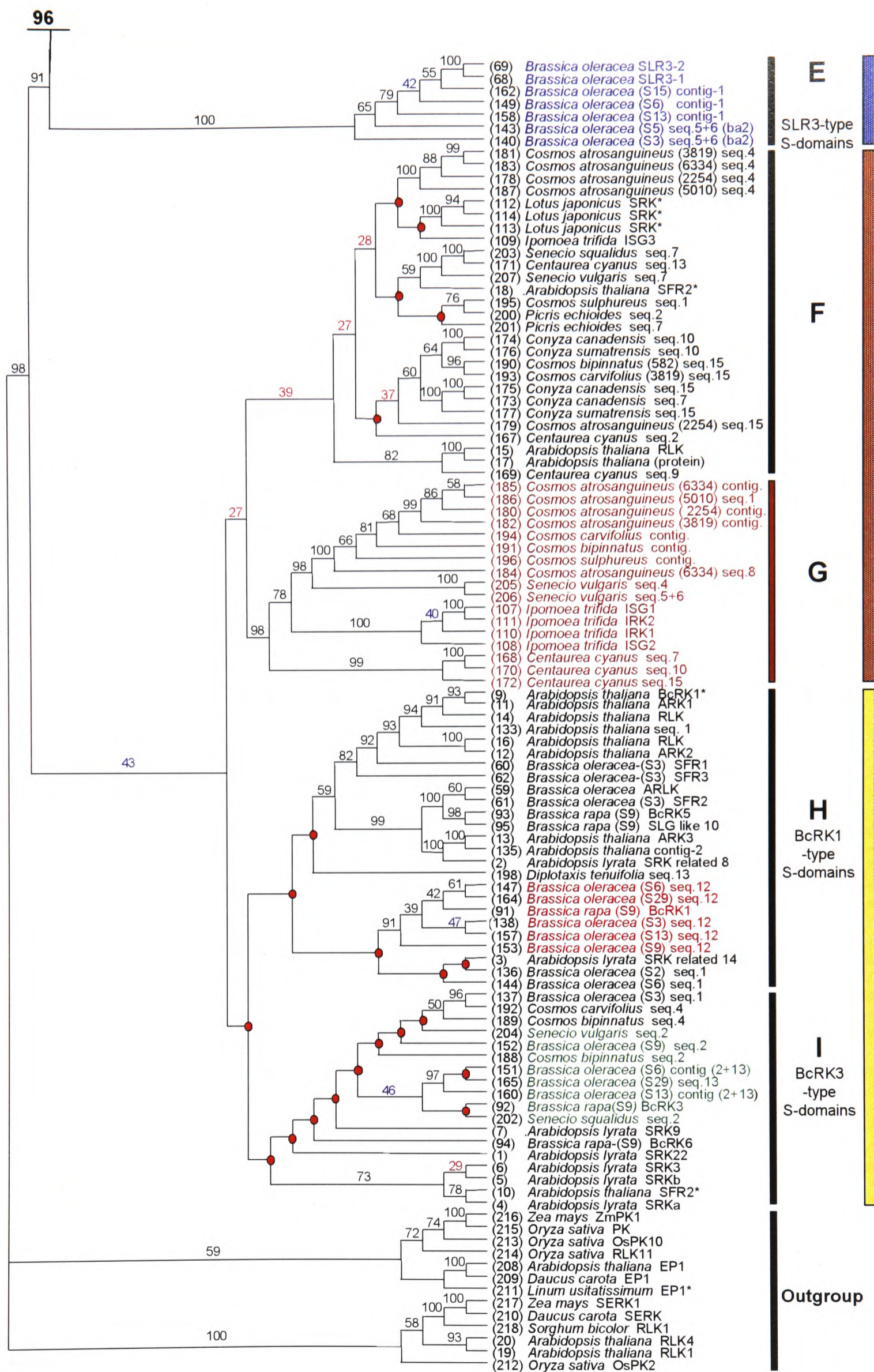
Species	RBG, Kew Acc. No.	Seq. No.	Name of CosPS Sequence	Sequence Length (amino acids)
<i>Picris echioides</i>	2002 3494	200	<i>Picris echioides</i> seq. 2	175
		201	<i>Picris echioides</i> seq. 7	248
<i>Senecio squalidus</i>	2002 3493	202	<i>Senecio squalidus</i> seq. 2	134
		203	<i>Senecio squalidus</i> seq. 7	227
<i>Senecio vulgaris</i>	2002 3492	204	<i>Senecio vulgaris</i> seq. 2	143
		205	<i>Senecio vulgaris</i> seq. 4	214
		206	<i>Senecio vulgaris</i> seq. 5+6	171
		207	<i>Senecio vulgaris</i> 7	237

Table 6.13c. List of NCBI S-domain protein sequences used as outgroup S-domain sequences in the construction the Neighbour-Joining (NJ) trees of plant S-domains illustrated in Figures 6.5a and 6.5b

Species	Seq. No.	Accession No.	Name of Protein	Information
<i>Arabidopsis thaliana</i>	208	AAN31898	EP1	Putative glycoprotein (EP1) coded by At1g78850 gene. (441 aa).
<i>Daucus carota</i>	209	AAA33136	EP1	The carrot secreted glycoprotein gene <i>EP1</i> is expressed in the epidermis and has sequence homology to <i>Brassica S</i> -locus glycoproteins. (389 aa).
	210	AAB61708	SERK	SERK somatic embryogenesis receptor-like kinase in carrot. (553 aa).
<i>Linum usitatissimum</i>	211	AAO15899	Secreted glycoprotein similar to EP1	Cultivar ariane DNA sequence, similar to EP1 glycoprotein from carrot. (430 aa).
<i>Oryza sativa</i> cultivar <i>Nipponbare</i>	212	AAL29303	OSPK2	OSPK2: putative histidine kinase for ethylene receptor-like protein 2. (836 aa).
	213	AAA33915	OSPK10	OSPK10 receptor type serine/threonine kinase. (824 aa).
	214	AAM90696	RLK11	<i>S</i> -locus receptor-like kinase RLK11. (820 aa).
	215	BAB90164	PK	Putative receptor-like protein kinase encoded by gene P0408G07.10 on chromosome 1. (823 aa).
<i>Zea mays</i>	216	CAA36611	ZmPK1	Protein kinase. (817 aa).
	217	CAC37638	SERK1	<i>SERK1</i> gene for putative LRR receptor-like kinase. (622 aa).
<i>Sorghum bicolor</i>	218	CAB51480	RLK1	Putative protein serine /threonine kinase that accumulates in mesophyll cells is encoded by 14600.1:164.2023. (619 aa).
Plus sequence (19) <i>Arabidopsis thaliana</i> RLK1 and sequence (20) <i>Arabidopsis thaliana</i> RLK4. (See Table 6.13a).				

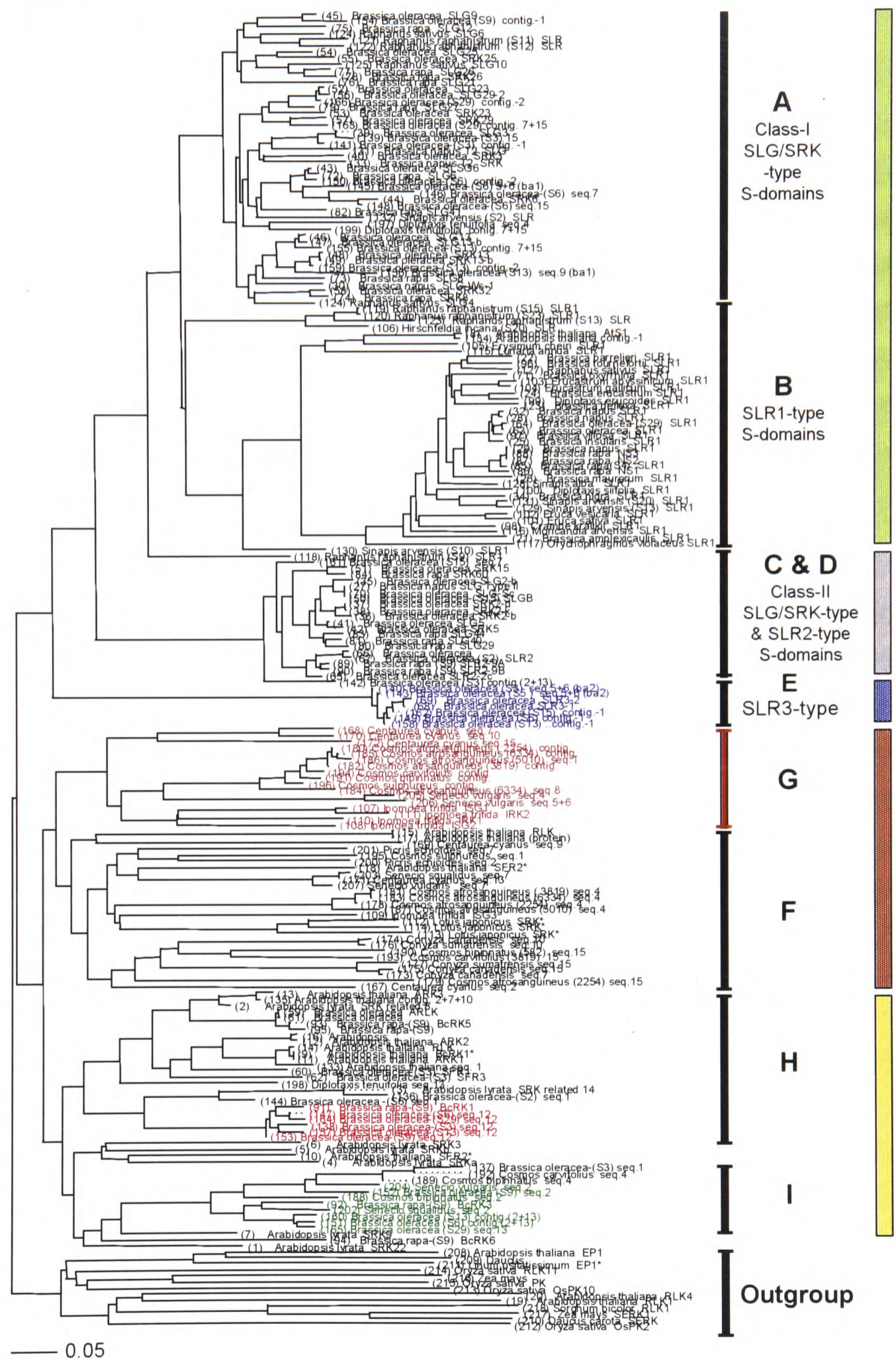
Figure 6.5a – NJ Tree of encoded CosPS S-domain sequences and S-domains from Brassicaceae, Convolvulaceae and Fabaceae





■ - SLR3-type S-proteins ■ = Non-Brassica-type S-proteins. ■ = Brassica-type RLKs.
Red circles indicate nodes that are not supported in the bootstrap tree. Numbers on tree represent the percentage bootstrap support per 1000 replications. Bootstrap percentages of less than 50% and 40% are highlighted in blue and red respectively. Number of taxa = 218; Number of characters = 567 Outgroups = 13. Distance settings: (i) objective function = Minimum Evolution (ME); (ii) negative branch length allowed but set to zero for tree score; (iii) distance measure = mean character difference. Tree score = ME = 28.84456.

Figure 6.5b. Phylogram of encoded CosPS S-domain sequences compared with S-domains from Brassicaceae, Convolvulaceae and Fabaceae



- = Brassicaceae class-I S-proteins.
- = Brassicaceae class-II S-proteins.
- = SLR3-type S-proteins
- = Non-Brassica-type S-proteins.
- = Brassica-type RLKs.

Phylogram showing distance relationships between clades A to I. Clades labelled and coloured as in Figure 6.5a.

The NJ tree in Figure 6.5a divides into two distinct subsections. The first sub-section includes the S-domains of Brassicaceae class-I (green bar, clades A-B) class-II (grey bar, clade C-D) and SLR3-type S-proteins (blue bar, clade E) in a well-supported division of the tree (BP 91). The second subsection contains the S-domains of non-*Brassica* type S-proteins (brown bar, clades F-G) and *Brassica*-type RLKs (yellow bar, H-I). In the first subsection (clades A-E), there is a clear well-supported separation of class-I and class-II S-domains (BP 96), and a further well-defined, well-supported division of SLR3-type Brassicaceae S-domains (BP 99). In contrast, the second subsection of the tree has very weak support (BP 43) for the separation of non-*Brassica*-type S-proteins and *Brassica*-type RLKs. However, the relationship between the two subsections of the tree is extremely well supported (98 BP), and confirms the relatedness of Brassicaceae and non-Brassicaceae S-domains, indicating that the encoded CosPS S-domains and those of Convolvulaceae, Fabaceae and non-*Brassica* Brassicaceae are probably members of the S-multigene family..

Brassicaceae class-I proteins (green bar) contain S-domains of Brassicaceae SLGs/SRKs/SLRs (clade A, 97 BP), and a group consisting of SLR1 S-domains (clade B). Clade A contains some interesting associations of S-domains. The S-domains of *Brassica oleracea* SLG₆, SRK₆, and *B. rapa* SLG₆ form a distinct and very well-supported (100 BP) group, hereafter referred to as the S₆-group. There is weak support for including the S-domains of *B. rapa* SLG₄₁ (49 BP) and *Sinapis arvensis* (S₂) SLR (BP 57) in the S₆-group, and hence these two latter sequences are not included in the S₆-group. The S-domains of *B. oleracea* SLG/SRK₃ and *B. napus* (T2) SLG/SRK form a moderately well supported group (66 BP) hereafter identified as the S₃/T2-group. A third well-resolved and well-supported (96 BP) group, identified hereafter as the S₂₃/S₂₉-group, consists of the S-domains of *B. oleracea* SLG/SRK₂₃ and SLG/SRK₂₉, but also *B. rapa* SLG₂₇. The relationships between the S₆-, S₃/T2- and S₂₃/S₂₉- groups of clade A are not well supported (BP 46). However, the three groups collectively form a well-supported subclade (82 BP) that is sister to an extensive and well supported S₁₃-group (92 BP), consisting predominantly of *B. oleracea* SLG/SRK₁₃ S-domains, but also the S-domains of *B. rapa* SLG/SRK₈, *B. oleracea* SRK₃₂, *B. napus* SLG-Ws-1 and *Raphanus sativus* SLG₄. The close relationship of *B. oleracea* S₁₃ and *B. rapa* S₈ haplotypes has been noted previously (Nasrallah and Nasrallah 1993; Boyes *et al.*, 1997; Suzuki *et al.*, 2000a; Watanabe *et al.*, 2000; Nasrallah *et al.* 2002) and these two haplotypes are believed to be derived from a common ancestral haplotype, to which it appears the *B. oleracea* S₃₂ haplotype, the *B. napus* SLG-Ws-1 and the *Raphanus sativus* SLG₄, a class-I SLG, also belong.

The *Diplotaxis tenuifolia* encoded CosPS.4 and CosPS contig.7+15 sequences are nested within the S_6 -, $S_3/T2$ - and S_{23}/S_{29} -groups, with the tree topography giving weak support (36 BP) for their inclusion between the $S_3/T2$ -group and the S_{23}/S_{29} -group of clade A. Although the precise location of these two *D. tenuifolia* encoded S-domains within the three *Brassica* SLG/SRK groups is unclear, their location in clade A, and their non-segregation with SLR1s of *D. silifolia* and *D. eruroides* in class B, suggests they encode class-I SLG/SRK S-domains or represent an SLR protein. Aside from SLRs of *Sinapis arvensis*, *Raphanus raphanistrum*, and the *R. sativus* SLGs, the encoded *Diplotaxis tenuifolia* CosPS.4 and CosPS-contig.7+15 sequences are the non-*Brassica* sequences most similar to *Brassica* SI proteins, again indicating that these sequences represent SLG/SRK. Since species-specific SLG/SRKs in clade A do not cluster together, the diversification of class-I SLG/SRK proteins would appear to predate the differentiation of *Brassica* species. Likewise, since genera-specific SLGs do not cluster together, the diversification of class-I SLGs probably predates the differentiation of *Raphanus*, *Brassica* and possibly *Diplotaxis* genera.

A heterogeneous, but well supported group of S-domains (92 BP) consisting of *B. oleracea* SLG9 and SLG/SRK26, *R. sativus* SLG6 and SLG10, *B. rapa* SLG12, SLG21 and SLG26, and SLR11 and SLR12 of *R. raphanistrum* makes up the fifth and final group of clade A, hereafter referred to as the S_9 -heterogeneous group. An interesting observation, is the inclusion within this group, of *R. sativus* class-I (S_6) and class-II (S_{10}) SLGs. The class-II *R. sativus* SLGs might have been expected to appear near to clades C or D, which contain the *Brassica* class-II type S-domains. According to the distance relationship described in these NJ trees (Figures 6.5a-b), class-II *R. sativus* SLGs, which were identified by non-binding of the *Brassica* class-I specific antibody (Sakamoto *et al.*, 1998), show greater similarity to *Brassica* class-I S-proteins than to *Brassica* class-II S-proteins. Perhaps these *R. sativus* class-II SLGs should more accurately be described as “non-class-I antibody-binding SLGs” to distinguish them from class-II type SLGs, which segregate into a distinct well-resolved major clade (grey bar BP 100), consisting of class-II *Brassica* S-proteins.

Another interesting observation is the location of the SLR11 and SLR12 proteins of *R. raphanistrum* in the S_9 -heterogeneous group of clade A. Another anomalous observation is the location of *R. raphanistrum* (S_{13}) SLR protein and the *Hirschfeldia incana* (S_{20}) SLR protein at the base of clade B, a clade which otherwise contains only SLR1 proteins. Their location in the NJ tree suggests that the SLR proteins of *R. raphanistrum* S_{13} and *Hirschfeldia incana* S_{20} may actually be SLR1 sequences. Or,

alternatively, that these two sequences and the SLR1 sequences of *R. raphanistrum* S₉, S₁₅ and S₂₃ represent sequences that are intermediate between SLR and SLR1 proteins. The very low support for this basal SLR1 group (45 BP) of clade B suggest the latter. Hence a propose of this thesis is that the SLR1 sequences of *R. raphanistrum* S₉, S₁₅, S₂₃, and the SLRs of *R. raphanistrum* S₁₃ and *H. incana* S₂₀ represent composite or intermediate S-domains encompassing characteristic of both SLG/SRK/SLR and SLR1 proteins. *Sinapis arvensis* SLR1 sequence may also constitute an intermediate S-domain as it segregates with this putative intermediate basal SLR1 group, rather than with the other *Sinapis* SLR1 sequences that locate deep within the SLR1 region of clade B. In contrast, the SLR11 and SLR12 of the *R. raphanistrum* are distinctively SLG-like in their homology, as they segregate to the S₉-heterogeneous group within clade A, which consists of class-I SLG/SRK-type domains.

The *Brassica* S-locus exhibits sequence and structural polymorphism, and extensive restructuring of the S-locus is known to have preceded speciation (Boyes and Nasrallah, 1993; Nasrallah and Nasrallah 1993; Boyes *et al.*, 1997; Suzuki *et al.*, 2000a; Watanabe *et al.*, 2000; Nasrallah *et al.* 2002). It is possible that these anomalous SLR/SLR1 sequences represent another lineage of Brassicaceae S-domain structural and sequence polymorphism.

None of the encoded CosPS sequences or S-domains from published sequences located with the *Arabidopsis thaliana* RLK1 or RLK4 S-domains. This observation supports the low percentage pairwise data that these *A. thaliana* S-domains have with known S-domain proteins (~22-25%). Interestingly, these two sequences associate with the outgroup clade containing SERK proteins of *Zea mays* and *Daucus carota* and not with the outgroup clade containing the S-like domains ZmPK1 and EP1, however separation of outgroups into two clades is not resolved and so the precise association of outgroup members with respect to each other is not clear.

Although the relationships between the S₆-, S₃/T2- and S₂₃/S₂₉-groups of clade A are not clear (BP 45), the topology and bootstrap support show a clear separation of these three groups from the S₁₃-group (BP 82) and S₉-heterogeneous group (BP 97) (Figures 6.5a-b). Unless orthology can be demonstrated, congruency of gene and species trees cannot be assumed (Koch *et al.*, 2001). However, if one accepts the hypothesis that S-domains in clade A arose from a single ancestor by common descent, then these data suggest a distinct separation between the S-domains of the S₁₃-group and S₉-heterogeneous group from those of the S₆-, S₃/T2- and S₂₃/S₂₉-groups, with the S₉-

heterogeneous group diverging first within clade A (BP 97), followed by the differentiation of the S_{13} -group (BP 82) from the S_6 -, $S_3/T2$ - and S_{23}/S_{29} -groups.

The Brassicaceae family is considered to have arisen ~50 million years ago and has since undergone rapid radiation (Koch *et al.*, 2001). The rapid diversification and the highly homoplastic characters used in Brassicaceae tribal circumscription have led to the creation of many artificial taxonomic groups that do not reflect Brassicaceae phylogeny. Only Brassiceae and Lepidieae form natural monophyletic tribes within the family (Janchen, 1942, Heywood, 1993; Koch *et al.*, 2001). In most phylogenies, *Brassica*, *Raphanus* and *Sinapis* form a natural grouping within Brassiceae, with *Raphanus* and *Brassica* related more to each other than to *Sinapis* (Yang *et al.*, 1999). The topology of Brassicaceae class-I S-domains (Figures 6.54-b, clades A & B) supports the natural grouping of *Brassica*, *Raphanus* and *Sinapis*, but does not identify a definitive relationship between *Raphanus* and *Brassica*. A single fossil record suggests differentiation of Brassicaceae species occurred in the upper Miocene between 5-11 million years ago (Hinata *et al.*, 1995). If diversification of the S-haplotype is placed at ~10 million years ago in accordance with the fossil record for speciation, then the estimated rate of molecular change of S-haplotypes would be very high, and much higher than those recorded for other plant genes (Hinata *et al.*, 1995). If diversification of the S-haplotype is assumed to have taken place ~50 million years ago, then the estimated rate of molecular change of S-haplotypes would accord with estimated rates of change observed for other plant genes, and S-haplotype diversification equates with the origin of the Brassicaceae (Hinata *et al.* 1995). Depending on which data are accepted, SI in Brassicaceae may predate familial diversification, or is a more recent condition acquired after differentiation of tribes and/or genera.

The separation of clades A and B identifies two distinct lineages within class-I proteins (BP 96), consisting of SLG/SRK/SLR S-domains and those of SLR1. Aside from sequence *Sinapis arvensis* (S_{10}) SLR1, a member of the tribe Brassiceae, that appears more closely related to S-domains of tribes Lepidieae and Lunarieae and may possibly be a composite SLG/SLR1-type S-domain (Table 6.14) and the weakly supported basal clade (BP 45) within clade B consisting of putative composite S-domains of *Raphanus raphanistrum* S-domains and *Hirschfeldia incana* SLR20, the phylogeny of Brassicaceae SLR1 proteins accords with the species, genera and tribal phylogeny of Brassicaceae. Within this phylogeny, the tribes Brassiceae and Sisymbrieae are more closely related to each other than they are to the Lunarieae and Lepidieae (Zunk *et al.*,

1996; Koch *et al.*, 2001), and *Brassica* species are divided into two evolutionary lineages: the *nigra* lineage and the *rapa/oleracea* lineage, either of which *Raphanus* is considered to belong (Palmer and Herbon, 1988; Song *et al.*, 1988, 1990; Warwick and Black, 1991; Thormann *et al.*, 1994; Pradhan *et al.*, 1992; Yang *et al.*, 1999). In Figure 6.5a, *Raphanus sativa* SLR1 is located within a well-supported (BP81) subclade of clade B that contains all the *Brassica rapa* and *B. oleracea* SLR1s, hereafter referred to as the SLR1-*rapa/oleracea* subclade. This SLR1-*rapa/oleracea* subclade is sister to a moderately well-supported group (BP 63) that contains *Brassica nigra*, *Sinapis ssp.* and *Diplotaxis siifolia*, suggesting that *Raphanus* SLR1 proteins are more closely related to SLR1s of *B. rapa* and *B. oleracea* than they are to *B. nigra*, and thus supporting the chloroplast and mitochondrial restriction site variation data, that place *Raphanus* in the *rapa/oleracea* lineage (Palmer and Herbon, 1988; 1990; Warwick and Black, 1991; Pradhan *et al.*, 1992).

Table 6.14 – Four Brassicaceae tribes and some respective genera

Brassicaceae	Lunarieae	Lepidieae	Sisymbrieae
<i>Brassica</i>	<i>Lunaria</i>	<i>Erysimum</i>	<i>Arabidopsis</i>
<i>Diplotaxis</i>			
<i>Raphanus</i>			
<i>Sinapis</i>			
<i>Moricandia</i>			
<i>Crambe</i>			
<i>Hirschfeldia</i>			
<i>Eruca</i>			
<i>Erucastrum</i>			
<i>Orychophragmus</i>			

The topology of clade B shows a distinct separation of SLR1s of the tribe Brassicaceae, i.e. *Brassica oleracea* (S29) to *Orychophragmus violaceus*, from those of the Sisymbrieae (*Arabidopsis*), Lepidieae (*Erysimum*) and Lunarieae (*Lunaria*). With genera from the latter three tribes forming a distinct well-supported clade (BP97) that is sister to the clade containing Brassicaceae SLR1s. However, the relationship of *Arabidopsis*, *Erysimum* and *Lunaria* SLR1s, illustrated by Figure 6.5a do not identify Sisymbrieae (*Arabidopsis*) as being sister to Brassicaceae. With the addition of more SLR1 sequences from genera of the Sisymbrieae, Lepidieae and Lunarieae, the resolution of the this part of the tree would be improved and may give support to the accepted tribal phylogeny that identifies the Brassicaceae and Sisymbrieae as being more closely related to each other than they are to the Lunarieae and Lepidieae (Zunk *et al.*, 1996; Koch *et al.*, 2001)

Sister to the major clade of Brassicaceae class-I S-proteins (green bar) are the Brassicaceae class-II S-proteins (grey bar), consisting of class-II SLG/SRK-type S-domains (clade C) and SLR2-type S-domains (clade D). There is 100% bootstrap support for this grouping of Brassicaceae class-II proteins and their separation from Brassicaceae class-I proteins is also very well supported (96 BP). Likewise, the SLR3-type S-domains form a well-resolved, well-supported group (clade E, blue bar, 100 BP) that is sister to class-II S-proteins (91 BP). If the S-domains represented in clades A, B, C and D are considered to be orthologous, having arisen from a single ancient common ancestor, then the high bootstrap support for the separation of class-I, class-II and SLR3-type S-domains confirms distinct phylogenies for these three groups of *Brassica* S-domains.

Almost half the encoded *B. oleracea* CosPS sequences are situated in clades A to E, and none of the *Brassica* CosPS sequences encoded SLR or SLR1 sequences, indicating that in *Brassica*, primer pairs 1-15 amplify predominantly SLG/SRK-type S-domains. In summary, the encoded CosPS *B. oleracea*-(S₆) sequences; seq.5+6(ba1) [145]¹², seq.7 [146] and seq.15 [148] are related to *B. oleracea* SRK₆ (clade A; S₆ group, 89 BP), while *B. oleracea*-(S₆) contig-2 (3+4+8) [150] appear to be homologues of *B. oleracea* SLG₆ (clade A; S₆ group, BP 95). The encoded CosPS *B. oleracea*-(S₃) sequences, seq.15 [139] and contig-1 (3+4+7+8) [141] are homologues of SLG₃ (clade A; S₃/T2 group, BP 100), while *B. oleracea*-(S₃) contig 2+13 [142] locates with *B. oleracea*-(S₁₅) seq.7 [161] to clade D (SLR2-type S-domains). *Brassica* class-II S-proteins are known to be more closely related to SLR2 protein sequences than they are to class-I S-proteins (Scutt and Croy, 1992), and the topography of the NJ tree (Figures 6.5a-b) supports this relationship and appears also to identify *B. oleracea*-(S₃) contig. 2+13 [142] as an SLR-2 type sequence (BP 83). The encoded CosPS *B. oleracea*-(S₂₉) sequences contig (7+15) [163] and contig-2 (3+4+8) [166] locate to the S₂₃/S₂₉ group of clade A, with the former being a homologue of *B. oleracea* SRK₂₉ (BP 97) and the latter a homologue of *B. oleracea* SLG₂₉ (BP 100). The encoded CosPS *B. oleracea*-(S₁₃) sequences seq.9(ba1) and [156] contig-2 (1+3+4+8+10) [159] are related to *B. oleracea* SRK₁₃ (clade A; S₁₃ group, BP 88), while contig.7+15 [155] is a homologue of *B. oleracea* SLG₁₃ (BP 100). The encoded CosPS *B. oleracea* (S₉) sequence contig-1 [154] is a *B. oleracea* SLG₉ homologue (Clade A; S₉ heterogeneous group, BP 100). As expected from SSEARCHs, the encoded CosPS *Arabidopsis thaliana* sequence

¹² Numbers in square brackets correspond to the sequence numbers in Tables 6.13a-c and Figures 6.5a-b

contig-1 [134] is a homologue of AtS1 [8], an *A. thaliana* SLR1 homologue (clade B, BP 100). *A. thaliana* seq.1 [133] located with ARK1 [11] and an unspecified *A. thaliana* RLK sequence [14] in clade H, (BcRK1-type S-domains, BP 94), and *A. thaliana* contig-2 [135] also located to clade H, where it appears to be a homologue of ARK3 (BP 100). All encoded CosPS-5+6(ba2) and CosPS-9(ba2) sequences located to clade E (*B. oleracea* SLR3-type S-domains) and appear to be homologues of SLR3-1 [68] (BP 100). The remaining encoded CosPS *B. oleracea* sequences identified as *Brassica* RLKs and located to clade H or clade I (Figure 6.5a-b).

Although the separation of Brassicaceae class-I, (green bar) class-II (grey bar) and SLR3-type (blue bar) S-proteins from non-*Brassica*-type S-proteins (brown bar) and *Brassica*-type RLKs is well supported (BP 98), the relationships within the second subsection of the NJ tree have weak statistical support. Much of the difficulty in resolving lineages in this subsection is due to the variable lengths of the encoded CosPS sequences comprising clades F-I. Many of the 5'-end CosPS sequences are particularly short and align in only ~150 out of the ~400 residues (~40%) of the full-length S-proteins used in the matrix (Table 6.16). It is noticeable that the greater the length of the CosPS sequences, the better the resolution and bootstrap support of the clades in which these sequences appear. Comparison of clade G, composed predominantly of wholepiece and contig CosPS sequences, with clades I, consisting of a mixture 3'-end 5'-end, and contig CosPS sequences, shows how variable sequence length affects tree resolution and topography. Considering the limitations in the length of some CosPS sequences, 47% bootstrap support for the separation of clades F-G, and clades H-I is not unacceptable, and so this tree topography is maintained for the foregoing discussion. Despite the very low support for the separation of clades F and G (22 BP), and H and I (30 BP), these divisions are likewise maintained as they serve clarity of discussion.

In general, the terminal branches of clades F to G are well supported, but the relationships of groups within a clade are not clear (Figure 6.5a, clades F and G). Clade G and F support the conclusions made previously that the phylogeny of encoded CosPS sequences from the five Asteraceae genera *Cosmos*, *Conyza*, *Senecio*, *Centaurea* and *Picris* accord with Asteraceae tribal phylogeny. Clade G (Figure 6.5a) is the most fully resolved and well-supported clade (97 BP) of this subsection, and it confirms the conclusions made for clade A in Figure 6.4a, that encoded contiguous, wholepiece and 3'-end CosPS sequences of *Senecio* spp, *Cosmos* spp. and *Centaurea cyanus* are more closely related to ISG1-2 and IRK1-2 of *Ipomoea trifida*

(Convolvulaceae) than to any other S-protein in the matrix. These data accord with the familial phylogeny wherein Convolvulaceae (euasterids I) and Asteraceae (euasterids II) are more closely related to each other than they are to Brassicaceae (eurosids II) (Figure 6.3). Interestingly, *Arabidopsis thaliana* RLK sequences, [15], [17] and [18] are more closely related to encoded Asteraceae S-domains than they are to other *A. thaliana* RLK sequences (clade F), an association that probably reflects a functional orthology for these sequences. Clade F suggests there is a relationship between the SRK S-domains of *Lotus japonicus* (Fabaceae), the encoded CosPS.4 S-domains of *C. atrosanguineus* and *Ipomoea trifida* ISG3 (Figure 6.3), although statistical support and topography of the bootstrap tree does not support this precise relationship. More data, in the form of greater sequence length will be needed before appropriate conclusions can be drawn about this cladal association. Furthermore, the tentative relationship identified for these sequences does not agree with the familial phylogeny as Fabaceae (eurosids I) is more closely related to *Brassica* (eurosids II) than it is to Convolvulaceae (asterids I) or Asteraceae (asterids II), (Figure 6.3), and so the closeness of these sequences probably reflects the closeness of their protein domains identifying them as possible paralogues. In contrast, there is very strong support for the relationship of the encoded CosP.7 sequences of *Senecio spp.* and *Centaurea cyanus* seq.13 (clade F, BP 100), and moderate support for identifying these sequences as being SFR2-type S-domains similar to SFR2 of *Arabidopsis thaliana* (BP 59). This latter relationship is interesting because *Senecio* and *Centaurea* come from different subfamilies (Figures 1.5 and 1.6) and *A. thaliana* from a different plant family. Since their nucleotide sequences show no relationship to each other (Table 6.5), it is unlikely these four S-sequences are orthologues. Their similarity is probably a consequence of homology in their protein domains. Protein-domain homology in paralogous genes can occur through concerted evolution of functionally orthologous protein domains, and often identifies proteins that are functionally similar (Koonen *et al.*, 2000). CosPS sequence-15 of *Cosmos bipinnatus* and *C. carvifolius* appear to be homologues (BP 96), as are *Conyza canadensis* seq.10 and *C. sumatrensis* seq.10 (clade F), with these two pairs of homologues forming a weakly-supported group in clade F (BP 64). The encoded S-domain of *Conyza canadensis* seq.7, seq.15 and the *C. sumatrensis* seq.15 are homologues (BP 100) and form a weakly-supported subclade that includes the encoded S-domains of seq.10 and seq.15 of *Conyza spp.* and *Cosmos spp.* respectively (BP 60).

The sequences in clade H were nominally described as BcRK1-type S-domains, but might equally have been designated SFR-type or ARK-type S-domains. Clade H

segregates into three well-supported subclades. The first subclade, forms a well-supported group (BP 82) of *Arabidopsis thaliana* BcRK1, ARK1, ARK2 homologues, and *Brassica oleracea* (S₃) SFR1 and SFR2 S-domains. There is weak support (BP 59) for accepting this subclade as being sister to the second extremely well-supported subclade that consists of *Brassica oleracea* ARLK, SFR2, *B. rapa*-(S₉) BcRK5, SLG-like 10, *A. thaliana* ARK3 homologues and *A. lyrata* SRK-related 8 S-domains (BP 99). The segregation of encoded CosPS *Brassica oleracea* BcRK1 homologues with *B. rapa* BcRK1 forms a third well-supported subclade of H (BP 91), although separation of clade H from the former two subclades is not supported statistically or topologically by the bootstrap tree. Likewise, clade I, (BcRK3-type S-domains), forms a weakly supported clade with dubious topography. The tree identifies a very odd relationship between encoded CosPS.4 sequences of *C. carvifolius* and *C. bipinnatus* with *B. oleracea*-(S₃) seq.1. The top SSEARCH protein match identified for *B. oleracea*-(S₃) seq.1 was *A. thaliana* ARK1, while the highest protein match for CosPS.4 *C. bipinnatus* and *C. carvifolius* S-domains was an *A. lyrata* S-related sequence and an unspecified *A. thaliana* RLK respectively (Table 6.5) The three CosPS sequences have similar lengths ranging from 139-174 residues and as a consequence they show a greater relationship to each other than they do to their highest pairwise match. If the full-length *Brassica* and *Cosmos* CosPS sequences were available then the relationship of these sequences in the tree would more properly reflect their pairwise homology, and the encoded *Cosmos* CosPS.4 sequences would probably form a well-supported group that associates with *Lotus japonicus* SRKs and *Ipomoea trifida* ISG3. Although it is not clear where the BcRK3-type S-domains sit in this subsection of the tree, the BcRK3-type encoded S-domains of *B. oleracea* (seqs. 13 and contigs. 2+13) and *Senecio squalidus* (seq.2) form a weakly-supported (BP 46) minor clade with *B. rapa* (S₉) BcRK3. However, the resolution of clade H is seriously compromised due to the variability in sequence length such that the encoded *C. bipinnatus* and *S. vulgaris* BcRK3 homologues are excluded from this minor clade.

6.4.6 – Summary

The topography illustrated in Figures 6.5a-b, identifies a split between the Brassicaceae class-I, class-II and SLR3-type S-domains (clades A-E respectively) and those of non-*Brassica* S-proteins (clades G-F) and *Brassica*-type RLKs (clades H-I). Although, the relative relationships of clades G to I are not clear, those of clades A to E identify distinct clusters of Brassicaceae S-domains that may reflect their relative points of divergence. In this part of the NJ tree, SLR3-type S-domains (clade E) form a distinct grouping of S-proteins and are the most distant from class-I S-domains (green

bar), forming the most basal clade of Brassicaceae S-proteins. Clade C and D are made up of class-II S-proteins (grey bar) and form a distinct subset of S-domains that show more similarity to SLR3-type S-domains than to class-I S-domains.

Within Brassicaceae class-I S-proteins, divergence of class-I SLG/SRK-type S-domains from SLR1-type S-domains has occurred with SLR1s appearing to be the most recently diverged of the Brassicaceae S-domains. A small basal SLR1 group, consisting of SLR1s of *Raphanus raphanistrum* (S_9), (S_{15}), (S_{23}), and the SLRs of *R. raphanistrum* (S_{13}) and *Hirschfeldia incana* (S_{20}) is composed of a set of putative hybrid S-domains that appear to be composites of class-I SLGs/SRKs and SLR1-type S-domains.

Fractured homology and structural polymorphism of the *Brassica* S-locus is becoming apparent, and is possibly also a characteristic of non-Brassicaceae S-genes (Boyes and Nasrallah, 1993; Nasrallah and Nasrallah 1993; Boyes *et al.*, 1997; Schopfer *et al.* 1999; Suzuki *et al.*, 2000a; Watanabe *et al.*, 2000; Nasrallah *et al.* 2002). The rearranged haplotypic configuration and the fractured homology identified in specific *Brassica* haplotypes appear to have contributed to a reduction in recombination at the S-locus (Watanabe *et al.*, 2000), and it may be that the ubiquitous S-associated conserved domains serve a similar role in conserving specific sequences in other S-domain genes

Interestingly the split in class-I S-proteins between SLGs/SRKs (clade A) and SLR1s (clade B) is mirrored in class-II S-proteins, where class-II SLGs/SRKs (clade C) and SLR2s (clade D) also form two distinct groupings. According to the NJ Trees in Figures 6.5a-b, there is a greater similarity between Brassicaceae class-I SLGs/SRKs and SLR1s, and between class-II SLGs/SRKs and SLR2s, than there is between class-I and class-II SLGs/SRKs, or between SLR1s and SLR2s. These data suggest that class-I SLGs/SRKs and SLR1s show greater sequence similarity to each other than they do to their respective class-II SLG/SRK and SLR2 sequences, and vice versa, and identifies a possibly a class-I and class-II lineage of Brassicaceae S-proteins.

CHAPTER 7. – Concluding comments and future prospects

7.1 – Discussion

Cosmos atrosanguineus is a self-incompatible Mexican endemic species of Asteraceae now believed to be extinct in the wild, and exists today only as a cultivated species. Cultivated specimens are not known to set seed, although the wild parental population from which cultivated specimens are derived are known to have produced seed in quantities large enough to support commercial sale. The loss of *C. atrosanguineus* from the natural environment is attributed to habitat destruction, particularly human exploitation of the pine-oak-forest mountain regions of Mexico. Human exploitation of Mexican forests has removed approximately 40% of temperate forest, but has affected disproportionately the pine-oak forest habitat specific to atrosanguinate *Cosmos* species, with more than 60% of this ecoregion lost to logging, agriculture and urban expansion (Toledo *et al.* 1989; Cárdenas-Hernández *et al.* 1994). The two known localities of wild *C. atrosanguineus* populations underwent rapid development in the late 19th-early 20th century as a result of the copper mining industry and subsequent urbanisation. Furthermore, during the 19th century, the Americas were frontier countries that attracted aspiring pioneers from many professions, not least from the field of the natural sciences. The plant collecting mentality that prevailed at the time, led to the removal of tonnes of living material from native environments and their transportation, as seed or dried specimens, to Europe, where they expanded considerably the living and herbarium material of European Botanical Gardens and private/commercial collections. The story of *C. atrosanguineus* exemplifies this culture of botanical appropriation and habitat destruction, with Benedict Roezl, the first to collect *C. atrosanguineus*, being one of its foremost proponents. As a means of financing his many plant-collecting trips, Roezl collected, for botanical posterity and commercial exploitation, vast amounts of plant material throughout North and Central America, often removing entire populations of interesting and novel plants in this pursuit (Appendix 2a-c). The two *C. atrosanguineus* collections in San Luis Potosí and Zimapan may have represented the only two regions of wild *C. atrosanguineus* populations, and were possibly composed of newly established individuals undergoing repeated events of polyploidization. It is conceivable that overzealous plant collection led to the loss of *C. atrosanguineus* from the wild, and that the narrow genetic base in these small isolated populations gave rise to European cultivars with limited numbers of S-alleles. Continual loss of progeny from genetically narrow cultivated *C. atrosanguineus* populations, and the inability to replenish cultivated genomes with wild genets, may have resulted in the development of a clonal species. It appears that the

combination of genetic bottlenecks, over-zealous plant collecting, and habitat destruction has eradicated wild sources of *C. atrosanguineus* and led to its development as a clonal cultivated species. The AFLP data (Wilkinson *et al.*, 2003) and monomorphism of certain primer-specific CosPS sequences isolated from *C. atrosanguineus* accessions in this study support the hypothesis that European *C. atrosanguineus* populations are probable clones.

Cosmos atrosanguineus is one example of seven known dark-atrosanguinate ligulate *Cosmos* species of the section *Discopoda*. Atrosanguinate *Cosmos* species are endemic to the pine-oak forest ecoregion of the sub-humid temperate ecological zones that occur between 1500-3000 metres in the mountain ranges of Mexico, and probably existed throughout the Mexican pine-oak forests that once formed a continuous ecological corridor linking the mountain chains of Mexico. Pioneers from these atrosanguinate *Cosmos* populations likely traversed Mexico via this pine-oak-forest corridor, diversifying as a result of their passage through the complex composition of microhabitats that exist in these environments. The destruction and fragmentation of the pine-oak forest may have disrupted the genetic flow between atrosanguinate *Cosmos* populations, isolating them into small ecologically vulnerable outcrossing populations that experienced narrowing genetic bottlenecks during the past 100-150 years of rampant deforestation. The two isolated collections of *C. atrosanguineus* in San Luis Potosí and Zimapan may represent such populations, as could the isolated populations of *C. montanus* and *C. concolor* in the HST region. In addition, the slash and burn methods, most often used in Mexico to clear the low stratum vegetation of pine-oak forests, disadvantages perennial tuberous species in particular by disrupting their sexual means of reproduction, through destruction of insect pollinators' habitats, and their vegetative means of reproduction through fire damage to tubers.

Based on its distribution and cytology, a likely progenitor of *C. atrosanguineus* is *C. scabiosoides*, although *C. montanus*, *C. concolor*, and *C. jaliscensis* also may have participated in the hybridisation and polyploidization events that gave rise to this species. The likely origin of atrosanguinate *Cosmos* species is the pine-oak forests of the Transvolcanic belt (TVB). The TVB possesses an abundance of unique microhabitats with the dry temperate climates conducive to growth of atrosanguinate *Cosmos* species. In addition, its recent turbulent geological history has given rise to diverse altitudes that have driven radiation and speciation, creating a region that is rich in endemics and polyploids. However, urban expansion into the TVB has been

extensive, with almost half the population of Mexico residing in this region, and so it is unlikely that the original habitat that gave rise to atrosanguinate *Cosmos* still exists.

Future directions in cytogenetics require the sampling of a broader range of *C. atrosanguineus* cultivated populations, and the collection, for cytogenetic analysis, of wild atrosanguinate *Cosmos* species and those perennial *Cosmos* species restricted to the area of San Luis Potosí and Hidalgo in Mexico. It would be interesting also to investigate the reproductive biology of atrosanguinate *Cosmos* species and to attempt interspecific pollinations. Molecular methods such as whole-genome *in situ* hybridisation (GISH) could be used to identify the putative ancestors of *C. atrosanguineus*, by testing the DNA homology of part or all of the *C. atrosanguineus* genome with wild-collected atrosanguinate *Cosmos* species. Elucidating the origins of *C. atrosanguineus* may be suitably tested through the production of artificial allopolyploids from candidate *Cosmos* progenitor species. In addition, the gene markers reviewed in Chapter 2 could be used to produce a phylogeny of *Cosmos* that may facilitate identification of *C. atrosanguineus*' closest relatives. Finally, it may be possible to investigate the estimated time of the *C. atrosanguineus* hybridization/polyploidization event using methods similar to the approach of Gaut and Doebley (1997).

Cosmos atrosanguineus, *C. bipinnatus* and *C. sulphureus* have normal microsporogenesis resulting in the formation of structurally coherent pollen. The pollen coats in *C. atrosanguineus*, *C. bipinnatus* and *C. sulphureus* appear normal, however, the methods used in Chapter 3 were not sensitive enough to identify minor aberrations in pollen-coat structure or chemistry. It would be interesting to make an assessment of the pollen-coat chemistry of the three *Cosmos* species, as the lack of a chemical component crucial to pollen function, may cause minor, but deleterious structural distortions in the *Cosmos* pollen coat not observable at the light-microscope or SEM level. The sterility of the *Arabidopsis cer6-2* (or *pop1*) mutants for example, is caused by defects in pollen-coat chemistry, with lesions in very-long chain acyl lipid synthesis pathways resulting in a lack of all, or part of the pollen-coat structure (Preuss *et al.* 1993). Although the pollen of these mutants is viable and able to germinate *in vitro* or in conditions of high humidity, they fail to hydrate on the stigma surface. Preuss *et al.* (1993) suggest that the inability of the *cer6-2* mutant pollen grains to hydrate is due to failures in pollen-stigma signalling, and could be a consequence of the absence of the putative very long-chain lipid signalling molecules, or more probably, because very long-chain lipid molecules solubilise or stabilise ligands held within the pollen coat.

Cosmos pollen-stigma interactions are characteristic of Asteraceae species, exhibiting four categories of pollen-stigma interaction and anomalous compatibility results. There is strong evidence to suggest that a gametophytic-sporophytic SI system operates in *Cosmos* and that dominance interaction of S-alleles is prevalent in the genus, with certain combinations of S suppressed by the activity of unmatched combinations of G. Pseudo self-compatibility (PSC) was observed in *C. bipinnatus* but not in *C. atrosanguineus*, where outcrossing and selfing produced the same strong self-incompatibility reaction. Bud pollinations and application of saline solution to stigmas were unable to override the *Cosmos* SI mechanism, and unless a method of producing selfed progeny can be found, investigations on *Cosmos* self-incompatibility will be difficult to quantify

The most interesting aspect to emerge from pollination studies in Asteraceae, and other SSI species, is the diverse interplay within in the S-locus and between the S-locus and unlinked S-modifier loci, with SSI revealing itself to be a possible model system for epigenetic and epistatic interactions (Nasrallah *et al.*, 1992; Conner *et al.*, 1997). If epistasis is accepted to mean the hierarchical interaction of non-allelic genes, then several S-unlinked loci in Asteraceae appear to be epistatic to the S-locus, affecting a range of SI weakening reactions. In addition to epistatic interactions, the sporophytic S-locus often exhibits complex dominance interactions between alleles, with control of dominance in stigma and pollen achieved through different mechanisms (Hiscock and McInnes, 2003). On the male side, reversible epigenetic interactions prevail, with the presence of dominant SCR alleles repressing the expression of recessive alleles, and dominance or recessiveness of SCR alleles depending on allelic partners (Hiscock and McInnes, 2003). In contrast, control of dominant and recessive S-alleles in the female is controlled post-transcriptionally (Kemp and Doughty 2003). A high frequency of recessive S-alleles in populations is associated with an increase in the proportion of PSC phenotypes, and appear to be the result of epistatic modification of recessive S-alleles (Reinartz and Les, 1994). In *Senecio*, PSC was associated with a loss in the ability of the stigma, but not the pollen, to discriminate S-specificities (Hiscock, 2000b) and may be achieved via activation of unlinked S-modifier loci that in some way down regulate the SI signalling pathway. Lewis (1994) noted that *Brassica* unmatched G-alleles were expressed in the presence of matched S-alleles high in the dominance series, but not in the presence of matched recessive S-alleles, resulting in semi-compatibility or full compatibility where cross-incompatibility was predicted. The weakening or silencing of matched S-alleles could be attributed to epistatic interactions

of *G*, and SI weakening in general may be a consequence of hierarchical interactions of non-*S*-genes with *S*. The differential action of the *G*-locus on dominant and recessive *S*-alleles could be explained by such hierarchical relationships. It is important to the heterozygosity and outbreeding behaviour of a species that dominance interactions of *S*-alleles is maintained, particularly in small SSI populations, where these interactions dramatically increases cross-compatibility. However, when rebounding from a genetic bottleneck, it may be advantageous for some matched *S*-alleles, particularly those higher in the dominance series to be weakened by unmatched *G*. The remnant *G*-gene, like the PSC modifier loci, may have survived its primitive beginnings because it weakens only certain dominant matched *S*-allele combinations, without adversely affecting overall interactions between dominant and recessive *S*-alleles (Larson, 1983).

Although, much was revealed through the study of the *Cosmos* pollen-stigma interaction, there were weaknesses in the method. Compatibility relationships could have been more accurately identified had the pollen-stigma interaction for each cross been equated with seed set per cross. There were mitigating circumstances why this was not undertaken, but nevertheless this was a weakness. Since selfed Asteraceae species are known to produce a high proportion of empty, (sterile) achenes, it is suggested that the number of viable achenes be recorded in selfed pollinations, cross-incompatible and cross-compatible phenotypes. In the microscope work, the use of the transmission electron microscope (TEM) would have improved visualisation of the *Cosmos* tryphine-pellicle-cuticle interface, and may have given better insight into the formation of this layer in the four types of Asteraceae pollen-stigma interaction. In future, larger populations of *Cosmos* species with known *S*-allele specificities should be used and the number of category-2 type incompatible pollen, *P*-type incompatible pollen and compatible pollen tubes produced per stigma should be recorded. Application of 1%, 0.5% and 0.1% saline solution did not suppress the SI reaction in *Cosmos atrosanguineus* or *C. bipinnatus*, as *Cosmos* stigmas were severely dehydrated by these applications. However, this method might yet prove successful, as it is known to work in *Senecio*, and should therefore be continued using decreasing concentrations of saline and perhaps different detergents. Other methods, such as bud pollination and high humidity environments, although affective in germinating some *Cosmos* pollen tubes, did not override *Cosmos* SI.

The use of degenerate *S*-specific primers isolated 41 *S*-domain-encoding Asteraceae sequences that were related to *S*-domains of Brassicaceae, Convolvulaceae and

Fabaceae. These putative Asteraceae S-domains show a stronger relationship to S-domain RLKs of *Ipomoea*, *Arabidopsis*, *Lotus japonicus*, and *Brassica* S-domain RLKs, than they do to *Brassica* SLG, SRK and SLR proteins. *Cosmos* S-domains exhibited no sequence polymorphism and hence did not contain hypervariable regions expected of SI molecules. Consequently, none of the encoded *Cosmos* S-domains identified as putative *Cosmos* SI molecules, and it appears, as suggested by Hiscock *et al.* (2003) and Kowiyama *et al.* (2000), that control of SI in Asteraceae and Convolvulaceae is probably afforded by a different molecular system than occurs in the Brassicaceae.

The NJ tree-building method used in this study was the best method available to assess the disparate data and produced an S-domain tree that equated in part with relationships and phylogenies of known S-sequences. On reflection, the S-domain tree constructed in this study would have been improved by including a greater number of *Brassica* SRK S-domains and SLGs, particularly from anomalous haplotypes such as the *B. oleracea* S₁₈ and S₆₀ haplotypes whose genomes contain mutated *SLG* alleles that produce truncated SLGs, and by incorporating SRKs from *SLG*-less haplotypes such as *B. oleracea* S₂₄, *B. rapa* S₃₂, S₃₃ and S₃₆. It would be interesting to see if these *SLG*-less haplotypes and those producing truncated SLGs and SRKs form distinctive phylogenetic groups within this S-domain tree. Interestingly, the haplotypes of *Brassica oleracea* S₂₄, *B. rapa* S₃₂ and *B. rapa* S₃₆ are thought to be derived from the same allelic ancestor (Sato *et al.*, 2002). A further three sets of S-haplotype pairs from *Brassica oleracea* (*Bo*) and *B. rapa* (*Br*) have been found to share the same S-haplotype specificity, with the *Bo*S₇-haplotype and the *Bra*S₄₆-haplotype showing themselves to be functionally identical, as are the *Bo*S₆₄- and the *Bra*S₄₁-haplotypes, and the *Bo*S₂₄- and the *Bra*S₃₆-haplotypes (Kimura *et al.*, 2002). These haplotypes would make an interesting inclusion to the tree, as would the inclusion of the *Senecio squalidus* SSRK sequences (Tabah *et al.*, 2004)

As more plant S-domain molecules are isolated and their functions identified, no doubt further S-gene or S-domain trees will be produced and the assembly of supermatrices may be possible. When this stage is reached super-tree methods, such as Matrix Representation Parsimony (MRP) or Matrix Representation Flip-distance supertrees (MRF) may reveal new insightful topological relationships between S-genes and/or S-domains. Whatever methods used, it is important that these methods are reliable, robust, computationally accessible, and provide an inclusive methodology capable of uniting and serving disparate realms of S-gene/S-domain research. The NJ trees

generated in this study are part of this process and are seen as one starting point in an analysis of S-domain sequences.

Plant S-domains are proving to be a ubiquitous family of molecules. Isolating the full-length CosPS sequences and identifying their expression patterns is the next logical step in this work. However, it is doubtful whether further use of S-specific degenerate primers will uncover the *Cosmos* SI molecule, and a more profitable approach may be found in the method developed by Nasrallah and Nasrallah (1989) and others. These researchers used isoelectric focussing (IEF) to identify polymorphic stigma proteins that cosegregate with specific S-genotypes (Kowyama *et al.*, 2000; Hiscock and McInnis, 2003; Hiscock *et al.*, 2003). However, before this method can be attempted in *Cosmos*, cross-compatible individuals will need to be identified. For *Cosmos bipinnatus* this may not prove difficult, but for the putative clonal *C. atrosanguineus*, other methods will need to be developed.

BIBLIOGRAPHY

- Aarts, M.G.M., Keijzer, C.J., Stiekma, W.J. and Pereira, A. (1995). Molecular characterisation of the *CER1* gene of *Arabidopsis* involved in epicuticular wax biosynthesis and pollen fertility. *Plant Cell* **7**, 2115-2127.
- Abbot, R.J. and Forbes, D.G. (2002). Extinction of the Edinburgh lineage of the allopolyploid neospecies *Senecio cambrensis* Rosser (Asteraceae). *Heredity* **88**, 267-269.
- Abbot, R.J. and Lowe, A.J. (2004) Origins, establishment and evolution of new polyploid species: *Senecio cambrensis* and *S. eboracensis* in the British Isles. *Biological Journal of the Linnean Society* **82**, 467-474.
- Abdul-Baki, A.A. (1992). Determination of pollen viability in tomatoes. *Journal of American Society of Horticultural Science* **117**, 473-476.
- Adams, K.L., Cronn, R., Percifield, R. and Wendel, J.F. (2003). Genes duplicated by polyploidy show unequal contributions to the transcriptome and organ-specific reciprocal silencing. *Proceedings of the National Academy of Sciences of the United States of America* **100**, 4649-4654.
- Ai, Y.J., Singh, A., Coleman, C.E., Ioerger, T.R., Kheypour, A. and Kao, T-h (1990). Self incompatibility in *Petunia inflata*: isolation and characterisation of cDNAs encoding 3 *S*-allele-associated proteins. *Sexual Plant Reproduction* **3**, 130-139
- Aizen, M.A. and Rovere, A.E. (1995). Does pollen viability decrease with ageing – a cross-population examination in *Austrocedrus chilensis* (Cupressaceae). *International Journal of Plant Sciences* **156**, 227-231.
- Akisha, T., Yasukawa, K., Oinuma, H., Kasahara, Y., Yamanouchi, S., Takido, M., Kumaki, K. and Tamura, T. (1996). Triterpene alcohols from the flowers of Compositae and their anti-inflammatory effects. *Phytochemistry* **43**, 1255-1260.
- Albertsen, M.C. and Palmer, R.G. (1979). A comparative light and electron-microscope study of microsporogenesis in male-sterile (*msl*) and male-fertile soybeans [*Glycine max* (L.) Merr.]. *American Journal of Botany* **66**, 253-265.
- Alexander, M.P. (1969). Differential staining of aborted and non-aborted pollen. *Stain Technology* **44**, 117-122.
- Alexander, M.P. (1980). A versatile stain for pollen, fungi, yeast and bacteria. *Stain Technology* **55**, 13-18.
- Allphin, L., Wiens, D. and Harper, K.T. (2002). The relative effects of resources and genetics on reproductive success in the rare Kachina daisy, *Erigeron kachinensis* (Asteraceae) *International Journal of Plant Sciences* **163**, 599-612.
- Altschul, SF., Gish, W., Miller, W., Myers, E.W. and Lipman, D.J. (1990). Basic local alignment search tool. *Journal of Molecular Biology* **215**, 403-410.

- Altschul, S.F., Boguski, M.S., Gish, W. and Wootton, J.C. (1994). Issues in searching molecular sequence databases. *Nature Genetics* **6**, 119-129.
- Altschul, S.F., Madden, T.L., Schäffer, A.A., Zhang, J., Zhang, Z., Miller, W., and Lipman, D.J. (1997). Gapped BLAST and PSI-BLAST: a new generation of protein database search programs. *Nucleic Acids Research* **25**, 3389-3402.
- Amela Garcia, M.T., Galati, B.G. and Anton, A.M. (2002). Microsporogenesis, microgametogenesis and pollen morphology of *Passiflora* spp. (Passifloraceae). *Botanical Journal of the Linnean Society* **139**, 383-394.
- Anderson, M.A., Cornish, E.C., Mau, S.L., Williams, E.G., Hoggart, R., Atkinson, A., Bonig, I., Grego, B., Simpson, R., Roche, P.J., Haley, J.D., Penschow, J.D., Niall, H.D., Tregear, G.W., Gochlan, J.P., Crawford, R.J. and Clarke, A.E. (1986). Cloning of cDNA for a stylar glycoprotein associated with the expression of self incompatibility in *Nicotiana glauca*. *Nature* **321**, 38-44.
- Anderson, M.A., McFaddon, G.I., Bernatzky, R., Atkinson, A., Orpin, T, Dedman, H., Tregear, G., Fernley, R. and Clarke, A.E. (1989). Sequence variability of 3 alleles of the self-incompatibility gene in *Nicotiana glauca*. *Plant Cell* **1**, 483-491.
- Angiosperm Phylogeny Group (APG). (1998). An ordinal classification for the families of flowering plants. *Annals of the Missouri Botanical Garden* **85**, 531-553.
- Angiosperm Phylogeny Group (APG II) (2003). An update of the Angiosperm Phylogeny Group classification for the orders and families of flowering plants: APGII. *Botanical Journal of the Linnean Society* **141**, 399-436.
- Ansaldi, R., Chaboud, A., and Dumas, C. (2000). Multiple *S* gene family members including natural antisense transcripts are differentially expressed during development of maize flowers. *The Journal of Biological Chemistry* **275**, 24146-24155.
- Aravind, L. and Koonin, E.V. (2000). The U-box is a modified RING finger – a common domain in ubiquitination. *Current Biology* **10**, pp. R132-R134.
- Atwood, S. S. (1944). Oppositional alleles in natural populations of *Trifolium repens*. *Genetics* **29**, 428-435.
- Azevedo, C. Santos-Rosa, M.J. and Shirasu, K. (2001). The U-box protein family in plants. *Trends in Plant Science* **6**, 354-358.
- Bae, E., Inamoto, K., Doi, M. and Imanishi, H. (1998). Retardation of hypocotyl elongation of ornamental and vegetative seedlings by ultraviolet irradiation. *Journal of the Japanese Society for Horticultural Science* **67**, 945-950.
- Bai, C., Sen, P., Hofmann, K., Ma, L., Goebel, M., Harper, W. and Elledge, S. (1996) Skp1 connects cell-cycle regulation to the ubiquitin proteolysis machinery through a novel motif, the F-box. *Cell* **86**, 263-274.

- Banerjee, A.K. (1971). Cytological investigation on some Indian members of the tribe Helianthoideae (Family – Compositae). *Journal of Cytology and Genetics* **6**, 90-109.
- Barnes, S.H. and Blackmore, S. (1988). Pollen ontogeny in *Catananche caerulea* L. (Compositae; Lactuceae) II. Free microspore stage to formation of the male germ unit. *Annals of Botany* **62**, 615-623.
- Bateman, A.J. (1952). Self-incompatibility systems in angiosperms I. Theory. *Heredity* **6**, 285-310
- Bateman, A.J. (1954). Self-incompatibility systems in angiosperms II. *Iberis amara*. *Heredity* **8**, 305-332.
- Bateman, A.J. (1955). Self-incompatibility systems in angiosperms III. Cruciferae. *Heredity* **9**, 52-68.
- Batesmith, E.C. (1980). Astringency of leaves. 4. Astringent tannins of *Cosmos bipinnatus*. *Phytochemistry* **19**, 982.
- Bayer, R.J. and Starr, J.R. (1998). Tribal phylogeny of the Asteraceae based on two non-coding chloroplast sequences, the *trnL* intron and *trnL/trnF* intergenic spacer. *Annals of the Missouri Botanical Gardens* **85**, 242-256.
- Becraft, P.W. (1998). Receptor kinases in plant development. *Trends in Plant Science* **3**, 384-388.
- Becraft, P.W., Stinard, P.S. and McCarty, D.R. (1996). CRINKLY4: A TNFR-Like receptor kinase involved in maize epidermal differentiation. *Science* **273**, 1406-1409.
- Becraft, P.W., Kang, S-H. and Suh, S-G. (2001). The maize CRINKLY4 receptor kinase controls a cell-autonomous differentiation response. *Plant Physiology* **127**, 486-496.
- Bell, P.R. (1995). Incompatibility in flowering plants: adaptation of an ancient response. *The Plant Cell* **7**, 5-16.
- Bennett, M.D. and Leitch, I.J. (1995). Nuclear DNA amounts in angiosperms. *Annals of Botany* **76**, 113-176.
- Bennett, M.D. and Leitch, I.J. (1997). Nuclear DNA amounts in angiosperms – 583 New Estimates. *Annals of Botany* **80**, 169-196.
- Bennett, M.D. and Leitch, I.J. (2003). Plant DNA C-values Database (Release 2.0). <http://www.rbgekew.org.uk/cval/homepage.html>. Email: dnac-value@kew.org.uk Jodrell Laboratory, Royal Botanic Gardens, Kew, Richmond Surrey.
- Bergthorsson, U., Richardson, A.O., Young, G.J., Goertzen, L.R. and Palmer, J.D. (2004). Massive horizontal transfer of mitochondrial genes from diverse land plant donors to the basal angiosperm *Amborella*. *Proceedings of the National Academy of Sciences of the United States of America* **101**, 17747-17752.

- Berry, P.E. and Calvo, R.N. (1989). Wind pollination, self-incompatibility, and altitudinal shifts in pollination systems in the high Andean genus *Espeletia* (Asteraceae). *American Journal of Botany* **76**, 1602-1614.
- Blackmore, S. and Barnes, S.H. (1985). *Cosmos* pollen ontogeny: A scanning electron microscope study. *Protoplasma* **126**, 91-99.
- Blackmore, S. and Barnes, S.H. (1987). Pollen wall morphogenesis in *Tragopogon porrifolius* L. (Compositae: Lactuceae) and its taxonomic significance. *Review of Palaeobotany and Palynology* **52**, 233-246.
- Blackmore, S. and Barnes, S.H. (1988). Pollen ontogeny in *Catananche caerulea* L. (Compositae; Lactuceae) I. Premeiotic phase to establishment of tetrads. *Annals of Botany* **62**, 605-614.
- Blackmore, S. and Barnes, S.H. (1990). Pollen wall development in angiosperms. In: *Microspore: Evolution and Ontogeny*. S. Blackmore, R.B. Knox (eds.). Academic Press. pp. 173-192.
- Boff, T. and Schifino-Wittman, M.T. (2003). Segmental allopolyploidy and paleopolyploidy in species of *Leucaena* Benth: evidence from meiotic behaviour analysis. *Hereditas* **138**, 27-35.
- Bork, P. and Gobson, T.J (1996). Applying motif and Profile searches. *Methods in Enzymology* **266**: 162-184.
- Boscaiu, M. and Guemes, J. (2001). Breeding system and conservation strategy of the extremely endangered *Cistus carthaginensis* Pau (Cistaceae) of Spain. *Israel Journal of Plant Sciences* **49**, 213-220
- Bouchez, D. and Hofte, H. (1998). Functional Genomics in Plants. *Plant Physiology* **118**: 725-732.
- Bower, M.S., Matias, D.D., Fernandes-Carvalho, E., Mazzurco, M., Gu, T., Rothstein, S.J. and Goring, D.R. (1996). Two members of the Thioredoxin-h family interact with the kinase domain of a *Brassica S* locus receptor kinase. *The Plant Cell* **8**, 1641-1650.
- Boyes, D.C. and Nasarallah, J.B. (1993). Physical linkage of the *SLG* and *SRK* genes at the self-incompatibility locus of *Brassica oleracea*. *Molecular and General Genetics* **236**, 269-272.
- Boyes, D.C. and Nasarallah, J.B. (1995). An anther-specific gene encoded by an *S* locus haplotype of *Brassica* produces complementary and differentially regulated transcripts. *The Plant Cell* **7**, 1283-1294.
- Boyes, D.C., Chen, C-H., Tantikanjana, T., Esch, J.J., and Nasrallah, J.B. (1991). Isolation of a second S-locus-related cDNA from *Brassica oleracea*: genetics relationship between the *S* locus and two related loci. *Genetics* **127**, 221-228

- Boyes, D.C., Chen, C-H., Tantikanjana, T., Esch, J.J., and Nasarallah, J.B. (1991). Isolation of a second S-locus-related cDNA from *Brassica oleracea*: genetic relationships between the S locus and the two related loci. *Genetics* **127**, 221-228.
- Boyes, D.C., Nasarallah, M.E., Vrebalov, J. and Nasarallah, J.B. (1997). The self-incompatibility (S) haplotypes of *Brassica* contain highly divergent and rearranged sequences of ancient origin. *The Plant Cell* **9**, 237-247.
- Brace, J. Ockendon, D.J. and King, G.J. (1993). Development of a method for the identification of S alleles in *Brassica oleracea* based on the digestion of PCR-amplified DNA with restriction endonucleases. *Sexual Plant Reproduction* **6**, 133-138.
- Brace, J. Ockendon, D.J. and King, G.J. (1994). A molecular approach to the identification of S-alleles in *Brassica oleracea*. *Sexual Plant Reproduction* **7**, 203-208.
- Brand, U., Fletcher, J.C., Hobe, M., Meyerowitz, E.M. and Simon, R. (2000). Dependence of stem cell fate in *Arabidopsis* on the feedback loop regulated by CLV3 activity. *Science* **289**, 617-619.
- Braun, D.M. and Walker, J.C. (1996). Plant transmembrane receptors: new pieces in the signalling puzzle. *Trends in Biochemical Science* **21**, 70-73.
- Braun, D.M., Stone, J.M. and Walker, J.C. (1997). Interaction of the maize and *Arabidopsis* kinase interaction domains with a subset of receptor-like proteins kinases: implication for transmembrane signalling in plants. *The Plant Journal* **12**, 83-95.
- Bremer, K. (1994). Asteraceae cladistics and classification. Oregon: Timber Press.
- Bremer, K. (1996). Major clades of the Asteraceae. In, *Compositae Systematics, Proceedings of the International Compositae Conference, Kew 1996*. D.J.N. Hind. and H.J. Beenjte (eds.). The Royal Botanic Gardens, Kew. pp 1-7.
- Brennan, A.C., Harris, S.A., Tabah, D.A. and Hiscock, S.J. (2002). The population genetics of sporophytic self-incompatibility in *Senecio squalidus* L. (Asteraceae) I: S allele diversity in a natural population. *Heredity*. **89**, 430-8.
- Brewbaker, J.L. (1967). The distribution and phylogenetic significance of binucleate and trinucleate pollen grains in angiosperms. *American Journal of Botany* **54**, 1069-1083.
- Brewbaker, J.L. and Majumder, S.K. (1961). Cultural studies of the pollen population effect and the self-incompatibility inhibition. *American Journal of Botany* **48**, 457-464.
- Brewbaker, J. and Kwack, B.H. (1963). The essential role of calcium ion in pollen germination and pollen tube growth. *American Journal of Botany* **50**, 859-865.

- Brickell, C. and Sharman, F. (1986). *The Vanishing Garden; a conservation guide to garden plants*. London: John Murray. pp.76-77.
- Britten, R.J. (1996). DNA sequence insertion and evolutionary variation in gene regulation. *Proceedings of the National Academy of Sciences of the United States of America* **93**, 9374-9377.
- Brochmann, C. and Elven, R. (1992). Ecological and genetic consequences of polyploidy in arctic *Draba*-(Brassicaceae). *Evolutionary Trends in Plants* **6**, 111-124.
- Brochmann, C., Stedje, B. and Borgen, L. (1992a). Gene flow across ploidal level in *Draba* (Brassicaceae). *Evolutionary Trends in Plants* **6**, 125-134.
- Brochmann, C., Soltis, P.S. and Soltis, D.E. (1992b). Recurrent formation and polyphyly of Nordic polyploid in *Draba* (Brassicaceae). *American Journal of Botany* **79**, 673-688.
- Broothaerts, W.J., Vanlaere, A., Witters, R., Preaux, G., Decock, B., Vandamme, J. and Vendrig, J.C. (1990). Purification and N-terminal sequencing of style glycoproteins associated with self incompatibility in *Petunia hybrida*. *Plant Molecular Biology* **14**, 93-102.
- Brubaker, C.L. Paterson, A.H. and Wendel J.F. (1999). Comparative genetic mapping of allotetraploid cotton and its diploid progenitors. *Genome*, **42**, 184-203.
- Bruckner, C.H., Casali, V.W.D, de Moraes, C.F., Regazzi, A.J and da Silva, E.A.M (1995). Self-incompatibility in passion fruit (*Passiflora edulis sims*). *Acta Horticulturae. (ISHS)* **370**, 45-58.
- Cabrillac, D., Delorme, V., Garin, J., Ruffio-Châble, V., Giranton, J-L., Dumas, C., Gaude, T. and Cock J.M. (1999). The *S*₁₅ self-incompatibility haplotype in *Brassica oleracea* includes three *S* gene family members expressed in stigmas. *The Plant Cell* **11**, 971-986.
- Cabrillac, D., Cock J.M, Dumas, C. and Gaude, T. (2001). The *S*-locus receptor kinase is inhibited by thioredoxins and activated by pollen coat proteins. *Nature* **410**, 220-223.
- Campbell, I.D. and Bork, P. (1993). Epidermal growth factor-like modules. *Current Opinion in Structural. Biology* **3**, 385-392.
- Campbell, J.M. and Lawrence, M.J. (1981). The population genetics of the self-incompatibility polymorphism in *Papver rhoeas*. I. The number and distribution of *S*-alleles in families from three localities. *Heredity* **46**, 69-79.

- Cárdenas-Hernández, O.G., Santana, E., Sánchez-Velázquez, L.R. (1994). *Abundancia de epífitas y cavidades en cuatro tipos de vegetación en la Estación Científica Las Joyas, Reserva de la Biósfera Sierra de Manantlán*. International Meeting of the Society for Conservation Biology and the Association for Tropical Biology, June 7-11, 1994. Universidad de Guadalajara, Guadalajara, Jalisco. Instituto Manantlán de Ecología y Conservación de la Biodiversidad y Centro Universitario de Ciencias biológicas y Agropecuarias. Universidad de Guadalajara, Mexico.
- Cassab, G.I. (1998). Plant cell wall proteins. *Annual Review of Plant Physiology and Plant Molecular Biology* **49**, 281-309.
- Centres of Plant Diversity website (2004). Volume 3, *The Americas, Mexico Regional Overview*. At, <http://www.nmnh.si.edu/botany/projects/cpd/ma/mamexico.htm>. V. M. Toledo, J. Rzedowski and J. Villa-Lobos (eds.). U.S.A, Washington, D.C.: Smithsonian Institution, Department of Systematic Biology-Botany.
- Challenger, A. (1998). Utilización y conservación de los ecosistemas terrestres de México. Pasado, presente, y futuro. Conabio, IBUNAM y Agrupación Sierra Madre, México.
- Chang, C., Schaller, G.E., Patterson, S.E. Kwok, S.F., Meyerowitz, E.M. and Bleecker, A.B. (1992). The TMK1 gene from *Arabidopsis* codes for a protein with structural and biochemical characteristics of a receptor protein kinase. *The Plant Cell* **4**, 1263-1271.
- Chapman, G.P. (1987). The tapetum. *International Review of Cytology* **107**, 111-125.
- Charlesworth, D. (1985). Distribution of dioecy and self-incompatibility in angiosperms. In: *Evolution: Essays in Honour of J. Maynard Smith*. P.J Greenwood, P.H. Harvey and M. Slatkin (eds.). Cambridge: Cambridge University Press. pp.237-268.
- Charlesworth, D. (1995). Multi-allelic self-incompatibility polymorphisms in plants. *BioEssays* **17**, 31-38.
- Charlesworth, D., Awadalla, P., Mable, B.K. and Schierup, M.H. (2000). Population-level studies of multiallelic self-incompatibility loci, with particular reference to Brassicaceae. *Annals of Botany* **85**, 227-239.

- Chase, M.W., Soltis, D.E., Olmstead, R.G., Morgan, D., Les, D., Mishler, B.D., Duvall, M.R. Price, R.A., Hills, H.G., Qiu, Y., Kron, K.A., Rettig, J.H. Conti, E., Palmer, J.D., Manhart, J.R., Sytsma, K.J., Michaels, H.J., Kress, W.J., Donoghue, M.J., Clark, W.D., Hedrén, M., Gaut, B.S., Jansen, R.K., Kim, K-J, Wimpee, C.F., Smith, J.F., Furnier, G.R., Strauss, S., Xiang, Q., Plunkett, G.M. Soltis, P.S. Swenson, S., Equiarte, L.E., Learn, G.H. Jr., Barret S.C.H., Graham, S., Dayanandan, S. and Albert, V.A. (1993). Phylogenetics of seed plants: an analysis of nucleotide sequences from the plastid gene *rbcL*. *Annals of the Missouri Botanical Gardens* **80**, 528-580.
- Chawla, B., Bernatzky, R., Liang, W. and Marcotrigiano, M. (1997). Breakdown of self-incompatibility in tetraploid *Lycopersicon peruvianum*: inheritance and expression of *S*-related proteins. *Theoretical and Applied Genetics* **95**, 992-996.
- Chen, C-H and Nasrallah, J.B. (1990). A new class of *S* sequences defined by a pollen recessive self-incompatibility allele of *Brassica oleracea*. *Molecular and General Genetics* **222**, 241-248.
- Chen, Q. and Armstrong, K. (1994). Genomic *in situ* hybridization in *Avena sativa*. *Genome* **37**, 607-612.
- Cheun, W.Y., Champagne, G., Hubert, N. and Landry, B.S. (1997). Comparison of the genetic maps of *Brassica napus* and *Brassica oleracea*. *Theoretical and Applied Genetics* **94**, 569-582.
- Cheptou, P.O., Lepart, J. and Escarre, J. (2002). Mating system variation along a successional gradient in the allogamous and colonizing plant *Crepis sancta* (Asteraceae) *Journal of Evolutionary Biology* **15**, 753-762.
- Cheung, A.Y. (1996). Pollen-pistil interactions during pollen-tube growth. *Trends in Plant Science* **1**, 45-51.
- Ciampolini, F. and Cresti, M. (1998). The structure and cytochemistry of the stigma-style complex of *Corylus avellana* L. 'Tonda Gentile delle Langhe' (Corylaceae). *Annals of Botany* **81**: 513-518.
- Clark, S.E., Williams R.W. and Meyerowitz, E.M. (1997). The *CLAVATA1* gene encodes a putative receptor kinase that controls shoot and floral meristem size in *Arabidopsis*. *Cell* **89**, 575-585.
- Clarke, A.E., Abbot, A., Mandel, T.E. and Pettitt, J.M. (1980). Organisation of the wall layers of the stigmatic papillae of *Gladiolus gandavensis*: freeze-fracture study. *Journal of Ultrastructure Research* **73**, 269-281.
- Clarke, A.E., Anderson, M.A., Atkinson, A., Bacic, A., Ebert, P.R. Jahnene, W., Lush, W.M., Mau, S.L. and Woodward, J.R. (1989). Recent developments in the molecular genetics and biology of self incompatibility. *Plant Molecular Biology* **13**, 267-271.

- Cock, J.M. and McCormick, S. (2001). A large family of genes that share homology with *CLAVATA3*. *Plant Physiology* **126**, 939-942.
- Cock, J.M., Stanchev, B., Delorme, V., Croy, R.R.D. and Dumas, C. (1995). *SLR3*: a modified receptor kinase gene that has been adapted to encode a putative secreted glycoprotein similar to the *S* locus glycoprotein. *Molecular and General Genetics* **248**, 151-161.
- Cock, J.M., Vanoosthuyse, V. and Gaude, T. (2002). Receptor kinase signalling in plants and animals: distinct molecular systems with mechanistic similarities. *Current Opinion in Cell Biology* **14**, 230-236.
- Coleman, A.W. and Goff L.J. (1985). Applications of fluorochromes to pollen biology I. Mithramycin and 4', 6-diamidino-2-phenylindole (DAPI). as vital stains and for quantitation of nuclear DNA. *Stain Technology* **60**, 145-154.
- Comai, L., Tyagi, A.P., Winter, K., Holmes-Davis, R., Reynolds, S.H., Stevens, Y. and Byers, B. (2000). Phenotypic instability and rapid gene silencing in newly formed *Arabidopsis* allotetraploids. *The Plant Cell*, **12**, 1551-1567.
- Conaway, R.C., Brower, C.S. and Conaway, J.W. (2002). Gene expression-emerging role of ubiquitin in transcription regulation. *Science* **296**, 1254-1258.
- Conn, H.J. and Lillie, R.D. (1977). *Biological Stains*. Baltimore: William and Wilkins, p.289.
- Conner, J.A., Tantikanjana, T., Stein, J.C., Kandasamy, M.K., Nasrallah, J.B. and Nasrallah, M.E. (1997). Transgene-induced silencing of *S*-locus genes and related genes in *Brassica*. *The Plant Journal* **11**, 809-823.
- Cook, L.M. and Soltis, P.S. (1999). Mating systems of diploid and allotetraploid populations of *Tragapogon* (Asteraceae). I. Natural populations. *Heredity* **82**, 237-244.
- Cook, L.M. and Soltis, P.S. (2000). Mating systems of diploid and allotetraploid populations of *Tragapogon* (Asteraceae). II. Artificial populations. *Heredity* **84**, 410-415.
- Cook, L.M., Soltis, P.S., Brunfield, S.J. and Soltis, D.E. (1998). Multiple independent formations of *Tragopogon* tetraploids (Asteraceae): evidence from RAPD markers. *Molecular Ecology* **7**, 1293-1302.
- Cooke, J. Noval, M.A., Boerlijst, M. and Maynard-Smith, J. (1997). Evolutionary origins and maintenance of redundant gene expression during metazoan development. *Trends in Genetics* **13**, 360-364.
- Cope, F.W. (1962a). The mechanism of pollen incompatibility in *Theobroma cacao* L. *Heredity* **17**, 156-182.
- Cope, F.W. (1962b). The effects of incompatibility and compatibility on the genotype proportions in populations of *Theobroma cacao* L. *Heredity* **17**, 183-195.

- Crane, M. B. and Brown, A. G (1937). Incompatibility and sterility in the sweet cherry. *Journal of Pomology* **15**, 86
- Cronn, R.C., Small, R.L. and Wendel, J.F. (1999). Duplicated genes evolve independently after polyploid formation in cotton. *Proceedings of the National Academy of Sciences of the United States of America* **96**, 14406-14441.
- Crowe L.K. (1954). Incompatibility in *Cosmos bipinnatus*. *Heredity* **8**, 1-11.
- Crowe L.K. (1964). The evolution of outbreeding in plants I. The Angiosperms. *Heredity* **19**, 435-457.
- Cruz-Garcia, F, Hancock, C.N. and McClure, B.A. (2003). S-RNase complexes and pollen rejection. *Journal of Experimental Botany* **54**, 123-130.
- Dafni, A. (1992). *Pollination ecology: a practical approach*. Oxford: Oxford University Press.
- Dana, M.N. and Ascher, P.D. (1986a). Sexually localized expression of pseudo-self compatibility (PSC) in *Petunia x hybrida* Hort. 1. Pollen activation. *Theoretical and Applied Genetics* **71**, 573-577.
- Dana, M.N. and Ascher, P.D. (1986b). Sexually localized expression of pseudo-self compatibility (PSC) in *Petunia x hybrida* Hort. 1. Styler inactivation. *Theoretical and Applied Genetics* **71**, 578-584.
- Dangl, J.L. (1995). Pièce de résistance: Novel classes of plant disease resistance genes. *Cell* **80**, 363-366.
- Daum, G., Eisenmann-Tappe, I., Fries, H-W., Troppmair, J. and Rapp, U.R. (1994). The ins and outs of Raf kinases. *Trends in Biochemical Science* **19**, 474-79.
- Decken, R. and Kaldenhoff, R. (1997). Light repressible receptor protein kinase: a novel photo-regulated gene from *Arabidopsis thaliana*. *Planta* **202**, 479-486.
- Delorme, V., Giranton, J-L., Hatzfeld, Y., Friry, A. Heizmann, P. Ariza, M.J., Dumas, C., Gaude, T. and Cock, J.M. (1995). Characterization of the *S* locus genes, SLG and SRK of the *Brassica* S3 haplotype: identification of a membrane-localized protein encoded by the *S* locus receptor kinase gene. *The Plant Journal* **7**, 429-440.
- DeMauro, M.M (1993). Relationship of breeding system to rarity in Lakeside Daisy (*Hymenoxys acaulis* var. *glabra*). *Conservation Botany* **7**, 542-450.
- de Nettancourt, D. (1977). *Incompatibility in Angiosperms*. Berlin, Heidelberg, New York: Springer-Verlag.
- de Nettancourt, D. (1997). Incompatibility in angiosperms. *Sexual Plant Reproduction* **10**, 185-199.
- de Nettancourt, D. (2001). *Incompatibility and Incongruity in Wild and Cultivated Plants*. Berlin, Heidelberg, New York: Springer-Verlag.

- Detchepare, S., Heizmann, P. and Duma, C. (1989). Changes in protein patterns in protein synthesis during anther development in *Brassica oleracea*. *Journal of Plant Physiology* **135**, 129-137.
- Devey, F., Fearon, C.H. Hayward, M.D. and Lawrence, M.J. (1994). Self incompatibility in ryegrass. 11: Number and frequency of alleles in a cultivar of *Lolium perenne* L. *Heredity* **73**, 254-261.
- Dickinson, H.G. (1973). The role of plastids in the formation of pollen grain coatings. *Cytobios* **8**, 25-40
- Dickinson, H.G. (1987). The physiology and biochemistry of meiosis in the anther *International Review of Cytology* **107**, 79-109.
- Dickinson, H.G. (1990). Self-incompatibility in flowering plants *BioEssays* **12**, 155-161.
- Dickinson, H.G. (1995). Dry stigmas, water and self-incompatibility in *Brassica*. *Sexual Plant Reproduction* **8**, 1-10.
- Dickinson, H.G. and Elleman, C.J. (1985). Structural changes in the pollen grain of *Brassica oleracea* during dehydration in the anther and development of the stigma as revealed by anhydrous fixation techniques. *Micron and Microscopica Acta* **16**, 225-270.
- Dickinson, H.G. and Elleman, C.J. (1994). Pollen hydrodynamics and self-incompatibility in *Brassica oleracea*. *Sexual Plant Reproduction*. **8**, 1-10.
- Dickinson, H.G. and Lewis, D (1973a). The formation of the tryphine coating the pollen grains of *Raphanus*, and its properties relating to the self-incompatibility system. *Proceedings of the Royal Society of London, Series B*, **184**, 149-165.
- Dickinson, H.G. and Lewis, D (1973b). Cytochemical and ultrastructural differences between intraspecific compatible and incompatible pollinations in *Raphanus*. *Proceedings of the Royal Society of London, Series B*, **183**, 31-38.
- Dickinson, H.G. and Potter, U. (1976). The development of patterning in the alveolar sexine of *Cosmos bipinnatus*. *New Phytologist*. **76**, 543-550.
- Dickinson, H.G. and Potter, U. (1979). Post-meiotic nucleo-cytoplasmic interaction in *Cosmos bipinnatus*. *Planta* **145**, 449-457.
- Dickinson, H.G., Crabbe, M.J.C. and Gaude, T. (1992). Sporophytic self-incompatibility systems: *S* gene products. *International Review of Cytology*. **140**, 525-561.
- Dickinson, H.G., Elleman, C.J. and Doughty, J. (2000). Pollen coatings – chimeric genetics and new functions. *Sexual Plant Reproduction* **12**, 302-309.
- Dirzo, R. and Gómez, G. (1996). Ritmos temporales de la investigación taxonómica de plantas vasculares en México y una estimación del número de especies conocidas. *Annals of the Missouri Botanical Gardens* **83**, 396-403.

- Dixit, R. Nasrallah, M.E. and Nasrallah, J.B. (2000). Post-transcriptional maturation of the *S* receptor kinase of *Brassica* correlates with coexpression of the *S*-locus glycoprotein in stigmas of two *Brassica* strains and in transgenic tobacco plants. *Plant Physiology* **124**, 297-311.
- Dodds, P.N., Clarke, A.E. and Newbigin, E. (1996). A molecular perspective on pollination in flowering plants. *Cell* **85**, 141-144.
- Doughty, J., Hedderson, F., McCubbin, A. and Dickinson, H.G (1993). Interaction between a coating-borne peptide of the *Brassica* pollen grain and stigmatic *S* (self-incompatibility)-locus-specific glycoproteins. *Proceedings of the National Academy of Sciences of the United States of America* **90**, 467-471.
- Doughty, J., Dixon, S., Hiscock, S.J., Willis, A.C. Parkin, A.P. and Dickinson, H.G. (1998). PCP-A1, a defensin-like *Brassica* pollen coated protein that binds the *S* locus glycoprotein, is the product of gametophytic gene expression. *The Plant Cell* **10**, 1333-1347.
- Doughty, J., Wong, H.Y. and Dickinson, H.G (2000). Cysteine-rich pollen coat proteins (PCPs) and their interactions with stigmatic *S*-incompatibility and *S*-related proteins in *Brassica* putative roles in SI and pollination. *Annals of Botany*, **85 supplement A**, 161-169.
- Doyle, J.J and Doyle, J.S. (1987). A rapid DNA isolation procedure for small quantities of fresh leaf tissue. *Phytochemical Bulletin* **19**: 11-15
- Dumas, C. and Gaude, T. (1981). Stigma-pollen recognition and pollen hydration. *Phytomorphology* **31**, 191-201.
- Dumas, C., Gaude, T., Heizmann, P. and Rougier, M. (1994). The cell biology of pollen development in *Brassica*. In, *Genetic Control of Self-incompatibility and Reproductive Development in Flowering Plants*. ed. E.G Williams, A.E. Clarke and R.B. Knox. London: Kluwer Academic press. pp. 309-335.
- Dwyer, K.G., Chao, A. Cheng, B., Chen, C-H. and Nasrallah, J.B. (1989). The *Brassica* self-incompatibility multigene family. *Genome* **31**, 969-972.
- Dwyer, K.G., Balent, M.A., Nasrallah, J.B. and Nasrallah, M.E. (1991). DNA sequences of self-incompatibility genes from *Brassica campestris* and *B. oleracea*: polymorphism predating speciation. *Plant Molecular Biology* **16**, 481-486.
- Dwyer, K.G., Lalonde, B.A., Nasrallah, J.B. and Nasrallah, M.E. (1992). Structure and expression of *AtS1*, an *Arabidopsis* gene homologous to the *S*-locus related genes of *Brassica*. *Molecular and General Genetics* **231**, 442-448.
- Dwyer, K.G., Kandasamy, M., Mahosky, D.I., Acciai, J., Kudish, B.I., Miller, J.E., Nasrallah, M.E. and Nasrallah, J.B. (1994). A superfamily of *S*-locus-related sequences in *Arabidopsis*: diverse structures and expression patterns. *The Plant Cell* **6**, 1229-1243.

- Dytham, C. (2003). *Choosing and Using Statistics: a biologist's guide*. Oxford: Blackwell.
- Dzelzkalns, V.A., Nasrallah, J.B. and Nasrallah, M.E. (1992). Cell-cell communication in plants: self-incompatibility in flower development. *Developmental Biology* **153**, 70-82.
- Dzelzkalns, V.A., Thorsness, M.K., Dwyer, K.G., Baxter, J.S., Balent, A., Nasrallah M.E. and Nasrallah, J.B (1993). Distinct *cis*-acting elements direct pistil-specific and pollen-specific activity of the *Brassica S* locus glycoproteins gene promoter. *The Plant Cell* **5**, 855-863.
- East, E.M. and Mangelsdorf, A.J. (1925). A new interpretation of the heredity behaviour of self-sterile plants. *Proceedings of the National Academy of Sciences of the United States of America*, **11**, 166-171.
- Echlin, P. and Godwin, H. (1968a). The ultrastructure and ontogeny of pollen in *Heleborus foetidus* L. I. The development of the tapetum and Ubisch bodies. *Journal of Cell Science* **3**, 161-174.
- Echlin, P. and Godwin, H. (1968b). The ultrastructure and ontogeny of pollen in *Heleborus foetidus* L. II. Pollen grain development through the callose special wall stage. *Journal of Cell Science* **3**, 175-186.
- Ellard-Ivey, M. Demura, T., Lomax, T and Carpita, N (1997). Connections: The hard wiring of the plant cell for perception, signalling, and Response. *Plant Cell* **9**, 2105-2117.
- Elleman, C.J. and Dickinson, H.G. (1986). Pollen stigma interactions in *Brassica oleracea* IV: Structural reorganisation in the pollen grains during hydration. *Journal of Cell Science* **80**, 141-157.
- Elleman, C.J. and Dickinson, H.G. (1990). The role of the exine coating in pollen-stigma interactions in *Brassica oleracea* L. *New Phytologist* **114**, 511-518.
- Elleman, C.J. and Dickinson, H.G. (1994). Pollen–stigma interaction during sporophytic self-incompatibility in *Brassica oleracea*. In: *Genetic control of self-incompatibility and reproductive development in flowering plants*. Ed. E.G Williams, A.E. Clarke, R.B. Knox. Dordrecht: Kluwer Academic. pp.67-87.
- Elleman, C.J., Willson, C.E., Sarker, R.H. and Dickinson, H.G. (1988). Interaction between the pollen tube and stigmatic cell wall following pollination in *Brassica oleracea*. *New Phytologist* **109**, 111-117.
- Elleman, C.J. Franklin-Tong, V. and Dickinson, H.G. (1992). Pollination in species with dry stigmas: the nature of the early stigmatic response and the pathway taken by pollen tubes. *New Phytologist* **121**, 413-424.
- Emerson, S. (1940). Growth of incompatible pollen tubes in *Oenothera organensis*. *Botanical Gazette* **100**, 890-911.

- Endre, G. Kereszi, A., Kevei, Z., Mihacea, S., Kalo, P. and Kiss, G.B. (2002). A receptor kinase gene regulating symbiotic nodule development. *Nature* **417**, 962-966.
- Entani, T., Iwano, M., Shiba, H., Che, F.S., Isogai, A. and Takayama, S. (2003). Comparative analysis of the self-incompatibility (*S*-) locus region of *Prunus mume*: identification of a pollen-expressed F-box gene with allelic diversity. *Genes to Cells* **8**, 203-213.
- Esau, K. (1977). *Anatomy of seed plants*. John Wiley & Sons.
- Estes, J.R. and Thorp, R.W. (1975). Pollination ecology of *Pyrrhopappus carolinianus* (Compositae). *American Journal of Botany* **62**, 148-159.
- Evans, D.E., Taylor, P.E. Singh, M.B. and Knox, R.B. (1992). The interrelationship between the accumulation of lipids, protein and the level of acyl carrier proteins during the development of *Brassica napus* L. pollen. *Planta* **186**, 343-354.
- Fantl, W.J., Johnson, D.E. and Williams, L.T. (1993). Signalling by receptor tyrosine kinases. *Annual Review of Biochemistry* **62**, 453-481.
- Fearon, C.H. Cornish, M.A., Hayward M.D. and Lawrence, M.J. (1994). Self incompatibility in ryegrass. 10: Number and frequency of alleles in a natural population of *Lolium perenne* L. *Heredity* **73**, 254-261.
- Ferreira, M.A., Almeida Engler, J. de., Miguens, F.C. Van Montagu, M. Engler, G. and Oliveira D.C., de. (1997). Oleosin gene expression in *Arabidopsis thaliana* tapetum coincides with accumulation of lipids in plastids and cytoplasmic bodies. *Plant Physiology and Biochemistry* **35**, 729-739.
- Ferris, S.D. and Whitt, G.S. (1977). Loss of duplicate gene expression after polyploidization. *Nature* **265**, 258-260.
- Ferris, S.D. and Whitt, G.S. (1979). Evolution of the differential regulation of duplicate genes after polyploidization. *Journal of Molecular Evolution* **12**, 267-317.
- Ferrusquía-Villafranca, I. (1993). Geology of Mexico: a synopsis. In, *Biological diversity of Mexico: origins and distribution*. T.P. Ramamoorthy, R. Bye, A. Lot, and J.E. Fa. (eds.). New York: Oxford University Press. pp. 3-107.
- Feuillet, C., Schachermayr, G. and Kellet, B. (1997). Molecular cloning of a new receptor-like kinase gene encoded at the *Lr10* disease resistance locus of wheat. *The Plant Journal* **11**, 45-52.
- Feuillet, C., Reuzeau, C., Kjellbom, P. and Kellet, B. (1998). Molecular characterization of a new type of receptor-like kinase (wlrk) gene family in wheat. *Plant Molecular Biology* **37**, 943-953.
- Fitzgerald, M.A. and Knox, R.B. (1995). Initiation of primexine in freeze-substituted microspores of *Brassica campestris*. *Sexual Plant Reproduction* **8**, 99-104.

- Foote, H.C.C., Rise, J.P., Franklin-Tong, V.E., Walker, E.A., Lawrence, M.J. and Franklin, F.C.H. (1994). Cloning and expression of a distinctive class of self-incompatibility (*S*) gene from *Papaver rhoeas* L. *Proceedings of the National Academy of Science Sciences of the United States of America*, **91**, 2265-2269.
- Force, A. Lynch, M., Pickett, F.B. Amores, A., Yan, Y.L. and Postlethwait, J. (1999). Preservation of duplicate genes by complementary degenerative mutations. *Genetics* **151**, 1531-1545.
- Ford, M.A and Kay, Q.O.N. (1985). The genetics of incompatibility in *Sinapis arvensis* L. *Heredity* **54**, 99-102.
- Franklin-Tong, V.E. and Franklin, F.C.H. (2003). Gametophytic self-incompatibility inhibits pollen tube growth using different mechanisms. *Trends in Plant Science* **8**, 598-605.
- Franklin, F.C.H., Hackett, R.M. and Franklin-Tong, V.E. (1992). The molecular biology of self-incompatible responses. In: Society for Experimental Biology Seminar series 48: *Perspectives in Plant Cell Recognition*, ed. J.A. Callow and J.R. Green. Cambridge, New York: Cambridge University Press. pp.79-103.
- Franklin, F.C.H., Lawrence, M.J. and Franklin-Tong, V.E. (1995). Cell and molecular biology of self-incompatibility in flowering plants. *International Review of Cytology* **158**, 1-64.
- Franklin-Tong, V.E., Ruuth, E., Marmey, P., Lawrence, M.J. and Franklin, F.C.H (1989). Characterisation of a stigmatic component from *Papaver rhoeas* L. which exhibits the specific activity of a self-incompatibility (*S*-) gene product. *New Phytologist* **112**, 307-315.
- Franklin-Tong, V. E., Atwal, K.K., Howell, E.C., Lawrence, M.J. and Franklin, F.C.H (1991). Self-incompatibility in *Papaver rhoeas*: there is no evidence for the involvement of stigmatic ribonuclease activity. *Plant Cell and Environment* **14**, 423-429.
- Franklin-Tong, V. E., Ride, J.P., Read N.D., Trewavas, A.J.. and Franklin, F.C.H (1993). The self-incompatibility response in *Papaver rhoeas*: is mediated by cytosolic free calcium. *Plant Journal* **4**, 163-177.
- Frova, C. and Pè, M.E. (1992). Gene expression during pollen development. In, *Sexual Plant Reproduction* , ed. M. Cresti and A Tiezzi. Berlin, Heidelberg, New York: Springer-Verlag. pp. 31-39.
- Fryxell, P.A. (1988). Malvaceae of Mexico. *Systematic Botany Monograph*. **25**.
- Fujita, H., Takemura, M., Tani, E., Nemoto, K., Tokota, A. and Kohchi, T. (2003). An *Arabidopsis* MADS-box protein, AGL24, is specifically bound to and phosphorylated by Meristematic Receptor-Like Kinase (MRLK). *Plant Cell Physiology* **44**, 735-742.

- Furness, C.A. and Rudall, P.J. (1998). The tapetum and systematics of monocotyledons. *The Botanical Review* **64**, 201-239.
- Furuyama, T. and Dzelzkalns, V.A. (1999). A novel calcium-binding protein is expressed in *Brassica* pistils and anthers late in flower development. *Plant Molecular Biology* **39**, 719-737.
- Gange, J.M., Downes, B.P., Shiu, S-H., Durski, A. and Vierstra, R.D. (2002). The F-box subunit of the SCF E3 complex is encoded by a diverse-superfamily of genes in *Arabidopsis*. *Proceedings of the National Academy of Sciences of the United States of America* **99**, 11519-11524.
- García, E. (1973). *Modificaciones al sistema de clasificación climática de Köppen (para adaptarlo a las condiciones de la república mexicana)*, 2nd edition. Instituto de Geografía, UNAM, Mexico, D.F.
- Garg, S. and Sastry, T.C.S (1996). Indian Compositae in foods and flavours – a review. In: *Compositae: Biology and Utilization, Proceedings of the International Compositae Conference, Kew 1994. Volume 2*, ed. P.D.S. Caligari and D.J.N. Hind. The Royal Botanic Gardens, Kew. pp.361-382.
- Gaude, T. and Dumas, C. (1984). A membrane-like structure on the pollen wall surface in *Brassica*. *Annals of Botany* **54**, 821-825.
- Gaut, B.S. and Doebley, J.F. (1997). DNA sequence evidence for the segmental allotetraploid origin of maize. *Proceedings of the National Academy of Sciences of the United States of America* **94**, 6809-6814.
- Gentry, A.H. (1978). Floristic knowledge and needs in Pacific tropical America. *Brittonia* **30**: 134-153.
- Gerstel, D.U. (1950). Self-incompatibility studies in Guayule II. Inheritance. *Genetics* **35**, 483-506.
- Gerstel, D.U. and Riner, M.E. (1950). Self-incompatibility studies in Guayule I. Pollen-tube behaviour. *Journal of Heredity* **41**, 49-55.
- Gibbs, P.E. and Bianchi, M.B. (1999). Does late-acting self-incompatibility (LSI) show family clustering? Two more species of Bignoniaceae with LSI: *Dolichandra cynanchoides* and *Tabebuia nodosa* *Annals of Botany* **84**, 449-457.
- Gibbs, P.E., Oliveira, P.E. and Ranga, N.T. (2003). Homomorphic self incompatibility, with stylar rejection site, in *Luehea grandiflora* Mart. And Zucc. (Tiliaceae-Malvaceae *s.l.*). *Plant Biology* **5**, 419-422.
- Gibson, T.J. and Spring, J. (1998). Genetic redundancy in vertebrates: polyploidy and persistence of genes encoding multidomain proteins. *Trends in Genetics* **14**, 46-49.

- Gifford, M., Dean, S. and Ingram, G.C. (2003). The *Arabidopsis ACR4* gene plays a role in cell layer organisation during ovule integument and sepal margin development. *Development* **130**, 4249-4258.
- Gigord, L., Lavigne, C. and Shykoff, J.A. (1998). Partial self-incompatibility and inbreeding depression in a native tree species of La Reunion (Indian Ocean) *Oecologia* **117**, 342-352.
- Giot, L., Bader, J.S., Brouwer, C., Chaudhuri, A., Kuang, B., Li, Y., Hao, Y.L. Ooi, C.E., Godwin, B., Vitols, Vijayadamodar, G., Pochart, P., Machineni, H., Welsh, M, Kong, Y., Zerhusen, B., Malcolm, R., Varrone, Z., Collis, A., Minto, M., Burgess, S., McDaniel, L., Stimpson, E., Spriggs, F., Williams, J., Neurath, K., Ioime, N., Agee, M., Voss, E., Furtak, K., Renzulli, R., Aanensen, N., Carrolla, S., Bickelhaup, E., Lazovatsky, Y., DaSilva, A., Zhong, J., Stanyon, C.A., Finley Jr., L., White, K.P., Braverman, M., Jarvie, T., Gold, S., Leach, M., Knight, J., Shimkets, A., Pckenna, M.P., Chant, J. and Rothberg, J.M.. (2003). A protein interaction map of *Drosophila melanogaster*. *Science* **302**, 1727-1736.
- Giranton, J-L., Dumas, C. Cock, J.M. and Gaude, T. (2000). The integral membrane S-locus receptor kinase of *Brassica* has serine/threonine kinase activity in a membranous environment and spontaneously forms oligomers in *planta*. *Proceedings of the National Academy of Sciences of the United States of America* **97**, 3759-3764.
- Glavin, T.L., Goring, D.R., Schafer, U. and Rothstein, S.J. (1994). Feature of the extracellular domain of the S-locus receptor kinase from *Brassica*. *Molecular and General Genetics* **244**, 630-637.
- Godt, M.J.W. and Hamrick, J.L. (1995). The Mating System Of *Liatris helleri* (Asteraceae), A threatened plant-species. *Heredity* **75**, 398-404.
- Goertzen, L.R., Cannone, J.J., Gutell, R.R. and Jansen, R.K. (2003). ITS secondary structure derived from comparative analysis: implications for the sequence alignment and phylogeny of the Asteraceae. *Molecular Phylogenetics and Evolution* **29**, 216-234.
- Goldblatt, P. (1980). Polyploidy in angiosperms: monocotyledons in *Polyploidy: Biological Relevance*, ed. D.A. Levin. New York: Plenum, pp.219-239
- Golz, J.F., Clarke, A.E., Newbigin, E. and Anderson, M. (1998). R relic S-RNase is expressed in the styles of self-compatible *Nicotiana sylvestris*. *The Plant Journal* **16**, 591-599.
- Gómez-Gómez, L., Felix, G. and Boller, T. (1999). A single locus determines sensitivity to bacterial flagellin in *Arabidopsis thaliana*. *Plant Journal* **18**, 277-284.

- Gómez-Gómez, L. and Boller, T. (2000). FLS2: an LRR receptor-like kinase involved in the perception of the bacterial elicitor flagellin in *Arabidopsis*. *Molecular Cell* **5**, 1003-1011.
- Gómez-Gómez, L., Bauer, Z. and Boller, T. (2001). Both the extracellular leucine-rich repeat domain and the kinase activity of FLS2 are required for flagellin binding and signalling in *Arabidopsis*. *The Plant Cell* **13**, 1155-1163.
- Gómez-Pompa, A. and Dirzo, R. with Kaus, A., Noguerón-Chang, C.R. and Ordoñez, M. de J. (1994). *Las áreas naturales protegidas de México de la Secretaría de Desarrollo Social*. SEDESOL, Mexico, D.F. 331 pp. Unpublished.
- Good-Avila, S.V., Frey, F, and Stephenson, A.G. (2001). The effect of partial self-incompatibility on the breeding system of *Campanula rapunculoides* L. (Campanulaceae) under conditions of natural pollination. *International Journal of Plant Sciences* **162**, 1081-1087.
- Goodwillie, C. (1997). The genetic control of self-incompatibility in *Linanthus parviflorus* (Polemoniaceae). *Heredity* **79**, 424-432.
- Goodwillie, C. (1999). Multiple origins of self-compatibility in *Linanthus* Section *Leptosiphon* (Polemoniaceae): phylogenetic evidence from internal-transcribed-spacer sequence data. *Evolution* **53**, 1387-1395.
- Goring, D.R. and Rothstein, S.J. (1992). The *S*-locus receptor kinase gene in a self-incompatible *Brassica napus* line encodes a functional serine/threonine kinase. *The Plant Cell* **4**, 1273-1281.
- Goring D.R. Banks, P., Fallis, L., Baszcynski, C., Beversdorf, W.D. and Rothstein, S. (1992a). Identification of an *S*-locus glycoprotein allele introgressed from *B. napus* ssp. *rapifera* to *B. napus* ssp. *oleifera*. *The Plant Journal* **2**, 963-989.
- Goring D.R. Banks, P., Wallace, D., Beversdorf, W.D. and Rothstein, S. (1992b). Use of the polymerase chain reaction to isolate an *S*-locus glycoprotein cDNA introgressed from *Brassica campestris* into *B. napus* ssp. *oleifera*. *Molecular and General Genetics* **234**, 185-192.
- Goring D.R. Glavin, T.L., Schafer, U. and Rothstein, S. (1993). An *S* receptor kinase gene in self-compatible *Brassica napus* has a 1-bp deletion. *The Plant Cell* **5**, 531-539.
- Grant, V. (1963). *The origin of adaptations*. New York: Columbia University Press
- Greyson, R.I. (1994). *The Development of Flowers*. New York Oxford University Press.
- Green, P.J. (1994). The ribonucleases of higher plants. *Annual Review of Plant Physiology and Plant Molecular Biology* **45**, 421-445.

- Grote, M. and Fromme, H.G. (1984). Ultrastructural demonstration of a glycoprotein surface coat in allergenic pollen grains by combined cetylpyridinium chloride precipitation and silver proteinate staining. *Histochemistry* **81**, 171-176.
- Graham, A. (1993). Historical factors and biological diversity in Mexico. In, *Biological diversity of Mexico: origins and distribution*. T.P. Ramamoorthy, R. Bye, A. Lot and J.E. Fa. (eds.). New York: Oxford University Press. pp. 577-591.
- Gruber, F. (1932). Über die verträglichkeitsverhältnisse bei einigen selbsterilen wildsippen von *Antirrhinum* und über eine selbstfertile mutande. *Z. Indukt. Abstammungs-Vererbungsl.* **62**, 426-462.
- Gu, T.S., Mazzurco, M. Sulaman, W. Matias, D.D. and Goring, D.R. (1998). Binding of an arm repeat to the kinase domain of the S-locus receptor kinase. *Proceedings of the National Academy of Sciences of the United States of America* **95**, 382-387
- Gupta, P., Shivanna, K.R. and Nohan Ram, H.Y. (1998). Pollen-pistil interaction in a non-pseudogamous apomict, *Commiphora wightii*. *Annals of Botany* **81**, 589-594.
- Gupta, P.K., Agarwal, D.K. and Srivastava, A.K. (1972). Further cytological investigations in Indian Compositae. *Cytologia* **37**, 581-593.
- Haffani, Y.Z, Gaude, T., Cock, M. and Goring, D.R. (2004). Antisense suppression of thiredoxin h nRNA in *Brassica napus* cv. Westar pistils causes a low level constitutive pollen rejection response. *Plant Molecular Biology* **5**, 619-630
- Hanks, S.K., Quinn, A.M. and Hunter, T. (1988). The protein kinase family: conserved features and deduced phylogeny of the catalytic domains. *Science* **241**, 43-52.
- Haring, V. Gray, J.E., McClure, B.A., Anderson, M.A. and Clarke, A.E. (1990). Self-incompatibility: a self-recognition system in plants. *Science* **250**, 937-941.
- Harris, P.J., Anderson, M.A., Bacic, A. and Clarke, A.E. (1984). Cell-cell recognition in plants with special reference to the pollen-stigma interaction. *Oxford Surveys of Plant Molecular and Cell Biology* **1**, 161-302.
- Hatakeyama, K., Takasaki, T., Watanabe, M. and Hinata, K. (1998). Molecular characterization of S locus genes, SLG and SRK, in a pollen-recessive self-incompatibility haplotype of *Brassica rapa* L. *Genetics* **149**, 1587-1597.
- Hatakeyama, K., Tkasaki, T., Suzuki, G., Nishio, T., Watanabe, M., Isogai, A. and Hinata, K. (2001). The S receptor kinase gene determines dominance relationships in stigma expression of self-incompatibility in *Brassica*. *Plant Journal* **26**, 69-76.
- He, Z-H., Fujiki, M. and Kohorn, B.D. (1996). A cell wall-associated receptor-like protein kinase. *Journal of Biological Chemistry* **271**, 19789-19793.
- He, Z-H. and Kohorn, B.D. (1998). Requirement for the induced expression of a cell wall-associated receptor-like kinase for survival during the pathogen attack. *Plant Journal* **14**, 55-63.

- Hearn, M.J., Franklin, F.C.H. and Ride, J.P. (1996). Identification of a membrane glycoprotein in pollen of *Papaver rhoeas* which binds stigmatic self-incompatibility (S-) proteins. *The Plant Journal* **9**, 467-475.
- Hecht, V., Vielle-Calzada, J.P., Hartog, M.V. Schmidt, E.D., Boutillier, K., Grossniklaus, U. and de Vries, S.C. (2001). The Arabidopsis *SOMATIC EMBRYOGENESIS RECEPTOR KINASE 1* gene is expressed in developing ovules and embryos and enhances embryogenic competence in culture. *Plant Physiology* **127**, 803-816.
- Heckadon, S.P. (1992). Central America: tropical land of mountains and volcanoes. In *Toward a green Central America: integrating conservation and development*. V. Barzetti. and Y. Rovinski. (eds.). Hartford, Connecticut, U.S.A: Kumarian Press. pp. 5-20.
- Heinrich, M (1996). Ethnobotany of Mexican Compositae: an analysis of historical and modern sources Compositae. In: *Compositae: Biology and Utilization, Proceedings of the International Compositae Conference, Kew 1994. Vol 2*, ed. P.D.S. Caligari and D.J.N. Hind. The Royal Botanic Gardens, Kew.
- Henny, R.J. and Ascher, P.D. (1977). Sporophytic recognition of pollen S alleles in gametophytic self incompatibility system *Nemesia strumosa* Benth. *Theoretical and Applied Genetics* **49**, 15-19.
- Hernández-Pinzón, I., Ross, J. H. E., Barnes, K. A., Damant, A.P. and Murphy, D. J. (1999). Composition and role of tapetal lipid bodies in the biogenesis of the pollen coat of *Brassica napus*. *Planta* **208**, 588-598.
- Hershko, A. and Ciechanover, A. (1998). The ubiquitin system. *Annual Review of Biochemistry* **67**, 425-479.
- Hervé, C., Dablos, P., Galaud, J-P., Rouge, P. and Lescure, B. (1996). Characterisation of an *Arabidopsis thaliana* gene that defines a new class of putative plant receptor kinases with an extracellular lectin-like domain. *Journal of Molecular Biology* **258**, 778-788.
- Heslop-Harrison, J. (1968). Tapetal origin of pollen coat substances in *Lilium*. *New Phytologist* **67**, 779-786.
- Heslop-Harrison, J. (1969). An acetolysis-resistant membrane investing tapetum and sporogenous tissue in the anthers of certain Compositae. *Canadian Journal of Botany* **47**, 512-542.
- Heslop-Harrison, J. (1975). Incompatibility and the pollen-stigma interaction. *Annual Review of Plant Physiology* **26**, 403-425.
- Heslop-Harrison, J. (1987). Pollen germination and pollen-tube growth. In: *Pollen: Cytology and Development; International Review of Cytology* **107**. (eds.) G.H. Bourne. London; Academic Press pp. 1-78.

- Heslop-Harrison, J. (1992a). The angiosperm stigma. In: *Sexual Plant Reproduction*, ed. M. Cresti, A. Tiezzi. Berlin: Springer-Verlag. pp. 59-68.
- Heslop-Harrison, J. (1992b). Pollen, capture, adhesion and hydration. In: *Sexual Plant Reproduction*, ed. M. Cresti, A. Tiezzi. Berlin: Springer-Verlag. pp. 81-88.
- Heslop-Harrison, J. (1992c). Cytological techniques to assess pollen quality. In: *Sexual Plant Reproduction*. M. Cresti, and A. Tiezzi (eds.). Berlin: Springer-Verlag. pp. 41-48.
- Heslop-Harrison, J. and Heslop-Harrison, Y. (1970). The evaluation of pollen viability by enzymatically induced fluorescence-intracellular hydrolysis of fluorescein diacetate. *Stain Technology* 45, 115.
- Heslop-Harrison, J. and Heslop-Harrison, Y. (1975a). Fine structure of the stigmatic papilla of *Crocus*. *Micron* 6, 45-52.
- Heslop-Harrison, J. and Heslop-Harrison, Y. (1975b). Enzymatic removal of the proteinaceous pellicle of the stigma papilla prevents pollen tube entry in the Caryophyllaceae. *Annals of Botany* 39, 163-165.
- Heslop-Harrison, J., Heslop-Harrison, Y., Knox, R.B. and Howlett, B (1973). Pollen-wall proteins; gametophytic and sporophytic fractions in the pollen walls of the Malvaceae. *Annals of Botany* 37, 403-412.
- Heslop-Harrison, J., Heslop-Harrison, Y. and Barber, J.B. (1975). The stigma surface in incompatibility responses. *Proceedings of the Royal Society of London Series B*. 188, 287-297.
- Heslop-Harrison, Y. and Shivanna, K.R (1977). The receptive surface of the angiosperm stigma. *Annals of Botany* 41, 1233-1258.
- Heslop-Harrison, Y. and Shivanna, K.R (1984). The evaluation of pollen quality, and a further appraisal of fluorochromatic (FCR) test procedure. *Theoretical and Applied Genetics* 67, 367-375.
- Heywood V.W., Harborne, J.B. and Turner, B.L. (1977). An overture to the Compositae, in *The Biology and Chemistry of the Compositae* Volume 1. V.H. Heywood, J.B. Harborne, and B.L. Turner. (eds.). London: Academic Press.
- Hill, J.P and Lord, E.M. (1987). Dynamics of the pollen tube growth in the wild radish *Raphanus raphanistrum* (Brassicaceae) II. Morphology, cytochemistry and ultrastructure of the transmitting tissue, and the path of pollen tube growth. *American Journal of Botany* 74, 988-997.
- Hinata, K. and Nishio, T. (1978). S-allele specificity of stigma proteins in *Brassica oleracea* and *B. campestris*. *Heredity* 41, 93-100
- Hinata, K. Watanabe, M. Toriyama, K. and Isogai, A. (1993). A review of recent studies on homomorphic self-incompatibility. *International Review of Cytology* 143, 257-296.

- Hinata, K. Watanabe, M., Yamakawa S., Satta, Y. and Isogai, A. (1995). Evolutionary aspects of the *S*-related genes of the *Brassica* self-incompatibility system: synonymous and nonsynonymous base substitutions. *Genetics* **140**, 1099-1104.
- Hiscock S.J. (2000a). Genetic control of self-incompatibility in *Senecio squalidus* L. (Asteraceae): a successful colonizing species. *Heredity*. **85**, 10-19.
- Hiscock S.J. (2000b). Self-incompatibility in *Senecio squalidus* L. (Asteraceae). *Annals of Botany*, **85 supplement A**, 181-190.
- Hiscock, S.J. and Dickinson, H.G. (1993). Unilateral incompatibility within the Brassicaceae: further evidence for the involvement of the self-incompatibility (*S*) locus. *Theoretical and Applied Genetics* **86**, 744-753.
- Hiscock, S.J. and Kües, U. (1999). Cellular and molecular mechanisms of sexual incompatibility in plants and fungi. *International Review of Cytology* **193**, 165-295.
- Hiscock, S.J. and McInnis, S.M. (2003). Pollen recognition and rejection during the sporophytic self-incompatibility response: *Brassica* and beyond. *Trends in Plant Science* **8**, 606-613.
- Hiscock, S.J. and Tabah, D.A. (2003). The different mechanisms of sporophytic self incompatibility in flowering plants. *Philosophical Transactions of the Royal Society of London Series B. Biological Science* **358**, 1037-1045.
- Hiscock, S.J., Dewey, F.M., Coleman, J.O.D. and Dickinson, H.G. (1994). Identification and localisation of an active cutinase in the pollen of *Brassica napus*. *Planta* **193**, 377-384.
- Hiscock, S.J., Doughty, J., and Dickinson, H.G. (1995a). Synthesis and phosphorylation of pollen proteins during the pollen–stigma interaction self-compatible *Brassica napus* L. and self-incompatible *Brassica oleracea* L. *Sexual Plant Reproduction* **8**, 345-353.
- Hiscock, S.J., Doughty, J., Willis, A.C. and Dickinson, H.G. (1995b). A 7-kDa pollen coating-borne peptide from *Brassica napus* interacts with *S*-locus glycoprotein and *S*-locus related glycoprotein. *Planta* **196**, 367-374.
- Hiscock, S.J., Kües, U. and Dickinson, H.G. (1996). Molecular mechanisms of self-incompatibility in flowering plants and fungi – different means to the same end. *Trends in Cell Biology* **6**, 421-428.
- Hiscock, S.J., Hoedemaekers, K., Friedman, W.E. and Dickinson, H.G. (2002). The stigma surface and pollen-stigma interactions in *Senecio squalidus* L. (Asteraceae) following cross (compatible) and self (incompatible) pollinations. *International Journal of Plant Sciences* **163**, 1-16.

- Hiscock, S.J., McInnis, S.M., Tabah, D.A., Henderson and C.A., Brennan A.C. (2003). Sporophytic self-incompatibility in *Senecio squalidus* L. (Asteraceae) the search for S. *Journal of Experimental Botany* **54**, 169-74.
- Hoekstra, F.A. and Bruinsma, J. (1975). Respiration and vitality of binucleate and trinucleate pollen. *Physiologia Plantarum* **34**, 221-225.
- Hoffmann, K. and Bucher, P. (1995). The FHA domain: a putative nuclear signalling domain found in protein kinases and transcription factors. *Trends in Biochemical Sciences* **20**, 347-349.
- Hokanson, K. and Hancock, J. (2000). Early-acting inbreeding depression in three species of *Vaccinium* (Ericaceae). *Sexual Plant Reproduction* **13**, 145-150.
- Holmgren, A. (1995). Thioredoxin structure and mechanism: conformational changes on oxidation of the active-site sulfhydryls to a disulfide. *Structure* **3**, 239-243.
- Hong, S.W., Jon, J.H. Kwak, J.M. and Nam, H.G. (1997). Identification of a receptor-like protein kinase gene rapidly induced by abscisic acid dehydration, high salt and cold treatments in *Arabidopsis thaliana*. *Plant Physiology* **113**, 1203-1212.
- Hooker, W. (1861). *Cosmos diversifolius* var. *atrosanguineus*. *Curtis Botanical Magazine* **87**: pl 5227.
- Horn, M.A. and Walker, J.C. (1994). Biochemical properties of the autophosphorylation of RLK5, a receptor-like protein kinase from *Arabidopsis thaliana*. *Biochimica et Biophysica Acta* **1208**, 65-74.
- Horner, H.T Jr. (1977). A comparative light- and electron-microscopic study of microsporogenesis in male-fertile and cytoplasmic male-sterile sunflower (*Helianthus annuus*). *American Journal of Botany* **64**, 745-759.
- Horner, H.T. Jr. and Pearson, C.B. (1978). Pollen wall and aperture development in *Helianthus annuus* (Compositae: Heliantheae) *American Journal of Botany* **65**, 293-309.
- Howell, G.J., Slater, A.T. and Knox, R.B. (1993). Secondary pollen presentation in angiosperms and its biological significance. *Australian Journal of Botany* **41**, 417-438.
- Howlett, B.J., Knox, R.B. and Heslop-Harrison, J. (1973). Pollen-wall proteins: release of the allergen antigen E from intine and exine sites in pollen grains of ragweed and *Cosmos*. *Journal of Cell Science* **13**, 603-619.
- Howlett, B.J., Knox, R.B., Paxton, J.D. and Heslop-Harrison, J. (1975). Pollen-wall proteins: physicochemical characterization and role in self-incompatibility in *Cosmos bipinnatus*. *Proceedings of the Royal Society of London Series B* **188**, 167-182.
- Hughes, A.L. (1994). The evolution of functionally novel proteins after genome doubling. *Proceedings of the Royal Society of London Series B*, **256**, 119-124.

- Hughes, M.B. and Babcock, E.B. (1950). Self-incompatibility in *Crepis foetida* (L.) subsp. *rhoeadifolia* (Bieb.) Schinz et Keller. *Genetics* **35**, 570-585.
- Hülkamp, M., Schneitz, K. and Pruitt, R.E. (1995). Genetic evidence for a long-range activity that directs pollen tube guidance in *Arabidopsis*. *The Plant Cell* **7**, 57-64.
- Humeau, L., Pailler, T. and Thompson, J.D. (1999). Variation in the breeding system of two sympatric *Dombeya* species on La Reunion Island. *Plant Systematics and Evolution* **218**, 77-87.
- Hunter, T. (1998). The Croonian Lecture 1997. The phosphorylation of proteins on tyrosine: its role in cell growth and disease. *Philosophical Transactions. Proceedings of the Royal Society London Series B* **353**, 583-605.
- Husani S.W. and Iwo, G.A. (1990). Cytology of some weedy species of the family Compositae (Asteraceae) from Jos plateau, Nigeria. *Feddes Repertorium* **101**, 49-62.
- Huang, S., Lee, H-S., Karunanandaa, B. and Kao, T-h. (1994). Ribonuclease activity of *Petunia inflata* S proteins is essential for rejection of self-pollen. *The Plant Cell* **6**, 1021-1028.
- Igic, B. and Kohn, J.R. (2001). Evolutionary relationships among self-incompatibility RNases. *Proceedings of the National Academy of Sciences of the United States of America* **98**, 13167-13171.
- Ikeda, S., Nasrallah, J.B., Dixit, R., Preiss, S. and Nasrallah, M.E. (1997). An aquaporin-like gene required for the *Brassica* self-incompatibility response. *Science* **276**, 1564-1566.
- Inazu, A. and Mato (1992). Expression of color-controlling Gene-C on *Cosmos bipinnatus* Cav. In relation to the anthocyanin biosynthetic pathway. *Japanese Journal of Breeding* **42**, 605-613.
- Ioerger, T.R., Gohlke, J.R., Xu, B. and Kao, T-h. (1991) Primary structural features of the self-incompatibility protein in solanaceae. *Sexual Plant Reproduction* **4**, 81-87.
- Imler, J-L. and Hoffman, J.A. (2001). Toll receptors in innate immunity. *Trends in Cell Biology* **11**, 305-311.
- Imrie, R.C. and Knowles, P.F. (1971). Genetic studies of self-incompatibility in *Carthamus flavescens* Spreng. *Crop Science* **11**, 6-9.
- Ishimizu, T., Miyagi, M., Norioka, S., Liu, Y-H., Clarke, A.E. and Sakiyama, F. (1995). Identification of Histidine 31 and Cysteine 95 in the active site of self-incompatibility associated S₆-RNase in *Nicotiana alata*. *Journal of Biochemistry* **118**, 1007-1013.

- Ishimizu, T., Norioka, S., Nakanishi, T., Kanai .M., Clarke, A.E. and Sakiyama, F. (1996a). Location of cysteine and cystine residues in S-ribonucleases associated with gametophytic self-incompatibility. *European Journal of Biochemistry*. **242**, 627-635.
- Ishimizu, T., Shinkawa, T., Sakiyama, F. and Norioka, S. (1996b). Identification of partial amino acid sequences of seven S-RNases associated with self-incompatibility of Japanese pear *Pyrus pyrifolia* Nakai. *Journal of Biochemistry* **120**, 326-334.
- Isogai, A., Takayama, S., Tsukamoto, C., Ueda, Y., Shiozawa, H., Hinata, K., Okazaki, K. and Suzuki, A. (1987). S-locus-specific glycoproteins associated with self-incompatibility in *Brassica campestris*. *Plant Cell Physiology* **28**, 1279-1291.
- Isogai, A., Takayama, S., Shiozawa, H., Tsukamoto, C., Kanbara, T., Hinata, K., Okazaki, K., and Suzuki, A. (1988). Existence of a common glycoprotein homologous to S-glycoproteins in two self incompatible homozygotes of *Brassica campestris*. *Plant Cell Physiology* **29**: 1331-1336.
- Isogai, A., Yamakawa, S., Shiozawa, H., Takayama, S., Tanaka, H., Kono, T., Watanabe, M., Hinata, K. and Suzuki, A. (1991). The cDNA sequence of NS₁ glycoprotein of *Brassica campestris* and its homology to S-locus-related glycoproteins of *Brassica oleracea*. *Plant Molecular Biology* **17**, 269-271.
- Jacob, V.J. (1973). Self-incompatibility mechanisms in *Cola nitida*. *Incompatibility Newsletter* **3**, 60-61.
- James, E.A. and Knox, R.B. (1993). Reproductive-biology of the Australian species of the genus *Pandorea* (Bignoniaceae) *Australian Journal of Botany* **41**, 611-626.
- Jansen, R.K. and Palmer, J.D. (1987). A chloroplast DNA inversion marks an ancient evolutionary split in the sunflower family (Asteraceae). *Proceedings of the National Academy of Sciences USA*, **84**, 5818-5822.
- Jansen, R.K., Michaels, H.J. and Palmer, J.D. (1991). Phylogeny and character evolution in the Asteraceae based on chloroplast DNA restriction site mapping. *Systematic Botany* **16**, 98-115.
- Jeanmougin F, Thompson JD, Gouy M, Higgins DG, Gibson TJ. (1998). Multiple sequence alignment with Clustal X. *Trends Biochemical Science* **23** (10): 403-5.
- Jeffree, C.E. (1996). Structure and ontogeny of plant cuticles. In, Plant cuticles, and integrated functional approach . Environmental Plant Biology Series. G. Kerstiens (ed.) Oxford: BIOS Scientific publishers. PP. 33-82.
- Jeong, S. Trotochaud, A.E. and Clarke, S.E. (1999). The *Arabidopsis CLAVATA2* gene encodes a receptor-like protein required for the stability of the receptor kinase. *The Plant Cell* **11**, 1925-1934.

- Jinn, T., Stone, J. and Walker, J. (2000). HESA, an *Arabidopsis* leucine-rich repeat receptor kinase, controls floral organ abscission. *Genes and Development* **14**, 108-117.
- Jones, G.H. and Vincent, J.E. (1994). Meiosis in autopolyploid *Crepis capillaris*. II. Autotetraploids. *Genome* **37**, 497-505.
- Koch, M., Haubold, B. and Mitchel-Olds, T. (2001). Molecular systematics of the Brassicaceae: evidence from coding plastid *MatK* and nuclear *CHS* sequences. *American Journal of Botany* **88**, 534-544.
- Kachroo, A., Schopfer, C.R., Nasrallah, M.E. and Nasrallah, J.B. (2001). Allele-specific receptor-ligand interactions in *Brassica* self incompatibility. *Science* **293** 1824-1826.
- Kachroo, A., Nasrallah, M.E. and Nasrallah, J.B. (2002). Self-incompatibility in the Brassicaceae: receptor-ligand signalling and cell-to-cell communication. *The Plant Cell*. **14**, 227-238.
- Kahmann, R. and Bölker, M. (1996). Self/nonsel recognition in fungi: old mysteries and simple solutions. *Cell* **85**, 145-148.
- Kai, N., Suzuki, G., Watanabe, M., and Hinata, K. (2001). Sequence comparisons among dispersed members of the *Brassica S* multigene family in an S^{θ} genome. *Mol Genet Genomics* **265**, 526-534.
- Kakizaki, T., Takada, Y., Ito, A., Suzuki, G., Shiba, H., Yakayama, S., Isogai, A. and Watanabe, M. (2003). Linear dominance relationships among four class-II *S* haplotypes in pollen is determined by the expression of SP11 in *Brassica* self-incompatibility. *Plant Cell Physiology* **44**, 70-75.
- Kamath, R.S., Fraser, A.G., Dong, Y., Poulin, G., Durbib, R., Gotta, M. Kampink, A., Le Bot, N., Moreno, S., Sohrmann, M., Welchman, D.P., Zipperlen, P. and Ahringer, J. (2003). Systematic functional analysis of the *Caenorhabditis elegans* genome using RNAi. *Nature* **421**, 231-237.
- Kandasamy, M.K., Paolillo, D.J., Faraday, C.D., Nasrallah, J.B. and Nasrallah, M.E. (1989). The *S*-locus specific glycoproteins of *Brassica* accumulate in the cell wall of developing stigma papillae. *Developmental Biology*. **134**, 462-72.
- Kandasamy, M.K., Dwyer, K.G., Paolillo, D.J., Doney, R.C., Nasrallah, J.B. and Nasrallah, M.E. (1990). *Brassica S*-proteins accumulate in the intercellular matrix along the path of pollen tubes in transgenic tobacco pistils. *The Plant Cell* **2**, 39-49.
- Kandasamy, M.K., Thorsness, M.K., Rundle, S.J., Goldberg, M.L. Nasrallah, J.B. and Nasrallah, M.E. (1993). Ablation of papillar cell function in *Brassica* flowers results in the loss of stigma receptivity to pollination. *The Plant Cell* **5**, 263-275.

- Kanellos, E.A.G. and Pearson, S. (2000). Environmental regulation of flowering and growth of *Cosmos atrosanguineus* (Hook.) Voss. *Scientia Horticulturae* **83**, 265-274.
- Kanno, T. and Hinata, K. (1969). An electron microscope study of barrier against pollen-tube growth in self-incompatible Cruciferae. *Plant and Cell Physiology* **10**, 213.
- Kao, T-h. and McCubbin, A.G. (1996a). How flowering plants discriminate between self and non-self pollen to prevent inbreeding. *Proceedings of the National Academy of Sciences USA*, **93**, 12059-12065.
- Kao, T-h. and McCubbin, A.G. (1996b). Molecular mechanisms of self-incompatibility. *Current Opinions in Biotechnology* **7**, 150-154.
- Kao, T-h. and McCubbin, A.G. (1997). Molecular and biochemical bases of gametophytic self-incompatibility in Solanaceae. *Plant Physiology and Biochemistry* **35**. 171-176.
- Karis, P.O. and Ryding, O. (1994). Tribe Heliantheae in *Asteraceae, cladistics and classification* by K. Bremer, Oregon: Timber Press.
- Karron, J.D., Marshall, D.L and Oliveras, D.M. (1990). Numbers of sporophytic self-incompatibility alleles in populations of wild radish. *Theoretical and Applied Genetics* **79**, 457-460.
- Karunanandaa, B., Huang, S. and Kao, T-h. (1994). Carbohydrate moiety of the *petunia inflata* S3 protein is not required for self-incompatibility interactions between pollen and pistil. *The Plant Cell* **6**, 1933-1940.
- Katoh, N. Goto, K., Asano, J., Fukushima, K., Yamada, K., Kasai, A., Li, T.Z., Takanoha, M., Miyairi, K. and Okuno, T. (2002). S-RNases from self-incompatible and self-compatible apple cultivars: purification, cloning, enzymic properties, and pollen tube growth inhibitory activity. *Bioscience, Biotechnology and Biochemistry* **66**, 1185-1195.
- Kaufmann, H., Kirch, H., Wemmer, T., Peil, A., Lottspeich, F., Uhrig, H. Salamini, F. and Thompson, R. (1992). Sporophytic and gametophytic self-incompatibility. In, *Sexual Plant Reproduction*. M. Cresti and A. Tiezzi. (eds.). Berlin: Springer-Verlag. pp. 117-125.
- Kearns, C.A. and Inouye, D.W. (1993). *Techniques for the pollination biologists*. Niwot: University Press of Colorado.
- Keijzer, C.J. (1987). The process of anther dehiscence and pollen dispersal II. The formation and the transfer mechanism of pollenkit, cell-wall development of the loculus tissues and a function of orbicles in pollen dispersal. *New Phytologist* **105**: 499-507.
- Keijzer, C.J. and Cresti M. (1987). A comparison of anther tissue development in male sterile *Aloe vera* and male fertile *Aloe ciliaris*. *Annals of Botany* **59**, 533-542

- Keil, D.J. and Stuessy, T.F. (1977). Chromosome counts of Compositae from Mexico and the United States. *American Journal of Botany* **6**, 791-798.
- Kemp, B.P. and Doughty, J. (2003). Just how complex is the *Brassica* S-receptor complex. *Journal of Experimental Botany*, **54**, 157-168.
- Kenton, A. Parakonny, A.S. Gleba, Y.Y and Bennett, M.D. (1993). Characterization of the *Nicotiana tabacum* L. genome by molecular cytogenetics. *Molecular and General Genetics* **240**, 159-169.
- Khatum, S. and Flowers, T.J. (1995). The estimation of pollen viability in rice. *Journal of Experimental Botany* **46**, 151-154.
- Kianian, S.F. and Quiros, C.F. (1992). Genetic analysis of major multigene families in *Brassica oleracea* and related species. *Genome* **35**, 516-527.
- Kidwell, M.G. and Lisch, D. (1997). Transposable elements as sources of variation in animals and plants. *Proceedings of the National Academy of Sciences of the United States of America* **94**, 7704-7711.
- Kim, K-J and Jansen, R.K. (1995). *ndhF* sequence evolution and the major classes in the sunflower family. *Proceedings of the National Academy of Sciences of the United States of America* **92**, 10379-10383.
- Kim, K-J, Jansen, R.K., Wallace, R.S., Michaels, H.J. and Palmer, J.D. (1992). phylogenetic implications of *rbcl* sequence variation in the Asteraceae. *Annals of the Missouri Botanical Gardens* **79**, 428-445.
- Kim, M., Cho, H.S., Kim, D-M., Lee, J.H. and Pai, H-S. (2003). CHRK1, a chitinase-related receptor-like kinase, interacts with NtPUB4, an armadillo repeat protein, in tobacco. *Biochimica et Biophysica Acta* **1651**, 50-59.
- Kimura, R., Sato, K., Fujiimoto, R. and Nishio, T. (2002). Recognition specificity of self-incompatibility maintained after the divergence of *Brassica oleracea* and *Brassica rapa*. *Plant Journal* **29**, 215-223
- King, J.R. (1960). The peroxidase reaction as an indicator of pollen viability. *Stain Technology* **55**, 225-227.
- Kirch, H.H., Uhrig, H., Lottspeich, F., Salamini, F., and Thompson, R.D. (1989). Characterization of proteins associated with self-incompatibility in *Solanum tuberosum*. *Theoretical and Applied Genetics* **78**, 581-588.
- Kirch, H-H., Li, T-Q., Seul, U. and Thompson, R.D. (1995). The expression of a potato (*Solanum tuberosum*) S-RNase gene in *Nicotiana tabacum* pollen. *Sexual Plant Reproduction* **8**, 77-84.
- Knight, R. and Rogers, H.H. (1955). Incompatibility in *Theobroma cacao*. *Heredity* **9**, 69-77.
- Knox, R.B. (1973). Pollen wall proteins: pollen-stigma interactions in ragweed and *Cosmos* (Compositae) *Journal of Cell Science* **12**, 421-443.

- Knox, R.B. (1984). Pollen-pistil interactions. In, *Encyclopedia of Plant Physiology* Eds. H.F Linskens and J. Heslop-Harrison. New Series, pp. 508-623.
- Knox, R.B. and Heslop-Harrison, J. (1970). Pollen-wall proteins: localization and enzyme activity. *Journal of Cell Science* **6**, 1-27.
- Knox, R.B. and Heslop-Harrison, J. (1971). Pollen-wall proteins: localization of antigenic and allergenic proteins in the pollen-grain walls of *Ambrosia* spp. (ragweeds) *Cytobios* **4** (13), 49-54.
- Knox, R.B. Dickinson, H.G. and Heslop-Harrison J. (1970). Cytochemical observations on the changes in RNA content and acid phosphatase activity during meiotic prophase in anther of *Cosmos bipinnatus* Cav. *Acta Botanica Neerlandica* **19**, 1.
- Kohorn, B.C., Lane, S. and Smith, T.A. (1992). An *Arabidopsis* serine/threonine kinase homologue with an epidermal growth factor repeat selected in yeast for its specificity for a thylakoid membrane protein. *Proceedings of the National Academy of Science, USA*, **89**, 10989-10992.
- Konarev, A.V., Anisimova, I.N., Gavrilova, V.A. Vachrusheva, T.E., Konechnaya, G.Y., Lewis, M., and Shewry, P.R. (2002). Serine proteinase inhibitors in the Compositae: distribution, polymorphism and properties. *Phytochemistry* **59**, 279-291.
- Koonin, E.V. (2003). Horizontal gene transfer: the path to maturity. *Molecular Microbiology* **50**, 725-727.
- Koonin, E.V., Aravind, L. and Kondrashov, A.S. (2000). The Impact of comparative genomics on our understanding of evolution. *Cell* **101**, 573-576.
- Koul, A.K. and Gohil, R.H. (1973). Cytotaxonomical conspectus of the flora of Kashmir (1) Chromosome numbers of some common plants. *Phyton* **15**, 57-66.
- Kowyama, Y., Shimano, N. and Kawase, T. (1980). Genetics of incompatibility in the diploid *Ipomoea* species closely related to the sweet potato. *Theoretical and Applied Genetics* **58**, 149-155.
- Kowyama, Y., Takahashi, H., Muraoka, K., Tani, T., Hara, K. and Shiotani, I. (1994). Number, frequency and dominance relationships of S-alleles in diploid *Ipomoea trifida*. *Heredity* **73**, 275-283.
- Kowyama, Y., Kakeda, K., Nakano, R. and Hattori, T. (1995). SLG/SRK-like sequences are expressed in the reproductive tissues of *Ipomoea trifida*. *Sexual Plant Reproduction* **8**, 333-338.
- Kowyama, Y., Kakeda, K., Kondo, K., Imada, T. and Hattori, T. (1996). A putative receptor protein kinase gene in *Ipomoea trifida*. *Plant Cell Physiology* **37**, 681-685.

- Kowyama, Y., Tsuchiya, T. and Kakeda, K. (2000). Sporophytic self-incompatibility in *Ipomoea trifida*, a close relative of sweet potato. *Annals of Botany*, **85 supplement A**, 191-196.
- Krusell, L., Madsen, L.H., Sato, S., Aubert, G., Genua, A., Szczyglowski, K., Duc, G., Kaneko, T., Tabata, S., de Bruijn, F., Pajuelo, E., Sandal, N. and Stougaard, J. (2002). Shoot control of root development and nodulation is mediated by a receptor-like kinase. *Nature* **420**, 422-435.
- Kumar, V. and Trick, M. (1994). Expression of the S-locus receptor kinase multigene family in *Brassica oleracea*. *The Plant Journal* **6**, 807-813.
- Kumar, A., Chowdhury, R.K. and Dahiya, O.S. (1995). Pollen viability and stigma receptivity in relation to meteorological parameters in pearl-millet. *Seed Science and Seed Technology* **23**, 147-156.
- Kurland, C.G., Canback, B. and Berg, O.G. (2003). Horizontal gene transfer: a critical review. *Proceedings of the National Academy of Sciences of the United States of America*. **100**: 9658-9662.
- Kusaba, M. and Nishio, T. (1999). Comparative analysis of *S* haplotypes with very similar *SLG* alleles in *Brassica rapa* and *Brassica oleracea*. *The Plant Journal* **17**, 83-91.
- Kusaba, M., Nishio, T., Satta, Y., Hinata, K. and Ockendon, D. (1997). Striking sequence similarity in inter- and intra-specific comparisons of class I *SLG* alleles from *Brassica oleracea* and *Brassica campestris*: Implications for the evolution and recognition mechanism. *Proceedings of the National Academy of Sciences, USA* **94**, 7673-7678.
- Kusaba, M., Matsushita, M., Okazaki, K. Satta, Y. and Nishio, T. (2000). Sequence and structural diversity of the *S* locus genes from different lines with the same self recognition specificities in *Brassica oleracea*. *Genetics* **154**, 413-420.
- Kusaba, M., Tung C-W., Nasrallah, M.E. and Nasrallah, J.B. (2002). Monoallelic expression and dominance interactions in anthers of self-incompatible *Arabidopsis lyrata*. *Plant Physiology*, **128**, 17-20.
- Lack, A.J. (1982). Competition for pollinators in the ecology of *Centaurea scabiosa* and *Centaurea nigra* L. III. Insect visits and the number of successful pollinations. *New Phytologist* **91**, 321-329.
- Lagercrantz, U. (1998). Comparative mapping between *Arabidopsis thaliana* and *Brassica nigra* indicates that *Brassica* genomes have evolved through extensive genome replication accompanied by chromosome fusions and frequent recombinations. *Genetics* **150**, 1217-1228.

- Lagercrantz, U. and Lydiate, D.J. (1996). Comparative genome mapping in *Brassica*. *Genetics* **144**, 1903-1910.
- Lai, Z., Ma, W.S., Han, B., Liang, L.Z., Zhang, Y.S., Hong, G.F. and Xue, Y.B. (2002). An F-box gene linked to the self-incompatibility (*S*) locus of *Antirrhinum* is expressed specifically in pollen and tapetum. *Plant Molecular Biology* **50**, 29-42
- Lalonde, B.A., Nasrallah, M.E., Dwyer, K.G., Chen, C-H., Barlow, B. and Nasrallah, J.B. (1989). A highly conserved *Brassica* gene with homology to the *S*-locus-specific glycoprotein structural gene. *The Plant Cell* **1**, 249-258.
- Lammertink, J.M., Rojas-Tomé, J.A., Casillas-Orona, F.M. & Otto, R.L. (1997). Situación y conservación de los bosques antiguos de pino-encino de la Sierra Madre Occidental y sus aves endémicas. México D.F. Consejo Internacional para la preservación de las aves, Sección Mexicana,
- Lankford, R.R. (1977). Coastal lagoons of Mexico: their origin and classification. In, *Estuarine processes*. M.L. Wiley (ed). San Diego, California: Academic Press. pp. 182-215.
- Lantin, S., Poliquin, J. and Matton, D.P. (1997). Pollen-pistil interactions in *Solanum chacoense*. *Plant Physiology* **114 Supplement S**, 1233-1233.
- La Porta, N. and Roselli, G. (1991). Relationships between pollen germination in vitro and fluorochromatic reaction in cherry clone F12/1 (*Prunus avium* L.) and some of its mutants. *Journal of Horticultural Science* **66**, 171-175.
- Larsen, K. (1977). Self-incompatibility in *Beta vulgaris* L. I. Four gametophytic, complementary *S*-loci in sugar beet. *Hereditas* **85**, 227-248.
- Larsen, K. (1978). Oligoallelism in the multigenic incompatibility of *Beta vulgaris* L. *Incompatibility Newsletter* **10**, 23-28.
- Larsen, K. (1983). Incompatibility, pseudo-compatibility and preferential fertilization in *Beta vulgaris* L. In: *Pollen: Biology and Implications for Plant Breeding*. ed. D.L. Mulcahy and E. Otaviano. Elsevier Science Publishing Co. pp.205-210.
- Lashermes, P., Couturon, E., Moreau, N., Paillard, M. and Louarn, J. (1996). Inheritance and genetic mapping of self-incompatibility in *Coffea canephora* Pierre. *Theoretical and Applied Genetics* **93**, 458-462.
- Lavthis, M. and Bhalla, P.L. (1995). Esterases in pollen and stigma of *Brassica*. *Sexual Plant Reproduction* **8**, 289-298.
- Lawrence, W.J.C. (1930). Incompatibility in polyploids. *Genetica* **12**, 269-294.
- Lawrence, J.G. and Hendrickson, H. (2003). Lateral gene transfer: when will adolescence end? *Molecular Biology* **50**, 739-749.
- Lawrence, M.J. Afzal, M. and Kenrick, J. (1978). The genetical control of self-incompatibility in *Papver rhoeas*. *Heredity* **40**, 239-253.

- Lawrence M.J., Lane, M.D., O'Donnell, S. and Franklin -Tong, V.E. (1993). The population genetics of the self-incompatibility polymorphism in *Papaver rhoeas*. 5. Cross-classification of the *S*-alleles of samples from 3 natural populations. *Heredity* **71**, 581-590.
- Leduc, N., Monner, M. and Douglas, G.C (1990). Germination of trinucleate pollen: Formulation of a new medium for *Capsella bursa-pastoris* L. *Sexual Plant Reproduction* **3**, 228-235.
- Lee, G-H., Ding, Z., Walker, J.C. and Van Doren, S.R. (2003). NMR structure of the forkhead-associated domain from the *Arabidopsis* receptor kinase associated phosphatase. *Proceedings of the National Academy of Sciences of the United States of America* **100**, 11261-11266.
- Lee, H.S., Huang, S. and Kao, T-h. (1994). S proteins control rejection of incompatible pollen in *Petunia inflata*. *Nature* **375**, 560-563.
- Lee, H.S., Karunanandaa, B., McCubbin, A., Gilroy, S. and Kao, T-h. (1996). PRK1, a receptor-like kinase of *Petunia inflata*, is essential for postmeiotic development of pollen. *The Plant Journal* **9**, 613-624.
- Lei, H.Y., Zhou, B., Hong, G.F. and Han, B. (2002). Characterisation of a *S*-locus-related receptor-like kinase cluster in rice chromosome 4. *Acta Botanica Sinica* **44**, 1346-1350.
- Lersten, N.R. and Curtis, J.D. (1990). Invasive tapetum and tricolled pollen in *Ambrosia trifida* (Asteraceae, tribe *Heliantheae*). *Plant Systematics and Evolution* **169**, 237-243.
- Levin, D.A. (1983). Polyploidy and novelty in flowering plants. *The American Naturalist* **122**, 1-25
- Levin, D.A. (1993). *S*-gene polymorphism in *Phlox drummondii*. *Heredity* **71**:193-198.
- Levin, D.A. (1996). The evolutionary significance of pseudo-self-fertility. *American Naturalist* **148**, 321-332.
- Lewis, D. (1954). Comparative incompatibility in angiosperms and fungi. *Advances in Genetics* **6**, 235-285.
- Lewis, D. (1977). Sporophytic incompatibility with 2 and 3 genes. *Proceedings of the Royal Society, London Series B* **196**, 161-170.
- Lewis, D. (1979). *Sexual Incompatibility in Plants*; Studies in Biology series No. 110. London: Edward Arnold.
- Lewis, D. (1994). Gametophytic-sporophytic incompatibility. In: *Genetic control of self-incompatibility and reproductive development in flowering plants*. Ed. E.G Williams, A.E. Clarke, R.B. Knox. Dordrecht: Kluwer Academic, 88-101.
- Lewis, D. and Crowe, L.K. (1958). Unilateral interspecific incompatibility in flowering plants. *Heredity* **12**, 233-256.

- Lewis, D., Verma, S.C. and Zuberi, M.I. (1988). Gametophytic-sporophytic incompatibility in the Cruciferae-*Raphanus sativus*. *Heredity* **61**, 355-366.
- Li, J. (2003). Brassinosteroids signal through two receptor-like kinases. *Current Opinion in Plant Biology* **6**, 494-499.
- Li, J. and Chory, J. (1997). A putative leucine-rich repeat receptor kinase involved in Brassinosteroid signal transduction. *Cell* **90**, 929-938.
- Li, J., Smith, G.P. and Walker, J.C. (1999). Kinase interaction domain of kinase-associated protein phosphatase, a phosphoprotein-binding domain. *Proceedings of the National Academy of Sciences of the United States of America* **96**, 7821-7826
- Li, J., Lease, K.A., Tax, F.E. and Walker, C. (2001). BRS1, a serine carboxypeptidase, regulates BRI1 signalling in *Arabidopsis thaliana*. *Proceedings of the National Academy of Sciences USA* **98**, 5916-5921.
- Li, J., Wen, J., Lease, K.A., Doke, J.T., Tax, F.E. and Walker, J.C. (2002). BAK1, an *Arabidopsis* LRR receptor-like protein kinase interacts with BRI1 and modulates brassinosteroid signalling. *Cell* **110**, 213-222.
- Li, X., Nield, J., Hayman, D. and Langridge, P. (1994). Cloning putative self-incompatibility gene from the grass *Phalaris coerulescens*. *The Plant Cell* **6**, 1923-1932
- Li, X., Nield, J., Hayman, D. and Langridge, P. (1995). Thioredoxin activity in the C terminus of *Phalaris* S protein. *The Plant Journal* **8**, 133-138.
- Li, X., Nield, J., Hayman, D. and Langridge, P. (1996). A self-fertile mutant of *Phalaris* produces an S protein with reduced thioredoxin activity. *The Plant Journal* **10**, 505-513.
- Li, Z and Wurtzel, E.T. (1998). The *ltk* gene family encodes novel receptor-like kinases with temporal expression in developing maize endosperm. *Plant Molecular Biology* **37**, 749-761.
- Lindberg, R.A. Quinn, A.M. and Hunter, T. (1992). Dual-specificity protein kinases: will any hydroxyl do? *Trends in Biochemical Science* **17**, 114-119.
- Linskens, H.F. and Esser, K. (1957). Über eine spezifische Anfärbung der Pollenschläuche im Griffel und die Zahl der Kallosepfropfen nach selbstung and fremdung. *Naturweiss* **44**, 16.
- Linville, S.U. (1995). Resources-allocation in sequentially flowering *Cosmos bipinnatus*. *American Midland Naturalist* **134**, 84-89.
- Little, T. M., Kantor, J.H. and Robinson, Jr, B. A. (1940). Incompatibility studies in *Cosmos bipinnatus*. *Genetics* **25**, 150-156.

- Lolle, S.J., Berlyn, G.P., Engstrom, E.M. Krolikowski, K.A., Reiter, W-D and Pruitt, R.E. (1997). Developmental regulation of cell interactions in the *Arabidopsis fiddlehead-1* mutant: a role for the epidermal cell wall and cuticle. *Developmental Biology* **189**, 311-321.
- Lopez-Casillas, F. Wrana, J.L. and Massague, J. (1993a). Betaclycan presents ligand to the TGF-*beta* signalling receptor. *Cell* **73**, 1435-1444.
- Lopez-Casillas, F. Doody, J., Wrana, J.L. and Zentella, A. (1993b). Signalling through TGF-*beta* receptors. *Journal of Cellular Biochemistry Supplement* **17A**, 224-224.
- Lot, A., Novelo, A. and Ramírez-García, P. (1993). Diversity of Mexican aquatic vascular plant flora. In, *Biological diversity of Mexico: origins and distribution*. T.P. Ramamoorthy, R. Bye, A. Lot and J.E. Fa. (eds.). New York: Oxford University Press. pp. 577-591.
- Love, E.M. (1949). La citologia como ayuda practica al mejoramiento de los cereales. *Review of Argentinean Agronomy* **16**, 1-13.
- Lowe, A.J. and Abbot, R.J. (2001996) Origins, of the new allopolyploid species: *Senecio cambrensis* (Asteraceae) and its relationship to the Canary Islands endemic *Senecio teneriffea*. *American Journal of Botany* **83**, 1365-1372.
- Luijten, S.H., Gerard, J., Oostermeijer, M.J.B., van Leeuwen, N.C. and den Nijs, H.C.M. (1996). Reproductive success and clonal genetic structure of the rare *Arnica montana* (Compositae) in the Netherlands *Plant Systematics and Evolution* **201**, 15-30.
- Lundqvist, A. (1962). The nature of the two-loci incompatibility system in grasses I. The hypothesis of a duplicative origin. *Hereditas* **48**, 153-168.
- Lundqvist, A. (1969). The identification of the self-incompatibility alleles in a grass population. *Hereditas* **61**, 345-352.
- Lundqvist, A. (1979). One-locus sporophytic self-Incompatibility in the Carnation family, Caryophyllaceae. *Hereditas* **91**, 307-307.
- Lundqvist, A. (1990). One locus sporophytic S-gene system with traces of gametophytic pollen control in *Cerastium arvense* ssp. *strictum* (Caryophyllaceae). *Hereditas* **113**, 204-215.
- Lundqvist A (1991). 4-locus S-gene control of self-incompatibility made probable in *Lilium-martagon* (Liliaceae). *Hereditas* **114**, 57-63.
- Lundqvist, A. (1994). "Slow" and "quick" S-alleles without dominance interaction in the sporophytic one-locus self-incompatibility system of *Stellaria holostea* (Caryophyllaceae). *Hereditas* **120**, 191-202.
- Lundqvist, A. (1995). Concealed genes for self-incompatibility in the carnation family Caryophyllaceae? *Hereditas* **122**, 85-89.

- Lundqvist, A., Østerbye, U., Larsen, K. and Linde-Laursen, I. (1973). Complex self-incompatibility systems in *Ranunculus acris* L. and *Beta vulgaris* L. *Hereditas* **74**, 161-168.
- Luu, D-T., Heizmann, P. and Dumas, C. (1997). Pollen-stigma adhesion in kale is not dependent on the self-(In)Compatibility genotype. *Plant Physiology* **115**, 1221-1230.
- Luu, D-T., Marty-Mazars, D., Trick, M., Dumas, C. and Heizmann, P. (1999). Pollen-stigma adhesion in *Brassica* spp involves SLG and SLR1 glycoproteins. *The Plant Cell* **11**, 251-262.
- Luu, D-T., Qin, X., Morse, D. and Cappadocia, M. (2000). S-RNase uptake by compatible pollen tubes in gametophytic self-incompatibility. *Nature* **407**, 649-651.
- Luu, D-T., Qin, X., Laubin, G., Yang, Q., Morse, D. and Cappadocia, M. (2001a). Rejection of S-heteroallelic pollen by a dual-specific S-RNase in *Solanum chacoense* predicts a multimeric SI pollen component. *Genetics* **159**, 329-335.
- Luu, D.-T., Hughes, S., Passelègue, E. and Heizmann, P. (2001b). Evidence for orthologous S-locus-Related 1 genes in several general of Brassicaceae *Molecular and General Genetics* **264**, 735-745.
- Ma, W.S., Zhou, J.L., Lai, Z., Zhang, Y.S. and Xue, Y.B. (2003). The self-incompatibility (S) locus of *Antirrhinum* resides in a pericentromeric region. *Acta Botanica Sinica* **45**, 47-52.
- Mable, B.K., Schierup, M.H. and Charlesworth, D. (2003). Estimating the number, frequency, and dominance of S-alleles in a natural population of *Arabidopsis lyrata* (Brassicaceae) with sporophytic control of self-incompatibility. *Heredity* **90**, 422-31.
- Mackay, G.R. (1977). A diallele cross method for the recognition of S allele homozygotes in turnip, *Brassica campestris* L. ssp. *Rapifera*. *Heredity* **38**, 301-308.
- Maddison, W.P and Maddison, D.R. (2000). MacClade 4. Sinauer: Massachusetts: USA
- Maddox, D.M., Joley, D.B. Supkoff, D.M. and Mayfield, A. (1996). Pollination biology of yellow starthistle (*Centaurea solstitialis*) in California. *Canadian Journal of Botany* **74**, 262-267.
- Madsen, E.B., Madsen, L.H., Radutolu, S., Olbryt, M. Rakawalska, M. Szczyglowski, K., Sayo, S., Kaneko, T., Tabata, S., Sandal, N. and Stougaard, J. (2003). A receptor kinase gene of the LysM type is involved in legume perception of rhizobial signals. *Nature* **425**, 637-640.
- Madsen, G.C. (1947). Influence of photoperiod on microsporogenesis in *Cosmos sulphureus* Cav. var. Klondike. *Botanical Gazette* **109**, 120-132.

- Manning, J.C. (1996). Diversity of the endothelial patterns in the angiosperms. In: *The Anther: Form, function and phylogeny*. ed. W.G. D'Arcy and R.C. Keating. Cambridge: Cambridge University Press. pp. 136-158.
- Marchler-Bauer, A. Anderson, J.B., DeWeese-Scott, C., Fedorova, N.D., Geer, L.Y., He, S., Hurwitz, D.I., Jackson, J.D., Jacobs, A.R., Lanczycki, C.J., Liebert, C.A., Liu, C., Madej, T., Marchler, G.H., Mazumder, R., Nikolskaya, A.N., Panchenko, A.R., Rao, B.S., Shoemaker, B.A., Simonyan, V., Song, J.S., Thiessen, P.A., Vasudevan, S., Wang, Y., Yamashita, R.A., Yin, J.J. and Bryant, S.H. (2003). CDD: a curated Entrez database of conserved domain alignments. *Nucleic Acid Research* **31**, 383-387.
- Marsden-Jones, E.M. and Turrill, W.B. (1954). British knapweeds. Allard and Son Ltd. Dorking, UK: Bartholomew Press.
- Marshall, C.J. (1994). Signal transduction: hot lips and phosphorylation of protein kinases. *Nature* **367**, 686-686.
- Marshall, C.J. (1995). Specificity of receptor tyrosine kinase signalling: transient versus sustained extracellular signal-regulated kinase activation. *Cell* **80**, 179-185.
- Martin, F.W. (1968). The system of self-incompatibility in *Ipomoea*. *Journal of Heredity* **59**, 263-267.
- Mascarenhas, J.P. (1975). The biochemistry of angiosperm pollen development. *The Botanical Review* **41**, 259-314.
- Mascarenhas, J.P. (1990). Gene activity during pollen development. *Annual Review of Plant Physiology and Plant Molecular Biology* **41**, 317-338.
- Masera, O., Ordóñez, M. de J. and Dirzo, R. (1997). Carbon emissions from Mexican forests: current situation and long-term scenarios. *Climate Change*, **35**, 265-295.
- Mastenbroek, I., Dewet, J.M.J. and Lu, C-Y (1982). Chromosome behaviour in early and advanced generations of tetraploid maize. *Caryologia* **35**, 463-470.
- Masterson, J. (1994). Stomatal size in fossil plants: evidence for polyploidy in majority of angiosperms. *Science* **264**, 421-423.
- Mather, K. (1944). Genetical control of incompatibility in angiosperms and fungi. *Nature* **153**, 392-395
- Mathew, A. and Mathew, P.M. (1988). Cytological studies of the South Indian Compositae. In: *Glimpses in Plant Research, Cytological Research monographs Vol. 8*. ed. P.K.K. Nair New Dehli, India. Today & Tomorrow's Printers & Publishers. pp 1-139.
- Mathew, P.M. and Thomson, R. (1984). Induced polyploidy in *Cosmos sulphureus* Cav. *New Botanist* **11**, 131-137.
- Matsubayashi, Y. (2003). Ligand-receptor pairs in plant-peptide signalling. *Journal of Cell Science* **116**, 3863-3870.

- Matsushita, Y., Suzuki, T., Kubota, R., Mori, M., Shimosato, H., Watanabe, M., Kayano, T. and Nishio, T. (2002). Isolation of a cDNA for a nucleoside diphosphate kinase capable of phosphorylating the kinase domain of the self-incompatibility factor SRK of *Brassica campestris*. *Journal of Experimental Botany* **53**, 765-767.
- Matton, D.P., Mau, S-L., Okamoto, S., Clarke, A.E. and Newbigin, E. (1995). The *S*-locus of *Nicotiana alata*: genomic organisation and sequence analysis of two *S*-RNase alleles. *Plant Molecular Biology* **28**, 847-858.
- Matton, D.P., Maes, C., Laublin, G., Qin, X.K., Bertrand, C., Morse, D. and Cappadocia, M. (1997). Hypervariable domains of self-incompatibility RNases mediate allele-specific pollen recognition. *The Plant Cell* **9**, 1757-1766.
- Mattsson, O., Knox, R.B., Heslop-Harrison, J. and Heslop-Harrison, Y. (1974). Protein pellicle of stigmatic papillae as a probable recognition site in incompatibility reaction. *Nature* **247**, 298-300.
- Mau, S.L., Williams, E.G., Atkinson, A., Anderson, M.A., Cornish, E.C., Grego, B., Simpson, R.J. Kheyr-Pour, A. and Clarke, A.E. (1986). Style proteins of wild tomato (*Lycopersicon peruvianum*) associated with the expression of self-incompatibility. *Planta* **169**, 184-191.
- Mau, S.L., Anderson, M.A., Haring, V., McClure, B.A. and Clarke, A.E. (1991). Molecular and evolutionary aspects of self-incompatibility in flowering plants. In: *Molecular Biology of Plant Development; Symposia of the Society for Experimental Biology* **45**. G.I. Jenkins and W. Schuch. (eds.). Cambridge: The Company of Biologists. pp.245-269.
- Mauseth, J.D. (1988). *Plant Anatomy*. California USA: Benjamin-Cummings.
- Mavrodiev, E.V. and Soltis, D.E. (2001). Recurring polyploid formation: an early account from the Russian literature. *Taxon* **50**, 469-473.
- Mayer, E. and Gottsberger, G. (2000). Pollen viability in the genus *Silene* (Caryophyllaceae) and its evaluation by means of different test procedures. *Flora* **195**, 349-353.
- Mazzurco, M. Sulaman, W. Matias, D.D. Elina, H., Cock, J.M. and Goring, D.R. (2001). Further analysis of the interactions between the *Brassica* S receptor kinase and three interaction proteins (ARC1, THL1 and THL2) in the yeast two-hybrid system. *Plant Molecular Biology* **45**, 336-376.
- McCabe, J.B. and Berthiaume, L.G. (1999). Functional roles for fatty acylated amino-terminal domains in subcellular localization. *Molecular Biology of the Cell* **10**, 3771-3786.
- McCarty, D.R. and Chory, J. (2000). Conservation and innovation in plant signaling pathways. *Cell* **103**, 201-209.

- McCormick, S. (1993). Male Gametophyte Development. *The Plant Cell* **5**, 1265-1275.
- McCormick, S., Twell, D., Vancanneyt, G. and Yamaguchi, J. (1991). Molecular analysis of gene regulation and function during male gametophyte development. In *Molecular Biology of Plant Development*. G.I. Jenkins and W. Schuch (eds.). Cambridge: The Company of Biologists. pp.229-269.
- McClure, B.A., Haring, V., Ebert, P.R., Anderson, M.A., Simpson, R.J., Sakiyami, F. and Clarke, A.E. (1989). Style self-incompatibility gene products of *Nicotiana glauca* are ribonucleases. *Nature* **342**, 955-957.
- McDonald, J.F. (1993). Evolution and consequences of transposable elements. *Current Opinion in Genetics and Development*, **3**, 855-864.
- McDonald, J.F. (1998). Transposable elements, gene silencing and macroevolution. *Trends in Ecology and Evolution*, **13**, 94-95.
- McIlvaine, T.C. (1921). A buffer solution for colorimetric comparison. *Journal of Biological Chemistry* **49**, 183-186.
- McKone, M.J., Lund, C.P. and O'Brien, J.M. (1998). Reproductive biology of two dominant prairie grasses (*Andropogon gerardii* and *Sorghastrum nutans*, Poaceae): Male-biased sex allocation in wind-pollinated plants? *American Journal of Botany* **85**, 776-783.
- McVaugh, R. (1984). *Flora Novo-Galiciana: A descriptive account of vascular plants of western Mexico*, Volume 12 Compositae. pp. 1-298
- Maslov, S., Sneppen, K., Eriksen, K.A. and Yan, K-K. (2004). Upstream plasticity and downstream robustness in evolution of molecular networks. *BMC Evolutionary Biology* **4**, 1-12.
- Mehlenbacher, S.A. and Thompson, M.M. (1988). Dominance relationships among *S* alleles in *Corylus avellana* L. *Theoretical and Applied Genetics* **76**, 669-672.
- Mehlenbacher, S.A. (1997). Revised dominance hierarchy for *S*-alleles in *Corylus avellana* L. *Theoretical and Applied Genetics* **94**, 360-366.
- Mehra, P.N. and Remanadan, P. (1974). Cytological investigations of the Indian Compositae. II Astereae, Heliantheae, Helenieae and Anthemideae. *Caryologia* **27**, 255-284.
- Melchert, T.E. (1968). Systematic studies in the Coreopsidinae: cytotaxonomy of Mexican and Guatemalan *Cosmos*. *American Journal of Botany* **55**, 345-353.
- Messmore, N.A. and Knox, J.S. (1997). The breeding system of the narrow endemic, *Helenium virginicum* (Asteraceae) *Journal of the Torrey Botanical Society* **124**, 318-321.
- Miege, C., Ruffio-Chable, V., Schierup, H. Cabrillac, D., Dumas, C., Gaude, T. and Cock, J.M. (2001). Intrahaplotype polymorphism at the *Brassica S* locus. *Genetics* **159**, 811-822.

- MINITAB (2000a). *MINITAB users' guide 1. Data, graphics, and Macros*. Release 13 for Windows®.
- MINITAB (2000b). *MINITAB users' guide 2. Data analysis and quality tools*. Release 13 for Windows®.
- Mittermeier, R.A. (1988). Primate diversity and the tropical forest: case studies from Brazil and Madagascar and the importance of the megadiversity countries. In *Biodiversity*, E. Wilson (ed.). Washington DC: National Academic Press.
- Molder, M. and Owens, J.N. (1972). Ontogeny and histochemistry of vegetative apex of *Cosmos bipinnatus* var. *sensation*. *Canadian Journal of Botany* **50**, 1171.
- Molder, M. and Owens, J.N. (1973). Ontogeny and histochemistry of intermediate and reproductive apices of *Cosmos bipinnatus* var. *sensation* in response to gibberellin A3 and photoperiod. *Canadian Journal of Botany* **51**, 535.
- Montoya, T., Nomura, T., Farrar, K., Kaneta, T., Yokota, T. and Bishop, G.J. (2002). Cloning the tomato *Curl3* gene highlights the putative dual role of the leucine-rich repeat receptor kinase tBRI1/SR160 in plant steroid hormone and peptide hormone signaling. *The Plant Cell* **14**, 3163-3176.
- Moon, J., Parry, G. and Estelle, M. (2004). The ubiquitin-proteasome pathway and plant development. *The Plant Cell* **16**, 3181-3195.
- Mu, J-H., Lee, H-S. and Kao, T-h. (1994). Characterization of a pollen-expressed receptor-like kinase gene of *Petunia inflata* and the activity of its kinase. *The Plant Cell* **6**, 709-721.
- Muller, J (1981). The fossil pollen records of extant angiosperms. *The Botanical Review* **47**, 1-142.
- Murase, K., Shiba, H, Iwano, M., Che, F-S., Watanabe, M., Isogai, A. and Takayama, s. (2004) A membrane-anchored protein kinase involved in *Brassica* self-incompatibility signaling. *Science* **303**, 1516-1519.
- Murfett, J., Atherton T.L., Mou, B., Gasser, C.S. and McClure, B.A. (1994). S-RNase expressed in transgenic *Nicotiana* causes S-allele-specific pollen rejection. *Nature* **367**, 563-566.
- Murfett, J., Stabala, J. Zurek, D.M., Mou, B., Beecher, B. and McClure, B.A. (1996). S-RNase and interspecific pollen rejection in the genus *Nicotiana*: multiple pollen-rejection pathways contribute to unilateral incompatibility between self-incompatible and self-compatible species. *The Plant Cell* **8**, 943-958.
- Murphy D.J. and Ross J.H.E. (1998). Biosynthesis and processing of the major pollen coat proteins of *Brassica napus*. *Plant Journal* **13**, 1-16.
- Murray, B.G. (1974). Breeding systems and floral biology in the genus *Briza*. *Heredity* **33**, 285-292.

- Murray, B.G. (1979). The genetics of self-incompatibility in *Briza spicata*. *Incompatibility Newsletter*. **11**, 42-45.
- Muschietti, J. Eyal, Y. and McCormick, S. (1998). Pollen tube localization implies a role in pollen-pistil interactions for the tomato receptor-like protein kinases LePRK1 and LePRK2. *The Plant Cell* **10**, 319-330.
- Nam, K.H. and Li, J. (2002). BRI1/BAK, a receptor kinase pair mediating brassinosteroid signaling. *Cell* **110**, 203-212.
- Naranjo, C.A., Poggio, L. and Brandham, P.E. (1983). A practical method of chromosome classification on the basis of centromere position. *Genetica* **62**, 51-53.
- Nasrallah, J.B. and Nasrallah, M.E. (1989). The molecular genetics of self-incompatibility in *Brassica*. *Annual Review of Genetics* **23**, 121-139.
- Nasrallah, J.B. and Nasrallah, M.E. (1993). Pollen-stigma signaling in the sporophytic self-incompatibility response. *The Plant Cell* **5**, 1325-1335.
- Nasrallah, J.B., Kao, T-h., Goldberg, M.L. and Nasrallah, M.E. (1985a). A cDNA clone encoding an S-locus-specific glycoprotein from *Brassica oleracea*. *Nature* **318**, 263-267.
- Nasrallah, J.B., Doney, R.C. and Nasrallah, M.E. (1985b). Biosynthesis of glycoproteins involved in the pollen-stigma interaction of incompatibility in developing flowers of *Brassica oleracea* L. *Planta* **165**, 100-107.
- Nasrallah, J.B., Kao, T-h., Chen, C-H., Goldberg, M.L. and Nasrallah, M.E. (1987). Amino-acid sequence of glycoproteins encoded by three alleles of the S locus of *Brassica oleracea*. *Nature* **326**, 617-619.
- Nasrallah, J.B., Yu, S-M. and Nasrallah, M.E. (1988). Self-incompatibility genes of *Brassica oleracea*: Expression, isolation and structure. *Proceedings of the National Academy of Sciences USA* **85**, 5551-5555.
- Nasrallah, J.B., Nishio, T. and Nasrallah, M.E. (1991). The self-incompatibility genes of *Brassica*; expression and use in genetic ablation of floral tissue. *Annual Review of Plant Physiology* **42**, 393-422.
- Nasrallah, J.B., Rundle, S.J. and Nasrallah, M.E. (1994). Genetic evidence for the requirement of the *Brassica* S-locus receptor kinase gene in the self-incompatibility response. *The Plant Journal* **5**, 373-384.
- Nasrallah, M.E., Liu, P. and Nasrallah, J.B. (2002). Generation of self-incompatible *Arabidopsis thaliana* by transfer of two S locus genes from *A. lyrata*. *Science* **297**, 247-249.
- Nasrallah, M.E., Muthugapatti, K. Kandasamy, K. and Nasrallah, J.B. (1992). A genetically defined *trans*-acting locus regulates S-locus function in *Brassica*. *The Plant Journal* **2**, 497-506.

- Navarro-Gochicoa, M-T., Camut, S., Timmers, A.C.J., Niebel, A., Hervé, C., Boulet, E. Bono, J-J., Imberty, A. and Cullimore, J. (2003). Characterization of four lectin-like receptor kinases expressed in roots of *Medicago truncatula*. Structure, location, regulation of expression, and potential role in the symbiosis with *Sinorhizobium meliloti*. *Plant Physiology* **133**, 1893-1910.
- Nielsen, L.R., Siegismund, H.R. and Philipp, M. (2003). Partial self-incompatibility in the polyploid endemic species *Scalesia affinis* (Asteraceae) from the Galapagos: remnants of a self-incompatibility system? *Botanical Journal of the Linnean Society* **142**, 93-101.
- Newbigin, E., Anderson, M.A. and Clarke, A.E. (1993). Gametophytic self-incompatibility systems. *The Plant Cell* **5**, 1215-1224.
- Nielsen, L.R., Philipp, M., Adsersen, H., and Siegismund, H.R. (2000). Breeding system of *Scalesia divisa* Andersson an endemic Asteraceae from the Galápagos Islands. *Det Norske Videnskaps-Akademi I. Matematisk-Naturvidenskapelige Klasse, Skrifter, Ny Serie* **39**, 127-138.
- Nielsen, L.R., Siegismund, H.R. and Philipp, M. (2003). Partial self-incompatibility in the polyploid endemic species *Scalesia affinis* (Asteraceae) from the Galápagos: remnants of a self-incompatibility system? *Botanical Journal of the Linnean Society* **142**, 93-101.
- Nishiguchi, M., Yoshida, K., Sumizono, T. and Tazaki, K. (2002). A receptor-like protein kinase with a lectin-like domain from lombardy poplar; gene expression in response to wounding and characterization of phosphorylation activity. *Molecular Genetics and Genomics* **267**, 506-514.
- Nishimura, R., Hayashi, M., Wu, G.-J., Kouchi, H., Imaizumi-Anraku, H., Murakami, Y., Kawasaki, S., Akao, S., Ohmori, M., Nagasawa, M., Harada, K. and Kawaguchi, M. (2002). HAR1 mediates systemic regulation of symbiotic organ development *Nature* **420**, 426-429
- Nishio, T., Sakamoto, K. and Yamaguchi, J. (1994). PCR-RFLP of *S* locus for identification of breeding lines in cruciferous vegetables. *Plant Cell Reports* **13**, 546-550.
- Nishio, T., Kusaba, M., Watanabe, M. and Hinata, K. (1996). Registration of *S* alleles in *Brassica campestris* L. by the restriction fragment sizes of SLGs. *Theoretical and Applied Genetics* **92**, 388-394.
- Nishio, T., Kusaba, M., Sakamoto, K. and Ockendon, D.J (1997). Polymorphism of the kinase domain of the *S*-locus receptor kinase gene (SRK) in *Brassica oleracea* L. *Theoretical and Applied Genetics* **95**, 335-342.

- Nixon, K.C. (1993). El género *Quercus* en México. In, *Biological diversity of Mexico: origins and distribution*. T.P. Ramamoorthy, R. Bye, A. Lot, & J.E Fa (eds.). Mexico: Instituto de Biología, UNAM.
- Nomura, T., Bishop, G.J., Kaneta, T., Reid, J.B., Chory, J. and Yokota, T. (2003). The *LKA* gene is a *BRASSINOSTEROID INSENSITIVE 1* homolog of pea. *Plant Journal* **36**, 291-300.
- Norioka, N., Norioka, S., Ohnishi, Y., Ishimizu, T., Oneyama, C., Nakabishi, Y. and Sakiyama, F. (1996). Molecular cloning and nucleotide sequences of cDNAs encoding *S*-allele specific stylar RNases in a self-incompatible cultivar and a self-compatible mutant of Japanese pear, *Pyrus pyrifolia* Nakai. *Journal of Biochemistry* **120**, 335-345.
- Norton, R.B. (1966). Testing of plum pollen viability with tetrazolium salts. *American Society of Horticultural Science* **89**, 132-134.
- Nou, I.S., Watanabe, M., Isogai, A., Shiozawa, H., Suzuli, A. and Hinata, K. (1991). Variation of *S*-alleles and S-glycoproteins in a naturalized population of self-incompatible *Brassica campestris* L. *Japanese Journal of Genetics* **66**, 227-239.
- Nou, I.S., Watanabe, M., Isogai, A. and Hinata, K. (1993). Comparison of *S*-alleles and S-glycoproteins between two wild populations of *Brassica campestris* in Turkey and Japan. *Sexual Plant Reproduction* **6**, 79-86.
- Ockendon, D.J. (1972). Pollen tube growth and site of incompatibility in *Brassica*. *New Phytologist* **71**, 519-522.
- Ockendon, D.J. (1974). Distribution of self-incompatibility alleles and breeding structure of open-pollinated cultivars of Brussels sprouts. *Heredity* **33**, 159-171.
- Ockendon, D.J. (1982). An *S*-allele survey of cabbage (*Brassica oleracea* var. *capitata*). *Euphytica* **31**, 325-331.
- Ockendon, D.J. and Gates, P.J. (1975). Growth of cross and self-pollen tubes in the styles of *Brassica oleracea*. *New Phytologist* **75**, 155-160.
- O'Donnell, S. and Lawrence, M.J. (1984). The population genetics of the self-incompatibility polymorphism in *Papaver rhoeas*. 4. The estimation of the number of *S*-alleles in a population. *Heredity* **53**, 495-507.
- Ohno, S. (1973). Ancient linkage groups and frozen accidents. *Nature* **244**, 259-262.
- Ohri, D. Kumar, A. and Pal, M. (1988). Variation in Nuclear DNA and karyotype in *Cosmos*. *Cytologia* **53**, 365-367.
- Ohta, T. (1991). Multigene families and the evolution of complexity. *Journal of Molecular Evolution* **33**, 34-41.
- Ohta, T. (1994). Further examples of evolution by gene duplication revealed through DNA sequence comparison. *Genetics* **138**, 1331-1337.

- Ohtake, T., Takahashi, T. and Komeda, Y. (2000). Salicylic acid induces the expression of a number of receptor-like kinase genes in *Arabidopsis thaliana*. *Plant Cell Physiology* **41**, 1038-1044.
- Okazaki, K., Kusaba, M. Ockendon, D.J. and Nishio, T. (1999). Characterization of S tester lines in *Brassica oleracea* polymorphism of restriction fragment length of SLG homologues and isoelectric points of S-locus glycoproteins. *Theoretical and Applied Genetics* **98**, 1329-1334.
- Okazaki, K. and Hinata, K. (1984). Analysis of S-alleles and S-glycoproteins in F1-hybrid varieties of Japanese radish (*Raphanus sativus* L.) *Japan. Journal of Breeding*. **34**, 237-245.
- Olsen, J. (1980). In, IOPB Chromosome number reports LXVII. *Taxon* **29**, 366-367.
- Ortega-Larrocea, M.P., Chavez, V.M. and Bye-Boettler, R. (1997). Microprogacion y establecimiento *ex vitro* de *Cosmos atrosanguineus* (Hook.) A. Voss. En el Jardin Botanico del Instituto de Biologia de la UNAM. *Amaranto* **10**, 1-9.
- Ortega-Olivencia, A. and Devesa, J.A. (1998). Taxonomy and breeding system in a new species of *Scrophularia* L. (Scrophulariaceae) from Morocco. *Botanical Journal of the Linnean Society* **128**, 185-202
- Osborn, T.C., Pires, J.C., Birchler, J.A., Augaer, D.L., Chen, Z.J., Lee, H-S, Comai, L., Madlung, A., Doerge, R.W., Colot, V. and Martienssen, R.A. (2003). Understanding mechanisms of novel gene expression in polyploids. *Trends in Genetics* **19**, 141-147.
- Østerbye, U. (1975). Self-incompatibility in *Ranunculus acris* L. I. Genetic interpretation and evolutionary aspects. *Hereditas* **80**, 91-112.
- Østerbye, U. (1977). Self-incompatibility in *Ranunculus acris* L. II. Four S-loci in a German population. *Hereditas* **87**, 173-178.
- Østerbye, U. (1978). The calculation and interpretation of S-genotype segregation in complex incompatibility systems. *Hereditas* **88**, 139-145
- Østerbye, U. (1986). Self-incompatibility in *Ranunculus acris* L. *Hereditas* **104**, 61-73.
- Østerbye, U., Larsen, K. and Lundqvist, A. (1980). Comments on the self-incompatibility in the Gramineae. *Incompatibility Newsletter* **12**. 45-57.
- Otto, S.P. (2003). In polyploids, one plus one does not equal two. *Trends in Ecology and Evolution* **18**, 431-433.
- Otto, S.P. and Whitton, J. (2000). Polyploid incidence and evolution. *Annual Review of Genetics* **34**, 401-437.
- Owen, H.A. and Makaroff, C.A. (1995). Ultrastructure of microsporogenesis and microgametogenesis in *Arabidopsis thaliana* (L.) Heynh. Ecotype *Wassilewskija* (Brassicaceae). *Protoplasma* **185**, 7-21.

- Ozkan, H., Levy, A.A and Feldman, M. (2001). Allopolyploidy-induced rapid genome evolution in the wheat (*aegilops-triticum*) group. *The Plant Cell* **13**, 1735-1759.
- Pacini, E. (1990). Tapetum and microspore function. In, *Microspores: Evolution and Ontogeny*, ed S. Blackmore and R.B. Knox. London: Academic Press. pp. 213-237.
- Pacini, E. (1994). Cell biology of anther and pollen development. In, *Genetic Control of Self-incompatibility and Reproductive Development in Flowering Plants*. E.G Williams, A.E. Clarke and R.B. Knox (eds.). London: Kluwer Academic press. pp.289-308.
- Pacini, E. (1996a). Tapetum types in: forms and function. In, *Compositae Systematics, Proceedings of the International Compositae Conference, Kew 1996*. D.J.N. Hind. and H.J. Beenjte (eds.). The Royal Botanic Gardens, Kew. pp 21-29.
- Pacini, E. (1996b). Types and meaning of pollen carbohydrate reserves. *Sexual Plant Reproduction* **9**, 362-366.
- Pacini, E. (1997). Tapetum character states: analytical keys for tapetum types and activities. *Canadian Journal of Botany* **75**, 1448-1459.
- Pacini, E. and Juniper, B.E. (1979). The ultrastructure of pollen-grain development in olive (*Olea europaea*). 2. Secretion by the tapetal cells. *New Phytologist* **83**, 165-174.
- Pacini, E. and Keijzer, C.J. (1989). Ontogeny of intruding non-plasmodial tapetum in the wild chicory, *Cichorium intybus* (Compositae). *Plant Systematics and Evolution* **167**, 149-164.
- Palmer, J.D. and Herbon, L.A. (1988). Plant mitochondrial DNA evolves rapidly in structure, but slowly in sequence. *Journal of Molecular Evolution* **28**, 87-97.
- Pandey, K.K. (1958). Time of the S allele action. *Nature* **181**, 1220.
- Pandey, K.K. (1960). Evolution of Gametophytic and sporophytic systems of self-incompatibility in angiosperms. *Evolution* **14**: 98-115.
- Pandey, K.K. (1967). Elements of the S-gene complex II. Mutation and complementation at the S₁ Locus in *Nicotiana glauca*. *Heredity* **22**. 255-282.
- Panero, J.L. and Funk, V.A. (2002). Toward a phylogenetic subfamilial classification for the Compositae (Asteraceae). *Proceedings of the Biological Society of Washington* **115**, 909-922.
- Park, A.E., Cho, S.K., Yun, U.J, Jin, M.Y., Lee, S.H., Sachetto-Martins, G. and Park, O.K. (2001). Interaction of the *Arabidopsis* receptor protein kinase Wak1 with glycine-rich protein, AtGRP-3. *Journal of Biochemistry* **276**, 26688-26693.
- Pastuglia, M., Roby, D., Dumas, C. and Cock, J.M. (1997). Rapid induction by wounding and bacterial infection of an S gene family receptor-like kinase gene in *Brassica oleracea*. *The Plant Cell* **9**, 46-60.

- Pastuglia, M., Swarup, R., Rocher, A., C. Saindrenan, P. Roby, D., Dumas, C. and Cock, J.M. (2002). Comparison of the expression patterns of two small gene families of *S* gene family receptor kinase genes during the defence response in *Brassica oleracea* and *Arabidopsis thaliana*. *Gene* **282**, 215-225.
- Paxman, G.J. (1963). The maximum likelihood estimation of the number of self-sterility alleles in a population. *Genetics* **48**, 1029-1032.
- Pearson, W.R. (1996). Effective protein sequence comparison. *Methods in Enzymology* **266**: 227-258.
- Pearson W.R. & Lipman D.J. (1988). *Proceedings of the National Academy of Sciences USA* **85**: 2444-2448
- Pickett, F.B. and Meeks-Wagner, D.R. (1995). Seeing double: appreciating genetic redundancy. *The Plant Cell* **7**: 1347-1336.
- Piffanelli, P., Ross, J.J.E. and Murphy, D.J. (1998). Biogenesis and function of the lipidic structures of pollen grains. *Sexual Plant Reproduction* **11**, 65-80.
- Pikaard, C.S. (2001). Genomic change and gene silencing in polyploids. *Trends in Genetics* **17**, 675-677.
- Pikaard, C.S. and Lawrence R.J. (2002). Uniting the paths of gene silencing. *Nature Genetics* **32**, 340-341.
- Pinkava, D.J. and Keil, D.J. (1977). Chromosome counts of Compositae from the United States and Mexico. *American Journal of Botany* **64**, 680-686.
- Powell, A.M. and Turner, B.L. (1963). Chromosome numbers in the Compositae VII, additional species from the south-western United States and Mexico. *Madroño* **17**, 128-140.
- Prabha, K., Sood, R. and Gupta S.C. (1982). High temperature-induced inactivation of sporophytic self-incompatibility in *Ipomoea-fistulosa*. *New Phytologist* **92**, 115-122.
- Pradhan, A.K., Prakash, S., Mukopadhyay, A. and Pental, D. (1992). Phylogeny of *Brassica* and allied genera based on variation in chloroplast and mitochondrial DNA patterns: Molecular and taxonomic classifications are incongruous. *Theoretical and Applied Genetics* **85**, 331-340.
- Preuss, D., Lemieux, B. Yen, G. and Davis, R.W. (1993). A conditional sterile mutation eliminates surface components from *Arabidopsis* pollen and disrupts cell signalling during fertilization. *Genes and Development* **7**, 974-985.
- Qioa, H., Wang, F., Zhao, L. Zhou, J., Huang, J. Zhang, Y. and Xue, Y. (2004a). The F-box protein AhSLF-S₂ physically interacts with S-RNases that may be inhibited by the ubiquitin/26S proteasome pathway of protein degradation during compatible pollination in *Antirrhinum*. *The Plant Cell* **16**, 582-595.

- Qioa, H., Wang, F., Zhao, L. Zhou, J., Lai, Z., Zhang, Y. and Robbins, T.P. (2004b). The F-box protein AhSLF-S₂ controls the pollen function of S-RNase-based self-incompatibility. *The Plant Cell* **16**, 2307-2322.
- Rabe, A.J. and Soltis, D.E. (1999). Pollen tube growth and self-incompatibility in *Heuchera micrantha* var. *diversifolia* (Saxifragaceae) *International Journal of Plant Sciences* **160**, 1157-1162.
- Radutolu, S., Madsen, L.H., Madsen, E.B., Felle, H.H., Umehara, Y., Grenlund, M., Sato, S., Nakamura, Y., Tabata, S., Sandal, N. and Stougaard, J. (2003). Plant recognition of symbiotic bacteria requires two LysM receptor-like kinases. *Nature* **425**, 585-592.
- Rain, J.C., Selig, L. Reuse, H.D. Battaglia, V. Reverdy, C., Simon, S. Lenzen, G., Petal, F., Wojcik, J., Schachter, V., Chemama, Y., Labigne, A. and Legrain, P.(2001). The protein-protein interaction map of *Helicobacter pylori*. *Nature* **409**, 211-215.
- Ramamoorthy, T.P. (1984). Notes on the genus *Salvia* (Lamiaceae) in Mexico with three new species. *J. Arnold Arbor.* **65**: 135-143.
- Ramamoorthy, T.P. and Elliott, M. (1993). Mexican Lamiaceae: diversity, distribution, endemism and evolution. In *Biological diversity of Mexico: origins and distribution*. eds T.P. Ramamoorthy, R. Bye, A. Lot and F.E. Fa, J.E., New York: Oxford University Press. pp. 513-539.
- Ramamoorthy, T.P. and Lorence, D.H. (1987). Species vicariance in Mexican flora and a new species of *Salvia* from Mexico. *Adansonia* **2**: 167-175.
- Ramamoorthy, T.P., Bye, R, Lot, A. and Fa, J.E (1993). Introduction. In, *Biological diversity of Mexico: origins and distribution*. T.P. Ramamoorthy, R. Bye, A. Lot, & J.E Fa (eds.). Mexico: Instituto de Biología, UNAM.
- Ramsey, J. and Schemske, D.W. (1998). Pathways, mechanisms and rates of polyploid formation in flowering plants. *Annual Review of Ecology and Systematics* **29**, 467-501.
- Ramsey, J. and Schemske, D.W. (2002). Neopolyploidy in flowering plants. *Annual Review of Ecology and Systematics* **33**, 589-639.
- Raspé, O. and Kohn, J.R. (2002). S-allele diversity in *Sorbus aucuparia* and *Crataegus monogyna* (Rosaceae : Maloideae). *Heredity* **88**, 458-465.
- Raven, P.H. and Axelrod, D.I. (1974). Angiosperm biogeography and past continental movements. *Annals of Missouri Botanical Garden* **61**:539-673.
- Rebay, I. (2002). Keeping the receptor tyrosine kinase signalling pathway in check: Lessons from *Drosophila*. *Developmental Biology* **251**, 1-17.
- Rebay, I., Fleming, R.J., Fehon, R.G., Cherbas, L., Cherbas, P. and Artavanistsakon, S.(1991). Specific EGF repeats of Notch mediate interactions with the Delta and serrate – implications for Notch as a multifunctional receptor. *Cell* **67**, 687-699.

- Redman, P.B., Dole, J.M., Maness, N.O. and Anderson, J.A. (2002). Post harvest handling of nine speciality cut flowers species. *Scientia Horticulturae* **92**, 293-303.
- Regal, E.A. (1861). *Gartenflora*. Vol. **10**, 406-409.
- Reinartz, J.A. and Les, D.H. (1994). Bottleneck-induced dissolution of self incompatibility and breeding system consequences in *Aster furcatus* (Asteraceae). *American Journal of Botany* **81**, 446-455.
- Reinisch, A.J., Dong, J., Brubaker, C.L. Stelly, D.M. Wendel, J.F. and Paterson, A.H. (1994). A detailed RFLP map of cotton *Gossypium hirsutum* x *G. barbdenses*: chromosome organization and evolution of disomic polyploid genomes. *Genetics* **138**: 829-847.
- Renault, L., Nasser, N., Vetter, I., Becker, J., Klebe, C., Roth, M. and Wittinhofer, A. (1998). The 1.7 angstrom crystal structure of the regulator of chromosome condensation (RCC1) reveals a seven-bladed propeller. *Nature* **392**, 97-101.
- Richards, A.J. (1997). *Plant Breeding Systems*. London, Weinheim, New York, Tokyo, Melbourne, Madras: Chapman and Hall.
- Richman, A.D., Kao, T-h., Schaeffer, S.W. and Uyenoyama, M.K: (1995). S-allele sequence diversity in natural populations of *Solanum carolinense* (Horsenettle). *Heredity*, **75**, 405–415.
- Richman, A.D., Uyenoyama, M.K. and Kohn, J.R.: (1996a). Allelic diversity and gene genealogy at the self-incompatibility locus in the Solanaceae. *Science*, **273**, 1212–1216.
- Richman, A.D., Uyenoyama, M.K. and Kohn, J.R.: (1996b). S-allele diversity in a natural population of *Physalis crassifolia* (Solanaceae)(Ground cherry) assessed by RT-PCR. *Heredity* **76**, 497-505.
- Richman, A.D., Broothaerts, W. and Kohn, J.R. (1997). Self-incompatibility RNases from three plant families: homology or convergence. *American Journal of Botany* **84**, 912-917.
- Ride, J.P. (1992). Recognition signals and initiation of host responses controlling basic incompatibility between fungi and plants. In, In, Society for Experimental Biology Seminar Series 48: *Perspectives in Plant Cell Recognition*, ed. J.A. Callow and J.R. Green. pp.213-237.
- Riley, H. P.(1934). Self-sterility and self-fertility in species of the genus *Nemesia*. *American Journal of Botany* **22**, 889-894.
- Robert, L.S., Gerster, J., Allard, S., Cass, L. and Simmonds, J. (1994). Molecular characterisation of two *Brassica napus* genes related to oleosins which are highly expressed in the tapetum. *Plant Journal* **6**, 927-933.
- Roberts, I.N. and Dickinson, H.G. (1981). Intraspecific incompatibility on the stigma of *Brassica*. *Phytomorphology* **31**, 165-174.

- Roberts, I.N. Harrod, G. and Dickinson, H.G. (1984a). Pollen-stigma interaction in *Brassica oleracea*. I. The ultrastructure and physiology of the stigmatic papillar cells. *Journal of Cell Science* **66**, 241-253.
- Roberts, I.N. Harrod, G. and Dickinson, H.G. (1984b). Pollen-stigma interaction in *Brassica oleracea* II. The fate of stigma surface proteins following pollination and their role in the self-incompatibility response. *Journal of Cell Science* **66**, 255-264.
- Robinson, H., Powel, A.M., King, R.M. and Weedin, J.F. (1981). Chromosome numbers in Compositae, XII: Heliantheae. *Smithsonian Contributions to Botany* **52**, 1-28.
- Rodriguez-Riano, T. and Dafni, A. (2000). A new procedure to assess pollen viability. *Sexual Plant Reproduction* **12**, 241-244.
- Roezl, B. (1874). Benedict Roezl. *Gardeners Chronicle* **2:28**. 73.
- Ronald, W.G and Ascher, P.D. (1975). Self-compatibility in garden *Chrysanthemum*: occurrence, inheritance and breeding potential. *Theoretical and Applied Genetics* **46**, 45-54.
- Ross J.H.E. and Murphy, D.J. (1996). Characterisation of anther-expressed genes encoding a major class of extracellular oleosin-like proteins in the pollen coat of Brassicaceae. *Plant Journal* **9**, 625-637.
- Rowley, J.R. (1990). The fundamental structure of the pollen exine. *Plant Systematics and Evolution* **5**, 13-29.
- Rowley, J.R., Dahl, A.O. and Rowley, J.S. (1981). Substructure in exines of *Artemesia vulgaris* (Asteraceae). *Review of Palaeobotany and Palynology* **35**, 1-38.
- Rudramuniyappa, C.K. (1985). A histochemical study of developing sporogenous tissue and periplasmial tapetum in the anther of *Parthenium* (Compositae). *Cytologia* **50**, 891-898.
- Ruffio-Châble, V., Hervé, Y., Dumas, C. and Gaude, T. (1997). Distribution of S-haplotypes and its relationship with the self-incompatibility in *Brassica oleracea*. Part 1. In inbred lines of cauliflower (*B. oleracea* var 'botrytis'). *Theoretical and Applied Genetics* **94**, 338-346.
- Ruffio-Châble, V., Hervé, Y., Dumas, C. and Gaude, T. (1999). Distribution of S-haplotypes and its relationship with the self-incompatibility in *Brassica oleracea*. Part 2. In varieties of broccoli and romanesco. *Theoretical and Applied Genetics* **98**, 541-550.
- Ruiter, R.K., Eldik, G.J. van., Herpen, M.M.A. van. and Schrauwen, J.A.M. (1997). Characterisation of oleosins in the pollen coat of *Brassica oleracea*. *Plant Cell* **9**, 1621-1631.
- Ryding, O. and Bremer, K. (1992). Phylogeny, distribution and classification of the Coreopsidae (Asteraceae). *Systematic Botany* **17**, 649-659.

- Rzedowski, J. (1973). Geographical relationships of the flora of Mexican dry regions. In, *Vegetation and vegetational history of northern Latin America*, ed. A. Graham. New York: Elsevier. pp. 61-72.
- Rzedowski, J. (1978). *Vegetación de México*. Mexico, D.F.: Editorial Limusa,
- Rzedowski, J. (1991). El endemismo en la flora fanerogámica mexicana: una apreciación analítica preliminar. *Acta Botanica Mexicana*. **15**: 47-64.
- Rzedowski, J. (1993). Diversity and Origins of the Phanerogamic flora of Mexico. In, *Biological diversity of Mexico: origins and distribution*. T.P. Ramamoorthy, R. Bye, A. Lot and J.E. Fa (eds.). New York: Oxford University Press. pp. 129-144
- Sage, T.L., Bertin, R.I. and Williams, E.G. (1994). Ovarian and other late-acting self-incompatibility systems. In: *Genetic Control of Self-incompatibility and Reproductive Development in Flowering Plants*. ed. E.G Williams, A.E. Clarke and R.B. Knox. London: Kluwer Academic press. pp.116-140.
- Sage, T.L., Griffin, S.R., Pontieri, V., Drobac, P., Cole, W.W. and Barrett, S.C.H. (2001). Stigmatic self-incompatibility and mating patterns in *Trillium grandiflorum* and *Trillium erectum* (Metanthiaceae) *Annals of Botany* **88**, 829-841.
- Saha, S., Nagar, P.K. and Sircar, P.K. (1985). Changes in cytokinin activity during flower development in *Cosmos bipinnatus* Cav. *Plant Growth Regulation* **3**, 27-35.
- Saito, K. (1976). Flavone glycosides in ray flowers of *Cosmos bipinnatus*. *Planta Medica* **30**, 349-355.
- Saitoh, M., Nishitoh, H. Fujii, M., Takeda, K., Tobiume, K., Sawada, Y., Kawabata, M. Miyazono, K. and Ichijo, H. (1998). Mammalian thioredoxin is a direct inhibitor of apoptosis signal-regulating kinase (ASK) 1. *The European Molecular Biology Organization (EMBO) Journal* **17**, 2596-2606.
- Sakamoto, K. Kusaba, M. and Nishio, T. (1998). Polymorphism of the *S*-locus glycoprotein gene (SLG) and the *S*-locus related gene (SLR1) in *Raphanus sativus* L. and self-incompatible ornamental plants in the Brassicaceae. *Molecular and General Genetics* **258**, 397-403.
- Sampson, D.R. (1967). Frequency and distribution of self-incompatibility alleles in *Raphanus raphanistrum*. *Genetics* **56**, 241-251.
- Sanderson, M.J. and Driskell, A.C. (2003). The challenge of constructing large phylogenetic trees. *Trends in Plant Science* **8**, 374-379.
- Sarker, R.H., Elleman, C.J. and Dickinson, H.G. (1988). Control of pollen hydration in *Brassica* requires continued protein synthesis, and glycosylation is necessary for intraspecific incompatibility. *Proceedings of the National Academy of Sciences, USA* **85**, 4340-4344.
- Sassa, H., Hirano, H. and Ikehashi, H. (1992). Self-incompatibility-related RNases in styles of Japanese pear (*Pyrus serotina* Rehd.). *Plant Cell Physiology* **33**, 811-814.

- Sassa, H., Hirano, H. and Ikehashi, H. (1993). Identification and characterization of stylar glycoproteins associated with self-incompatibility genes of Japanese pear, *Pyrus serotina* Rehd. *Molecular and General Genetics* **241**, 17-25.
- Sassa, H., Mase, N., Hirano, H. and Ikehashi, H. (1994). Identification of self-incompatibility-related glycoproteins in styles of apple (*Malus x domestica*) *Theoretical and Applied Genetics* **89**, 201-205.
- Sassa, H., Nishio, T., Kowayama, Y. Hirano, H., Koba, T. and Ikehashi, H. (1996). Self-incompatibility (*S*) alleles of the Rosaceae encode members of a distant class of the T₂/S ribonuclease superfamily. *Molecular and General Genetics* **250**, 547-557.
- Sato, K., Nishio, T., Kimura, R., Kusaba, M., Suzuki, T., Hatakeyama, K. Ockendon, D.J. and Satta, Y. (2002). Coevolution of the *S*-locus genes *SRK*, *SLG* and *SP11/SCR* in *Brassica oleracea* and *B. rapa*. *Genetics* **162**, 931-940.
- Sato, T., Thorsness, M.K., Kandasamy, M.K., Nishio, T., Hirai, M., Nasrallah, J.B. and Nasrallah, M.E. (1991). Activity of an *S* locus gene promoter in pistils and anthers of transgenic *Brassica*. *The Plant Cell* **3**, 867-876.
- Saupe, S.J. and Glass, N.L. (1997). Allelic specificity at the *het-c* heterokaryon incompatibility locus of *Neurospora crassa* is determined by a highly variable domain. *Genetics* **146**, 1299-1309.
- Scheer, J.M. and Ryan, Jr. C.A. (2002). The systemin receptor SR160 from *Lycopersicon peruvianum* is a member of the LRR receptor kinase family. *Proceedings of the National Academy of Sciences of the United States of America* **99**, 9585-9560.
- Schierup, M.H., Vekemans, X. and Christiansen, F.B. (1997). Evolutionary dynamics of sporophytic self-incompatibility alleles in plants. *Genetics* **147**, 835-846.
- Schierup, M.H., Mable, B.K., Awadalla, P., and Charlesworth, D. (2001). Identification and characterisation of a polymorphic receptor kinase gene linked to the self-incompatibility locus of *Arabidopsis lyrata*. *Genetics* **158**, 387-399.
- Schmidt, E.D.L., Guzzo, T., Toonen, M.A.J., and de Vries, S.C. (1997). A leucine-rich repeat containing receptor-like kinase marks somatic plant cells competent to form embryos. *Development* **124**, 2049-2062.
- Schopfer, C.R., Nasrallah, M.E. and Nasrallah, J.B. (1999). The male determinant of self-incompatibility in *Brassica*. *Science* **286**, 1697-1700.
- Schulze,-Muth, P., Irmeler, S., Schroder, G. and Schroder, J. (1996). Novel type of receptor-like protein kinase from a higher plant (*Catharanthus roseus*) cDNA gene, intramolecular autophosphorylation and identification of a threonine important for auto- and substrate phosphorylation. *Journal of Biological Chemistry* **271**, 26684-26689.

- Schumacher, K. and Chory, J. (2000). Brassinosteroid signal transduction: still casting the actors. *Current Opinion in Plant Biology* **3**, 79-84.
- Schlunegger, M.P. and Grutter, M.P. (1993). Refined crystal-structure of human transforming growth factor beta-2 at 1.95 angstrom resolution. *Journal of Molecular Biology* **231**, 445-458.
- Scott, D. and Carbonell, M. (eds.) (1986). *A directory of neotropical wetlands*. Cambridge, U.K: IUCN. pp. 684.
- Scutt, C.P. and Croy, R.D. (1992). An S5 self-incompatibility allele-specific cDNA sequence from *Brassica oleracea* shows high homology to the SLR2 gene. *Molecular and General Genetics* **232**, 240-246.
- Seagraves, K.A., Thompson, J.N., Soltis, P.S. and Soltis, D.E. (1999). Multiple origins of polyploidy and the geographical structure of *Heuchera grossularifolia*. *Molecular Ecology* **8**, 253-262.
- Searle, I., Men, A., Laniya, T., Buzas, D., Iturbep-Ormaetxe, I., Carroll, B. and Gressoff, P. (2003). Long-distance signalling in nodulation directed by a CLAVATA1-like receptor kinase. *Science* **299**, 109-112.
- Shah, K., Russinova, E., Gadella, T.W., Jr., Willemse, J.S. and De Vries, S.C. (2002). The *Arabidopsis* kinase-associated protein phosphatase controls internalization of the somatic embryogenesis receptor kinase 1. *Genes and Development* **16**, 1707-1720.
- Shaked, H. Kashkush, K., Ozkan, H. Feldman, M. and Levy, A. (2001). Sequence elimination and cytosine methylation are rapid and reproducible responses of the genome to wide hybridization and allopolyploidy in wheat. *The Plant Cell* **13**, 1749-1759.
- Shan, F., Yan, G. and Plummer, J.A. (2003). Meiotic chromosome behaviour and *Boronia* (Rutaceae) genome reorganisation. *Australian Journal of Botany* **51**, 599-607.
- Sharma, A.K. (1947). A cytological investigation of incompatibility between *Cosmos bipinnatus* Cav. and *C. sulphureus* Cav. *Bulletin of the Botanical Society of Bengal* Botanical Society of Bengal, Calcutta. **Volume I**, pp.19-26.
- Sherff, E.E. (1932). Revision of the Genus *Cosmos*. In: *Field Museum of Natural History Publication 313, Botanical Series 8 (No. 6)* B.E. Dahlgren (ed.). Chicago: Field Museum of Natural History. pp.401-447.
- Sherff, E.E. (1934). Some new or otherwise noteworthy members of the families Labiate and Compositae. *Botanical Gazette* **96**, 136-153.
- Sherff, E.E. (1935). New or otherwise noteworthy Compositae. X. *American Journal of Botany* **22**, 705-710.

- Sherff, E.E. (1937). Certain new plants from Hawaii and Mexico.. *American Journal of Botany* **24**, 88-90.
- Sherff, E.E. and Alexander, E.J. (1955). Compositae-Heliantheae-Coreopsidinae. In, *North American Flora*, series 2 part 2. New York: New York Botanical Gardens. pp. 1-190.
- Shiba, H., Takayama, S. and Iwano, M (2001). A pollen coat protein, SP11/SCR, determines the pollen S-receptivity in the self-incompatibility of *Brassica* species. *Plant Physiology* **125**, 2095-2103.
- Shiba, H., Iwano, M., Entani, T., Isimoto, K., Shimosato, H., Che, F-S., Satta, Y., Ito, A., Takada, Y., Watanabe, M., Isogai, A. and Takayama, S. (2002). The dominance of alleles controlling self incompatibility in *Brassica* pollen is regulated at the RNA level. *The Plant Cell* **14**, 491-504.
- Shiu, S-H. and Bleecker, A.B. (2001) Receptor-like kinases from *Arabidopsis* form a monophyletic gene family related to animal receptor kinases. *Proceedings of the National Academy of Sciences of the United States of America* **98**, 10763-10768.
- Shiu, S-H. and Bleecker, A.B. (2003) Expansion of the receptor-like kinase/Pelle gene family and receptor-like proteins in *Arabidopsis*. *Plant Physiology* **132**, 530-543.
- Shivanna, K.R. and Heslop-Harrison, J. (1981). Membrane state and pollen viability. *Annals of Botany* **47**, 759-770.
- Shivanna, K.R. and Johri, B.M. (1985). *The angiosperm pollen: structure and function*. New York: John Wiley and Son.
- Shivanna, K.R. and Rangaswamy (1992). *Pollen biology – a laboratory manual*. Berlin, Heidelberg, New York: Springer-Verlag
- Shivanna, K.R., Linskens, H.F. and Cresti, M. (1991). Pollen viability and pollen vigour. *Theoretical and Applied Genetics* **81**, 38-42.
- Shoemaker, R.C., Polzin, K., Labate, J., Specht, J., Brummer, E.C., Olson, T., Young, N., Concibido, V., Wilcox, J., Tamulonis, J.P. Kochert, G. and Boerma, H.R. (1996). Genome duplication in soybean (*Glycine* subgenus *soja*). *Genetics* **144**, 329-338.
- Sijacic, P., Wang, X., Skirpan, A.L., Wang, Y., Dowd, P.E., McCubbin, A.G., Huang, S. and Kao, T-h. (2004). Identification of the pollen determinant of S-Rnase-mediated self-incompatibility. *Nature* **249**, 302-305.
- Silva, N.F. and Goring, D.R. (2002). The proline-rich, extensin-like receptor kinase-1 (PERK1) gene is rapidly induced by wounding. *Plant Molecular Biology* **50**, 667-685.
- Singh, M.B., O'Neill, P.M. and Knox, R.B. (1985). Initiation of postmeiotic β -galactosidase synthesis during microsporogenesis in oilseed rape. *Plant Physiology* **77**, 225-228.

- Skowrya, D., Craig, K.L., Tyers, M., Elledge, S.J. and Harper, J.W. (1997). F-box proteins are receptors that recruit phosphorylated substrates to the SCF ubiquitin-ligase complex. *Cell* **91**, 209-219.
- Smith, E.B. (1975). The chromosome numbers of North American *Coreopsis* with phyletic interpretations. *Botanical Gazette* **136**, 78-86.
- Smith, R.D. and Walker, J.C. (1996). Plant protein phosphatases. *Annual Review of Plant Physiology and Plant Molecular Biology* **47**, 101-125.
- Solbrig, O.T., Donald, W.K., Powell, M. and Raven, P.H. (1972). Chromosome numbers in Compositae VIII: Heliantheae. *American Journal of Botany* **59**, 869-878.
- Solbrig, O.T. (1977). Chromosomal cytology and evolution in the family Compositae, in *The Biology and Chemistry of the Compositae*, Volume 2. V.H. Heywood, J.B. Harborne, B.L. Turner (eds.). London: Academic Press.
- Soltis, D.E. and Soltis, P.S. (1995). The dynamic nature of polyploid genomes. *Proceedings of the National Academy of Sciences of the United States of America* **92**, 8089-8091.
- Soltis, D.E. and Soltis, P.S. (1999). Polyploidy: recurrent formation and genome evolution. *Trends in Ecology and Evolution* **14**, 348-352.
- Soltis, P.S. and Soltis, D.E. (2000). The role of genetic and genomic attributes in the success of polyploids. *Proceedings of the National Academy of Sciences of the United States of America* **97**, 7051-7057.
- Soltis, P.S. and Soltis, D.E. (2001). Molecular systematics: assembling and using the Tree of Life. *Taxon* **50**, 663-677.
- Soltis, P.S., Plunkett, G.M., Novak, S.J. and Soltis, D.E. (1995). Genetic variation in *Tragapogon* species: additional origins of the allotetraploids *T. mirus* and *T. miscellus* (Compositae). *American Journal of Botany* **82**, 1329-1241.
- Song, K., Lu, P., Tang, K. and Osborn, T.C. (1995a). Rapid genome change in synthetic polyploids of *Brassica* and its implications for polyploid evolution. *Proceedings of the National Academy of Sciences of the United States of America*, **92**, 7719-7723.
- Song, K.M., Osborn, T.C. and Williams, P.H. (1990). *Brassica* taxonomy based on nuclear restriction fragment length polymorphisms (RFLPs) 3. Genome relationship in *Brassica* and related genera and the origin of *B. oleracea* and *B. rapa* (syn. *Campestris*). *Theoretical and Applied Genetics* **79**, 497-506.
- Song, W-H., Wang, G-L., Chen, L-L., Kim, H-S., Pi, L-Y., Holsten, T., Gardener, J., Wang, B., Zhal, W-X., Zhu, L-H., Fauquet, C. and Ronald, P. (1995b). A receptor kinase-like protein encoded by the rice disease resistant gene, *Xa21*. *Science* **270**, 1804-1806.
- Sood, R., Prabha, K., Govil, S. and Gupta, S. (1982). Overcoming self-incompatibility in *Ipomoea cairica* by IAA. *Euphytica* **31**, 333-339.

- Srivastava, V.K. (1983). Genetic-evolutionary studies on the ornamental *Cosmos*: cytological investigations in diploid *Cosmos*. *Journal of Cytology and Genetics* **18**, 11-14.
- Stanchev, B.S., Doughty, J., Scutt, C.P. Dickinson, H.G. and Croy, R.R.D. (1996). Cloning of PCP1, a member of a family of pollen coat protein (PCP) genes from *Brassica oleracea* encoding novel cysteine-rich proteins involved in pollen-stigma interactions. *The Plant Journal* **10**, 303-313.
- Stanley, R.G. and Linskens, H.F. (1974). *Pollen – biology, biochemistry, management*. Berlin, Heidelberg, New York: Springer-Verlag.
- Stapf, O. (1929) *Botanical magazine*. Vol. **153**, pl. 9180.
- Starman, T.W., Cerny, T.A. and Mackensie, A.J. (1995). Productivity and profitability of some field-grown speciality cut flowers. *Horscience* **30**, 1217-1220.
- Stead, A.D., Roberts, I.N. and Dickinson, H.G. (1979). Pollen-pistil interaction in *Brassica oleracea*. Events prior to pollen germination. *Planta* **146**, 211-216.
- Stead, A.D., Roberts, I.N. and Dickinson, H.G. (1980). Pollen-stigma interaction in *Brassica oleracea*. The role of stigmatic proteins in pollen grain adhesion. *Journal of Cell Science* **42**, 417-423.
- Stebbins, G.L. (1938). Cytological characteristics associated with the different growth habits in the dicotyledons. *American Journal of Botany* **25**, 189-198.
- Stebbins, G.L. (1947). Types of polyploid: their classification and significance. *Advances in Genetics* **1**, 403-429.
- Stebbins, G.L. (1950). *Variation and Evolution in Plants*. New York, Columbia University Press.
- Stebbins, G.L. (1971). *Chromosomal Evolution in Higher Plants*. London, Edward Arnold.
- Stebbins, G.L. (1975). The role of polyploid complexes in the evolution of North American grasslands. *Taxon* **24**: 91-106.
- Steen, A., Buist, G., Leenhouts, K.J., El Khattabi, M., Grijpstra, F., Zomer, A.L. Venema, G. Kuipers, O.P. and Kok, J. (2003). Cell wall attachment of a widely distributed peptidoglycan binding domain is hindered by cell wall constituents. *Journal of Biological Chemistry* **278**, 23874-23881.
- Stein, J.C. and Nasrallah, J.B. (1993). A plant receptor-like gene, the *S*-locus receptor kinase of *Brassica oleracea* L. encodes a functional serine threonine kinase. *Plant Physiology* **101**, 1103-1106.
- Stein, J.C., Howlett, B., Boyes, D.C., Nasrallah, M.E. and Nasrallah, J.B. (1991). Molecular cloning of a putative receptor protein kinase gene encoded at the self-incompatibility locus of *Brassica oleracea*. *Proceedings of the National Academy of Sciences, USA*, **88**, 8816-8820.

- Stein, J.C., Dixit, R., Nasrallah, M.E. and Nasrallah, J.B. (1996). SRK, the stigma-specific S locus receptor kinase of *Brassica*, is targeted to the plasma membrane in transgenic tobacco. *The Plant Cell* **8**, 249-445.
- Stephenson A.G., Doughty, J., Dixon, S., Elleman, C., Hiscock, S. and Dickinson, H.G. (1997). The male determinant of self-incompatibility in *Brassica oleracea* is located in the pollen. *The Plant Journal* **12**, 1351-1359.
- Stephenson, A.G., Good, S.V. and Vogler, D.W. (2000). Interrelationships among inbreeding depression, plasticity in the self-incompatibility system, and the breeding system of *Campanula rapunculoides* L-(Campanulaceae) *Annals of Botany* **85 Supplement. A**, 211-219.
- Steven, J.C., Rooney, T.P., Boyle, O.D. and Waller, D.M. (2003). Density-dependent pollinator visitation and self-incompatibility in upper Great Lakes populations of *Trillium grandiflorum*. *Journal of the Torrey Botanical Society* **130**, 23-29
- Stevens, J.P. and Kay, Q.O.N. (1988). The number of loci controlling the sporophytic self-incompatibility system in *Sinapis arvensis* L. *Heredity* **61**, 411-418.
- Stevens, J.P. and Kay, Q.O.N. (1989). The number, dominance relationships and frequencies of self-incompatibility alleles in a natural population of *Sinapis arvensis* L. in South Wales. *Heredity* **62**, 199-205.
- Stone, J.L., Thomson, J.D. and Dentacosta, S.J. (1995). Assessment of pollen viability in hand pollination experiments – A review. *American Journal of Botany* **82**, 1186-1197.
- Stone, J.M. and Walker, J.C. (1995). Plant protein kinase families and signal transduction. *Plant Physiology* **108**, 451-457.
- Stone, J.M., Trotochaud, A.E., Walker, J.C. and Clark, S.E. (1998). Control of meristem development by CLAVATA1 receptor kinase and kinase-associated protein phosphatase interactions. *Plant Physiology* **117**, 1217-1225.
- Stone, S.L., Anderson, E.M., Mullen, R.T. and Goring, D.R. (1999). ARC1 is an E3 ubiquitin ligase and promotes the ubiquitination of proteins during the rejection of self-incompatible *Brassica* pollen. *The Plant Cell* **15**, 885-898.
- Stone, S.L., Anderson, Arnoldo, M. and Goring, D.R. (2003). A breakdown of *Brassica* self-incompatibility in ARC1 antisense transgenic plants. *Science* **286**, 1729-1731.
- Stout, A.B. (1918). Fertility in *Cichorium Intybus*: self-compatibility and self-incompatibility among offspring of self-fertile lines of descent. *Journal of Genetics* **7**, 71-103.
- Stout, A.B. (1920). Further experimental studies on self-incompatibility in hermaphrodite plants. *Journal of Genetics* **9**, 6-129.

- Stracke, S., Kistner, C., Yoshida, S., Mulder, L., Sato, S., Kaneko, T., Tabata, S., Sandal, N., Stougaard, J., Szczyglowski, K. and Parniske, M. (2002). A plant receptor-like kinase required for both bacterial and fungal symbiosis. *Nature* **417**, 959-961.
- Strother, J.L. and Panero, J.L. (2001). Chromosome studies: Mexican Compositae. *American Journal of Botany* **88**, 499-502.
- Stuessy, T.F. (1977). Heliantheae – systematic review in *The Biology and Chemistry of the Compositae*, Volume 2. V.H. Heywood, J.B. Harborne, B.L. Turner (eds.). London: Academic Press.
- Styles, T.B. (1993). Genus *Pinus*: A Mexican purview. In, *Biological diversity of Mexico: origins and distribution*. T.P. Ramamoorthy, R. Bye, A. Lot and J.E. Fa (eds.). New York: Oxford University Press. pp. 397-420.
- Sugiura, T (1936). Studies on the chromosome numbers of higher plants, with special reference to cytokinesis, I. *Cytologia* **7**, 543-595.
- Sun, X., Cao, Y., Yang, Z. Xu, C., Li, X., Wang, S. and Zhang, O. (2004). *Xa26*, a gene conferring resistance to *Xanthomonas oryzae* pv. *oryzae* in rice, encodes an LRR receptor kinase-like gene. *Plant Journal* **37**, 517-727.
- Suzuki, G., Watanabe, M., Kai, N., Matsuda, N., Toriyama K., Nishio, T., Takayama, S., Isogai, A., and Hinata, K. (1997). Three members of the *S* multigene family are linked to the *S* locus of *Brassica*. *Molecular and General Genetics* **256**, 257-264.
- Suzuki, G., Kai, N., Hirose, T., Fukui, K., Nishio, T., Takayama, S., Isogai, A., Watanabe, M. and Hinata, K. (1999). Genomic organization of the *S* locus: identification and characterization of genes in SLG/SRK region of S⁹ haplotype of *Brassica campestris* (syn. *rapa*). *Genetics* **153**, 391-400.
- Suzuki, G., Watanabe and M. and Nishio, T. (2000a). Physical distance between *S*-locus genes in various *S* haplotypes of *Brassica rapa* and *B. oleracea*. *Theoretical and Applied Genetics* **101**, 80-85.
- Suzuki, G., Kakizaki, T., Takada, Y., Shiba, H., Takayama, S., Isogai, A. and Watanabe, M. (2003). The *S* haplotypes lacking *SLG* in the genome of *Brassica rapa*. *Plant Cell Reports* **21**, 911-915.
- Suzuki, T., Kusaba, M., Matsushita, M., Okazaki, K. and Nishio, T. (2000b). Characterization of *Brassica S*-haplotypes lacking *S*-locus glycoprotein. *FEBS Letters* **482**, 102-108.
- Swofford, D.L. (2002). PAUP*. Phylogenetic Analysis Using Parsimony (*and Other Methods) Version 4. Sinauer Associates inc., Sunderland, MA.
- Sybenga, J. (1992). *Cytogenetics in Plant Breeding. Monographs on theoretical and applied genetics*. Berlin, Heidelberg, New York: Springer-Verlag.
- Sybenga, J. (1994). Preferential pairing estimates from multivalent frequencies in tetraploids. *Genome* **37**, 1045-1055.

- Sybenga, J. (1996). Chromosome pairing affinity and quadrivalent formation in polyploids: do segmental allopolyploids exist. *Genome* **39**, 1176-1184.
- Tabah, A., McInnis, S.M., Hiscock, S.J. (2004). Members of the *S*-receptor kinase multigene family in *Senecio squalidus* L. (Asteraceae), a species with sporophytic self-incompatibility. *Sexual Plant Reproduction* **17**, 131-140.
- Takahashi, T. Mu, J-H., Gasch, A. and Chua, N-H. (1998). Identification of PCR receptor-like protein kinases from *Arabidopsis* flowers. *Plant Molecular Biology* **37**, 587-596.
- Takasaki, T., Hatakeyama, K., Watanabe, M., Toriyama, K., Isogai, A. and Hinata, K. (1999). Introduction of SLG (*S* locus glycoprotein) alters the phenotype of endogenous *S* haplotype, but confers no new haplotype specificity in *Brassica rapa* L. *Plant Molecular Biology* **40**, 659-668.
- Takasaki, T., Hatakeyama, K., Suzuki, G., Watanabe, M., Isogai, A. and Hinata, K. (2000). The *S* receptor kinase determines self-incompatibility in *Brassica* stigma. *Nature* **403**, 913-915.
- Takayama, S., Isogai, A., Tsukamoto, C., Shiozawa, H., Ueda, Y., Hinata, K., Okazaki, K., Koseki, K. and Suzuki, A. (1989). Structures of *N*-glycosidic saccharide chains in *S*-glycoproteins, products of *S*-genes associated with self-incompatibility in *Brassica campestris*. *Agricultural and Biological Chemistry* **53**, 713-722.
- Takayama, S., Shiba, H., Iwano, M., Shimosato, H., Che, F-S., Kai, N., Watanabe, M., Suzuki, G., Hinata, K. and Isogai, A. (2000a). The pollen determinant of self-incompatibility in *Brassica campestris*. *Proceedings of the National Academy of Sciences of the United States of America* **97**, 1920-1925.
- Takayama, S., Shiba, H., Iwano, M., Asano, K., Hara, M., Che, F-S., Watanabe, M., Hinata, K. and Isogai, A. (2000b). Isolation and characterisation of pollen coat proteins of *Brassica campestris* that interact with *S* locus-related glycoprotein 1 involved in pollen-stigma adhesion. *Proceedings of the National Academy of Sciences of the United States of America* **97**, 3765-3770.
- Takayama, S., Shimosato, H. Shiba, H., Funato, Che, F-S., Watanabe, M., M. Iwano, and Isogai, A. (2001). Direct ligand receptor complex interaction controls *Brassica* self incompatibility *Nature* **413**, 534-538.
- Talavera, S., Gibbs, P. E., Fernández-Piedra, M. P. and Ortiz-Herrera, M. A. (2001). Genetic control of self-incompatibility in *Anagallis monelli* (Primulaceae: Myrsinaceae). *Heredity* **87**, 589.
- Tandon, R., Manohara, T.N., Nijalingappa, H.M. and Shivanna, K.R. (2001). Pollinations and pollen-pistil interaction in Oil Palm, *Elaeis guineensis*. *Annals of Botany* **87**, 831-832.

- Tangmitcharoen, S. and Owens, J.N. (1997). Pollen viability and pollen-tube growth following controlled pollination and their relation to low fruit production in teak (*Tectona grandis* Linn. f.). *Annals of Botany* **80**, 401-410.
- Tantikanjana, T., Nasrallah, M.E., Stein, J.C., Chen, H-H. and Nasrallah, J.B. (1993). An alternative transcript of the *S* locus glycoprotein gene in a class II pollen-recessive self-incompatibility haplotype of *Brassica oleracea* encodes a membrane-anchored protein. *The Plant Cell* **5**, 657-666.
- Tao, R., Yamane, H., Sassa, H., Mori, H., Gradziel, T.M., Dandekar, A.M. and Sugiura, A. (1997). Identification of stylar RNases associated with gametophytic self-incompatibility in almond (*Prunus dulcis*). *Plant Cell Physiology* **38**, 304-311.
- Tao, R., Yamane, H., Murayama, H., Sassa, H., Mori, H. and Sugiura, A. (1999). Molecular typing of *S*-alleles through identification, characterization and cDNA cloning for *S*-RNases in sweet cherry. *Journal of the American Society of Horticultural Science* **124**, 224-233.
- Tatusaov, R.L., Natsle, D.A. Garkavtsev, I.V. a, T.A., Shankavaram, U.T. and Rao, B.S (2001). The COG database: new developments in phylogenetic classification of proteins from complete genomes. *Nucleic Acids Research* **29**, 22-28.
- Terryn, N. and Rouzé, P. (2000). The sense of naturally transcribed antisense RNAs in plants. *Trends in Plant Science* **5**, 394-396.
- Thomas, S.G. and Franklin-Tong, V.E. (2004). Self-incompatibility triggers programmed cell death in *Papaver* pollen. *Nature* **249**, 305-309.
- Thompson, K.F. and Taylor, J.P. (1966a). Non-linear dominance relationships between *S* alleles. *Heredity* **21**, 347-362.
- Thompson, K.F. and Taylor, J.P. (1966b). The breakdown of self-incompatibility in cultivars of *Brassica oleracea*. *Heredity* **21**, 637-648.
- Thompson, M. M. (1979). Genetics of incompatibility in *Corylus avellana*. *Theoretical and Applied Genetics* **54**, 113-116.
- Thomson, J.D., Rigney, L.P., Karoly, K.M. and Thomson, B.A. (1994). Pollen viability, vigor and competitive ability in *Erythronium grandiflorum* (Liliaceae). *American Journal of Botany* **8**, 1257-1266.
- Thormann, C.E., Ferreira, M.E., Camargo, L.E.A., Tivang, J.G. and Osborn, T.C. (1994). Comparison of RFLP and RAPD markers to estimating genetic relationships within and among cruciferous species. *Theoretical and Applied Genetics* **88**, 973-980.
- Tobias, C.M. and Nasrallah, J.B. (1996). An *S* locus-related gene in *Arabidopsis* encodes a functional kinase and produces two classes of transcript. *The Plant Journal* **10**, 523-531.

- Tobias, C.M. Howlett, B. and Nasrallah, J.B. (1992). An *Arabidopsis thaliana* gene with sequence similarity to the S-locus receptor kinase of *Brassica oleracea*. *Plant Physiology* **99**, 284-290.
- Toledo, V.M. (1985). *A critical evaluation of the floristic knowledge in Latin America and the Caribbean*. A report presented to The Nature Conservancy International Program. Washington, D.C.
- Toledo, V.M. (1995). Los habitats naturales de México: una visión sintética. In, *Fauna mexicana en peligro de extinción*, G. Ceballos and D. Navarro (eds.). Mexico, D.F: UNAM.
- Toledo, V.M. and Ordóñez, M. de J. (1993). The biodiversity scenarios of Mexico: an analysis of terrestrial habitats. In, *Biological diversity of Mexico: origins and distribution*. T.P. Ramamoorthy, R. Bye, A. Lot and J.E. Fa (eds.). New York: Oxford University Press. pp. 757-777.
- Toledo, V.M. and Sosa, V. (1993). Floristics in Latin America and the Caribbean: an evaluation of plant collections and botanists. *Taxon* **42**: 355-364.
- Toledo, V.M., Carabias, J., Toledo, C. and González-Pacheco, C. (1989). *La producción rural en México: alternativas ecológicas*. Fundación Universo Veintiuno, Mexico, D.F.
- Tori, K.U. (2000). Receptor kinase activation and signal transduction in plants: an emerging picture. *Current Opinion in Plant Breeding* **3**, 361-367.
- Torii, K.U. and Clark, S. (2000). Receptor-like kinases in plant development. *Advances in Botanical Research* **32**, 235-267.
- Torii, K.U., Mitsukawa, N., Oosumi, T., Matsuura, Y., Yokoyama, R., Whittier, R.F. and Komeda Y. (1996). The *Arabidopsis ERECTA* gene encodes a putative receptor protein kinase with extracellular leucine-rich repeats. *The Plant Cell* **8**, 735-745.
- Trick, M. and Flavell, R.B. (1989). A homozygous *S* genotype of *Brassica oleracea* expresses two S-like genes. *Molecular and General Genetics* **218**, 112-117.
- Trick, M. and Heizmann, P. (1992). Sporophytic self-incompatibility systems: *Brassica* S gene family. *International Review of Cytology* **140**, 485-524.
- Trognitz, B.R. (1991). Comparison of different pollen viability assays to evaluate pollen fertility of potato dihaploids. *Euphytica* **66**, 143-148.
- Trotochaud, A.E., Hao, T., Wu, G., Yang, Z. and Clark, S.E. (1999). The CLAVATA1 receptor-like kinase requires CLAVATA3 for its assembly into a signalling complex that includes KAPP and a Rho-related protein. *The Plant Cell* **11**, 393-405.

- Trotochaud, A.E., Hao, T., Wu, G., Yang, Z. and Clark, S.E. (2000). CLAVATA3, a multimeric ligand for the CLAVATA1 receptor kinase. *Science* **289**, 613-616.
- Tsukamoto, T., Ando, T., Kokubun, H., Watanabe, H., Masada, M., Zhu, X., Marchesi, E. and Kao, T. H (1999). Breakdown of self-incompatibility in a natural population of *Petunia axillaris* (Solanaceae) in Uruguay containing both self-incompatible and self-compatible plants. *Sexual Plant Reproduction* **12**, 6-13.
- Tsukamoto, T., Ando, T., Kokubun, H., Watanabe, H., Sato, T., Masada, M., Marchesi, E. and Kao, T.H (2003). Breakdown of self-incompatibility in a natural population of *Petunia axillaris* caused by a modifier locus that suppresses the expression of an S-RNase gene. *Sexual Plant Reproduction* **15**, 255-263. 2003.
- Tsuruhara A, Tezuka T (2001). Relationship between the self-incompatibility and cAMP level in *Lilium longiflorum*. *Plant and Cell Physiology* **42**, 1234-1238.
- Turner, B.L. and Flyr, D. (1966). Chromosome numbers in the Compositae. X. North American species. *American Journal of Botany* **53**, 24-33.
- Turner, B.L., Powell, A.M. and Watson, T.J. (1973). Chromosome numbers in Mexican Asteraceae. *American Journal of Botany* **60**, 592-596.
- Turner, B.L. (1977a). Fossil history and geography. *The Biology and Chemistry of the Compositae*, Volume 1. V.H. Heywood, J.B. Harborne, B.L. Turner (eds.). London: Academic Press.
- Turner, B.L. (1977b). *Henricksonia* (Asteraceae-Coreopsidinae), a newly discovered genus with a paleaceous pappus from north-central Mexico. *American Journal of Botany* **64**, 78-80.
- Turner, B.L. Bacon, J., Urbatsch, L. and Simpson, B. (1979). Chromosome numbers in the South-American Compositae. *American Journal of Botany* **66**, 173-178.
- Turner, B.L. and Nesom, G.L. (1993). Biogeography, diversity, and endangered or threatened status of Mexican Asteraceae. In, *Biological diversity of Mexico: origins and distribution*. T.P Ramamoorthy, R. Bye, A. Lot. and J.E. Fa (eds.). New York: Oxford University Press. pp. 559-575.
- Turner, B.L., Powell, A.M. and Watson, Jr. T.J (1973). Chromosome numbers in Mexican Asteraceae. *American Journal of Botany* **60**, 592-596.
- Turner, B.L., Bacon, J. Urbatsch, L and Simpson B. (1979). Chromosome numbers in South American Compositae. *American Journal of Botany* **66**, 173-178.
- Ushijima, K., Sassa, H., Tao, R., Yamane, H., Dandekar, A.M., Gradziel, T.M., and Hirano, H. (1998). Cloning and characterization of cDNAs encoding S-RNases from almond (*Prunus dulcis*): primary structural features and sequence diversity of the S-RNases in Rosaceae. *Molecular and General Genetics* **241**, 17-25.

- Valdés-Reyna, J. and Cabral-Cordero, I. (1993). Chorology of Mexican grasses. In, *Biological diversity of Mexico: origins and distribution*. T.P. Ramamoorthy, R. Bye, A. Lot and J.E. Fa (eds.). New York :Oxford University Press. pp. 439-446.
- Van der Geer, P. and Hunter, T. (1993). Mutation of Tyr 697, a GRB2-binding site, and Tyr 721, a PI 3-kinase binding site, abrogates signal transduction by the murine CSF-1 receptor expressed in Rat-2 fibroblast. *The EMBO Journal* **12**, 5161-5172.
- Van der Geer, P., Hunter, T. and Lindberg, R.A. (1994). Receptor protein tyrosine kinases and their signal transduction pathways. *Annual Review of Cell Biology* **10**. 251-337.
- van der Knaap, E., Sauter, M., Wilford, R. and Kende, H. (1996). Identification of a gibberellin-induced receptor-like kinase in deepwater rice (Accession no. Y07748) (PGR96-100). *Plant Physiology* **112**, 1397.
- van der Knaap, E., Song, W.Y., Ruan, D.L., Sauter, M., Ronald, P.C. and Kende, H. (1999). Expression of a gibberellin-induced leucine-rich repeat receptor-like kinase in deepwater rice and its interaction with kinase-associated protein phosphatase. *Plant Physiology* **120**, 559-569.
- Vanoosthuysse, V. Tichtinsky, G. Dumas, C., Gaude, T. and Cock, J.M. (2003). Interaction of Calmodulin, a sorting nexin and kinase-associated protein phosphatase with *Brassica oleracea* S locus receptor kinase. *Plant Physiology* **133**, 919-929.
- Varotto, S., Pizzoli, M., Lucchin, M. and Parrini, P. (1995). The incompatibility system in Italian red chicory (*Cichorium intybus* L.) *Plant Breeding* **114**, 535-538.
- Vassiliadis, C., Lepart, J., Saumitou-Laprade, P. and Vernet, P. (2000). Self-incompatibility and male fertilization success in *Phillyrea angustifolia* (Oleaceae) *International Journal of Plant Sciences* **161**, 393-402.
- Verica, J and He, Z-H. (2002). The cell wall-associated kinase (WAK) and WAK-like kinase gene family. *Plant Physiology* **129**, 455-459.
- Villaseñor, J.L. (1991). Las Heliantheae endemics a Mexico: una guia hacia la conservacion. *Acta Botanica Mexicana*. **15**: 29-46.
- Villaseñor, J.L. (1994). The Asteraceae of Mexico. Its present knowledge based on activities carried out by the National herbarium of Mexico. (Abstract 56). In, D.J.N. Hind (coordinator). *Abstracts of the International Compositae Conference*, Kew: Royal Botanic Gardens, Kew.
- Vinckier, S. and Smets, E. (2003). Morphological and ultrastructural diversity of orbicles in Gentianaceae. *Annals of Botany* **92**, 657-672.
- Vithanage, H.I.M.V. and Knox, R.B. (1977). Development and cytochemistry of stigma surface and response to self and foreign pollination in *Helianthus annuus*. *Phytomorphology* **27**, 168-179.

- Vithanage, H.I.M.V. and Knox, R.B. (1979). Pollen development and quantitative cytochemistry of exine and intine enzymes in sunflower *Helianthus annuus* L. *Annals of Botany* **44**, 95-106.
- Vithanage, H.I.M.V. Howlett, B.J., Jobson, S. and Knox, R.B. (1982). Immunocytochemical localization of water-soluble glycoproteins, including group 1 allergen, in pollen of ryegrass, *Lolium perenne*, using ferritin-labelled antibody. *Histochemical Journal* **14**, 949-966.
- Voß, A. (1894). *Vilmorin's Blumengärtnerei*. Berlin: Paul Parey Volume 1, p.485-486.
- Wagstaff, S.J. and Breitwieser, I. (2002). phylogenetic relationships of New Zealand Asteraceae inferred from ITS sequences. *Plant Systematics and Evolution* **231**, 203-224.
- Walker, J.C. (1993). Receptor-like protein kinase genes of *Arabidopsis thaliana*. *The Plant Journal* **3**, 451-456.
- Walker, J.C. (1994). Structure and function of the receptor-like proteins kinases of higher plants. *Plant Molecular Biology* **26**, 1699-1609.
- Walker, J.C. and Zhang, R. (1990). Relationship of a putative receptor protein kinase from maize to the *S*-locus glycoprotein of *Brassica*. *Nature* **345**, 743-746.
- Wang, A., Xia, Q., Xie, W., Datla, R. and Selvaraj, G. (2003). The classical Ubisch bodies carry a sporophytically produced structural protein (RAFTIN) that is essential for pollen development. *Proceedings of the National Academy of Sciences of the United States of America* **100**, 14487-14492.
- Wang, C-H' Möller' M. and Cronk' QCB. (2004). Aspects of sexual failure in the reproductive processes of a rare bulbiferous plant, *Titanotrichum oldhamii* (Gesneriaceae), in subtropical Asia. *Sexual Plant Reproduction* **17**, 23 – 31.
- Wang, G.L., Ruan, D-L., Song, W-Y., Sideris, S., Chen, L., Pi, L-Y., Zhang, S., Zhang, Z., Fauquet, C., Gaut, B.S., Whalen, M.C. and Ronald, P.C. (1998). *Xa21D* encodes a receptor-like molecule with a leucine-rich repeat domain that determines race-specific recognition and is subject to adaptive evolution. *The Plant Cell* **10**, 765-779.
- Wang, T-W., Balsamo, R.A., Ratnayake, C. Platt, K.A., Ting, J.T.L. and Huang, A.H.C. (1997). Identification, subcellular localisation and developmental studies of oleosins in the anther of *Brassica napus*. *Plant Journal* **11**, 475-487.
- Wang, X., Zafian, P., Choudhary, M. and Lawton, M. (1996). The PR5K receptor protein kinase from *Arabidopsis thaliana* is structurally related to a family of plant defense proteins. *Proceedings of the National Academy of Sciences of the United States of America* **93**, 2598-2602.

- Ward, C.W., Hoyne, P.A. and Flegg, R.H. (1995). Insulin and epidermal growth factor receptors contain the cysteine repeat motif found in the tumor necrosis factor receptor. *Proteins: Structure, Function and Genetics* **22**, 141-153.
- Warwick, S.I. and Black, L.D. (1991). Molecular systematics of *Brassica* and allied genera (subtribe Brassicinae, Brassiceae) – Chloroplast genome and cytodeme congruence. *Theoretical and Applied Genetics* **82**, 81-92.
- Watanabe, M., Takasaki, T., Toriyama, K., Yamakawa, S., Isogai, A., Suzuki, A. and Hinata, K. (1994). A high degree of homology exists between the protein encoded by *SLG* and the S receptor domain encoded by *SRK* in self-incompatible *Brassica campestris* L. *Plant Cell Physiology* **35**, 1221-1229.
- Watanabe, M., Suzuki, G., Takayama, S., Isogai, A. and Hinata, K. (2000). Genomic organization of the *SLG/SRK* region of the *S*-locus in *Brassica* species. *Annals of Botany*, **85 supplement A**, 155-160.
- Wehling, P., Hackauf, B. and Wricke, G. (1995). Characterization of the two-factor self-incompatibility system in *Secale cereale* L. *Advances in Plant Breeding* **18**, 149-161.
- Weiblen, G.D. and Brehm, B.G. (1996). Reproductive strategies and barriers to hybridization between *Tellima grandiflora* and *Tolmeia menziesii* (Saxifragaceae) *American Journal of Botany* **83**, 910-918.
- Weiss, H. and Maluszynska, J. (2000). Chromosomal rearrangement in autotetraploid plants of *Arabidopsis thaliana*. *Hereditas* **133**, 255-261.
- Wells, R., Gilboa, L., Sun, Y., Liu, X., Henis, Y.I. and Lodish, H.F. (1999). Transforming growth factor- β induces formation of a dithiothreitol-resistant Type I/Type II receptor complex in live cells. *Journal of Biochemistry* **274**, 5716-5722.
- Wendel, J.F. (2000). Genome evolution in plants. *Plant Molecular Biology* **42**, 225-249.
- White, S.E., Habera, L.F. and Wessler, S.R. (1994). Retrotransposons in the flanking regions of normal plant genes: A role for *copia*-like elements in the evolution of gene structure and expression. *Proceedings of the National Academy of Sciences of the United States of America* **91**, 11792-11796.
- Whitkus, R., Doebley, J. and Lee, M. (1992). Comparative mapping of sorghum and maize. *Genetics* **132**, 119-1130.
- Wilkinson, K. (1999). Ubiquitin-dependent signalling: the role of ubiquitination in the response of cells to their environment. *Journal of Nutrition* **129**, 1933-1936.
- Wilkinson, T., Wetten, A. and Fay, M.F. (1998). Cryopreservation of *Cosmos atrosanguineus* shoot tips by a modified encapsulation/dehydration method. *Cryo-Letters* **19**, 293-302.

- Wilkinson, T.; Wetten, A. Prychid, C. and Fay, M.F (2003). Suitability of cryopreservation for the long-term storage of rare and endangered plant species: a case history for *Cosmos atrosanguineus*. *Annals of Botany* **91**, 65-74.
- Williams, L.O. (1956). An enumeration of the Orchidaceae of Central America, British Honduras, and Panama. *Ceiba* **5**, 1-256.
- Wistow, G.J., Mulders, J.W.M. and de Jong, W.W. (1987). The enzyme lactate dehydrogenase as a structural protein in avian and crocodilian lenses. *Nature* **326**, 622-624.
- Wrana, J.L. Attisano, L., Wieser, R., Ventura, F. and Massagué, J (1994). Mechanism of activation of the TGF- β receptor. *Nature* **370**, 341-346.
- Xu, B.B., Mu, J.H., Nevins, D.L., Grun, P. and Kao T-h (1990). Cloning and sequencing of cDNAs encoding 2 self-incompatibility associated proteins in *Solanum chacoense*. *Molecular and General Genetics* **224**, 341-346.
- Xue, Y.B, Carpenter, R., Dickinson, H.G. and Coen, E.S. (1996). Origin of allelic diversity in *Antirrhinum S* locus RNases. *The Plant Cell* **8**, 805-814.
- Yacine, A. and Bouras, F. (1997). Self- and cross-pollination effects on pollen tube growth and seed set in holm oak *Quercus ilex* L (Fagaceae). *Annales Des Sciences Forestieres* **54**, 447-462.
- Yamamuro, C., Ihara, Y. Wu, X., Noguchi, T., Fujioka, S., Takasuto, S., Ashikari, M. Kitano, H. and Matsuoka, M. (2000). Loss of function of a rice *brassinosteroid insensitive 1* homology prevents internode elongation and bending of the lamina joint. *The Plant Cell* **12**, 1591-1605.
- Yamakawa, S., Shiba, H., Watanabe, M., Shiozawa, H. Takayama, S., Hinata, K., Isogai, A. and Suzuki, A. (1994). The sequences of S-glycoproteins involved in self-incompatibility of *Brassica campestris* and their distribution among Brassicaceae. *Bioscience, Biotechnology and Biochemistry* **58**, 921-925.
- Yamakawa, S., Watanabe, M., Hinata, K., Suzuki, A. and Isogai, A. (1995). The sequences of S-receptor kinases (SRK) involved in self-incompatibility and their homologies to S-locus glycoproteins of *Brassica campestris*. *Bioscience, Biotechnology and Biochemistry* **59**, 161-162.
- Yang, Y-W., Lai, K-N., Tai, P-Y., Ma, D-P. and Li, W-H. (1999). Molecular phylogenetic studies of *Brassica*, *Rorippa*, *Arabidopsis* and allied genera based on the internal transcribed spacer region of 18S-25S rDNA. *Molecular Phylogenetics and Evolution* **13**, 455-462.
- Young A., Miller, C., Gregory, E. and Langston, A. (2000). Sporophytic self-incompatibility in diploid and tetraploid races of *Rutidosia leptorrhynchoides* (Asteraceae) Australian Journal of Botany **48**, 667-672.

- Young, A.G., Hill, J.H., Murray, B.G. and Peakall, R. (2002). Breeding system, genetic diversity and clonal structure in the sub-alpine forb *Rutidosia leiolepis* F. Muell. (Asteraceae) *Biological Conservation* **106**, 71-78.
- Zhou, J., Wang, F., Ma, W., Zhang, Y., Han, B. and Xue, Y. (2003). Structural and transcriptional analysis of *S*-Locus F-box genes in *Antirrhinum*. *Sexual Plant Reproduction* **16**, 165-167.
- Zhou, S.L., Hong, D.Y. and Pan, Y.K. (1999). Pollination biology of *Paeonia jishanensis* T. Honf & W.Z. Zhao (Paeoniaceae) with special emphasis on pollen and stigma biology. *Botanical Journal of the Linnean Society* **130**, 43-52.
- Zhao, Y., Feng, X.H., Watson, J.C., Bottino, P.J. and Kung, S.D. (1994). Molecular cloning and biochemical characterization of a receptor-like serine-threonine kinase from rice. *Plant Molecular Biology* **26**, 791-803.
- Zimmer, K. (1988). Photoperiodic responses of *Cosmos bipinnatus*. *Gartenbauwissenschaft* **53** 257-260.
- Zinkl, G.M., Zwiebel, B.I., Grier, D.G. and Preuss, D. (1999). Pollen-stigma adhesion in *Arabidopsis*: a species-specific interaction mediated by lipophilic molecules in the pollen exine. *Development* **126**, 5431-5440.
- Zuberi, M.I. and Lewis, D. (1988). Gametophytic-sporophytic incompatibility in the Cruciferae-*Brassica campestris*. *Heredity* **61**, 367-377.
- Zunk, K., Mummenhoff, K., Koch, M. and Hurka, H. (1996). Phylogenetic relationships of *Thlaspi s.l.* (subtribe Thlaspidinae, Lepidieae) and allied genera based on chloroplast DNA restriction-site variation. *Theoretical and Applied Genetics* **92**, 375-381.
- Zwierzykowski, Z., Tavyar, R. Brunnell, M. and Lukaszewski, A.J. (1998). Genome recombination in intergeneric hybrids between tetraploid *Festuca pratensis* and *Lolium multiflorum*. *Journal of Heredity* **89**, 324-328.

APPENDIX 1 - Names descriptions and abbreviations of RLKs, RTKs and associated molecules

Acronym	Full Name	Description of Protein
ARK1 to 3	Arabidopsis Receptor Kinase 1 to 3	S-domain transmembrane serine/threonine receptor kinases in <i>Arabidopsis thaliana</i> .
ARC1	Arm-Repeat-Containing protein 1	ARC1 is a modular protein of 661 amino acids expressed specifically in <i>Brassica stigmas</i> and shown to interact with the kinase domain of <i>Brassica</i> SRKs in a phosphorylation-dependent manner.
AtGRP-3	Arabidopsis thaliana Glycine-Rich Protein-3	AtGRP-3 is a 48-kDa protein of the GRP glycine-rich protein family. AtGRP-3 is a putative cell-wall protein with a high glycine (31%) content. AtGRP-3 positively regulates <i>wak1</i> by binding to the WAK1 cell-wall domain in a pathogenesis-related manner.
BAK1	BRI1-Associated Receptor Kinase	An LRR II receptor kinase with a short LRR extracellular domain containing five LRR motifs and lacks the 70 amino acid island characteristic of BRI1 homologues. In <i>Arabidopsis</i> , BAK1 physically interacts with BRI1.
BL	Brassinolide	A C-28 polyhydroxy-steroid with an unusual lactone B-ring structure; one of the most bioactive BRs (Brassinosteroids) in plants.
BR	BRASSINOSTEROID	Plant steroid hormones essential for normal plant growth.
BRI1	BRASSINOSTEROID INSENSITIVE 1	A transmembrane serine/threonine receptor kinase with LRR extracellular domain containing 25 LRR motifs and a 70 AA island between the 22 nd and 23 rd LRR repeat. BRI1 is a putative BR receptor.
BRS1	BRASSINOSTEROID 1	A secreted serine carboxypeptidase involved early in the BRI1 signalling pathway in <i>Arabidopsis thaliana</i> .
CHRK1	Chitinase-like Receptor Kinase	A transmembrane receptor kinase of <i>Nicotiana tabacum</i> that has an ectodomain closely related to the class-V chitinases of tobacco, and microbial chitinases.
CSF-1	Colony Stimulating Factor 1	A PDGF β (platelet-derived growth factor- β) protein needed for the proliferation of myeloid precursor cells and their differentiation into macrophages.

CLV1	CLAVATA1	LRR extracellular domain transmembrane serine/threonine receptor kinase required for the proper balance between cell proliferation, differentiation and organ formation in <i>Arabidopsis</i> shoot and flower meristems.
CLV2	CLAVATA2	A receptor-like protein (RLP) with an LRR extracellular domain and a very short non-catalytic cytoplasmic tail.
CLV3	CLAVATA3	A small secreted protein. CLV3 is the ligand of CLV1 and is required for the active CLV1 receptor complex.
CR4	CRINKLY4	TNFR-like receptor serine/threonine receptor kinase involved in epidermal differentiation in <i>Zea mays</i> .
ER	ERECTA	LRR extracellular domain transmembrane serine/threonine receptor kinase required for appropriate organ shape in <i>Arabidopsis</i> .
FLS2	<u>FLAGELLIN SENSITIVITY 2</u>	A transmembrane serine/threonine receptor kinase with an LRR extracellular domain associated with sensing bacterial flagellin and inducing pathogenesis-related responses in <i>Arabidopsis</i> .
HAESA	(formerly RLK5)	A transmembrane serine/threonine receptor kinase with LRR extracellular domain, required for floral abscission in <i>Arabidopsis</i> .
HAR1 gene	Hypernodulation aberrant root 1 gene	<i>HAR1</i> controls the autoregulation of nodulation in legumes whereby earlier nodulation events in legume roots inhibit nodulation in younger root tissue.
HAR1	<i>HAR1</i> protein product	A transmembrane serine/threonine receptor kinase with LRR extracellular domain, required for autoregulation of nodulation in legumes.
ISG1-3	Ipomoea S-domain like Glycoprotein 1-3	S-domain like secreted glycoproteins found in <i>Ipomoea trifida</i> .
IRK1-2	Ipomoea Receptor Kinases 1 & 2	S-domain transmembrane serine/threonine receptor kinases found in <i>Ipomoea trifida</i> .
KAPP	Kinase Associated Protein Phosphatase	Protein phosphatase that interact via their KI domains with receptor kinases. KAPP molecules have been isolated from <i>Arabidopsis thaliana</i> and <i>Zea mays</i> .
KI	Kinase interaction domain	The kinase interaction (KI) domain occurs in KAPP molecules. In <i>Arabidopsis thaliana</i> , the KI of KAPP interacts with a phosphorylated form of RLK5 (now known as HAESA) and WAK1. In <i>Zea mays</i> , the KI domain of KAPP interacts with KIK1.

KIK1	KI interacting Kinase 1	S-domain transmembrane serine/threonine receptor kinase found in <i>Zea mays</i> that interacts with the KI domain of KAPP.
LB	Leghaemoglobin	A haemoglobin compound found in legumes that functions as an oxygen buffer in mature nodules and has additional roles in the early detection of Nod factors.
LecRK1	Lectin-like Receptor Kinase	Serine/threonine transmembrane receptor kinase with extracellular domain similar to carbohydrate-binding proteins of the legume lectin family first isolated in <i>Arabidopsis thaliana</i> .
LTK1-3	Leucine-rich repeat Transmembrane Kinase	LRR-transmembrane serine/threonine receptor kinases with putative functions in endosperm development in <i>Zea mays</i> seeds.
MLPK	<i>M</i> locus protein kinase	MPLK is receptor-like cytoplasmic kinase (RLCK) that has no apparent signal sequence or transmembrane domain and exhibits autophosphorylation at specific serine and threonine residues. MLPK is localised to the plasma membrane of <i>Brassica</i> stigma cells and positively regulates <i>Brassica</i> SI through down-stream mediation of SRK signalling. Its expression in the stigmas increases with the onset of self-incompatibility and reaches a maximum one day before anthesis.
MRLK	Meristem Receptor-Like Kinase	LRR-transmembrane serine/threonine receptor kinases with putative functions in transitions from vegetative to flowering stage in <i>A. thaliana</i> .
NARK	Nodule Autoregulation Receptor Kinase	LRR-transmembrane serine/threonine receptor kinases identified initially in soybean (GmNARK for <i>Glycine max</i> Nodule Autoregulation Receptor Kinase) shown to control autoregulation of nodulation (AON). NARK corresponds in function with HAR1.
NF or Nod factors	Nodulation factors	Symbiotic signalling compounds identified as lipochitin oligosaccharides that are synthesized by rhizobia and induce root hair deformation.
NORK	Nodulation Receptor Kinase	LRR-transmembrane serine/threonine receptor kinases with functions in the Nod-factor perception/transduction system that initiates a signal cascade leading to nodulation in <i>Medicago sativa</i> and other legumes.
OsBRI1	<i>Oryza sativa</i> Brassinosteroid Insensitive 1	The rice homologue of BRI1.

OsPK10	<i>Oryza sativa</i> protein kinase 10	S-domain transmembrane serine/threonine receptor kinase found in rice (<i>Oryza sativa</i>).
PH domains	Pleckstrin Homology domains	PH domains consist of ~120 amino-acid residues. PH domains bind phospholipids allowing association of the molecule containing the PH domain with the cytoplasmic face of the plasma membrane.
PnLPK	<i>Poplar nigra</i> var. <i>italica</i> Lectin-like Protein Kinase	A poplar homologue of the Ath.LecRK1 (<i>Arabidopsis thaliana</i> LecRK1).
PRs	Pathogenesis-Related proteins	Plant defence proteins which are expression products of <i>PR</i> genes that control resistance to specific plant infections.
PR5K	PR5-like Receptor Kinase	Serine/threonine transmembrane receptor kinase in <i>Arabidopsis thaliana</i> that has an extracellular domain similar to PR5 (pathogenesis related protein 5).
PsBRI1	<i>Pisium sativum</i> Brassinosteroid Insensitive 1	The pea homologue of BRI1.
PTB	Phosphotyrosine binding domain	PTB domains are made up of ~150 amino-acid residues. PTB domains interact in a phosphorylation-dependent manner with 1-8 residues upstream towards the N-terminal region of P.Tyr residue in proteins that contain the general consensus sequence Asn-Pro-X-Tyr. Some PTBs bind this consensus sequence in a phosphorylation-independent manner.
RLK1 & 4	Receptor-Like Kinases 1 & 4	S-domain transmembrane serine/threonine receptor kinases found in <i>Arabidopsis thaliana</i> .
RLK11	Receptor-Like Kinase 11	LRR-transmembrane serine/threonine receptor kinase isolated from <i>Oryza sativa</i> .
SCR	S-locus Cysteine-Rich Protein	The male determinant of self-incompatibility in <i>Brassica</i> . The putative ligand for SRK.
SERK	Somatic Embryogenesis Receptor Kinase	LRR-transmembrane serine/threonine receptor kinase that is associated embryogenic competence or potential of somatic cells.
SFR1-3	S-gene Family Receptor kinases 1-3	S-domain transmembrane serine/threonine receptor kinases found in <i>Brassica oleracea</i> .
SLG	S-Locus Glycoprotein	A secreted glycoprotein that contains the characteristic features of S-domains. SLG was the first S-domain to be fully described and from which the S-domain was named.

SH2 domain	Scr homology 2 domain	SH2 domains are made up of ~100 amino-acid residues. SH2 domains react in a sequence specific manner with proteins that contain a P.Tyr residue embedded in a specific sequence. Usually between 1-5 residues on the C-terminal side of the P.Tyr are recognised. SH2 interacts in a phosphorylation-dependent manner.
SH3 domain	Scr homology 3 domain	SH3 domains are made up of ~60 amino-acid residues. SH3 domains react in a sequence specific but phosphorylation-independent manner. SH3 domains bind to proteins that have short sequences containing Pro-X-X-Pro.
SLR	S-Locus Related glycoprotein	A secreted glycoprotein that contains the characteristic features of S-domains.
SR160	System Receptor 160	LRR-transmembrane serine/threonine receptor kinase isolated from <i>Lycopersicon peruvianum</i> that is the putative receptor for the plant polypeptide wound signal systemin.
SRK	S-Receptor Kinase	S-domain transmembrane serine/threonine receptor kinase. SRK is the female component of the self-incompatibility response in <i>Brassica</i> and is the putative receptor molecule for SCR.
SYMRK	Symbiosis Receptor-like Kinase	A NORK homologue. SYMRK is an LRR-transmembrane serine/threonine receptor kinase isolated from the legumes <i>Lotus japonicus</i> and <i>Pisium sativum</i> , and is required for bacterial and fungal symbiosis.
SYM29	Symbiosis 29 gene receptor kinase	The pea orthologue of HARI1.
tBRI1	tomato Brassinosteroid Insensitive 1	The tomato homologue of BRI1.
TβR I	TGF- β type I receptor	A type-I transmembrane serine/threonine receptor kinase that forms the TGF- β receptor complex with T β R II after binding of the TGF- β ligand with T β R-II.
TβR II	TGF- β type II receptor	A type-II transmembrane serine/threonine receptor kinase for the transforming growth factor- β (TGF- β) peptide growth-factor signalling molecule.
TβR III	Betaglycan	A membrane-anchored proteoglycan TGF- β type-III receptor that presents TGF- β ligand to T β R-II receptor.

TGF-β	Transforming growth factor β	Transforming growth factor- β (TGF- β) is a peptide growth-factor signalling molecule ligand of the T β R-II receptor.
WAK1-5	Wall Associated Kinases 1-5	EGF (epidermal growth factor-containing domain) serine/threonine receptor kinase isoforms found in <i>Arabidopsis thaliana</i> . WAKs are cell-wall associated receptor kinases that link the plasma membrane to the extracellular membrane.
WLRK	Wheat Leaf Receptor Kinase	Serine/threonine transmembrane receptor kinase encoded by <i>Lrk10</i> that is located at the leaf rust <i>Lr10</i> (Leaf resistant 10) disease resistance locus in wheat.
XA21	<i>Xanthomonas</i> 21	A transmembrane serine/threonine receptor kinase with LRR extracellular domain that bestows resistance to the <i>Xanthomonas oryzae</i> pv. <i>oryzae</i> race 6 (<i>Xoo</i>).
ZmPK1	Zea mays Protein Kinase 1	S-domain transmembrane serine/threonine receptor kinases of <i>Zea mays</i> .

APPENDIX 2 – The Story of *Cosmos atrosanguineus*

2.1 – Life and times of Benedict Roezl

(a) – Reproduction of an article on the life of Benedict Roezl printed in *The Gardeners Chronicle*, July 18, 1874. (p.73),

JULY 18, 1874.] THE GARDENERS' CHRONICLE. 73

lined three such boxes on the top of each other, covering the top of all with a thick board, and the bottom resting on the ordinary foot-board. I have had some of these in use for some time, and am so far satisfied with them that I do not intend to change them until I see some very promising thing turn up. I can take off the top division pretty easily, and if the whole box is pretty full there will not be many bees in the top. I put on an empty one where I take the fall one off, but perhaps it is better to add the empty one below, and screw the top board on what was before the second division. So much for my general experience. Another time I will give you a few more particulars. G. S.

ANNUALS FOR BEE-KEEPERS.—Having during the last two days taken notes of more than 350 kinds of flowering plants, of which a very large proportion consisted of varieties of annuals, and the weather having been extremely hot, I have had an unusually good opportunity of seeing hymenoptera on the feed. Amongst vegetables, the flowers of Parsley appeared to be much approved of by bees. Amongst flowers there was a slight hum going on over beds of *Bastonia azraea*, but the bees were neither large nor conspicuous. There was, however, one variety of a well-known plant which was liberally beset with bees—*Clarkia pulchella alba*. I counted no less than five species of bees on it, and heard their music several yards off. H. T. P.

BENEDICT ROEZL.

Few people are aware of the amount of zeal and endurance experienced by our botanical collectors, and of the degree of enterprise manifested by importers of new plants. Judging from the history of many collectors, there are few occupations more fatal to health, and we may sorrowfully say to existence. When we remember the sad fate of a very large proportion of botanical collectors we may the more rejoice that such men as Fortune, Roezl, Bruchmüller and others, will remain to us. Among the most indefatigable of the class to which he belongs is certainly M. Benedict Roezl, whose portrait we give with the present number, and this remark applies equally to the numbers of first-class plants introduced by him and to the extent of his travels. If ever man deserved to be free of the Travellers' Club and of the Royal Geographical Society it is M. Roezl. This will be made apparent in the following notes, for the substance of which we are indebted to M. Roezl himself, and which, in their literal, unadorned statements, will convey a deeper impression than if a more detailed account were given. Few travellers, it is to be hoped, can say, as M. Roezl does, that he has been robbed of all his possessions seventeen times. One thing we beg of M. Roezl, and others who like him can boast of the tons of rare plants they send to Europe, that, ere they exterminate, as they most surely do, the plants from their native haunts, they carefully preserve a few pounds' weight only of dried specimens, to serve as records for the future.

"I started in my horticultural career," writes M. Roezl, "in my thirteenth year—in 1836; I was apprenticed in the gardens of the Count of Thun, at Töschau, in Bohemia, from which, after three years, I went to the gardens of Count Pawlikowsky, at Melica, Galicia. At that time these gardens contained the largest collection of plants in Europe, and I was there enabled to gain most of my botanical knowledge of plants. After staying there three years I went to Vienna to the famous gardens of Baron von Hügel; from there I went to Tesch, in Moravia, to Count Lichtenstein, and from there to Ghent, to M. Van Houtte, where I stayed five years. I was *chef de culture* in the School of Horticulture of the Belgian Government. After this I served for two years as foreman to M. Wagner, in Riga (Rania). From Riga I went again to M. Van Houtte for two years, but I could no longer restrain my ardent wish to see the tropics, and I proceeded, via New Orleans, to Mexico; this was in 1854. In Mexico I started a nursery for European fruit trees; there also I collected a large number of Mexican Finex. From thence I sent to Europe *Dahlia imperialis*, *Bourbaixii Humboldtii*, *Zinnia Hasseana*, *Cosmos atropurpureus*, *Agave schottigera* and many other plants. I introduced into Mexico the culture of Ramie (*Bombyx tenacissima*), and planted many acres of land with it. I invented, also, a machine for extracting and cleaning the fibre of Ramie and Hemp, and took out a patent for my machine from the Government of the United States on September 17, 1867. The Agricultural Exhibition awarded a diploma for it in February, 1868. This discovery was the cause, in the year 1868, of the loss of one of my arms. Many people in Havana solicited me to exhibit my machine there, and I was asked by some gentlemen to try if the machine would extract the fibre from *Agave americana*. The result of the trial proved that my assertion, that the fibre would come out green, was correct; but in endeavouring to show

me that they were right in their assertions they managed in some way or the other to fasten some screws tighter, so as to get the cylinders closer together, and I not knowing this, in putting a leaf between the cylinders (making 360 revolutions per minute), in consequence lost my left arm. Afterwards I again travelled in Mexico, and discovered *Dalechampia Roezliana rosea*, *Apelandra americana Roezlii*, *Campylobotris Origiesii*, *C. Roezlii*, *Negreria fulgida* and *digitaliflora*. From Mexico I went again to Havana and Cuba, and discovered *Mitrocycas* species.

"Afterwards I proceeded to New York, to start on my Californian travels over the Rocky Mountains and Sierra Nevada. I discovered here the new Lilies *Washingtonianum*, *puberulum*, *parvum* and *Humboldtii*; the latter I found on the hundredth memorial day of Alexander von Humboldt, and hence named one of the species after him. The Lily in question does not come from the Humboldt County, as some catalogues


proceeding to New Mexico, found the beautiful *Abies concolor* (Engelmann), *Yucca laccaea*, many hardy Cacti, and many annual and perennial. From there I went again to the Sierra Nevada, where I found *Pinus edulis*, *Pinus Bolanderi*, and collected Californian Lilies, and went to San Francisco, from thence via Acapulco into the Sierra Madre, where I found *Odotoglossum maxillare*, *pulchellum*, *citrosum*, *roseum*, and many others—altogether, 3500 Orchids, which arrived in London in fine condition. From there I went to Panama over the Isthmus, and went to La Guayra to get to Caracas in Venezuela, where I found *Cattleya labiata Roezlii*. I forwarded in all no less than 8 tons of Orchids to London. From there to St. Thomas, and to Havana and Vera Cruz, then to the Isthmus of Tehuantepec, and into the State of Oajaca in Mexico, where I found a real "new wonder," the double *Foinsettia pulcherrima*, which has already flowered in New York, and many Cacti and Agaves, Dios, and Orchids—in all, 10 tons of plants. From the city of Mexico I returned to Vera Cruz to go to New York, from New York to Panama, from there to Lima and Peru, over the Oriza railroad, crossed the Andes at a height of 17,000 feet to Tarma and Chanchamayo; brought back with me 20,000 bulbs of various sorts, *Filices* molle, many *Cactaceae*, new *Bromelias*, *Lourea*, *Calceolarias*, *Fuchsia*, *Mitella*, and many other new plants. From thence I returned to Lima and Callao, to South Peru, to Mollenda and Arigipa, to Puno on the Lake of Titicaca; from there I went to La Paz in Bolivia, and from thence I went over the Snowy Mountains of Illimani to the province of Yungas, there I found *Odotoglossum selligerum*, *Telopogon Benedictii*, *Mastrevallia aspera*, many new beautiful *Begonias* and *Lourea*, *Tacsonia*, *Tropaeolum*, and others. From thence I returned to Tarma and Arica to Lima; from there again I went to Payta, crossed the Andes to Huanuco-Camba, from whence I sent home many *Mastrevallias* and *Odotoglossums*, *Filices* *Pearcockii* and *Telopogon Hercules*, and went to Guayaquil (Ecuador), from there down the Chimbras, found a new *Zinnia*, *Pentstemon Roezlii* (Reich.), *Batemani*, *Wallii* (Reich.), and others. I returned to Guayaquil and went to Buenaventura to visit once more the Valley of Cauca, where I found *Mastrevallia chimera*, *Odotoglossum Roezlii*, *Pentstemon Dayana*, and many others. With these I started once more for London."

Such, in more outline, is the account of M. Roezl's wanderings, and of the results of his travels.

GREENHOUSE PLANTS.—XIII.
THEIR CULTURE AND MANAGEMENT.

Analysis.—Of all the plants in cultivation, either as specimens for the exhibition stage, for conservatory decoration, or simply grown for producing cut flowers, there are few that equal the Azalea, especially if we take into account its excellent constitution and immunity from disease when fairly treated. To those commencing their cultivation a little judgment is required in the selection of plants. Taking all things into consideration, it is much better to select grafted plants; some of the stronger-growing varieties will certainly do equally well on their own roots, but I do not think they are so long-lived, and by far the greater number do much better when grafted. The object in view ought to be to grow them up to something like the size required as quickly as possible; such plants are always more likely to live and bloom satisfactorily than those that have been grown slowly and indifferently; hence the necessity of selecting free-growing young plants. On no account commence with such as are at all stunted, either through having been too long in small pots, or being kept too cold in the winter. I would much rather have a newly-struck cutting, which, with proper treatment, will grow a way and far outstrip plants that are stunted. I much prefer those that have a few strong vigorous shoots, to those that have had their shoots stopped so as to form little bushy plants.

We will suppose the plants to be in something like 6-inch pots, with from six to a dozen stout shoots; if procured in the autumn do not winter them in a lower temperature than 45° to 50° by night, if at all stunted keep them 20° higher. Perceptibly they will make little or no progress through the winter months, but they will cast very few leaves, and their roots will be actively at work all the winter; such plants will make more progress the ensuing summer than those that have been starved through the winter will do in two seasons. Towards the beginning of March they will require potting; give them a liberal shift, say from a 6 to a 9-inch pot; use nothing but good fibrous peat, broken into pieces about the size of acorns, and sufficient silver sand to insure porosity. After potting keep the house a little close. Through April and May give them a night temperature of 60° to 65°, day 70° to 75°; syringe regularly overhead every afternoon; do not stop the shoots, as is often done, unless it be some one that is much stronger than the rest; if



BENEDICT ROEZL.

(b) – Enlarged extract of columns 1 and 2 from the Article on the Life of Benedict Roezl printed in *The Gardeners Chronicle*, July 18, 1874. (p.73). Arrowheads highlight reference to Roezl's prodigious collection of tropical and subtropical plants. Roezl makes reference to a plant "*Cosmos atropurpureus*" (arrow), that he sent from Mexico to Europe. "*Cosmos atropurpureus* could be Roezl's synonym for *Cosmos atosanguineus*."



BENEDICT ROEZL

FEW people are aware of the amount of zeal and endurance experienced by our botanical collectors, and of the degree of enterprise manifested by importers of new plants. Judging from the history of many collectors, there are few occupations more fatal to health, and we may sorrowfully say to existence. When we remember the sad fate of a very large proportion of botanical collectors we may the more rejoice that such men as Fortune, Roezl, Bruchmuller and others, still remain to us. Among the most indefatigable of the class to which he belongs is certainly M. Benedict Roezl, whose portrait we give with the present number, and this remark applies equally to the numbers of first-class plants introduced by him and to the extent of his travels. If ever man deserved to be free of the Travellers' Club and of the Royal Geographical Society it is M. Roezl. This will be made apparent in the following notes, for the substance of which we are indebted to M. Roezl himself, and which, in their literal, unadorned statements, will convey a deeper impression than if a more detailed account were given. Few travellers, it is to be hoped, can say, as M. Roezl does, that he has been robbed of all his possessions seventeen times. One thing we beg of M. Roezl, and others who like him can boast of the tons of rare plants they send to Europe, that, ere they exterminate, as they must surely do, the plants from their native haunts, they carefully preserve a few pounds' weight only of dried specimens, to serve as records for the future.

"I started in my horticultural career," writes M. Roezl, "in my thirteenth year—in 1836; I was apprenticed in the gardens of the Count of Thun, at Tötschen, in Bohemia, from which, after three years, I went to the gardens of Count Pawlikowsky, at Medica, Galicia. At that time these gardens contained the largest collection of plants in Europe, and I was there enabled to gain most of my botanical knowledge of plants. After staying there three years I went to Vienna to the far-famed gardens of Baron von Hügel; from there I went to Telsch, in Moravia, to Count Lichtenstein, and from there to Ghent, to M. Van Houtte, where I stayed five years. I was *chef de culture* in the School of Horticulture of the Belgian Government. After this I served for two years as foreman to M. Wagner, in Riga (Russia). From Riga I went again to M. Van Houtte for two years, but I could no longer restrain my ardent wish to see the tropics, and I proceeded, *via* New Orleans, to Mexico; this was in 1854. In Mexico I started a nursery for European fruit trees; there also I collected a large number of Mexican Pines. From thence I sent to Europe *Dahlia imperialis*, *Bouvardia Humboldtii*, *Zinnia Haageana*, *Cosmos atropurpureus*, *Agave schidigera* and many other plants. I introduced into Mexico the culture of Ramie (*Böhmeria tenacissima*), and planted many acres of land with it. I invented, also, a machine for extracting and cleaning the fibre of Ramie and Hemp, and took out a patent for my machine from the Government of the United States on September 17, 1867. The Agricultural Exhibition awarded a diploma for it in February, 1868. This discovery was the cause, in the year 1868, of the loss of one of my arms. Many people in Havanna solicited me to exhibit my machine there, and I was asked by some gentlemen to try if the machine would extract the fibre from *Agave americana*. The result of the trial proved that my assertion, that the fibre would come out green, was correct; but in endeavouring to show me that they were right in their assertions they managed in some way or the other to fasten some screws tighter, so as to get the cylinders closer together, and I not knowing this, in putting a leaf between the cylinders (making 360 revolutions per minute), in consequence lost my left arm. Afterwards I again travelled in Mexico, and discovered *Dalechampia Roezliana rosea*, *Aphelandra aurantiaca Roezlii*, *Campylobotris Ortgiesii*, *C. Roezlii*, *Nægelia fulgida* and *digitaliflora*. From Mexico I went again to Havanna and Cuba, and discovered *Microcycas* species.

"Afterwards I proceeded to New York, to start on my Californian travels over the Rocky Mountains and Sierra Nevada. I discovered here the new Lilies *Washingtonianum*, *puberulum*, *parvum* and *Humboldtii*; the latter I found on the hundredth memorial day of Alexander von Humboldt, and hence named one of the species after him. The Lily in question does not come from the Humboldt County, as some catalogues

(c) – Enlarged extract of columns 2 and 3 from the Article on the Life of Benedict RoezI printed in *The Gardeners Chronicle*, July 18, 1874. (p.73), Arrowheads highlight reference to RoezI sending tons of plant material from Mexico to Europe.

assert. I also found here *Saxifraga peltata*, *Calochortus Leichtlinii*, *Abies magnifica*, and many others that have been published from time to time. From there I went to Panama and Ocaña, in New Grenada, where I found *Utricularia montana*, *Anæctochilus Ortgiesii*, and forwarded about 10,000 Orchids to Europe, and something like 500 species of plants. From there I went to the Sierra Nevada, from Santa Martha; I found there *Telipogon Roezlii* (Reich.), and of which I collected 800 plants. These died in one night, owing to the great heat in Rio de Hacha. I also found many new varieties of *Odontoglossum*, and forwarded upwards of 3000 to Europe.

“Then, at the beginning of the Franco-German I went to Panama and to San Francisco, and owing to the war many of my consignments arrived dead at their destination. Wishing to await the end of the war, I went to the Washington territory, and found *Lilium columbianum* and a great variety of Conifer seeds. From there I proceeded to Sierra Nevada, California, to gather Conifer seeds, but the harvest was lost, on account of the severe frost. From there I went to South California, then to Panama and Bonaventura, in Choco; there I found *Zamia Roezlii* and *Lindeni*, and *Cypripedium palmifolium* and *Roezlii*. Here I also gathered *Cattleya chocoensis*, and brought them to Bonaventura, to ship them, and returned through the valley of Cauca. Now a very difficult journey commenced, through the State of Cauca to Antioquia, where I discovered large quantities of many varieties of *Masdevallias* described by Professor Reichenbach, and *Odontoglossum vexillarium*, *Curmeria picturata*, *Cattleya gigas*, *Phyllotænum Lindeni*, and many *Dieffenbachias* and other Aroids. After a journey of six months I travelled down the Magdalen River and to Colon and Panama, thence to North Peru, crossed the Andes where I found a scarlet Violet, a new species of *Heliotrope*, *Tillandsia argentea*, *Epidendrum Frederici Guilielmi*, *Masdevallia amabilis*, &c. I returned to Payta, to ship my plants and myself too, and went to Bonaventura, found *Odontoglossum Roezlii*, and when almost exhausted I found on the way *Masdevallia chimæra* and several new Aroids, which I brought myself to Europe. After staying about four months, and visiting the principal towns and nurseries, and seeing my parents again, I started once more for a new series of travels.

“On August 3, 1872, I went from Liverpool *via* New York, into the Colorado territory, and in Denver City I was robbed of 2000 dols., the whole of my possessions. There I collected *Yucca angustifolia*, *Calochortus Krelagii*, *Ipomœa leptophylla*, and,


proceeding to New Mexico, found the beautiful *Abies concolor* (Engelmann), *Yucca baccata*, many hardy Cacti, and many annuals and perennials. From there I went again to the Sierra Nevada, where I found *Pinus edulis*, *Pinus Bolanderi*, and collected Californian Lilies, and went to San Francisco, from thence *via* Acapulco into the Sierra Madra, where I found *Odontoglossum maxillare*, *pulchellum*, *citrosimum*, *roseum*, and many others—altogether, 3500 Orchids, which arrived in London in fine condition. From there I went to Panama over the Isthmus, and went to La Guayra to get to Caracas in Venezuela, where I found *Cattleya labiata Roezlii*. I forwarded in all no less than 8 tons of Orchids to London. From there to St. Thomas, and to Havanna and Vera Cruz, then to the Isthmus of Tehuantepec, and into the State of Oajaca in Mexico, where I found a real “new wonder,” the double *Poinsettia pulcherrima*, which has already flowered in New York, and many Cacti and Agaves, Dion, and Orchids—in all, 10 tons of plants. From the city of Mexico I returned to Vera Cruz to go to New York, from New York to Panama, from there to Lima and Peru, over the Oroja railroad, crossed the Andes at a height of 17,000 feet to Tarma and Chanchamaga; brought back with me 10,000 bulbs of various sorts, *Pilocereus mollis*, many *Cantuas*, new *Bromelias*, *Loasas*, *Calceolarias*, *Fuchsias*, *Mutisias*, and many other new plants. From thence I returned to Lima and Callao, to South Peru, to Molienda and Arigipa, to Puno on the Lake of Titicaca; from there I went to La Paz in Bolivia, and from thence I went over the Snowy Mountains of Illimani to the province of Yungas, there I found *Odontoglossum selligerum*, *Telipogon Benedictii*, *Masdevallia aspera*, many new bulbous *Begonias* and *Loasas*, *Tacsonias*, *Tropæolums*, and others. From thence I returned to Tacna and Arica to Lima; from there again I went to Payta, crossed the Andes to Huaca-Camba, from whence I sent home many *Masdevallias* and *Odontoglossums*, *Pilocereus Peacockii* and *Telipogon Hercules*, and went to Guayaquil (Ecuador), from there down the Chimbazo, found a new *Zamia*, *Pescatorea Roezlii* (Reich.), *Batemanii*, *Wallisii* (Reich.), and others. I returned to Guayaquil and went to Bonaventura to visit once more the Valley of Cauca, where I found *Masdevallia chimæra*, *Odontoglossum Roezlii*, *Pescatorea Dayana*, and many others. With these I started once more for London.”

Such, in mere outline, is the account of M. RoezI's wanderings, and of the results of his travels.

2.2 – Front cover of the fax that accompanied copies of the 1885, 1902 Thompson's seed catalogues and the 1942 Thompson and Morgan seed catalogue.

Relevant pages from Thompson's/Thompson and Morgan's seed catalogues pertaining to *Cosmos diversifolius* var. *atrosanguineus* kindly supplied by Claire Horne, Horticultural Quality Control Manager at Thompson and Morgan.

19-MAY-2000 14:12 FROM THOMPSON & MORGAN	TO 02083325310 P. 01/07
--	-------------------------



Fax

Thompson & Morgan (UK) Ltd.
Poplar Lane, Ipswich, Suffolk IP8 3BU
United Kingdom
Main Switchboard: (+44) 01473 688588
Customer Care: (+44) 01473 688821
Fax: (+44) 01473 680199
Email: chorne@thompson-morgan.com
Website: www.thompson-morgan.com

To: Sarah Lewendon	From: Claire Horne
Fax: 0208 3325310	Pages: Seven
Re: <i>Cosmos atrosanguineus</i>	Date: 19 May, 2000

Urgent For Your Info Please Comment Please Reply Please Recycle

Here are the photocopies of the catalogues I spoke about on the phone. I hope they help you with your PhD and any other research you are doing.

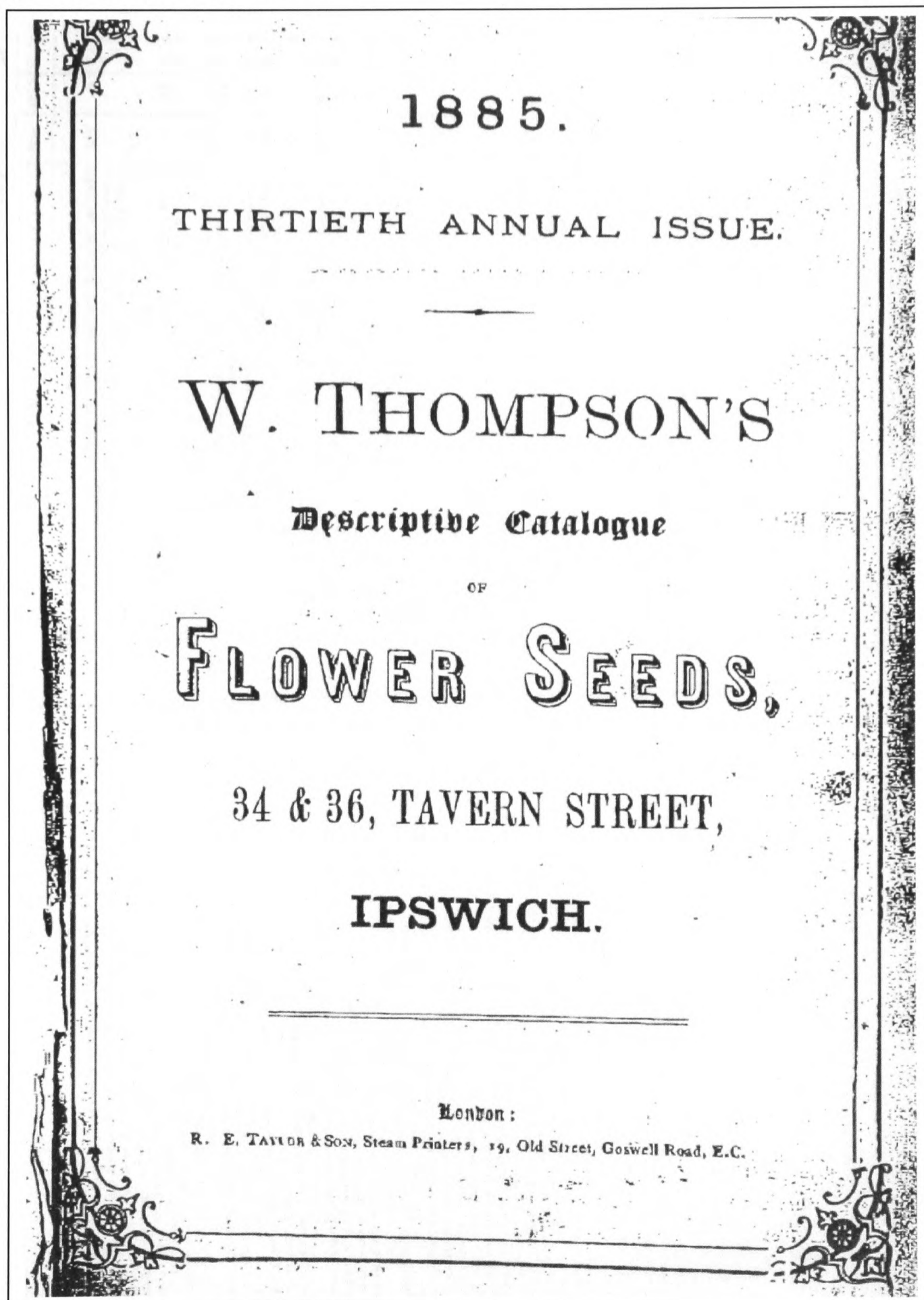
Page 2 & 3 are from the earliest catalogue that we have 1885. 4 & 5 are from the 1902 catalogue and show the selected form. 6 & 7 are the last catalogue with it listed in any form! I have included the inside cover as it talks about 'prohibition of importation of flower seed from any country due to the war.' I can find no mention of this variety in any further catalogues.

All the best

Claire Horne
Horticultural Quality Control Manager

2.3 - Thompson's 1885 Seed Catalogue

(a) - Thompson's 1885 Seed Catalogue (Front Cover)



(b) - Thompson's 1885 Seed Catalogue (pages 12-13). *Cosmos diversifolius atrosanguineus* listed on page 13 catalogue number 469 (arrow).

W. THOMPSON'S DESCRIPTIVE CATALOGUE.

W. THOMPSON'S DESCRIPTIVE CATALOGUE.		18	
NAME.		Dur.	Hgt. s. d.
CLEMATIS —			
420	CEREA, interesting species, white flowers stained with crimson	hP	0 6
421	GRAVELAND, new yellow-flowered species from Tibet	"	0 6
422	HYBRIDA, fine new hybrids of <i>Jacquinii</i> , &c., in mixture	"	0 6
423	KANTONIA, very large pale lilac flowers, fine wall climber	"	0 6
424	SOGOMIA, new dwarf white flowered species, fragrant, very distinct	"	0 6
* Most <i>Clematis</i> seeds vegetate only after an interval of from 6 to 12 months, when they will grow with tolerable certainty. No. 421 grows readily and has been known to flower the first year.			
OLEANTHUS —			
425	DAMPNUS, <i>Foa</i> Tribe, Leguminosae. Loam and peat.	QSh	1 0
426	DAMPNUS, splendid, dark red and black, does best in warm border	"	0 6
428	PUMIUS, crimson, hardy against a wall, with slight protection	hbA	0 3
429	PUMIUS, crimson, hardy against a wall, with slight protection	"	0 3
430	PUMIUS, crimson, hardy against a wall, with slight protection	"	0 3
431	PUMIUS, crimson, hardy against a wall, with slight protection	"	0 3
432	PUMIUS, crimson, hardy against a wall, with slight protection	"	0 3
433	PUMIUS, crimson, hardy against a wall, with slight protection	"	0 3
434	PUMIUS, crimson, hardy against a wall, with slight protection	"	0 3
435	PUMIUS, crimson, hardy against a wall, with slight protection	"	0 3
436	PUMIUS, crimson, hardy against a wall, with slight protection	"	0 3
437	PUMIUS, crimson, hardy against a wall, with slight protection	"	0 3
438	PUMIUS, crimson, hardy against a wall, with slight protection	"	0 3
439	PUMIUS, crimson, hardy against a wall, with slight protection	"	0 3
440	PUMIUS, crimson, hardy against a wall, with slight protection	"	0 3
441	PUMIUS, crimson, hardy against a wall, with slight protection	"	0 3
442	PUMIUS, crimson, hardy against a wall, with slight protection	"	0 3
443	PUMIUS, crimson, hardy against a wall, with slight protection	"	0 3
444	PUMIUS, crimson, hardy against a wall, with slight protection	"	0 3
445	PUMIUS, crimson, hardy against a wall, with slight protection	"	0 3
446	PUMIUS, crimson, hardy against a wall, with slight protection	"	0 3
447	PUMIUS, crimson, hardy against a wall, with slight protection	"	0 3
448	PUMIUS, crimson, hardy against a wall, with slight protection	"	0 3
449	PUMIUS, crimson, hardy against a wall, with slight protection	"	0 3
450	PUMIUS, crimson, hardy against a wall, with slight protection	"	0 3
451	PUMIUS, crimson, hardy against a wall, with slight protection	"	0 3
452	PUMIUS, crimson, hardy against a wall, with slight protection	"	0 3
453	PUMIUS, crimson, hardy against a wall, with slight protection	"	0 3
454	PUMIUS, crimson, hardy against a wall, with slight protection	"	0 3
455	PUMIUS, crimson, hardy against a wall, with slight protection	"	0 3
456	PUMIUS, crimson, hardy against a wall, with slight protection	"	0 3
457	PUMIUS, crimson, hardy against a wall, with slight protection	"	0 3
458	PUMIUS, crimson, hardy against a wall, with slight protection	"	0 3
459	PUMIUS, crimson, hardy against a wall, with slight protection	"	0 3
460	PUMIUS, crimson, hardy against a wall, with slight protection	"	0 3
461	PUMIUS, crimson, hardy against a wall, with slight protection	"	0 3
462	PUMIUS, crimson, hardy against a wall, with slight protection	"	0 3
463	PUMIUS, crimson, hardy against a wall, with slight protection	"	0 3
464	PUMIUS, crimson, hardy against a wall, with slight protection	"	0 3
465	PUMIUS, crimson, hardy against a wall, with slight protection	"	0 3
466	PUMIUS, crimson, hardy against a wall, with slight protection	"	0 3
467	PUMIUS, crimson, hardy against a wall, with slight protection	"	0 3
468	PUMIUS, crimson, hardy against a wall, with slight protection	"	0 3
469	PUMIUS, crimson, hardy against a wall, with slight protection	"	0 3
470	PUMIUS, crimson, hardy against a wall, with slight protection	"	0 3
471	PUMIUS, crimson, hardy against a wall, with slight protection	"	0 3
472	PUMIUS, crimson, hardy against a wall, with slight protection	"	0 3
473	PUMIUS, crimson, hardy against a wall, with slight protection	"	0 3
474	PUMIUS, crimson, hardy against a wall, with slight protection	"	0 3
475	PUMIUS, crimson, hardy against a wall, with slight protection	"	0 3
476	PUMIUS, crimson, hardy against a wall, with slight protection	"	0 3
477	PUMIUS, crimson, hardy against a wall, with slight protection	"	0 3
478	PUMIUS, crimson, hardy against a wall, with slight protection	"	0 3
479	PUMIUS, crimson, hardy against a wall, with slight protection	"	0 3
480	PUMIUS, crimson, hardy against a wall, with slight protection	"	0 3
481	PUMIUS, crimson, hardy against a wall, with slight protection	"	0 3
482	PUMIUS, crimson, hardy against a wall, with slight protection	"	0 3
483	PUMIUS, crimson, hardy against a wall, with slight protection	"	0 3
484	PUMIUS, crimson, hardy against a wall, with slight protection	"	0 3
485	PUMIUS, crimson, hardy against a wall, with slight protection	"	0 3
486	PUMIUS, crimson, hardy against a wall, with slight protection	"	0 3
487	PUMIUS, crimson, hardy against a wall, with slight protection	"	0 3
488	PUMIUS, crimson, hardy against a wall, with slight protection	"	0 3
489	PUMIUS, crimson, hardy against a wall, with slight protection	"	0 3
490	PUMIUS, crimson, hardy against a wall, with slight protection	"	0 3
491	PUMIUS, crimson, hardy against a wall, with slight protection	"	0 3
492	PUMIUS, crimson, hardy against a wall, with slight protection	"	0 3
493	PUMIUS, crimson, hardy against a wall, with slight protection	"	0 3
494	PUMIUS, crimson, hardy against a wall, with slight protection	"	0 3
495	PUMIUS, crimson, hardy against a wall, with slight protection	"	0 3
496	PUMIUS, crimson, hardy against a wall, with slight protection	"	0 3
497	PUMIUS, crimson, hardy against a wall, with slight protection	"	0 3
498	PUMIUS, crimson, hardy against a wall, with slight protection	"	0 3
499	PUMIUS, crimson, hardy against a wall, with slight protection	"	0 3
500	PUMIUS, crimson, hardy against a wall, with slight protection	"	0 3
501	PUMIUS, crimson, hardy against a wall, with slight protection	"	0 3
502	PUMIUS, crimson, hardy against a wall, with slight protection	"	0 3
503	PUMIUS, crimson, hardy against a wall, with slight protection	"	0 3
504	PUMIUS, crimson, hardy against a wall, with slight protection	"	0 3
505	PUMIUS, crimson, hardy against a wall, with slight protection	"	0 3
506	PUMIUS, crimson, hardy against a wall, with slight protection	"	0 3
507	PUMIUS, crimson, hardy against a wall, with slight protection	"	0 3
508	PUMIUS, crimson, hardy against a wall, with slight protection	"	0 3
509	PUMIUS, crimson, hardy against a wall, with slight protection	"	0 3
510	PUMIUS, crimson, hardy against a wall, with slight protection	"	0 3

(2)

19-MAY-2008 14:13 FROM THOMPSON & MORGAN TO 02083325310 P.03/07

2.4 - Thompson's 1902 Seed Catalogue (pages 24-25).

Two forms of *Cosmos diversifolius atrosanguineus* are listed on page 25, catalogue numbers 690 and 691 (arrows).

NAME	Dur.	Hgt.	Price	Notes
GLIANTHUS. - Continued.				
640 <i>punicus</i> albus, beautiful new white var., should prove good for	OSh	4	0 6	
641 <i>magnificus</i> , improved var., colour brighter crimson (outling	"	4	1 0	
CLINTONIA. <i>Lobelia</i> Family, Lobeliaceae.				
642 <i>pulethella</i> , elegant, blue, yellow and white, syn. <i>Downingii pulchella</i>	hA	3	0 4	
COBEA. <i>Phlox-worts</i> . Polemoniaceae. Ordinary soil.				
643 <i>macrostema</i> , new species, flowers yellowish, very distinct	hP	cl	0 3	
644 <i>scandens</i> , deep violet, handsome climber of rapid growth	"	cl	0 3	
CODONOPSIS. <i>Ball-worts</i> , Campanulaceae. Mixed soil. [violet				
645 <i>grandiflora</i> , rather large flowers, of an attractive purple or	hP	1	0 4	
646 <i>ovata</i> , pale, purple flowers, very pretty half-twinning plant	"	1	0 4	
647 <i>vividiflora</i> , rare species with green, grey, and violet fls., beautiful	"	1	0 5	
COLEUS. <i>Lip-worts</i> , Labiales. Rich mixed soil. [collection				
648 <i>hybridus</i> , splendid ornamental foliage; from a magnificent	hP	1 1/2	0 3	
649 <i>Bizarro</i> , striking novelty; leaves of remarkable form and	"	1 1/2	1 0	
650 <i>flammea</i> , another wonderful strain of this popular plant,	"	1 1/2	1 0	
651 <i>ornatus</i> , splendid new large-leaved variety, very striking	"	1 1/2	1 0	
652 <i>salignifolius</i> , "Parrot," improved var. of the willow-	"	1 1/2	1 0	
leaved <i>Coleus</i> in the brightest colours, and most marvellous	"	1 1/2	1 0	
designs	"	1 1/2	1 0	
COLLINSIA. <i>Libinaria</i> , Scrophulariaceae. Common soil.				
653 <i>bartschifolia</i> alba, very neat pure white variety for edging, &c.	hA	3	0 3	
654 <i>bleu</i> , lilac and white, good border annual	"	3	0 3	
655 <i>candidissima</i> , pure white variety	"	3	0 3	
656 <i>tinctoria purpurea</i> , flowers large deep red-violet, very showy	"	3	0 3	
657 <i>verna</i> , blue and wh., very early; seed supplied in <i>Autumn only</i>	"	3	0 3	
COLLOMIA. <i>Phlox-worts</i> , Polemoniaceae. Common soil.				
658 <i>coccinea</i> , bright red, neat dwarf annual, very hardy	"	3	0 2	
COLUMBINE. long-spurred and others, see <i>Aquilegia</i> . Common soil.				
COMMELINA. <i>Spider-wort</i> Family, Commelinaceae.				
659 <i>caelestis</i> , fine blue, abundant bloomer, tuberous-rooted	hP	2	0 2	
660 <i>alba</i> , pure white variety, comes partially true from seed	"	2	0 2	
CONVOLVULUS. <i>Convolvulus</i> Family, Convolvulaceae. Common soil.				
661 <i>althoides</i> , pale rosy-purple, pretty trailing sp., flowers golden yellow	hP	cl	0 3	
662 <i>aureus superbus</i> , pale rose, non-climbing, neat dwarf species	hP	tr	0 4	
663 <i>Gantabrica</i> , pale blue, very pretty dwarf trailing species	hP	tr	0 4	
664 <i>mauritanicus</i> , violet blue, pretty dwarf trailing species	hP	tr	0 4	
665 <i>Soldanella</i> , pretty trailer for sandy soil, fls. rose and white	hP	tr	0 4	
666 <i>tricolor</i> (<i>minor Convolvulus</i>), deep blue, yellow, and white	hA	1 1/2	0 2	
667 <i>compactus</i> , new dwarf, compact variety, very floriferous	"	1 1/2	0 2	
668 <i>Crimson Beauty</i> , rich crimson-violet in clusters, upright hbt.	"	1 1/2	0 3	
major. See <i>Igonia purpurea</i> .				
COREOPSIS. <i>Composites</i> . Common soil.				
669 <i>grandiflora</i> , large deep yellow, very distinct, grand for cutting	hP	3	0 3	
670 <i>lancofolata</i> , large yellow heads, very showy border plant	"	3	0 3	
671 <i>palmata</i> , rare dwarfish species, yellow flower-heads	"	3	0 3	
672 <i>verticillata</i> , graceful slender habit, fls. yellow with dark disk	"	3	0 4	
CORNFLOWER. see <i>Centaurea</i> .				
CORONILLA. <i>Pea</i> Family, Leguminosae. Common soil.				
673 <i>elegans</i> , rosy-purple flowers, neat dwarf sp., from Asia Minor	hP	1 1/2	0 4	
674 <i>ibogea</i> , showy sp., large yellow pea-shaped flowers	"	1 1/2	0 4	
CORTUSA. <i>Primrose</i> Family, Primulaceae. Peat and loam.				
675 <i>Martholli</i> , deep red flowers, in drooping umbels, pretty Alpine	"	1 1/2	0 6	
676 <i>ansylvanica</i> , allied to <i>Martholli</i> , but foliage densely covered	"	1 1/2	0 6	
with rose hairs, flowers darker	"	1 1/2	0 6	
677 <i>villosa</i> , neat Alpine, reddish-purple in small umbels, rare	"	1 1/2	0 6	

TRY I. & M.'S SPECIAL LAWN GRASS MIXTURE.

Conceptus conf.

Handwritten note: This eye is not thick

NAME	Dur.	Hgt.	Price	Notes
CORYDALIS. <i>Poppie-worts</i> , Papaveraceae. Sandy loam.				
678 <i>chellanthifolia</i> , fine novelty, fern-like fol., yellow flowers	hP	1	0 3	
679 <i>glauca</i> , reddish-purple fls., neat indigenous sp., for walls, &c.	hA	3	0 3	
680 <i>lutea</i> , snowy golden-yellow fls., glaucous foliage, dwarf habit	hB	1 1/2	0 4	
681 <i>alba</i> , very pretty creamy-white fls.; dry border or rockery	hP	3	0 3	
682 <i>nobilis</i> , fine border plant, yellow fls., seeds slow to vegetate	"	3	0 3	
683 <i>ochroleuca</i> , charming little rock plant, fls. delicate pale yellow	"	3	0 3	
684 <i>thalictrifolia</i> , beautiful new sp., handsome; fol., yellow fls.	"	3	0 3	
all summer, requires slight protection	"	3	0 3	
COSMOS. <i>Composites</i> . Light soil.				
685 <i>bipinnatus purpureus</i> , deep purple-red, showy, late bloomer	hA	2	0 3	
686 <i>hybridus purpureus</i> , fine mix. pink, crimson, purple, white, &c.	"	2	0 3	
687 <i>crimson</i> } Separate vars. of this elegant early strain, sown	"	2	0 3	
688 <i>rose</i> } in heat and plant out in full sun in poor soil	"	2	0 3	
689 <i>white</i> } in May, will flower in July	"	2	0 3	
690 <i>diversifolius atrosanguineus</i> (<i>Black Dablia</i>), dark purple,	"	2	0 3	
dwarf, tuberous	"	2	0 3	
691 <i>king of the Blacks</i> , improved form of the interesting Black	"	2	0 3	
CRUCIANELLA. <i>Madder</i> Family, Rubiaceae. Sandy soil.				
692 <i>stylosa</i> , pink, in large heads; pretty trailer, dry banks or rocks	hA	1	0 3	
CUCURBIT. <i>Gourd</i> Family, Cucurbitaceae. Light soil.				
693 <i>acutangulus</i> , interesting and curious species, good for trellis	cl	0 3	0 3	
694 <i>Dudaim</i> , pretty small melon-like fruit, mottled green	cl	0 3	0 3	
695 <i>erythraeus</i> (<i>Hedgehog</i>), curious spiny fruit	cl	0 3	0 3	
696 <i>myriocarpus</i> (<i>Gooseberry</i>), small gooseberry-like fruit	cl	0 3	0 3	
CUCURBITA. <i>Gourd</i> Family, Cucurbitaceae. Light rich soil.				
697 <i>melanosperma</i> , very handsome variegated fruit and foliage	"	"	"	
698 <i>Pepo</i> , small apple-shaped Gourd, very pretty variety	"	"	"	
699 <i>small</i> , small egg-shaped Gourd, white, ornamental	"	"	"	
700 <i>small</i> , small egg-shaped Gourd, very pretty	"	"	"	
701 <i>pear-shaped</i> , Gourd, several varieties mixed	"	"	"	
702 <i>small striped</i> , Gourd, flattish in shape, pretty	"	"	"	
703 <i>small</i> , small variegated Gourd, an attractive kind	"	"	"	
704 <i>small</i> , small variegated Gourd, mixed small fruited varieties	"	"	"	
CUPHEA. <i>Loose-stives</i> , Lythraceae. Ordinary soil.				
705 <i>ignea</i> , red & bl., useful border, incorrectly sold for <i>C. platycentra</i>	hP	1	0 6	
CYANANTHUS. <i>Belt-worts</i> , Campanulaceae. Sandy peat and leaf				
mould on rockery.				
707 <i>lobatus</i> , choice Himalayan Alpine for rockery, fls. blue blue	hP	tr	0 6	
CYCLAMEN. <i>Primrose</i> Family, Primulaceae. Peat and loam.				
708 <i>alatum</i> , pretty early-flowering sp., very dwarf, rosy-crimson	hP	1	0 6	
709 <i>album</i> , choice variety of this lovely species	"	1	0 6	
710 <i>europaeum</i> , white, foliage cordate, very hardy (part	"	1	0 6	
711 <i>macropetalum</i> , nearly allied to <i>heterophyllum</i> , but larger in all its	"	1	0 6	
712 <i>neapolitanum</i> , red-purple and white, good hardy species	"	1	0 6	
713 <i>persicatum</i> , saved from a choice sweet-scented strain, mixed	"	1	0 6	
714 <i>pushhilli</i> , "remarkable novelty," petals with	"	1	0 6	
715 <i>Emperor William</i> , very fine dark red var. feathered crest	"	1	0 6	
716 <i>giganteum</i> , Low's improved, very large flowers choicest	"	1	0 6	
717 <i>Mont Blanc</i> , the finest pure white var., extra fine (mixed	"	1	0 6	
718 <i>odoratum</i> , lovely strain of sweet-scented <i>Cyclamen</i> in mix	"	1	0 6	
719 <i>Papilio</i> , beautifully fringed flowers, mixed colours	"	1	0 6	
720 <i>Alpine</i> , new var. <i>Ritardata</i> , variety, flowers large	"	1	0 6	
721 <i>pure white</i> with red eye, the fringed petals being broadly	"	1	0 6	
adged with bright red, a lovely novelty	"	1	0 6	
722 <i>Salmon King</i> , grand novelty, lovely salmon flowers	"	1	0 6	
Out <i>Cyclamen</i> seeds are very highly recommended, the	"	1	0 6	

It is really EXTRA FINE and RELIABLE. For Prices see end of List.

6

19-MAY-2000 14:15 FROM THOMPSON & MORGAN TO 02083325310 P.05/07

SPECIAL WAR TIME NOTICE.

IN renewing our grateful acknowledgments to our customers and friends for their past favours and confidence, we regret to announce that it has been necessary to further reduce the present Edition of our Catalogue from 80 to 64 pages. This has been necessary partly through the shortage of paper, but chiefly owing to the prohibition of importation of flower seeds from any country. We have omitted all Coloured and Black and White Illustrations, also 32 pages of Notes on Novelities and seeds of recent introductions.

With these reductions, however, we are still able to offer over 3,000 different kinds of Flower Seeds, many of them unobtainable elsewhere.

To anyone who still retains a 1939 Catalogue we would like to state that the numbers in this issue are the same as in the 1939 Edition and several seeds not offered now can be supplied. We have several hundred copies of our 1939 Catalogue and will be pleased to send a copy on request, while they last.

We have, however, been able to retain and offer splendid stocks of the more common seeds of many beautiful Hardy and Half-Hardy Annuals, which can be depended upon to make a brilliant show at very little cost.

As we have served you well with the more uncommon seeds we now respectfully solicit your order for general list of flower and vegetable seeds. Our vegetable seeds are of the finest strains and gave good results to all who grew them last season.

January, 1942.

Telegrams: HORTUS, IPSWICH.

Telephone: 2780 IPSWICH.

It is particularly requested that intending Customers will kindly read the following notice prior to ordering seeds.

TERMS OF BUSINESS.

All Seeds are sent Post Free or C carriage Paid to any Station in the United Kingdom except small lots of less value than 2s. 6d.. Artichokes and Shallots. Postal Orders offer the readiest means of remitting small sums. When stamps are sent, 1d., 2d. or 2½d. will be preferred, if convenient to the sender. We do not specially acknowledge the receipt of sums under 2/- unless an extra stamp be sent.

Accounts are rendered quarterly. Five per cent. discount is allowed on amounts of £1 and upwards paid within a month of date of invoice.

We shall be particularly obliged by Names and Addresses being given in a distinct and legible manner, especially in the case of new customers, of whom we are annually receiving a large number. BLOCK LETTERS PREFERRED.

In ordering Flower Seeds, only the number prefixed to the name in the Catalogue need be given and it will be a GREAT CONVENIENCE if this is in all cases given, as far as possible; it is indispensable to give the DATE of the Catalogue. Customers will greatly oblige by making out their orders by using Order Form enclosed with Catalogue. As it must often happen that some particular seed cannot be supplied, either from its being early sold out or from failure of the seed crop, it will be well to add a few duplicate numbers, from which the deficiency may be made up.

The price of each packet is that of the smallest quantity that can be supplied.

We hope our friends will excuse our pointing out that as the seeds are packed in advance of the spring trade, no variation in the size of the packets is possible without great inconvenience to us.

2.5 - Thompson and Morgan's 1942 Seed Catalogue (a) - (front and back pages).

Back page includes a notice about war-time restrictions.

THOMPSON & MORGAN'S DESCRIPTIVE CATALOGUE OF Flower and Vegetable Seeds

SPECIAL IMPORTATION NOTICE.—All Seeds marked * require a Permit from the Ministry of Agriculture for importation into U.S.A.

SECTION 1.

FLOWER SEEDS

ARRANGED ALPHABETICALLY

The following arrangement needs but little explanation: it may, however, be desirable to remark that the information so briefly given, with regard to the duration, hardiness, and height of each plant, is to be regarded as only approximate. Some plants which are quite hardy in the Southern Counties, will not resist a Yorkshire or a Scottish winter and plants will vary considerably in height according to the character of the soil and situation in which they are cultivated, especially in pots. A few plants which flower the first year, but are really perennial, if protected, are more conveniently treated as half-hardy annuals, and are classed as such in the following pages.

EXPLANATIONS AND ABBREVIATIONS EMPLOYED.

H Hardy. HH Half-hardy. T Tender. A Annual. P Perennial. B Biennial. Sh Shrub. Bb Biennial or tuber. S Stone. G Greenhouse. d Climber. tr. Trailer. An Asterisk (*) signifies that a biennial or perennial plant will flower the first season, if sown early.

PRICES.

All Seeds are priced per packet. The packets vary in size according to the value and rareness of the seed.

NAME	Dur.	Height, ft.
ABRONIA. (Sand Verbena). Nymphaeaceae. Light sandy soil.		
ABUTILON. Malvaceae. Common soil. Light sandy soil.	HHA	tr. 0 4
*ACACIA. Leguminosae. Common soil. Quick growing.	HHSN	10 0 6
14 Abneyana. Dicotyled. Silvery-blue foliage. Brilliant yellow flowers.		5 0 6
15 Acahuala (Yellow Mimosa). Fabaceae. Foliage resembles plenty of room.		5 0 4
16 Acahuala (Yellow Mimosa). Fabaceae. Foliage resembles plenty of room.		5 0 4
*ACENA. New Zealand Star. Rosaceae. Light dry soil.	HP	tr. 0 3
20 Buchananii. Foliage very pretty bluish-green, dwarf trailing habit.		tr. 0 3
21 Breviflora. Minute purple flowers, very early.		tr. 0 6
*ACANTHOPHYLLUM SPINOSUM. See Dianthus nemorosus.		
*ACER (Maple). Aceraceae. Deep loamy soil.	HT	30 0 6
25 Acahuala (Yellow Mimosa). Fabaceae. Light soil.	HP	1 0
26 Acahuala (Yellow Mimosa). Fabaceae. Light soil.	HP	1 0
27 Acahuala (Yellow Mimosa). Fabaceae. Light soil.	HP	1 0
28 Acahuala (Yellow Mimosa). Fabaceae. Light soil.	HP	1 0
29 Acahuala (Yellow Mimosa). Fabaceae. Light soil.	HP	1 0
30 Acahuala (Yellow Mimosa). Fabaceae. Light soil.	HP	1 0
31 Acahuala (Yellow Mimosa). Fabaceae. Light soil.	HP	1 0
32 Acahuala (Yellow Mimosa). Fabaceae. Light soil.	HP	1 0
33 Acahuala (Yellow Mimosa). Fabaceae. Light soil.	HP	1 0
34 Acahuala (Yellow Mimosa). Fabaceae. Light soil.	HP	1 0
35 Acahuala (Yellow Mimosa). Fabaceae. Light soil.	HP	1 0
36 Acahuala (Yellow Mimosa). Fabaceae. Light soil.	HP	1 0
37 Acahuala (Yellow Mimosa). Fabaceae. Light soil.	HP	1 0
38 Acahuala (Yellow Mimosa). Fabaceae. Light soil.	HP	1 0
39 Acahuala (Yellow Mimosa). Fabaceae. Light soil.	HP	1 0
40 Acahuala (Yellow Mimosa). Fabaceae. Light soil.	HP	1 0
41 Acahuala (Yellow Mimosa). Fabaceae. Light soil.	HP	1 0
42 Acahuala (Yellow Mimosa). Fabaceae. Light soil.	HP	1 0
43 Acahuala (Yellow Mimosa). Fabaceae. Light soil.	HP	1 0
44 Acahuala (Yellow Mimosa). Fabaceae. Light soil.	HP	1 0
45 Acahuala (Yellow Mimosa). Fabaceae. Light soil.	HP	1 0
46 Acahuala (Yellow Mimosa). Fabaceae. Light soil.	HP	1 0
47 Acahuala (Yellow Mimosa). Fabaceae. Light soil.	HP	1 0
48 Acahuala (Yellow Mimosa). Fabaceae. Light soil.	HP	1 0
49 Acahuala (Yellow Mimosa). Fabaceae. Light soil.	HP	1 0
50 Acahuala (Yellow Mimosa). Fabaceae. Light soil.	HP	1 0
51 Acahuala (Yellow Mimosa). Fabaceae. Light soil.	HP	1 0
52 Acahuala (Yellow Mimosa). Fabaceae. Light soil.	HP	1 0
53 Acahuala (Yellow Mimosa). Fabaceae. Light soil.	HP	1 0
54 Acahuala (Yellow Mimosa). Fabaceae. Light soil.	HP	1 0
55 Acahuala (Yellow Mimosa). Fabaceae. Light soil.	HP	1 0
56 Acahuala (Yellow Mimosa). Fabaceae. Light soil.	HP	1 0
57 Acahuala (Yellow Mimosa). Fabaceae. Light soil.	HP	1 0
58 Acahuala (Yellow Mimosa). Fabaceae. Light soil.	HP	1 0
59 Acahuala (Yellow Mimosa). Fabaceae. Light soil.	HP	1 0
60 Acahuala (Yellow Mimosa). Fabaceae. Light soil.	HP	1 0
61 Acahuala (Yellow Mimosa). Fabaceae. Light soil.	HP	1 0
62 Acahuala (Yellow Mimosa). Fabaceae. Light soil.	HP	1 0
63 Acahuala (Yellow Mimosa). Fabaceae. Light soil.	HP	1 0
64 Acahuala (Yellow Mimosa). Fabaceae. Light soil.	HP	1 0
65 Acahuala (Yellow Mimosa). Fabaceae. Light soil.	HP	1 0
66 Acahuala (Yellow Mimosa). Fabaceae. Light soil.	HP	1 0
67 Acahuala (Yellow Mimosa). Fabaceae. Light soil.	HP	1 0
68 Acahuala (Yellow Mimosa). Fabaceae. Light soil.	HP	1 0
69 Acahuala (Yellow Mimosa). Fabaceae. Light soil.	HP	1 0
70 Acahuala (Yellow Mimosa). Fabaceae. Light soil.	HP	1 0

(b) - Thompson and Morgan's 1942 Seed Catalogue (pages 12-13).
Cosmos diversifolius atrosanguineus on page 13, catalogue number 1354 (arrow),
described as King of the Blacks (Black Dahlia).

NAME	Dur.	Hgt. in ft.	d.
CLARKIA —continued.			
1222 elegans Salmon Queen, double salmon-rose, very pretty	HA	2	0.3
1223 — Scarlet Queen, most brilliant double variety, for border or cutting	"	2	0.3
1224 — patchella fl. pl., beautiful double varietals, fine mixed	"	1 1/2	0.3
1225 — crimson, extra select, really double	"	1 1/2	0.4
1226 — Tom Thumb, finest mixed	"	1 1/2	0.4
CLEMATIS , Ranunculaceae. Ordinary soil.			
1237 cocinea, various shades of red flowers, very distinct	"	cl.	0.6
1240 globosa, a rare species, rather fine dark claret flowers	"	cl.	0.6
1241 graveolens, fine yellow-flowered species from Tibet	"	cl.	0.4
1242 heracleaefolia campanula, pale blue flowers in great profusion, erect habit	"	cl.	0.6
1243 hybrida, fine new hybrids of Jockmac, etc. in mixture	"	cl.	0.6
1244 integrifolia, erect habit, drooping blue flowers, herbaceous	"	cl.	0.4
1245 macropetala, large violet flowers, a rare and beautiful climber	"	cl.	0.6
1246 montana, small pure white flowers, freely produced, a favourite	"	cl.	0.6
1250 recta, erect habit, non-climbing, white flowers in clusters	"	cl.	0.6
1252 serratifolia, bright yellow flowers, Autumn flowering	"	cl.	0.6
1253 tangutica, golden yellow flowers, rapid grower	"	cl.	0.6
1259 Vitalba, the common "Old Man's Beard," or "Traveller's Joy," of British hedges, rampant climber, white flowers	"	cl.	0.3
**Most Clematis seeds vegetate only after an interval of some months, when they will grow with tolerable certainty. Graveolens, and some others grow readily and have been known to flower the first year. Light soil.			
GLEOME (Sibley flower). Cappariaceae. Light soil.			
1262 pungens. Rose Queen, bright rose flowers	HHA	3	0.4
CLEODONOPSIS , Verbenaceae. Peat and loam.			
1263 fallax, handsome plant, large spikes of scarlet flowers	GSh	6	1.0
1264 Fargessi, large leaves, purple in spring, white flowers followed by blue fruits	HSh	5	0.9
CLYANTHUS , Leguminosae. Loam and peat.			
1267 Damptieri, dark red and black flowers, does best in warm border	GSh	2	0.6
1268 purpureus, crimson, hardy against a wall with slight protection	"	4	0.4
COBÆA , Polemoniaceae. Ordinary garden soil.			
1275 scandens, deep violet, handsome climber of rapid growth	HHA	cl.	0.4
1276 — alba, variety with white flowers, partially true from seed	"	cl.	0.4
COCKSCOMB , See <i>Celosia cristata</i> .			
CODONOPSIS , Campanulaceae. Mixed soil.			
1279 clematidea, blue bell-shaped flowers, white and yellow centre	HP	1	0.6
1280 ovata, pale purple flowers, very pretty half-wooling plant	"	1	0.4
COLEUS , Labiaceae. Rich mixed soil.			
1283 hybridus, splendid ornamental foliage; from a magnificent collection	HHP*	1 1/2	0.6
1284 — Pyrenean Giant, large leaves, mostly with white ground, richly marked	"	1 1/2	0.6
1285 thyrsoides, light blue flowers in panicles, fine foliage	"	2	2.5
COLLINSIA , Scrophulariaceae. Common soil.			
1286 bicolor, lilac and white, good border annual	HA	1 1/2	0.3
1289 — Salmon Beauty, pure salmon-rose flowers, a really good annual	"	1	0.6
1290 grandiflora carminea, flowers large deep red-violet, very showy	"	1	0.3
COLLOMIA , Polemoniaceae. Common soil.			
1292 cocinea, bright red, neat dwarf annual, very hardy	"	1 1/2	0.3
1293 grandiflora, soft pink to salmon-apricot scented flowers	"	1 1/2	0.5
COLUMBINE , Long spurred and others. See <i>Aquilegia</i> .			
COLUTEA , Bladder Senna, Leguminosae. Common soil.			
1294 arborescens, yellow pea-shaped flowers, strong-growing shrub	HSh	10	0.6
COMMELINA , Commelinaceae. Common soil.			
1297 caelestis, fine blue, abundant bloomer, tuberous-rooted	HP*	1 1/2	0.3
1299 Sallowiana, flowers very large, of a beautiful cobalt blue	"	1 1/2	0.4
CONVALLARIA , Lily of the Valley, Liliaceae. Common soil.			
1300 majalis, large-flowered Lily of the Valley	HP	1	0.4
CONVOLVULUS , Convolvulaceae. Common soil.			
1301 althaeoides floribundus, charming soft pink flowers all summer, whitish leaves	"	cl.	0.4
1303 aureus superbus, pretty trailing species, flowers golden-yellow	HHP*	d.	0.3
1306 mauritanicus, violet-blue, pretty dwarf trailing species	"	d.	0.4
1308 tricolor (Miser Cordulatus), deep blue, yellow and white	"	d.	0.2
1309 — azureus, deep Wedgwood blue, golden centre	HA	1 1/2	0.3
1310 — roseus, delicate rose-pink flowers	"	1	0.3
COREOPSIS , Compositae. Common soil.			
1313 auriculata superba. See pubescens superba.	"	"	"
1314 grandiflora, large deep yellow, very distinct, grand for cutting	HB	3	0.3
1315 — lanceolata, large yellow heads, very showy border plant	HP	2 1/2	0.4
1316 — Mayfield Giant, taller and more vigorous than type	"	3	0.6
1317 — Perry's Double, semi-double with golden-yellow flowers	"	2 1/2	0.6
1318 pubescens superba, very fine growing, large yellow flowers with dark blotch in centre	"	3	0.6
1319 verticillata, slender habit, linear whorled leaves, dark yellow disk, elegant	"	2	0.6
CORARIA , Coriariaceae. Peaty soil.			
1321 myrsinifolia, evergreen shrub of spreading habit	HSh	5	0.6
1322 vermicillata, a small growing shrub, with yellow ornamental fruit	"	2	0.6
CORNFLOWER . See <i>Centaurea</i> .			
CORNUS , Cornaceae. Sand and peat.			
1323 Baileyi, berries white, often tinged pale blue	HT	3	0.6
1325 Kouss chinensis, has very large white bract, scarlet foliage in Autumn	HSh	12	1.0
1327 sanguinea, common Dog-wood, red wood effective during Winter	"	6	0.4
1328 alabrica, crimson bark, robust habit	"	8	0.4
CORONIA , Cornaceae. Light soil.			
1329 Coronaster, small shrub from New Zealand, yellow flowers, large red berries	HSh	6	1.0
1330 Virgata, rather larger foliage than preceding, yellow berries	"	4	1.0
CONOMILIA , Leguminosae. Common soil.			
1331 Emerici, a quick-growing species, suitable for covering banks	HSh	3	0.6
1332 glauca, beautiful yellow flowers, fragrant in the daytime	HHP	3	0.4
1333 vaginalls, a distinct herbaceous species	"	2	0.6
CORYDALIS (formosa). Papaveraceae. Sandy loam.			
1337 cheilanthifolia, fine Spring bloomer, fern-like foliage, yellow flowers	"	1	0.5
1338 lutea, showy golden-yellow flowers, glaucous foliage, dwarf habit	"	1	0.3
1340 achroelea, charming little rock plant, flowers delicate pale yellow	"	1	0.4
COSMOS , Compositae. Light soil.			
1343 bipinnatus hybridus praecox, fine mixture of early varieties	HHA	3	0.3
1344 — crimson, bright crimson flowers, slow early	"	3	0.3
1348 — Pink Beauty, double pink variety, good novelty	"	3	0.4
1349 — Rose Queen, early-flowered rose variety	"	3	0.4
1350 — Sensation, large pink and white flowers, very early	"	3	0.6
1351 — Giant Blush Queen, large-flowered, pale lilac rose	"	3	0.6
1352 — Hybrids, much improved strain and very early	"	3	0.6
1354 diversifolius atrosanguineus, King of the Blacks (Black Dahlia), dark purple, dwarf	HHP*	1 1/2	0.3
1355 Klondyke Orange Flame, large vivid orange flowers, should be sown early under glass	HHA	2	0.6
COTONEASTER , Rosaceae. Common soil.			
1359 adpressa, valuable for rock garden, spreading habit	HSh	1 1/2	0.6
1359 appianata, strong grower, white flowers followed by brilliant scarlet berries	"	1 1/2	0.6
1361 bullata, leaves dark red, covered beneath with grey down, flowers rosy-white, red fruit	"	12	0.6
1365 divaricata, dark green leaves, bright red egg-shaped berries	"	6	0.6
1366 Francocheti, erect-growing shrub, bright red berries	"	12	0.6
1367 frigida, makes fine standard tree, brilliant scarlet berries	"	tr.	0.6
1369 horizontalis, dense spreading branches, brilliant vermilion berries; fine for rocky	"	tr.	0.6
1370 humifusa, dark green prostrate foliage, brilliant red berries	"	5	0.6
1371 Lindleyi, dark stems, crimson berries	"	5	0.6
1372 — cochlearia, quite prostrate growth, pinkish flowers, followed by bright red berries	"	5	0.6
1373 microphylla, prostrate evergreen, pinkish flowers, crimson berries	"	tr.	0.3
1378 radcliffeana, a spreading shrub, small showy orange berries in Autumn	"	tr.	0.6
1379 Simonii, evergreen, red berries, makes a fine hedge	"	6-8	0.6
1380 thymaeifolia, neat-growing dwarf variety, suitable for rockeries, pinky-white flowers	"	tr.	0.6
COTULA , Compositae. Common soil.			
1381 barbata, small globular golden-yellow flowers, dwarf habit, fine for rockery or border	HA	1	0.4
COTYLEDON , Cruciferae. Light soil, warm position.			
1382 simplicifolia, a beautiful species, deep yellow flowers in drooping racemes	HP	1	0.6
CRABAPPLE , Cruciferae. Common garden soil.			
1383 cordifolia, loam soil, small white flowers in abundance	"	6	0.4
CRATAEGUS , Thorn, Rosaceae. Common soil.			
1384 Carrierei, single white flowers, clusters of pale yellowish fruit in Autumn	HSh	10	0.6
1385 cocinea, dark glossy leaves, large scarlet fruit	HT	15	0.6
1386 Crougalli, white flowers tinged with red, scarlet fruit	HSh	10	0.6
1387 Douglasi, this makes a fine ornamental tree, purplish fruit and fine foliage in the Autumn	"	15	0.6
CRIBRIS , Compositae. Common soil.			
1388 arborea, a pretty little hawkweed, rosy-pink flowers	HA	1	0.3
CROCUS , Iridaceae. Common soil.			
1392 Tommasinianus, pale bluish-lavender, beautiful	HBB	1	0.4
CRUCIATELLA , Rubiaceae. Sandy soil.			
1395 stylosa, pink, in large heads, pretty trailer, dry banks or rocks	HP	1	0.3
CUCURBITA , Gourd, Cucurbitaceae. Light rich soil.			
1397 melanosperma, very handsome variegated fruit and foliage	HHA	cl.	0.3
1399 — apple-shaped Gourd, creamy white	"	"	"
1400 — bicolor Gourd, very pretty variety, green and yellow	"	"	"
1401 — Carabass, strange shaped warty fruits	"	"	"
1402 — egg-shaped (Japanese Niac Egg), white ornamental	"	"	"
1403 — Miniature, fruits round, dark green yellow stripe	"	"	"
1404 — orange Gourd (Mock Orange), very pretty	"	"	"
1405 — pear-shaped Gourd, green and yellow striped, naked	"	"	"
1406 — green Gourd	"	"	"
1407 — striped Gourd, flatish in shape, dark green striped, yellow	"	"	"
1408 — varied Gourd, an attractive kind	"	"	"
CUPHEA , Lythraeae. Ordinary soil.			
1410 Avalon hybrid, a wonderful variety of colours	HHP	1 1/2	0.6
1411 miniata, Mexican species, purplish-rose flowers	"	"	"
CUPRESSUS , Coniferae. Common soil.			
1414 laevifolia, well-known ornamental tree	"	"	"
1415 — alberti, an attractive glaucous variety, erect growth	"	"	"
1417 — aurea, golden foliage, beautiful tree	"	"	"
CYANTHUS , Campanulaceae. Peat and leaf mould.			
1424 lobatus, very choice Alpine for rockery, flowers fine blue; rare	HP	tr.	1.0
CYCLAMEN , Primulaceae. Peat and loam.			
1427 Caum, charming miniature species for rockery, Winter flowering	"	"	"
1428 europaeum, purple and white, foliage cordate, very hardy, Summer flowering	"	"	"
1431 ibenicum, Winter flowering, purple flowers and marbled leaves	"	"	"
1432 neapolitanum, red-purple and white, good hardy species, Autumn flowering	"	"	"
1433 — album, dainty pure white flowers, followed by silver-marbled foliage	"	"	"
1434 parvicorn, saved from a choice selected strain, mixed	"	"	"
1435 — "Bushy Pioneer," remarkable strain, petals with feathered crest; in fine mixture	"	"	"
1436 — signatum Improved, very large-flowered strain of every shade of colour	"	"	"

2.6 – Correspondence between Sarah Lewendon and Brian Halliwell

- (a) – Letter from Sarah Lewendon (28-3-99) to Brian Halliwell requesting information on the *Cosmos atrosanguineus*' accessions at the Royal Botanic Gardens, Kew.

Royal Botanic Gardens, Kew, Richmond, Surrey TW9 3AB, UK

Telephone *direct*: +44 - (0)181-332 Fax *direct*: +44 - (0)181-332



Sarah Lewendon
Royal Botanic Gardens, Kew
Richmond
Surrey TW9 3DS

Brian Halliwell

28 March 1999

Dear Brian Halliwell

Mike Sinnott put your name forward, as some that might be able to help me. My name is Sarah Lewendon and I am a PhD student at the Jodrell Laboratory under the supervision of Simon Owens. Our research focus is self-incompatibility in *Cosmos atrosanguineus*. Presently I am attempting to track down the history and source of the Accessions we are using at RBG, Kew to see how these relate to the Hooker/Thompson 1861 record.

Mike Fay assures me that the *Cosmos atrosanguineus* of Hooker/Thompson died out at RBG, Kew in the mid 1970s and that the plant on which you and Fred Larkby developed the tuber propagation technique came from America, via Le Roy Davidson. Unfortunately, the records at Kew do not give the source of Le Roy Davidson's *Cosmos atrosanguineus* plants and so I am writing to you in the hope that you may be able to help. I would be grateful for any information about the source of the Davidson plant and whether this was the accession on which you worked.

Mike Fay thinks, that as a result of your propagation method, the Davidson Accession is probably the plant from which most of the present-day cultivated species are derived. He bases this view on his recent genetic fingerprinting work which appears to show all *Cosmos atrosanguineus* species to be clones.

I can be reached on my home number most evenings on (There is an answerphone at this number). Otherwise I can be reached at the Jodrell Laboratory, RBG, Kew (.....) on Thursdays and Fridays. I hope this request does not inconvenience you too greatly.

Looking forward to hearing from you

Yours sincerely

Email:@rbgkew.org.uk

Telephone *central*: +44 - (0)181- 332 5000 24hr recorded information: +44 - (0)181- 940 1171 Fax *central*: +44 - (0)181- 332 5197 Telex: 296694 KEWGAR

The Royal Botanic Gardens, Kew has charitable status

100% recycled paper

(b) – Reply from Brian Halliwell (5-4-99) to Sarah Lewendon's letter dated (28-3-99)

5th April 1999

Sarah Lewendon
Royal Botanic Gardens Kew
Richmond
Surrey TW9 3DS

Dear Sarah Lewendon,

I refer to your letter of 28th March seeking information about Cosmos atrosanguineus.

Some of the information you include is correct, some doubtful. I came to Kew in 1968 and there was no plant of this name or under its various synonyms at that time in what was the old Decorative nor in what was Albine when I transferred. If it was at Kew, I can only assume it was in the Temperate Department. I did receive a plant from Le Roy Davidson but this was most likely in the 30s; I met Davidson for the first time in 1976. Le Roy Davidson was an assembler of plants. He collected anything that was out of the ordinary from many different sources. Only some of them were planted in his garden, others died or were given away.

It was discovered that although this plant had a tuber, cuttings had to be taken in early summer to ensure there was a large enough tuber before the plant went dormant. The Davidson plant was planted on the Duchess Border and it was still there on my retirement in 1989. There were other plants of this species in England, probably even before I acquired the Davidson plant from North America.

Assuming that Le Roy Davidson is still alive I have no address for him; Tony Hall might. Even if you could make contact I feel you would be wasting your time for I would not expect him to remember his gift to me nor its origin.

Yours faithfully

Brian Halliwell

APPENDIX 3

3.1 - Protocol 1 – Wax embedding

- 90% alcohol for 2 hours
- 95% alcohol for 2hrs
- 100% alcohol for 2hrs (twice)
- 90 : 10 parts alcohol : HistoClear for 2hrs
- 70 : 30 alcohol : HistoClear for 2hrs
- 50 : 50 alcohol : HistoClear + ($\frac{1}{10}$ g eosin) for 6hrs
- 30 : 70 alcohol : HistoClear for 2hrs
- 10 : 90 alcohol : HistoClear for 2hrs
- 100% HistoClear for 2hrs.

3.2 - Protocol 2 – Staining schedule (safranin and Alcian blue)

- 100% HistoClear for 3 minutes (twice)
- 100% alcohol for 2 mins. (twice)
- 95% alcohol for 2 mins.
- 90% alcohol for 2 mins.
- 70% alcohol for 2 mins.
- 50% alcohol for 2 mins.
- safranin (1g safranin in 50% alcohol) for 2 mins.
- distilled water for 2 mins.
- Alcian blue (1% solution) for 4 mins.
- 50% alcohol for 2 mins.
- 70% alcohol for 2 mins.
- 90% alcohol for 2 mins.
- 95% alcohol for 2 mins.
- 100% alcohol for 2 mins. (twice)
- 100% HistoClear for 3 mins. (twice)

3.3 - Protocol 3 – Alcohol series for CPD

- 70% alcohol for 2 hrs
- 90% alcohol for 2 hrs
- 100% alcohol for 2 hrs (twice)

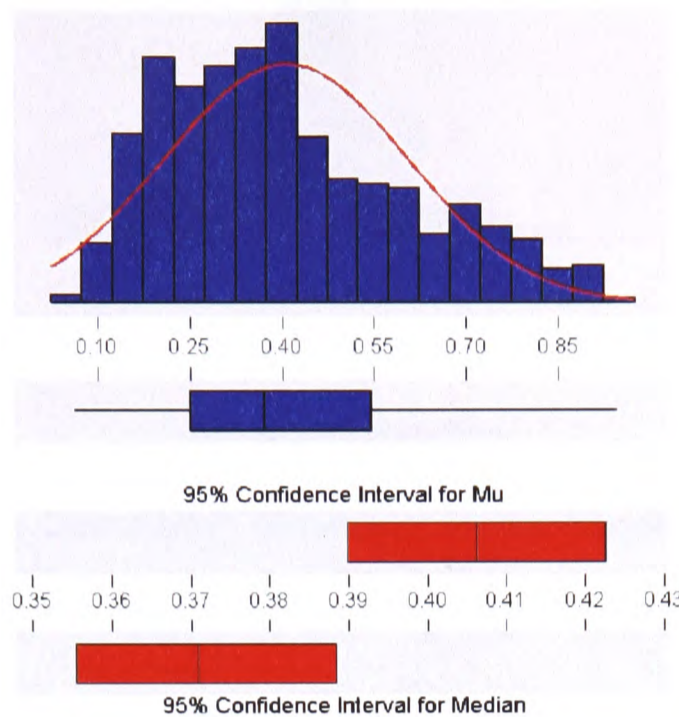
3.4 - Protocol 4 – Resin embedding

- Karnovsky's fixative (2% paraformaldehyde and 2.5% glutaraldehyde in 0.05M phosphate buffer) for 3 hours at 5°C
- buffer (0.1M phosphate buffer at pH 7.2) for 30 minutes at 5°C
- 1% osmium tetroxide solution for 2 hrs. at 5°C
- buffer for 10 mins. at 8°C
- buffer for 10 mins. at 11°C
- buffer for 10 mins. at 14°C
- 30% ethanol (EtOH) for 30 mins. at 17°C
- 50% EtOH for 30 mins. at 20°C
- 70% EtOH for 45 mins. at 20°C
- 90% EtOH for 1 hr. at 20°C
- 100% EtOH for 1 hr. at 20°C (twice)
- 1 : 3 resin (LR white) : EtOH for 1 hr. at 17°C
- 1 : 1 resin : EtOH for 1 hr. 30 mins. at 14°C
- 3 : 1 resin : EtOH for 2 hrs. at 11°C
- 100% resin for 2 hrs. at 8°C
- 100% resin for 4 hrs. at 5°C (four times)

APPENDIX 4 – Statistical analyses for Chapter 4

4.1 – Descriptive Statistics for pollen viability, pollen number and pollen size

Descriptive Statistics for Pollen Viability in Cosmos species



Variable: Pollen Viability

Anderson-Darling Normality Test

A-Squared: 8.117
P-Value: 0.000

Mean 0.406290
StDev 0.197254
Variance 3.89E-02
Skewness 0.630437
Kurtosis -3.8E-01
N 560

Minimum 0.062500
1st Quartile 0.250000
Median 0.370900
3rd Quartile 0.544550
Maximum 0.944400

95% Confidence Interval for Mu
0.389917 0.422662

95% Confidence Interval for Sigma
0.186339 0.209539

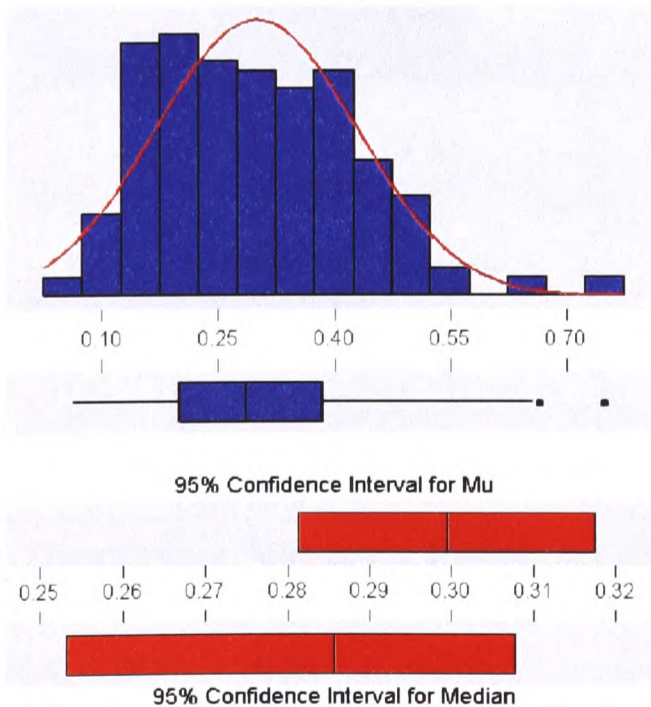
95% Confidence Interval for Median
0.355552 0.388311

4.1.1 - Descriptive Statistics: Pollen Viability

Variable	N	Mean	Median	TrMean	StDev	SE Mean
Viability	560	0.40629	0.37090	0.39803	0.19725	0.00834

Variable	Minimum	Maximum	Q1	Q3
Viability	0.06250	0.94440	0.25000	0.54455

Descriptive Statistics for Pollen viability in C. atrosanguineus accessions



Variable: Pollen Viability

Anderson-Darling Normality Test

A-Squared: 1.231
P-Value: 0.003

Mean 0.299456
StDev 0.129642
Variance 1.68E-02
Skewness 0.676838
Kurtosis 0.610947
N 200

Minimum 0.062500
1st Quartile 0.200000
Median 0.285700
3rd Quartile 0.383700
Maximum 0.750000

95% Confidence Interval for Mu
0.281379 0.317533

95% Confidence Interval for Sigma
0.118060 0.143763

95% Confidence Interval for Median
0.253299 0.307700

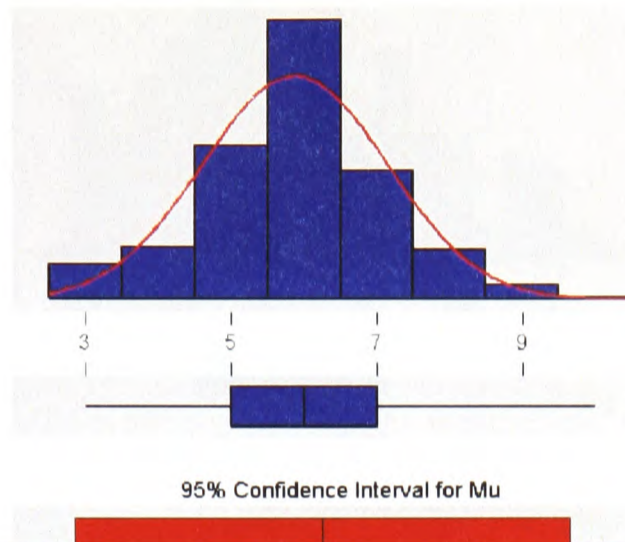
4.1.2 - Descriptive Statistics: Pollen Viability in C. atrosanguineus accessions

Variable	N	Mean	Median	TrMean	StDev	SE Mean
Viability	200	0.29946	0.28570	0.29406	0.12964	0.00917

Variable	Minimum	Maximum	Q1	Q3
Viability	0.06250	0.75000	0.20000	0.38370

4.1 – continued

Descriptive Statistics for Pollen Number in Cosmos species



Variable: Pollen Number

Anderson-Darling Normality Test

A-Squared: 15.805
P-Value: 0.000

Mean 5.87400
StDev 1.26702
Variance 1.60533
Skewness -7.0E-02
Kurtosis 0.363491
N 500

Minimum 3.0000
1st Quartile 5.0000
Median 6.0000
3rd Quartile 7.0000
Maximum 10.0000

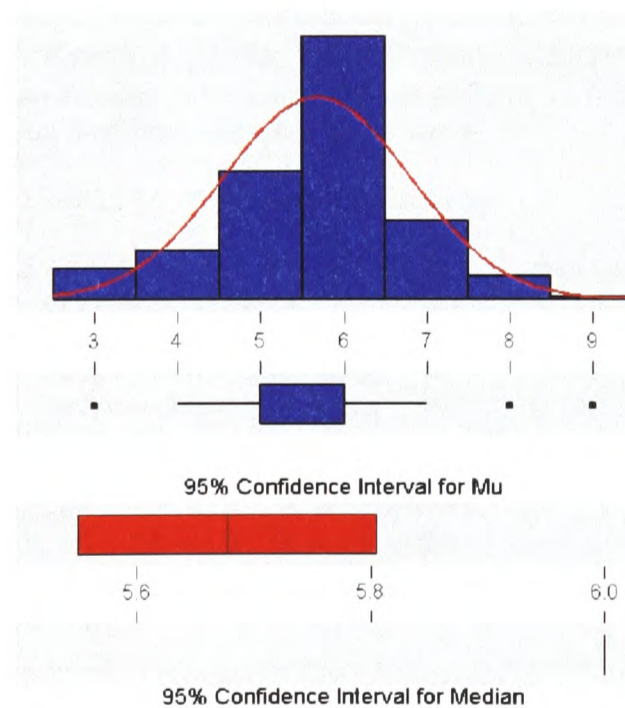
95% Confidence Interval for Mu

4.1.3 - Descriptive Statistics: Pollen Number

Variable	N	Mean	Median	TrMean	StDev	SE Mean
Number	500	5.8740	6.0000	5.8889	1.2670	0.0567

Variable	Minimum	Maximum	Q1	Q3
Number	3.0000	10.0000	5.0000	7.0000

Descriptive Statistics for Pollen Number in C. atrosanguineus accessions



Variable: Pollen Number

Anderson-Darling Normality Test

A-Squared: 14.150
P-Value: 0.000

Mean 5.67667
StDev 1.12383
Variance 1.26300
Skewness -3.8E-01
Kurtosis 0.460263
N 300

Minimum 3.00000
1st Quartile 5.00000
Median 6.00000
3rd Quartile 6.00000
Maximum 9.00000

95% Confidence Interval for Mu

5.54898 5.80435

95% Confidence Interval for Sigma

1.04052 1.22175

95% Confidence Interval for Median

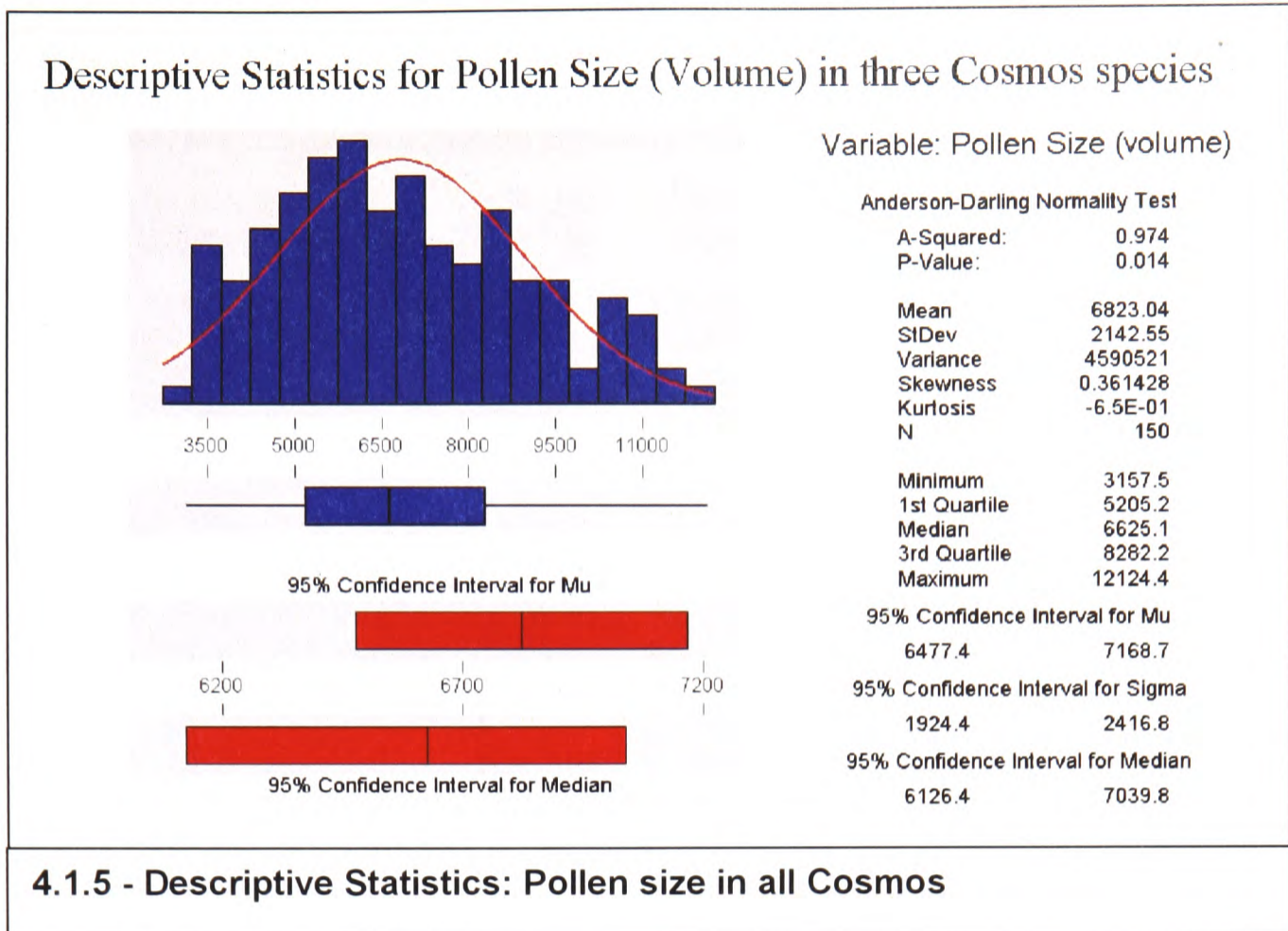
6.00000 6.00000

4.1.4 - Descriptive Statistics: Pollen Number vs. C. atrosanguineus accessions

Variable	N	Mean	Median	TrMean	StDev	SE Mean
Number	300	5.6767	6.0000	5.7000	1.1238	0.0649

Variable	Minimum	Maximum	Q1	Q3
Number	3.0000	9.0000	5.0000	6.0000

4.1 – continued



4.1.5 - Descriptive Statistics: Pollen size in all *Cosmos*

4.2 – Statistical analysis of pollen viability, pollen number and pollen size in *Cosmos*

Box 1 - Kruskal-Wallis Test: Pollen viability versus *Cosmos* species to test 1H_0 that pollen viability of *Cosmos atosanguineus*, *C. bipinnatus*, *C. sulphureus* (Spring) and *C. sulphureus* (Autumn) samples is the same

Kruskal-Wallis Test on Viability

Species	N	Median	Ave Rank	Z
<i>Cosmos atosanguineus</i>	200	0.2857	194.1	-9.42
<i>Cosmos bipinnatus</i>	200	0.4000	298.5	1.96
<i>Cosmos sulphureus</i> (Spring)	80	0.7157	493.8	12.73
<i>Cosmos sulphureus</i> (Autumn)	80	0.3504	238.5	-2.51
Overall	560	280.5		

H = 203.94 DF = 3 P = 0.000**

H = 203.99 DF = 3 P = 0.000** (adjusted for ties)

Reject 1H_0 .

Box 2 - Mann-Whitney U Test and CI: Pollen viability in *Cosmos atosanguineus* vs. pollen viability in *Cosmos bipinnatus* to test 2H_0 that pollen viability of *C. atosanguineus* and *C. bipinnatus* samples is the same

<i>C. atosanguineus</i>	N = 200	Median =	0.28570
<i>C. bipinnatus</i>	N = 200	Median =	0.40000

Point estimate for ETA1-ETA2 is -0.11420

95.0 Percent CI for ETA1-ETA2 is (-0.14580, -0.08220)

W = 32180.5

Test of ETA1 = ETA2 vs ETA1 not = ETA2 is significant at 0.0000**

The test is significant at 0.0000** (adjusted for ties)

Reject 2H_0 .

4.2 continued

Box 3 - Mann-Whitney U Test and CI: Pollen viability in *Cosmos bipinnatus* vs. pollen viability in *Cosmos sulphureus* (Spring) to test 3H_0 that pollen viability of *C. bipinnatus* and *C. sulphureus* (Spring) samples is the same

<i>C. bipinnatus</i>	N = 200	Median =	0.40000
<i>C. sulphureus</i> (Spring)	N = 80	Median =	0.71565

Point estimate for ETA1-ETA2 is -0.30000
 95.0 Percent CI for ETA1-ETA2 is (-0.34311,-0.25619)
 W = 21707.5

Test of ETA1 = ETA2 vs ETA1 not = ETA2 is significant at 0.0000**
 The test is significant at 0.0000** (adjusted for ties)

Reject 3H_0 .

Box 4 - Mann-Whitney U Test and CI: Pollen viability in *Cosmos bipinnatus* vs. pollen viability in *Cosmos sulphureus* (Autumn) to test 4H_0 that pollen viability of *C. bipinnatus* and *C. sulphureus* (Autumn) samples is the same.

<i>C. bipinnatus</i>	N = 200	Median =	0.40000
<i>C. sulphureus</i> (Autumn)	N = 80	Median =	0.35035

Point estimate for ETA1-ETA2 is 0.07010
 95.0 Percent CI for ETA1-ETA2 is (0.02778,0.11429)
 W = 30132.0

Test of ETA1 = ETA2 vs ETA1 not = ETA2 is significant at 0.0009**
 The test is significant at 0.0009** (adjusted for ties)

Reject 4H_0 .

Box 5 - Mann-Whitney U Test and CI: Pollen viability in *Cosmos atosanguineus* vs. pollen viability in *Cosmos sulphureus* (Spring) to test 5H_0 that pollen viability of *C. atosanguineus* and *C. sulphureus* (Spring) samples is the same

<i>C. atosanguineus</i>	N = 200	Median =	0.28570
<i>C. sulphureus</i> (Spring)	N = 80	Median =	0.71565

Point estimate for ETA1-ETA2 is -0.42065
 95.0 Percent CI for ETA1-ETA2 is (-0.45552,-0.38652)
 W = 20443.0

Test of ETA1 = ETA2 vs ETA1 not = ETA2 is significant at 0.0000**
 The test is significant at 0.0000** (adjusted for ties)

Reject 5H_0 .

Box 6 - Mann-Whitney U Test and CI: Pollen viability in *Cosmos atosanguineus* vs. pollen viability in *Cosmos sulphureus* (Autumn) to test 6H_0 that pollen viability of *C. atosanguineus* and *C. sulphureus* (Autumn) samples is the same

<i>C. atosanguineus</i>	N = 200	Median =	0.28570
<i>C. sulphureus</i> (Autumn)	N = 80	Median =	0.35035

Point estimate for ETA1-ETA2 is -0.04450
 95.0 Percent CI for ETA1-ETA2 is (-0.07689,-0.01288)
 W = 26420.0

Test of ETA1 = ETA2 vs ETA1 not = ETA2 is significant at 0.0061**
 The test is significant at 0.0061** (adjusted for ties)

Reject 6H_0 .

4.2 continued

Box 7 - Mann-Whitney U Test and CI: Pollen viability in *Cosmos sulphureus* (Spring) vs. pollen viability in *Cosmos sulphureus* (Autumn) to test 7H_0 that pollen viability of *C. sulphureus* (Spring) and *C. sulphureus* (Autumn) samples is the same

<i>C. sulphureus</i> (Spring)	N = 80	Median =	0.71565
<i>C. sulphureus</i> (Autumn)	N = 80	Median =	0.35035

Point estimate for ETA1-ETA2 is 0.38065
 95.0 Percent CI for ETA1-ETA2 is (0.34030,0.41671)
 W = 9451.5

Test of ETA1 = ETA2 vs ETA1 not = ETA2 is significant at 0.0000**
 The test is significant at 0.0000** (adjusted for ties)

Reject 7H_0 .

Box 8 - Kruskal-Wallis Test: Pollen viability of *C. atosanguineus* vs. accession number to test 8H_0 that pollen viability recorded for the three *C. atosanguineus* accessions; 1999 3819, 1999 2254, and 1997 6334 are the same

<i>C. atro</i> accs.	N	Median	Ave Rank	Z
1999 3189	80	0.2584	88.3	-2.44
1999 2254	60	0.3000	107.1	1.05
1997 6334	60	0.3038	110.2	1.55
Overall	200		100.5	

H = 6.04 DF = 2 P = 0.049
 H = 6.04 DF = 2 P = 0.049 (adjusted for ties)

Reject 8H_0 . There is weak support indicating a difference in the pollen viability of the three *C. atosanguineus* accessions; 1999 3819, 1999 2254 and 1997 6334

Box 9 - Mann-Whitney U Test and CI: Pollen viability in *Cosmos atosanguineus* accession 1999 3819 vs. *C. atosanguineus* 1999 2254 to test 9H_0 that the pollen viability of *C. atosanguineus* 1999 3819 and *C. atosanguineus* 1999 2254 samples are the same.

1999 3819	N = 80	Median =	0.25840
1999 2255	N = 60	Median =	0.30000

Point estimate for ETA1-ETA2 is -0.04170
 95.0 Percent CI for ETA1-ETA2 is (-0.08947,0.00000)
 W = 5202.5

Test of ETA1 = ETA2 vs ETA1 not = ETA2 is significant at 0.0658
 The test is significant at 0.0656 (adjusted for ties)

Cannot reject 9H_0 at alpha = 0.05

Box 10 - Mann-Whitney U Test and CI: Pollen viability in *Cosmos atosanguineus* accession 1999 2254 vs. *C. atosanguineus* 1997 6334 to test $^{10}H_0$ that pollen viability in samples of *C. atosanguineus* 1999 3819 and *C. atosanguineus* 1997 6334 are the same.

1999 3810	N = 80	Median =	0.25840
1997 6334	N = 60	Median =	0.30385

Point estimate for ETA1-ETA2 is -0.04760
 95.0 Percent CI for ETA1-ETA2 is (-0.08431,-0.00720)
 W = 5099.5

Test of ETA1 = ETA2 vs ETA1 not = ETA2 is significant at 0.0230
 The test is significant at 0.0229 (adjusted for ties)

Reject $^{10}H_0$.

4.2 continued

Box 11 - Mann-Whitney U Test and CI: Pollen viability in *Cosmos atrosanguineus* accession 1999 3819 vs. *C. atrosanguineus* 1997 6334 to test $^{11}H_0$ that pollen viability in samples of *C. atrosanguineus* 1999 2254 and *C. atrosanguineus* 1997 6334 are the same

1999 225 N = 60 Median = 0.30000
 1997 633 N = 60 Median = 0.30385

Point estimate for ETA1-ETA2 is -0.00475
 95.0 Percent CI for ETA1-ETA2 is (-0.05110,0.04707)
 W = 3587.5
 Test of ETA1 = ETA2 vs ETA1 not = ETA2 is significant at 0.8255
 The test is significant at 0.8254 (adjusted for ties)

Cannot reject $^{11}H_0$ at alpha = 0.05

Box 12 - Kruskal-Wallis Test: Pollen number vs. *Cosmos* species to test $^{12}H_0$ that pollen grain numbers in samples of *C. atrosanguineus*, *C. bipinnatus* and *C. sulphureus* (Spring) are the same

Species	N	Median	Ave Rank	Z
<i>C. atrosanguineus</i>	300	6.000	229.8	-3.92
<i>C. bipinnatus</i>	100	7.000	319.8	5.36
<i>C. sulphureus</i>	100	6.000	243.3	-0.56
Overall	500		250.5	

H = 29.38 DF = 2 P = 0.000**
 H = 31.83 DF = 2 P = 0.000** (adjusted for ties).

Reject $^{12}H_0$

Box 13 - Mann-Whitney Test and CI. Pollen number: *C. atrosanguineus* vs. *C. bipinnatus* to test $^{13}H_0$ that the number of pollen grains produced by samples *C. atrosanguineus* and *C. bipinnatus* are same

C. atrosanguineus N = 300 Median = 6.0000
C. bipinnatus N = 100 Median = 7.0000

Point estimate for ETA1-ETA2 is -1.0000
 95.0 Percent CI for ETA1-ETA2 is (-0.9999,-0.9999)
 W = 54782.0
 Test of ETA1 = ETA2 vs ETA1 not = ETA2 is significant at 0.0000**
 The test is significant at 0.0000** (adjusted for ties).

Reject $^{13}H_0$

Box 14 - Mann-Whitney Test and CI. Pollen number: *C. atrosanguineus* vs. *C. sulphureus* to test $^{14}H_0$ that the number of pollen grains produced by samples from populations of *C. atrosanguineus* and *C. sulphureus* are the same

C. atrosanguineus N = 300 Median = 6.0000
C. sulphureus N = 100 Median = 6.0000

Point estimate for ETA1-ETA2 is -0.0000
 95.0 Percent CI for ETA1-ETA2 is (0.0001,0.0000)
 W = 59312.0
 Test of ETA1 = ETA2 vs ETA1 not = ETA2 is significant at 0.4029
 The test is significant at 0.3780 (adjusted for ties)

Cannot reject $^{14}H_0$ at alpha = 0.05

4.2 continued

Box 15 - Mann-Whitney Test and CI. Pollen number: *C. bipinnatus* vs. *C. sulphureus* to test $^{15}H_0$ that the number of pollen grains produced samples from populations of by *C. bipinnatus* and *C. sulphureus* are the same

C. bipinnatus N = 100 Median = 7.0000
C. sulphureus N = 100 Median = 6.0000

Point estimate for ETA1-ETA2 is 1.0000

95.0 Percent CI for ETA1-ETA2 is (-0.0000,1.0000)

W = 11608.0

Test of ETA1 = ETA2 vs ETA1 not = ETA2 is significant at 0.0001**

The test is significant at 0.0001** (adjusted for ties).

Reject $^{15}H_0$

Box 16 - Kruskal-Wallis Test. *C. atrosanguineus* pollen grain number vs. *C. atrosanguineus* accession number to test $^{16}H_0$ that the number of pollen grains produced in the three *C. atrosanguineus* accessions; are the same

Accession	N	Median	Ave Rank	Z
1999 3819	100	6.000	156.8	0.88
1999 2254	100	6.000	148.7	-0.25
1997 6334	100	6.000	146.0	-0.63
Overall	300		150.5	

H = 0.83 DF = 2 P = 0.661

H = 0.93 DF = 2 P = 0.627 (adjusted for ties).

Cannot reject $^{16}H_0$ at alpha = 0.05

Box 17 - Mann-Whitney Test and CI. Pollen number in *C. atrosanguineus* accession 3819: plant 2 vs. plant 3 to test $^{17}H_0$ that the number of pollen grains produced by *C. atrosanguineus* plants 2 and 3 are the same

Plant No.2 N = 50 Median = 6.0000

Plant No.4 N = 50 Median = 6.0000

Point estimate for ETA1-ETA2 is -0.0000

95.0 Percent CI for ETA1-ETA2 is (0.0000,0.0002)

W = 2520.5

Test of ETA1 = ETA2 vs ETA1 not = ETA2 is significant at 0.9780

The test is significant at 0.9764 (adjusted for ties)

Cannot reject $^{17}H_0$ at alpha = 0.05

Box 18 - Mann-Whitney Test and CI: Pollen number in *C. atrosanguineus* accession 2254: plant 5 vs. plant 6 to test $^{18}H_0$ that the number of pollen grains produced by *C. atrosanguineus* plants 5 and 6 are the same

Plant No.5 N = 50 Median = 6.0000

Plant No.6 N = 50 Median = 6.0000

Point estimate for ETA1-ETA2 is -0.0000

95.0 Percent CI for ETA1-ETA2 is (0.0000,-0.0000)

W = 2534.5

Test of ETA1 = ETA2 vs ETA1 not = ETA2 is significant at 0.9505

The test is significant at 0.9482 (adjusted for ties)

Cannot reject $^{18}H_0$ at alpha = 0.05

Box 19 - Mann-Whitney Test and CI: Pollen number in *C. atrosanguineus* 6334: plant 9 vs. plant 10 to test $^{19}H_0$ that the number of pollen grains produced by *Cosmos atrosanguineus* plants 9 and 10 are the same

Plant No. 9 N = 50 Median = 6.0000

Plant No. 10 N = 50 Median = 6.0000

Point estimate for ETA1-ETA2 is 0.0000

95.0 Percent CI for ETA1-ETA2 is (-0.0003,0.0000)

W = 2616.0

Test of ETA1 = ETA2 vs ETA1 not = ETA2 is significant at 0.5327

The test is significant at 0.5052 (adjusted for ties)

Cannot reject $^{19}H_0$ at alpha = 0.05

4.2 continued

Box 20 - Mann-Whitney Test and CI. Pollen number in *C. bipinnatus*: plant 3 vs. plant 8 to test $^{20}H_0$ that the number of pollen grains produced by *C. bipinnatus* plants 3 and 8 are the same

Plant No.3 N = 50 Median = 7.000
 Plant No.8 N = 50 Median = 7.000
 Point estimate for ETA1-ETA2 is -0.000
 95.0 Percent CI for ETA1-ETA2 is (0.000,1.000)
 W = 2601.5
 Test of ETA1 = ETA2 vs ETA1 not = ETA2 is significant at 0.6003
 The test is significant at 0.5928 (adjusted for ties)

Cannot reject $^{20}H_0$ at alpha = 0.05

Box 21 Mann-Whitney Test and CI. Pollen number in *C. sulphureus* (Spring) plant 6 vs. plant 7 to test $^{21}H_0$ that the number of pollen grains produced by *C. sulphureus* plants 5 and 6 are the same

Plant No.6 N = 50 Median = 6.0000
 Plant No.7 N = 50 Median = 6.0000
 Point estimate for ETA1-ETA2 is 0.0000
 95.0 Percent CI for ETA1-ETA2 is (-1.0002,-0.0000)
 W = 2444.5
 Test of ETA1 = ETA2 vs ETA1 not = ETA2 is significant at 0.5813
 The test is significant at 0.5666 (adjusted for ties)

Cannot reject $^{21}H_0$ at alpha = 0.05

Box 22 - Results for Spearman rank-order-correlation to test $^{22}H_0$ that no significant correlation exists between pollen viability and pollen number of: *C. atosanguineus*; plants 2 vs. 3 (1999 3819), plants 5 vs. 6 (1999 2254), plants 9 vs.10 (1997 6334); *C. bipinnatus*; plants 3 vs. 8 (1996 582); and *C. sulphureus*; plants 6 vs. 7 (1996 980)

Correlations: ranked pollen viability vs. ranked pollen number

Spearman rank-order correlation of Pollen viability and Pollen Number $r_s = -0.020$; $r_s^2 = 0.0004$; $P = 0.774$

Cannot reject $^{22}H_0$

Box 23 - Kruskal-Wallis Test. Pollen size (volume) vs. *Cosmos* species to test hypothesis $^{23}H_0$ that pollen size in the three *Cosmos* species are the same.

Species	N	Median	Ave Rank	Z
<i>C. atro</i>	50	8787	119.5	8.76
<i>C. bip</i>	50	5847	56.2	-3.85
<i>C. sul</i>	50	5278	50.8	-4.92
Overall	150		75.5	

H = 77.20 DF = 2 P = 0.000**
 H = 77.22 DF = 2 P = 0.000** (adjusted for ties)

Reject $^{23}H_0$

Box 24 - Mann-Whitney Test and CI. Pollen size in *C. atosanguineus* vs. pollen size in *C. bipinnatus* to test $^{24}H_0$ that pollen size in populations of *C. atosanguineus* and *C. bipinnatus* are the same.

C. atro N = 50 Median = 8787.1
C. bip N = 50 Median = 5847.4
 Point estimate for ETA1-ETA2 is 3133.2
 95.0 Percent CI for ETA1-ETA2 is (2614.3,3647.8)
 W = 3660.5

Test of ETA1 = ETA2 vs ETA1 not = ETA2 is significant at 0.0000
 The test is significant at 0.0000 (adjusted for ties)

Reject $^{24}H_0$

4.2 continued

Box 25 - Mann-Whitney Test and CI. Pollen size in *C. atrosanguineus* vs. pollen size in *C. sulphureus* to test $^{25}H_0$ that pollen size in populations of *C. atrosanguineus* and *C. sulphureus* are the same.

C. atro N = 50 Median = 8787.1
C. sul N = 50 Median = 5278.2
Point estimate for ETA1-ETA2 is 3512.1
95.0 Percent CI for ETA1-ETA2 is (2869.7,4148.8)
W = 3588.0

Test of ETA1 = ETA2 vs ETA1 not = ETA2 is significant at 0.0000
The test is significant at 0.0000 (adjusted for ties)

Reject $^{25}H_0$

Box 26 - Mann-Whitney Test and CI: Pollen size in *C. bipinnatus* vs. pollen size in *C. sulphureus* to test $^{26}H_0$ that pollen size in populations of *C. bipinnatus* and *C. sulphureus* are the same.

C. bip N = 50 Median = 5847.4
C. sul N = 50 Median = 5278.2
Point estimate for ETA1-ETA2 is 371.7
95.0 Percent CI for ETA1-ETA2 is (-256.3,984.3)
W = 2695.0

Test of ETA1 = ETA2 vs ETA1 not = ETA2 is significant at 0.2426
The test is significant at 0.2425 (adjusted for ties)

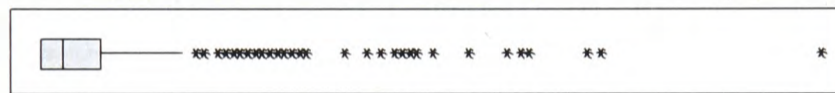
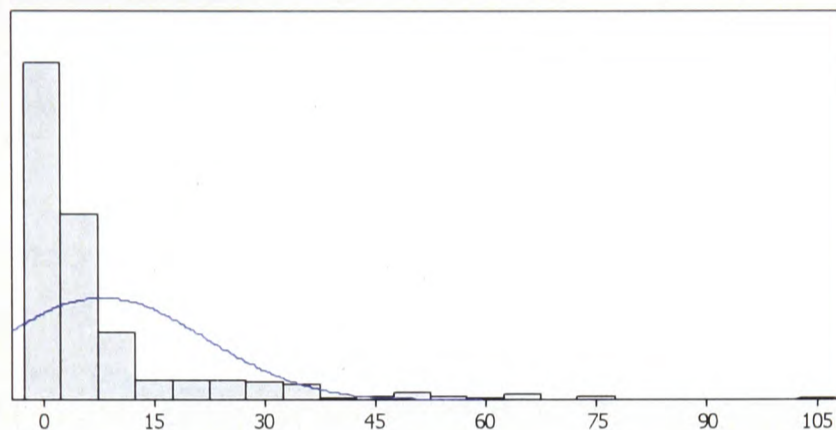
Cannot reject $^{26}H_0$ at alpha = 0.05

Appendix 5 - Statistical analyses and plant data for Chapter 5

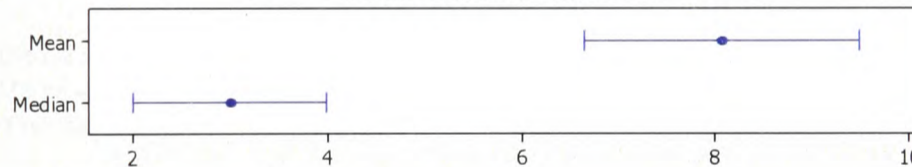
5.1 - Descriptive Statistics for compatible pollen tubes and incompatible pollen tubes produced in all *Cosmos bipinnatus* compatibility groups

Box 1a – Descriptive statistics to test null hypothesis $^{1a}H_0$ = that compatible pollen tubes produced in all *C.-bipinnatus* compatibility groups have normal distribution.

Summary for compatible pollen tubes



95% Confidence Intervals



Anderson-Darling Normality Test

A-Squared 47.66
P-Value < 0.005

Mean 8.069
StDev 13.880
Variance 192.664
Skewness 3.0619
Kurtosis 11.7624
N 375

Minimum 0.000
1st Quartile 0.000
Median 3.000
3rd Quartile 8.000
Maximum 106.000

95% Confidence Interval for Mean

6.660 9.479

95% Confidence Interval for Median

2.000 4.000

95% Confidence Interval for StDev

12.953 14.952

Descriptive Statistics: compatible pollen tubes (pts.) in all *Cosmos bipinnatus* compatibility groups

Variable	N	N*	Mean	SE Mean	StDev	Minimum	Q1
compatible pts.	375	0	8.069	0.717	13.880	0.000000000	0.000000000

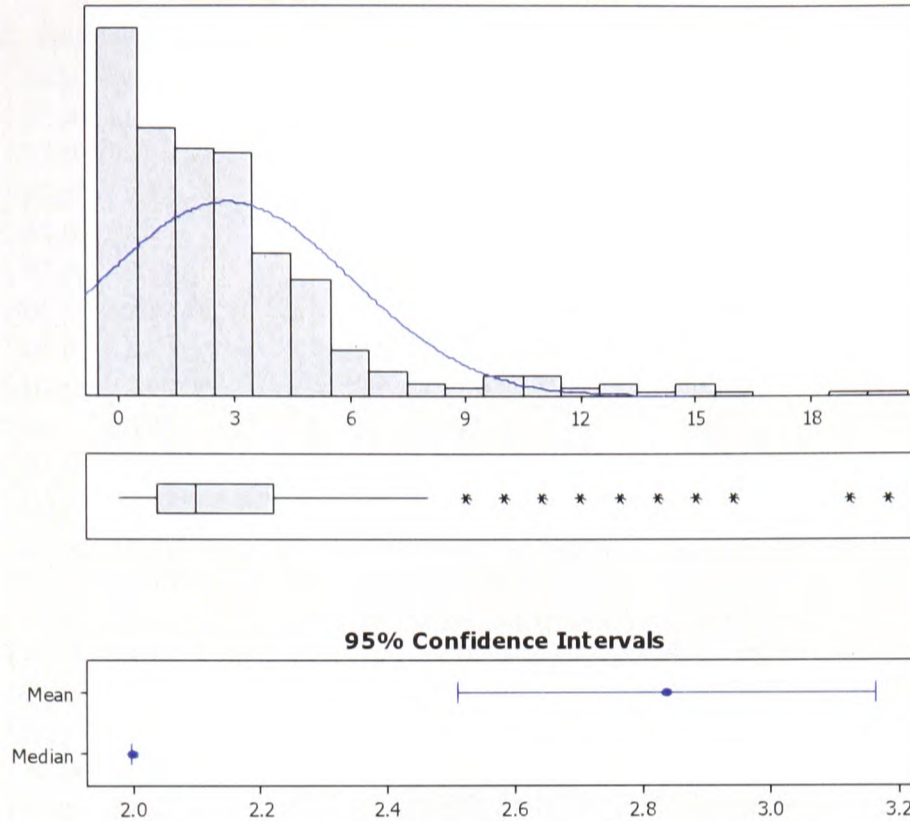
Variable	Median	Q3	Maximum
compatible pts.	3.000	8.000	106.000

Reject $^{1a}H_0$ ($p = < 0.05$) therefore can assume that compatible pollen tubes produced in all *C. bipinnatus* compatibility groups do not have normal distribution (p -value = < 0.05).

5.1 - continued

Box 1b – Descriptive statistics to test null hypothesis 1H_0 = that incompatible pollen tubes produced in all *C.-bipinnatus* compatibility groups have normal distribution.

Summary for Incompatible pollen tubes



Anderson-Darling Normality Test

A-Squared 21.45
P-Value < 0.005

Mean 2.8373
StDev 3.2205
Variance 10.3719
Skewness 2.18473
Kurtosis 6.13673
N 375

Minimum 0.0000
1st Quartile 1.0000
Median 2.0000
3rd Quartile 4.0000
Maximum 20.0000

95% Confidence Interval for Mean
2.5103 3.1643

95% Confidence Interval for Median
2.0000 2.0000

95% Confidence Interval for StDev
3.0054 3.4692

Descriptive Statistics: incompatible pollen tubes (pts.) in all *Cosmos bipinnatus* compatibility groups

Variable	N	N*	Mean	SE Mean	StDev	Minimum	Q1
Incompatible pts	375	0	2.837	0.166	3.221	0.000000000	1.000

Variable	Median	Q3	Maximum
Incompatible pts	2.000	4.000	20.000

Reject 1H_0 ($p = < 0.05$), therefore can assume that incompatible pollen tubes produced in all *C.-bipinnatus* compatibility groups do not have normal distribution (p -value = < 0.05).

5.2 - Statistical analysis for compatible pollen tubes and incompatible pollen tubes produced in all *Cosmos bipinnatus* compatibility groups

Box 1c – Kruskal-Wallis Test: Compatible pollen tubes versus C.bip cross to test 1H_0 , that the number of compatible pollen tubes produced in all *Cosmos-bipinnatus* compatibility groups is the same.

C.bip cross	N	Median	Ave Rank	Z
[Bip 1x1]	15	0.000000000	77.3	-4.04
[Bip 1x2]	15	3.50000E+01	353.1	6.02
[Bip 1x3]	15	0.000000000	67.7	-4.39
[Bip 1x4]	15	5.30000E+01	361.9	6.34
[Bip 1x5]	15	3.000000000	169.0	-0.69
[Bip 2x1]	15	3.000000000	191.9	0.14
[Bip 2x2]	15	0.000000000	81.1	-3.90
[Bip 2x3]	15	4.000000000	203.3	0.56
[Bip 2x4]	15	9.000000000	279.7	3.35
[Bip 2x5]	15	7.000000000	274.0	3.14
[Bip 3x1]	15	2.000000000	169.6	-0.67
[Bip 3x2]	15	8.000000000	271.8	3.06
[Bip 3x3]	15	0.000000000	58.0	-4.74
[Bip 3x4]	15	7.000000000	263.3	2.75
[Bip 3x5]	15	8.000000000	271.8	3.05
[Bip 4x1]	15	1.000000000	114.7	-2.67
[Bip 4x2]	15	3.000000000	182.3	-0.21
[Bip 4x3]	15	3.000000000	166.7	-0.78
[Bip 4x4]	15	0.000000000	81.1	-3.90
[Bip 4x5]	15	1.000000000	151.7	-1.32
[Bip 5x1]	15	1.30000E+01	315.9	4.67
[Bip 5x2]	15	1.10000E+01	277.9	3.28
[Bip 5x3]	15	3.000000000	188.4	0.02
[Bip 5x4]	15	0.000000000	69.6	-4.32
[Bip 5x5]	15	0.000000000	58.0	-4.74
Overall	375		188.0	

H = 284.66 DF = 24 P = 0.000

H = 293.67 DF = 24 P = 0.000 (adjusted for ties)

Reject 1H_0 ($p = < 0.05$), therefore can assume there is significant difference in the number of compatible pollen tubes produced by all *Cosmos bipinnatus* compatibility groups in POLL-01 pollination experiments.

5.3 – Statistical analysis of *Cosmos bipinnatus* pollination groups

Box 2 Kruskal-Wallis Test: $^{2a}H_0$, that the number of compatible pollen tubes produced by selfed *Cosmos bipinnatus* (Bip) groups is the same.

Bip Pollination	N	Median	Ave Rank	Z
Bip 1 selfed	15	0.00E+00	41.5	0.69
Bip 2 selfed	15	0.00E+00	42.3	0.85
Bip 3 selfed	15	0.00E+00	32.0	-1.19
Bip 4 selfed	15	0.00E+00	42.3	0.85
Bip 5 selfed	15	0.00E+00	32.0	-1.19
Overall	75		38.0	

H = 3.80 DF = 4 P = 0.433

H = 9.37 DF = 4 P = 0.053 (adjusted for ties)

Cannot reject $^{2a}H_0$ ($p = 0.053$), there is very weak support for assuming that there is no significant difference in the number of compatible pollen tubes produced by selfed *Cosmos bipinnatus* (Bip) groups. However Bip 3 and Bip 5 identify as the most extreme groups, and when the data from these two selfed individuals are removed from the Kruskal-Wallis test, then the significance in number of compatible pollen tubes produced in selfed Bip 1, Bip 2 and Bip 3 individuals increases greatly (see $^{2b}H_0$ below)

$^{2b}H_0$, that the number of compatible pollen tubes produced by *Cosmos bipinnatus* selfed groups; Bip 1, Bip 2 and Bip 4 is the same.

C. bip

pollination	N	Median	Ave Rank	Z
Bip 1 (selfed)	15	0.000000000	22.5	-0.19
Bip 2 (selfed)	15	0.000000000	23.3	0.10
Bip 4 (selfed)	15	0.000000000	23.3	0.10
Overall	45		23.0	

H = 0.04 DF = 2 P = 0.982

H = 0.06 DF = 2 P = 0.970 (adjusted for ties)

Cannot reject $^{2b}H_0$, therefore can assume that the number of compatible pollen tubes produced by selfed *Cosmos bipinnatus* groups; Bip 1, Bip 2 and Bip 4 is the same.

Box 3 - Kruskal-Wallis Test: 3H_0 , that the number of compatible pollen tubes produced in selfed *Cosmos bipinnatus* groups and cross-incompatible groups is the same

C. bip

pollination	N	Median	Ave Rank	Z
Bip 1 x 1	15	0.000000000	77.3	-2.49
Bip 2 x 2	15	0.000000000	81.0	-2.28
Bip 3 x 3	15	0.000000000	58.0	-3.60
Bip 4 x 4	15	0.000000000	81.0	-2.28
Bip 5 x 5	15	0.000000000	58.0	-3.60
Bip 1 x 3	15	0.000000000	67.7	-3.04
Bip 1 x 5	15	3.000000000	160.2	2.29
Bip 2 x 1	15	3.000000000	177.8	3.30
Bip 2 x 3	15	4.000000000	187.0	3.83
Bip 3 x 1	15	2.000000000	162.5	2.42
Bip 4 x 1	15	1.000000000	114.1	-0.37
Bip 4 x 2	15	3.000000000	166.8	2.67
Bip 4 x 3	15	3.000000000	152.4	1.84
Bip 4 x 5	15	1.000000000	138.6	1.04
Bip 5 x 3	15	3.000000000	176.0	3.20
Bip 5 x 4	15	0.000000000	69.5	-2.94
Overall	240		120.5	

H = 111.58 DF = 15 P = 0.000

H = 125.98 DF = 15 P = 0.000 (adjusted for ties)

Reject 3H_0 ($p = < 0.05$), therefore can assume there is significant difference in the number of compatible pollen tubes produced by *Cosmos bipinnatus* selfed groups and cross-incompatible groups.

5.3 – continued

Box 4 - Kruskal-Wallis Test: 4H_0 , that the number of compatible pollen tubes produced by strong cross-incompatible groups [Bip 1x3], [Bip 4x1], [Bip 4x5], [Bip 5x4] are the same as the number of compatible pollen tubes produced by selfed *Cosmos bipinnatus* (Bip) groups.

C. bip				
pollination	N	Median	Ave Rank	Z
Bip 1 x 1	15	0.000000000	66.6	-0.15
Bip 2 x 2	15	0.000000000	68.4	0.04
Bip 3 x 3	15	0.000000000	51.0	-1.79
Bip 4 x 4	15	0.000000000	68.4	0.04
Bip 5 x 5	15	0.000000000	51.0	-1.79
Bip 1 x 3	15	0.000000000	58.8	-0.97
Bip 4 x 1	15	1.000000000	91.9	2.51
Bip 4 x 5	15	1.000000000	96.2	2.96
Bip 5 x 4	15	0.000000000	59.7	-0.87
Overall	135		68.0	

H = 20.59 DF = 8 P = 0.008
H = 35.56 DF = 8 P = 0.000 (adjusted for ties)

Reject 4H_0 ($p = < 0.05$), therefore can assume there is significant difference between the number of compatible pollen tubes produced by strong cross incompatible groups and selfed *Cosmos bipinnatus*. The cross incompatible groups [Bip 4 x 1] and [Bip 4 x 5] identify as the highest extreme results in this test.

Box 5 - Kruskal-Wallis Test: 5H_0 , that the number of compatible pollen tubes produced by strong reciprocally cross-incompatible groups [Bip 1 x 3] and [Bip 5 x 4] are the same as the number of compatible pollen tubes produced by selfed *Cosmos bipinnatus* (Bip) groups.

C. bip				
pollination	N	Median	Ave Rank	Z
Bip 1 x 1	15	0.000000000	58.3	0.73
Bip 2 x 2	15	0.000000000	59.4	0.88
Bip 3 x 3	15	0.000000000	45.0	-1.10
Bip 4 x 4	15	0.000000000	59.4	0.88
Bip 5 x 5	15	0.000000000	45.0	-1.10
Bip 1 x 3	15	0.000000000	51.7	-0.18
Bip 5 x 4	15	0.000000000	52.2	-0.11
Overall	105		53.0	

H = 3.89 DF = 6 P = 0.691
H = 9.99 DF = 6 P = 0.125 (adjusted for ties)

Cannot reject 5H_0 , therefore can assume that the number of compatible pollen tubes produced by strong reciprocally cross-incompatible groups [Bip 1 x 3], [Bip 5 x 4] and selfed *Cosmos bipinnatus* groups are the same.

5.3 – continued

Box 6 - Kruskal-Wallis Test: 6H_0 that the number of compatible pollen tubes produced by *C. bipinnatus* cross-incompatible groups having a median >0 is the same.

C. bip					
pollination	N	Median	Ave Rank	Z	
Bip 1 x 5	15	3.000	68.3	0.03	
Bip 2 x 1	15	3.000	78.8	1.13	
Bip 2 x 3	15	4.000	84.5	1.73	
Bip 3 x 1	15	2.000	64.5	-0.37	
Bip 4 x 1	15	1.000	36.3	-3.33	
Bip 4 x 2	15	3.000	75.3	0.77	
Bip 4 x 3	15	3.000	68.3	0.03	
Bip 4 x 5	15	1.000	59.4	-0.91	
Bip 5 x 3	15	3.000	76.8	0.92	
Overall	135		68.0		

H = 15.80 DF = 8 P = 0.045

H = 16.13 DF = 8 P = 0.041 (adjusted for ties)

Reject 6H_0 therefore can assume that there is significant difference in the number of compatible pollen tubes produced by *C. bipinnatus* cross-incompatible groups having a median >1. Cross incompatible groups [Bip 4 x 1] and [Bip 4 x 5] identify as the lowest extreme results.

Box 7 – Mann-Whitney Test and CI: 7H_0 that the number of compatible pollen tubes produced by cross-incompatible *C. bipinnatus* groups having a median of 1 compatible pollen grain per stigma is the same

C. bip		
Poll.	N	Median
Bip 4 x 1	15	1.000
Bip 4 x 5	15	1.000

Point estimate for ETA1-ETA2 is 0.000

95.4 Percent CI for ETA1-ETA2 is (-3.999,0.999)

W = 210.5

Test of ETA1 = ETA2 vs ETA1 not = ETA2 is significant at 0.3725

The test is significant at 0.3535 (adjusted for ties)

Cannot reject 7H_0 therefore can assume that the number of compatible pollen tubes produced by cross-incompatible groups [Bip 4 x 1] and [Bip 4 x 5] is the same

Box 8 - Kruskal-Wallis Test: 8H_0 that the number of compatible pollen tubes produced by cross-incompatible *C. bipinnatus* groups having a median of 2-4 compatible pollen tubes per stigma is the same.

C. bip					
pollinations	N	Median	Ave Rank	Z	
Bip 1 x 5	15	3.000	48.5	-0.61	
Bip 2 x 1	15	3.000	56.9	0.54	
Bip 2 x 3	15	4.000	61.5	1.17	
Bip 3 x 1	15	2.000	44.5	-1.17	
Bip 4 x 2	15	3.000	54.8	0.25	
Bip 4 x 3	15	3.000	49.7	-0.45	
Bip 5 x 3	15	3.000	55.0	0.27	
Overall	105		53.0		

H = 3.22 DF = 6 P = 0.781

H = 3.28 DF = 6 P = 0.773 (adjusted for ties)

Cannot reject 8H_0 therefore can assume that the number of compatible pollen tubes produced by *C. bipinnatus* cross-incompatible groups with a median of 2-4 compatible pollen tubes per stigma is the same...

5.3 – continued

Box 9 - Kruskal-Wallis Test: 9H_0 that the number of incompatible category-2 pollen tubes produced by *C.-bipinnatus* selfed and cross-incompatible groups is the same.

C. bip pollination	N	Median	Ave Rank	Z
Bip 1 x 1	15	2.000000000	121.6	0.06
Bip 2 x 2	15	1.000000000	99.2	-1.23
Bip 3 x 3	15	0.000000000	88.5	-1.84
Bip 4 x 4	15	2.000000000	131.5	0.64
Bip 5 x 5	15	0.000000000	48.9	-4.12
Bip 1 x 3	15	2.000000000	120.2	-0.02
Bip 1 x 5	15	1.20000E+01	221.0	5.79
Bip 2 x 1	15	1.000000000	98.8	-1.25
Bip 2 x 3	15	1.000000000	105.3	-0.88
Bip 3 x 1	15	2.000000000	124.1	0.21
Bip 4 x 1	15	3.000000000	145.2	1.42
Bip 4 x 2	15	2.000000000	132.6	0.70
Bip 4 x 3	15	3.000000000	151.7	1.80
Bip 4 x 5	15	1.000000000	113.9	-0.38
Bip 5 x 3	15	5.000000000	168.8	2.78
Bip 5 x 4	15	0.000000000	56.6	-3.68
Overall	240		120.5	

H = 80.05 DF = 15 P = 0.000
H = 83.57 DF = 15 P = 0.000 (adjusted for ties)

Reject 9H_0 ($p = < 0.05$) therefore can assume that there is significant difference in number of incompatible category-2 pollen tubes produced by *C.-bipinnatus* selfed and cross-incompatible groups..

Box 10 - Kruskal-Wallis Test: $^{10}H_0$ that the number of incompatible category-2 pollen tubes produced by selfed *C.-bipinnatus* groups is the same.

Kruskal-Wallis Test on Incompatible pollen tubes

C. bip pollination	N	Median	Ave Rank	Z
Bip 1 x 1	15	2.000000000	46.1	1.60
Bip 2 x 2	15	1.000000000	38.9	0.19
Bip 3 x 3	15	0.000000000	34.4	-0.71
Bip 4 x 4	15	2.000000000	48.9	2.16
Bip 5 x 5	15	0.000000000	21.7	-3.24
Overall	75		38.0	

H = 14.60 DF = 4 P = 0.006
H = 16.38 DF = 4 P = 0.003 (adjusted for ties)

Reject $^{10}H_0$ ($p = < 0.05$), therefore can assume that there is significant difference in number of incompatible category-2 pollen tubes produced by selfed *C.-bipinnatus* groups..

5.3 – continued

Box 11 - Kruskal-Wallis Test: $^{11}H_0$ that the number of incompatible category-2 pollen tubes produced by all *C.-bipinnatus* cross-incompatible groups is the same.

C. bip					
pollination	N	Median	Ave Rank	Z	
Bip 1 x 3	15	2.000000000	75.0	-0.68	
Bip 1 x 5	15	1.20000E+01	148.8	5.60	
Bip 2 x 1	15	1.000000000	60.7	-1.90	
Bip 2 x 3	15	1.000000000	64.8	-1.55	
Bip 3 x 1	15	2.000000000	77.3	-0.48	
Bip 4 x 1	15	3.000000000	92.3	0.79	
Bip 4 x 2	15	2.000000000	83.3	0.03	
Bip 4 x 3	15	3.000000000	96.5	1.15	
Bip 4 x 5	15	1.000000000	71.8	-0.95	
Bip 5 x 3	15	5.000000000	110.0	2.29	
Bip 5 x 4	15	0.000000000	32.4	-4.30	
Overall	165		83.0		

H = 58.76 DF = 10 P = 0.000

H = 60.46 DF = 10 P = 0.000 (adjusted for ties)

Reject $^{11}H_0$ ($p = < 0.05$), therefore can assume that there is significant difference in the number of incompatible category-2 pollen tubes produced by all *C.-bipinnatus* cross-incompatible groups.

Box 12 - Kruskal-Wallis Test: $^{12}H_0$ that the number of incompatible category-2 pollen tubes produced by strong cross incompatible groups [Bip 1 x 3], [Bip 4 x 1], [Bip 4 x 5] and [Bip 5 x 4] is the same.

C. bip					
pollination	N	Median	Ave Rank	Z	
Bip 1 x 3	15	2.000000000	33.4	0.74	
Bip 1 x 1	15	3.000000000	40.2	2.48	
Bip 4 x 5	15	1.000000000	31.5	0.26	
Bip 5 x 4	15	0.000000000	16.9	-3.48	
Overall	60		30.5		

H = 14.19 DF = 3 P = 0.003

H = 15.20 DF = 3 P = 0.002 (adjusted for ties)

Reject $^{12}H_0$ ($p = < 0.05$), therefore can assume that there is significant difference in the number of incompatible category-2 pollen tubes produced by selfed *C.-bipinnatus* groups and strongly cross-incompatible groups.

Box 13 - Spearman rank-order correlation: Rank-F compatible pollen tubes, Rank-G incompatible pollen tubes in *C. bipinnatus* selfed and cross incompatible groups to test, $^{13}H_0$ that there is no correlation between the number of compatible pollen tubes and the number of incompatible pollen tubes in *C. bipinnatus* selfed and cross incompatible groups

Pearson correlation of Rank-F and Rank-G = $r_s = 0.368$

P-Value = 0.000

$r^2 = 0.135424$

Reject $^{13}H_0$ ($p = < 0.05$), therefore can assume that there is a significant weak positive correlation between compatible pollen tubes and incompatible pollen tubes in self and cross incompatible groups ($r_s = 0.367$; $p = < 0.05$). With ~13% of the variation in the number of compatible pollen tubes explained by the number of incompatible pollen tubes ($r^2 = 0.135424$). These data suggest stigmas of selfed and cross-incompatible groups that germinate more compatible pollen tubes tend to germinate more incompatible pollen tubes.

5.3 – continued

Box 14 - Kruskal-Wallis Test: $^{14}H_0$ that the number of compatible pollen tubes produced by *C. bipinnatus* semi-compatible and cross-compatible groups is the same.

C. bip				
pollination	N	Median	Ave Rank	Z
Bip 1x2 (+)	15	35.000	113.1	4.73
Bip 1x4 (+)	15	53.000	121.9	5.66
Bip 2x4 (semi)	15	9.000	55.4	-1.32
Bip 2x5 (semi)	15	7.000	48.7	-2.03
Bip 3x2 (semi)	15	8.000	52.0	-1.68
Bip 3x4 (semi)	15	7.000	42.6	-2.67
Bip 3x5 (semi)	15	8.000	46.5	-2.26
Bip 5x1 (semi)	15	13.000	77.3	0.97
Bip 5x2 (semi)	15	11.000	54.6	-1.40
Overall	135		68.0	

H = 69.59 DF = 8 P = 0.000

H = 69.73 DF = 8 P = 0.000 (adjusted for ties)

Reject $^{14}H_0$ ($p = < 0.05$), therefore can assume that there is significance difference in the number of compatible pollen tubes produced by *C. bipinnatus* semi-compatible groups and cross compatible groups. (Results of semi-compatible groups are highlighted).

Box 15 - Kruskal-Wallis Test: $^{15}H_0$ that the number of compatible pollen tubes on stigmas of *C. bipinnatus* semi-compatible (inconclusive) groups and cross-incompatible groups having a median of 2-4 compatible pollen tubes per stigma is the same.

C. bip				
pollination	N	Median	Ave Rank	Z
Bip 1x5 (x-in)	15	3.000	57.3	-3.19
Bip 2x1 (x-in)	15	3.000	71.0	-2.28
Bip 2x3 (x-in)	15	4.000	77.8	-1.83
Bip 3x1 (x-in)	15	2.000	51.5	-3.57
Bip 4x2 (x-in)	15	3.000	70.4	-2.32
Bip 4x3 (x-in)	15	3.000	64.0	-2.74
Bip 5x3 (x-in)	15	3.000	67.4	-2.52
Bip 2x4 (semi)	15	9.000	145.5	2.65
Bip 2x5 (semi)	15	7.000	140.9	2.34
Bip 3x2 (semi)	15	8.000	138.5	2.18
Bip 3x4 (semi)	15	7.000	130.2	1.63
Bip 3x5 (semi)	15	8.000	138.7	2.20
Bip 5x1 (semi)	15	13.000	179.6	4.90
Bip 5x2 (semi)	15	11.000	144.2	2.56
Overall	210		105.5	

H = 98.44 DF = 13 P = 0.000

H = 98.99 DF = 13 P = 0.000 (adjusted for ties)

Reject $^{15}H_0$ ($p = < 0.05$), therefore can assume that there is significance difference in the number of compatible pollen tubes produced by *C. bipinnatus* semi-compatible groups and cross incompatible groups.

Results of semi-compatible groups are highlighted.

5.3 – continued

Box 16 - Kruskal-Wallis Test: $^{16}H_0$, that the number of compatible pollen tubes on stigmas of *C. bipinnatus* semi compatible (inconclusive) groups is the same

C. bip					
pollination	N	Median	Ave Rank	Z	
Bip 2x4 (semi)	15	9.000	53.9	0.12	
Bip 2x5 (semi)	15	7.000	48.5	-0.62	
Bip 3x2 (semi)	15	8.000	50.9	-0.29	
Bip 3x4 (semi)	15	7.000	41.9	-1.52	
Bip 3x5 (semi)	15	8.000	46.4	-0.90	
Bip 5x1 (semi)	15	13.000	75.7	3.11	
Bip 5x2 (semi)	15	11.000	53.8	0.11	
Overall	105		53.0		

H = 11.42 DF = 6 P = 0.076

H = 11.47 DF = 6 P = 0.075 (adjusted for ties)

Cannot reject $^{16}H_0$, therefore can assume that the number of compatible pollen tubes produced by semi-incompatible (inconclusive) groups is the same.

[Bip 5 x 1] is highlighted as it has a much higher median and average rank than the other semi-compatible groups. Its inclusion within this group considerably reduces the significance of the Kruskal-Wallis p -value. When [Bip 5 x 1] is excluded from the Kruskal-Wallis test, the significance is greatly increased for this compatibility group (See Box 17 below).

Box 17 - Kruskal-Wallis Test: $^{17}H_0$, that the number of compatible pollen tubes on stigmas of *C. bipinnatus* semi-compatible groups with [Bip 5 x 1] excluded is the same and highly significant

C. bip					
pollination	N	Median	Ave Rank	Z	
Bip 2x4 (semi)	15	9.000	49.3	0.62	
Bip 2x5 (semi)	15	7.000	45.4	-0.02	
Bip 3x2 (semi)	15	8.000	46.4	0.15	
Bip 3x4 (semi)	15	7.000	39.5	-0.97	
Bip 3x5 (semi)	15	8.000	43.7	-0.29	
Bip 5x2 (semi)	15	11.000	48.7	0.51	
Overall	90		45.5		

H = 1.42 DF = 5 P = 0.923

H = 1.42 DF = 5 P = 0.922 (adjusted for ties)

Cannot reject $^{17}H_0$, therefore can assume that the number of compatible pollen tubes produced by all semi-compatible groups, with semi-compatible group [Bip 5 x 1] excluded, is the same and highly significant.

Box 18 - Kruskal-Wallis Test: $^{18}H_0$, that the number of compatible pollen tubes produced by *C.-bipinnatus* semi-compatible [Bip 5 x 1] cross compatible [Bip 1 x 2] and [Bip 1 x 4] is the same.

C. bip					
pollination	N	Median	Ave Rank	Z	
Bip 1 x 2	15	35.00	26.0	1.08	
Bip 1 x 4	15	53.00	33.4	3.76	
Bip 5 x 1 (semi)	15	13.00	9.6	-4.84	
Overall	45		23.0		

H = 25.80 DF = 2 P = 0.000

H = 25.82 DF = 2 P = 0.000 (adjusted for ties)

Reject $^{18}H_0$ ($p < 0.05$), therefore can assume that there is significance difference in the number of compatible pollen tubes produced by *C.-bipinnatus* semi-compatible [Bip 5 x 1] cross compatible [Bip 1 x 2] and [Bip 1 x 4]. The semi compatible group [Bip 5 x 1] identifies as the lowest extreme result (data highlighted).

5.3 – continued

Box 19 - Mann-Whitney Test and CI: $^{19}H_0$ that the number of compatible pollen tubes produced by *C. bipinnatus* compatible groups is the same.

Mann-Whitney Test and CI: compatible pollen tubes in [Bip 1 x 2] vs. [Bip 1 x 4]

<i>C. bip</i> pollination	N	Median
Bip 1 x 2	15	35.00
Bip 1 x 4	15	53.00

Point estimate for ETA1-ETA2 is -15.00

95.4 Percent CI for ETA1-ETA2 is (-30.00,-2.00)

W = 180.0

Test of ETA1 = ETA2 vs ETA1 not = ETA2 is significant at 0.0310

The test is significant at 0.0309 (adjusted for ties)

Reject $^{19}H_0$ ($p = < 0.05$), therefore can assume that there is significant difference in the number of compatible pollen tubes produced by *C. bipinnatus* compatible groups

Box 20 - Mann-Whitney Test and CI: $^{20}H_0$ that the number of compatible pollen tubes produced by *C. bipinnatus* semi-compatible group [Bip 5 x 1] and compatible group [Bip 1 x 2] are the same.

Mann-Whitney Test and CI: compatible pollen tubes in [Bip 5 x 1] vs. [Bip 1 x 2]

<i>C. bip</i> pollination	N	Median
Bip 5 x 1(semi)	15	13.00
Bip 1 x 2(compatible)	15	35.00

Point estimate for ETA1-ETA2 is -19.00

95.4 Percent CI for ETA1-ETA2 is (-27.00,-13.00)

W = 135.0

Test of ETA1 = ETA2 vs ETA1 not = ETA2 is significant at 0.0001

The test is significant at 0.0001 (adjusted for ties)

Reject $^{20}H_0$ ($p = < 0.05$), therefore can assume that there is a large and significant difference in the number of compatible pollen tubes produced by *C. bipinnatus* semi-compatible cross [Bip 5 x 1] and compatible cross [Bip 1 x 2].

Box 21 - Mann-Whitney Test and CI: $^{20}H_0$ that the number of compatible pollen tubes produced by *C. bipinnatus* semi-compatible group [Bip 5 x 1] and compatible group [Bip 1 x 4] are the same.

Mann-Whitney Test and CI: compatible pollen tubes in [Bip 5 x 1] vs. [Bip 1 x 4]

<i>C. bip</i> pollination	N	Median
Bip 5 x 1(semi)	15	13.00
Bip 1 x 4(compatible)	15	53.00

Point estimate for ETA1-ETA2 is -37.00

95.4 Percent CI for ETA1-ETA2 is (-50.00,-19.99)

W = 129.0

Test of ETA1 = ETA2 vs ETA1 not = ETA2 is significant at 0.0000

The test is significant at 0.0000 (adjusted for ties)

Reject $^{21}H_0$ ($p = < 0.05$), therefore can assume that there is large and significant difference in the number of compatible pollen tubes produced by *C. bipinnatus* semi-compatible cross [Bip 5 x 1] and compatible cross [Bip 1 x 4].

5.3 – continued

Box 22 - Kruskal-Wallis Test: $^{18}H_0$ that the number of category-2 type incompatible pollen tubes produced by semi-compatible groups is the same

C. bip

pollination	N	Median	Ave Rank	Z
Bip 2x4 (semi)	15	3.000	51.8	-0.17
Bip 2x5 (semi)	15	2.000	54.1	0.15
Bip 3x1 (semi)	15	2.000	38.8	-1.96
Bip 3x4 (semi)	15	2.000	47.4	-0.77
Bip 3x5 (semi)	15	5.000	66.5	1.85
Bip 5x1 (semi)	15	4.000	68.9	2.18
Bip 5x2 (semi)	15	2.000	43.7	-1.28
Overall	105		53.0	

H = 12.24 DF = 6 P = 0.057

H = 12.49 DF = 6 P = 0.052 (adjusted for ties)

Cannot reject $^{18}H_0$ there is weak support for assuming that the number of incompatible category-2 type pollen tubes produced by semi-incompatible groups is the same.

Box 23 - Kruskal-Wallis Test: $^{19}H_0$ that the number of category-2 type incompatible pollen tubes produced by *C. bipinnatus* compatible groups is the same.

C. bip

pollination	N	Median	Ave Rank	Z
1	120	2.000	82.3	-8.04
2	112	4.000	153.2	8.04
Overall	232		116.5	

H = 64.67 DF = 1 P = 0.000

H = 67.67 DF = 1 P = 0.000 (adjusted for ties)

Reject $^{19}H_0$ ($p < 0.05$) therefore can assume that there is significant difference in number of incompatible category-2 type pollen tubes produced by compatible groups.

Box 24 - Spearman rank-order correlation: Rank-H, compatible pollen tubes, Rank-I incompatible pollen tubes in *C. bipinnatus* semi-compatible and cross compatible groups to test, $^{20}H_0$ that there is no correlation between the number of compatible pollen tubes and the number of incompatible pollen tubes in *C. bipinnatus* semi-compatible and cross compatible groups.

Pearson correlation of Rank-H and Rank-I = $r_s = 0.403$

p-Value = 0.000

$r_s^2 = 0.162409$

Reject $^{20}H_0$ ($p < 0.05$) therefore can assume that there is a significant weak positive correlation between compatible pollen tubes and incompatible pollen tubes in semi-compatible and cross compatible groups ($r_s = 0.403$; $p = 0.000$). With ~16% of the variation in the number of compatible pollen tubes explained by the number of incompatible pollen tubes ($r_s^2 = 0.162409$). These data suggest semi-compatible and cross-compatible stigmas that germinate more compatible pollen tubes tend to germinate more incompatible pollen tubes.

5.3 – continued

Box 25 - Spearman rank-order correlation: Rank-J, compatible pollen tubes, Rank-K incompatible pollen tubes in all *C. bipinnatus* compatibility groups to test, H_0 that there is no correlation between the number of compatible pollen tubes and the number of incompatible pollen tubes in all *C.-bipinnatus* compatibility groups.

Pearson correlation of Rank-J and Rank-K = $r_s = 0.375$

$p = 0.000$

$r_s^2 = 0.140625$

Reject H_0 ($p = < 0.05$), therefore can assume that there is a significant weak positive association between compatible pollen tubes and incompatible pollen tubes in all *C.-bipinnatus* compatibility groups ($r_s = 0.375$; $p = 0.000$). With ~14% of the variation in the number of compatible pollen tubes explained by the number of incompatible pollen tubes ($r_s^2 = 0.140625$). These data suggest *C.-bipinnatus* stigmas that germinate more compatible pollen tubes tend to germinate more incompatible pollen tubes.

5.4 – Royal Botanic Gardens, Kew (RBG, Kew) Plant Data for *Cosmos* accessions used in POLL-01 pollinations (Chapter 5)

(a) – *Cosmos atrosanguineus*

1977-3447 **Alpine & Herb.**

COMPOSITAE *Cosmos atrosanguineus* (Hook.) Stapf

Location(s): area 153

area 157 65

Taxon notes: Tribe: Heliantheae, Family: Asteraceae

Range: Central Mexico

Mexican states: Hidalgo, San Luis Potosí

Batch: 420

Donated by: Le Roy Davidson (DAVI)

Material received: Plant

Field notes: (Via Tony Hall).

Identification notes: Verified. by F.G. Davies 14.8.78

Horticultural merit: Very high

Curation notes: + Loc.15765. **Part transferred to Technical 26/11/1999 see 1999-3819.**

Repeat propagation in April Vegetative propagation method: Cuttings

Tolerance: Needs winter protection

Habit: Perennial dying back

Sex: Hermaphrodite

Flowering period: -----JAS--- (July-August-September)

Scientific interest: Possible

Date Record Created:

Date record last amended: 26/11/1999

Date last resurrected:

→ **1999-3819 Technical**

COMPOSITAE *Cosmos atrosanguineus* (Hook.) Stapf

Location(s): Jodrell Glass (5 plants)

Taxon notes: Tribe: Heliantheae, Family: Asteraceae

Range: Central Mexico

Mexican states: Hidalgo, San Luis Potosí

Batch: 420

Donated by: Le Roy Davidson (DAVI)

Material received: Plant

Field notes: (Via Tony Hall).

Identification notes: Verified by F.G. Davies 14.8.78

Horticultural merit: Very high

Curation notes: + Loc.15765. **Part transferred from Alpine & Herb. 26/11/1999 see 1977-3447.**

Repeat propagation in April Vegetative propagation method: Cuttings

Tolerance: Needs winter protection.

Habit: Perennial dying back

Sex: Hermaphrodite

Flowering period: -----JAS---

Scientific interest: Possible

Date Record Created: 26/11/1999

Date record last amended:

Date last resurrected:

1998-490 Alpine & Herb.

DEAD

COMPOSITAE *Cosmos atrosanguineus* (Hook.) Stapf

Location(s): Decorative Nursery

Taxon notes: Tribe: Heliantheae, Family: Asteraceae

Range: Central Mexico

Mexican states: Hidalgo, San Luis Potosí

Donated by: Proculture Plants Ltd. (PROP) on 13/02/1998

Material received: Plant

Curation notes: Accessioned 13/02/1998. (For summer bedding displays 1998). (RBGARPB). CUTTINGS sent to Mr Tim Miles, Cotswold Wildlife Park,, Burford,, Oxon. on 15/09/1998. **Part transferred to Technical 07/07/1999 see 1999-2254.** Not required for displays in near future.

Deaded 09/07/1999 (Discarded).

Tolerance: Needs winter protection.

Habit: Perennial dying back

Sex: Hermaphrodite

Flowering period: -----JAS---

Scientific interest: Possible

Date Record Created: 13/02/1998

Date record last amended: 09/07/1999

Date last Deaded: 09/07/1999

Reason for Death: Discarded

→ **1999-2254 Technical**

COMPOSITAE *Cosmos atrosanguineus* (Hook.) Stapf

Location(s): Jodrell Glass (3 plants)

Taxon notes: Tribe: Heliantheae, Family: Asteraceae

Range: Central Mexico

Mexican states: Hidalgo, San Luis Potosí

Donated by: Proculture Plants Ltd. (PROP) on 13/02/1998

Material received: Plant

Curation notes: Accessioned 13/02/1998. (For summer bedding displays 1998). (RBGARPB). CUTTINGS sent to Mr Tim Miles,, Cotswold Wildlife Park,, Burford,, Oxon. on 15/09/1998. **Part transferred from Alpine & Herb. 07/07/1999 see 1998-490.**

Tolerance: Needs winter protection.

Habit: Perennial dying back

Sex: Hermaphrodite

Flowering period: -----JAS---

Scientific interest: Possible

Date Record Created: 07/07/1999

Date record last amended: 13/02/1998

Date last resurrected:

1998-1957 Alpine & Herb.

DEAD

COMPOSITAE *Cosmos atrosanguineus* (Hook.) Stapf

Location(s): Alpine Yard PROP

Taxon notes: Tribe: Heliantheae, Family: Asteraceae

Range: Central Mexico

Mexican states: Hidalgo, San Luis Potosí

Donated by: Jard.Bot.Nat.de Belgique (JB NB) on 14/05/1998

Material received: **Seeds**

Field notes: Verified by Institute.

Curation notes: Accessioned 14/05/1998. For Order Beds. RBGARP B

Habit: Perennial dying back

Sex: Hermaphrodite

Flowering period: -----

Scientific interest: **High**

Date Record Created: 14/05/1998

Date record last amended: 14/05/1998

Date last resurrected:

1979-1666 Wakehurst

COMPOSITAE *Cosmos atrosanguineus* (Hook.) Stapf

Location(s): area 751 HPG-B (1 plants)

Micropropagation

Wakehurst Nursery SP

Taxon notes: Tribe: Heliantheae, Family: Asteraceae

Range: Central Mexico

Mexican states: Hidalgo, San Luis Potosí

Batch: 178

Donated by: National Trust (NTTT)

Material received: Plant

Identification notes: Syn. *Cosmos diversifolius* Otto var. *atrosanguineus* Hook.f. F.G.Davies 17.7.81

Nursery Sort Code: B

Horticultural merit: High

Curation notes: Tuberous rooted. Repropagated regularly. Group planted 1980 1 PL to W.Ingwensen 29.9.86. 1 PL to J.Russell 3.3.89. Material to Micropropagation August 1993 for propagation and possible return to Mexico, where species is now thought to be extinct in wild. **Part transferred to Jodrell Glass 18/09/1997 - see 1997-6334.**

Repeat propagation in September Vegetative propagation method: Cuttings TPU no. 3497

Habit: Perennial dying back

Sex: Hermaphrodite

Flowering period: -----JJA---- (June-July-August)

Scientific interest: Possible

Date Record Created:

Date record last amended: 01/09/1999

Date last resurrected:

→ **1997-6334 Technical**

COMPOSITAE *Cosmos atrosanguineus* (Hook.) Stapf

Location(s): Jodrell Glass

Micropropagation

Taxon notes: Tribe: Heliantheae, Family: Asteraceae

Range: Central Mexico

Mexican states: Hidalgo, San Luis Potosí

Batch: 178

Donated by: National Trust (NTTT)

Material received: Plant

Identification notes: Syn. *Cosmos diversifolius* Otto var. *atrosanguineus* Hook.f. F.G.Davies 17.7.81

Nursery Sort Code: B

Horticultural merit: High

Curation notes: Part transferred from Wakehurst 18/09/1997 - see 1979-1666. 2 plant sent to Botanic Garden, University of Copenhagen,, Oster Farimagsgade 2 B, D-K 1353 Copenhagen K,, Denmark. on 19/09/1997

Repeat propagation in Sep Veg. propagation method: Cuttings

TPU no. 3497

Habit: Perennial dying back

Sex: Hermaphrodite

Flowering period: -----JJA----

Scientific interest: Possible

Date Record Created: 18/09/1997

Date record last amended: 05/02/1999

Date last resurrected:

(b) – Cosmos bipinnatus

1995-2162 Alpine & Herb.

COMPOSITAE *Cosmos bipinnatus* Cav.

Location(s): area 157 63 (5 plants)

Taxon notes: Tribe: Heliantheae, Family: Asteraceae

Range: Arizona, Mexico

Arizona, southeastward into the states of Puebla & Michoacan, Mexico.

Donated by: Dr. & Mrs. H. J. M. Bowen (BOHJ) on 31/05/1995

Collected by: Dr. & Mrs. H. J. M. Bowen (BOHJ)

Material received: Seeds

Field notes: Original collecting data: West Down, Dorset, collected 1994 from rubbish tip?

Curation notes: Accessioned 31/05/95: For Order Beds **Part transferred to Jodrell Glass 14/02/96 - see 1996-582.**

Habit: Annual

Sex: Hermaphrodite

Flowering period: -----

Scientific interest: Possible

Date Record Created: 31/05/1995

Date record last amended: 09/09/1996

Date last resurrected:

1996-582 Technical

COMPOSITAE *Cosmos bipinnatus* Cav.

Location(s): Jodrell Glass (5 plants)

Fully Verified by Sarah A. L. Smith (SMTS) on 15/08/1996

Taxon notes: Tribe: Heliantheae, Family: Asteraceae

Range: Arizona, Mexico

Arizona, southeastward into the states of Puebla & Michoacan, Mexico.

Donated by: Dr. & Mrs. H. J. M. Bowen (BOHJ) on 31/05/1995

Collected by: Dr. & Mrs. H. J. M. Bowen (BOHJ)

Material received: Seeds

Field notes: Original collecting data: West Down, Dorset, collected 1994 from rubbish tip?

Identification notes: Previously verified as COMPOSITAE *Cosmos bipinatus* Cav. (Dr. D. J. N. Hind 20/05/1996). Previously known as COMPOSITAE *Cosmos bipinnatus*.

Curation notes: **Part transferred from Alpine & Herbaceous 14/02/96 - see 1995-2162.**

Habit: Annual

Sex: Hermaphrodite

Flowering period: -----

Scientific interest: Possible

Date Record Created: 14/02/1996

Date record last amended: 09/09/1996

Date last resurrected:

(c) – Cosmos sulphureus

1988-1964 Alpine & Herb.

COMPOSITAE *Cosmos sulphureus* Cav.

Location(s): area 157 66

ARP Rating(s): A2 (Core research support)

Taxon notes: Tribe: Heliantheae, Family: Asteraceae

Range: Mexico

Native of Mexico, widespread as a pan-tropic weed and escape from cultivation

Batch: 241

Donated by: Mrs A.Hoffman (HOFF)

Material received: Seeds

Field notes: Cultivated, garden origin. 16.5.88. Submitted as *Cosmos*.

Identification notes: Verified by D.J.N.Hind 27.9.88.

Horticultural merit: Very high

Curation notes: + Loc.15766 **Part transferred to Jodrell Glass 14/02/96 - see 1996-583.**

Vegetative propagation method: Cuttings

Tolerance: Tender

Habit: Annual

Sex: Hermaphrodite

Flowering period: -----S---

Date Record Created:

Date record last amended: 14/02/1996

Date last resurrected:

1996-583 Technical

DEAD

COMPOSITAE *Cosmos sulphureus* Cav.

Location(s): Jodrell Glass (5 plants)

ARP Rating(s): A2 (Core research support)

Taxon notes: Tribe: Heliantheae, Family: Asteraceae

Range: Mexico

Native of Mexico, widespread as a pan-tropic weed and escape from cultivation

Batch: 241

Donated by: Mrs A.Hoffman (HOFF)

Material received: Seeds

Field notes: Cultivated, garden origin. 16.5.88. Subm.as *Cosmos*.

Identification notes: Ver. by D.J.N.Hind 27.9.88.

Horticultural merit: Very high

Curation notes: **Part transferred from Alpine & Herbaceous 14/02/96 - see 1988-1964.** Deaded 05/02/1999 (Failed to germinate).

Veg. propagation method: Cuttings

Tolerance: Tender

Habit: Annual

Sex: Hermaphrodite

Flowering period: -----S---

Date Record Created: 14/02/1996

Date record last amended: 05/02/1999

Date last Deaded: 05/02/1999

Reason for Death: Failed to germinate

(d) – Cosmos carvifolius

1994-552 Alpine & Herb. Natural Source
COMPOSITAE *Cosmos carvifolius*
Location(s): area 157 65
Taxon notes: Tribe: Heliantheae, Family: Asteraceae
Range: Mexico
Donated by: J.A.Compton (COMP) on 07/02/1994
Collected by: Compton, D'Arcy & Rix (CDRX) no. 1404
Geography: Durango Findspot: Sinaloa/Durango Province border, La
Cuidad to Copala road
Altitude: 2000 metres
Material received: Seeds
Field notes: Dissected leaves, pale pink flowers. Collected Oct-Nov
1991.
Curation notes: Accessioned 16/02/94. For O.B. Part transferred to
Technical 11/02/1999 - see 1999-383.
Tolerance: Tender
Habit: Annual
Sex: Hermaphrodite
Flowering period: -----
Date Record Created: 16/02/1994
Date record last amended: 24/03/1999
Date last resurrected:

1999-383 Alpine & Herb. Natural Source
COMPOSITAE *Cosmos carvifolius*
Location(s): Technical
Taxon notes: Tribe: Heliantheae, Family: Asteraceae
Range: Mexico
Donated by: J.A.Compton (COMP) on 07/02/1994
Collected by: Compton, D'Arcy & Rix (CDRX) no. 1404
Geography: Durango Findspot: Sinaloa/Durango Province border, La
Cuidad to Copala road
Altitude: 2000 metres
Material received: seeds
Field notes: Dissected leaves, pale pink flowers. Collected Oct-Nov
1991.
Curation notes: Accessioned 16/02/94. For O.B. **Part transferred from
from Alpine area 157 65 11/02/1999 - see. 1994-552**
Identification notes: Previously accessioned as COMPOSITAE *Cosmos
diversifolius* 16/02/94. Verified as *Cosmos carvifolius* (Dr. D.J.N.
Hind 24/03/1999).
Tolerance: Tender
Habit: Annual
Sex: Hermaphrodite
Flowering period: -----
Date Record Created: 16/02/1994
Date record last amended: 24/03/1999
Date last resurrected:

APPENDIX 6 - Review of *Brassica* S-primers

6.1 - Published *Brassica* S-primers used in PCR-amplification and cycle sequencing of S-genes in *Brassica* and *Arabidopsis*

Primer name	Priming Direction	Nucleotide Sequence (5' to 3')	Primer length (bases)	Class	Gene source	Genbank Accession	Ref.
PS1	⇒	¹ AGATGAAAGGAGTAAGAAAA ²⁰	20	I	Bol SLG6	Y00268	10, 11.
PS3	⇒	¹ ATGAAAGGGGTACAGAACAT ²⁰	20	II	Bol SLG2-b	AB024415	4, 8, 12.
PS5	⇒	¹ ATGAAAGGCGTAAGAAAAACCTA ²³	23	I	Bra SLG8	D84468	6,11,12,17.
PS4CM	⇒	[?] CGGAATATGGTATAAGAAAGTCTCCCA [?]	27	II	Bol SLGA (S15) Bol SLGB (S15)	Y18262 Y18261	2, 9.
PS5CM	⇒	[?] GGAATATGGTATAAAAAAGCCCCCTG [?]	26	II	Bol SLGA (S15) Bol SLGB (S15)	Y18262 Y18261	2, 9.
PS18	⇒	¹ ATGAAAGGTGTACGAAACATCTA ²³	23	I	Bra SLG9	D30050	12, 16.
PS22	⇒	¹⁹⁶ ATCGATGGGATGAAAAAGTCATCG ²¹⁹	24	I	Bol SLG13 promoter region	S82574	7, 13, 14.
PS24	⇒	¹ ATGAGAGGTGTAATACCAAAC ²¹	21	I	Bol SLR1-(S29)	X16122	13, 15.
PSA	⇒	¹³⁹ AGAACACTTGTATCTCCCGGT ¹⁵⁹	21	I & II	Bol SLG13	X55275	1, 6.
Oligo-C	⇒	⁻¹¹ TGGCTCGAGAGATGAAAGGCATAAGAAAAAC ²⁰	31	I	Bol SLG3	X79431	5.
SDOM1	⇒	²⁰² GWTGGTAYCTCGGRATRTGGTA ²²⁴	22	I	Bol SLG13	X55275	1, 6, 9.
SLGF	⇒	²⁴¹ AGAACCTATGCATGGGTTGC ²⁶⁰	20	I & II	Bol SLG13	X55275	3.
S11	⇒	¹⁷¹ GCTTGGTTTCTTCACTCC ¹⁸⁷	18	NA	Bol SLG13	X55275	3.
Ats1F	⇒	⁴²⁷ AACTTCGTGATGCGAGACTCC ⁴⁴⁷	21	NA	Ath AtS1	S84921	3.
SRK2-F	⇒	¹²⁰⁷ ACGGGTGTGTGATTTGGACTGGA ¹²³⁰	24	I	Bol SRK13	AB024419	3.

¹Brace *et al.* (1993); ²Cabrillac *et al.* (1999); ³Charlesworth *et al.* (2000); ⁴Chen & Nasrallah (1990); ⁵Delorme *et al.* (1995); ⁶Dwyer *et al.* (1991); ⁷Dzelzalns *et al.* (1993); ⁸Kusaba *et al.* (2000); ⁹Miege *et al.* (2001); ¹⁰Nasrallah *et al.* (1987); ¹¹Nishio *et al.* (1994); ¹²Nishio *et al.* (1996); ¹³Sakamoto *et al.* (1998); ¹⁴Stein *et al.* (1996); ¹⁵Trick and Flavell (1989); ¹⁶Watanabe *et al.* (1994); ¹⁷Yamakawa *et al.* (1994). Superscript numbers indicate the nucleotide position from the translation initiation site ATG.. Bol = *Brassica oleracea*; Bra = *Brassica rapa* (syn. *campestris*); Ath = *Arabidopsis thaliana*

6.1 - continued

Primer name	Priming Direction	Nucleotide Sequence (5' to 3')	Primer length (bases)	Class	Gene source	Genbank Accession	Ref.
PS2	↗	¹³²¹ ATCCGTGCTTTATTTAAGA ¹²⁴⁰	20	I	BoI <i>SLG6</i>	Y00268	11.
PS4	↗	¹³²⁶ CTAACCTAGATCAGCAGCAT ¹³⁰⁷	20	II	BoI <i>SLG2-b</i>	AB024415	4, 8, 11, 12.
PS15	↖	¹³³⁶ CCGTGTTTTATTTAAGAGAAAGAGCT ¹³¹⁰	27	I	Bca <i>SLG8</i>	D84468	6, 12, 17.
PS21	↖	¹⁰²⁵ CTCAAGTCCCCTGCTGCGG ¹⁰⁰⁶	20	II	BoI <i>SLG2A</i> BoI <i>SLG2-b</i>	AB024415	4, 8, 12.
PS25	↖	¹³⁰² GAGATAAAGATCTTGACCTC ¹²⁸³	20	I	BoI <i>SLR1 (S29)</i>	X16122	13, 15.
PSB	↖	¹²⁸⁷ CAATCTGACATAAAGATCTTG ¹²⁶⁷	21	I	BoI <i>SLG13</i>	X55275	1, 6.
PSD	↖	¹¹³³ AAGGTCAGCAGSAGCCAATC ¹¹¹⁴	20	I	BoI <i>SLG9</i>	D85200	1.
Oligo-D	↖	¹⁴⁷² AGGGAGATCAAATTTATGTGATTTTACATGG ¹⁴⁴²	31	I	BoI <i>SLG3</i>	X79431	5.
SG17	↖	? TGTTCGGTCTGTCAAGTCCCCTGCTGCGG ?	30	II	BoI <i>SLGA (S15)</i> BoI <i>SLGB (S15)</i>	Y18262 Y18261	2, 9.
SG2	↖	? GGCCTGCAGCAGCATTCAATCTGAC ?	25	II	BoI <i>SLGA (S15)</i> BoI <i>SLGB (S15)</i>	Y18262 Y18261	2, 9.
SG39	↖	? CTTTGCGTTTCAACACGTTGATTCA ?	25	II	BoI <i>SLGA (S15)</i> BoI <i>SLGB (S15)</i>	Y18262 Y18261	2, 9.
SK30	↖	¹⁸⁰⁵ TTCTCGCCCTCATAAACACAACAG ¹⁷⁸²	24	II	BoI <i>SRK2-b</i>	AB024416	8, 9.
SK38	↖	¹³⁷⁰ CTCCAACCTATGATTTTCCAGT ¹³⁴⁸	23	II	BoI <i>SRK2-b</i>	AB024416	8, 9.
SRK4-R	↖	¹⁷²² TTTCGGTGGCTTTGACAACAG ¹⁷⁰²	21	I	BoI <i>SRK13</i>	AB024419	3.
SK66DC	↖	¹⁴²⁷ CTCCTCCAAAAGCAGAACACGATAAACACTC ¹³⁹⁸	30	I	BoI <i>SRK2-b</i>	AB024416	1, 6, 9.
SLGR	↖	¹²⁸⁵ ATCTGACATAAAGATCTTGACC ¹²⁶⁴	22	I	BoI <i>SLG13</i>	X55275	3.
Ats1R	↖	¹²⁴⁹ CGGTCCAATGACACAACCCG ¹²²⁹	21	NA	Ath <i>AtS1</i>	S84921	3.

6 2 - Analysis of priming characteristics of published *Brassica S*-primer pairs

Primer Pairs	Primer Class	Specificity	Comments on PCR Product
PS1 + PS2	I	SLG	A single 1.3 kb DNA fragment thought to be a class-I SLG amplified in <i>Brassica oleracea</i> and <i>B. campestris</i> .
PS5 + PS15	I	SLG	A single 1.3 kb DNA fragment. thought to be a class-I SLG was amplified in <i>Brassica</i> spp. and <i>Raphanus sativus</i> .
PS3 + PS4	II	SLG, SLR2	Two 1.3 kb DNA fragments produced in <i>Brassica oleracea</i> . One thought to be SLR2, the other thought to be a class-II SLG because it was only detected in the 12 S-genotypes that were negative with class-I primer pair PS5 + PS15. PS4 is a class II SLG primer that has a nucleotide sequence similar to SLR2, so it is not possible to distinguish class II SLGs from SLR2 using PS4 as the reverse primer.
PS3 + PS21	II	SLG, SRK	A single 1.0 kb DNA fragment was amplified, which is the expected size of a class II-SLG fragment.
PS18 + PS15	I	SLG	A single 1.3 kb DNA fragment produced, which is the expected size of a class I-SLG fragment.
PSA + PSB	I & II	SLG, SRK, SLR1, SLR2 when annealed at 58°C	A single DNA fragment of 1150bp amplified. Some of this fragment was SLR2 and the other SLG (Nishio <i>et al.</i> 1996). Brace <i>et al.</i> (1993) used these primers to amplify a single 1150bp fragment from genomic DNA of different <i>Brassica oleracea</i> S haplotypes. This primer pair shows high homology to all members of the <i>Brassica S</i> -multigene family for which sequence data are available and consequently also amplifies a range of unidentified S-multigene family sequences. This is because PSA was designed from the highly conserved region located towards the 5' end (nt region = low 100 bp) and PSB from the extremely highly conserved region at the 3' end of SLG ¹³ (Bol) (nt region = low 1300 bp).
PSA + PSD	I	SLG, SRK, SLR2 when annealed at 65°C	SLR1 is not present in the amplification products when PSA + PSD are used at an annealing temperature of 65°C. At this Ta the proportion of SLR2 and the unknown S-multigene family sequences is also reduced or eliminated. PSD was designed from the extremely highly conserved sequence towards the 3' end (nt region = low 1.3 kb, but further downstream than PSB). Primer PSD was designed with the aim of eliminating SLR1 sequences, but also reduces the proportion of SLR2 fragments in the amplification products when an annealing temperature of 65°C is used.
PS22 + PS15	I	SLG	A single 1.5 kb fragment of DNA amplified in <i>Brassica campestris</i> (Nishio <i>et al.</i> , 1996) that has 85% to 90% sequence similarity to SLG ⁶ (Bol).
PS24 + PS25	SLR1	SLR1	DNA fragments of 1.3 kb amplified in <i>B. oleracea</i> and <i>B. campestris</i> . Sequences have a low intraspecific polymorphism typical of SLR1 sequences.
Oligo C + OligoD	I	S-domain	Used to amplify the S-domain region of SLG ³ (Bol) and SRK3(Bol) (Delorme <i>et al.</i> , 1995).
PS3 + SG17	II	SLG	Used to amplify 1.27 kb corresponding to SLGA, SLGB and the SRK-S-domain in S15 <i>Brassica oleracea</i> .
PS4CM + SG39	II	SLG	Used to amplify 1.27 kb corresponding to SLGA, SLGB and the of SRK-S-domain in S15 <i>Brassica oleracea</i> .
PS5CM + SG2	II	SRK	Amplifies Class II SRK in S15 <i>Brassica oleracea</i> .
SDOM1 + SK30	I	SRK	Amplifies Class I AND II SRK sequences.
SDOM1 + SK38	I	SRK	Amplifies Class I AND II SRK sequences.
SDOM1+SK66DC	I	SRK	Amplifies Class I AND II SRK sequences.